Universidad de Huelva

Departamento de Ingeniería Química, Química Física y Ciencias de los Materiales

Development of new lignocellulosic-based thickening agents for biodegradable oleogel formulations with several industrial applications

Memoria para optar al grado de doctor
presentada por:

Antonio María Borrero López

Fecha de lectura: 1 de julio de 2021

Bajo la dirección de los doctores:

José María Franco Gómez

Concepción Valencia Barragán

Huelva, 2021

University of Huelva

Department of Chemical Engineering, Physical Chemistry
and Materials Science

Development of new lignocellulosic-based thickening agents for biodegradable oleogel formulations with several industrial applications

Ph.D. Thesis

Doctoral Program in Industrial and Environmental Science and Technology

Antonio María Borrero López

2021

Supervisors:

Dr. José María Franco Gómez

Dr. Concepción Valencia Barragán

Universidad de Huelva

Departamento de Ingeniería Química, Química Física y Ciencias de los Materiales

Desarrollo de nuevos agentes espesantes basados en fracciones lignocelulósicas para formulaciones biodegradables tipo gel en fase oleosa con diversas aplicaciones industriales

Tesis Doctoral

Programa de Doctorado en Ciencia y Tecnología Industrial y Ambiental

Antonio María Borrero López

2021

Supervisores:

Dr. José María Franco Gómez

Dr. Concepción Valencia Barragán

Acknowledgments

In the first place, I would like to express how bad I feel when I think that this Doctoral Thesis will bear only my name as an author, since I have always seen this research more as a joint project among all those who have participated from the slightest contribution to those who have had more than one headache seeing a snarl of results and my crazy ideas about it.

For this reason, I would like to first name the pillars of this thesis, my two supervisors, José María Franco and Concepción Valencia, because without them, their trust and determination, all this research would have not been possible. All those moments in which Concha came to the laboratory with new ideas, so many times that it was difficult for me to remember them all, now seem distant, but they are very present in the success of this work. José María, although generally from his office, also contributed with his ideas and wisdom to transform points and lines on a graph into clearly observable trends and verifiable facts. Thank you both.

Again I want to reaffirm that this project is not only mine, since without the help of those who have been by my side in the laboratory, contributing with their knowledge, their ideas, or simply encouraging when something seemed that it would never go well, nothing of this would have been possible. For this reason, I want to make special mention of a prodigious mind, Adrián, for teaching me more about polyurethanes than any other book or publication, and thus guiding my steps far beyond of what I could have done alone. Special mention also to Esperanza, who never denied me help and who has always been there for me when I needed it. You have also been very good friends during these 5 years. Just thank you for everything. And special mention also to all those who have made an exceptional work environment, for those who were and those who are, and even at the risk of forgetting a name, I would never forgive myself for not including them here. Thanks Alex, Clara, Fran, Esteban, Mauricio, Alberto, Víctor, Belén, Rocío, Ortega, Cuadri, Quique, Alba, Coraima, María, José Fernando, Rodrigo, Ricardo, Manolo, Isa,… Thanks also to all the Chemical Process and Product Technology Research Centre (Pro2TecS), and the Complex Fluid Engineering Group (TEP-185), for their support and involvement in this research.

Thanks also to the Aalto University, University of Alcalá and INIA, for hosting me during the research stays, especially Professor Orlando Rojas, Manuel Hernández and María Eugenia Eugenio, and all those who have given me a hand both inside and outside the University,

Ling, Blaise, Tai, Bruno, Luiz, Melania, Jan, Ester, etc., with special mention to *Cadu*, simply a very good friend.

Thanks also to the *Ministerio de Educación, Cultura y Deporte*, which has given me the opportunity during the last years of my thesis to complete this project, that could have otherwise been a little shorter, with the grant *Beca de Formación del Profesorado Universitario* FPU16/03697, and the mobility grants (EST17/00875 and EST18/00577), without which all of this could have never been carried out. Thanks also to the projects CTQ2014-56038-C3-1R and CTQ2014-56038-C3-2R, which made the collaborative work between INIA, Universidad de Alcalá and our research centre possible.

Of course I cannot forget my family, who have suffered during all these years the question of *what does Antonio work for?* I hope that today they will be able to give an answer without mentioning *lignin* and *polyurethane*, so that they do not make me look like a freak. Thanks to my parents, for supporting me not only in this, but in everything I have done in my life, and giving me an unbeatable education, from which I am sure I have learned the most valuable thing I know, to be happy. Thanks to my brothers, two of the people I admire most in my life, you have been able to be everything I like, and above all, you have given it a personal touch that makes you unique and irreplaceable, you are really the best. Thanks to my Aunt María José, for being a second mother. Thanks to my grandparents, my aunts, my uncles, my godmother, in short, to all that group that showed up at my graduation and almost made the auditorium small when I told them only two days in advance, I know you love me very much, and so do I.

Thanks to Ana, the person who has probably experienced the worst part of all of this, when things did not go well and I was frustrated, or when I forgot something and my anger came to the surface, she has always been there to calm me down, and honestly, just by looking at her I thought many times about the insignificance of the situation, and I forgot about it. Thank you for making me so happy and making me laugh so much, thank you from the bottom of my heart.

Finally, thanks to Emilio for the cover design, to all my friends from the town, from my career, from my precious village, from the beach, from those places where I have worked far from home, you are all part of who I am and of what I have achieved.

Thank you all from the heart.

Agradecimientos

En primer lugar, me gustaría expresar lo mal que me siento al pensar que esta Tesis Doctoral llevará únicamente mi nombre como autor, ya que siempre he visto más esta investigación como un proyecto conjunto entre todos aquellos que han aportado desde la más mínima contribución hasta aquellos que han tenido más de un dolor de cabeza viendo una maraña de resultados y mis elucubraciones al respecto.

Por ello, me gustaría nombrar en primer lugar a los pilares de esta tesis, mis dos supervisores, José María Franco y Concepción Valencia, porque sin ellos, su confianza y determinación, toda esta investigación no habría sido posible. Todos esos momentos en los que Concha venía al laboratorio con nuevas ideas, tantas que muchas veces me costaba recordarlas todas, se antojan ahora lejanos, pero están muy presentes en el éxito de la totalidad de este trabajo. José María, aunque desde su despacho generalmente, también aportaba sus ideas y su sabiduría para transformar puntos y líneas en un gráfico en tendencias claramente observables y hechos contrastables. A los dos, mil gracias.

De nuevo quiero reafirmarme en que este proyecto no es mío sólo, ya que sin la ayuda de aquellos que han estado a mi lado en el laboratorio, aportando sus conocimientos, sus ideas, o simplemente animando cuando algo parecía que jamás saldría bien, nada de esto hubiera sido posible. Por ello, quiero hacer especial mención a una mente prodigiosa, Adrián, por enseñarme más de los poliuretanos que ningún otro libro ni publicación, y de este modo guiar mis pasos mucho más allá de lo que podría haberlo hecho solo. Especial mención también a Esperanza, la cual jamás me negó la ayuda y que siempre ha buscado un hueco cuando lo necesitaba. Habéis sido además muy buenos amigos durante estos 5 años. Simplemente, gracias por todo. Y especial mención también a todos aquellos que han hecho un ambiente de trabajo excepcional, para los que estuvieron y los que están, y aún a riesgo de olvidar algún nombre, jamás me perdonaría no incluirlos aquí. Gracias Alex, Clara, Fran, Esteban, Mauricio, Alberto, Víctor, Belén, Rocío, Ortega, Cuadri, Quique, Alba, Coraima, María, José Fernando, Rodrigo, Ricardo, Manolo, Isa, … Gracias también a todo el *Centro de Investigación en Tecnología de Productos y Procesos Químicos* (Pro^{2}TecS) y al *Grupo de Ingeniería de Fluidos Complejos* (TEP-185) por su apoyo y su implicación en la investigación.

Gracias también a la Universidad de Aalto, la Universidad de Alcalá, y el INIA por acogerme durante las estancias de investigación, en especial al Profesor Orlando Rojas, Manuel

Hernández y María Eugenia Eugenio, y a todos aquellos que me han echado una mano tanto dentro como fuera de la Universidad, Ling, Blaise, Tai, Bruno, Luiz, Melania, Jan, Ester, etc., con especial mención a *Cadu*, simplemente un muy buen amigo.

Gracias también al *Ministerio de Educación, Cultura y Deporte*, que me ha dado la posibilidad durante los últimos años de tesis de culminar este proyecto que de otro modo podría haberse quedado un poco corto, con la concesión de la *Beca de Formación del Profesorado Universitario* FPU16/03697, y las becas de movilidad (EST17/00875 y EST18/00577), sin las cuales todo esto jamás podría haberse llevado a cabo. Gracias también a los proyectos CTQ2014-56038-C3-1R y CTQ2014-56038-C3-2R, que hicieron posible la colaboración entre el INIA, la Universidad de Alcalá y nuestro centro de investigación.

Por supuesto no puedo olvidar a mi familia, los cuáles han sufrido durante todos estos años la pregunta *¿de qué trabaja Antonio?*, espero que a día de hoy sean capaces de dar una respuesta sin mencionar *lignina* y *poliuretan*o, de modo que no me hagan parecer un bicho raro. Gracias a mis padres, por apoyarme no sólo en esto, sino en todo lo que he hecho en mi vida, y darme una educación inmejorable, de la cual estoy seguro que he aprendido lo más valioso que sé, a ser feliz. Gracias a mis hermanos, dos de las personas que más admiro en mi vida, habéis sido capaces de ser todo lo que me gusta, y encima le habéis dado un toque personal que os hace únicos e irremplazables, de verdad sois lo mejor. Gracias a mi Tía María José, por ser una segunda madre. Gracias a mis abuelos, mis tías, mis tíos, mi madrina, en definitiva, a todo ese grupo que se presentó en mi graduación y casi hacen pequeño el auditorio cuando os avisé con dos días de antelación, sé que me queréis mucho, y yo a vosotros.

Gracias a Ana, la persona que probablemente haya vivido la peor parte de todo esto, cuando las cosas no salían bien y me frustraba, o cuando olvidaba algo y la rabia me salía a flor de piel, ella siempre ha estado ahí para calmarme, y la verdad, solo con mirarla muchas veces pensaba en lo nimio de la situación, y me hacía olvidarme de todo ello. Gracias por hacerme tan feliz y hacerme reír tanto, gracias de corazón.

Finalmente, gracias a Emilio por el diseño de la portada, a todos mis amigos del pueblo, de la carrera, de mi preciada aldea, de la playa, de aquellos lugares donde he trabajado lejos de casa, todos formáis parte de lo que soy y de lo que he conseguido.

Gracias de corazón a todos.

The most beautiful thing we can experience is the mysterious. It is the source of all true art and science. He to whom the emotion is a stranger, who can no longer pause to wonder and stand wrapped in awe, is as good as dead; his eyes are closed. To know what is impenetrable to us really exists, manifesting itself as the highest wisdom and the most radiant beauty, which our dull faculties can comprehend only in their most primitive forms.

Albert Einstein

La cosa más bella que podemos experimentar es el misterio. Es la fuente de toda verdad y ciencia. Aquel para quien esa emoción es ajena, aquel que ya no puede maravillarse y extasiarse ante el asombro, vale tanto como un muerto: sus ojos están cerrados. Saber que lo impenetrable para nosotros existe realmente, manifestándose como la sabiduría suprema y la belleza más radiante, que nuestras torpes capacidades pueden comprender tan sólo en sus formas más primitivas.

Albert Einstein

Por Dani y Andrés

Contents

Table of contents

Resumen

Debido a la creciente necesidad de encontrar productos que respeten el medio ambiente, el trabajo que conforma esta Tesis Doctoral está centrado en el uso y aprovechamiento de material lignocelulósico procedente de diversas fuentes, principalmente ligninas residuales, como polioles para la formación de poliuretanos, que pueden actuar como agentes gelificantes alternativos en medio oleoso. Para lograr tal fin, se han llevado a cabo modificaciones químicas y/o biológicas, a través de las cuales se ha conseguido mejorar y modular tanto las propiedades mecánicas como reológicas de los oleogeles de poliuretano resultantes. Se han empleado satisfactoriamente como material lignocelulósico residuos procedentes de la agricultura como son la paja de trigo y de cebada directamente, así como ligninas obtenidas de diversas fuentes y pasta de celulosa. Además, en función del tipo y concentración del material lignocelulósico, naturaleza y concentración del agente entrecruzante y protocolo de procesado, se han desarrollado sistemas tipo gel con propiedades lubricantes, adhesivos y elastómeros con excelentes propiedades de amortiguación.

Abstract

Propelled by the urgent need of finding more environmental-friendly products, the study comprising the present Ph.D. thesis is devoted to the use of different lignocellulosic materials from several sources, mainly waste lignins, as polyols for polyurethane formation, which have been targeted as alternative bio-based gelling agents in oil media. For achieving such purpose, chemical and/or biological modifications have been aimed, through which improved and tailored rheological and mechanical properties of the resulting polyurethane oleogels have been obtained. Agriculture residues such as barley and wheat straw, lignin from different origins, and cellulose pulp have successfully been employed as alternative lignocellulosic materials. Furthermore, depending on lignocellulose source type and concentration, nature and concentration of crosslinker and processing protocol, soft gel-like systems with lubricant properties, adhesives, and elastomeric materials with excellent cushioning properties have been developed.

Chapter 1: Introduction

1. Summary

Driven by the environmental awareness and the still lack of bio-based products that may replace the non-renewable-based systems, this Ph.D. thesis is devoted to the search for lignocellulosic-based networks that can act as thickening and/or gelling agents in oil media for several consumer goods such as lubricants, adhesives or cushioning materials. Therefore, the main purpose of this study is the finding of suitable combinations of lignocellulosic biomass with castor oil, as the vegetable oil selected for the accomplishment of eco-friendly gel-like systems, through proper crosslinking with diisocyanate compounds. In this sense, two different processing protocols have been studied, a two-step process dealing first with a functionalization of the biosource with the diisocyanate and followed by a proper chemical oleogelation; and a second more straightforward one-step process consisting of the reaction of both components with the diisocyanate, implying a simultaneous oleogel formation. A wide range of lignocellulosic biomass from different sources and submitted to different treatments has been used for these purposes. First of all, wheat and barley straws were treated with an actinobacteria strain, and without further separation, were combined with castor oil and hexamethylene diisocyanate to obtain oleogels for lubricating purposes. Cellulose pulps, likewise obtained from fermented procedures, with high cellulose and hemicellulose and low lignin contents were also tested. Finally, due to its scarce use for commercial purposes and lack of industrial applications, the most studied lignocellulosic source in this thesis was lignin. Commercial or technical kraft lignins (Kraft lignin from Merck and Indulin IAT, a Kraft lignin from pine (MeadWestvaco)), as well as residual lignin-containing fractions generated as side-streams in different conversion processes of eucalyptus and pine woods such as Kraft pulping and fermentable sugars extraction by autohydrolysis and steam explosion were used. Moreover, lignin of different agricultural wastes such as wheat and barley straws treated with two *Streptomyces* strains were also evaluated. All of them were modified and tested as gelling agents for either lubricating grease, adhesive or cushioning materials production.

The chemical structure and properties of the lignocellulosic sources and products obtained were investigated by means of different techniques: Fourier-transform infrared spectroscopy let functional groups be distinguished, curing process be monitored and the different urethane/urea-based structures within the polyurethane network be discerned. Thermogravimetric analysis was employed to establish the thermal stability and structure of

raw materials and final products, differential scanning calorimetry let both curing and glass transition temperatures be obtained, while nuclear magnetic resonance gave a deep insight of lignocellulosic chemical structure. In addition, the rheological properties of polyurethane-based products were also assessed, generally considering both viscoelastic and viscous behaviour. Moreover, depending on polyurethane functionality, those systems devoted to lubricating performance were eventually tested by tribological and mechanical resistance tests, whereas the stickiness of the adhesive products was evaluated by standardized mechanical analysis on different surfaces, and the cushioning properties were measured by both static and dynamic mechanical experiments.

Since many diisocyanates are commercially available, the preliminary study was to assess the rheological properties imparted by several diisocyanates which differed in their structure, i.e., two aromatic diisocyanates (toluene diisocyanate (TDI) and 4,4′-methylene bis (phenyl isocyanate) (MDI)), a linear one (hexamethylene diisocyanate (HDI)) and a cyclic saturated one (isophorone diisocyanate (IDI)). Thus, the oleogels obtained with technical kraft lignin provided completely different results according to the diisocyanate own structure. The strongest gel-like characteristics were observed using HDI as the crosslinker, while relatively liquid-like characteristics were obtained by using either aromatic or cyclic diisocyanates. It was also worth noticing the influence of lignin type and processing in the diverse bioproducts generated. Thus, both processing temperature and agitation speed turned out to be crucial for polyurethane development as a consequence of the diverse structural conformations obtained. The lower both temperature and agitation speed, the stronger the mechanical properties achieved. The diverse lignin types studied have also demonstrated to critically influence oleogel properties. The higher the carbohydrate content, the higher the viscoelastic properties obtained, while the inherent structure depending on the biosource origin also demonstrated remarkable differences. On the other hand, pretreatments have also shown the possibility of tuning the rheological properties of lignocellulosic biomass. Therefore, actinobacteria as *Streptomyces* have been used in order to induce structural changes within agricultural residues such as barley and wheat straws, which are responsible for severe modifications leading to the accomplishment of oleogels with enhanced rheological properties compared to the uninoculated ones. Furthermore, this influence caused by *Streptomyces* can be seen not only in the use of the lignocellulosic residues. Instead, it can be extrapolated to both lignin and cellulose pulps obtained from those fermented straws.

The systems may achieve exceptional adhesive properties if the crosslinker concentration is increased. As a result, adhesives performed with kraft lignin, castor oil and HDI were produced and characterized. Furthermore, both the origin and the pretreatment demonstrated to influence the adhesion performance in different surfaces by testing lignins from wheat and barley straws, treated with actinobacteria strains.

On the other hand, if the component proportions are carefully selected, then elastomers can also be obtained, some of them exhibiting outstanding cushioning properties for application in multiple fields and consumer goods.

Summarising, the ability of lignocellulosic materials to produce suitable thickening agents in oil media, via polyurethane formation, for lubricating, cushioning and adhesive applications has been demonstrated in this study, as well as how diverse lignocellulosic origin, processing and pretreatments may tune the oleogel properties.

2. Justification

The increasing challenge related to climate change, waste valorization and non-renewable resources depletion is driving the search for bio-based and renewable materials that could replace those systems, complying with the principles of *Green Chemistry*. Nonetheless, some industries are far from that commitment. Such is the case of the lubricating grease industry, which has traditionally used the combination of either mineral or synthetic oils with metallic-based soaps, being lithium the predominant metal employed, with the disadvantages of the lithium utilization in important competing applications like batteries and microelectronics. Regarding the adhesive industry, apart from the harmful synthetic materials usually utilised for the formulation of the most common commercial adhesives, these are well known to release harmful volatile organic compounds when processed and applied. Considering cushioning materials, once more, synthetic and petroleum-based products are the most common ones.

Therefore, there has been intense research during the last decades for the replacement of those petroleum-based raw materials for bio-based and renewable ones. It is at this point where lignocellulosic sources may play a significant role. Lignocellulosic sources are the most ubiquitously raw materials produced on Earth, and are composed of three interesting

biopolymers, i.e., cellulose, hemicellulose and lignin. Either by its use as pristine material or divided into the three different biopolymers, extensive research has been done to obtain energy, high-value added chemicals or end-use biomaterials from these.

However, not all of them possess similar characteristics or advantages. Whereas lignocellulose covers all existing plants on Earth, the main advantage lies in the preferential use of residues such as straws, which have low or non-valuable uses beyond. When separating the biopolymers, again advantage is preferably taken from cellulose in order to produce paper, while lignin and hemicellulose are generally considered as low-valuable or even residual products. For that reason, the use of lignin as a biological network for thickening purposes is the main purpose of this study.

For the production of oleogel systems, in addition to the thickening agent, obviously an oil phase is required, which in many industrial applications is a synthetic or mineral one, as above mentioned. Nonetheless, in this study, the use of a vegetable oil, i.e., castor oil, has been tested, due to its interesting and singular characteristics, i.e. high viscosity, high thermal resistance and hydroxyl groups functionality.

As both lignin and castor oil can act as polyols for polyurethane formation, the combination with diisocyanate may generate extensive networks of different characteristics, where both lignin and castor oil become entangled. Moreover, depending on the degree of crosslinking, from soft gels to strong elastomeric materials can be obtained, hereby applications may vary from lubricating greases to elastomers or even strong adhesives.

3. Objectives

The principal objective of the present thesis relies on the valorization of different lignocellulosic sources and biopolymers derived from them, especially lignin, by means of the production of thickening agents able to gelify vegetable oils, via polyurethane formation, for high-value added applications. For reaching that purpose, crosslinking of the different biosources with diisocyanate compounds was promoted, aiming to obtain suitable networks in combination with castor oil, where the rheological properties account for viscoelastic materials with different industrial possibilities.

The first specific objective was related to the study and optimization of the oleogel formulation and the processing protocol. First, the most suitable diisocyanate for the production of lignin- and castor oil-based polyurethane oleogels by means of a sequential two-step process was evaluated. Several aromatic, linear and cyclic aliphatic diisocyanates were tested, in different biosource/crosslinker ratios and castor oil/gelling agent concentration. Afterwards, the optimization of the processing protocol was addressed. For that, the search for a more environmentally friendly process was undertaken. Thus, temperature, agitation speed and diisocyanate type were evaluated in the implementation of a more straightforward one-step process, free of harmful solvents and catalysts.

The second specific objective was related to the study of the use of several residual lignin fractions from different physico-chemical treatments as gelling agents for lubricating grease formulations. Thus, several different lignin/HDI ratios and castor oil concentrations for the production of suitable bio-based substitutes for traditional lubricating grease formulations were assessed with residual fractions from eucalyptus. Lignin from different pretreatments, like steam explosion, autohydrolysis, and Kraft processes were also evaluated. With the lubricating grease application in mind, apart from a convenient rheological characterization, some of the specimens created were analysed tribologically in order to evaluate the frictional and anti-wear responses.

The third specific objective was also related to the use of lignocellulosic fractions as gelling agents for lubricating grease purposes, but treated with *Streptomyces* strains to evaluate the action of the biological pretreatment and the resulting modifications in the rheological and tribological response. Within this framework, three different goals were addressed. The first one implied to go a step backwards, and instead of using cellulose, lignin or hemicellulose, take the advantages of using the three biopolymers together, in the form of the original lignocellulosic material. Moreover, the use of two straws with different origin, barley and wheat straws, could let both pretreatment and original source be likewise evaluated. The following one consisted of the development of gel-like systems using cellulose pulp from the solid-state fermentation of those residual straws as gelling agent by applying the one-step process with optimized conditions previously described, and the successful modifications promoted by the *Streptomyces* action. Lastly, similar enzymatic action was evaluated for lignin-rich fractions, and the fermentation modifications were studied for both lignin and oleogels developed.

The fourth specific objective was to use lignin, also derived from solid-state fermentation, as binder in adhesive formulations, and evaluate both the influence of the lignocellulose source and further pretreatment on the rheological and adhesion performance of resulting polyurethane adhesives.

Finally, the fifth specific objective was to use lignin to develop a third type of formulation, a cushioning material, able to withstand extraordinary compression properties, both under static and dynamic modes, thus proving to be an outstanding bio-replacer for petroleum-based rubbers and elastomers. This was made by using a high hydroxyl content lignin and tailoring the lignin/HDI ratio and castor oil concentration.

4. Document Structure

The present thesis manuscript is divided into five chapters. In addition to this first chapter comprising the introduction, justification and objectives of the Ph.D. thesis, the second one includes an analysis of the state-of-the-art related to lignocellulose description, main techniques for lignocellulose pretreatment, main bioproducts obtained from lignocellulose and more specifically, bio-based polyurethanes.

The third one includes a detailed description of the materials, techniques, processing protocols and equipment utilized for the preparation, modification and characterization of raw materials, intermediates and final products obtained.

The fourth chapter contains the experimental results, formal analysis and discussion of the different studies that comprise this thesis. As the Ph.D. manuscript is presented as a compendium of articles, the fourth section is divided into five sections, related to the specific objectives, each one including at least one published article, or ready-to-send manuscript, in relevant scientific journals. Thus, the articles have been separated according to the objectives into the five sections, which are detailed hereunder:

1) Study and optimization of lignin-based polyurethane formulations and processing protocol
    a) Rheology of lignin-based chemical oleogels prepared using diisocyanate crosslinkers: effect of the diisocyanate and curing kinetics

   b) Green and facile procedure for the preparation of liquid and gel-like polyurethanes based on castor oil and lignin: Effect of processing conditions on the rheological properties
2) Use of residual lignin fractions obtained from different physico-chemical pretreatments as gelling agent for lubricating grease application
   a) Valorization of Kraft lignin as thickener in castor oil for lubricant applications
   b) Evaluation of lignin-enriched side-streams from different biomass conversion processes as thickeners in bio-lubricant formulations
3) Use of lignocellulose from solid-state fermentation with *Streptomyces* as thickening agent for lubricating grease formulations
   a) Influence of solid-state fermentation with *Streptomyces* on the ability of wheat and barley straws to thicken castor oil for lubricating purposes
   b) Cellulose pulp- and castor oil-based polyurethanes for lubricating applications: influence of *Streptomyces* action on barley and wheat straws
   c) Valorization of soda lignin from wheat straw solid-state fermentation: Production of oleogels
4) Use of lignin from solid-state fermentation with *Streptomyces* as binder for adhesive formulations
   a) Rheology and adhesion performance of bio-sourced adhesives formulated with lignins from agricultural waste straws submitted to solid-state fermentation
5) Use of lignin as filler for elastomeric cushioning formulations
   a) Lignin effect in castor oil-based elastomers: Reaching new limits in rheological and cushioning behaviors

The last chapter summarises the main general conclusions arisen from the experimental studies, and establishes possible future routes and pathways for the continuation of this research.

Annex I includes other articles and oral and poster presentations in national and international congresses derived from or related to the present thesis.

Chapter 2: State of the art

1. Environmental problematic

It is for all well known that with the increasing issue of climate change, waste management and the unstoppable resource exhaustion, politics and efforts need to be combined into the search of new materials and sources that can replace fossil fuels and non-renewable resources currently in use, which besides generally include hazardous/toxic manufacture protocols and problematic end-of-life. The anthropogenic imprint on global temperature has already been reported as an increase of 0.87ºC, and it is expected to be around 1.5ºC between 2030-2050, temperatures which may imply severe changes in the worldwide climate, increasing the probabilities of droughts and heavy precipitations in determined regions, along with many increasing risks in fields such as health, food security, water supply, etc. [1]. In order to mitigate these increments and minimize the human impact, stronger politics need to be applied, as well as worldwide research must provide the technology and resources necessary for the replacement of the contaminating sources by biomaterials and harmless products manufacturing [2,3]. It is at this point that lignocellulosic sources can play a fundamental role as a consequence of their natural origin, ubiquitous production all over the world, minimum carbon footprint and the interesting properties of their main components [3–6].

2. Lignocellulosic materials as a source for the production of Biomaterials, Biochemicals and Biofuels

Lignocellulosic biomass comprises the skeleton of all the living plants on Earth from their roots, leaves and stalks to their fruits and flowers. Wood is generally divided into two main groups, hardwood and softwood. Whereas hardwood refers to wood coming from angiosperm trees, like oak, eucalyptus and beech, softwood is originated from gymnosperm trees, such as conifers. Both of them are mainly composed by the joined combination of three natural polymers, i.e., cellulose, hemicellulose and lignin, and are nowadays widely targeted as they comprise promising renewable materials for bioproducts performance and biofuels [6–11]. Their content range varies between 40-50% of cellulose, 15-30% of lignin and 25-30% of hemicellulose, nonetheless, these concentrations depend significantly on the type of biomass selected, part and age of the plant, part of the cellulose wall (see Figure 1) and growth conditions [12,13] (see Table 1).

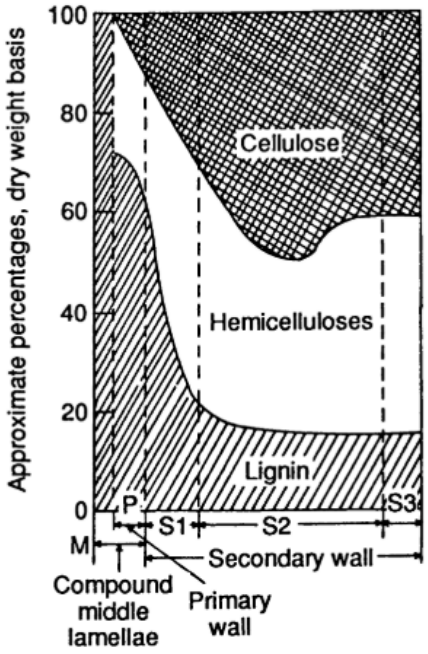

Figure 1. Distribution of cellulose, hemicellulose and lignin in the plant cell wall [14].

Each one of those biopolymers confers unique properties to the biomass due to their distinctive structure and the synergistic effect when they act as a whole for plant structuration. More detailed information about each one of them is included in the following section.

Table 1. Composition of representative lignocellulosic feedstocks [12].

Feedstocks	Carbohydrate composition (% dry weight)		
	Cellulose	Hemicellulose	Lignin
Barley hull	24	36	19
Barley straw	36-43	24-33	6.3-9.8
Bamboo	49-50	18-20	23
Banana waste	13	15	14
Corn cob	32.3-45.6	39.8	6.7-13.9
Corn stover	35.1-39.5	20.7-24.6	11.0-19.1
Cotton	85-95	5-15	0
Cotton stalk	31	11	30
Coffee pulp	33.7-36.9	44.2-47.5	15.6-19.1
Douglas fir	35-48	20-22	15-21
Eucalyptus	45-51	11-18	29
Hardwood stems	40-55	24-40	18-25
Rice straw	29.2-34.7	23-25.9	17-19
Rice husk	28.7-35.6	11.96-29.3	15.4-20
Wheat straw	35-39	22-30	12-16
Wheat bran	10.5-14.8	35.5-39.2	8.3-12.5
Grasses	25-40	25-50	10-30
Newspaper	40-55	24-39	18-30
Sugarcane bagasse	25-45	28-32	15-25
Sugarcane tops	35	32	14
Pine	42-49	13-25	23-29
Poplar wood	45-51	25-28	10-21
Olive tree biomass	25.2	15.8	19.1
Jute fibres	45-53	18-21	21-26
Switchgrass	35-40	25-30	15-20
Grasses	25-40	25-50	10-30
Winter rye	29-30	22-26	16.1
Oilseed rape	27.3	20.5	14.2
Softwood stem	45-50	24-40	18-25
Oat straw	31-35	20-26	10-15
Nut shells	25-30	22-28	30-40
Sorghum straw	32-35	24-27	15-21
Tamarind kernel powder	10-15	55-65	-
Water hyacinth	18.2-22.1	48.7-50.1	35.-5.4

2.1. Description and components

2.1.1. Cellulose

Cellulose comprises the most abundant biopolymer on Earth, as it is the most important skeletal component of plant cell walls (see Table 1). It is formed by the union of D-glucose units via β-1,4 glycosidic linkages, forming a semicrystalline fibrous structure, which can surpass polymerization degrees of 9000 units [15–17]. However, the cellulose homopolymer length can vary considerably, as it is strongly dependent on the plant source nature and pretreatment extraction method, hence ranging between hundreds to thousands of glucose units. Therefore, the number of glucose units per cellulose molecule coming from wood pulp may vary between 300-1700, whereas cotton, bacterial cellulose and other plant fibres vary between 800-10000 units [17]. By acid treatment or by cellulase catalysed hydrolysis, the number of glucose units can be critically reduced, reaching 250-500 monomer units. Nonetheless, it has been demonstrated that only 25-30 glucose units are enough for keeping all the outstanding properties of this biopolymer [18]. Between its main characteristics, chirality, hydrophilicity, degradability and reactivity (mainly consequence of the hydroxyl groups, found in C-2, C-3 and C-6) are the most important ones [17,19]. Nonetheless, not only the chemical sequence but the structural conformation has made this biopolymer to reach such importance. Cellulose, as a consequence of its linearity and hydroxyl groups present in its structure, possesses the ability to generate hydrogen bonds, which can confer a semicrystalline conformation to the biopolymer structure, in which ordered and disordered domains are randomly distributed (see Figure 2) [20]. Up to four types of crystalline structures have been accepted, but only cellulose II is chosen as relevant because it is the most stable structure compared to the others (see Figure 3).

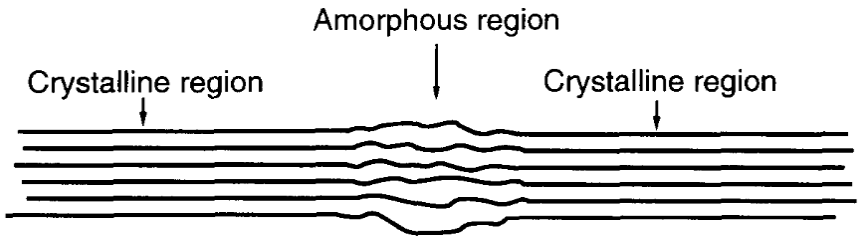

Figure 2. Schematic structure of a cellulose fibril [20].

As a consequence of the great abundance and the stunning properties, cellulose, in its pristine mode, by the formation of complex structures or by chemical or biological modification, has been used in a huge variety of applications. Among them, applications such as biofilms (barrier, antimicrobial or transparent films), reinforcing fillers for polymers and at the same time for flexible displays, biomedical implants, pharmaceuticals, drug delivery systems, fibres for textile production, templates for electrical and electronic devices, supercapacitors, highly-specialized separation membranes, carrier materials, batteries, electroactive polymers, nonwovens, colour pigments, enantioselective chromatography, fibre-optical biosensors, hydrophobic matrices for cosmetics, antimicrobial activity, emulsion stabilizer, etc. can be found [17,21–26].

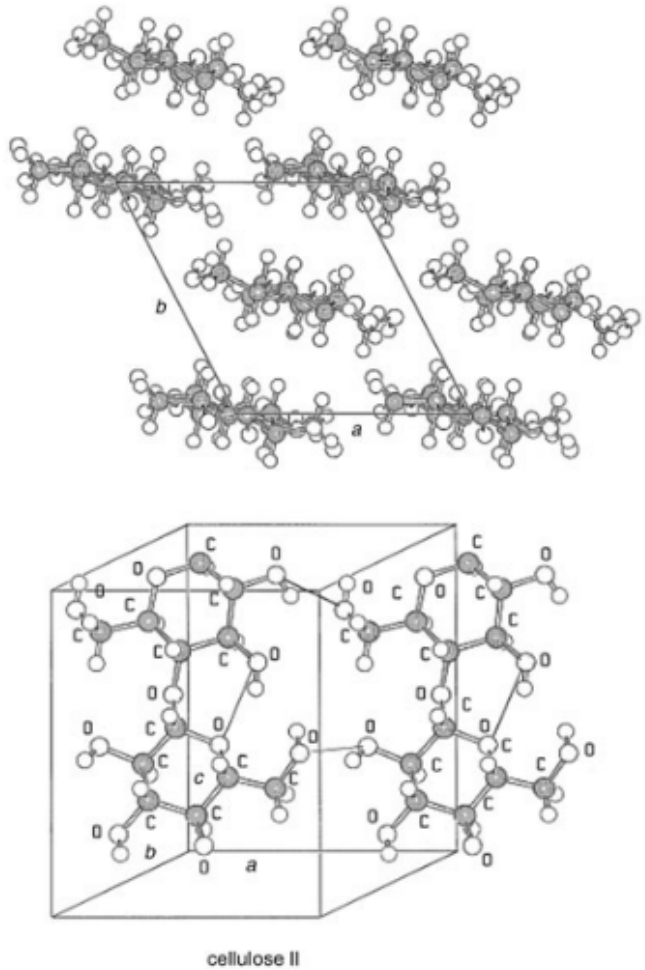

Figure 3. Crystal structures of cellulose II: a) projection of the unit cell along the a–b plane; b) projection of the UC parallel to the (010) lattice plane [17].

2.1.2. Hemicellulose

On the other hand, hemicellulose does not possess a defined structure, as it consists of a combination of several diverse monomers, i.e., xylose, arabinose, mannose, galactose, rhamnose, glucose, etc. (see detailed structures in Figure 4), whose concentrations depend on the biomass. Unlike cellulose, it is comprised of an amorphous and branched polymer in which monomer units are usually within the range of 500-3000 units [27,28]. The combination of the diverse units usually generates four main hemicellulose structures, i.e., xylan, xyloglucan, galactomannan and galactoglucomannan, which have been included in Figure 5. The main role of hemicellulose in biological growth resides in the toughening of the cell wall by the interaction with lignin and cellulose [27].

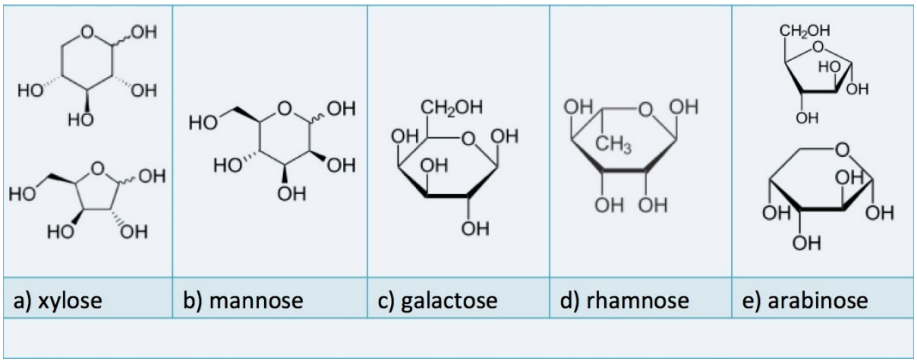

Figure 4. Hemicellulose main structural units [29].

Industrially, it is mainly obtained during the paper-making process as a byproduct, and has not been exploited properly on a large-production scale [30]. The main research focus had traditionally been paid in obtaining sugars, chemicals and fuels or other heat sources [31–34]. Recently, nevertheless, the attention has been redirected into the leveraging of the biopolymer with its inherent properties [30], being able to be utilised in fields such as ultrasensitive detection of metals [35], food biopackaging [36], sulfadimidine absorption [37], etc.

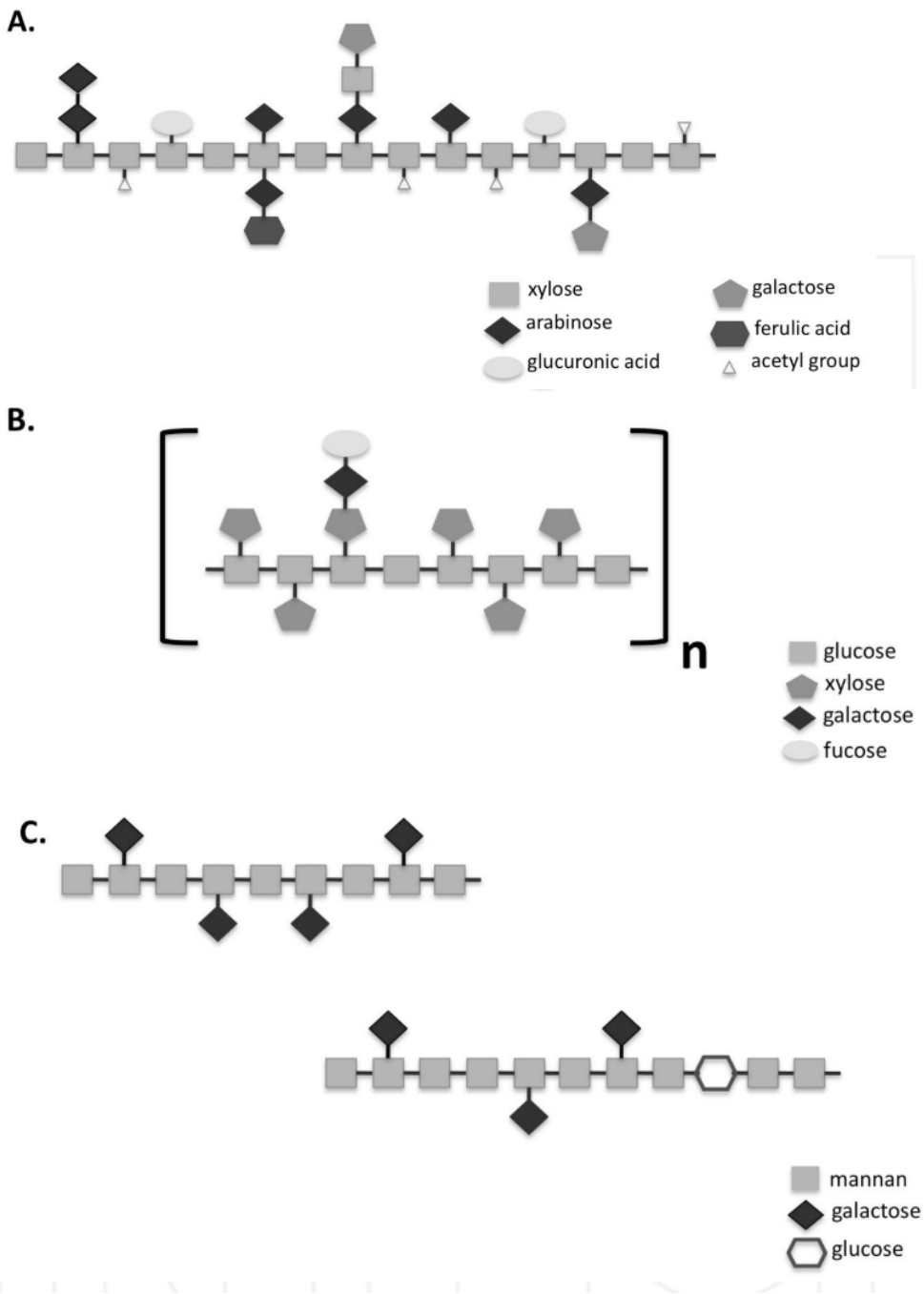

Figure 5. Schematic representation of the three major hemicellulose structures. A) xylan, B) xyloglucan, C) galactomannan (upper left) and galactoglucamannan (lower right) [38].

2.1.3. Lignin

Lignin constitutes the second most ubiquitous biopolymer around the world, just overtook by cellulose. It is responsible for biomass rigidity but it also acts as a defence against diseases and microbial attacks [39,40]. Its content in lignocellulosic sources follows the general trend softwoods > hardwoods > grasses [41]. Industrially, it is mainly generated as a residue or by-product of the pulping process, being its main use (98-99%) the direct incineration in an energy-recovering co-generation process within the own pulp and paper industry. The use of lignin as fuel, however, is not a profitable process, as the calculations make lignin-based fuel value not arise from 0.18 US $/kg [42]. The remaining 1-2% of the produced lignin is extracted and used for commercial purposes [40,41], where two opposed trends can be found, transforming lignin into those products which take advantage of the units that conform lignin (vanillin and dimethylsufoxide (DMSO) obtaining), and those products that make use of the polymer and polyelectrolyte properties of the aromatic chain (dispersants, binders, emulsifiers, sequestrants, adhesives or fillers) [43,44]. Albeit, it is still a promising raw material, since with suitable techniques, it could become a major and cheap source of high-added value aromatic compounds [40,41,44,45], such as syringaldehyde, phenol, syringol, coniferol or guaiacol [43,46]. Moreover, there are also great expectations based on those above-mentioned applications taking advantage of the 3-dimensional aromatic structure [47], as well as some new trends, like hydrogels with healing or adhesive characteristics [48,49]. Hence, currently, there is great attention in the research of this by-product [50–54]. Within this research, the work proposed in this thesis is mainly framed.

2.1.3.1. Lignin structure

Lignin consists of a highly-entangled biopolymer based on several phenyl propane aromatic units, known as monolignols, together with other aromatic and non-aromatic units. Basically, these monolignols are three, i.e., coniferyl alcohol, sinapyl alcohol and paracoumaryl alcohol, shown in Figure 6.

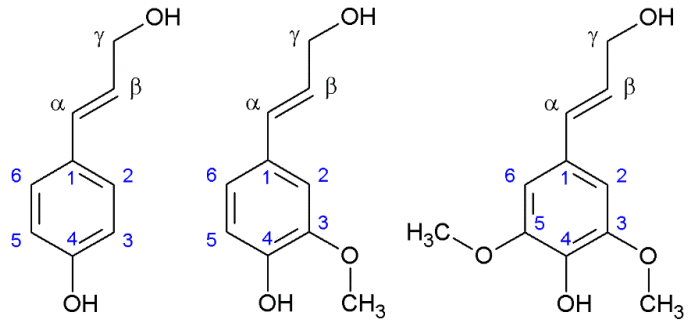

Figure 6. Main monolignols units. p-coumaryl alcohol, coniferyl alcohol and sinapyl alcohol from left to right.

However, the possibilities of the lignin structure are immense, as just by the combination of those three units, and having in mind the different resonance structures that can be generated for further reaction (see Figure 7), a complex and wide range of bonding alternatives are available, making lignin structure extremely difficult to predict [46]. Nonetheless, thanks to powerful nuclear magnetic resonance (NMR) techniques, as the two-dimensional NMR (2D-NMR) or ^{13}C NMR, some of the principal sequences have been elucidated, which are shown in Figure 8 [55–58]. Further information and extended work in 2D-NMR structural information of lignin can be seen elsewhere [59]. ^{13}C NMR detailed information of lignin structure can also be found in the literature [60,61].

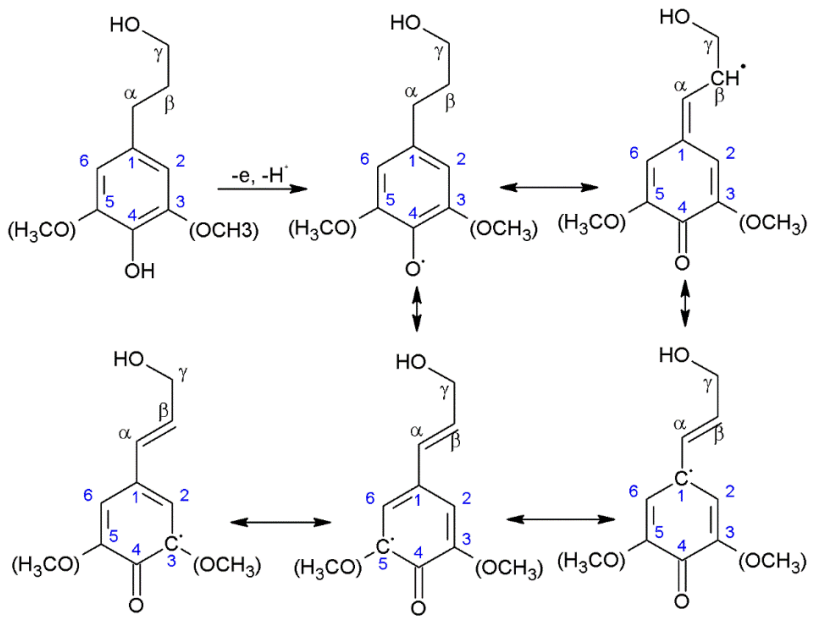

Figure 7. Resonance units of the radical intermediates of the diverse monolignols units during lignin synthesis.

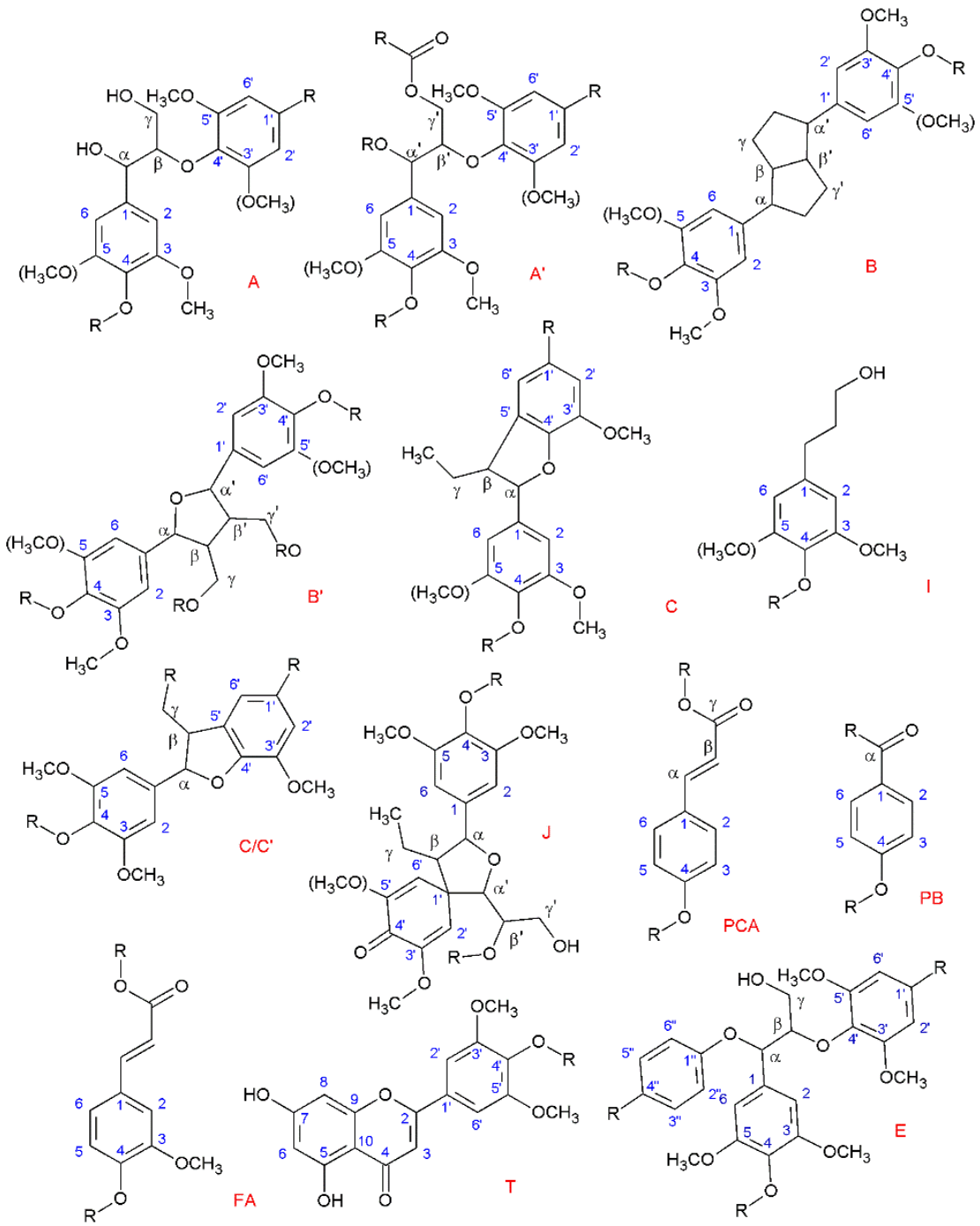

Figure 8. Main lignin structures identified by NMR. (R may indicate both aliphatic and aromatic chains). (A) β-O-4 alkyl-aryl ethers; (A') β-O-4 alkyl-aryl ethers with acylated γ'-OH with p-coumaric acid; (B) resinols; (B') di-c-acylated mono-tetrahydrofuran structure formed by β–β' coupling and subsequent α-O-a' bonding (R, acetyl/p-coumaroyl); (C) phenylcoumarans; (I) p-hydroxycinnamyl alcohol end-groups; (C') γ-acetylated phenylcoumaran (R, acetyl) (J) spirodienones (β-1') ; (PCA) p-coumarates; (PB) p-hydroxybenzoate; (FA) ferulates; (T) tricin incorporation into the lignin polymer through a G-type β-O-4 linkage; (E) α,β-diaryl ethers (α-O-4/ β-O-4).

2D-NMR technique also lets the different percentage of structural units be estimated [55,56,58,62,63]. Thus, the quantification of these interunit linkages has been widely reported, and as can be observed, β-O-4 is outlined as the most prevalent bond type (see Table 2) [41]. Figure 9 includes visual information about these different linkages in a possible partial lignin structure. As softwood and hardwood evidence significant differences, diverse lignin structures have been proposed for both of them, as shown in Figure 10.

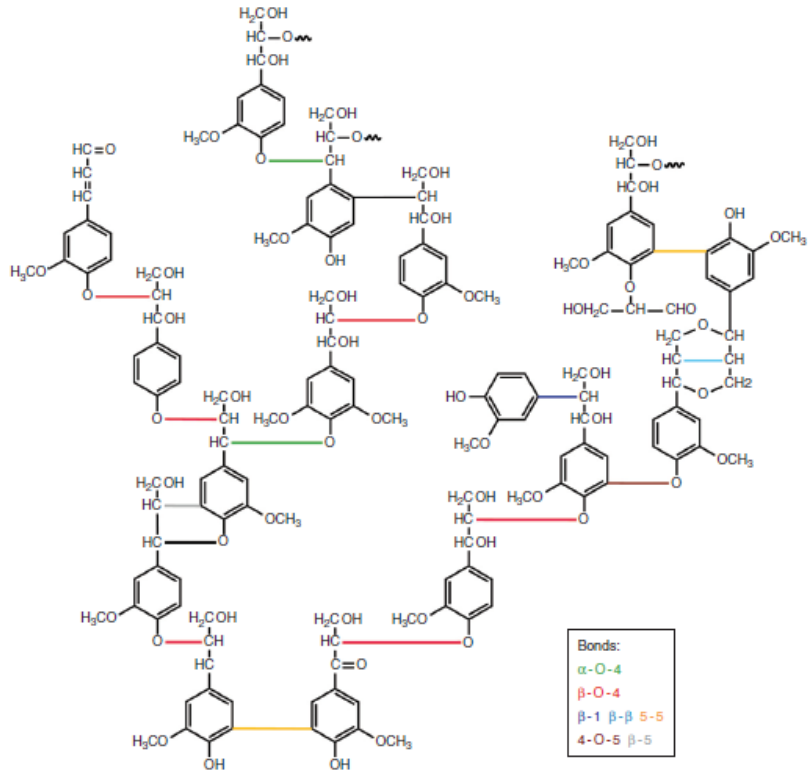

Figure 9. Main linkages of lignin: α-O-4 (green), β-O-4 (red), β-1 (blue), β-β (light blue), 5-5 (yellow), 4-O-5 (brown), β-5 (grey) [64].

Table 2. Approximate percentages of linkages found in softwood and hardwood lignin [44].

Linkage Type	Approximate Percentage (%)	
	Softwood	Hardwood
β-O-4	45-50	60
5-5	18-25	5
β-5	9-12	6
4-O-5	4-8	7
β-1	7-10	7
β- β	3	3

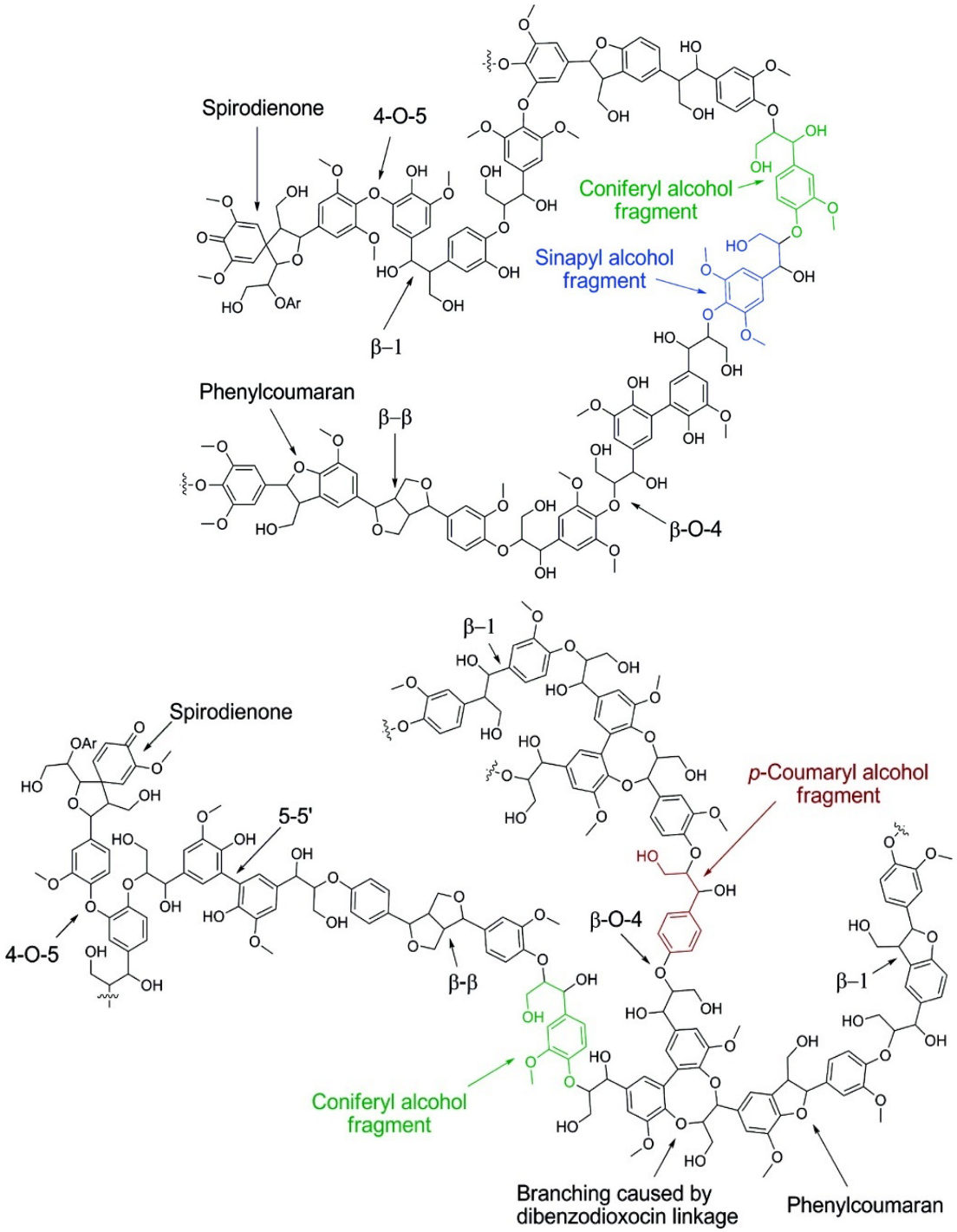

Figure 10. Proposed structures for hardwood (top) and softwood (bottom) lignins [41].

Moreover, the proportion of monolignol units may differ significantly, with the H:G:S ratio being an important parameter to define lignin. This ratio may be likewise acquired by ^{1}H NMR [65], a technique that lets hydroxyl groups proportion and aromatic/linear hydroxyl groups ratio be collected as well [66–68]. As expected, this H:G:S ratio is highly dependent on biomass selected, as illustrated in Table 3.

Table 3. Relative distributions of lignin monomers [69].

Biomass	S	G	H
Poplar[a]	63	37	-
Birch[a]	78	22	-
Spruce[a]	Trace	98	2
Miscanthus[b]	44	52	4
Wheat[a]	56	49	5
Alfalfa[c]	39	56	5

[a]Thioacidolysis of extractive-free cell walls; [b]Milled wood lignin; [c]Thioacidolysis and acetyl bromide treatment.

It is also worth noticing that some functional groups may be placed in different sites, which can put into compromise their ability to react with other functional groups by either chemical or biological attacks. That is the case, for example, of hydroxyl groups, which may be placed in syringyl, guaiacyl, p-hydroxyphenyl units, in linear aliphatic chains, etc. Hence, the elucidation of the diverse hydroxyl groups concentration may also play a fundamental role, which can be performed thanks to ^{31}P NMR [70].

Nonetheless, those differences between diverse types of plants have gone beyond, as other authors have demonstrated that significant variations are present depending even on the geographical location of similar species [44]. These deviations have always been explained based on lignin polymerization in any biomass source to be carried out by means of radical-radical random bonding, nonetheless, it is in fact directed by enzymatic procedures, since some proteins have been discovered as “orienting carriers” of this polymerization [71]. In Table 4, molecular formulas of lignin monomers can be found depending on diverse origins and pretreatments utilized. More information about the different lignin extraction processes is found somewhere else [41].

Table 4. Monomer molecular formulas and weight of lignin from various sources [41].

Type	Monomer molecular formula	Monomer M_w (g/mol)	ref
Kraft lignin	$C_9H_{8.5}O_{2.1}S_{0.1}(OCH_3)_{0.8}(CO_2H)_{0.2}$	180	[43]
Technical kraft lignin	$C_9H_{7.98}O_{2.28}S_{0.08}(OCH_3)_{0.77}$	176.52	[72]
Unreacted kraft lignin	$C_9H_{8.97}O_{2.65}S_{0.08}(OCH_3)_{0.89}$	189.73	[73]
Lignosulfonate lignin (softwood)	$C_9H_{8.5}O_{2.5}(OCH_3)_{0.85}(SO_3H)_{0.4}$	215-254	[43]
Lignosulfonate lignin (hardwood)	$C_9H_{7.5}O_{2.5}(OCH_3)_{0.39}(SO_3H)_{0.6}$	188	[43]
Organosolv lignin	$C_9H_{8.53}O_{2.45}(OCH_3)_{1.04}$	nd	[43]
Pyrolisis lignin	$C_8H_{6.3\text{-}7.3}O_{0.6\text{-}1.4}(OCH_3)_{0.3\text{-}0.8}(OH)_{1\text{-}1.2}$	nd	[43]
Steam explosion lignin	$C_9H_{8.53}O_{2.45}(OCH_3)_{1.04}$	~188	[43]
Dilute acid lignin	$C_9H_{8.53}O_{2.45}(OCH_3)_{1.04}$	~188	[43]
Alkaline oxidation lignin	$C_9H_{8.53}O_{2.45}(OCH_3)_{1.04}$	~188	[43]
Beech lignin	$C_9H_{8.83}O_{2.37}(OCH_3)_{0.96}$	nd	[74]
Lignophenol (bamboo)	$C_9H_{8.27}O_{3.11}N_{0.088}S_{0.0006}(OCH_3)_{1.16}$	203.35	[75]
Soluble kraft lignin (bamboo)	$C_9H_{8.77}O_{2.77}N_{0.093}S_{0.16}(OCH_3)_{0.75}$	187.76	[75]
Kraft lignophenol (bamboo)	$C_9H_{8.67}O_{3.36}N_{0.040}S_{0.11}(OCH_3)_{1.09}$	208.45	[75]
Milled bamboo lignin	$C_9H_{7.73}O_{3.81}(OCH_3)_{1.24}$	215.13	[76]

There are also new trends that aim to bioengineer lignin production in biomass [77–79], as the use of genome bioediting technologies [80], often aiming to reduce and ease their own recalcitrance. Thus, lignin can be tuned in order to make it more accessible and easy to separate from holocellulose [77]. And more importantly, these different characteristics provided to lignin structures may lead to diverse outcomes when considering final applications [39,40].

2.1.3.2. Molecular weight

The molecular weight of lignin also dependent largely on the biomass selected, but even more crucial is the technique used to isolate the lignin from biomass, as well as the characterization method chosen, which may interfere in lignin molecular weight calculations [69]. In some cases, an increase in molecular weight of around 100% is achieved when changing from one isolation technique to another. As an example, Kraft lignin has been studied and, depending on the biomass and processing, average molecular weights between 200 and 20000 $g \cdot mol^{-1}$ have been reported [69]. An extensive report on lignin molecular weight elucidation and differences depending on characterization techniques, nature of the biomass and pretreatments can be found elsewhere [69].

2.1.3.3. Thermal stability

The thermal stability of lignin has also been deeply studied in the literature. At relatively low temperatures (up to 125ºC), an initial loss of moisture is generally undergone. Later on, from 165 to 250ºC, small weight losses are a consequence of both residual hemicellulose [81] and dehydration of hydroxyl groups present on lignin structure [82]. In addition, one of the main weight losses is achieved around 250-350ºC, assigned to the β-O-4 linkages breakdown, leading to the formation of many volatile groups at these temperatures such as guaiacol, dimethoxyphenol, dimetoxyacetophenone and trimethoxyacetophenone. Overlapped to this weight loss and generally comprising an unique combined event, the β-aryl–alkyl–ether linkages scission (150-300ºC) are found, as well as the rupture of the aliphatic side chains joined to the aromatic units (around 300ºC), and the C-C cleavage of lignin structural units at higher temperatures (370-400ºC) (see Figure 11) [82–84]. No thermal events are displayed further on but a continuous decrease up to a final residue of around 22-32% at 900ºC [85], again highly dependent on the selected biomass [86].

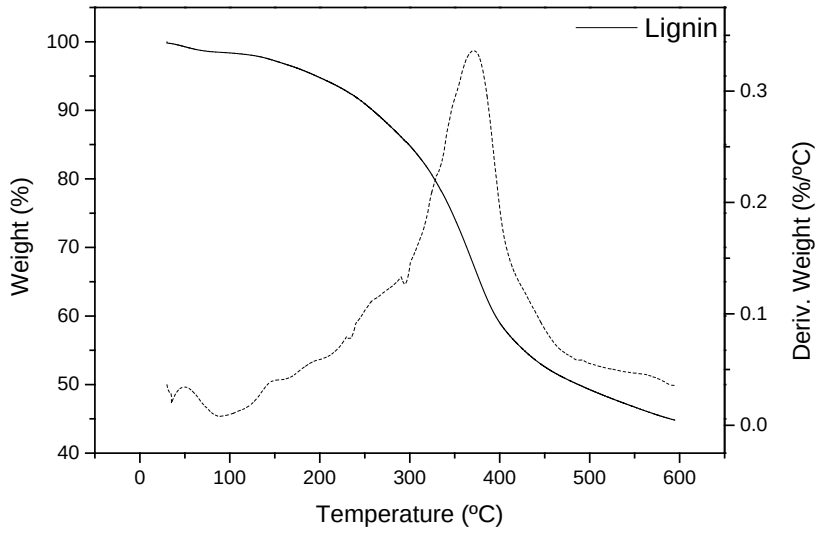

Figure 11. Thermogravimetric spectrum of lignin [83].

Once the main units and linkages have been elucidated, a final representation of the lignin structure can be envisioned in Figure 12.

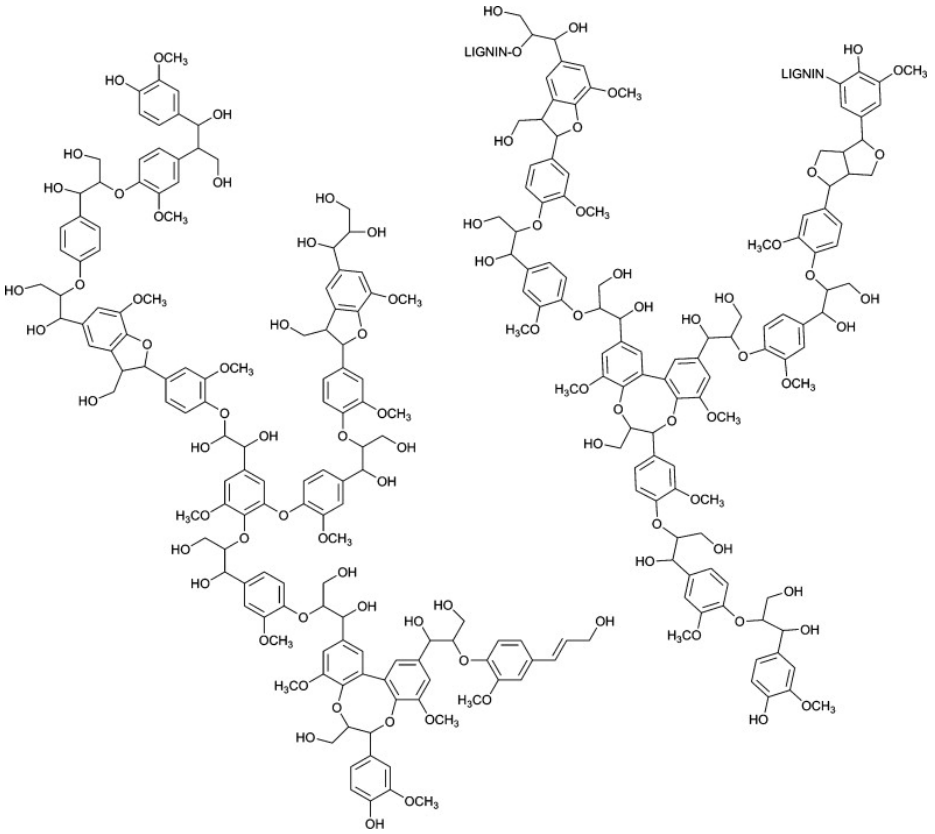

Figure 12. Lignin structure [87].

2.1.4. Lignocellulosic biorefinery

All these three materials together perform a highly-developed 3D network, which has made the separation of these biopolymers an extremely interesting topic, due to its inherent relationship with the papermaking industry. Such has been the case that meticulous research has been carried out in order to improve this separation and hence decrease energy costs [88]. As an example of the traditional pulp and paper industry, the Kraft process, the most followed procedure, is hereafter explained: Once the biomass has been properly milled, a Kraft process takes place (extensive information about this process can be found elsewhere [89]), where an aqueous solution containing sodium sulphide and sodium hydroxide is mixed together with the biomass at high temperature (around 170ºC), thus bonds among lignin, cellulose and hemicellulose are broken. Both hemicellulose and lignin are dissolved in the strongly basic solution whereas cellulose is obtained as a solid pulp. The final cellulose product is obtained after several stages of washing and purifying. Lignin, however, is obtained from the *black liquor* through acidification of the solution, appearing as a precipitate. Hemicellulose can be

extracted through precipitation with an ethanol solution [90]. In this process, both hemicellulose and lignin are considered low-valuable by-products, being both generally used as low-valuable fuels for recovering part of the energy consumed during the process. However, there are other pulping procedures, exploited in lower extents, which deserve mention, such as alkaline sulfite anthraquinone methanol pulping, soda-anthraquinone, Alcell® or Organocell processes [91].

Nonetheless, the full and/or alternative utilisation of the three components would lead to a much better economic performance, which is the basis of the biorefinery concept. In Figure 13, an example of how a paper industry could lead to complete exploitation of the raw biomass is presented.

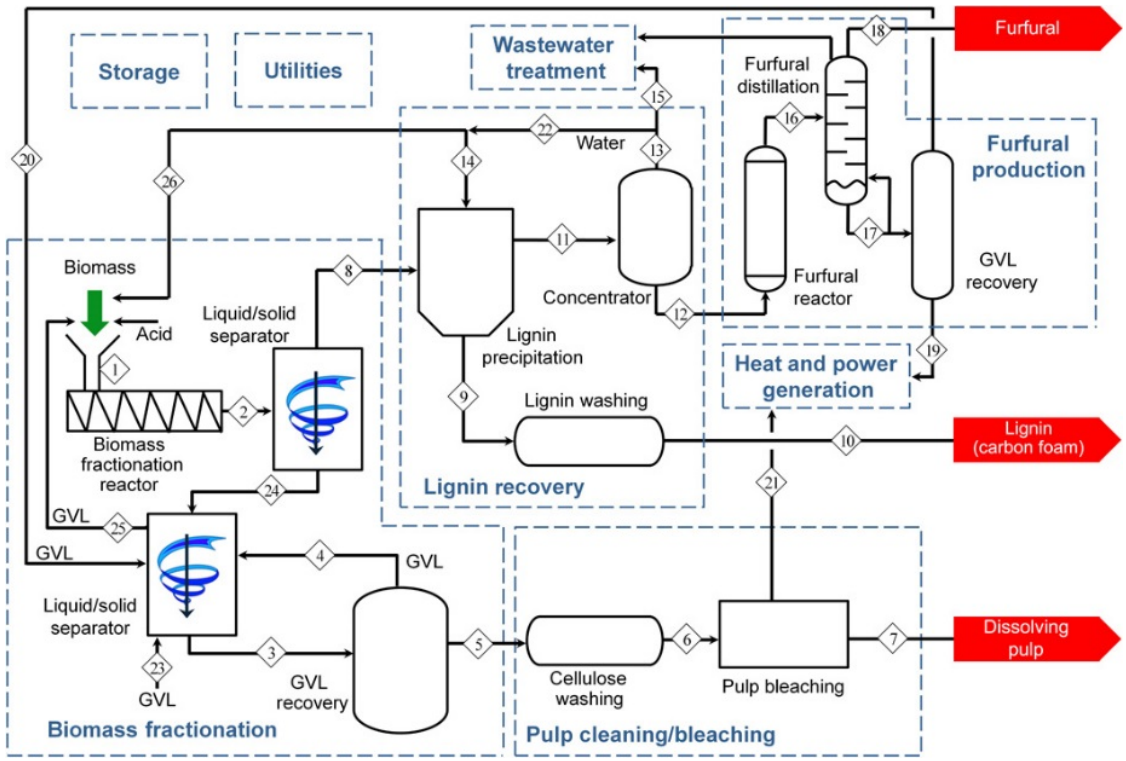

Figure 13. Overview of the process flow diagram to exploit potential fractions from lignocellulosic biomass [92].

Therefore, a wide range of more specific methodologies has been studied for the separation and purification of cellulose [93], hemicellulose and lignin [11,12,94], some of them including a proper biorefinery scheme for the valorisation of each lignocellulosic fraction [41].

Most of the biorefinery concepts, like the one shown in Figure 13, are based on the production of interesting chemicals derived from the lignocellulosic biopolymers. Even though this trend looks promising, it requires complex processing units and multiple byproducts formation. Therefore, a less-followed but likewise very appealing trend is based on the use of the interesting characteristics of those biopolymers to produce high-added value specific products. In this last framework, lignocellulosic materials have been previously investigated in our department and Research Centre aiming to be implemented in biobased lubricant formulations [95–99]. Cellulose and cellulose-derivatives have demonstrated outstanding results, however, they compete strongly with the paper industry, including the processing of paper and cardboard, as well as with other processes involving cellulose derivatives, which are used in fields as coatings, optical films, laminates, sorption media, additives in building materials, pharmaceuticals, food and cosmetics [17]. However, it is in the proper cellulose refining process where another extremely interesting biopolymer, which competes with a much smaller industrial market, can be found, i.e. lignin.

Within the following sections, the emerging possibilities and potential of lignin as a key component of high-value added bioproducts will be discussed in more detail. However, as established above, chemical processing is mandatory for the separation of the lignocellulosic fractions. Thus, the exploitation of the lignocellulosic biomass without further separation represents an even more appealing topic.

2.2. Agricultural residues: barley and wheat straws.

The use and leverage of agricultural residues are among the hottest topics currently aimed at research, as they consist of promising low-cost energy precursor of biofuels, high-value added chemicals sources [100–105], feedstock for soil fertilizer [106,107], together with potential precursors of some new applications which are currently being developed [108–111]. The main agricultural residues produced worldwide are originated from rice, wheat, soybean, tomato, sugarcane, maize, potatoes, etc. [112], where many of them are just open-field burned, with the consequent negative impact on climate change and the misuse of these materials [113]. The biofuels that may be obtained from these crops vary between bioethanol [103,114], biohydrogen [2,100], biobutanol [114–116], etc., but they can also be directly burned as low-energy fuels with heating values of around 4000 kcal/kg [117,118]. More concretely, studies regarding both barley and wheat straws are gaining more and more interest, as can be seen by

the peer-reviewed articles published recently containing either wheat or barley straw as keywords (see Figure 14).

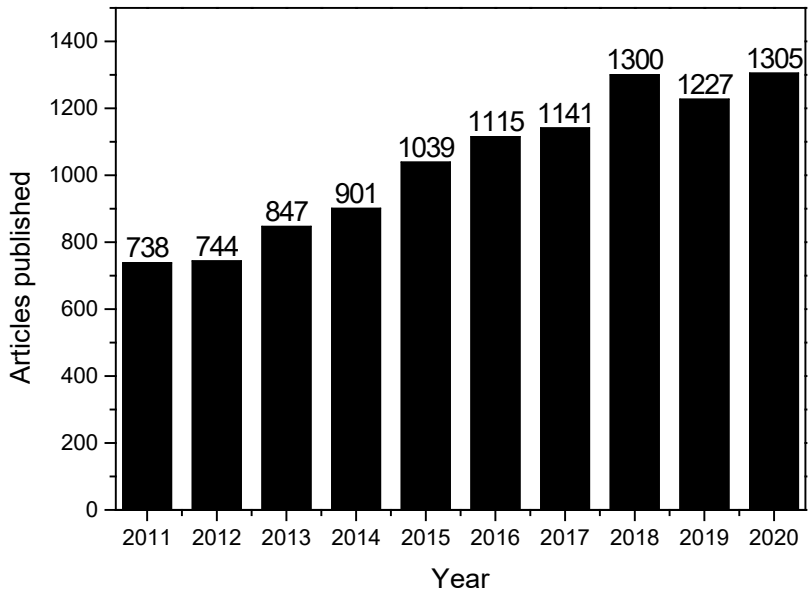

Figure 14. Peer-reviewed articles including either barley or wheat straw in recent years (in Web of Science).

Barley has been produced at around 124 Tg/year for the last decade, mostly centred in Europe, Asia and North America. Nevertheless, the production of wheat is much higher, raising 529 Tg/year, with larger production centred in Asia and Europe [103].

The use of these crops together with the residues yielded are depicted in Table 5. Thus, around 4.2 and 19.7 Tg of barley and wheat wastes are generated per year, which boosts the study of these residues leverage worldwide.

The lignocellulosic composition of the associated barley and wheat straws has already been depicted in Table 1, where close values between both biosources are apparent. Thus, the cellulose content varied from 39.5 to 37 wt%, hemicellulose from 28.5 and 26 wt% and lignin from 8 to 14 wt% regarding barley and wheat straw, respectively [12,119]. Nonetheless, there is scarce agreement in research data considering these contents, as wheat straw hemicellulose concentrations have been reported up to more than 50 wt% in some cases [118]. Other studies have once more highlighted its composition similarity, but have reported much higher lignin concentrations (around 25 wt%) [114,120]. In conclusion, the growing conditions, the source origin, together with many other factors become crucial to elucidate the lignocellulosic

composition of these agricultural residues and may lead to significant differences, as mentioned before. Thus, the concentration of the biopolymers estimated with proper analytical methods is mandatory.

Table 5. Uses of barley and wheat grains [103].

Barley	Feed (%)	Seed (%)	Waste (%)	Food manufacture (%)	Food (%)	Others (%)
Africa	30.20	6.98	5.77	12.14	44.57	0.34
Asia	54.18	5.93	6.73	19.91	9.70	3.82
Europe	75.19	9.52	2.59	11.05	1.38	0.27
North America	74.99	3.48	0.04	20.49	0.93	0.07
Central America	29.07	1.38	2.22	65.11	1.90	0.33
Oceania	78.47	5.50	3.08	12.77	0.15	0.03
South America	11.03	2.78	3.35	73.69	7.29	1.85
World	66.74	7.54	3.39	15.99	5.32	1.03
Wheat						
Africa	4.68	2.26	5.71	0.18	85.87	1.30
Asia	4.34	5.46	4.50	0.64	84.31	0.74
Europe	38.78	8.13	2.44	1.60	46.72	2.33
North America	28.69	8.07	0.03	0.00	73.08	9.95
Central America	7.95	0.95	8.07	0.00	73.08	9.95
Oceania	42.00	8.29	4.02	3.07	28.19	14.44
South America	4.35	3.73	5.11	0.00	86.80	0.01
World	16.72	6.11	3.72	0.84	71.13	1.48

Apart from the already-mentioned applications, less conventional uses have also been pointed out. Thus, wheat and barley straws have been targeted as insulation for bricks in construction materials [111], electricity production [110], phycoremediation of wastewater [108], as cement properties enhancer [109], biochar production [121], fibres in concrete [122], etc.

2.3. Pretreatments of lignocellulosic sources

Lignocellulosic biomass has naturally developed protection against enzymatic and pathogen activity through a great entangled network in which the three biopolymers are

covalent or hydrogen-bonded conforming a great resilient structure [123], which now plays against human needs when the disruption of the plant cell wall is aimed [124]. In order to ease the proper separation among the different lignocellulosic biopolymers, a wide range of pretreatments are available [125]. Furthermore, when specific purposes that require determined properties are aimed, the application of pretreatments of different nature becomes necessary. These pretreatments have been classified into four categories: physical, thermal, chemical and biological pretreatments [124,126]. Nevertheless, within a determined process, changes in parameter conditions may anyway lead to diverse structural changes [127].

2.3.1. Physical pretreatments

The physical pretreatments include those processes which aim to disrupt the plant cell wall mechanically, reducing the particle size and exposing a higher surface for later purposes. Frequently, these are often preliminary stages after which other pretreatments may be applied. Diverse ball milling procedures are some of the most researched examples [4,124].

2.3.2. Thermal pretreatments

Among the most used thermal pretreatments, examples such as steam explosion and hydrothermolysis (also known as autohydrolysis) can be found. By taking advantage of water at high temperatures, hemicellulose has been almost completely recovered [4], while lignin and cellulose have been mildly modified making it more accessible for further treatments. Albeit, the energy requirements in order to implement this technique industrially still remain too high [126].

2.3.3. Chemical pretreatments

With the chemical pretreatments, the solubilisation of the biopolymers which comprise the lignocellulosic biomass into different solvents is sought. The vast majority of the lignocellulosic separation processes are chemically-based, which can be classified into acidic, alkaline and oxidative pretreatments.

The three of them mainly affect both hemicellulose and lignin, leading to great solubilisation of these two biopolymers and making cellulose available to a greater extent for subsequent treatments [124]. For some authors, steam explosion and hydrothermolysis are considered acidic pretreatments as a consequence of the acidic characteristics of water at high

temperatures [124]. Detailed information about the diverse chemical pretreatments methods can be found elsewhere [4,123–126].

2.3.4. Biological pretreatments

In opposition to the other types of pretreatments, biological procedures have the advantage to be low-energy and low-chemical consuming processes, eco-friendly and without the formation of inhibitors such as aldehydes, furfurals and phenolics [123,124,126]. Carried out through the action of either fungi or bacteria, the degradation capacity relies on the production of a great variety of enzymes, which are able to digest the three biopolymer types. The main parameters affecting biological pretreatments are the incubation temperature and time, moisture content, pH, aeration, inoculum concentration, particle size and type of microorganism. Moreover, the biomass type also plays a fundamental role [128]. Hereby, the correct scalability of the pretreatment to an industrial process lies in the correct selection of the above-mentioned parameters [126,128]. Although the different biopolymer degradation by both fungi and bacteria will be discussed in the following sections separately, it is worth noticing that the synergistic activity of the different enzymes is responsible for the complete degradation carried out by the microorganisms [129].

2.3.4.1. Biodegradation by fungus activity

Fungi are able to secrete a wide range of enzymes with the capacity to degrade the three biopolymer types of plant cell walls. Within that range, enzymes can be divided into two types: hydrolytic, able to degrade both cellulose and hemicellulose and oxidative, mainly responsible for lignin degradation [130]. Fungi can be also divided into three diverse groups, soft-, white- and brown-rot fungi, a classification that is based on the degradation mechanism pattern for each lignocellulose biopolymer [131,132]. Therefore, the white-rot fungi are known to degrade successfully the three lignocellulosic biopolymers. The brown-rot fungi attack is mainly centred on the holocellulose instead, whilst action in lignin is only limited. Finally, the soft-rot fungi demonstrate no effect on lignin [132].

2.3.4.1.1. Cellulose biodegradation by fungus activity

Regarding cellulose biodegradation, those enzymes with the ability to digest cellulose are called cellulases. Three are the main cellulase groups generated by fungi, i.e., endoglucanases, cellobiohydrolases and β-glucosidases [131]. Endoglucanases are known to

attack randomly the amorphous region, opening suitable locations for the subsequent hydrolisation of crystalline structures by cellobiohydrolases and β-glucosidases, which are known to act synergistically [131,132].

2.3.4.1.2. Hemicellulose biodegradation by fungus activity

As a consequence of the greater heterogeneity of this biopolymer in comparison to cellulose, a greater number of enzymes are necessary in order to properly degrade the biopolymer. Each one of the typical monomers that compose hemicellulose, i.e., xylose, mannose, galactose, arabinose, etc. has its own range of enzymes suitable for its proper degradation and transformation [133]. Generally, at least two types of enzymes may be present for each monomer, a first one responsible for the transformation of the hemicellulose chain into oligosaccharides and a second one which acts for the ulterior degradation to the monomers and acetic acid [131].

2.3.4.1.3. Lignin biodegradation by fungus activity

The most common oxidative enzymes produced by fungi are phenol oxidases, from which lignin and manganese peroxidases and laccases have been more deeply studied. The first ones are responsible for the degradation of the non-phenolic units, whereas the second ones are known to attack both phenolic and non-phenolic units. Laccases, however, only degrade phenolics and other electron-rich groups. The different routes for lignin degradation by using both laccases and peroxidases have been depicted in Figure 15. The lignin breakdown by those enzymes could lead to the production of important aromatic chemicals. For instance, a wide range of aromatic carboxylic acids and acyclic 2,4-hexadiene-1,6-dioic acids were found when spruce-based lignin was degraded by *Phanerochaete chrysosporium.* In this particular case, lignin degradation is occurring by C_{α}–C_{β} oxidative cleavage as suggested by the benzoic-acid derivative nature of the compounds obtained [134]. Detailed information about the scheme and further information about fungi-based lignocellulosic degradation can be found elsewhere [131,135].

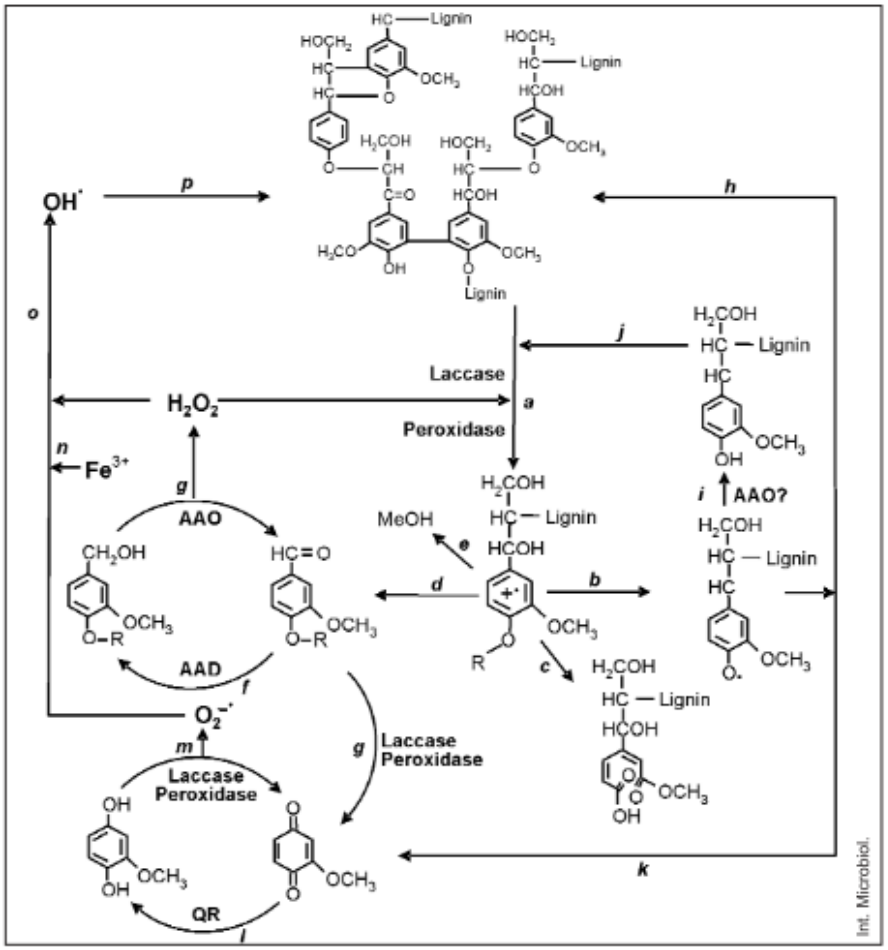

Figure 15. Lignin degradation by enzymatic process [135].

2.3.4.2. Biodegradation by bacterial activity

By producing different types of enzymes, bacteria are also able to degrade lignocellulosic biomass in the same way as fungi do. However, as bacteria generally do not produce lignanases, the aromatic biopolymer constitutes a barrier for many of these bacteria. Such is the interest of the bacterial ability to degrade lignocellulose that some genetic modifications have been carried out in order to improve the degradation capacity [136] or target some specific degradation products [137,138]. The search for bacterial activity related to lignocellulosic degradation has traditionally been performed in the animal gastrointestinal system, but also in landfill sites, interesting microorganisms have been found lately [139,140].

2.3.4.2.1. Cellulose biodegradation by bacterial activity

Many specific bacteria have shown the ability to degrade cellulose, such as those coming from the genera *Sporocytophaga, Trichonympha, Cellulomonas Erwinia, Clostridium, Acetivibrio, Thermobifida, Mucilaginibacter, Bacteroides, Streptomyces, Cytophaga, Butyrivibrio, Fibrobacter, Pedobacter, Ruminococcus, Methanobrevibacter, Caldicel-lulosiruptor* and *Clostridium* [38,141–143], which come from both aerobic and anaerobic types of bacteria. Generally, likewise fungi, aerobic bacteria possess the three types of enzymes acting synergistically [143], while the digestion by anaerobic procedures is based on the formation of complexes called cellulosomes (calcium-and-thiol-dependent multicomponent complexes) acting on the bacteria's surface [144,145]. Cellulases have also been divided into families that share a distinctive catalytic core, thus exhibiting similar reaction mechanism, i.e., either a single substitution with the inversion of the configuration or a double substitution leading to the maintenance of the β-arrangement at the anomeric carbon [20]. Cellulases possess very particular structures, where along with the usual catalytic domain, many also include domains related to the substrate, cell or cellulosomes binding, the last one leading to the formation of these enzyme-based complexes [20]. These bindings may avoid the elimination of the enzyme from the substrate, conduct hydrolysis to specific domains or facilitate the recovery of the digestion products [20].

Furthermore, often bacteria and microorganisms do not possess the three types, but they act synergistically between them instead. The enzymatic cellulose degradation is affected by both the structural characteristics of the biopolymer (crystallinity, degree of polymerization, etc.) and the own acting enzymes [129,146]. The enzyme-related factors which affect cellulose degradation are enzyme origin, temperature, specific product inhibition, binding to the substrate, activity balance for synergism, specific activity and both enzyme processibility and compatibility [129].

2.3.4.2.2. Hemicellulose biodegradation by bacterial activity

Once more, species from both aerobic and anaerobic bacteria were identified as hemicellulose degraders, counting *Ochrobactrum*, *Bacillus*, *Paenibacillus*, *Acinetobacter*, *Thermomonospora, Clostridia, Streptomyces, Cellvibrio* and *Pseudomonas* between the hemicellulase-producer genera [145,147]. In the same way as fungi, hemicellulose complete degradation is accomplished by the synergistic operation of a vast range of enzymes because of

the inherent variability of the hemicellulose biopolymer. Only for xylan, a wide range of enzymes have been reported mandatory for the degradation completion, which have been included in Table 6, together with a short explanation of their mode of action [32,147].

Table 6. Enzymes involved in the hydrolysis of complex heteroarabinoxylans [32].

Enzyme	Mode of action
Endo-β-l,4-xylanase	Hydrolyzes mainly interior β -1,4-xylose linkages of the xylan backbone
Exo-xylanase	Hydrolyzes β -1,4-xylose linkages releasing xylobiose
β -Xylosidase	Releases xylose from xylobiose and short-chain xylooligosaccharides
α-L-Arabinofuranosidase	Hydrolyzes terminal nonreducing α -arabinofuranose from arabinoxylans
α -Glucuronidase	Releases glucuronic acid from glucuronoxylans
Acetylxylan esterase	Hydrolyzes acetylester bonds in acetyl xylans
Ferulic acid esterase	Hydrolyzes feruloylester bonds in xylans
ρ-Coumaric acid esterase	Hydrolyzes ρ -coumaryl ester bonds in xylans

On the other hand, some xylanases are known not to provoke the breakdown of glycosidic linkages until a proper debranching has been performed. However, those debranching enzymes often require partial hydrolysis before a proper breakage can be obtained. Hence, these findings highlight the intricate complexity of hemicellulose degradation, which apart from the great numbers of enzymes involved, also requires a careful equilibrium and synergistic operation between the different enzymes [32,145,148].

2.3.4.2.3. Lignin biodegradation by bacterial activity

Although the ability to degrade lignin is exclusive of a few bacteria genus such as *Streptomyces, Rhodococcus, Nocardia* or several *Sphingomonas*, *Pseudomonas, Enterobacter* and *Actinomyces* species [38,137,149], it has often been reported to be comparable to that shown by well-known lignin-degrader fungi [149]. Furthermore, the difficulties found in the genetic modification together with the low enzymatic yields usually observed in fungi have propelled the interest in the lignin-degrader bacteria [150]. These bacteria have been found in

its vast majority within the digestive system of termites and other insects, though some other important species have also been found in soil and decaying vegetation [149–151].

Despite the enzymology of bacterial lignin digestion has not been developed as deeply as with fungi, some studies have helped to elucidate some of the enzymes which play a significant role in the lignin degradation by bacteria. Thus, four different types of bacterial lignin-degrader enzymes have been found up to date [150]. Multi-copper oxidase enzymes, also known as laccases, constitute the first one, which have been found in species from the *Streptomyces, Ochrobactrum, Pseudomonas, Paenibacillus* and *Amycolaptosis* genera. Laccases have been found in very different living organisms, in which they play different roles. Hence, they are related with morphogenesis, pathogen-host interaction, stress defence and lignin degradation in fungi, whereas they play an opposite role in plants, where they are responsible for the growth by lignin biosynthesis. Functions as morphogenesis, copper homeostasis and pigmentation have been found in bacteria, whereas they are related to the sclerotization of the cuticle in insects [140].

Other species from the *Rhodococcus, Enterobacter, Saccharomonospora, Pseudomonas, Amycolatopsis* and *Thermobifida* genera have otherwise shown the production of Dyp-type peroxidases [151,152], which form the second type of bacterial lignin-degrader enzymes. Recently, a lignin-oxidising manganese superoxide dismutase enzyme was found in *Sphingobacterium* sp. T2 [150], which establishes the third type of enzymes. The last group is formed by the glutathione-dependent β-etherase enzymes, which are known to act through the β-aryl ether linkage rupture [150]. The visual appearance of the active sites of the different lignin-degrader enzymes can be seen in Figure 16.

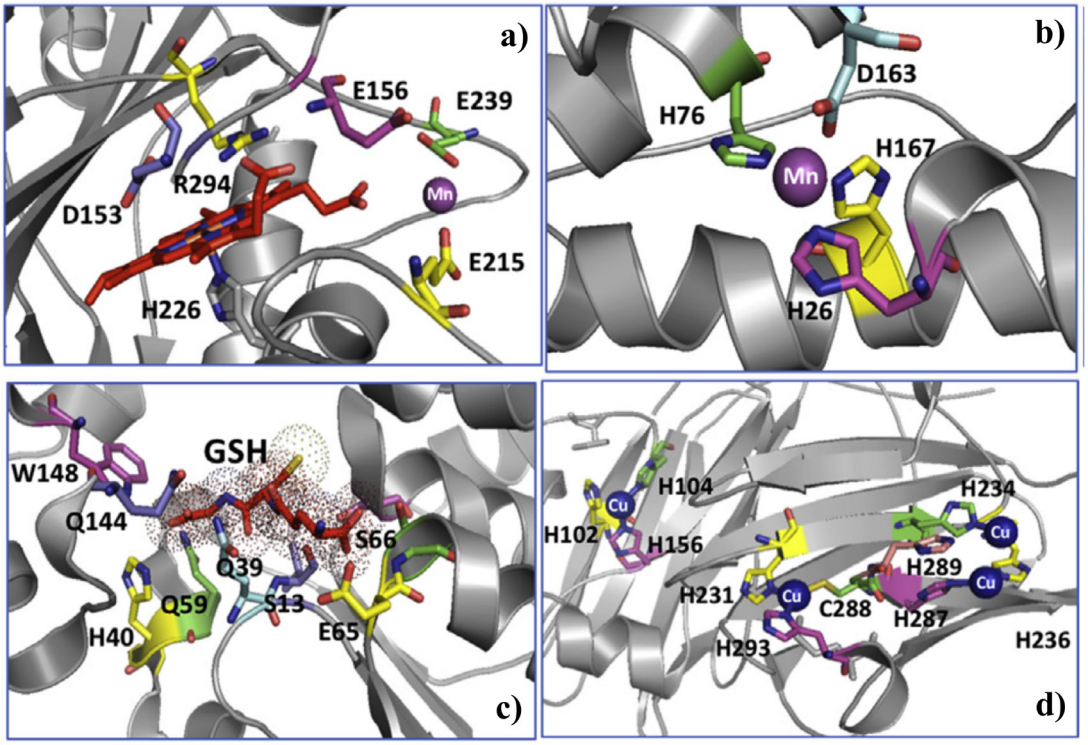

Figure 16. Active sites of lignin-degrading enzymes. a) DyP peroxidase, b) manganese superoxide dismutase, c) β-etherase LigF, d) Multi-copper oxidase [150].

The main aromatic species found through the biological pretreatment with lignin-degrader bacteria have been summarised in Table 7, which also includes fungi-related data to this production.

It is also worth mentioning that such products are not often directly obtained from the lignocellulosic chain, instead, oxidised polymeric intermediates are found. *Streptomyces viridosporus, Amycolatopsis* sp. 75iv3 and *Thermobifida fusca* have shown to produce a water-soluble intermediate described as acid-precipitable poly-phenolic polymeric lignin (APPL) [149,150]. But the production of either the polymeric intermediates or the direct phenolic-based molecules is based on the cleavage of the interunit linkages that join lignin. Thus, as diverse bonds have been found to form lignin, diverse pathways for lignin breakdown have also been reported, where the β-ketoadipate pathway has been considered the most usual one [140,149,150]. Figures 17 and 18 show diverse enzymatic pathways regarding the main interunits that comprise lignin.

Table 7. Aromatic products detected from lignin breakdown [137,149,150].

Compound		Fungal lignin degrader	Bacterial lignin degrader
Benzoic acid	4-hydroxy	*P. chrysosporium*	*A. aneurinilyticus, A.* sp. 75iv3
	4-hydroxy-3-methoxy	*P. chrysosporium*	*A. aneurinilyticus*
	4-hydroxy-3-methoxy-6-carboxy	*P. chrysosporium*	
	4-hydroxy-3-methoxy-5-carboxy		*P. putida, R. jostii* RHA1
	3,4-dimethoxy	*P. chrysosporium*	
	3,4-dimethoxy-2-carboxy	*P. chrysosporium*	
	2-hydroxy-3-methoxy		*A. aneurinilyticus, P. putida*
	2,3-dihydroxy		
	2,3,4-trihydroxy		*Bacillus sp.*
Benzaldehyde	4-hydroxy-3-methoxy		*S. paucimobilis*
	3,4,5-trimethoxy		*Bacillus sp.*
Cinnamic acid	4-hydroxy		*Bacillus sp.*
	4-hydroxy-3-methoxy		*Bacillus sp., P. putida, R. jostii* RHA1
Biphenyl-5,5'-dicarboxylic acid, 2,2'-dihydroxy, 3,3'-dimethoxy	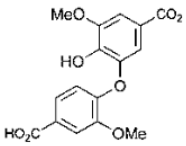	P. chrysosporium	
Diphenyl ether		P. chrysosporium	
Propiophenone-3'-hydroxy	4-hydroxy-3-methoxy		*S. paucimobilis. P. putida, R. jostii* RHA1
Acetophenone	4-hydroxy-3-methoxy		Soil metabolite
Phenol	2-methoxy		Soil metabolite
	2-methoxy-4-vinyl		Soil metabolite
Vanillin			*R. jostii* RHA1, *A.* sp. 75iv3

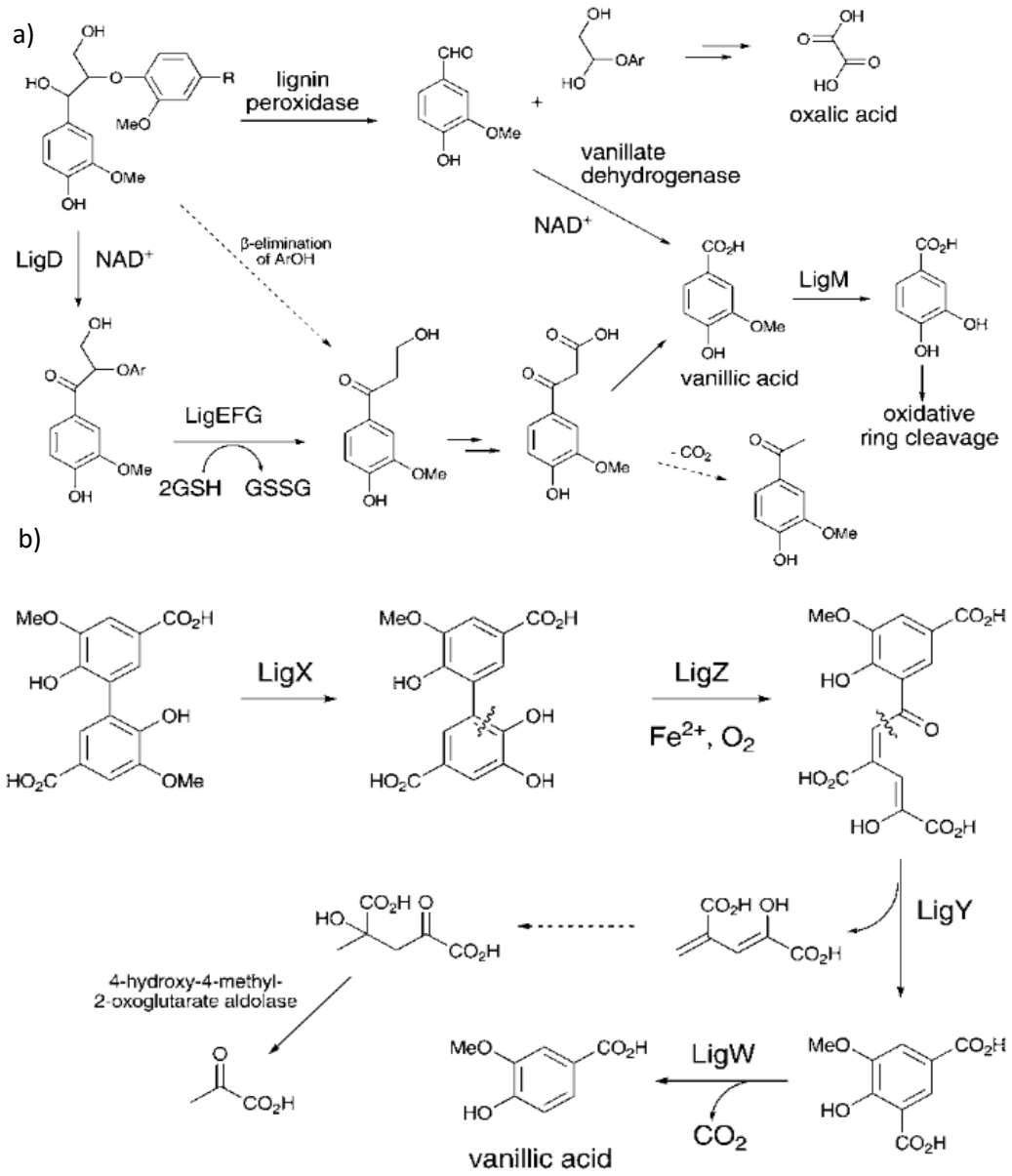

Figure 17. Different pathways for the bacterial metabolism of a) β-aryl ether and b) biphenyl components of lignin.

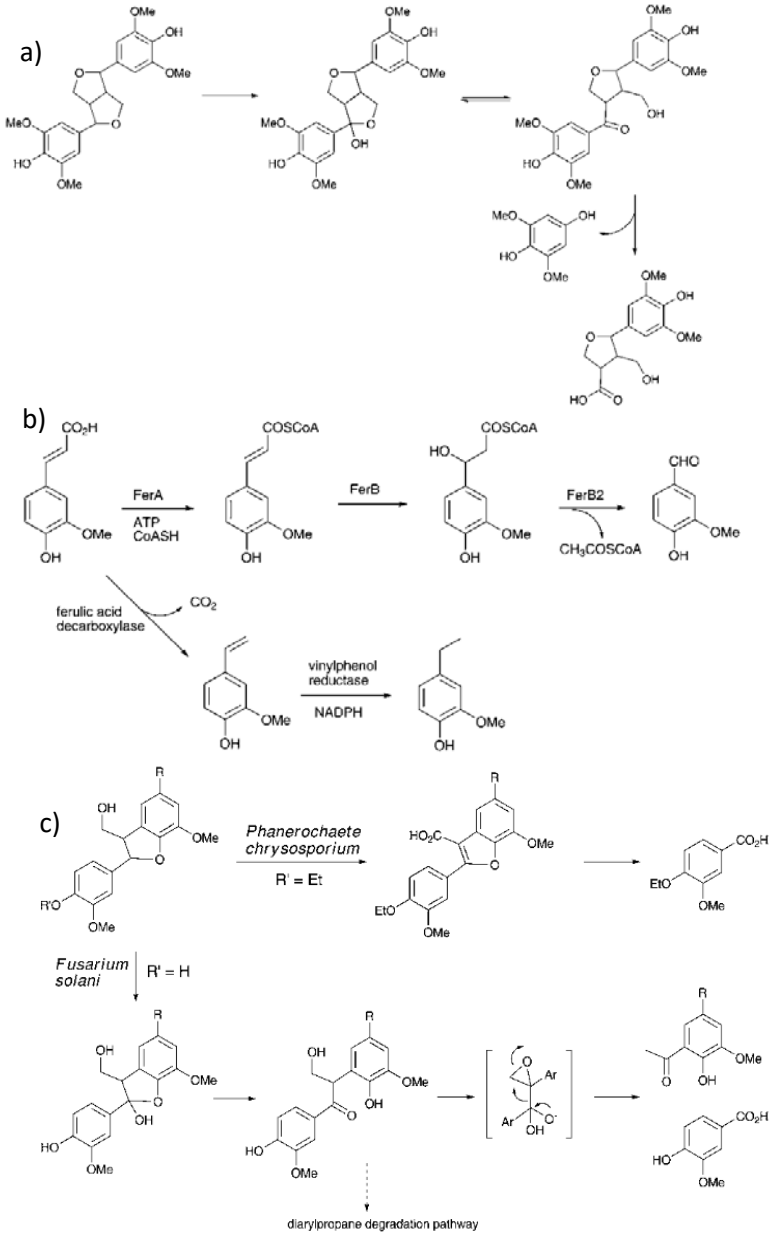

Figure 18. Different pathways for the bacterial metabolism of a) pinoresinol, b) ferulic acid and c) phenylcoumarane components of lignin.

As a summary for the pretreatment section, a table including the main pretreatment methods with remarkable characteristics and a description of their advantages/disadvantages has been included in Table 8.

Table 8. Comparison of the different pretreatment methods used for lignocellulosic degradation methods [146].

Pretreatment	Cost	Toxic by-product	Applicable to a wide range of biomass	Remarks
Acid pretreatment	Low	High	Yes	Dilute acid is used to limit inhibitors generation
Freezing	Low	Low	No	Cycles of freezing and thawing
Milling	Low	Low	Yes	Used for bioethanol and biogas production
Liquid hot water	Low	Low	No	High water and energy inputs
Organic solvent (Organosolv)	High	High	Yes	Low boiling point of solvent. Solvent recycling is required
Oxidation	High	No	Yes	High cost of ozone generation. Proper ozone handling is required
Steam explosion	High	High	Yes	High cost of steam generation
Extrusion	Low	Low	Yes	Hydrolysis efficiency is improved
Wet oxidation	High	Low	No	Less water use as no solid washing is required
CO_2 explosion	High	Low	Yes	High cost for pressure maintenance
Microwave irradiation	High	Low	Yes	More effective than conventional heating process
Ultrasound	High	Low	Yes	Low temperature and less time required
Ammonium fibre expansion	High	Low	Yes	Less effective for biomass with high lignin contents
Ionic liquid	High	Low	Yes	Stability and reuse. Instability may cause contamination
Biological pretreatment	Low	Low	Yes	Increases delignification and able to reduce polymerization
Hydrothermal liquefaction	High	Low	Yes	Lignocellulosic materials are depolymerized into bio-oil, biogas, biochar and water-soluble compounds

2.4. Lignocellulosic materials in the production of Biomaterials, Biochemicals and Biofuels

As previously mentioned, the great availability, wide range of biopolymers and renewable characteristics have propelled the research of biomaterials, biochemical and biofuels based on lignocellulosic components [153].

2.4.1. Biofuels

Compared to petroleum-based fuels, biofuels possess advantages such as renewability, sustainability, availability, biodegradability, safety, neutral greenhouse effects, and negligible SO_x and reduced NO_x gas emissions [154]. Lignocellulose represents the only sustainable, low-cost and scalable eco-friendly option for industrial fuel production [155]. Furthermore, it also represents a great opportunity for increasing the domestic energy production in those countries with large biomass supplies and/or land availability to produce energy crops [156]. The main drawback is found in lignin degradation, as it is considered the more energy-consuming step of the production process, due to the resilience of this biopolymer. Moreover, the cellulose efficiency, enzymatic and biomass costs and composition are other parallel parameters that critically affect the development of suitable technologies [155–157]. Furthermore, the obtaining of high-quality biofuels faces other problems, such as many of the most effective solvents for biomass pretreatment are simultaneously incompatible with enzymatic development, whereas those microbes with the highest yields in biofuels production do not often use the sugars present in hydrolysates as substrates [156]. Therefore, as mentioned before and widely discussed, massive attention has been paid to suitable pretreatments for advanced purposes.

Lately, the effort has been focused on genome editing technologies as a powerful tool for understanding and developing an integrated system to produce fuels in fast and lower energy-consuming processes [156]. Thus, some of the inhibitory compounds usually produced in natural plants, such as ferulic acid, can be substantially reduced by genomic editing, nonetheless, negative effects on crop yields, costs and environmental impacts can likewise take place [156]. Another approach that has been substantially developed is the preferential growth of cellulose in detriment of hemicellulose and lignin, as most industrial microbes generally take advantage of hexoses instead of pentoses for biofuel production. Lignin content reduction

and composition homogenization have also been targeted, the latter letting less complex product mixtures being generated, thus higher-valuable molecules being obtained. On the other hand, other strategies have been based on the incorporation of unusual monomers, which potentiate chain elongation or the incorporation of interchangeable linkages, resulting, once more, in higher saccharification yields [156].

Nevertheless, the use of lignocellulosic biomass as biofuel competes with the use as food supply. Hence, a step further can be taken when residual lignocellulosic biomass is considered, as it can be transformed into what is called *advanced biofuels*, i.e., biofuels which significantly reduce greenhouse emissions simultaneously with the preservation of the common use of landfills, and therefore do not compete with food or feed commerce [153,158]. In this sense, deep research and many industrial projects which include from aerospace to common fuels, biogas, bioethanol or biodiesel have been accomplished or are being carried out nowadays [153,155]. In order to obtain those products, three different routes have been targeted, i.e., thermochemical, biochemical and hybrid conversion. An overview of these alternatives is shown in Figure 19.

The thermomechanical route includes a variety of thermal treatments, from relatively low severity to strong processes where high temperatures are applied. Hence, torrefaction, pyrolysis, hydrothermal liquefaction and gasification are found between them.

The biochemical route relies on the enzymatic digestion of the different biopolymers that comprise lignin, which has been deeply described in previous sections, by either fungi or bacteria. The biomass digestion can lead to the production of small sugars, which can be directly used as fuels. However, a suitable separation process is generally needed as a consequence of the huge variety of products involved in lignocellulosic degradation. In addition, by following the biological route, certain compounds that cannot be obtained by chemical routes are produced, opening new areas of advanced biofuels [156].

Often, the products from biochemical routes are further converted by catalytic or thermomechanical processes into higher-added valuable fuels. Thus, the hybrid route is accomplished.

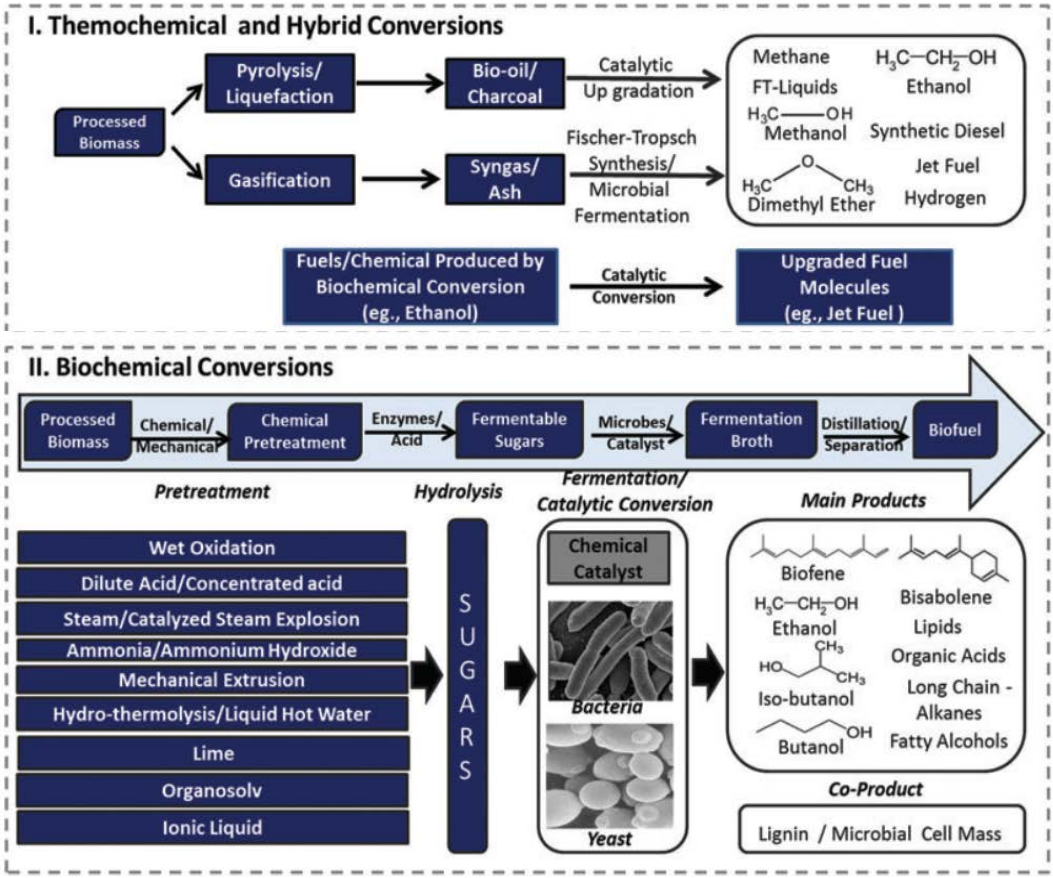

Figure 19. Overview of the different process to produce advanced biofuels [153].

The main biofuels that have been studied up to date are summarized in Table 9. More specific details about raw materials, final characteristics and conversion routes can be seen in the indicated references.

Table 9. Main biofuels and corresponding processing routes reported in the literature.

Biofuel	Reference
Biodiesel	[159]
Bioethanol	[159]
Biocrude	[159]
Bio-oil	[159,160]
Biogas	[154,161,162]
Biohydrogen	[154,161]
Biobutanol	[163]

2.4.2. Biochemicals

As a consequence of the great variety of monomeric units and linkages that comprise the three biopolymers, the range of biochemicals that can be obtained from them constitutes an even much wider range. These biochemicals critically depend on the original biopolymer, i.e., lignin generally provides outstanding aromatic-based compounds, whereas sugars resulting from the hydrolysis of cellulose and hemicellulose may produce valuable six- and five-carbon derived products [164].

In the case of cellulose and hemicellulose, many different products can be obtained [165,166]. Werpy and Petersen [167] analysed more than 50 compounds, from which they found glycerol, acetic acid, levulinic acid, 3-hydroxybutyrolactone, glutamic acid, malic acid, itaconic acid, aspartic acid, oxalic acid, 3-hydroxy propionic acid, succinic acid, fumaric acid, 2,5-furan dicarboxylic acid, glucaric acid, sorbitol, and xylitol/arabinitol among the more interesting ones. Most of them can also act as building blocks for the development of fine chemicals and derived compounds. Table 10 depicts the main processes to obtain those species, together with the main derived products that can be obtained from them.

Other important cellulose and hemicellulose-derived products are 5-hydroxymethyl furfural and furfural, which have been reported to be obtained by hydrothermal carbonization of those biopolymers, respectively. Both derived-furans can also be precursors of many other chemicals, biofuels, pharmaceutical and agrochemical products [164,166,168].

A detailed summary including the different chemical structures of both precursors and final products has been included in Figures 20, 21 and 22 [166].

Table 10. Main building blocks and their derivatives obtained from cellulose and hemicellulose [167].

Compound	Production	Derived products
Succinic, fumaric and malic acid	Biofermentation	Tetrahydrofuran (THF), 1,4-butanediol, 2-pyrrolidone, o-butyrolactone, N-methyl-2-pyrrolidone (NMP)
2,5-Furan dicarboxylic acid	Chemical (oxidative dehydration of glucose) and biological	(2,5-Bis(aminomethyl)-tetrahydrofuran, 2,5-dihydroxymethyl-tetrahydrofuran, 2,5-dihydroxymethyl-furan
3-Hydroxy propionic acid	Biofermentation	1,3-Propanediol, acrylic acid, acrylamide
Aspartic acid	Chemical and biological pathways	2-Amino-1,4-butanediol, aspartic anhydride, 3-aminotetrahydrofuran, amino-γ-butyrolactone
Glucaric acid	Chemical (starch oxidation by nitric acid or bleach)	Glucaro-γ-lactone, polyhydroxypolyamides, glucarodilactone, glucaro-δ-lactone
Glutamic acid	Biofermentation	Glutaminol, glutaric acid, norvoline, 1,5-pentandiol, 5-amino-1-butanol
Itaconic acid	Chemical and biofermentation	3-Methylpyrrolidine, 3- & 4-methyl NMP, 3-methyl THF, 2-methyl-1,4-butanediol.
Levulinic acid	Chemical (acid decomposition of six-carbon sugars)	Diphenolic acid, 2-methyl-THF, b-acetylacrylic acid, 1,4-pentanediol
3-Hydroxybutyrolactone	Chemical (oxidative degradation of starch)	3-Hydroxytetrahydrofuran, 3-aminotetrahydrofuran, acrylate-lactone
Glycerol	Transesterification (via chemical or biological pathways)	Glyceric acid, 1,3-propanediol, propylene glycol
Sorbitol	Chemical (glucose hydrogenation)	Isosorbide, propylene glycol, ethylene glycol, 1,4-sorbitan
Xylitol/arabinitol	Chemical (hydrogenation of xylose and arabinose) and biological	Xylaric acid, propylene glycol, ethylene glycol, lactic acid

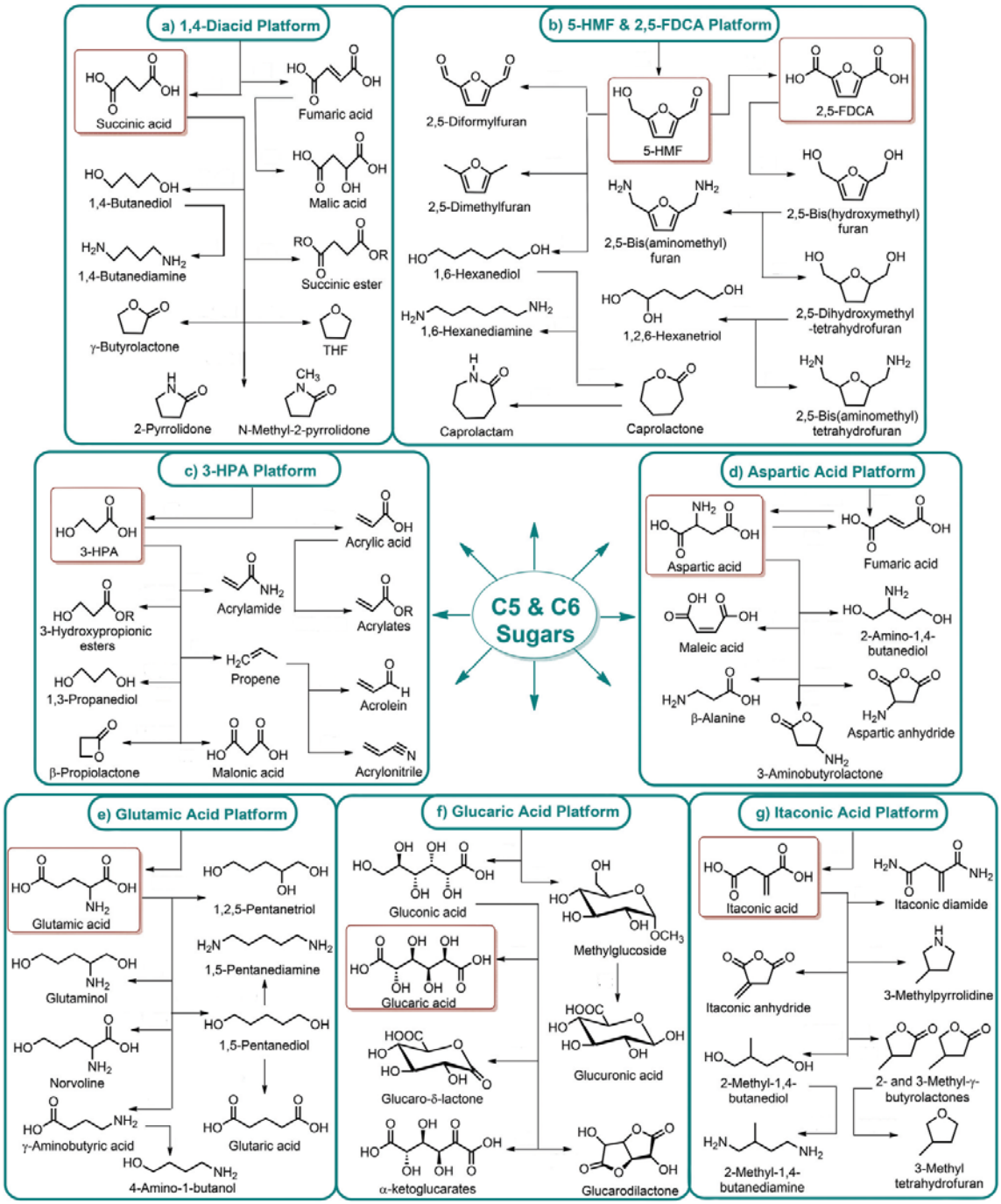

Figure 20. Main chemicals and building blocks obtained from cellulose and hemicellulose (I) [166].

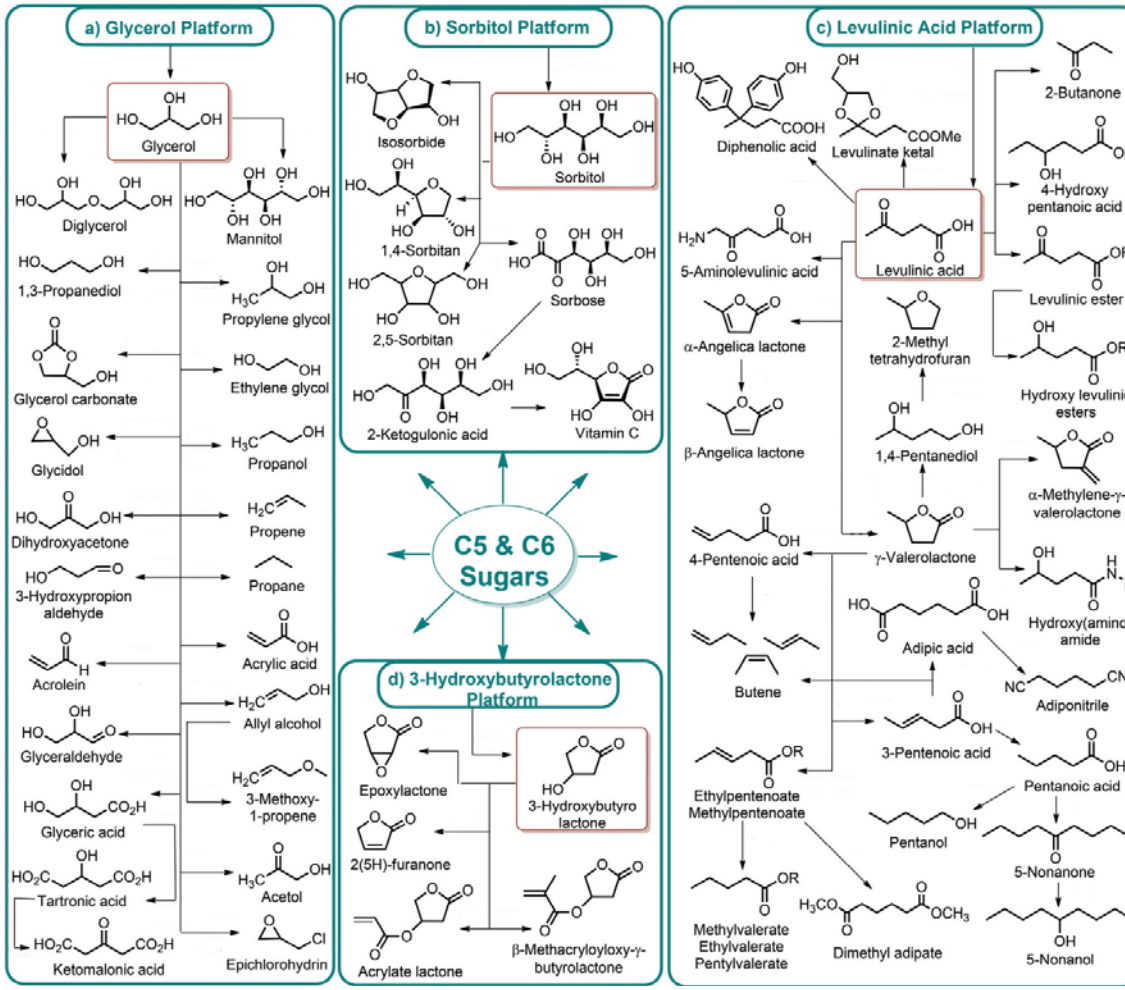

Figure 21. Main chemicals and building blocks obtained from cellulose and hemicellulose (II) [166].

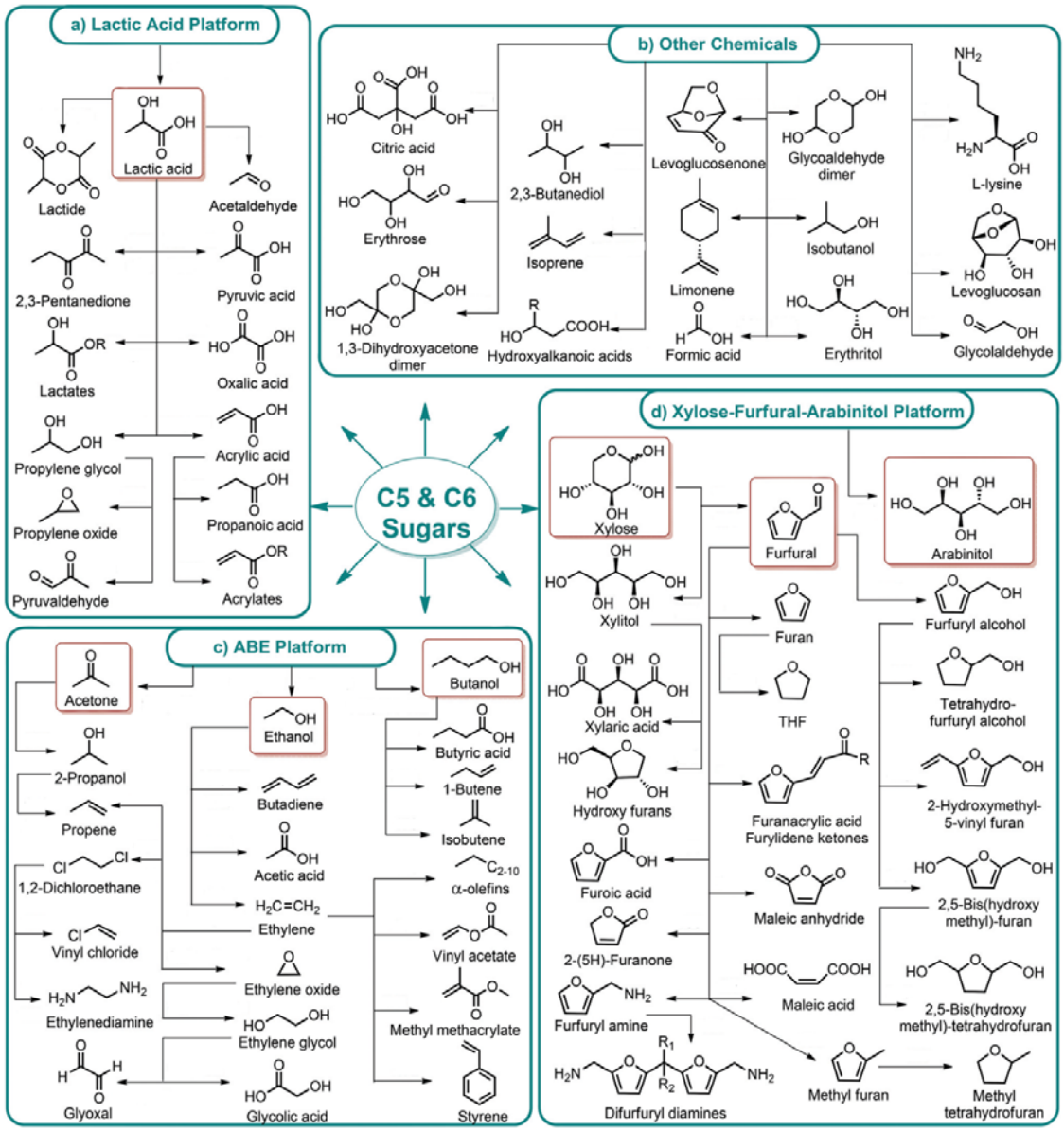

Figure 22. Main chemicals and building blocks obtained from cellulose and hemicellulose (III) [166].

Regarding lignin, as mentioned above, a vast range of aromatic-based chemicals can also be obtained by its decomposition and transformation. However, the success of the suitable formation of chemicals from lignin relies on several main aspects, i.e., lignin fractionation from raw biomass, proper degradation, depolymerisation, transformation into high-value added compounds and further separation. Depending on depolymerisation conditions, diverse products can be obtained, as shown in Table 11.

Table 11. Main procedures from lignin depolymerisation along with main products obtained.

Depolymerisation	Procedures	Products	Refs
Non-reductive depolymerisation	Thermal, hydrothermal, oxidative, acid and base catalysed, solvolytic	Vanillin, syringaldehyde, acetosyringone, guaiacylacetone, p-hydroxylated phenol acetovanillone, syringol, guaiacol, phenol, catechol, alkylcatechols, creosol, p-hydroxybenzaldehyde, vanillic, protocatechuic, syringic, homovanillic and p-hydroxybenzoic acid, aliphatic carboxylic acids (succinic, acetic and formic acid)	[164,169]
Reductive depolymerisation	Hydroprocessing, liquid phase reforming	Cresol, xylenol, phenol with long alkyl chains, p-substituted methoxyphenols,	[169]

The different processes do not only lead to the formation of different species but also the monomer yields depend on the procedure characteristics, as Figure 23 depicts.

Similar to cellulose and hemicellulose, several of the compounds obtained can be considered end products, while many others can likewise act as building blocks for possible upgraded compounds. A summary is included in Figure 24 [166].

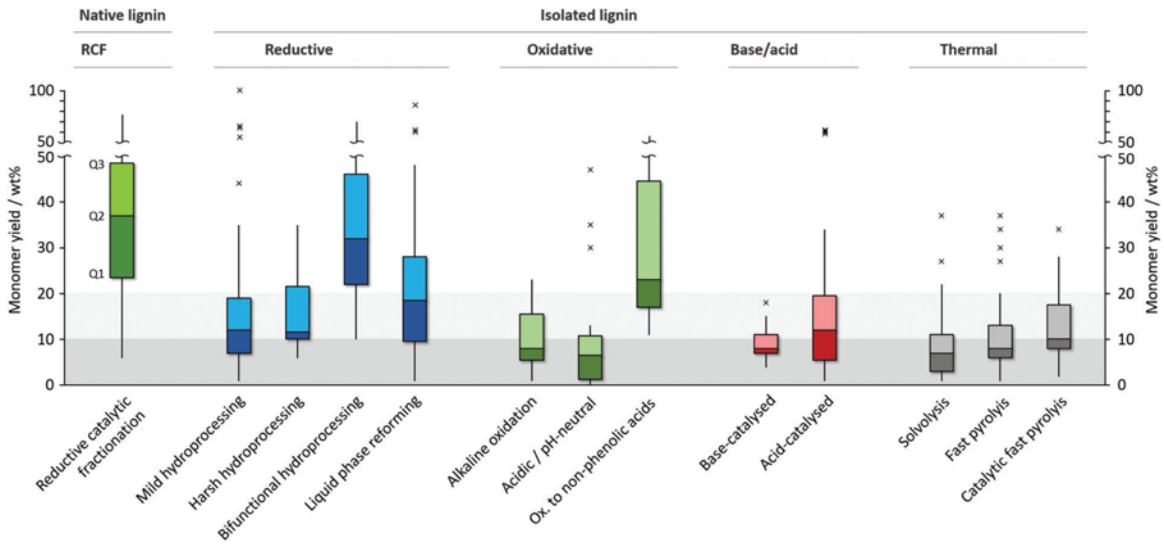

Figure 23. Monomer yields obtained by diverse lignin depolymerisation techniques [169].

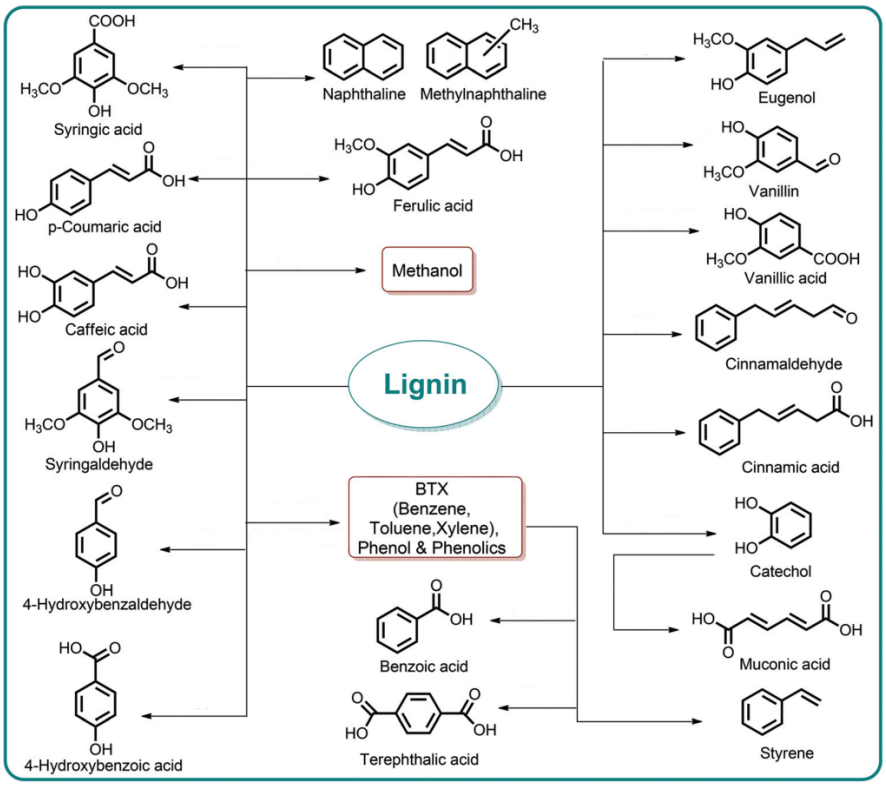

Figure 24. Main chemicals and building blocks obtained from lignin [169].

2.4.3. Biomaterials

Due to the extensive variety of molecular species obtained from lignocellulosic degradation, the possibilities of derived biomaterials are massive. Werpy and Petersen [167] included in their work an exhaustive review of the biomass components, their primary degradation products, main intermediates and a brief description of derived bioproducts and uses, as can be seen in Figure 25. Hence, lignocellulose derivatives may play a significant role in areas such as general industry, transportation, textiles, packaging and other food vessels, environment, plastic replacers, stationery, house and leisure items, health and hygiene.

However, those biomaterials that make use of the interesting biopolymer network characteristics without further fractionation into derived products are not included among those uses, thus, they will be discussed separately. When considering lignocellulose, frequently research has taken advantage of lignin, cellulose and hemicellulose biopolymers separately, however, also the whole biomass has been considered.

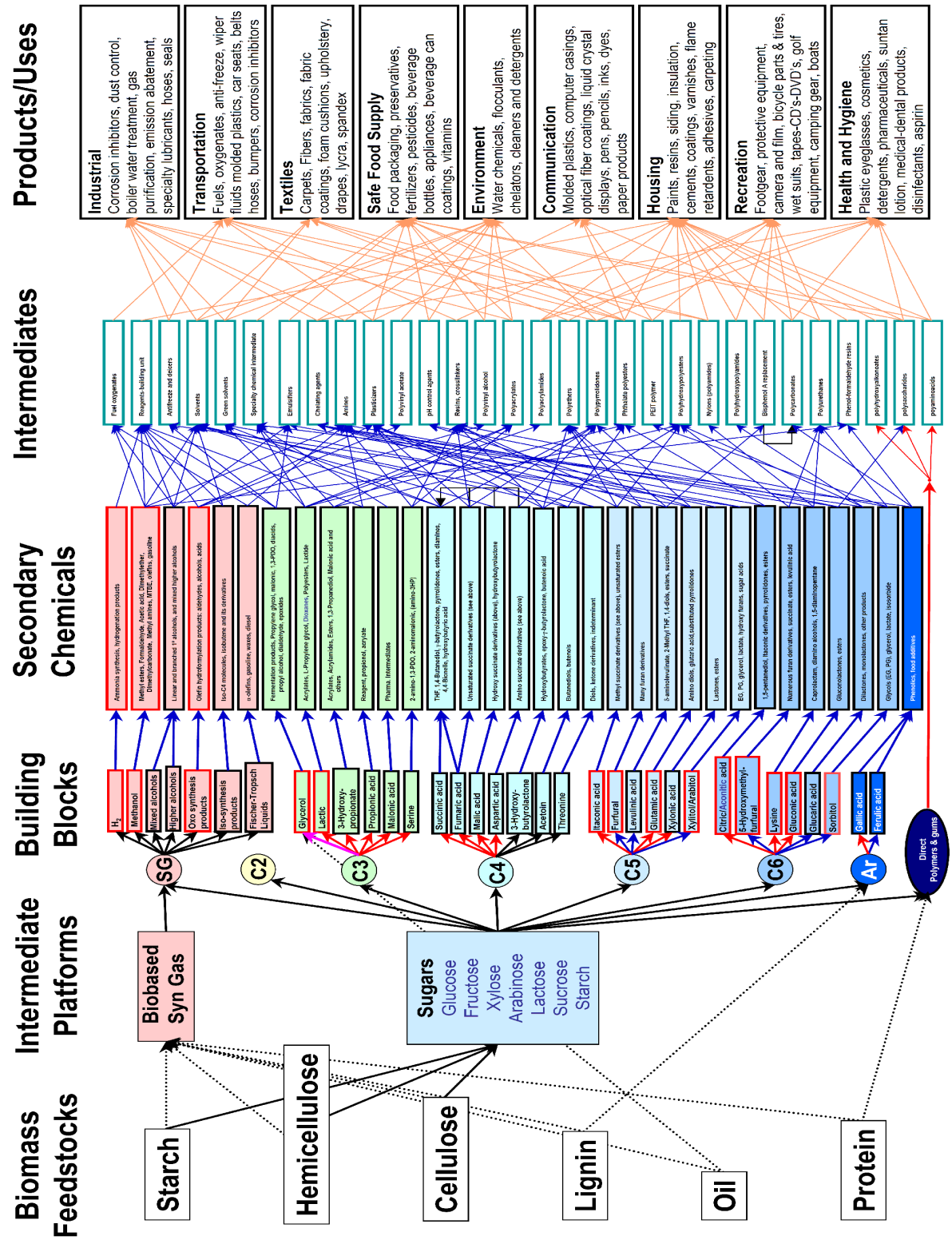

Figure 25. Bio-based products flowchart for biomass feedstocks [167].

2.4.3.1. Lignocellulose-derived biomaterials

There is an immense range of biosource applications nowadays, boosted by research possibilities, variety and exceptional properties. Some of them will be discussed further on in this section, nonetheless, a detailed revision of many of these applications is further beyond the scope of this work.

For wheat and barley straw, as introduced in section 2.2, advanced biomaterials for construction materials, phycoremediation of wastewater, cement properties enhancer and fibres in concrete were reported. Straws and stalks from other sources were also focused on board production, being potentially suitable for beaverboard, packing materials, one-use tableware or seeding devices [170–172].

One of the main applications that has been developed is the use of biomass as an adsorbent. In this sense, Rocha et al. [173] studied the adsorption of metal ions such as Cu(II), Zn(II), Hg(II) and Cd(II) on rice straw-derived solutions. By the formation of biochar from rice straw, other metal ions such as Pb and Zn can also be adsorbed [174,175], as well as nitrogen and phosphorous [176]. Abdel-Aal et al. [177] reported the ability of rice straw for the treatment of wastewater including several commercial dyes instead. Likewise, banana peel- and palm flower waste-based derived products were also able to remove methylene blue and malachite green dyes from polluted solutions [178,179]. Other studies obtained proper adsorbents from residual products such as orange peel and sugarcane bagasse [180].

On the other hand, electrocatalytic activity was also studied on biomass-derived materials. Thus, Gao et al. [181] produced N-doped porous carbon spheres based on rice straw, while Liu et al. [182] created soybean straw-based Fe-N co-doped porous carbons, both exhibiting excellent properties in electrochemical applications. Ma et al. [183] demonstrated cornstalks and pomelos skins to efficiently act as carbon sources for the construction of cathode catalysts for microbial fuel cells. Another biosource, watermelon, was used by Wu et al. [184] to create hydrogels and aerogels with electrochemical applications. Other biomass sources suitable for electrochemical applications are sawdust or grasses [185].

Composites containing residual lignocellulosic biosources have also been targeted. In those, lignocellulose acts as a reinforcing filler, and avoids problems such as lack of flexibility or respiratory illnesses [186]. Bugatti et al. [187] shown how tomato peels could form proper

composites with halloysite nanotubes for packaging applications. Ita-Nagy et al. [188] demonstrated sugarcane bagasse fibres to also reinforce properly composites structure. Pinhao and pecan nutshells were also used for reinforced composites preparation. The pinhao nutshell-based composite exhibited lower water absorption capacity than petcan-based one, based on the enhanced hydrophobic character of the pinhao-based composite [189]. Fibres from tropical maize and sweet sorghum bagasse were also studied as composite additives [190].

The use of biomass as catalysts or catalyst supports has also been deeply studied, as is the case of soybean and other biomass with high protein content [191].

In textile, bamboo fibres can provide comfortability, good dyeing and appealing characteristics. Hemp can also be utilised for textile application, as well as for making sacks and ropes, degumming, etc. [192].

In food, tomato peels have acted as an enhancer for colour and antioxidant properties for yoghurts [193], whereas tomato peel fibres have demonstrated the ability to produce a suitable network for edible gels, with enhanced stability and texture [194].

A singular case can be considered when lignocellulosic biomass acts as a hydrogel precursor, which have found interesting applications in fields such as film formation, high strength filaments, tissue engineering, among many others [195].

Nonetheless, the number of applications and studies are boosted when the different lignocellulosic biopolymers are considered separately. In the following sections, cellulose-, hemicellulose- and lignin-derived biomaterials have been examined.

2.4.3.2. Cellulose-derived biomaterials

The singular structure of cellulose, together with its possibilities of being modified by chemical reactions or converted into alkyl-derived or nano-systems have made a great range of biomaterials available nowadays from this biopolymer.

The high number of hydroxyl groups present in cellulose has attracted research attention to the formation of cellulose-based hydrogels. Even though the cellulose ability to be dissolved in water is limited, the development of many suitable solvents has made hydrogels

with stunning properties be obtained, with applications such as food packaging, smart swelling, controllable delivery and biomedical applications [196–198].

The well-known ability of some bacteria to produce cellulose (bacterial cellulose) has also been leveraged for the performance of hydrogels. In general, good tensile and compressive properties are shown, together with high water-absorption capacity, crystallinity and biocompatibility, which have made bacterial cellulose-based hydrogels to be focused on bioapplications such as dental and meniscus implants, or tissue engineering scaffolds [196].

Hydrogels from alkyl-cellulose-derived products have also been analysed, such as hydroxypropyl-, hydroxypropylmethyl-, carboxymethyl- or methyl-cellulose. The alkyl-derived chains introduce regions where physical crosslinking may be dampened, thus, chemical crosslinking has frequently been targeted, which has provided hydrogels with new characteristics, for instance, pH dependence in sorption capacity. These hydrogels have shown valuable in water body elimination through the absorption of water in the stomach [199], dyes elimination [200], food and drugs [196].

Nonetheless, the capacities of cellulose-based hydrogels can be further boosted by the combination of other synthetic or natural polymers. Hence, heavy metal elimination, food or tissue engineering have been targeted by the combination with chitosan, starch or alginate, respectively [196].

On the other hand, inorganic materials have also been added to the cellulose-based hydrogels structures, with applications in fields such as electricity, magnetics, optics and biology. A summarised insight on the potential applications of cellulose-based hydrogels has been depicted in Figure 26.

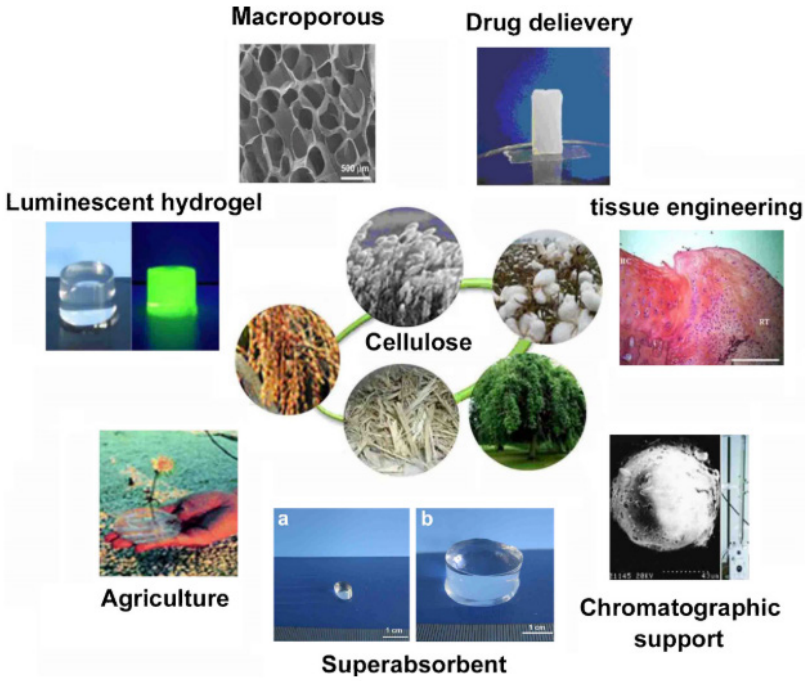

Figure 26. Insight on applications for cellulose-based hydrogels [195].

However, not only hydrogels have been reported to be developed from cellulose. Aerogels, usually obtained by freeze-drying of hydrogels or supercritical drying with CO_2, have also been performed. In the same way as with hydrogels, cellulose, bacterial cellulose and many derived systems (from alkyl- to nano-systems) have been reported to produce aerogels, affecting both the synthesis process and final properties [201].

Aerogels possess characteristics like very low density (up to 0.5 mg/mL), high specific surface area (up to 975 m^2/g) and highly porous structures (up to 99.9% porosity), while keeping good mechanical characteristics, which have propelled their use in applications such as shock absorbers, acoustic and thermal insulation, oil absorption, biomedical devices and implants, conductivity enhancers or carrier of metal nanoparticles and oxides [201–203].

On the other hand, by the combination with oily systems, oleogels have also been prepared. Once more prepared through the use of cellulose and cellulose-derived materials, a vast range of products have been documented. In food industry, it is ethyl cellulose the one which has attracted the most attention due to the appealing thickening properties, though pristine cellulose, methylcellulose and hydroxypropyl methylcellulose have also been studied [204]. Nonetheless, the rheology-modifier characteristics have been leveraged for its use in a

wider range of applications such as binders, films, adhesives, lubricating greases and hot blends [98,205].

The case of lubricating greases remains especially appealing, as regardless of the extensive work found in literature, the industry continues to employ almost entirely petroleum-based products, and using lithium- and other metal-based soaps as thickening agents. Hence, studies that explore the use of cellulose pulp as thickener can be found [206–208], but also pristine cellulose [98,209,210] and cellulose derivatives [209–211]. A wide range of these systems has demonstrated to impart suitable rheological and excellent tribological properties, along with appropriate mechanical stability comparable to lithium-based lubricating greases benchmarks.

As already introduced in this section, the formation of nanostructures from cellulose is also a very appealing approach for the development of potential systems with a broad range of applications. By the formation of nanofibres, excellent properties of water-based hydrogels have been shown, as only a very low concentration is needed in order to obtain good rheological properties. Furthermore, the formation of films and nanocomposites have also been extensively reported. Thus, applications such as reinforcing agent for paper, greaseproof paper, thermosetting resins, strengthened composites, obesity-precautionary thickener, suspension stabilizer, sanitary products, wound dressing, coatings, etc. can be found [212,213].

The formation of cellulose nanocrystals has also been extensively studied, with the majority of applications based on the formation of composites. Nonetheless, the suspensions containing these cellulose nanocrystals have shown nematic chirality, which boosts their applications in fields such as NMR spectroscopy and optical taggants [212,214].

In addition, not only mechanical and chemical processes have been documented to successfully produce cellulose nanostructures. Instead, some bacteria have also exhibited the possibility of directly obtaining cellulose nanostructures with the only presence of hydroxyl moieties as functional groups. The high yield for a biological process (up to 40%) and unique structure have propelled its use in fields such as regenerative medicine, wound healing, implants, membranes, films and barrier layers [212].

2.4.3.3. Hemicellulose-derived biomaterials

Even though hemicellulose does not possess the significance and properties of cellulose and cellulose derivatives, there are also many studies that take advantage of hemicellulose structure to produce interesting biomaterials. Due to the fact that hemicellulose is not formed by a single type of biopolymer, the possibilities are again raised. The main target of hemicellulose-based biomaterials has been based on the production of antioxidant agents, hydrogels and films for uses such as coatings, packaging or biomedicine, nonetheless, some other less common uses have also been studied.

Hydrogels have been mainly centred in drug delivery [215–217], tissue engineering and environmental protection, and have demonstrated pH, ioinic strength, media composition and organic solvent dependent behaviour. Thus, the removal of heavy metals like Ni (II), Cu(II), Pb (II), Cd(II), Pd(II) and Zn(II) or sulfadimidine has been successfully achieved by these hydrogels [37,218,219]. On the contrary, good adhesion in tissues like liver has also been documented, in which they may play a good replacement role in detriment to more expensive and lower available tissue and organ transplants [220]. In drug delivery, xylan- and galactomannan-based microcapsules have shown to be excellent colon-specific carriers [216,221,222], while xyloglucan mucoadhesive and surface tailoring properties have led to the development of many specific studies [217]. Galactomannans have also shown useful for drug delivery by the formation of an aerogel structure [223].

Hemicellulose-based films were also produced, whose significance is based on the outstanding properties against oxygen permeability, thus conforming a great replacement for oxygen-sensitive food packaging. Xylan, arabinoxylan, glucomannan and galactoglucomannan, alone, modified, or by combination with other biopolymers, are some of the biopolymers from hemicellulose which have shown suitable properties for film production [218,224,225].

The same oxygen permeability provides hemicellulose with interesting antioxidant and antimoisture properties, which make of them good replacements as coatings for food packaging.

Between the less common uses, there is still a vast range to be found. Peng et al. [226] demonstrated hemicellulose to act as stabilizer for the formation of silver nanoparticles. Jiang

et al. [35], instead, use hemicellulose for the synthesis of quantum dots to detect Ag(I) and L-Cysteyne in aqueous solutions. Farhat et al. [227] were able to produce hemicellulose from bleached hardwood pulp and switchgrass, which crosslinked with zirconium, exhibited excellent adhesive properties. Xylan has been analysed by Ebringerova [228], who evaluated other potential applications such as textile printing, antimicrobial additive, plant growth regulator, inmunoenhancing supplement, additives and thickening agent in food. On the other hand, xyloglucan has also been reported as texture enhancer, binder, dye absorption, emulsion stabilizer, syneresis control and food additive [229]. Some of these applications are shared by galactomannan-derived products, which have shown to act as binders, texture modifiers, emulsifiers, lubricators or stabilizers, mainly in food industry [230]. Galactoglucomannan has been also studied as food additive because of its prebiotic properties [231].

2.4.3.4. Lignin-derived biomaterials

The unique characteristics of lignin have propelled both research and industry to focus on this biosource acting as an additive for a wide range of polymers, such as polypropylene, polystyrene, polyethylene, polyamide, PVC, poly(vinyl alcohol), among others bio and synthetic polymers [232]. Thus, thermal and UV stabilizer, flame-retardant, reinforcing filler, plasticizer, lubricant, colour-adding pigment and antioxidant are among the most significant properties that lignin incorporation can enhance or modify [233], giving interesting biomaterials that can be applied in fields such as thermoplastic, thermoset, bioplastic and rubber composites, aerogels, carbon fibres and foams [232].

For instance, lignin addition in polyethylene and polystyrene matrices up to 20% has shown not to modify processability whilst significantly improving resistance against photodegradation [234]. In another study, Mishra et al. [235] demonstrated lignin to provide stronger resistance to UV in PVC films acting as UV absorber. Yang et al. [236] also showed poly(methyl methacrylate) thermal and mechanical properties to be enhanced by the lignin addition against UV light. Therefore, applications in fields such as automotive, acrylic glasses, vehicles and lenses have been targeted. On the other hand, different lignin fractions response to UV light as a function of the solvent utilised has also been studied, showing UV resistance to be dependent on the lignin extraction method [237,238]. In Pouteau et al. [238] study, lignin origin also demonstrated varied antioxidant properties.

Thermal resistance is frequently another weak point in conventional polymers and composites, thus, lignin addition as enhancer of the heat resistance has been a deeply studied topic. Canetti et al. [239] demonstrated lignin addition from 5 to 10% in polypropylene blends to successfully improve the thermal resistance. Working on natural rubber modification, Gregorová et al. [240] showed that the lignin addition also increased the thermo-oxidative long term resistance. On the contrary, Tavares et al. [241] reported a simple 1% lignin addition to reinforce the poly(butylene adipate-co-terephthalate) matrix. On the other hand, Lisperguer et al. [242] demonstrated lignin addition to recycled polystyrene could provide similar characteristics to the native polymer. Such is the interest in the improvement of the thermal properties by lignin addition of blends, composites and copolymers that Sen et al. [243] wrote an extensive review where lignin modification by different processes and the thermal response of the products obtained were evaluated.

Flame prevention is another powerful characteristic that lignin can provide to a biomaterial. Thus, De Chirico et al. [244] worked with lignin and various derivatives, which were able to provide the polypropylene matrix with enhanced combustion time and char yields, and reduced both heat liberation and mass loss rate while saving mechanical properties. The flame retardant properties of polylactic acid-based biopolymers were likewise improved by the use of lignin nanoparticles functionalized with diethyl (2-(triethoxysilyl)ethyl) phosphonate [245]. Another renewable polymer, polybutylene succinate, was also successfully treated with nitrogen-and-phosphorous doped lignin systems, improving both heat release rate and total heat release in around 30%, properties that could lead this biopolymer to be applied in wider fields [246]. Recently, some reviews concerning the flame retardant possibilities of lignin and its derivatives, as well as their future prospects, have been reported [247,248].

Lignin acting as reinforcing filler has also been extensively documented. Therefore, Ikeda et al. [249] showed that lignin potentially improves tensile stress and storage moduli of natural rubber, while reducing the dissipative loss. The tensile and flexural modulus of polylatic acid, poly(3-hydroxybutyrate), and thermoplastic elastomers after lignin addition were also raised [250]. Mechanical properties were also generally improved when lignin nanoparticles-poly (diallyldimethylammonium chloride) complexes were added to natural rubber [251]. In a study developed by Rozman et al. [252], coconut fiber and polypropylene were mixed using lignin as compatibilizer. The mixtures exhibited better flexural properties when lignin was included. On the other hand, Tanjung et al. [253] demonstrated that lignin

addition to polypropylene/chitosan composites successfully increased tensile strength, elongation at break, Young's modulus and impact strength. Extensive reports have been documented regarding lignin acting as filler for bioplastics, thermoplastic and thermoset composites [232]. Regarding bioplastics, Yang et al. [254] revised the most recent literature in lignin-reinforced bioplastics made of cellulose, protein, starch, polylatic acid and poly-hydroxybutyrate. Recently, an extensive review aiming to compile the latest advances on lignin reinforcing properties in the rubber industry has also been published [255].

As mentioned above, lignin can likewise act as plasticizer, which has been achieved frequently through structural modifications. Therefore, lignosulfonate has been used as an usual plasticizer for concrete. Through other modifications like alkylation, a plasticizing effect of lignin has also been achieved [243]. Working with PVC and different molecular weight lignin fractions, those with the lowest ones were reported to act as plasticizers by Yue et al. [256]. On the other hand, a novel process consisting of an alkali-O_2 oxidation technology for lignin revalorization has recently been addressed for plasticization (LigniOx), which was included in the annual report of the top 20 innovative bio-based products form the European Commission [257]. Moreover, by further modifications, superplasticizers have been targeted, which could replicate the performance of well-known commercial naphthalene plasticizers [258].

The presence of hydroxyl groups in lignin has provided it with the possibility of establishing H-bonds, which has been leveraged for its use as an additive for lubricants. Hereby, lignin has been added to many different base oils, in which the H-bonds formed have proved to generally decrease both wear and friction. Mu et al. [259] developed fully bio-based lubricants by utilizing lignin and ionic liquids, demonstrating outstanding tribological and anticorrosive properties on both aluminum and iron surfaces. Working with polyethylene glycol as the base oil in a more recent study, Mu et al. [260] compared lignins as additives from different origins and extraction processes, highlighting hydrogen bonding and molecular weight as crucial factors on thermal and lubricating properties. Up to 93.8% wear reduction was reported by the lignin incorporation. In another study, Hua et al. [261] created lignin-based green lubricants with excellent properties in diamond-like carbon-steel contact compared to commercial lubricants, showing lignin-based lubricants to be useful on surfaces with different characteristics. In addition, not only liquid lubricants but also semi-solid ones, i.e. lubricating greases, have been developed by using lignin [262].

Even though lignin is almost colourless in wood, its separation from cellulose and hemicellulose finally turns it into a dark brown colour [263]. For this reason, Balasubramanian et al. [264] used lignin as brown pigment and tested it in leather, where apart from dyeing the surface properly, exhibited compatibilization with common products for leather finishing. However, the use of lignin as pigment is not a new trend, as its use to produce inks by reaction with salts and tannin dates back to 1970 [265]. On the other hand, Araújo et al. [266] used lignin nanoparticles to encapsulate blue-pigments, which increased both solubilization and stabilization, making them more suitable for industrial applications.

Within lignin roles in plants resides the antioxidant capacity as a consequence of its aromatic structure, which has likewise been used for the incorporation of antioxidant properties in biomaterials production, with applications in cosmetics, healthcare agricultural products and pharmaceuticals [267,268]. Once more, the lignin varied characteristics depending on both the origin and extraction method have let adjustable antioxidant properties be obtained [267,269–271]. For instance, Li et al. [272] used different solvents (ether, ethyl acetate, methanol, acetone, and dioxane/water) in order to study the antioxidant properties of the different fractions obtained. The results showed that the higher the dissolving ability of the chemicals, the lower the antioxidant capacity of the resulting lignin fraction. Instead, Ma et al. [273] investigated the antioxidant activity as a function of pH in the lignin extraction method. High pHs led to low lignin content and low phenolic content, which exhibited low antioxidant activity. On the contrary, low pHs turned into lower molecular weight lignin fractions with high phenolic hydroxyl content, showing excellent antioxidant properties and highlighting the crucial effect of both molecular weight and phenolic hydroxyl group content in antioxidant properties.

Industrially, lignin has been used as dispersant, binder or chelator, as a substitute of phenolics powder resins, in polyurethane foams and epoxy resins or as biodispersant, among others. Thus, some North American companies have implemented lignin addition in products such as automotive brake pads and molds and oriented strand boards. The company Bioconsult Gesellschaft fuer Biotechnologie mbH, has developed a lignin-based system able to control the microbial growth in industrial wastewater ambits [274]. The company Nippon Paper Group has released diverse lignin-based biomaterials, SAN X®, VANILLEX®, PEARLLEX®, which can act as mentioned above according to their characteristics [275]. More concretely, the company TECNARO has been able to use lignin in thermoplastics with applications in fields such as

jewelry, construction, musical instruments, electronics, furniture, etc. In Figure 27, some headphones made of this lignin, ARBOFORM®, are presented. The Prisma Renewable Composites company developed a system named evolUTIA™, able to create lignins with similar characteristics from different plant sources, which have let them use lignin in biomaterials such as plastics, elastomers and carbon fibres. Their first product is BioLAN™, which has been declared as a substitute for ABS with enhanced both mechanical and UV resistant properties.

Figure 27. Headphones made of ARBOFORM®.

3. Bio-based polyurethanes

3.1. Diisocyanates and polyurethanes

Isocyanates are known to possess extraordinary reactive capability with many functional groups, which makes them suitable compounds to generate urethane and urea bonds. If isocyanates with more than one NCO group (di or tri-isocyanates) are considered, extensive polymers can be obtained [276].

The reactivity of the NCO group relies on its structure, which leads to a low electronic density focused on the carbon atom, a high electronic density on oxygen and a medium electronic density on nitrogen, as shown by the possible resonant structures in Figure 28. In this situation, a nucleophilic hydrogen compound can attack the electrophilic carbon atom, generating the new bond, as shown for the general reactions in Figure 29.

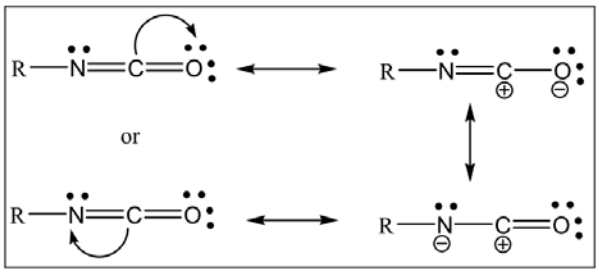

Figure 28. Resonance structures of an isocyanate group [277].

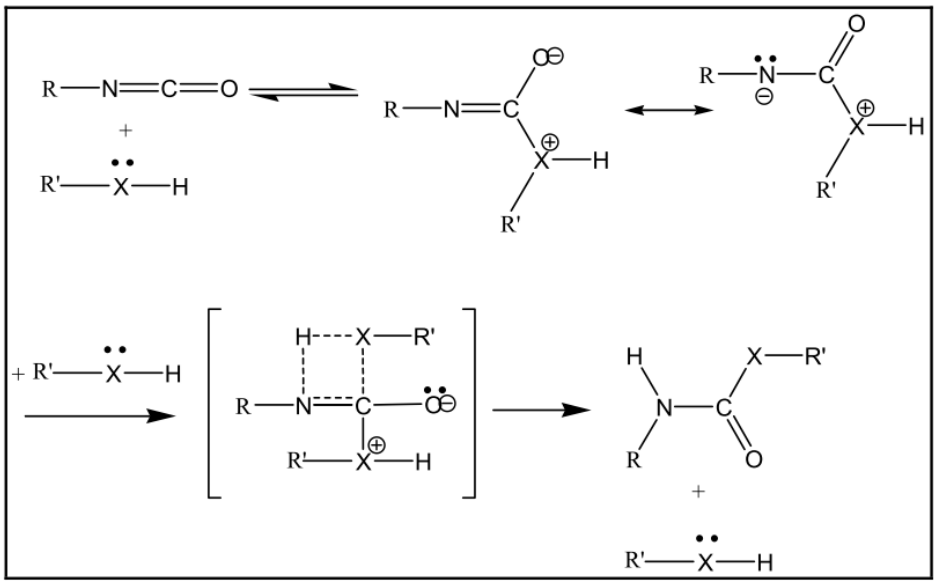

Figure 29. Reaction mechanism of isocyanate reaction in absence of catalyst [278].

The main functional groups for which isocyanates show affinity are included in Table 12, where the relative reactivity is also included.

Table 12. Relative reactivity of isocyanates groups with active hydrogen compounds at 25ºC with no catalyst involved [279].

Active Hydrogen Compound	Structure	Relative Reaction Rate
Primary aliphatic amine	R-NH_2	100000
Secondary aliphatic amine	RR'NH	20000 – 50000
Primary aromatic amine	Ar-NH_2	200 – 300
Primary hydroxyl	RCH_2-OH	100
Water	HOH	100
Carboxylic acid	RCOOH	40
Secondary hydroxyl	RR'CH-OH	30
Ureas	R-NH-CO-NH-R	15
Tertiary hydroxyl	RR'R"C-OH	0.5
Urethane	R-NH-CO-O-R	0.3
Amide	RCO-NH_2	0.1

This diverse reactivity of the different structures is based on both the steric hindrance and electroaffinity. In fact, the own diisocyanate can favour or dampen the reaction according to the same characteristics. It is because of this fact that aromatic diisocyanates show higher reactivity than non-aromatic ones [276,279]. In the market, there is a great number of diisocyanates available; the most significant ones, including their structure and main physical characteristics, are presented in Table 13.

Different species are formed by the combination of diisocyanates with the diverse reactive hydrogen compounds, thus forming characteristic linkages. The main species obtained have been included in Figure 30.

Table 13. Main diisocyanates present in the market.

Diisocyanate	Formula	Structure	Molecular weight (g/mol)	Melting point (ºC)	Density at 20ºC (kg/m^3)
Hexamethylene diisocyanate (HDI)	$C_8H_{12}O_2N_2$	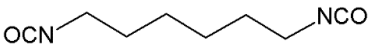	168.2	-67	1047
Tolylene-2,4-diisocyanate (TDI)	$C_9H_6O_2N_2$	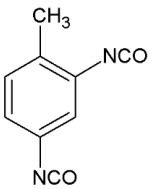	174.2	21.8	1061
4,4'-methylene diphenyl diisocyanate (MDI)	$C_{15}H_{10}O_2N_2$	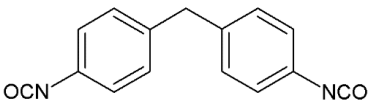	250.3	39.5	1180
Isophorone diisocyanate (IDI)	$C_{12}H_{18}O_2N_2$	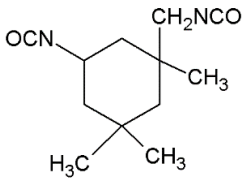	222.3	-60	1061
1,4-phenylene diisocyanate (PDI)	$C_8H_6O_2N_2$	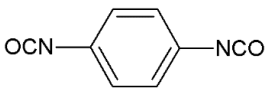	160.1	97.5	-
Poly(hexamethylene diisocyanate) (PhDI)	$(C_8H_{12}O_2N_2)_n$	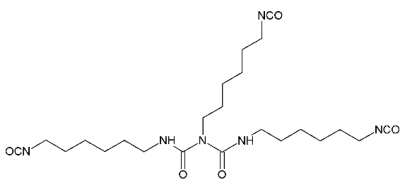	$(168.2)_n$	-	1120

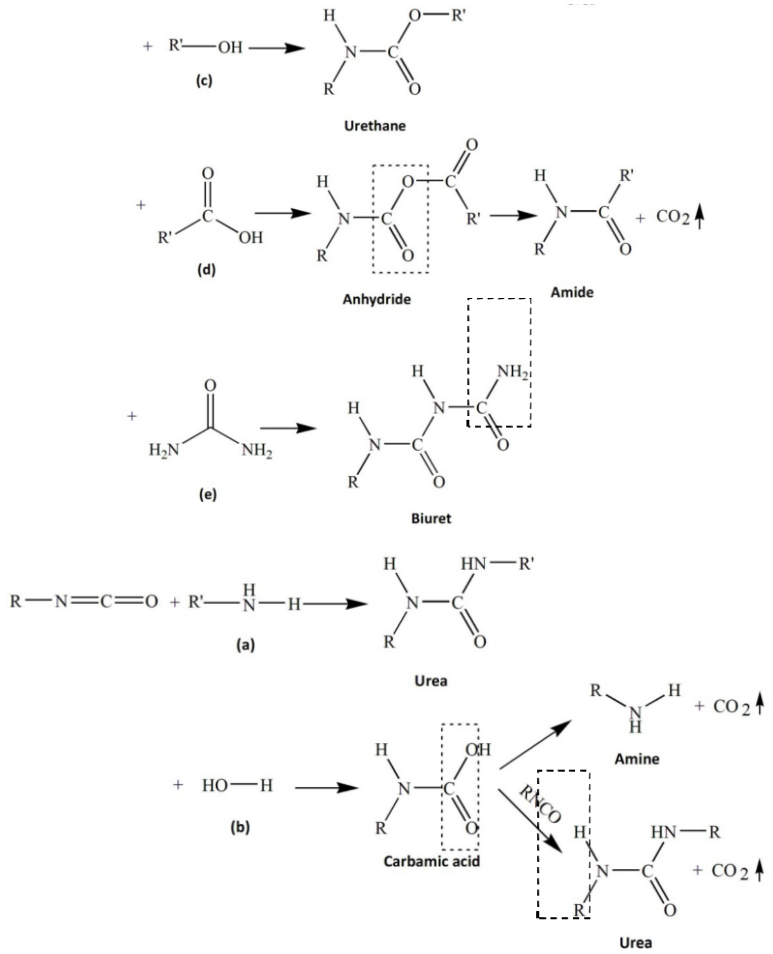

Figure 30. Different linkages generated through diisocyanate reaction with diverse functional groups [277].

Among all these possibilities, the most commercially available and deeply studied kind of polymer obtained from diisocyanate reactions is polyurethane. These polyurethanes were first discovered in 1937 by Otto Bayer and coworkers, and they have been synthesised commercially since 1952 [276]. Since the initial works dealing with the reactions of aliphatic diisocyanates and diamines obtaining polyureas, there has been a huge development in polyurethanes and polyureas, as well as in available diisocyanates, improving and managing their properties (light weight, high strength, heat stability, low cost, fine shape deformability, shape memory, etc.) to suit the wide range of characteristics that make them useful in many applications (see Figure 31) [277]. It is because of those facts that polyurethanes have become one of the most important polymers worldwide, with a prediction of reaching a $56.76 billion market in 2021, whilst top 10 plastic market is predicted to get $586.24 billion, according to the US market research company Markets and Markets (M&M).

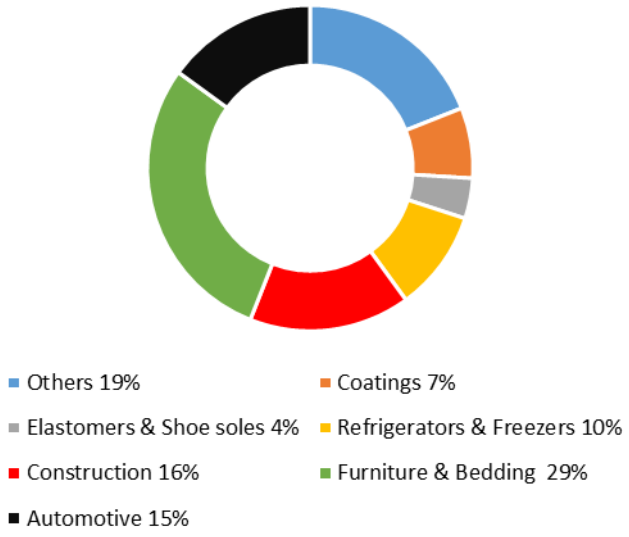

Figure 31. Polyurethanes market [279].

Nonetheless, in the frame of environmental protection, the substitution of the non-renewable chain extenders traditionally used to obtain renewable and/or bio-based competitive polyurethanes is still not totally resolved, and stands as a mandatory issue for reaching a sustainable future. Extensive research has been carried out according to this aim, achieving some outstanding outcomes with a huge variety of precursors, such as castor oil [280], lignin [40,281–283], dimethylolpropionic acid [284], ethylene diamine (EDA), adipic dihydrazide (ADH) and water [285], coumarin [286], CO_2-polyol [287], CO_2 [288], cotton seed plant oil [289], etc. and have also been extensively reviewed as a function of their applications, such as coatings [290,291], bone repair [292], removal of organic dyes from wastewater [293], aerospace, textile industry, sensors, drug delivery systems [294], flame retardant [295], adhesives [296], fibres, foams, elastomers [297], tissue engineering [298], etc.

In the following section, the formation of polyurethanes based on natural resources is discussed in detail.

3.2. Production of polyurethanes from natural vegetable resources

Around 75% of the polyols utilised in the industry for the formation of polyurethanes are obtained by the reaction between a ‘starter’ polyol and an alkylene oxide, forming what is known as polyether polyols. The remaining percentage are polyester polyols, which instead are

developed by following a polycondensation reaction between a polyol and a dicarboxylic acid [299].

During the last decades, wide research has been carried out regarding the replacement of traditional petroleum-based polyol precursors of polyurethanes by natural resources with many different applications. In the first attempts, small molecular weight precursors of those 'starters' such as sorbitol or sucrose in the case of polyether or glycerol and bio-based acids for polyesther formation were studied. More recently, the study has been deviated to the use of higher molecular weight compounds, which could directly act as polyols without the need for any polymeric reaction [299]. Such is the case of lignocellulose biomass, protein-based feedstocks and vegetable oils and their derivatives [296,300]. In this present thesis, those polyurethanes obtained from vegetable oils and lignocellulosic biomass are discussed.

3.2.1. Vegetable oil-based polyurethanes

The main differences that can be found in vegetable oil-based polyols rely on their own nature and the synthesis protocol. In addition, the vegetable oil characteristics may be likewise dependent on vegetable oil origin and environmental conditions. In order to use these vegetable oils or fatty acids derived from them as polyols for polyurethane production, often chemical modifications are necessary, as only castor and lesquerella oils possess hydroxyl groups in their structures. Herein, the carbon double bond and the ester linkage are the usual targets for the alteration of the structure. Different processes have been reported in the literature, epoxidation and oxirane ring-opening, hydroformylation and hydrogenation, ozonolysis, thiolene coupling and transesterification/amidation. Detailed information about those processes can be found elsewhere [300–302].

Albeit, avoiding this modification step, the use of castor oil has been propelled and extensive work has been performed. Castor oil-based polyurethanes generally possess semi-rigid and semi-flexible properties due to the secondary hydroxyl groups, which provide low reactivity. As a consequence, frequently transesterification/amidation or alkoxylation are conducted to increase its reactivity. Stirna et al. [303] submitted castor oil to a transesterification process with triethanolamine and amidation with diethanolamine, obtaining castor oil with different hydroxyl numbers ranging from 291 to 512 mg KOH/g. Both the physical and the mechanical properties were altered by the modification, always showing better properties than the original. Macalino et al. [304] created castor oil-based PUs by

combination with HDI to the formation of biofilms, which exhibited no swelling properties owing to the presence of triglycerides within the PU structure. Both the hardness and the elastic modulus exhibited a proportional relationship with HDI relative content. Castor oil-based films were also performed by Panda et al. [305], this time taking advantage of water-borne dispersions. Once more, the increase in the hard segment content led to an enhancement of the physicochemical properties.

In this sense, many companies have also developed their own bio-based polyester polyols, such as Oleon, Cargill, Huntsam or BASF, all of them based on vegetable oils, which have propelled the bio-based content of polyurethanes up to 60-70 wt%.

Nonetheless, it is worth mentioning that potential conflicts of interestes may emerge from the use of vegetable oils as building blocks since they are also widely used in food industry. Therefore, the use of non-edible oils (such as castor oil) or waste oils (cooking oil) is preferred [306].

3.2.2. Lignocellulose-based polyurethanes

Due to the ubiquitous production, environmentally-friendly character and the interesting properties of either lignocellulosic sources as a whole or separated into their main components, large research has been devoted to the formation of polyurethanes based on lignocellulosic materials [300]. For instance, the addition of wheat straw in polyethylene glycol-based PU foams was shown to provide both better thermal resistance and compressive strength compared to those systems only based on polyethylene glycol. Moreover, the biodegradability was likewise enhanced [307]. Wheat straw was once more used in combination with castor oil to produce suitable PU coatings for controlled-release fertilizer. Apart from the great controlled-release characteristics, the PUs exhibited good degradability and high density [308]. On the other hand, barley straw-derived foams for insulation were also performed, which demonstrated water intakes up to 986% after 48 h, better than those obtained with synthetic PUs [309]. PU foams were also considered by Ertas et al. [310], but obtained from *Eucalyptus camaldulensis* and *Pinus sylvestris* instead. Other biosources considered for the production of rigid foams were cotton stalk, peanut shell, pine bark and apricot stone [311–313]. Nonetheless, the range of available PUs for different applications has been greatly expanded by the use of cellulose, hemicellulose and lignin separately.

3.2.2.1. Cellulose-based polyurethanes

Cellulose-based polyurethanes have been performed by either taking advantage of the biopolymer structure and hydroxyl functional groups or by the cleavage and modification of the structure in order to get intermediate products for PU formation. The last one is the case, for instance, of isosorbide and 2,3-butanediol. Both derived from glucose, Calvo-Correas et al. [315] demonstrated they can act as copolymers in PU synthesis for film formulations, which can compete with non-renewable ones. On the other hand, Wei et al. [316] elaborated a synthetic route to produce adipic acid from cellulose, from which Nylon 66 or PUs can be obtained. Another approach was the transformation of cellulose into what is called cellulose-based ionic liquids. These systems were transformed into PUs from which excellent membranes were performed, able to adequately separate CO_2/CH_4 from natural gas sidestreams [317].

Cellulose has been frequently employed as Pickering emulsifying agent, from which porous monoliths can be formed. However, poor mechanical properties have been generally observed. Nonetheless, by the chemical interaction with diisocyanates, proper robustness can be obtained. Moreover, the system provides suitable and fast absorption capacity and tunable wettability from hydrophilicity/oleophilicity to hydrophobicity/oleophilicity [318]. Cellulose has also been used as grafting copolymer, which has led to interesting shape-memory products for smart applications [319]. Cellulose from industrial furniture waste has also been tested to absorb dye within a PU foam matrix. For the three dyes utilised, methylene blue, Procion yellow and Procion red, the kinetic studies suggested a pseudo-second-order absorption model. The maximum removal values were around 70, 90 and 80 wt%, respectively [320].

Using cellulose fibres, the reinforcement of polyurethane composites has been targeted [321,322]. Hadjad et al. [323] incorporated up to 30% of cellulose fibres and studied the conductivity and capacitance alterations of the composites. Up to 10% concentration, the main electrical characteristics were unaffected. But cellulose can also be used as chain extender due to the high molecular weight usually reported, thus, Ikhwan et al. [324] developed cellulose fibres and polyethylene glycol-based PUs, whose relative concentration demonstrated a strong influence on thermal properties. In order to provide PU composites with even superior performance, nanofibres have been utilised. The use of nanofibres has provided a fast response (less than 1 minute) in shape recovery, which propels the potential use of these

nanocomposites for biomedical applications [325]. The properties improvement by using cellulose nanofibers was also observed for flame retardant applications. Therefore, by assembling with anionic vermiculite, outstanding transparency, resistance to oxygen pass and record fire resistance characteristics have been reported [326]. On the other hand, aerogels with excellent flame retardant properties were also obtained by combination with hydroxyapatite [327].

Polyurethanes were also prepared by using bacterial cellulose. In Urbina et al. [328] study, biocompatible PU nanocomposites were once more reinforced by bacterial cellulose incorporation, displaying outstanding shape memory and mechanical results. Nonetheless, they could not be compared to the use of nanofibers, as 93% recovery took place in around 3 min.

The use of cellulose nanocrystals was also focused on the reinforcement of PU nanocomposites. An enhancement on both Young modulus and stress at break was usually recorded [329,330].

3.2.2.2. Hemicellulose-based polyurethanes

In the same way as happening with its glucose-based homonym, research has been devoted to the production of bio-PUs by following two pathways; using the complete hemicellulose structure and derived constituents or dividing it into smaller units, which can be further used as polyols. Hence, following the last approach, xylitol or furfural have been obtained and applied for PU formation by liquefaction or oxypropilation [331]. Along with xylitol, sorbitol was also produced by Robinson et al. [332]. On the other hand, Samavi and Rakshit [333] utilised hemicellulose liquor to produce epoxidized microbial oil, which could be further used as polyol in PU production. A summary of the main processes which can lead to hemicellulose division into polyols has been explained elsewhere [334].

Taking advantage of the hemicellulose and derivatives structure instead, Cheng et al. [335] reported the use of xylan to produce PUs with enhanced thermal stability. On the other hand, arabinoxylan was used to achieve PU films with application in the packaging field [336], or coatings by crosslinking with glutaraldehyde, which exhibited comparable properties to polyvinyl alcohol, becoming a sustainable substitute [337]. Simultaneously, studies using arabinogalactan have helped polyurethane scaffolds to improve cell attachment yields [338,339]. On the contrary, another hemicellulose-constituent biopolymer, galactomannan, has

been shown to provide PUs with excellent characteristics for drug release in specific body parts [340]. Nonetheless, the most used hemicellulose-derived biopolymer is glucomannan. Improving mechanical performance, the use of glucomannan in composites and nanocomposites has been deeply studied. Its combination with waterborne PUs has also provided excellent mechanical performance and thermal properties due to the strong H-bonding between the PU and glucomannan [341]. A summary of glucomannan-based products with their potential applications and techniques used for characterization is included hereinbelow.

Table 14. Glucomannan-based materials, characterization performed and future application prospects in various fields [341].

Components	Characterization techniques	Potential applications
Chitosan/Konjac glucomannan (KGM)	FTIR,SEM,XRD	Membrane with superior dehydration
KGM/Chitosan	SEM, XPS, FTIR, DSC, WAXD	Food industry, biomaterial matrix, biomedical material
KGM/Ethyl cellulose	SEM, FTIR, XRD,TGA	Films for food packaging
Glucomannan–Chitosan–Nisin	FTIR, DSC	Active packaging material
KGM/Gellan gum	FTIR, DSC, SEM WAXD	Food packaging material
KGM/Poly(acrylic acid)	FTIR, SEM	Specific drug delivery
KGM/Polyacrylamide/Sodium xanthate	FTIR, SEM	Hydrogels for drug delivery
KGM/ poly(methacrylic acid)	FTIR	Specific drug delivery
KGM/Polyvinyl alcohol	FTIR, SEM, XRD, DSX, WAXD	Pervaporation dehydration, food package film
KGM/Xanthan gum	FTIR, GPC	Gels for delivery systems, specific drug delivery
KGM/Alginate/ Chitosan	FTIR, SEM	Controlled release
KGM/Carboxymethyl cellulose	SEM	Emulsion stabilizer
KGM/Curdian	FTIR, XRD, SEM, DSC	Food films and coatings
KGM/Poly(aspartic acid)	FTIR, SEM	Carrier for drug delivery
KGM/Cellulose	FTIR, SEM, XRD	Separation
KGM/Whey protein		Edible food films
KGM/Sodium alginate	FTIR, SEM, DSC, WAXD	Food films
KGM/Gelatin	FTIR, XRD, SEM	Specific drug delivery
KGM/Starch	FTIR, SEM, XRD	Edible food films & coatings

Table 14. Glucomannan-based materials, characterization performed and future application prospects in various fields [341] *(continuation).*

KGM/Poly(diallydimethylammonium chloride)	FTIR, SEM, XRD, DSC, TGA	Antibacterial in biomedicine
KGM/xanthan gum	FTIR	Drug delivery
KGM-graft-Polyacrylamide-co-sodium xanthate	WAXD, SEM, TGA	Flocculant
KGM	FTIR, TEM, DMA, SEM	Coating

Furthermore, in a study elaborated by Shao et al. [342], no division but the whole hemicellulose extracted from corncob was used to perform PU films. These were compared to films originated from cellulose, lignin and diverse mixes between the three biopolymers, obtaining the hemicellulose-based PU films the highest glass transition temperature.

3.2.2.3. Lignin-based polyurethanes

Similar to the previous biopolymers, both the lignin as a whole structure or derivatives and small compounds obtained from it have successfully produced PUs. Thus, the production of ferulic acid and cresol-based monomers from lignin yielded PUs with superior thermal characteristics [343]. In the same way, vanillin-derived systems were also used as polyols for PU formation [344].

Extensive research has been carried out regarding the use of lignin in polyurethane formation due to the availability of hydroxyl groups, which makes of it an interesting biopolyol replacer. Moreover, both aromatic and aliphatic hydroxyl groups have been demonstrated to react with diisocyanates [345], however, some of these groups may be hindered due to steric encumbrance based on the network ordering and self-association [346]. Generally, lignin has been used alone or accompanied by other synthetic or natural polyols, while often it is first modified to enhance overall hydroxyl groups value, aliphatic hydroxyl value or improve access to them [346]. In this sense, demethylation stands as a very useful technique, through which lignin get methyl groups replaced by hydrogen, finally obtaining higher hydroxyl values. Another technique extensively used is hydroxyalkylation, which introduces primary and secondary alcohols to the lignin network by combination with different compounds, as shown in Figure 32. Another significant process that intends to enhance hydroxyl value is phenolation. Since diisocyanates also possess a great affinity to amine groups, lignin amination and nitration have likewise been focused [346–348]. Nonetheless, the high molecular weight

and structure stand for a too-high viscosity and difficulties with reactivity, thus, depolymerisation is often targeted as well.

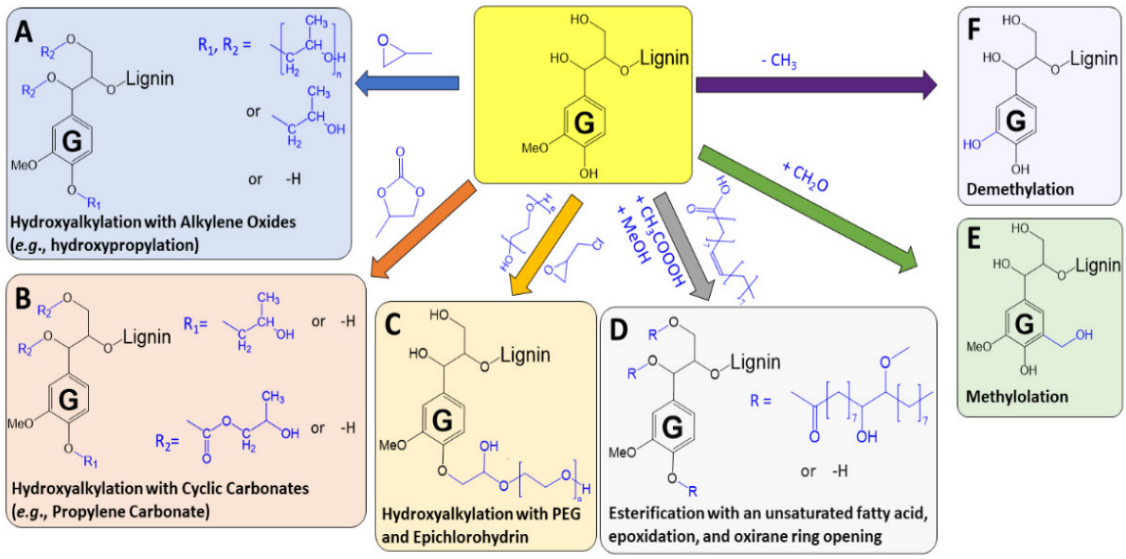

Figure 32. Examples of hydroxyalkylation of lignin with different compounds [346].

In any case, lignin can provide exceptional fire resistance, crosslink density, ultraviolet stability, biodegradability, insulation, compression, antioxidant, thermal and reinforcing properties to PUs [274,343,346,349], as well as high availability and low cost, reason why foams constitute one of the main formulations for lignin-based PUs, where it can act either as a polyol or as a filler. The mechanical performance usually gets improved as a consequence of the more entangled generated systems [349], however, lignin is also known to increase stiffness, and therefore brittleness, due to the aromatic and low flexible structural configuration, which has been usually reported for concentrations larger than 30 wt% [346]. As a consequence, flexible chains like castor oil, butanediol and polypropylene oxide have been proved valuable for improving this characteristic. It is also worth mentioning that different lignin-extraction procedures, origin, biomass source, etc. can likewise lead to lignin with different properties, with extends to derived PUs [345,350,351]. Therefore, new pathways are always being studied, as aldehyde-assisted fractionation, which provides lignin with enhanced solubility, functionality and purity compared to the well-extended Kraft process [352]. Despite the mentioned disadvantages, many authors have proved lignin-based foams to act similarly or even better than those petroleum-based ones [343,346]. But the use of lignin in PUs is not limited to foams. Elastomers, adhesives, coatings and more special products are also frequently

targeted [346]. Regarding coating applications, Griffini et al. [353] utilized non-modified lignin to produce suitable films with enhanced formation ability, adhesion on diverse substrates, tensile properties and hydrophobic behaviour. Nonetheless, other properties like antioxidation, gas impermeability and UV resistance have also been reported for lignin-PU-based coatings [354]. Thus, Zhang and Huang [355] developed PUs with nitrosonitric acid-modified lignin to improve UV and water resistance. On the other hand, Fuqiang and Xiangjiao [356] developed UV-cured lignin PUs with improved hydrophibicity. Peng and Chen [357] elaborated lignin-PU-based hydrogels, stabilized by the biopolymer, which could act as coatings with slow-release fertilizer properties. In general, weathering performance was also improved by the lignin inclusion into the polymeric matrix [346].

Even though to a lesser extent, lignin has also been used to produce composites that can act as tent fabrics [358], potentiometric chemical sensors [359], chromatographic and chemoselective membrane applications [360] and stereolithography 3D printing ink.

3.2.3. Non-isocyanate based PUs

It is also worth mentioning an alternative green option that consists of the formation of vegetable-oil or fatty acid-based isocyanates [300,361], eliminating some of the risks of using harmful isocyanates. However, reactivity is seriously reduced, since many diisocyanates, as seen in previous sections, are aromatic-based, which reactivity is significantly higher. Two synthesis routes have been reported, which are included in Figure 33.

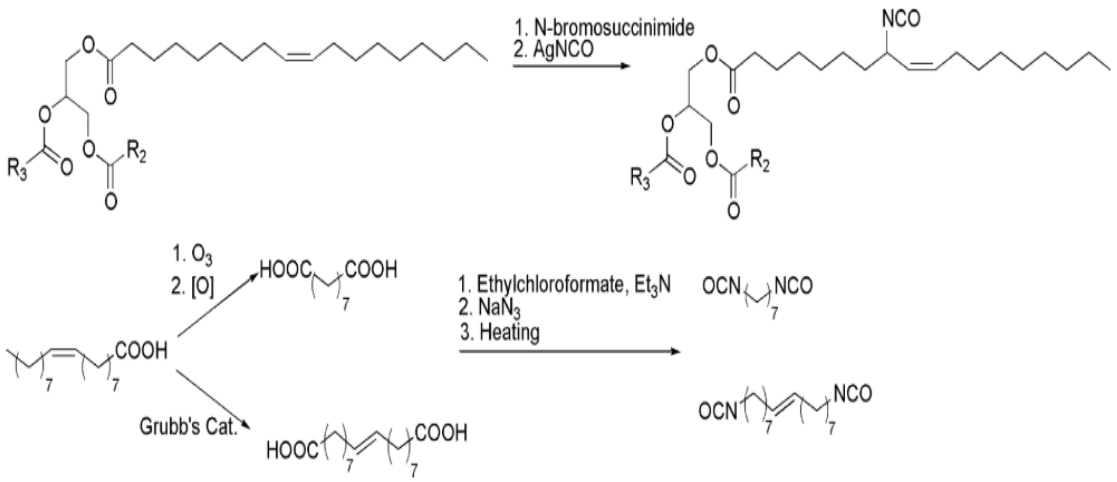

Figure 33. Synthetic routes for the production of vegetable-oil based isocyanates [299].

Nonetheless, the state-of-the-art technology has recently been focused on the formation of polyurethanes without isocyanate presence, what is known as polyhydroxyurethanes (PHUs), performed by polyaddition of polyamines to polycyclic carbonates (see Figure 34). In this sense, both the crosslinking agent and the polyol can be biobased materials [299,361]. With this new approach, the risk of producing and employing isocyanates is eliminated, and a newer and greener strategy is hereby presented. Due to the enhanced water absorption, porosity, chemical and thermal resistance compared to PUs, a wide range of applications have been addressed. Kalinina et al. [363] performed PHUs based on N-phenylmaleimide and 3-(2-vinyloxyethoxy)-1,2-propylene carbonate, which demonstrated outstanding properties acting as coatings with high chemical and impact resistance, low humidity absorbance and good adhesion to metal surfaces. On the other hand, Figovsky et al. [364] created very stable UV coatings with excellent adhesion properties by the combination of acrylic and siloxane cyclo-carbonates and dendro-polyfunctional siloxane primary amine oligomers. Other studies have shown PHUs to have applications in fields like sealants, construction, composites, biochemical and electrical equipment [299,362].

When vegetable oils are used, then PHUs can gain sustainability-related properties. One of the most interesting vegetable oils targeted is soybean oil, which can form carbonated soybean oil, then PHUs are obtained by the combination with several amines, giving outstanding elastomeric properties [299,362]. Carbonated linseed oil was also studied, which once more combined with amines generated PHUs with exceptional both stiffness and stability [362,365]. An even greener approach was obtained when carbonated linseed oil was utilised with a polyamine derived from nut shells [366]. Castor oil derived materials were also utilised to produce non-isocyanate polyurethanes and polyureas by AB-type self-condensation [367]. In a study conducted by Levina et al. [368], sunflower oil was used instead. A narrower distribution of fatty acids was obtained compared to soybean oil, whereas reactivity was similar. Another interesting compound that has been extensively studied as carbonated bio-based system is glycerol, from which various PHUs have been developed [299]. One of the last recent trends has been the use of nanotechnology to enhance the mechanical properties of the PHUs, therefore, the inclusion of SiO_2 nanoparticles has provided the systems with improved transparency, stiffness and rigidity. Furthermore, the particles could act as crosslinking points for enhanced both adhesion and reduction of water uptake [362].

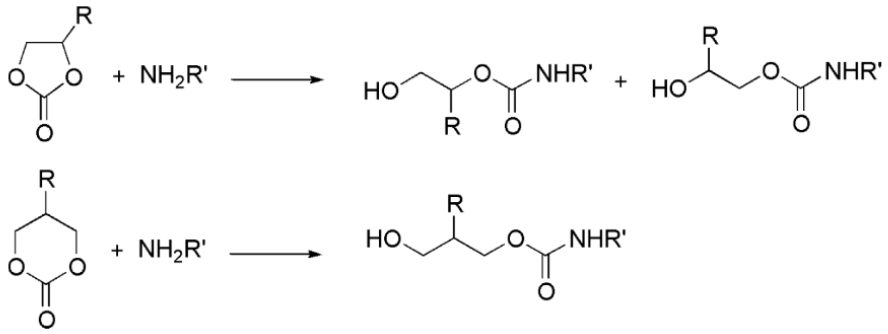

Figure 34. Aminolysis reaction of five- and six-membered cyclic carbonates [299].

In the next sections, the production of novelty bio-based adhesives, lubricants and elastomers from the main lignocellulosic sources and vegetable oils are deeply discussed, as they comprise the potential applications of the PU systems developed in this thesis.

A summarising table regarding the main advantages and disadvantages of the renewable sources used for PU formation is included hereunder:

Table 15. Advantages and disadvantages of the principal renewable sources used for PU production.

Renewable source	Advantages	Disadvantages
Vegetable oil	Great availability, easy to manipulate	Modification frequently needed, low reactivity, conflicts with food industry, low oxidation stability,
Cellulose	Great availability, presence of reactive groups, high molecular weight	Conflicts with paper industry, difficult to isolate, high operational costs, higroscopicity
Hemicellulose	Great availability, presence of reactive groups, high versatility, low cost, easy to isolate	Low homogeneity, low thermal resistance, hygroscopicity
Lignin	Great availability, residual character, presence of reactive groups, high molecular weight, low cost	Low homogeneity, bad solubilisation

3.3. Bio-based polyurethane adhesives

Since PUs arrival, great effort has been made to the production of high-performance PU-based adhesives. As can be observed within the landscape of adhesives established by Burchardt [369] (see Figure 35), PUs play a very significant role throughout the whole mechanical/adhesion response spectra.

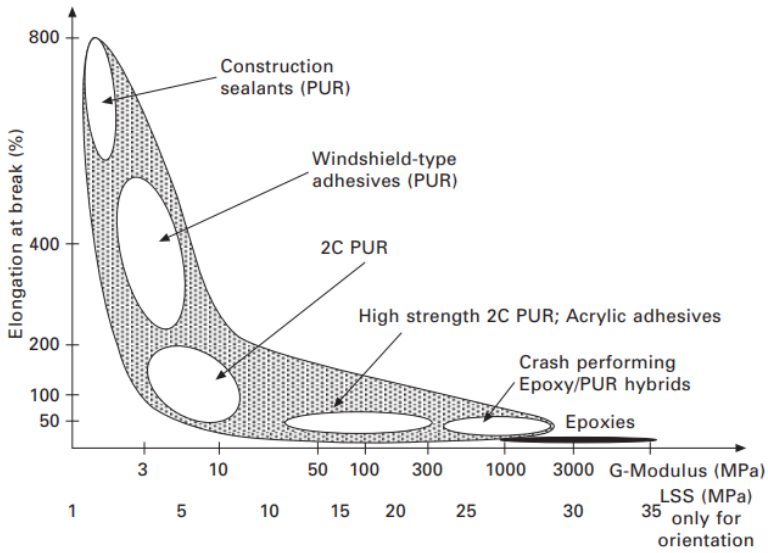

Figure 35. Landscape of polyurethane (PUR), epoxy and acrylic adhesives [369].

Nonetheless, recent advances in political and environmental restrictions are endangering the use of commercial PU adhesives since they are usually formed by the combination of non-renewable polyols and harmful diisocyanates. As already mentioned above, it is in the polyol substitution where biomass can play a significant role, however, other techniques aiming to reach 100% bio-based adhesives are also to be discussed in this section.

3.3.1. Vegetable oil-based polyurethane adhesives

According to the previous explanation, vegetable oils are a vast feedstock of biomaterials, with very different characteristics depending on oil nature, growth and variety [296]. As hydrophobic systems and due to the fatty acid chains, they can provide the adhesive with water resistance and thermal resilience [296]. Unlike castor and lesquerella oils, which possess hydroxyl groups in their structure, the remaining oils must undergo some processing if polyols are to be obtained, as previously mentioned. A detailed discussion about the different procedures is reported elsewhere [296]. For instance, palm oil has been extensively studied

during the last two decades, thus some authors have tested wood adhesion in solventless conditions after previous epoxidation [370], pressure-sensitive adhesives [371,372] or adhesives for automotive applications [373]. Other vegetable oils like Jatropha oil, have been previously modified and utilized to produce PU adhesives [374]. These adhesives were tested in hostile environments such as hot water, alkali and acid. On the other hand, tung oil was approached by Man et al. [375], who evaluated the adhesion of derived PUs in surfaces such as glass, silica gel, wood and metal, onto which exhibited strong adhesion, mainly attributed to hydrogen bonding. Another different application for soybean oil-based adhesives was evaluated by Orgilés-Calpena et al. [376], who focused on footwear adhesion. Two different diisocyanates were tested, MDI and HDI, demonstrating that both can fulfill the adhesives requirements up to 22 and 7 wt% oil content, respectively.

On the contrary, castor oil has been directly used in bioadhesive formulations. Tenorio-Alfonso et al. [377–379], Raghunanan et al. [380], Santan et al. [381], Oliveira et al. [382] or Ferreira et al. [383] are just a few examples of the use of castor oil in PU-based bio-adhesives. Alone or by combination with other polyols, castor oil-based adhesives were tested as pressure sensitive adhesives (PSA), long-term adhesives for wood, metal and metal/textile surfaces, or even surgical applications [384]. By the modification of humidity during the curing process, Raghunanan et al. [380] were able to reach more than 5 MPa stress at break for wood-wood surfaces, comparable to that achieved by Poh et al. [370] working with modified palm oil. Tenorio-Alfonso et al. [377–379] also reported outstanding results of castor oil- and cellulose acetate-based PUs with better adhesion performance than commercial adhesives except for polyethylene surfaces, where the bioadhesives shown poorer characteristics. In order to seek better performance, Oliveira et al. [382] introduced low-valuable fillers as cement or recycled rubber particles. Whereas the inclusion of only 3% cement significantly enhanced mechanical properties, it was rubber particles that raised single lap shear strength. Both mechanical and adhesive improvements were otherwise obtained when chitosan was included in a castor oil-based PU adhesive matrix [385]. On the other hand, Faria et al. [386] reached the conclusion that castor oil-based PU adhesives could successfully replace non-renewable-based adhesives in laminated veneer lumber. Deeper insight on castor oil-based adhesives was carried out by Gama et al. [387], who focused on different castor oil/diisocyanate ratios, and evaluated their mechanical response. The results let conclude that a 2.50 NCO/OH ratio turned out in optimum adhesion, being faster than the commercial adhesive used as benchmark.

Even though lesquerella oil also possesses hydroxyl groups in its structure, its use as polyol replacer has been not considered as deeply as castor oil. The reason behind this fact relies on the actual content of hydroxyl groups, as only around 57% of lesquerella oil is based on actual hydroxylated fatty acids [388], thus the overall hydroxyl group content may be much lower than castor oil, which fatty acid composition stands between 85-95 wt% ricinoleic acid [389]. Therefore, just a few studies regarding lesquerella oil-based PU with adhesive properties have been reported [390,391].

3.3.2. Lignocellulose-based polyurethane adhesives

Once more, the crosslinking ability of lignocellulose biopolymers, low cost and renewable character have been leveraged in order to produce bio-based PU adhesives. Therefore, liquefied products have demonstrated a great ability to develop a wide range of products [392]. Thus, the liquefaction of two plant species, China fir (*Cunninghamia lanceolata*) and Taiwan acacia (*Acacia confusa*) was carried out to subsequently produce PU adhesives by combining up to three types of poliisocyanates, i.e., Desmodur L (based on toluene diisocyanate and trimethylol propane), Desmodur N (based on hexamethylene diisocyanate) and poly-4,4'-diphenylmethane diisocyanate. The study allowed to conclude that liquefied Taiwan acacia and Desmodur L exhibit the best adhesion performance [393]. Different sources, such as the Japanese cherry blossom or Sakura (*Prunus cerasus*) [394], kenaf (*Hibiscus cannabinus* L.) [395] or Sugi (*Criptmeria Japonica*) [396] were likewise tested after liquefaction to produce polyurethane adhesives with poly-4,4′-diphenylmethane diisocyanate. Nonetheless, the fractionation of lignocellulose into its main components is much preferred for PU adhesive production, and is discussed in the next sections.

3.3.2.1. Cellulose-based polyurethane adhesives

Cellulose and its derivatives have also been employed to produce bioadhesives. Thus, cellulose acetate in combination with CO was used by Tenorio-Alfonso et al. in several studies [377–379], from which a wide range of concentrations, NCO:OH ratios and diverse diisocyanates were tested, always exhibiting excellent properties, comparable to commercial adhesives. Similar to lignocellulose, liquefaction was also used to formulate adhesives from cellulose pulp, thus, sugar beet derived-pulp adhesives with up to 87% biosource exhibited good adhesion ability, improved by increasing diisocyanate/biosource ratio. The stability of sugar beet pulp-adhesives was better than other biomass also tested [397].

3.3.2.2. Hemicellulose-based polyurethane adhesives

As previously mentioned, hemicellulose is formed by a combination of different monomers, such as xylose, arabinose, etc. Balcioglu et al. [398] utilised xylose for PU-adhesive formulations, obtaining adequate biocompatible adhesives with strength up to 415 kPa, at 15% xylose concentration. A patent has been registered where xylan inclusion in adhesives reported strengthening of the bonding [399]. Although any hemicellulose-derived polyol can actually be used as a precursor for PU-based adhesives, no such studies have been performed to our knowledge.

3.3.2.3. Lignin-based polyurethane adhesives

Lignin has also been widely studied over the last few decades for PU adhesion, as demonstrated by the vast number of publications and patents centred on this topic [346,347,360,400]. The use of lignin let overcome typical PU-adhesives drawbacks, as delamination resistance, cohesive failure, and gap-filling properties. Moreover, it generally enhances the thermal behaviour of the adhesive [346].

To mention some of the greatest advances reported, lignin in combination with vanillin-derived diisocyanates were able to withstand more than 9 MPa break at failure onto glass surface, while the results for other surfaces (wood, aluminium and steel) were much lower (around 1 MPa). Moreover, the use of diverse lignin sources demonstrated adhesive properties to be tailored [401]. Griffini et al. [353] also exhibited outstanding adhesive properties of lignin-based PUs, however, the maximum strength was found in wood specimens (more than 9 MPa), while in glass exhibited very good results still (7.6 MPa), as well as in aluminum and steel showing around 1 MPa. As hydroxyl groups are the main bonding point to form proper urethane bonds with diisocyanates, other studies have been focused on primarily increasing the hydroxyl group index of lignin by hydroxypropylation or demethylation in order to create a stronger adhesive network [360,402,403]. In this sense, improved tensile strength of more than 200% reference values was obtained by hydroxypropylation [402]. On the other hand, biological modifications with laccase were leveraged by Ibrahim et al. [404], who tested both uninoculated and inoculated lignin with other natural sources such as chitosan and soy protein as well as with polyethyleneimine to produce suitable adhesives. These exhibited close values to petroleum-based ones, and withstood hard thermal treatments with no significant performance loss. Regarding systematic studies aiming to elucidate main parameters for

adhesion evaluation, Lima-García et al. [405] tested different kinds of lignins, Kraft and organosolv, resulting in particle size, lignin source and dispersion processing being key parameters for lignin adequate incorporation into the adhesive, which exhibited more than 50% better mechanical properties than non-lignin-based ones. In another study, it was demonstrated that both isocyanate and lignin source together with solvent were critical for adhesive strength performance [400]. Looking for synergistic effects, the combination of epoxy-modified lignin with PU emulsion also demonstrated to significantly enhance the adhesive properties of lignin-based adhesives [406].

3.4. Bio-based polyurethane lubricating greases

As already mentioned in previous sections, the future prospects of lubricating grease industry rely on the finding of suitable thickening agents and base oils that can replace the metal-based soaps and mineral oils usually utilized for those purposes, respectively (see Table 16).

Table 16. Most-used base oils and thickeners for lubricating greases.

Base oils	Thickeners
Mineral oil	Sodium soap
Synthetic oil	Calcium soap
Diester	Lithium soap
Silicone liquid	Aluminium soap
Phosphate ester	Lithium complex
Fluorinated silicone	Calcium complex
Chlorinated silicone	Aluminum complex
Polyglycol	Bentonite
Castor oil	Silicon oxide
	Carbon/graphite
	Polyurea
	Polyethylene
	Indanthrene dye
	Phthalocyanine dye

In history, the use of natural materials as lubricating greases was widely carried out since the first mentions of the topic, dated back to Ancient Egypt. Nonetheless, the finding of metal-based soaps and mineral and synthetic oils crucially changed the course of the lubricating grease production (see Table 17) [407].

In this sense, once more, natural resources can play a decisive role, providing suitable replacers for both main lubricating grease components, aiming to fulfill current industrial demands and enhanced biodegradation properties of lubricants based on non-renewable resources. Via polyurethane formation, structural networks able to withstand and thicken oils can be obtained, making them suitable for lubricating purposes. Some of the most used natural sources for PUs formation will be discussed in the following sections regarding their application as lubricating greases.

Table 17. Lubricating greases evolution through history [407,408].

Date	Event
About 1400 BC	The use of animal fat and limestone for lubrication of axes of Hittite chariots was started. In the same period, lubricants based on olive oil and limestone were used in Ancient Egypt
1845	A lubricant consisting of mineral oil, animal fat, and limestone was invented in the United States
1853	The first sodium lubricant based on beef fat appeared in the United Kingdom
1912	The production of calcium lubricants with the dispersion medium based on mineral oil was started in Japan
1938	Lithium lubricants were developed. They quickly conquered the world and were used as multipurpose lubricants
1954	Invention of complex aluminum lubricants for operation at high temperatures
1955	Invention of urea greases in the United States
1960-Present	Resurgence of vegetable oil-based lubricating greases

3.4.1. Lignocellulose-based polyurethane lubricating greases

No studies have been devoted to the use of the whole lignocellulose structure as PU polyol source for lubricant applications, but some of the main constituents, i.e. cellulose and lignin, have been reported to be used as polyurethane-type thickening agents.

3.4.1.1. Cellulose-based polyurethane lubricating greases

Several studies have taken advantage of the polyol structure of cellulose and its derivatives for the production of lubricating greases. Thus, PU formulations proposed as bio-based lubricating greases were obtained by functionalization of methylcellulose with HDI and further mixing with castor oil. The different concentrations and methylcellulose/HDI ratios led to tunable characteristics, covering a wide range of lubricating grease consistencies [95,97]. Other studies have tested α-cellulose, 2-hydroxyethyl cellulose, methyl 2-hydroxyethyl cellulose and cellulose acetate propionate as precursors for PU-based lubricating grease formulations. The results let conclude that the balance and size of the polar and non-polar groups turned out crucial in order to predict the rheological behaviour of the bio-based PUs [98]. Nonetheless, less purified cellulose-based systems as industrial cellulose pulps were also evaluated as oil thickening agent, providing a more economical and industrial approach. Therefore, both *Eucalyptus globulus* and *Pinus radiata* cellulose pulps were assessed, the first one with two different purity grades, obtained by semi-mechanical cooking and commercial Kraft process. All of them exhibited gel-like rheological characteristics with well-developed plateau regions within the frequency range studied, and microstructures very similar to that found in commercial lithium lubricating greases [96]. On the other hand, tribological properties of many of these systems were also evaluated, as well as mechanical stability, showing most of them suitable values for being considered potential replacers of traditional petroleum-based lubricating greases [96,409].

3.4.1.2. Lignin-based polyurethane lubricating greases

Lignin, as shown in previous sections, can easily act as lubricant additive in composites and other materials, in both liquid and solid lubricants. Nonetheless, in this section, those few studies related to the production of lignin-based PUs with lubricating properties are overviewed. Thus, Ma et al. [410] developed lignin-based PUs, with lignin acting as an emulsifier for [BMIm]PF6 ionic liquid lubricant. The tribological results demonstrated very low friction coefficient and wear scars, as well as excellent thermal stability. Lignin-based lubricating greases formed with a polyurea-polyurethane thickener were patented lately [411]. Moreover, other patented lubricants also include lignin and polyurethane resins as components in their formulations [412].

3.5. Bio-based polyurethane elastomers

The substitution or at least minimization of the use of petroleum-based sources by the inclusion of biobased plant-derived components in PU elastomers is considered in this section. Different types of natural vegetable sources have been reviewed and discussed hereunder.

3.5.1. Vegetable oil-based polyurethane elastomers

Most common vegetable oils, as mentioned in previous sections, need previous modifications if polyurethane elastomers want to be obtained, due to the inherent lack of hydroxyl or other reactive functional groups within their structure. Thus, elastomers with epoxidized soybean oil have been recently studied [413,414]. The influence of molecular weight of soybean oil-derived polyols in related elastomers has also been studied, showing the best thermal and mechanical properties those performed with the lowest molecular mass [415]. Zheng et al. [416] also studied soy oil-based PU elastomers which, depending on concentration, showed from 7.5 to 31 MPa tensile strength, while at the same time the elongation was reduced from 228 to 20%. Not only concentration but isocyanate type allowed to modulate the rubbery properties of soy oil-based PUs. Therefore, aromatic triisocyanates provided the stiffest properties, while aliphatic triisocyanates and diisocyanates imparted the highest elongations. Aromatic and cycloaliphatic diisocyanates instead, exhibited intermediate properties [417]. On the other hand, palm oil was also used for PU elastomer formation. By modification through metathesis, and depending on the hydroxyl index obtained, elastomers behaved as soft or hard materials (tensile strength from 4.2 to 18 MPa) [418]. Esterification of the palm oil triglycerides was also performed to elaborate soft polyurethane elastomers, with pressure-sensitive adhesion characteristics [372]. In another study, Somarathna et al. [419] developed palm oil monoester polyols which, in combination with PEG and MDI, produced PU elastomers with very different mechanical properties, depending on PEG concentration. Other less common oils that have also been tested for developing elastomeric formulations but still worth to be mentioned are rapeseed [420–422], oleic [423], tall [424,425], linseed, tung and corn [426] oils.

On the other hand, as previously mentioned, certain oils do not need modification, as their own structure includes hydroxyl groups, such as lesquerella and castor oil. The last one has been much more targeted in research, as castor oil-based PU elastomer first studies on the

topic date from more than 50 years ago, where diverse diisocyanates were tested as crosslinker for castor oil [427]. Nonetheless, the dangling fatty acid chains do not generally provide high strains. For instance, Zhang et al. [428], by combining castor oil with IPDI, developed elastomers able to reach 120% strain tensile deformation at break. Also, Abdolhosseini and Givi [429], using IPDI as crosslinker, reported up to 430% elongation at break and tensile strength of 32 MPa. However, by using HDI instead, less than 32% was generally reported [430–432]. Nonetheless, even though the mechanical properties were not ideal, the bio-based character of the castor oil has propelled related elastomers to their use in medical applications such as cardiac, wound healing, bone tissue engineering and bioadhesive, where extensive work has been done [433]. Formulations of castor oil-based elastomers have in fact been patented for around 16 years [413].

The mechanical properties of castor oil-based elastomers are usually improved by the addition of alternative polyols; such is the case, for instance, of Oprea [434], who prepared elastomers by mixing castor oil with poly (1,4-butanediol). Thus, thermal and mechanical properties were tuned, and elongations at break of more than 600% were achieved. On the other hand, An et al. [435] incorporated isosorbide into the castor oil-PU matrix, which likewise improved mechanical properties. The modification of the isosorbide/castor oil ratio allowed to change from brittle samples with high Young modulus and relatively low elongations at break to high elongations but lower stiffness. The mixture of castor oil with polyethylene glycol also led to improved properties in the derived elastomers, as observed by Gao et al. [436], who reported elongations at break superior to 300%, and tensile strengths at break of 5-12MPa. Nonetheless, polyethylene glycol was also used by other authors, from which elastomers with up to 1180% strain at break and tensile strengths up to 27.5 MPa were obtained [437,438]. In other studies, polycaprolactone has also been used as copolyol [439].

3.5.2. Lignocellulose-based polyurethane elastomers

Lignocellulose-based PU elastomers have been widely studied due to the low cost, high availability, biodegradability and excellent performance. Once more, the properties of the related elastomers have shown great dependency on origin, composition, growth conditions, etc. Nonetheless, the lack of industrial advance on the topic relies on incompatibilities related to differences in hydrophilicity, compromising suitable dispersion [426].

Several are the lignocellulosic sources that have been analysed in literature for this purpose. For instance, sawdust has been tested for PU elastomeric formulations. Thus, acoustic panels with soundproof properties have been obtained from the combination of some multicomponents, being sawdust and PU elastomer binder two of them [440]. A close material, wood flour, was also used for composite formation with elastomeric properties, which were prepared in filaments by 3D-printing technology. The tensile strength exhibited a minimum when wood flour concentration varied between 0-40%, while elongation at break was seriously compromised by increasing concentration [441]. In another study, Mengeloğlu et Çavuş [442] tested different lignocellulose sources as fillers, such as teak wood flour and rice husk, which were previously milled and screened before used. The results showed that a 15% filler concentration potentially increased mechanical properties, while a 30% concentration caused a dramatic drop in the already mentioned properties. In general terms, the performance of teak based-systems was slightly better than that of rice husk. By using rice straw, the liquefied products from it have also led to the formation of polyurethane elastomers [443]. Following this tendency, straw liquefied products were also used by Zhao et al. [444] to perform PU elastomers where special attention in the obtaining procedure and its relation to mechanical performance was paid. In the following sections, the use of cellulose, hemicellulose and lignin in PU elastomeric formulations is discussed in more detail.

3.5.2.1. Cellulose-based polyurethane elastomers

Cellulose and cellulose-derived materials have been known to act as proper fillers and endow materials with though properties, due to the fibrous structure and hydrogen bonding possibilities. Regarding PU elastomers, the same can be applied, nonetheless, the use of micro and nanocellulose has been more lately targeted. For instance, microfibrillated cellulose has been leveraged as casting material for PU formation, then acting as tough elastomers for composite reinforcing [445]. The addition of up to 5% of microcrystalline cellulose to a PU based on MDI, butanediol and polytetramethylene glycol turned out in a better performance of more than 650% tensile strength compared to the reference system [446]. Pei et al. [447] demonstrated that incorporating cellulose nanocrystals to a MDI-poly(tetramethylene glycol)-based PU only at 1% weight concentration, stress at break could be 8-fold increased. In another work, the use of cellulose nanowhiskers prepared from microcrystalline cellulose allowed the formulation of shape-memory PU elastomers, triggered by water [448]. The addition of cellulose nanocrystals also demonstrated to improve the rheological properties of PU

elastomers, with an increase of several orders of magnitude of the still unreacted suspensions, due to strong interactions between the nanocrystals and the polyol [449]. In another study, Saralegi et al. [450] developed from elastomeric to rigid bio-based PUs by increasing cellulose nanocrystal concentration. Interestingly, Lee et al. [451] incorporated cellulose nanofibres to a PU-urea matrix, and reported a decrease in the elastic modulus by increasing cellulose concentration up to 1% and a further increase at 2%. Nonetheless, the mechanical properties were anyway enhanced. In castor oil/PEG-based PUs, the inclusion of cellulose nanocrystals obtained from *Eucalyptus globulus* was likewise positive for mechanical properties enhancement, reporting shifts from 5 to 12 MPa and from 1 to 5 MPa of tensile strength and Young modulus respectively, in comparison with the cellulose-free system [436].

3.5.2.2. Hemicellulose-based polyurethane elastomers

Only a few studies proposed either hemicellulose derivatives or the monomers that comprise its structure as suitable polyols for the preparation of PU elastomers. Glucommanan was used in different concentrations to tune castor oil-based PUs properties from elastomeric to very rigid systems within the range of 5-90 wt% concentration [452,453]. In a related work, films with elastomeric properties by modifying glucommanan molecular weight were elaborated [454]. It is also well known that very interesting furan derivatives can be obtained from hemicellulose, like furfural. Such compounds have also been used as sources for polyurethane formation, some of them serving as elastomers [166].

3.5.2.3. Lignin-based polyurethane elastomers

Lignin and lignin derivatives have also been occasionally used as polyols and fillers for elastomers production [455]. One of the most important derived-chemical that can be obtained from lignin is vanillin. Apart from the already mentioned uses in previous sections, PU elastomers have likewise been generated. Vanillin inclusion propelled mechanical properties, making Young modulus and strain at break to increase up to around 130 and 150% respectively [456]. Another lignin derivative that has been used as copolymer in PU elastomers is lignin-derived polycarboxylic acid. With a content of only 2.5%, the Young modulus and tensile stress at different strains (100 and 300%) were augmented 384, 135 and 90% respectively [457].

In the development of lignin-based PU elastomers, frequently lignin acted as polyol, becoming a structural part of the formulation, while sometimes it is only cast or mixed acting as filler. As examples of the first case, improved thermal and mechanical properties were reported by the use of unmodified lignin as polyol along with poly (propylene glycol) and TDI as crosslinker, yielding PUs with outstanding tensile performance (176 MPa, 33 MPa and 1394% of Young modulus, tensile strength and elongation at break respectively) by the addition of up to 40% lignin. In addition, the better performance of low-molecular-weight lignin fractions was reported [458]. The use of acetylated lignin and polyethylene glycol (PEG) as copolymers let elongations at break higher than 2000% be obtained [67]. Likewise, PEG with oxidised lignin was used by Zhang et al. [459], resulting once more in great tensile performance. On the other hand, Liu et al. [460] took advantage of enzymatic procedures to alter lignin structure, which decreased molecular weight, thus imparting stronger mechanical properties to the network, i.e. up to 60 MPa tensile strength. Using lignin as filler, Ciobanu et al. [461] performed PU elastomers based on poly(ethyleneadipate), ethylene glycol, and MDI where lignin was cast using DMF as solvent at concentrations from 4 to 23%. The results indicated, once more, improved performance on mechanical properties with only a 10% lignin concentration, where the tensile strength and elongation at break were augmented up to 370 and 160% respectively. Acting as filler, lignin is usually responsible for enhancing mechanical properties, such as Young modulus or compressive performance [247,346,462]. In general, the higher the lignin concentration, the higher both the storage and Young moduli up to a certain concentration depending on the formulation, since lignin acts as a rigid component [346]. In this sense, storage modulus has been raised 6-fold by the addition of up to 60% lignin to polypropylene glycol-based PUs [39]. In another study, Ortíz-Serna et al. [351] evaluated both the thermal and mechanical properties of Kraft and organosolv lignin also acting as fillers for PU elastomers based on castor oil and butanediol, exhibiting great differences between these products. Culebras et al. [463] tested Alcell organosolv and hydroxypropyl-modified Kraft hardwood lignin for the same purpose, being the first one able to achieve excellent mechanical properties, with Young modulus of 80 GPa, comparable to commercial elastomers. Other authors tested other different lignins, such as wheat straw soda-derived, Indulin AT softwood kraft, Protobind 1000 soda, corn stover or sulfite hardwood lignins [346,464]. Frigerio et al. [465] found particle size, polar surface and agglomeration tendency to be key points in lignin performance as fillers. Non-modified lignin was demonstrated to carry out the functions of both crosslinker and reinforcing agent in silicone-based PUs, matching some of the properties

of commercially-available silicone PUs [466]. Some of these elastomers can act as sealants, materials in surfboards, car interiors, household items and sportive indoor courts [467].

4. References

[1] Masson-Delmotte, V., P. Zhai, H.-O. Pörtner, D. Roberts, J. Skea, P.R. Shukla, A. Pirani, W. Moufouma-Okia, C. Péan, R. Pidcock, S. Connors, J.B.R. Matthews, Y. Chen, X. Zhou, M.I. Gomis, E. Lonnoy, T. Maycock, M. Tignor, T. Waterfield, Summary for Policymakers. In: Global Warming of 1.5°C. An IPCC Special Report on the impacts of global warming of 1.5°C above pre-industrial levels and related global greenhouse gas emission pathways, in the context of strengthening the global response to the threat of climate change, sustainable development, and efforts to eradicate poverty, 2018.

[2] C.L. Cheng, Y.C. Lo, K.S. Lee, D.J. Lee, C.Y. Lin, J.S. Chang, Biohydrogen production from lignocellulosic feedstock, Bioresour. Technol. 102 (2011) 8514–8523. https://doi.org/10.1016/j.biortech.2011.04.059.

[3] M.E. Himmel, S.Y. Ding, D.K. Johnson, W.S. Adney, M.R. Nimlos, J.W. Brady, T.D. Foust, Biomass recalcitrance: Engineering plants and enzymes for biofuels production, Science 315 (2007) 804–807. https://doi.org/10.1126/science.1137016.

[4] N. Mosier, C. Wyman, B. Dale, R. Elander, Y.Y. Lee, M. Holtzapple, M. Ladisch, Features of promising technologies for pretreatment of lignocellulosic biomass., Bioresour. Technol. 96 (2005) 673–686. https://doi.org/10.1016/j.biortech.2004.06.025.

[5] M. Bussemaker, N. Trokanas, L. Koo, F. Cecelja, Ontology Modelling for Lignocellulosic Biomass: Composition and Conversion, in: Comput. Aided Chem. Eng. 43 (2018) 1565–1570 . https://doi.org/10.1016/B978-0-444-64235-6.50273-4.

[6] G.W. Huber, S. Iborra, A. Corma, Synthesis of Transportation Fuels from Biomass: Chemistry, Catalysts, and Engineering, Chem. Rev. 106 (2006) 4044–4098. https://doi.org/10.1021/cr068360d.

[7] A.T.W.M. Hendriks, G. Zeeman, Pretreatments to enhance the digestibility of lignocellulosic biomass, Bioresour. Technol. 100 (2009) 10–18. https://doi.org/10.1016/j.biortech.2008.05.027.

[8] C. Li, X. Zhao, A. Wang, G.W. Huber, T. Zhang, Catalytic Transformation of Lignin for the Production of Chemicals and Fuels, Chem. Rev. 115 (2015) 11559–11624. https://doi.org/10.1021/acs.chemrev.5b00155.

[9] J.B. Binder, R.T. Raines, Simple chemical transformation of lignocellulosic biomass into furans for fuels and chemicals, J. Am. Chem. Soc. 131 (2009) 1979–1985. https://doi.org/10.1021/ja808537j.

[10] J. Domínguez-Robles, E. Espinosa, D. Savy, A. Rosal, Biorefinery Process Combining Specel® Process and Selective Lignin Precipitation using Mineral Acids, Bioresources 11 (2016) 7061–7077. https://doi.org/10.15376/biores.11.3.7061-7077.

[11] M. FitzPatrick, P. Champagne, M.F. Cunningham, R.A. Whitney, A biorefinery processing perspective: Treatment of lignocellulosic materials for the production of value-added products, Bioresour. Technol. 101 (2010) 8915–8922. https://doi.org/10.1016/j.biortech.2010.06.125.

[12] V. Menon, M. Rao, Trends in bioconversion of lignocellulose: Biofuels, platform chemicals & biorefinery concept, Prog. Energy Combust. Sci. 38 (2012) 522–550. https://doi.org/10.1016/j.pecs.2012.02.002.

[13] S. Yang, Chapter 1 . Bioprocessing – from Biotechnology to Biorefinery. In: Bioprocessing for Value-Added Products from Renewable Resources, Elsevier (2007). https://doi.org/10.1016/B978-044452114-9/50002-5.

[14] L.T. Fan, Y.-H. Lee, M.M. Gharpuray, The nature of lignocellulosics and their pretreatments for enzymatic hydrolysis. In: Microbial Reactions. Advances in Biochemical Engineering, Springer (1982). https://doi.org/10.1007/3540116982_4.

[15] K.-C. Cheng, C.-F. Huang, Y. Wei, S. Hsu, Novel chitosan–cellulose nanofiber self-healing hydrogels to correlate self-healing properties of hydrogels with neural regeneration effects, NPG Asia Mater. 11 (2019) 25. https://doi.org/10.1038/s41427-019-0124-z.

[16] M. Gao, J. Li, Z. Bao, M. Hu, R. Nian, D. Feng, D. An, X. Li, M. Xian, H. Zhang, A natural in situ fabrication method of functional bacterial cellulose using a microorganism, Nat. Commun. 10 (2019) 437. https://doi.org/10.1038/s41467-018-07879-3.

[17] D. Klemm, B. Heublein, H.P. Fink, A. Bohn, Cellulose: Fascinating biopolymer and sustainable raw material, Angew. Chemie - Int. Ed. 44 (2005) 3358–3393. https://doi.org/10.1002/anie.200460587.

[18] S. Kobayashi, J. Sakamoto, S. Kimura, In vitro synthesis of cellulose and related polysaccharides, Prog. Polym. Sci. 26 (2001) 1525–1560. https://doi.org/10.1016/S0079-6700(01)00026-0.

[19] R. Gallego, Functionalization of biopolymers with reactive groups to be used as thickeners in oil media, Ph. D. Thesis, Universidad de Huelva, (2015).

[20] P. Beguin, J.P. Aubert, The biological degradation of cellulose, FEMS Microbiol. Rev. 13 (1994) 25–58. https://doi.org/10.1111/j.1574-6976.1994.tb00033.x.

[21] R.J. Moon, A. Martini, J. Nairn, J. Simonsen, J. Youngblood, Cellulose nanomaterials review: structure, properties and nanocomposites, Chem. Soc. Rev. 40 (2011) 3941–3994. https://doi.org/10.1039/c0cs00108b.

[22] J. Xie, Y.C. Hung, Methodology to evaluate the antimicrobial effectiveness of UV-activated TiO2 nanoparticle-embedded cellulose acetate film, Food Control 106 (2019) 106690. https://doi.org/10.1016/j.foodcont.2019.06.016.

[23] H. Yang, L. Yang, H. Wang, Z. Xu, Y. Zhao, Y. Luo, N. Nasir, Y. Song, H. Wu, F. Pan, Z. Jiang, Covalent organic framework membranes through a mixed-dimensional assembly for molecular separations, Nat. Commun. 10 (2019) 2101. https://doi.org/10.1038/s41467-019-10157-5.

[24] H. Zhang, Y. Qian, S. Chen, Y. Zhao, Physicochemical characteristics and emulsification properties of cellulose nanocrystals stabilized O/W pickering emulsions with high $-OSO_3^-$ groups, Food Hydrocoll. 96 (2019) 267–277. https://doi.org/10.1016/j.foodhyd.2019.05.023.

[25] S.Y.H. Abdalkarim, H. Yu, C. Wang, Y. Chen, Z. Zou, L. Han, J. Yao, K.C. Tam, Thermo and light-responsive phase change nanofibers with high energy storage efficiency for energy storage and thermally regulated on-off drug release devices, Chem. Eng. J. 375 (2019) 121979. https://doi.org/10.1016/j.cej.2019.121979.

[26] Y. Wang, C. Wang, Y. Xie, Y. Yang, Y. Zheng, H. Meng, W. He, K. Qiao, Highly transparent, highly flexible composite membrane with multiple antimicrobial effects

used for promoting wound healing, Carbohydr. Polym. 222 (2019) 114985. https://doi.org/10.1016/j.carbpol.2019.114985.

[27] H.V. Scheller, P. Ulvskov, Hemicelluloses, Annu. Rev. Plant Biol. 61 (2010) 263–289. https://doi.org/10.1146/annurev-arplant-042809-112315.

[28] L.J. Gibson, The hierarchical structure and mechanics of plant materials, J. R. Soc. Interface. 9 (2012) 2749–2766. https://doi.org/10.1098/rsif.2012.0341.

[29] Alternative fuels from biomass sources, (last accessed 2021). https://www.e-education.psu.edu/egee439/node/664.

[30] A. Ebringerová, Z. Hromádková, H. Thomas, Hemicellulose. In: Polysaccharides I. Advances in Polymer Science, Springer (2005). https://doi.org/10.1007/b136816.

[31] Y. Sun, J. Cheng, Hydrolysis of lignocellulosic materials for ethanol production : a review, Bioresour. Technol. 83 (2002) 1–11. https://doi.org/10.1016/S0960-8524(01)00212-7

[32] B.C. Saha, Hemicellulose bioconversion, J. Ind. Microbiol. Biotechnol., 30 (2003) 279–291. https://doi.org/10.1007/s10295-003-0049-x.

[33] H. Kobayashi, A. Fukuoka, Synthesis and utilisation of sugar compounds derived from lignocellulosic biomass, Green Chem. 15 (2013) 1740–1763. https://doi.org/10.1039/c3gc00060e.

[34] C.O. Tuck, E. Pérez, I.T. Horváth, R.A. Sheldon, M. Poliakoff, Valorization of biomass: Deriving more value from waste, Science 338 (2012) 695–699. https://doi.org/10.1126/science.1218930.

[35] X. Jiang, J. Huang, T. Chen, Q. Zhao, F. Xu, X. Zhang, Synthesis of hemicellulose/deep eutectic solvent based carbon quantum dots for ultrasensitive detection of Ag^{+} and L-cysteine with “off-on” pattern, Int. J. Biol. Macromol. 153 (2020) 412–420. https://doi.org/10.1016/j.ijbiomac.2020.03.026.

[36] L.R. Mugwagwa, A.F.A. Chimphango, Enhancing the functional properties of acetylated hemicellulose films for active food packaging using acetylated nanocellulose reinforcement and polycaprolactone coating, Food Packag. Shelf Life. 24 (2020) 100481. https://doi.org/10.1016/j.fpsl.2020.100481.

[37] J. Wan, L. Liu, K.S. Ayub, W. Zhang, G. Shen, S. Hu, X. Qian, Characterization and adsorption performance of biochars derived from three key biomass constituents, Fuel. 269 (2020) 117142. https://doi.org/10.1016/j.fuel.2020.117142.

[38] W.R. de Souza, Microbial Degradation of Lignocellulosic. In: Sustainable Degradation of Lignocellulosic Biomass - Techniques, Applications and Commercialization, IntechOpen (2013). https://doi.org/10.5772/54325.

[39] J.M. Lang, U.M. Shrestha, M. Dadmun, The Effect of Plant Source on the Properties of Lignin-Based Polyurethanes, Front. Energy Res. 6 (2018) 4. https://doi.org/10.3389/fenrg.2018.00004.

[40] N. Mahmood, Z. Yuan, J. Schmidt, C. Xu, Depolymerization of lignins and their applications for the preparation of polyols and rigid polyurethane foams: A review, Renew. Sustain. Energy Rev. 60 (2016) 317–329. https://doi.org/10.1016/j.rser.2016.01.037.

[41] J. Zakzeski, P.C.A. Bruijnincx, A.L. Jongerius, B.M. Weckhuysen, The Catalytic

Valorization of Lignin for the Production of Renewable Chemicals, Chem. Rev. 110 (2010) 3552–3599. https://doi.org/10.1021/cr900354u.

[42] A.G. Vishtal, A. Kraslawski, Challenges in industrial applications of technical lignins, BioResources 6 (2011) 3547–3568.

[43] J.E. Holladay, J.F. White, J.J. Bozell, D. Johnson, Top Value-Added Chemicals from Biomass Volume II - Results of Screening for Potential Candidates from Biorefinery Lignin, Pacific Northwest Natl. Lab. II (2007). https://doi.org/10.2172/921839.

[44] N.D. Patil, N.R. Tanguy, N. Yan, Lignin Interunit Linkages and Model Compounds. In: Lignin in Polymer Composites, Elsevier (2016). https://doi.org/10.1016/B978-0-323-35565-0.00003-5.

[45] E.A.B. Da Silva, M. Zabkova, J.D. Araújo, C.A. Cateto, M.F. Barreiro, M.N. Belgacem, A.E. Rodrigues, An integrated process to produce vanillin and lignin-based polyurethanes from Kraft lignin, Chem. Eng. Res. Des. 87 (2009) 1276–1292. https://doi.org/10.1016/j.cherd.2009.05.008.

[46] C. Amen-Chen, H. Pakdel, C. Roy, Production of monomeric phenols by thermochemical conversion of biomass: A review, Bioresour. Technol. 79 (2001) 277–299. https://doi.org/10.1016/S0960-8524(00)00180-2.

[47] Q. Liu, Y. Matsushita, D. Aoki, K. Fukushima, Industrial utilizations of water-soluble sulfuric acid lignin prepared by hydrothermal treatment as flocculant and dispersant, J. Wood Sci. 65 (2019) 18. https://doi.org/10.1186/s10086-019-1797-1.

[48] D. Gan, W. Xing, L. Jiang, J. Fang, C. Zhao, F. Ren, L. Fang, K. Wang, X. Lu, Plant-inspired adhesive and tough hydrogel based on Ag-Lignin nanoparticles-triggered dynamic redox catechol chemistry, Nat. Commun. 10 (2019) 1487. https://doi.org/10.1038/s41467-019-09351-2.

[49] K. Ravishankar, M. Venkatesan, R.P. Desingh, A. Mahalingam, B. Sadhasivam, R. Subramaniyam, R. Dhamodharan, Biocompatible hydrogels of chitosan-alkali lignin for potential wound healing applications, Mater. Sci. Eng. C. 102 (2019) 447–457. https://doi.org/10.1016/j.msec.2019.04.038.

[50] F. Flores-Céspedes, I. Daza-Fernández, M. Villafranca-Sánchez, M. Fernández-Pérez, E. Morillo, T. Undabeytia, Lignin and ethylcellulose in controlled release formulations to reduce leaching of chloridazon and metribuzin in light-textured soils, J. Hazard. Mater. 343 (2018) 227–234. https://doi.org/10.1016/j.jhazmat.2017.09.012.

[51] S. Żółtowska-Aksamitowska, P. Bartczak, J. Zembrzuska, T. Jesionowski, Removal of hazardous non-steroidal anti-inflammatory drugs from aqueous solutions by biosorbent based on chitin and lignin, Sci. Total Environ. 612 (2018) 1223–1233. https://doi.org/10.1016/j.scitotenv.2017.09.037.

[52] Z. Chi, Z. Wang, Y. Liu, G. Yang, Preparation of organosolv lignin-stabilized nano zero-valent iron and its application as granular electrode in the tertiary treatment of pulp and paper wastewater, Chem. Eng. J. 331 (2017) 317–325. https://doi.org/10.1016/j.cej.2017.08.121.

[53] D. Yang, W. Huang, X. Qiu, H. Lou, Y. Qian, Modifying sulfomethylated alkali lignin by horseradish peroxidase to improve the dispersibility and conductivity of polyaniline, Appl. Surf. Sci. 426 (2017) 287–293. https://doi.org/10.1016/j.apsusc.2017.07.102.

[54] H. Wang, X. Qiu, W. Liu, D. Yang, Facile preparation of well-combined lignin-based

carbon/ZnO hybrid composite with excellent photocatalytic activity, Appl. Surf. Sci. 426 (2017) 206–216. https://doi.org/10.1016/j.apsusc.2017.07.112.

[55] Á.T. Martínez, J. Rencoret, G. Marques, A. Gutiérrez, D. Ibarra, J. Jiménez-Barbero, J.C. Del Río, Monolignol acylation and lignin structure in some nonwoody plants : A 2D NMR study, Phytochemistry 69 (2008) 2831–2843. https://doi.org/10.1016/j.phytochem.2008.09.005.

[56] S. Sun, J. Wen, M. Li, R. Sun, Revealing the Structural Inhomogeneity of Lignins from Sweet Sorghum Stem by Successive Alkali Extractions, J. Agric. Food Chem. 61 (2013) 4226–4235. https://doi.org/10.1021/jf400824p.

[57] S. Heikkinen, M.M. Toikka, P.T. Karhunen, I.A. Kilpeläinen, Quantitative 2D HSQC (Q-HSQC) via Suppression of J-Dependence of Polarization Transfer in NMR Spectroscopy : Application to Wood Lignin, J. Am. Chem. Soc. 125 (2003) 4362–4367. https://doi.org/10.1021/ja029035k.

[58] J.I. Santos, U. Fillat, R. Martín-Sampedro, I. Ballesteros, P. Manzanares, M. Ballesteros, M.E. Eugenio, D. Ibarra, Lignin-enriched Fermentation Residues from Bioethanol Production of Fast-growing Poplar and Forage Sorghum Lignin-enriched Fermentation Residues from Bioethanol Production of Fast-growing Poplar and Forage Sorghum, Bioresources 10 (2015) 5215–5232. https://doi.org/10.15376/biores.10.3.5215-5232.

[59] C. Heitner, D. Dimmel, J. Schmidt, Lignin and Lignans: Advances in Chemistry, CRC Press (2010). https://doi.org/10.1201/EBK1574444865.

[60] B.K.P. Kringstad, R. Mörck, ^{13}C-NMR Spectra of Kraft Lignins 1 C-NMR Spectrum of Milled Wood Lignin, Holzforschung 37 (1983) 237–244.

[61] Z. Xia, L.G. Akim, D.S. Argyropoulos, Quantitative ^{13}C NMR analysis of lignins with internal standards, J. Agric. Food Chem. 49 (2001) 3573–3578. https://doi.org/10.1021/jf010333v.

[62] J.I. Santos, R. Martín-Sampedro, U. Fillat, J.M. Oliva, M.J. Negro, M. Ballesteros, M.E. Eugenio, D. Ibarra, Evaluating lignin-rich residues from biochemical ethanol production of wheat straw and olive tree pruning by FTIR and 2D-NMR, Int. J. Polym. Sci. 2015 (2015) 314891. https://doi.org/10.1155/2015/314891.

[63] L. Zhang, G. Gellerstedt, Quantitative 2D HSQC NMR determination of polymer structures by selecting suitable internal standard references, Magn. Reson. Chem. 45 (2007) 37–45. https://doi.org/10.1002/mrc.1914.

[64] E. Windeisen, G. Wegener, Lignin as Building Unit for Polymers, In. Polymer Science: A Comprehensive Reference, Elsevier (2012). https://doi.org/10.1016/B978-0-444-53349-4.00263-6.

[65] N.A. Abdul Halim, N. Ngadi, M.N. Mohammad Ibrahim, S.M. Ansari, Monomeric Structure Characterization of Different Sources Biomass Lignin, Key Eng. Mater. 700 (2016) 42–49. https://doi.org/10.4028/www.scientific.net/KEM.700.42.

[66] E.A. Capanema, M.Y. Balakshin, and J.F. Kadla, A Comprehensive Approach for Quantitative Lignin Characterization by NMR Spectroscopy, J. Agric. Food Chem. 52 (2004) 1850–1860.

[67] H. Jeong, J. Park, S. Kim, J. Lee, N. Ahn, H.G. Roh, Preparation and characterization of thermoplastic polyurethanes using partially acetylated Kraft lignin, Fibers Polym. 14

(2013) 1082–1093. https://doi.org/10.1007/s12221-013-1082-7.

[68] C.A. Cateto, M.F. Barreiro, A.E. Rodrigues, M.C. Brochier-Salon, W. Thielemans, M.N. Belgacem, Lignins as Macromonomers for Polyurethane Synthesis: A Comparative Study on Hydroxyl Group Determination, J. Appl. Polym. Sci. 109 (2008) 3008–3017. https://doi.org/10.1002/app.28393.

[69] A. Tolbert, H. Akinosho, R. Khunsupat, A.K. Naskar, A.J. Ragauskas, Characterization and analysis of the molecular weight of lignin for biorefi ning studies, Biofuels, Bioprod. Biorefining 6 (2012) 836–856. https://doi.org/10.1002/bbb.1500.

[70] M. Balakshin, E. Capanema, On the quantification of lignin hydroxyl groups with ^{31}P and ^{13}C NMR spectroscopy, J. Wood Chem. Technol. 35 (2015) 220–237. https://doi.org/10.1080/02773813.2014.928328.

[71] L.B. Davin, N.G. Lewis, Lignin primary structures and dirigent sites, Curr. Opin. Biotechnol. 16 (2005) 407–415. https://doi.org/10.1016/j.copbio.2005.06.011.

[72] C.L. Chen, Determination of Methoxyl Groups. In: Methods in Lignin Chemistry, Springer (1992). https://doi.org/10.1007/978-3-642-74065-7_32.

[73] J.F. Kadla, H. Chang, H. Jameel, The Reactions of Lignins with High Temperature Hydrogen Peroxide Part 2. The Oxidation of Kraft Lignin, Holzforschung. 53 (1999) 277–284. https://doi.org/10.1515/hf.1999.047.

[74] H. Nimz, Beech Lignin—Proposal of a Constitutional Scheme, Angew. Chemie Int. Ed. English. 13 (1974) 313–321. https://doi.org/10.1002/anie.197403131.

[75] H. Ren, X.. Dai, H. Zhai, Z. Liu, S. Omori, Comparison of Bamboo Native Lignin and Alkaline Lignin Modified By Phase-Separation Method, Cellul. Chem. Technol. 49 (2015) 429–438.

[76] D. Fengel, X. Shao, Studies on the lignin of the bamboo species *Phyllostachys makinoi* Hay, Wood Sci. Technol. 19 (1985) 131–137. https://doi.org/10.1007/BF00353073.

[77] E.L. Mahon, S.D. Mansfield, Tailor-made trees: engineering lignin for ease of processing and tomorrow's bioeconomy, Curr. Opin. Biotechnol. 56 (2019) 147–155. https://doi.org/10.1016/j.copbio.2018.10.014.

[78] C. Halpin, Lignin engineering to improve saccharification and digestibility in grasses, Curr. Opin. Biotechnol. 56 (2019) 223–229. https://doi.org/10.1016/j.copbio.2019.02.013.

[79] S.R. Verma, U.N. Dwivedi, Lignin genetic engineering for improvement of wood quality: Applications in paper and textile industries, fodder and bioenergy production, South African J. Bot. 91 (2014) 107–125. https://doi.org/10.1016/j.sajb.2014.01.002.

[80] A. Eudes, Y. Liang, P. Mitra, D. Loqué, Lignin bioengineering, Curr. Opin. Biotechnol. 26 (2014) 189–198. https://doi.org/10.1016/j.copbio.2014.01.002.

[81] S.H.F. da Silva, P.S.B. dos Santos, D. Thomas da Silva, R. Briones, D.A. Gatto, J. Labidi, Kraft Lignin-Based Polyols by Microwave: Optimizing Reaction Conditions, J. Wood Chem. Technol. 37 (2017) 1–16. https://doi.org/10.1080/02773813.2017.1303513.

[82] C. Liu, H. Wang, A.M. Karim, J. Sun, Y. Wang, Catalytic fast pyrolysis of lignocellulosic biomass, Chem. Soc. Rev. 43 (2014) 7594–7623. https://doi.org/10.1039/C3CS60414D.

[83] D.R. De Oliveira, I.M. Nogueira, F.J.N. Maia, M.F. Rosa, S.E. Mazzetto, D. Lomonaco, Ecofriendly modification of acetosolv lignin from oil palm biomass for improvement of PMMA thermo-oxidative properties, J. Appl. Polym. Sci. 134 (2017) e45498. https://doi.org/10.1002/app.45498.

[84] H. Yang, R. Yan, H. Chen, D.H. Lee, C. Zheng, Characteristics of hemicellulose, cellulose and lignin pyrolysis, Fuel 86 (2007) 1781–1788. https://doi.org/10.1016/j.fuel.2006.12.013.

[85] N.A. Sa'don, A.A. Rahim, M.N.M. Ibrahim, N. Brosse, M.H. Hussin, Modification of oil palm fronds lignin by incorporation of m-cresol for improving structural and antioxidant properties, Int. J. Biol. Macromol. 104 (2017) 251–260. https://doi.org/10.1016/j.ijbiomac.2017.06.038.

[86] J. Domínguez-Robles, R. Sánchez, P. Díaz-Carrasco, E. Espinosa, M.T. García-Domínguez, A. Rodríguez, Isolation and characterization of lignins from wheat straw: Application as binder in lithium batteries, Int. J. Biol. Macromol. 104 (2017) 909–918. https://doi.org/10.1016/j.ijbiomac.2017.07.015.

[87] C. Crestini, M. Crucianelli, M. Orlandi, R. Saladino, Oxidative strategies in lignin chemistry: A new environmental friendly approach for the functionalisation of lignin and lignocellulosic fibers, Catal. Today. 156 (2010) 8–22. https://doi.org/10.1016/j.cattod.2010.03.057.

[88] A. Lawrence, P. Thollander, M. Karlsson, Drivers, barriers, and success factors for improving energy management in the pulp and paper industry, Sustain. 10 (2018) 1851. https://doi.org/10.3390/su10061851.

[89] F.S. Chakar, A.J. Ragauskas, Review of current and future softwood Kraft lignin process chemistry, Ind. Crops Prod. 20 (2004) 131–141. https://doi.org/10.1016/j.indcrop.2004.04.016.

[90] R.J. Stoklosa, Fractionation and characterization of solubilized biopolymers from alkaline pulping liquors, Ph. D. Thesis, Michigan State University (2014).

[91] B.I. Fleming, Alternative & emerging pulping technologies: Non-Kraft processes. In: "International symposium on pollution in the manufacture of pulp & paper.", Washington D.C., (1992).

[92] D.M. Alonso, S.H. Hakim, S. Zhou, W. Won, O. Hosseinaei, J. Tao, V. Garcia-negron, A.H. Motagamwala, M.A. Mellmer, K. Huang, C.J. Houtman, N. Labbé, D.P. Harper, C. Maravelias, T. Runge, J.A. Dumesic, Increasing the revenue from lignocellulosic biomass : Maximizing feedstock utilization, Sci. Adv. 3 (2017) e1603301. https://doi.org/10.1126/sciadv.1603301.

[93] L. Liu, T. Jiang, J. Yao, A Two-Step Chemical Process for the Extraction of Cellulose Fiber and Pectin from Mulberry Branch Bark Efficiently, J. Polym. Environ. 19 (2011) 568–573. https://doi.org/10.1007/s10924-011-0300-x.

[94] J. Li, Isolation of lignin from wood. In: Methods in Lignin Chemistry, Springer (1992). https://doi.org/10.1007/978-3-642-74065-7_5.

[95] R. Gallego, J.F. Arteaga, C. Valencia, J.M. Franco, Chemical modification of methyl cellulose with HMDI to modulate the thickening properties in castor oil, Cellulose 20 (2013) 495–507. https://doi.org/10.1007/s10570-012-9803-4.

[96] R. Gallego, J.F. Arteaga, C. Valencia, M.J. Díaz, J.M. Franco, Gel-Like Dispersions of

HMDI-Cross-Linked Lignocellulosic Materials in Castor Oil: Toward Completely Renewable Lubricating Grease Formulations, ACS Sustain. Chem. Eng. 3 (2015) 2130–2141. https://doi.org/10.1021/acssuschemeng.5b00389.

[97] R. Gallego, J.F. Arteaga, C. Valencia, J.M. Franco, Rheology and thermal degradation of isocyanate-functionalized methyl cellulose-based oleogels, Carbohydr. Polym. 98 (2013) 152–160. https://doi.org/10.1016/j.carbpol.2013.04.104.

[98] R. Gallego, J.F. Arteaga, C. Valencia, J.M. Franco, Thickening properties of several NCO-functionalized cellulose derivatives in castor oil, Chem. Eng. Sci. 134 (2015) 260–268. https://doi.org/10.1016/j.ces.2015.05.007.

[99] L.A. García-Zapateiro, C. Valencia, J.M. Franco, Formulation of lubricating greases from renewable basestocks and thickener agents: A rheological approach, Ind. Crops Prod. 54 (2014) 115–121. https://doi.org/10.1016/j.indcrop.2014.01.020.

[100] Z.M.A. Bundhoo, Potential of bio-hydrogen production from dark fermentation of crop residues: A review, Int. J. Hydrogen Energy. 44 (2019) 17346–17362. https://doi.org/10.1016/j.ijhydene.2018.11.098.

[101] H. Zhang, P.C. Lopez, C. Holland, A. Lunde, M. Ambye-Jensen, C. Felby, S.T. Thomsen, The multi-feedstock biorefinery – Assessing the compatibility of alternative feedstocks in a 2G wheat straw biorefinery process, GCB Bioenergy. 10 (2018) 946–959. https://doi.org/10.1111/gcbb.12557.

[102] Y. Sun, Z. He, R. Tu, Y. Wu, E. Jiang, X. Xu, The mechanism of wet/dry torrefaction pretreatment on the pyrolysis performance of tobacco stalk, Bioresour. Technol. 286 (2019) 121390. https://doi.org/10.1016/j.biortech.2019.121390.

[103] S. Kim, B.E. Dale, Global potential bioethanol production from wasted crops and crop residues, Biomass Bioenergy 26 (2004) 361–375. https://doi.org/10.1016/j.biombioe.2003.08.002.

[104] D. Nabarlatz, A. Ebringerová, D. Montané, Autohydrolysis of agricultural by-products for the production of xylo-oligosaccharides, Carbohydr. Polym. 69 (2007) 20–28. https://doi.org/10.1016/j.carbpol.2006.08.020.

[105] A.M. Borrero-López, V. Fierro, A. Jeder, A. Ouederni, E. Masson, A. Celzard, High added-value products from the hydrothermal carbonisation of olive stones, Environ. Sci. Pollut. Res. 24 (2017) 9859–9869. https://doi.org/10.1007/s11356-016-7807-6.

[106] S.S. Malhi, R. Lemke, Z.H. Wang, B.S. Chhabra, Tillage, nitrogen and crop residue effects on crop yield, nutrient uptake, soil quality, and greenhouse gas emissions, Soil Tillage Res. 90 (2006) 171–183. https://doi.org/10.1016/j.still.2005.09.001.

[107] M. Piekarczyk, M. Kobierski, I. Jaskulska, L. Gałęzewski, Content of available forms of boron, copper, manganese, zinc and iron in sandy soil fertilised with barley, wheat and oilseed rape straw ash, J. Elem. 23 (2018) 107–118. https://doi.org/10.5601/jelem.2017.22.1.1281.

[108] J. Sharma, S.S. Kumara, V. Kumar, S.K. Malyan, T. Mathimani, N.R. Bishnoi, A. Pugazhendhi, Upgrading of microalgal consortia with CO_2 from fermentation of wheat straw for the phycoremediation of domestic wastewater, Bioresour. Technol. 305 (2020) 123063. https://doi.org/10.1016/j.biortech.2020.123063.

[109] M.R. Ahmad, B. Chen, H. Duan, Improvement effect of pyrolyzed agro-food biochar on the properties of magnesium phosphate cement, Sci. Total Environ. 718 (2020)

137422. https://doi.org/10.1016/j.scitotenv.2020.137422.

[110] Y.A. Chen, H. Yang, D. Ouyang, T. Liu, D. Liu, X. Zhao, Construction of electron transfer chains with methylene blue and ferric ions for direct conversion of lignocellulosic biomass to electricity in a wide pH range, Appl. Catal. B Environ. 265 (2020) 118578. https://doi.org/10.1016/j.apcatb.2019.118578.

[111] R. Ahmadi, B. Souri, M. Ebrahimi, Evaluation of wheat straw to insulate fired clay hollow bricks as a construction material, J. Clean. Prod. 254 (2020) 120043. https://doi.org/10.1016/j.jclepro.2020.120043.

[112] "FAOSTAT". www.fao.org., (last accessed 2020).

[113] J. Medina, C.M. Monreal, L. Orellana, M. Calabi-Floody, M.E. González, S. Meier, F. Borie, P. Cornejo, Influence of saprophytic fungi and inorganic additives on enzyme activities and chemical properties of the biodegradation process of wheat straw for the production of organo-mineral amendments, J. Environ. Manage. 255 (2020) 109922. https://doi.org/10.1016/j.jenvman.2019.109922.

[114] B. Branska, L. Fořtová, M. Dvořáková, H. Liu, P. Patakova, J. Zhang, M. Melzoch, Chicken feather and wheat straw hydrolysate for direct utilization in biobutanol production, Renew. Energy 145 (2020) 1941–1948. https://doi.org/10.1016/j.renene.2019.07.094.

[115] G. Qi, L. Xiong, H. Li, Q. Huang, M. Luo, L. Tian, X. Chen, C. Huang, X. Chen, Hydrotropic pretreatment on wheat straw for efficient biobutanol production, Biomass Bioenergy 122 (2019) 76–83. https://doi.org/10.1016/j.biombioe.2019.01.039.

[116] N. Qureshi, T.C. Ezeji, Butanol, 'a superior biofuel' production from agricultural residues (renewable biomass): recent progress in technology, Biofuels, Bioprod. Biorefining 2 (2008) 319–330. https://doi.org/10.1002/bbb.85.

[117] S. Naik, V.V. Goud, P.K. Rout, K. Jacobson, A.K. Dalai, Characterization of Canadian biomass for alternative renewable biofuel, Renew. Energy 35 (2010) 1624–1631. https://doi.org/10.1016/j.renene.2009.08.033.

[118] C.S. Fermanelli, A. Córdoba, L.B. Pierella, C. Saux, Pyrolysis and copyrolysis of three lignocellulosic biomass residues from the agro-food industry: A comparative study, Waste Manag. 102 (2020) 362–370. https://doi.org/10.1016/j.wasman.2019.10.057.

[119] A.G. Froese, T.N. Nguyen, B.T. Ayele, R. Sparling, Digestibility of Wheat and Cattail Biomass Using a Co-culture of Thermophilic Anaerobes for Consolidated Bioprocessing, Bioenergy Res. 13 (2020) 325–333. https://doi.org/10.1007/s12155-020-10103-0.

[120] P. Poletto, G.N. Pereira, C.R.M. Monteiro, M.A.F. Pereira, S.E. Bordignon, D. De Oliveira, Xylooligosaccharides: Transforming the lignocellulosic biomasses into valuable 5-carbon sugar prebiotics, Process Biochem. 91 (2020) 352–363. https://doi.org/10.1016/j.procbio.2020.01.005.

[121] S. Martos, S. Mattana, A. Ribas, E. Albanell, X. Domene, Biochar application as a win-win strategy to mitigate soil nitrate pollution without compromising crop yields: a case study in a Mediterranean calcareous soil, J. Soils Sediments 20 (2020) 220–233. https://doi.org/10.1007/s11368-019-02400-9.

[122] S. Luhar, T.W. Cheng, I. Luhar, Incorporation of natural waste from agricultural and aquacultural farming as supplementary materials with green concrete: A review,

Compos. Part B Eng. 175 (2019) 107076. https://doi.org/10.1016/j.compositesb.2019.107076.

[123] J. Baruah, B.K. Nath, R. Sharma, S. Kumar, R.C. Deka, D.C. Baruah, E. Kalita, Recent trends in the pretreatment of lignocellulosic biomass for value-added products, Front. Energy Res. 6 (2018) 141. https://doi.org/10.3389/fenrg.2018.00141.

[124] L. Da Costa Sousa, S.P. Chundawat, V. Balan, B.E. Dale, "Cradle-to-grave" assessment of existing lignocellulose pretreatment technologies, Curr. Opin. Biotechnol. 20 (2009) 339–347. https://doi.org/10.1016/j.copbio.2009.05.003.

[125] J.D. McMillan, Pretreatment of Lignocellulosic Biomass, In: Enzymatic Conversion of Biomass for Fuels Production, ACS (1994). https://doi.org/10.1021/bk-1994-0566.ch015.

[126] B. Yang, C.E. Wyman, Pretreatment: the key to unlocking low-cost cellulosic ethanol, Biofuels Bioprod. Biorefin. 2 (2007) 26–40. https://doi.org/10.1002/bbb.49.

[127] R. El Hage, N. Brosse, P. Sannigrahi, A. Ragauskas, Effects of process severity on the chemical structure of Miscanthus ethanol organosolv lignin, Polym. Degrad. Stab. 95 (2010) 997–1003. https://doi.org/10.1016/j.polymdegradstab.2010.03.012.

[128] R. Sindhu, P. Binod, A. Pandey, Biological pretreatment of lignocellulosic biomass - An overview, Bioresour. Technol. 199 (2016) 76–82. https://doi.org/10.1016/j.biortech.2015.08.030.

[129] B. Yang, Z. Dai, S.Y. Ding, C.E. Wyman, Enzymatic hydrolysis of cellulosic biomass, Biofuels 2 (2011) 421–449. https://doi.org/10.4155/bfs.11.116.

[130] M. Andlar, T. Rezić, N. Marđetko, D. Kracher, R. Ludwig, B. Šantek, Lignocellulose degradation: An overview of fungi and fungal enzymes involved in lignocellulose degradation, Eng. Life Sci. 18 (2018) 768–778. https://doi.org/10.1002/elsc.201800039.

[131] C. Sánchez, Lignocellulosic residues: Biodegradation and bioconversion by fungi, Biotechnol. Adv. 27 (2009) 185–194. https://doi.org/10.1016/j.biotechadv.2008.11.001.

[132] M.P. Coughlan, Cellulose degradation by fungi, In: W.M. Forgarty (Ed.), Microbial Enzymes and Biotechnology, Springer (1990). https://doi.org/10.1007/978-94-009-0765-2_1.

[133] R.F.H. Dekker, Biodegradation of the Hemicelluloses, In: Biosynthesis and Biodegradation of Wood Components, Academic Press, (1985). https://doi.org/10.13140/2.1.2266.2081.

[134] C. Chen, H. Chang, T.K. Kirk, Carboxylic Acids Produced Through Oxidative Cleavage of Aromatic Rings During Degradation of Lignin in Spruce Wood by Phanerochaete Chrysosporium, J. Wood Chem. Technol. 3 (1983) 35–57. https://doi.org/10.1080/02773818308085150.

[135] Á.T. Martínez, M. Speranza, F.J. Ruiz-Dueñas, P. Ferreira, S. Camarero, F. Guillén, M.J. Martínez, A. Gutiérrez, J.C. Del Río, Biodegradation of lignocellulosics: Microbial, chemical, and enzymatic aspects of the fungal attack of lignin, Int. Microbiol. 8 (2005) 195–204.

[136] M. Thornbury, J. Sicheri, P. Slaine, L.J. Getz, E. Finlayson-Trick, J. Cook, C. Guinard, N. Boudreau, D. Jakeman, J. Rohde, C. McCormick, Characterization of novel lignocellulose-degrading enzymes from the porcupine microbiome using synthetic

metagenomics, PLoS One 14 (2019) e0209221. https://doi.org/10.1371/journal.pone.0209221.

[137] P.D. Sainsbury, E.M. Hardiman, M. Ahmad, H. Otani, N. Seghezzi, L.D. Eltis, T.D.H. Bugg, Breaking down lignin to high-value chemicals: The conversion of lignocellulose to vanillin in a gene deletion mutant of *Rhodococcus jostii* RHA1, ACS Chem. Biol. 8 (2013) 2151–2156. https://doi.org/10.1021/cb400505a.

[138] C.R. Strachan, R. Singh, D. VanInsberghe, K. Ievdokymenko, K. Budwill, W.W. Mohn, L.D. Eltis, S.J. Hallam, Metagenomic scaffolds enable combinatorial lignin transformation, PNAS 111 (2014) 10143–10148. https://doi.org/10.1073/pnas.1401631111.

[139] E. Ransom-Jones, A.J. McCarthy, S. Haldenby, J. Doonan, J.E. McDonald, Lignocellulose-Degrading Microbial Communities in Landfill Sites Represent a Repository of Unexplored Biomass-Degrading Diversity, Appl. Environ. Sci. 2 (2017) e00300-17. https://doi.org/10.1128/mSphere.00300-17.

[140] R.S. Granja-Travez, G.F. Persinoti, F.M. Squina, T.D.H. Bugg, Functional genomic analysis of bacterial lignin degraders: diversity in mechanisms of lignin oxidation and metabolism, Appl. Microbiol. Biotechnol. 104 (2020) 3305–3320. https://doi.org/10.1007/s00253-019-10318-y.

[141] R. López-Mondéjar, D. Zühlke, D. Becher, K. Riedel, P. Baldrian, Cellulose and hemicellulose decomposition by forest soil bacteria proceeds by the action of structurally variable enzymatic systems, Sci. Rep. 6 (2016) 25279. https://doi.org/10.1038/srep25279.

[142] P. Gupta, K. Samant, A. Sahu, Isolation of cellulose-degrading bacteria and determination of their cellulolytic potential, Int. J. Microbiol. 2012 (2012) 578925. https://doi.org/10.1155/2012/578925.

[143] M.E. Himmel, W.S. Adney, J.O. Baker, R.A. Nieves, S.R. Thomas, Cellulases: structure, function, and applications, In: Handbook on bioethanol: production and utilization, Taylor & Francis (1996). https://doi.org/10.1201/9780203752456-8.

[144] M.P. Coughlan, Mechanisms of cellulose degradation by fungi and bacteria, Anim. Feed Sci. Technol. 32 (1991) 77–100. https://doi.org/10.1016/0377-8401(91)90012-H.

[145] D. Shallom, Y. Shoham, Microbial hemicellulases, Curr. Opin. Microbiol. 6 (2003) 219–228. https://doi.org/10.1016/S1369-5274(03)00056-0.

[146] W.Y. Cheah, R. Sankaran, P.L. Show, T. Ibrahim, T.N. Baizura, K.W. Chew, A. Culaba, J-S. Chang, Pretreatment methods for lignocellulosic biofuels production: current advances, challenges and future prospects, Biofuel Res. J. 7 (2020) 1115–1127. https://doi.org/10.18331/BRJ2020.7.1.4.

[147] A. Schäfer, R. Konrad, T. Kuhnigk, P. Kämpfer, H. Hertel, H. König, Hemicellulose-degrading bacteria and yeasts from the termite gut, J. Appl. Bacteriol. 80 (1996) 471–478. https://doi.org/10.1111/j.1365-2672.1996.tb03245.x.

[148] J.S. Brigham, W.S. Adney, M.E. Himmel, Hemicellulases: Diversity and Applications, In: Handbook on bioethanol: production and utilization, Taylor & Francis (1996). https://doi.org/10.1201/9780203752456-7.

[149] T.D.H. Bugg, M. Ahmad, E.M. Hardiman, R. Rahmanpour, Pathways for degradation of lignin in bacteria and fungi, Nat. Prod. Rep. 28 (2011) 1883–1896.

https://doi.org/10.1039/c1np00042j.

[150] T.D.H. Bugg, J.J. Williamson, G.M.M. Rashid, Bacterial enzymes for lignin depolymerisation: new biocatalysts for generation of renewable chemicals from biomass, Curr. Opin. Chem. Biol. 55 (2020) 26–33. https://doi.org/10.1016/j.cbpa.2019.11.007.

[151] M. Ahmad, J.N. Roberts, E.M. Hardiman, R. Singh, L.D. Eltis, T.D.H. Bugg, Identification of DypB from *Rhodococcus jostii* RHA1 as a lignin peroxidase, Biochemistry 50 (2011) 5096–5107. https://doi.org/10.1021/bi101892z.

[152] R. Rahmanpour, D. Rea, S. Jamshidi, V. Fülöp, T.D.H. Bugg, Structure of *Thermobifida fusca* DyP-type peroxidase and activity towards Kraft lignin and lignin model compounds, Arch. Biochem. Biophys. 594 (2016) 54–60. https://doi.org/10.1016/j.abb.2016.02.019.

[153] V. Balan, D. Chiaramonti, S. Kumar, Review of US and EU initiatives toward development, demonstration, and commercialization of lignocellulosic biofuels, Biofuels, Bioprod. Biorefining. 7 (2013) 732–759. https://doi.org/10.1002/bbb.1436.

[154] R. Ruan, Y. Zhang, P. Chen, S. Liu, L. Fan, N. Zhou, K. Ding, P. Peng, M. Addy, Y. Cheng, E. Anderson, Y. Wang, Y. Liu, H. Lei, B. Li, Biofuels: Introduction, In: Biofuels: Alternative Feedstocks and Conversion Processes for the Production of Liquid and Gaseous Biofuels, Elsevier (2019). https://doi.org/10.1016/B978-0-12-816856-1.00001-4.

[155] S.G. Wi, E.J. Cho, D.S. Lee, S.J. Lee, Y.J. Lee, H-J. Bae, Lignocellulose conversion for biofuel: A new pretreatment greatly improves downstream biocatalytic hydrolysis of various lignocellulosic materials, Biotechnol. Biofuels 8 (2015) 228. https://doi.org/10.1186/s13068-015-0419-4.

[156] N.R. Baral, E.R. Sundstrom, L. Das, J. Gladden, A. Eudes, J.C. Mortimer, S.W. Singer, A. Mukhopadhyay, C.D. Scown, Approaches for More Efficient Biological Conversion of Lignocellulosic Feedstocks to Biofuels and Bioproducts, ACS Sustain. Chem. Eng. 7 (2019) 9062–9079. https://doi.org/10.1021/acssuschemeng.9b01229.

[157] N.R. Baral, O. Kavvada, D. Mendez-Perez, A. Mukhopadhyay, T.S. Lee, B.A. Simmons, C.D. Scown, Techno-economic analysis and life-cycle greenhouse gas mitigation cost of five routes to bio-jet fuel blendstocks, Energy Environ. Sci. 12 (2019) 807–824. https://doi.org/10.1039/c8ee03266a.

[158] L. Machineni, Lignocellulosic biofuel production: review of alternatives, Biomass Convers. Biorefinery 10 (2019) 779–791. https://doi.org/10.1007/s13399-019-00445-x.

[159] A. Demirbas, Competitive liquid biofuels from biomass, Appl. Energy 88 (2011) 17–28. https://doi.org/10.1016/j.apenergy.2010.07.016.

[160] W.N.R.W. Isahak, M.W.M. Hisham, M.A. Yarmo, T.Y. Yun Hin, A review on bio-oil production from biomass by using pyrolysis method, Renew. Sustain. Energy Rev. 16 (2012) 5910–5923. https://doi.org/10.1016/j.rser.2012.05.039.

[161] S. Prasad, M.S. Dhanya, N. Gupta, A. Kumar, Biofuels from biomass : a sustainable alternative to energy and environment, Biochem. Cell. Arch. 12 (2012) 255–260.

[162] C. Da Costa Gomez, Biogas as an energy option, an overview, In: The biogas handbook, Science, Products and Applications, Woodhead Publishing (2013). https://doi.org/10.1533/9780857097415.1.

[163] L.D. Gottumukkala, A.K. Mathew, A. Abraham, R.K. Sukumaran, Biobutanol production: Microbes, feedstock, and strategies, In: Biofuels: Alternative Feedstocks and Conversion Processes for the Production of Liquid and Gaseous Biofuels, Elsevier (2019). https://doi.org/10.1016/B978-0-12-816856-1.00015-4.

[164] A.M. Borrero-López, E. Masson, A. Celzard, V. Fierro, Modelling the reactions of cellulose, hemicellulose and lignin submitted to hydrothermal treatment, Ind. Crops Prod. 124 (2018) 919–930. https://doi.org/10.1016/j.indcrop.2018.08.045.

[165] J.A. Geboers, S. Van De Vyver, R. Ooms, B. Op De Beeck, P.A. Jacobs, B.F. Sels, Chemocatalytic conversion of cellulose: Opportunities, advances and pitfalls, Catal. Sci. Technol. 1 (2011) 714–726. https://doi.org/10.1039/c1cy00093d.

[166] F.H. Isikgor, C.R. Becer, Lignocellulosic biomass: a sustainable platform for the production of bio-based chemicals and polymers, Polym. Chem. 6 (2015) 4497–4559. https://doi.org/10.1039/c5py00263j.

[167] T. Werpy, G. Petersen, Top Value Added Chemicals from Biomass Volume I - Results of Screening for Potential Candidates from Sugars and Synthesis Gas (2004). https://doi.org/10.2172/15008859.

[168] A.S. Mamman, J-M. Lee, J-S.H. Y-C. Kim, I.T. Hwang, N-J. Park, Y.K. Hwang, J-S. Chang, J-S. Hwang, Furfural: Hemicellulose/xylose- derived biochemical, Biofuels, Bioprod. Biorefining 2 (2008) 438–454. https://doi.org/10.1002/bbb.95.

[169] W. Schutyser, T. Renders, S. Van Den Bosch, S.F. Koelewijn, G.T. Beckham, B.F. Sels, Chemicals from lignin: An interplay of lignocellulose fractionation, depolymerisation, and upgrading, Chem. Soc. Rev. 47 (2018) 852–908. https://doi.org/10.1039/c7cs00566k.

[170] H. Chen, Lignocellulose biorefinery product engineering, In: Lignocellulose Biorefinery Engineering, Woodhead Publishing (2015). https://doi.org/10.1016/b978-0-08-100135-6.00005-3.

[171] A.H. Basta, E.S. Abd El-Sayed, H. El-Saied, Lignocellulosic materials in building elements. Part IV - Economical manufacture and improvement of properties of light-weight agro-panels, Int. J. Polym. Mater. Polym. Biomater. 53 (2004) 709–723. https://doi.org/10.1080/00914030490472917.

[172] A. Buzarovska, G. Bogoeva-Gaceva, A. Grozdanov, M. Avella, G. Gentile, M. Errico, Potential use of rice straw as filler in eco-composite materials, Aust. J. Crop Sci. 1 (2008) 37–42.

[173] C.G. Rocha, D.A.M. Zaia, R.V. da S. Alfaya, A.A. da S. Alfaya, Use of rice straw as biosorbent for removal of Cu(II), Zn(II), Cd(II) and Hg(II) ions in industrial effluents, J. Hazard. Mater. 16 (2009) 383–388. https://doi.org/10.1016/j.jhazmat.2008.11.074.

[174] L. Wang, N.S. Bolan, D.C.W. Tsang, D. Hou, Green immobilization of toxic metals using alkaline enhanced rice husk biochar: Effects of pyrolysis temperature and KOH concentration, Sci. Total Environ. 720 (2020) 137584. https://doi.org/10.1016/j.scitotenv.2020.137584.

[175] M. Zhao, Y. Dai, M. Zhang, C. Feng, B. Qin, W. Zhang, N. Zhao, Y. Li, Z. Ni, Z. Xu, D.C.W. Tsang, R. Qiu, Mechanisms of Pb and/or Zn adsorption by different biochars: Biochar characteristics, stability, and binding energies, Sci. Total Environ. 717 (2020) 136894. https://doi.org/10.1016/j.scitotenv.2020.136894.

[176] Y. Dai, W. Wang, L. Lu, L. Yan, D. Yu, Utilization of biochar for the removal of nitrogen and phosphorus, J. Clean. Prod. 257 (2020) 120573. https://doi.org/10.1016/j.jclepro.2020.120573.

[177] S.E. Abdel-Aal, Y.H. Gad, A.M. Dessouki, Use of rice straw and radiation-modified maize starch/acrylonitrile in the treatment of wastewater, J. Hazard. Mater. 129 (2006) 204–215. https://doi.org/10.1016/j.jhazmat.2005.08.041.

[178] S. Nethaji, A. Sivasamy, G. Thennarasu, S. Saravanan, Adsorption of Malachite Green dye onto activated carbon derived from *Borassus aethiopum* flower biomass, J. Hazard. Mater. 181 (2010) 271–280. https://doi.org/10.1016/j.jhazmat.2010.05.008.

[179] R-L. Liu, Y. Liu, X-Y. Zhou, Z-Q. Zhang, J. Zhang, F-Q. Dang, Biomass-derived highly porous functional carbon fabricated by using a free-standing template for efficient removal of methylene blue, Bioresour. Technol. 154 (2014) 138–147. https://doi.org/10.1016/j.biortech.2013.12.034.

[180] Á.I. Licona-Aguilar, J.A. Lois-Correa, A.M. Torres-Huerta, M.A. Domínguez-Crespo, H.J. Dorantes-Rosales, D.S. García-Zaleta, Sugarcane Bagasse-, Orange Peel-Derived Adsorbent Materials: Thermal and Morphological Studies, J. Nanosci. Nanotechnol. 20 (2020) 4563–4573. https://doi.org/10.1166/jnn.2020.17866.

[181] S. Gao, Y. Chen, H. Fan, X. Wei, C. Hu, H. Luo, L. Qu, Large scale production of biomass-derived n-doped porous carbon spheres for oxygen reduction and supercapacitors, J. Mater. Chem. A. 2 (2014) 3317–3324. https://doi.org/10.1039/c3ta14281g.

[182] Y. Liu, M. Su, D. Li, S. Li, X. Li, J. Zhao, F. Liu, Soybean straw biomass-derived Fe-N co-doped porous carbon as an efficient electrocatalyst for oxygen reduction in both alkaline and acidic media, RSC Adv. 12 (2020) 6763–6771. https://doi.org/10.1039/c9ra07539a.

[183] M. Ma, Y. Dai, J.L. Zou, L. Wang, K. Pan, H.G. Fu, Synthesis of iron oxide/partly graphitized carbon composites as a high-efficiency and low-cost cathode catalyst for microbial fuel cells, ACS Appl. Mater. Interfaces 6 (2014) 13438–13447. https://doi.org/10.1021/am501844p.

[184] X-L. Wu, T. Wen, H-L. Guo, S. Yang, X. Wang, A-W. Xu, Biomass-Derived Sponge-like Carbonaceous Hydrogels and Aerogels for Supercapacitors, ACS Nano 7 (2013) 3589–3597. https://doi.org/10.1021/nn400566d.

[185] G. Kumar Gupta, S. De, A. Franco, A.M. Balu, R. Luque, Sustainable Biomaterials: Current Trends, Challenges and Applications, Molecules 21 (2015) 48. https://doi.org/10.3390/molecules21010048.

[186] H.M.N. Iqbal, G. Kyazze, T. Keshavarz, Advances in the valorization of lignocellulosic materials by biotechnology: An overview, BioResources 8 (2013) 3157–3176. https://doi.org/10.15376/biores.8.2.3157-3176.

[187] V. Bugatti, P. Brachi, G. Viscusi, G. Gorrasi, Valorization of tomato processing residues through the production of active bio-composites for packaging applications, Front. Mater. 6 (2019) 34. https://doi.org/10.3389/fmats.2019.00034.

[188] D. Ita-Nagy, I. Vázquez-Rowe, R. Kahhat, I. Quispe, G. Chinga-Carrasco, N.M. Clauser, M.C. Area, Life cycle assessment of bagasse fiber reinforced biocomposites, Sci. Total Environ. 720 (2020) 137586.

https://doi.org/10.1016/j.scitotenv.2020.137586.

[189] J.B. Engel, M. Mac Ginity, C.L. Luchese, I.C. Tessaro, J.C. Spada, Reuse of Different Agroindustrial Wastes: *Pinhão* and Pecan Nutshells Incorporated into Biocomposites Using Thermocompression, J. Polym. Environ. 28 (2020) 1431–1440. https://doi.org/10.1007/s10924-020-01696-w.

[190] B. Chen, Z. Luo, H. Chen, C. Chen, D. Cai, P. Qin, H. Cao, T. Tan, Wood Plastic Composites from the Waste Lignocellulosic Biomass Fibers of Bio-Fuels Processes: A Comparative Study on Mechanical Properties and Weathering Effects, Waste and Biomass Valorization 11 (2020) 1701–1710. https://doi.org/10.1007/s12649-018-0413-8.

[191] W.F. Chen, S. Iyer, S. Iyer, K. Sasaki, C.H. Wang, Y. Zhu, J.T. Muckerman, E. Fujita, Biomass-derived electrocatalytic composites for hydrogen evolution, Energy Environ. Sci. 6 (2013) 1818–1826. https://doi.org/10.1039/c3ee40596f.

[192] H. Chen, Integrated industrial lignocellulose biorefinery chains, In: Lignocellulose Biorefinery Engineering, Principles and Applications, Woodhead Publishing (2015). https://doi.org/10.1016/b978-0-08-100135-6.00007-7.

[193] T.I. Horuz, K.B. Belibağli, Encapsulation of tomato peel extract into nanofibers and its application in model food, J. Food Process. Preserv. 43 (2019) 14090. https://doi.org/10.1111/jfpp.14090.

[194] Y. Niu, Q. Xia, M. Gu, L. Yu, Interpenetrating network gels composed of gelatin and soluble dietary fibers from tomato peels, Food Hydrocoll. 89 (2019) 95–99. https://doi.org/10.1016/j.foodhyd.2018.10.028.

[195] R. Ajdary, B.L. Tardy, B.D. Mattos, L. Bai, O.J. Rojas, Plant nanomaterials and inspiration from nature: water interactions and hierarchically structured hydrogels, Adv. Mater. (2020) 2001085. https://doi.org/10.1002/adma.202001085.

[196] C. Chang, L. Zhang, Cellulose-based hydrogels: Present status and application prospects, Carbohydr. Polym. 84 (2011) 40–53. https://doi.org/10.1016/j.carbpol.2010.12.023.

[197] G. Zhao, X. Lyu, J. Lee, X. Cui, W.N. Chen, Biodegradable and transparent cellulose film prepared eco-friendly from durian rind for packaging application, Food Packag. Shelf Life 21 (2019) 100345. https://doi.org/10.1016/j.fpsl.2019.100345.

[198] S.M.F. Kabir, P.P. Sikdar, B. Haque, M.A.R. Bhuiyan, A. Ali, M.N. Islam, Cellulose-based hydrogel materials: chemistry, properties and their prospective applications, Prog. Biomater. 7 (2018) 153–174. https://doi.org/10.1007/s40204-018-0095-0.

[199] A. Sannino, M. Madaghiele, M.G. Lionetto, T. Schettino, A. Maffezzoli, A cellulose-based hydrogel as a potential bulking agent for hypocaloric diets: An *in vitro* biocompatibility study on rat intestine, J. Appl. Polym. Sci. 102 (2006) 1524–1530. https://doi.org/10.1002/app.24468.

[200] L. Yan, Q. Shuai, X. Gong, Q. Gu, H. Yu, Synthesis of microporous cationic hydrogel of hydroxypropyl cellulose (HPC) and its application on anionic dye removal, Clean - Soil, Air, Water 37 (2009) 392–398. https://doi.org/10.1002/clen.200900006.

[201] L-Y. Long, Y-X. Weng, Y-Z. Wang, Cellulose aerogels: Synthesis, applications, and prospects, Polymers 10 (2018) 623. https://doi.org/10.3390/polym10060623.

[202] A. Tripathi, G.N. Parsons, O.J. Rojas, S.A. Khan, Featherlight, Mechanically Robust Cellulose Ester Aerogels for Environmental Remediation, ACS Omega 2 (2017) 4297–4305. https://doi.org/10.1021/acsomega.7b00571.

[203] A. Tripathi, G.N. Parsons, S.A. Khan, O.J. Rojas, Synthesis of organic aerogels with tailorable morphology and strength by controlled solvent swelling following Hansen solubility, Sci. Rep. 8 (2018) 2106. https://doi.org/10.1038/s41598-018-19720-4.

[204] A. Puscas, V. Muresan, C. Socaciu, S. Muste, Oleogels in food: A review of current and potential applications, Foods 9 (2020) 70. https://doi.org/10.3390/foods9010070.

[205] A.J. Gravelle, A.G. Marangoni, M. Davidovich-Pinhas, Ethylcellulose Oleogels, In: Edible Oleogels, AOCS Press (2018). https://doi.org/10.1016/b978-0-12-814270-7.00014-9.

[206] N. Núñez, J.E. Martín-Alfonso, M.E. Eugenio, C. Valencia, M.J. Díaz, J.M. Franco, Preparation and characterization of gel-like dispersions based on cellulosic pulps and castor oil for lubricant applications, Ind. Eng. Chem. Res. 50 (2011) 5618–5627. https://doi.org/10.1021/ie1025584.

[207] N. Núñez, J.E. Martín-Alfonso, C. Valencia, M.C. Sánchez, J.M. Franco, Rheology of new green lubricating grease formulations containing cellulose pulp and its methylated derivative as thickener agents, Ind. Crops Prod. 37 (2012) 500–507. https://doi.org/10.1016/j.indcrop.2011.07.027.

[208] E. Cortés-Triviño, C. Valencia, M.A. Delgado, J.M. Franco, Rheology of epoxidized cellulose pulp gel-like dispersions in castor oil: Influence of epoxidation degree and the epoxide chemical structure, Carbohydr. Polym. 199 (2018) 563–571. https://doi.org/10.1016/j.carbpol.2018.07.058.

[209] R. Sánchez, M. Fiedler, E. Kuhn, J.M. Franco, Tribological characterization of green lubricating greases formulated with castor oil and different biogenic thickener agents: A comparative experimental study, Ind. Lubr. Tribol. 63 (2011) 446–452. https://doi.org/10.1108/00368791111169034.

[210] R. Sánchez, J.M. Franco, M.A. Delgado, C. Valencia, C. Gallegos, Rheological and mechanical properties of oleogels based on castor oil and cellulosic derivatives potentially applicable as bio-lubricating greases: Influence of cellulosic derivatives concentration ratio, J. Ind. Eng. Chem. 17 (2011) 705–711. https://doi.org/10.1016/j.jiec.2011.05.019.

[211] J.E. Martín-Alfonso, N. Núñez, C. Valencia, J.M. Franco, M.J. Díaz, Formulation of new biodegradable lubricating greases using ethylated cellulose pulp as thickener agent, J. Ind. Eng. Chem. 17 (2011) 818–823. https://doi.org/10.1016/j.jiec.2011.09.003.

[212] D. Klemm, F. Kramer, S. Moritz, T. Lindström, M. Ankerfors, D. Gray, A. Dorris, Nanocelluloses: A new family of nature-based materials, Angew. Chemie - Int. Ed. 50 (2011) 5438–5466. https://doi.org/10.1002/anie.201001273.

[213] N. Mittal, F. Ansari, V. Gowda Krishne, C. Brouzet, P. Chen, P.T. Larsson, S. V. Roth, F. Lundell, L. Wågberg, N.A. Kotov, L.D. Söderberg, Multiscale Control of Nanocellulose Assembly: Transferring Remarkable Nanoscale Fibril Mechanics to Macroscale Fibers, ACS Nano 12 (2018) 6378–6388. https://doi.org/10.1021/acsnano.8b01084.

[214] B.L. Peng, N. Dhar, H.L. Liu, K.C. Tam, Chemistry and applications of nanocrystalline

cellulose and its derivatives: A nanotechnology perspective, Can. J. Chem. Eng. 89 (2011) 1191–1206. https://doi.org/10.1002/cjce.20554.

[215] W. Farhat, R. Venditti, N. Mignard, M. Taha, F. Becquart, A. Ayoub, Polysaccharides and lignin based hydrogels with potential pharmaceutical use as a drug delivery system produced by a reactive extrusion process, Int. J. Biol. Macromol. 104 (2017) 564–575. https://doi.org/10.1016/j.ijbiomac.2017.06.037.

[216] A.E. da Silva, H.R. Marcelino, M.C.S. Gomes, E.E. Oliveira, T. Nagashima Jr, E.S.T. Egito, Xylan, a Promising Hemicellulose for Pharmaceutical Use, In: Products and Applications of Biopolymers, IntechOpen (2012). https://doi.org/10.5772/33070.

[217] C. V. Pardeshi, A.D. Kulkarni, V.S. Belgamwar, S.J. Surana, Xyloglucan for drug delivery applications, In: Fundamental Biomaterials: Polymers, Woodhead Publishing (2018). https://doi.org/10.1016/B978-0-08-102194-1.00007-4.

[218] P. Peng, D. She, Isolation, structural characterization, and potential applications of hemicelluloses from bamboo: A review, Carbohydr. Polym. 112 (2014) 701–720. https://doi.org/10.1016/j.carbpol.2014.06.068.

[219] A. Ayoub, R.A. Venditti, J.J. Pawlak, A. Salam, M.A. Hubbe, Novel hemicellulose-chitosan biosorbent for water desalination and heavy metal removal, ACS Sustain. Chem. Eng. 1 (2013) 1102–1109. https://doi.org/10.1021/sc300166m.

[220] S-J. Seo, I-K. Park, M-K. Yoo, M. Shirakawa, T. Akaike, C-S. Cho, Xyloglucan as a synthetic extracellular matrix for hepatocyte attachment, J. Biomater. Sci. Polym. Ed. 15 (2004) 1375–1387. https://doi.org/10.1163/1568562042368059.

[221] J.L.M. Silveira, T.M.B. Bresolin, Pharmaceutical use of galactomannans, Quim. Nova 34 (2011) 292–299. https://doi.org/10.1590/S0100-40422011000200023.

[222] M. Landin, M.M. Echezarreta, Galactomannans: Old and new pharmaceutical materials, In: Polysaccharides: Development, Properties and Applications, Nova Science (2010).

[223] B. Rossi, E. Ponzini, L. Merlini, R. Grandori, Y.M. Galante, Characterization of aerogels from chemo-enzymatically oxidized galactomannans as novel polymeric biomaterials, Eur. Polym. J. 93 (2017) 347–357. https://doi.org/10.1016/j.eurpolymj.2017.06.016.

[224] N.M.L. Hansen, D. Plackett, Sustainable films and coatings from hemicelluloses: A review, Biomacromolecules 9 (2008) 1493–1505. https://doi.org/10.1021/bm800053z.

[225] K. Prakobna, V. Kisonen, C. Xu, L.A. Berglund, Strong reinforcing effects from galactoglucomannan hemicellulose on mechanical behavior of wet cellulose nanofiber gels, J. Mater. Sci. 50 (2015) 7413–7423. https://doi.org/10.1007/s10853-015-9299-z.

[226] H. Peng, A. Yang, J. Xiong, Green, microwave-assisted synthesis of silver nanoparticles using bamboo hemicelluloses and glucose in an aqueous medium, Carbohydr. Polym. 91 (2013) 348–355. https://doi.org/10.1016/j.carbpol.2012.08.073.

[227] W. Farhat, R. Venditti, A. Quick, M. Taha, N. Mignard, F. Becquart, A. Ayoub, Hemicellulose extraction and characterization for applications in paper coatings and adhesives, Ind. Crops Prod. 107 (2017) 370–377. https://doi.org/10.1016/j.indcrop.2017.05.055.

[228] A. Ebringerova, The potential of xylans as biomaterial resources, In: Polysaccharide Building Blocks: A Sustainable Approach to the Development of Renewable

Biomaterials, Wiley (2006). https://doi.org/10.1002/9781118229484.ch13.

[229] D.M. Martínez-Ibarra, J. López-Cervantes, D.I. Sánchez-Machado, A. Sanches-Silva, Chitosan and Xyloglucan-Based Hydrogels: An Overview of Synthetic and Functional Utility, In: Chitin-Chitosan - Myriad Functionalities in Science and Technology, IntechOpen (2018). https://doi.org/10.5772/intechopen.74646.

[230] V.D. Prajapati, G.K. Jani, N.G. Moradiya, N.P. Randeria, B.J. Nagar, N.N. Naikwadi, B.C. Variya, Galactomannan: A versatile biodegradable seed polysaccharide, Int. J. Biol. Macromol. 60 (2013) 83–92. https://doi.org/10.1016/j.ijbiomac.2013.05.017.

[231] L. Polari, P. Ojansivu, S. Mäkelä, C. Eckerman, B. Holmbom, S. Salminen, Galactoglucomannan extracted from spruce (*Picea abies*) as a carbohydrate source for probiotic bacteria, J. Agric. Food Chem. 60 (2012) 11037–11043. https://doi.org/10.1021/jf303741h.

[232] O. Faruk, M. Sain, Lignin in Polymer Composites, Elsevier (2015). https://doi.org/10.1016/C2014-0-01101-X.

[233] O. Gordobil, New Products From Lignin (PhD Thesis) (2018).

[234] R. Pucciariello, V. Villani, C. Bonini, M. D'Auria, T. Vetere, Physical properties of straw lignin-based polymer blends, Polymer 45 (2004) 4159–4169. https://doi.org/10.1016/j.polymer.2004.03.098.

[235] S.B. Mishra, A.K. Mishra, N.K. Kaushik, M.A. Khan, Study of performance properties of lignin-based polyblends with polyvinyl chloride, J. Mater. Process. Technol. 183 (2007) 273–276. https://doi.org/10.1016/j.jmatprotec.2006.10.016.

[236] W. Yang, M. Rallini, D.Y. Wang, D. Gao, F. Dominici, L. Torre, J.M. Kenny, D. Puglia, Role of lignin nanoparticles in UV resistance, thermal and mechanical performance of PMMA nanocomposites prepared by a combined free-radical graft polymerization/masterbatch procedure, Compos. Part A Appl. Sci. Manuf. 107 (2018) 61–69. https://doi.org/10.1016/j.compositesa.2017.12.030.

[237] S.Y. Park, J-Y. Kim, H.J. Youn, J.W. Choi, Utilization of lignin fractions in UV resistant lignin-PLA biocomposites via lignin-lactide grafting, Int. J. Biol. Macromol. 138 (2019) 1029–1034. https://doi.org/10.1016/j.ijbiomac.2019.07.157.

[238] C. Pouteau, P. Dole, B. Cathala, L. Averous, N. Boquillon, Antioxidant properties of lignin in polypropylene, Polym. Degrad. Stab. 81 (2003) 9–18. https://doi.org/10.1016/S0141-3910(03)00057-0.

[239] M. Canetti, F. Bertini, A. De Chirico, G. Audisio, Thermal degradation behaviour of isotactic polypropylene blended with lignin, Polym. Degrad. Stab. 91 (2006) 494–498. https://doi.org/10.1016/j.polymdegradstab.2005.01.052.

[240] A. Gregorová, B. Košíková, R. Moravčík, Stabilization effect of lignin in natural rubber, Polym. Degrad. Stab. 91 (2006) 229–233. https://doi.org/10.1016/j.polymdegradstab.2005.05.009.

[241] L.B. Tavares, D. dos S. Rosa, Stabilization effect of Kraft lignin into PBAT: Thermal analyses approach, Materia 24 (2019) 12405. https://doi.org/10.1590/s1517-707620190003.0718.

[242] J. Lisperguer, C. Nuñez, P. Perez-Guerrero, Structure and thermal properties of maleated lignin-recycled polystyrene composites, J. Chil. Chem. Soc. 58 (2013) 1937–

1940. https://doi.org/10.4067/S0717-97072013000400005.

[243] S. Sen, S. Patil, D.S. Argyropoulos, Thermal properties of lignin in copolymers, blends, and composites: a review, Green Chem. 17 (2015) 4862–4887. https://doi.org/10.1039/c5gc01066g.

[244] A. De Chirico, M. Armanini, P. Chini, G. Cioccolo, F. Provasoli, G. Audisio, Flame retardants for polypropylene based on lignin, Polym. Degrad. Stab. 79 (2003) 139–145. https://doi.org/10.1016/S0141-3910(02)00266-5.

[245] B. Chollet, J.M. Lopez-Cuesta, F. Laoutid, L. Ferry, Lignin nanoparticles as a promising way for enhancing lignin flame retardant effect in polylactide, Materials 12 (2019) 2132. https://doi.org/10.3390/ma12132132.

[246] S. Chen, S. Lin, Y. Hu, M. Ma, Y. Shi, J. Liu, F. Zhu, X. Wang, A lignin-based flame retardant for improving fire behavior and biodegradation performance of polybutylene succinate, Polym. Adv. Technol. 29 (2018) 3142–3150. https://doi.org/10.1002/pat.4436.

[247] H. Yang, B. Yu, X. Xu, S. Bourbigot, H. Wang, P. Song, Lignin-derived bio-based flame retardants toward high-performance sustainable polymeric materials, Green Chem. 22 (2020) 2129–2161. https://doi.org/10.1039/d0gc00449a.

[248] N. Mandlekar, A. Cayla, F. Rault, S. Giraud, F. Salaün, G. Malucelli, J.-P. Guan, An Overview on the Use of Lignin and Its Derivatives in Fire Retardant Polymer Systems, In: Lignin - Trends and Applications, IntechOpen (2018). https://doi.org/10.5772/intechopen.72963.

[249] Y. Ikeda, T. Phakkeeree, P. Junkong, H. Yokohama, P. Phinyocheep, R. Kitano, A. Kato, Reinforcing biofiller “lignin” for high performance green natural rubber nanocomposites, RSC Adv. 7 (2017) 5222–5231. https://doi.org/10.1039/c6ra26359c.

[250] A. Al Mamun, M.A. Nikousaleh, M. Feldmann, A. Rüppel, V. Sauer, S. Kleinhans, H.P. Heim, Lignin Reinforcement in Bioplastic Composites, In: Lignin in Polymer Composites, William Andrew (2016). https://doi.org/10.1016/B978-0-323-35565-0.00008-4.

[251] C. Jiang, H. He, H. Jiang, L. Ma, D.M. Jia, Nano-lignin filled natural rubber composites: Preparation and characterization, Express Polym. Lett. 7 (2013) 480–493. https://doi.org/10.3144/expresspolymlett.2013.44.

[252] H.D. Rozman, K.W. Tan, R.N. Kumar, A. Abubakar, Z.A. Mohd. Ishak, H. Ismail, The effect of lignin as a compatibilizer on the physical properties of coconut fiber-polypropylene composites, Eur. Polym. J. 36 (2000) 1483–1494. https://doi.org/10.1016/S0014-3057(99)00200-1.

[253] F.A. Tanjung, S. Husseinsyah, K. Hussin, Chitosan-filled polypropylene composites: The effect of filler loading and organosolv lignin on mechanical, morphological and thermal properties, Fibers Polym. 15 (2014) 800–808. https://doi.org/10.1007/s12221-014-0800-0.

[254] J. Yang, Y.C. Ching, C.H. Chuah, Applications of Lignocellulosic Fibers and Lignin in Bioplastics: A review, Polymers 11 (2019) 751. https://doi.org/10.3390/polym11050751.

[255] N.A. Mohamad Aini, N. Othman, M.H. Hussin, K. Sahakaro, N. Hayeemasae, Lignin as Alternative Reinforcing Filler in the Rubber Industry: A Review, Front. Mater. 6

(2020) 329. https://doi.org/10.3389/fmats.2019.00329.

[256] X. Yue, F. Chen, X. Zhou, G. He, Preparation and characterization of poly (vinyl chloride) polyblends with fractionated lignin, Int. J. Polym. Mater. Polym. Biomater. 61 (2012) 214–228. https://doi.org/10.1080/00914037.2011.574659.

[257] Study on Support to R&I Policy in the Area of Bio-based Products and Services on the Top 20 Innovative Bio-Based Products (2019). https://doi.org/10.2777/85805.

[258] G. Yu, B. Li, H. Wang, C. Liu, X. Mu, Preparation of concrete superplasticizer by oxidation- sulfomethylation of sodium lignosulfonate, BioResources 8 (2013) 1055–1063. https://doi.org/10.15376/biores.8.1.1055-1063.

[259] L. Mu, Y. Shi, X. Guo, T. Ji, L. Chen, R. Yuan, L. Brisbin, H. Wang, J. Zhu, Non-corrosive green lubricants: strengthened lignin-[choline][amino acid] ionic liquids interaction via reciprocal hydrogen bonding, RSC Adv. 5 (2015) 66067–66072. https://doi.org/10.1039/C5RA11093A.

[260] L. Mu, J. Wu, L. Matsakas, M. Chen, U. Rova, P. Christakopoulos, J. Zhu, Y. Shi, Two important factors of selecting lignin as efficient lubricating additives in poly (ethylene glycol): Hydrogen bond and molecular weight, Int. J. Biol. Macromol. 129 (2019) 564–570. https://doi.org/10.1016/j.ijbiomac.2019.01.175.

[261] J. Hua, Y. Shi, Non-corrosive Green Lubricant With Dissolved Lignin in Ionic Liquids Behave as Ideal Lubricants for Steel-DLC Applications, Front. Chem. 7 (2019) 857. https://doi.org/10.3389/fchem.2019.00857.

[262] T. Litters, A. Liebenau, Lubricating greases containing lignosulfonate, the production thereof, and the use thereof (2011).

[263] J. Wang, Y. Deng, Y. Qian, X. Qiu, Y. Ren, D. Yang, Reduction of lignin color via one-step UV irradiation, Green Chem. 18 (2016) 695–699. https://doi.org/10.1039/c5gc02180d.

[264] P. Balasubramanian, S. Ramalingam, M.A. Javid, J.R. Rao, Lignin Based Colorant: Modified Black Liquor for Leather Surface Coating Application, J. Am. Leather Chem. Assoc. 113 (2018) 311–317.

[265] R.K. Kemer., Ink comprising lignin-based colorants (1970).

[266] P. Araújo, A. Costa, I. Fernandes, N. Mateus, V. de Freitas, B. Sarmento, J. Oliveira, Stabilization of bluish pyranoanthocyanin pigments in aqueous systems using lignin nanoparticles, Dye. Pigment. 166 (2019) 367–374. https://doi.org/10.1016/j.dyepig.2019.03.020.

[267] V. Ugartondo, M. Mitjans, M.P. Vinardell, Comparative antioxidant and cytotoxic effects of lignins from different sources, Bioresour. Technol. 99 (2008) 6683–6687. https://doi.org/10.1016/j.biortech.2007.11.038.

[268] J.L. Espinoza-Acosta, P.I. Torres-Chávez, B. Ramírez-Wong, C.M. López-Saiz, B. Montaño-Leyva, Antioxidant, antimicrobial, and antimutagenic properties of technical lignins and their applications, BioResources 11 (2016) 5452–5481. https://doi.org/10.15376/biores.11.2.Espinoza_Acosta.

[269] Z. Mahmood, M. Yameen, M. Jahangeer, M. Riaz, A. Ghaffar, I. Javid, Lignin as Natural Antioxidant Capacity, In: Lignin – Trends and Applications, IntechOpen (2018). https://doi.org/10.5772/intechopen.73284.

[270] A. Alzagameem, B. El Khaldi-Hansen, D. Büchner, M. Larkins, B. Kamm, S. Witzleben, M. Schulze, Lignocellulosic biomass as source for lignin-based environmentally benign antioxidants, Molecules 23 (2018) 2664. https://doi.org/10.3390/molecules23102664.

[271] B. Jiang, Y. Zhang, L. Gu, W. Wu, H. Zhao, Y. Jin, Structural elucidation and antioxidant activity of lignin isolated from rice straw and alkali-oxygen black liquor, Int. J. Biol. Macromol. 116 (2018) 513–519. https://doi.org/10.1016/j.ijbiomac.2018.05.063.

[272] M-F. Li, S-N. Sun, F. Xu, R-C. Sun, Sequential solvent fractionation of heterogeneous bamboo organosolv lignin for value-added application, Sep. Purif. Technol. 101 (2012) 18–25. https://doi.org/10.1016/j.seppur.2012.09.013.

[273] P. Ma, Y. Gao, H. Zhai, Fractionated wheat straw lignin and its application as antioxidant, BioResources 8 (2013) 5581–5595. https://doi.org/10.15376/biores.8.4.5581-5595.

[274] J.H. Lora, W.G. Glasser, Recent industrial applications of lignin: A sustainable alternative to nonrenewable materials, J. Polym. Environ. 10 (2002) 39–48. https://doi.org/10.1023/A:1021070006895.

[275] Nippon Paper Group, (last accessed in March 2020). https://www.nipponpapergroup.com/english/products/chemical/lignin_products/#:~:text=Lignin is one of the,are used in many industries.

[276] M. Szycher, Szycher's handbook of polyurethanes, CRC Press (2012). https://doi.org/10.1201/b12343.

[277] E. Sharmin, F. Zafar, Polyurethane : An Introduction, In: Polyurethane, IntechOpen (2012).

[278] Polyurethanes, In: Handbook of Plastics Joining, William Andrew (2009). https://doi.org/10.1016/b978-0-8155-1581-4.50038-x.

[279] W.D. Vilar, Quimica e tecnologia dos poliuretanos, Vilar Consultoria, 1998.

[280] S. Das, P. Pandey, S. Mohanty, S.K. Nayak, Insight on Castor Oil Based Polyurethane and Nanocomposites: Recent Trends and Development, Polym. Plast. Technol. Eng. 56 (2017) 1556–1585. https://doi.org/10.1080/03602559.2017.1280685.

[281] C.S. Carriço, T. Fraga, V.M.D. Pasa, Production and characterization of polyurethane foams from a simple mixture of castor oil, crude glycerol and untreated lignin as bio-based polyols, Eur. Polym. J. 85 (2016) 53–61. https://doi.org/10.1016/j.eurpolymj.2016.10.012.

[282] N. Mahmood, Z. Yuan, J. Schmidt, C. Xu, Preparation of bio-based rigid polyurethane foam using hydrolytically depolymerized Kraft lignin via direct replacement or oxypropylation, Eur. Polym. J. 68 (2015) 1–9. https://doi.org/10.1016/j.eurpolymj.2015.04.030.

[283] J. Bernardini, P. Cinelli, I. Anguillesi, M.B. Coltelli, A. Lazzeri, Flexible polyurethane foams green production employing lignin or oxypropylated lignin, Eur. Polym. J. 64 (2015) 147–156. https://doi.org/10.1016/j.eurpolymj.2014.11.039.

[284] Y. Li, B.A.J. Noordover, R.A.T.M. Van Benthem, C.E. Koning, Bio-based poly(urethane urea) dispersions with low internal stabilizing agent contents and tunable

thermal properties, Prog. Org. Coatings. 86 (2015) 134–142. https://doi.org/10.1016/j.porgcoat.2015.04.018.

[285] Y. Li, B.A.J. Noordover, R.A.T.M. Van Benthem, C.E. Koning, Chain extension of dimer fatty acid- and sugar-based polyurethanes in aqueous dispersions, Eur. Polym. J. 52 (2014) 12–22. https://doi.org/10.1016/j.eurpolymj.2013.12.007.

[286] R.H. Aguirresarobe, L. Martin, N. Aramburu, L. Irusta, M.J. Fernandez-Berridi, Coumarin based light responsive healable waterborne polyurethanes, Prog. Org. Coatings 99 (2016) 314–321. https://doi.org/10.1016/j.porgcoat.2016.06.011.

[287] J. Wang, H. Zhang, Y. Miao, L. Qiao, X. Wang, F. Wang, UV-curable waterborne polyurethane from CO_2-polyol with high hydrolysis resistance, Polymer 100 (2016) 219–226. https://doi.org/10.1016/j.polymer.2016.08.039.

[288] S. Liu, X. Wang, Polymers from carbon dioxide: Polycarbonates, polyurethanes, Curr. Opin. Green Sustain. Chem. 3 (2017) 61–66. https://doi.org/10.1016/j.cogsc.2016.08.003.

[289] C.K. Patil, S.D. Rajput, R.J. Marathe, R.D. Kulkarni, H. Phadnis, D. Sohn, P.P. Mahulikar, V. V. Gite, Synthesis of bio-based polyurethane coatings from vegetable oil and dicarboxylic acids, Prog. Org. Coatings. 106 (2017) 87–95. https://doi.org/10.1016/j.porgcoat.2016.11.024.

[290] A. Noreen, K.M. Zia, M. Zuber, S. Tabasum, A.F. Zahoor, Bio-based polyurethane: An efficient and environment friendly coating systems: A review, Prog. Org. Coatings. 91 (2016) 25–32. https://doi.org/10.1016/j.porgcoat.2015.11.018.

[291] L. Poussard, J. Lazko, J. Mariage, J-M. Raquez, P. Dubois, Biobased waterborne polyurethanes for coating applications: How fully biobased polyols may improve the coating properties, Prog. Org. Coatings. 97 (2016) 175–183. https://doi.org/10.1016/j.porgcoat.2016.04.003.

[292] M. Marzec, J. Kucińska-Lipka, I. Kalaszczyńska, H. Janik, Development of polyurethanes for bone repair, Mater. Sci. Eng. C. 80 (2017) 736–747. https://doi.org/10.1016/j.msec.2017.07.047.

[293] M. Sultan, Polyurethane for removal of organic dyes from textile wastewater, Environ. Chem. Lett. 15 (2017) 347–366. https://doi.org/10.1007/s10311-016-0597-8.

[294] A. Kausar, Review on Technological Significance of Photoactive, Electroactive, pH Sensitive, Water-active, and Thermo-Responsive Polyurethane Materials, Polym. Plast. Technol. Eng. 56 (2017) 606–616. https://doi.org/10.1080/03602559.2016.1233279.

[295] J. Jin, Q-X. Dong, Z-J. Shu, W-J. Wang, K. He, Flame retardant Properties of Polyurethane/expandable Praphite Composites, Procedia Eng. 71 (2014) 304–309. https://doi.org/10.1016/j.proeng.2014.04.044.

[296] A. Tenorio-Alfonso, M.C. Sánchez, J.M. Franco, A Review of the Sustainable Approaches in the Production of Bio - based Polyurethanes and Their Applications in the Adhesive Field, J. Polym. Environ. 28 (2020) 749–774. https://doi.org/10.1007/s10924-020-01659-1.

[297] Q. Zhang, G. Zhang, J. Xu, C. Gao, Y. Wu, Recent advances on ligin-derived polyurethane polymers, Rev. Adv. Mater. Sci. 40 (2015) 146–154.

[298] I. Adipurnama, M-C. Yang, T. Ciach, B. Butruk-Raszeja, Surface modification and

endothelialization of polyurethane for vascular tissue engineering applications: a review, Biomater. Sci. 5 (2017) 22–37. https://doi.org/10.1039/C6BM00618C.

[299] B. Nohra, L. Candy, J.F. Blanco, C. Guerin, Y. Raoul, Z. Mouloungui, From petrochemical polyurethanes to biobased polyhydroxyurethanes, Macromolecules 46 (2013) 3771–3792. https://doi.org/10.1021/ma400197c.

[300] Y. Li, X. Luo, S. Hu, Bio-based Polyols and Polyurethanes, Springer (2015).

[301] G. Lligadas, J.C. Ronda, M. Galiá, V. Cádiz, Plant oils as platform chemicals for polyurethane synthesis: Current state-of-the-art, Biomacromolecules 11 (2010) 2825–2835. https://doi.org/10.1021/bm100839x.

[302] M. Desroches, M. Escouvois, R. Auvergne, S. Caillol, B. Boutevin, From vegetable oils to polyurethanes: Synthetic routes to polyols and main industrial products, Polym. Rev. 52 (2012) 38–79. https://doi.org/10.1080/15583724.2011.640443.

[303] U. Stirna, B. Lazdiņa, D. Vilsone, M.J. Lopez, M. Del Carmen Vargas-Garcia, F. Suárez-Estrella, J. Moreno, Structure and properties of the polyurethane and polyurethane foam synthesized from castor oil polyols, J. Cell. Plast. 48 (2012) 476–488. https://doi.org/10.1177/0021955X12445178.

[304] A.D. Macalino, V.A. Salen, L.Q. Reyes, Castor Oil Based Polyurethanes: Synthesis and Characterization, IOP Conf. Ser. Mater. Sci. Eng. 229 (2017) 012016. https://doi.org/10.1088/1757-899X/229/1/012016.

[305] S.S. Panda, B.P. Panda, S. Mohanty, S.K. Nayak, The castor oil based water borne polyurethane dispersion ; effect of -NCO/OH content : synthesis, characterization and properties, Green Process Synth. 6 (2016) 0144. https://doi.org/10.1515/gps-2016-0144.

[306] M.I. Attia, S. Zoorob, K. Hassan, H. El-Husseini, J.M. Reid, M.S. Al Kuwari, Development of building blocks using vegetable oil and recycled aggregate. MATEC Web Conf. 120 (2017) 03006. https://doi.org/10.1051/matecconf/201712003006.

[307] F. Chen, Z. Lu, Liquefaction of wheat straw and preparation of rigid polyurethane foam from the liquefaction products, J. Appl. Polym. Sci. 111 (2009) 508–516. https://doi.org/10.1002/app.29107.

[308] P. Lu, Y. Zhang, C. Jia, C. Wang, X. Li, M. Zhang, Polyurethane from liquefied wheat straw as coating material for controlled release fertilizers, BioResources 10 (2015) 7877–7888.

[309] T. Gürsoy, Water absorption and biodegradation properties of barley straw-contained polyurethane foams, In: Book of Abstract Proceedings, 8TH International Adavanced Technologies Symposium IATS (2017).

[310] M. Ertas, M.S. Fidan, M.H. Almat, Preparation and characterization of biodegradable rigid polyurethane foams from the liquefied eucalyptus and pine woods, Wood Res. 59 (2014) 97–108.

[311] Q. Wang, N. Tuohedi, Polyurethane Foams and Bio-Polyols from Liquefied Cotton Stalk Agricultural sustainability Polyurethane Foams and Bio-Polyols from Liquefied Cotton Stalk Agricultural Waste, Sustainability 12 (2020) 4214. https://doi.org/10.3390/su12104214.

[312] M.S. Fidan, M. Ertas, Biobased Rigid Polyurethane Foam Prepared from Apricot Stone Shell-based Polyol for Thermal Insulation Application - Part 2: Morphological,

Mechanical, and Thermal Properties, BioResources 15 (2020) 6080–6094.

[313] G. Zhang, Y. Wu, W. Chen, D. Han, X. Lin, G. Xu, Q. Zhang, Open-Cell Rigid Polyurethane Foams from Peanut Shell-Derived Polyols Prepared under Different Post-Processing Conditions, Polymers 11 (2019) 1392. https://doi.org/10.3390/polym11091392.

[314] Q. Zhang, X. Lin, W. Chen, H. Zhang, D. Han, Modification of rigid polyurethane foams with the addition of nano-SiO_2 or lignocellulosic biomass, Polymers 12 (2020) 107. https://doi.org/10.3390/polym12010107.

[315] T. Calvo-Correas, L. Ugarte, J.R. Ochoa-Gómez, T. Roncal, C. Diñeiro, M.A. Corcuera, A. Eceiza, Lignocellulosic Biomass as a Source of Raw Materials for the Synthesis of Polyurethanes, Proceedings 2 (2018) 1493. https://doi.org/10.3390/proceedings2231493.

[316] L. Wei, J. Zhang, W. Deng, S. Xie, Q. Zhang, Y. Wang, Catalytic transformation of 2,5-furandicarboxylic acid to adipic acid over niobic acid-supported Pt nanoparticles, Chem. Commun. 55 (2019) 8013–8016. https://doi.org/10.1039/c9cc02877c.

[317] F.L. Bernard, L.M. dos Santos, F.W. Cobalchina, M.B. Schwab, S. Einloft, Polyurethane/poly (ionic liquids) cellulosic composites and their evaluation for separation of CO_2 from natural gas, Mater. Res. 22 (2019) 20180827. https://doi.org/10.1590/1980-5373-MR-2018-0827.

[318] T. Zhang, Y. Zhao, M.S. Silverstein, Cellulose-based, highly porous polyurethanes templated within non-aqueous high internal phase emulsions, Cellulose 27 (2020) 4007–4018. https://doi.org/10.1007/s10570-020-03059-z.

[319] W. Wang, F. Wang, C. Zhang, Z. Wang, J. Tang, X. Zeng, X. Wan, Robust, Reprocessable, and Reconfigurable Cellulose-Based Multiple Shape Memory Polymer Enabled by Dynamic Metal-Ligand Bonds, ACS Appl. Mater. Interfaces. 12 (2020) 25233–25242. https://doi.org/10.1021/acsami.9b13316.

[320] M.M. Góes, M. Keller, V. Masiero Oliveira, L.D.G. Villalobos, J.C.G. Moraes, G.M. Carvalho, Polyurethane foams synthesized from cellulose-based wastes: Kinetics studies of dye adsorption, Ind. Crops Prod. 85 (2016) 149–158. https://doi.org/10.1016/j.indcrop.2016.02.051.

[321] L.J.Y. Jabber, J.C. Grumo, J.N. Patricio, M.R. Magdadaro, A.C. Alguno, A. Lubguban, Effect of cellulose-based fibers extracted from pineapple (*Ananas comosus*) leaf in the formation of polyurethane foam, J Fundam Appl Sci. 9 (2017) 134–143.

[322] L.J.Y. Jabber, J.C. Grumo, A.C. Alguno, A.A. Lubguban, R.Y. Capangpangan, The effect of cellulose fibers on the formation of petroleum-based and bio-based polyurethane foams, Key Eng. Mater. 803 (2019) 371–376. https://doi.org/10.4028/www.scientific.net/KEM.803.371.

[323] A. Hadjadj, O. Jbara, A. Tara, M. Gilliot, F. Malek, E.M. Maafi, L. Tighzert, Effects of cellulose fiber content on physical properties of polyurethane based composites, Compos. Struct. 135 (2016) 217–223. https://doi.org/10.1016/j.compstruct.2015.09.043.

[324] F.H. Ikhwan, S. Ilmiati, H. Kurnia Adi, R. Arumsari, M. Chalid, Novel route of synthesis for cellulose fiber-based hybrid polyurethane, IOP Conf. Ser. Mater. Sci. Eng. 223 (2017) 012019. https://doi.org/10.1088/1757-899X/223/1/012019.

[325] Y. Wang, Z. Cheng, Z. Liu, H. Kang, Y. Liu, Cellulose nanofibers/polyurethane shape memory composites with fast water-responsivity, J. Mater. Chem. B. 11 (2018) 1668–1677. https://doi.org/10.1039/c7tb03069j.

[326] S. Qin, M.G. Pour, S. Lazar, O. Köklükaya, J. Gerringer, Y. Song, L. Wågberg, J.C. Grunlan, Super Gas Barrier and Fire Resistance of Nanoplatelet/Nanofibril Multilayer Thin Films, Adv. Mater. Interfaces. 6 (2019) 1801424. https://doi.org/10.1002/admi.201801424.

[327] W. Guo, X. Wang, P. Zhang, J. Liu, L. Song, Y. Hu, Nano-fibrillated cellulose-hydroxyapatite based composite foams with excellent fire resistance, Carbohydr. Polym. 195 (2018) 71–78. https://doi.org/10.1016/j.carbpol.2018.04.063.

[328] L. Urbina, A. Alonso-Varona, A. Saralegi, T. Palomares, A. Eceiza, M.Á. Corcuera, A. Retegi, Hybrid and biocompatible cellulose/polyurethane nanocomposites with water-activated shape memory properties, Carbohydr. Polym. 216 (2019) 86–96. https://doi.org/10.1016/j.carbpol.2019.04.010.

[329] V. Kupka, Q. Zhou, F. Ansari, H. Tang, M. Šlouf, L. Vojtová, L.A. Berglund, J. Jančář, Well-dispersed polyurethane/cellulose nanocrystal nanocomposites synthesized by a solvent-free procedure in bulk, Polym. Compos. 40 (2019) 456–465. https://doi.org/10.1002/pc.24748.

[330] G.W. Yun, J.H. Lee, S.H. Kim, Flame retardant and mechanical properties of expandable graphite/polyurethane foam composites containing iron phosphonate dopamine-coated cellulose, Polym. Compos. (2020). https://doi.org/10.1002/pc.25578.

[331] X. Ge, C. Chang, L. Zhang, S. Cui, X. Luo, S. Hu, Y. Qin, Y. Li, Conversion of Lignocellulosic Biomass Into Platform Chemicals for Biobased Polyurethane Application, In: Advances in Bioenergy, Elsevier (2018). https://doi.org/10.1016/bs.aibe.2018.03.002.

[332] J.M. Robinson, C.E. Burgess, M.A. Bently, C.D. Brasher, B.O. Horne, D.M. Lillard, J.M. Macias, H.D. Mandal, S.C. Mills, K.D. O'Hara, J.T. Pon, A.F. Raigoza, E.H. Sanchez, J.S. Villarreal, The use of catalytic hydrogenation to intercept carbohydrates in a dilute acid hydrolysis of biomass to effect a clean separation from lignin, Biomass Bioenerg. 26 (2004) 473–483. https://doi.org/10.1016/j.biombioe.2003.09.005.

[333] M. Samavi, S. Rakshit, Utilization of Microbial Oil from Poplar Wood Hemicellulose Prehydrolysate for the Production of Polyol Using Chemo-enzymatic Epoxidation, Biotechnol. Bioprocess Eng. 25 (2020) 327–335. https://doi.org/10.1007/s12257-019-0416-8.

[334] J. Fernández-Rodríguez, X. Erdocia, P.L. de Hoyos, A. Sequeiros, J. Labidi, Catalytic Cascade Transformations of Biomass into Polyols, In: Production of Biofuels and Chemicals with Bifunctional Catalysts, Springer (2017). https://doi.org/10.1007/978-981-10-5137-1_6.

[335] H.N. Cheng, R.F. Furtado, C.R. Alves, M. do Socorro Rocha Bastos, S. Kim, A. Biswas, Novel polyurethanes from xylan and TDI: Preparation and characterization, Int. J. Polym. Anal. Charact. 22 (2017) 35–42. https://doi.org/10.1080/1023666X.2016.1222491.

[336] M. Magnusson, A study of alternative Polyurethane films with Hemicellulose Preparation and characterization methods, Ph. D. Thesis, Chalmers University of Technology (2017).

[337] Z. Hu, Z. Xiang, T. Song, F. Lu, Effects of crosslinking degree on the coating properties of arabinoxylan, BioResources 14 (2019) 70–86.

[338] B. Pakzad, M. Daryaei, M.D. Ashkezari, Coating of Polyurethane Scaffold With Arabinogalactan Leads to Increase of Adhesion to Fibroblast Cells by Integrin Molecules Pathway, Colloids Interface Sci. Commun. 22 (2018) 1–4. https://doi.org/10.1016/j.colcom.2017.11.003.

[339] A.F. Bafghi, M.D. Ashkezari, M. Vakili, S. Pournasir, Polyurethane sheet impregnated with Arabinogalactan can lead to increase of attachment of promastigotes and Amastigote of *Leishmania major* (MRHO/IR/75/ER) by *GP63* and *HSP70* genes, Mater. Sci. Eng. C. 91 (2018) 292–296. https://doi.org/10.1016/j.msec.2018.05.044.

[340] A.W. Sarkiliotis, K.H. Bauer, Synthesis and investigation of polyurethanes with galactomannan segment as auxiliary materials for the release of peptide drugs in the colon, Pharm. Ind. 54 (1992) 873–880.

[341] F. Zia, K.M. Zia, M. Zuber, H.B. Ahmad, M.I. Muneer, Glucomannan based polyurethanes: A critical short review of recent advances and future perspectives, Int. J. Biol. Macromol. 87 (2016) 229–236. https://doi.org/10.1016/j.ijbiomac.2016.02.058.

[342] M. Shao, Z-Q. Liu, D. Li, Y. Zhao, N. Özkan, X.D. Chen, Thermal properties of polyurethane films prepared from mixed cellulose, hemicelluloses and lignin, Int. J. Food Eng. 8 (2012) 1. https://doi.org/10.1515/1556-3758.1935.

[343] B.M. Upton, A.M. Kasko, Strategies for the conversion of lignin to high-value polymeric materials: Review and perspective, Chem. Rev. 116 (2016) 2275–2306. https://doi.org/10.1021/acs.chemrev.5b00345.

[344] C. Zhao, C. Huang, Q. Chen, I.D.V. Ingram, X. Zeng, T. Ren, H. Xie, Sustainable aromatic aliphatic polyesters and polyurethanes prepared from vanillin-derived diols via green catalysis, Polymers 12 (2020) 586. https://doi.org/10.3390/polym12030586.

[345] A. Gandini, M.N. Belgacem, Z-X. Guo, S. Montanari, Lignins as Macromonomers for Polyesters and Polyurethanes, In: Chemical Modification, Properties, and Usage of Lignin, Springer (2002). https://doi.org/10.1007/978-1-4615-0643-0_4.

[346] M. Alinejad, C. Henry, S. Nikafshar, A. Gondaliya, S. Bagheri, N. Chen, S.K. Singh, D.B. Hodge, M. Nejad, Lignin-Based Polyurethanes: Opportunities for Bio-Based Foams, Elastomers, Coatings and Adhesives, Polymers 11 (2019) 1202. https://doi.org/10.3390/polym11071202.

[347] S. Laurichesse, L. Avérous, Chemical modification of lignins: Towards biobased polymers, Prog. Polym. Sci. 39 (2014) 1266–1290. https://doi.org/10.1016/j.progpolymsci.2013.11.004.

[348] S. Nikafshar, Z. Fang, M. Nejad, Development of a Novel Curing Accelerator-Blowing Agent for Formulating Epoxy Rigid Foam Containing Aminated-Lignin, Ind. Eng. Chem. Res. 59 (2020) 15146–15154. https://doi.org/10.1021/acs.iecr.0c02738.

[349] N. Obaid, M.T. Kortschot, M. Sain, Lignin-Based Foaming Materials, In: Lignin in Polymer Composites, Elsevier (2016). https://doi.org/10.1016/B978-0-323-35565-0.00012-6.

[350] C.A. Cateto, M.F. Barreiro, A.E. Rodrigues, M.N. Belgacem, Kinetic study of the formation of lignin-based polyurethanes in bulk, React. Funct. Polym. 71 (2011) 863–869. https://doi.org/10.1016/j.reactfunctpolym.2011.05.007.

[351] P. Ortíz-Serna, M. Carsí, M. Culebras, M.N. Collins, M.J. Sanchis, Exploring the role of lignin structure in molecular dynamics of lignin/bio-derived thermoplastic elastomer polyurethane blends, Int. J. Biol. Macromol. 158 (2020) 1369–1379. https://doi.org/10.1016/j.ijbiomac.2020.04.261.

[352] R. Vendamme, J.T. Behaghel de Bueren, J. Gracia-Vitoria, F. Isnard, M. Monga Mulunda, P. Ortiz, M. Wadekar, K. Vanbroekhoven, C. Wegmann, R. Buser, F. Héroguel, J.S. Luterbacher, W. Eevers, Aldehyde-Assisted Lignocellulose Fractionation Provides Unique Lignin Oligomers for the Design of Tunable Polyurethane Bioresins, Biomacromolecules 21 (2020) 4135–4148. https://doi.org/10.1021/acs.biomac.0c00927.

[353] G. Griffini, V. Passoni, R. Suriano, M. Levi, S. Turri, Polyurethane Coatings Based on Chemically Unmodified Fractionated Lignin, ACS Sustain. Chem. Eng. 3 (2015) 1145–1154. https://doi.org/10.1021/acssuschemeng.5b00073.

[354] S.I.S. Shahabadi, J. Kong, X. Lu, Aqueous-Only, Green Route to Self-Healable, UV-Resistant, and Electrically Conductive Polyurethane/Graphene/Lignin Nanocomposite Coatings, ACS Sustain. Chem. Eng. 5 (2017) 3148–3157. https://doi.org/10.1021/acssuschemeng.6b02941.

[355] L. Zhang, J. Huang, Effects of nitrolignin on mechanical properties of polyurethane-nitrolignin films, J. Appl. Polym. Sci. 80 (2001) 1213–1219. https://doi.org/10.1002/app.1206.

[356] F.Q. Chu, X.J. Wu, Water-based UV-curable polyurethane based on wheat straw lignin obtained by ethanol extraction, Adv. Mater. Res. 295–297 (2011) 278–281. https://doi.org/10.4028/www.scientific.net/AMR.295-297.278.

[357] Z. Peng, F. Chen, Synthesis and properties of lignin-based polyurethane hydrogels, Int. J. Polym. Mater. Polym. Biomater. 60 (2011) 674–683. https://doi.org/10.1080/00914037.2010.551353.

[358] Y. Zhang, T-T. Li, C-W. Lou, J-H. Lin, Facile method for tent fabrics with eco-friendly/durable properties using waterborne polyurethane/lignin: Preparation and evaluation, J. Ind. Text. 0 (2020) 1–18. https://doi.org/10.1177/1528083720931884.

[359] S.S.L. Gonçalves, A. Rudnitskaya, A.J.M. Sales, L.M.C. Costa, D. V. Evtuguin, Nanocomposite polymeric materials based on eucalyptus lignoboost® Kraft lignin for liquid sensing applications, Materials 13 (2020) 1637. https://doi.org/10.3390/ma13071637.

[360] M.S. Karunarathna, R.C. Smith, Valorization of lignin as a sustainable component of structural materials and composites: Advances from 2011 to 2019, Sustain. 12 (2020)734 . https://doi.org/10.3390/su12020734.

[361] L. Hojabri, X. Kong, S.S. Narine, Fatty Acid-Derived diisocyanate and biobased polyurethane produced from vegetable oil: Synthesis, polymerization, and characterization, Biomacromolecules 10 (2009) 884–891. https://doi.org/10.1021/bm801411w.

[362] M.S. Kathalewar, P.B. Joshi, A.S. Sabnis, V.C. Malshe, Non-isocyanate polyurethanes: From chemistry to applications, RSC Adv. 3 (2013) 4110–4129. https://doi.org/10.1039/c2ra21938g.

[363] F.E. Kalinina, D.M. Mognonov, L.D. Radnaeva, Poly(hydroxy urethane) coatings prepared from copolymers of 3-(2-vinyloxyethoxy)-l,2-propylene carbonate and N-

phenylmaleimide, Russ. J. Appl. Chem. 81 (2008) 1302–1304. https://doi.org/10.1134/S1070427208070367.

[364] O. Figovsky, L. Shapovalov, F. Buslov, Ultraviolet and thermostable non-isocyanate polyurethane coatings, Surf. Coatings Int. Part B Coatings Trans. 88 (2005) 67–71. https://doi.org/10.1007/BF02699710.

[365] M. Bähr, R. Mülhaupt, Linseed and soybean oil-based polyurethanes prepared *via* the non-isocyanate route and catalytic carbon dioxide conversion, Green Chem. 2 (2012) 483–489. https://doi.org/10.1039/c2gc16230j.

[366] A.R. Mahendran, N. Aust, G. Wuzella, U. Müller, A. Kandelbauer, Bio-Based Non-Isocyanate Urethane Derived from Plant Oil, J. Polym. Environ. 20 (2012) 926–931. https://doi.org/10.1007/s10924-012-0491-9.

[367] M. Calle, G. Lligadas, J.C. Ronda, M. Galià, V. Cádiz, Non-isocyanate route to biobased polyurethanes and polyureas via AB-type self-polycondensation, Eur. Polym. J. 84 (2016) 837–848. https://doi.org/10.1016/j.eurpolymj.2016.04.022.

[368] M.A. Levina, D.G. Miloslavskii, M. V. Zabalov, M.L. Pridatchenko, A. V. Gorshkov, V.T. Shashkova, V.L. Krasheninnikov, R.P. Tiger, Green Chemistry of Polyurethanes: Synthesis, Functional Composition, and Reactivity of Cyclocarbonate-Containing Sunflower Oil Triglycerides—Renewable Raw Materials for New Urethanes, Polym. Sci. - Ser. B 61 (2019) 540–549. https://doi.org/10.1134/S1560090419050117.

[369] B. Burchardt, Advances in polyurethane structural adhesives, In: Advances in Structural Adhesive Bonding, Woodhead Publishing (2010). https://doi.org/10.1533/9781845698058.1.35.

[370] A.K. Poh, L.C. Sin, C.S. Foon, C.C. Hock, Polyurethane wood adhesive from palm oil-based polyester polyol, J. Adhes. Sci. Technol. 28 (2014) 1020–1033. https://doi.org/10.1080/01694243.2014.883772.

[371] M.H. Mahmood, S.N. Baharom, R. Tajau, M.Z. Salleh, K.Z.M. Dahlan, R.C. Ismail, Effect of structure and molecular weight on properties of pressure sensitive adhesives (PSA) formulated from palm oil based urethane acrylate (POBUA), J. Nucl. Relat. Technol. 1 (2004) 51–62.

[372] S.M. Norhisham, T.I.T.N. Maznee, H.N. Ain, P.P.K. Devi, A. Srihanum, M.N. Norhayati, S.K. Yeong, A.H. Hazimah, C.M. Schiffman, A. Sendijarevic, V. Sendijarevic, I. Sendijarevic, Soft polyurethane elastomers with adhesion properties based on palm olein and palm oil fatty acid methyl ester polyols, Int. J. Adhes. Adhes. 73 (2017) 38–44. https://doi.org/10.1016/j.ijadhadh.2016.10.012.

[373] N.M. Zain, E.N. Roslin, S. Ahmad, Preliminary study on bio-based polyurethane adhesive/aluminum laminated composites for automotive applications, Int. J. Adhes. Adhes. 71 (2016) 1–9. https://doi.org/10.1016/j.ijadhadh.2016.08.001.

[374] M.M. Aung, Z. Yaakob, S. Kamarudin, L.C. Abdullah, Synthesis and characterization of Jatropha (*Jatropha curcas* L.) oil-based polyurethane wood adhesive, Ind. Crops Prod. 60 (2014) 177–185. https://doi.org/10.1016/j.indcrop.2014.05.038.

[375] L. Man, Y. Feng, Y. Hu, T. Yuan, Z. Yang, A renewable and multifunctional eco-friendly coating from novel tung oil-based cationic waterborne polyurethane dispersions, J. Clean. Prod. 241 (2019) 118341. https://doi.org/10.1016/j.jclepro.2019.118341.

[376] E. Orgilés-Calpena, F. Arán-Aís, A.M. Torró-Palau, C. Orgilés-Barcelo, Biodegradable polyurethane adhesives based on polyols derived from renewable resources, Proc. Inst. Mech. Eng. Part L J. Mater. Des. Appl. 228 (2014) 125–136. https://doi.org/10.1177/1464420713517674.

[377] A. Tenorio-Alfonso, M.C. Sánchez, J.M. Franco, Preparation, Characterization and Mechanical Properties of Bio-Based Polyurethane Adhesives from Isocyanate-Functionalized Cellulose Acetate and Castor Oil for Bonding Wood, Polymers 9 (2017) 132. https://doi.org/10.3390/polym9040132.

[378] A. Tenorio-alfonso, M.L. Pizarro, M.C. Sánchez, J.M. Franco, Assessing the rheological properties and adhesion performance on di ff erent substrates of a novel green polyurethane based on castor oil and cellulose acetate : A comparison with commercial adhesives, Int. J. Adhes. Adhes. 82 (2018) 21–26. https://doi.org/10.1016/j.ijadhadh.2017.12.012.

[379] A. Tenorio-Alfonso, M.C. Sánchez, J.M. Franco, Synthesis and mechanical properties of bio-sourced polyurethane adhesives obtained from castor oil and MDI-modified cellulose acetate: Influence of cellulose acetate modification, Int. J. Adhes. Adhes. 95 (2019) 102404. https://doi.org/10.1016/j.ijadhadh.2019.102404.

[380] L.C. Raghunanan, S. Fernandez-Prieto, I. Martínez, C. Valencia, M.C. Sánchez, J.M. Franco, Molecular insights into the mechanisms of humidity-induced changes on the bulk performance of model castor oil derived polyurethane adhesives, Eur. Polym. J. 101 (2018) 291–303. https://doi.org/10.1016/j.eurpolymj.2018.02.041.

[381] H.D. Santan, C. James, E. Fratini, I. Martínez, C. Valencia, M.C. Sánchez, J.M. Franco, Structure-property relationships in solvent free adhesives derived from castor oil, Ind. Crops Prod. 121 (2018) 90–98. https://doi.org/10.1016/j.indcrop.2018.05.012.

[382] P.R. Oliveira, M. May, T.H. Panzera, F. Scarpa, S. Hiermaier, Reinforced biobased adhesive for eco-friendly sandwich panels, Int. J. Adhes. Adhes. 98 (2020) 102550. https://doi.org/10.1016/j.ijadhadh.2020.102550.

[383] P. Ferreira, R. Pereira, J.F.J. Coelho, A.F.M. Silva, M.H. Gil, Modification of the biopolymer castor oil with free isocyanate groups to be applied as bioadhesive, Int. J. Biol. Macromol. 40 (2007) 144–152. https://doi.org/10.1016/j.ijbiomac.2006.06.023.

[384] Q. Su, D. Wei, W. Dai, Y. Zhang, Z. Xia, Designing a castor oil-based polyurethane as bioadhesive, Colloids Surfaces B Biointerfaces 181 (2019) 740–748. https://doi.org/10.1016/j.colsurfb.2019.06.032.

[385] Y.L. Uscátegui, S.J. Arévalo-Alquichire, J.A. Gómez-Tejedor, A. Vallés-Lluch, L.E. Díaz, M.F. Valero, Polyurethane-based bioadhesive synthesized from polyols derived from castor oil (*Ricinus communis*) and low concentration of chitosan, J. Mater. Res. 32 (2017) 3699–3711. https://doi.org/10.1557/jmr.2017.371.

[386] D.L. Faria, T.A. Lopes, M.V. Scatolino, T. de P. Protásio, M.F. Do Nascimento, F.A.R. Lahr, L.M. Mendes, J.B. Guimarães Júnior, Studying the grammage in LVL panels glued with castor oil-based polyurethane adhesive: A possible alternative to formaldehyde releasing adhesives, Cerne 26 (2020) 140–149. https://doi.org/10.1590/01047760202026012691.

[387] N. Gama, A. Ferreira, A. Barros-Timmons, Cure and performance of castor oil polyurethane adhesive, Int. J. Adhes. Adhes. 95 (2019) 102413. https://doi.org/10.1016/j.ijadhadh.2019.102413.

[388] D.A. Babb, Polyurethanes from renewable resources, In: Synthetic Biodegradable Polymers, Springer (2012). https://doi.org/10.1007/12_2011_130.

[389] B. Sreenivasan, N.R. Kamath, J.G. Kane, Studies on castor oil. I. Fatty acid composition of castor oil, J. Am. Oil Chem. Soc. 33 (1956) 61–66. https://doi.org/10.1007/BF02612549.

[390] S.F. Thames, M.O. Bautista, M.D. Watson, M.D. Wang, Application of Lesquerella Oil in Industrial Coatings, In: Polymers from Agricultural Coproducts, ACS (1994). https://doi.org/10.1021/bk-1994-0575.ch015.

[391] S.F. Thames, M.O. Bautista, H. Yu, K.G. Panjnani, M.D. Wang, Lesquerella: renewable resource for industrial coatings and polyurethane foams, Int. SAMPE Symp. Exhib. 41 (1996) 1191–1202.

[392] W. Jiang, A. Kumar, S. Adamopoulos, Liquefaction of lignocellulosic materials and its applications in wood adhesives—A review, Ind. Crops Prod. 124 (2018) 325–342. https://doi.org/10.1016/j.indcrop.2018.07.053.

[393] W-J. Lee, M.S. Lin, Preparation and application of polyurethane adhesives made from polyhydric alcohol liquefied taiwan acacia and china fir, J. Appl. Polym. Sci. 109 (2008) 23–31. https://doi.org/10.1002/app.28007.

[394] R. Mori, Inorganic–organic hybrid biodegradable polyurethane resin derived from liquefied Sakura wood, Wood Sci. Technol. 49 (2015) 507–516. https://doi.org/10.1007/s00226-015-0707-y.

[395] M.F. Juhaida, M.T. Paridah, M.M. Hilmi, Z. Sarani, H. Jalaluddin, A.R. Mohamad Zaki, Liquefaction of kenaf (*Hibiscus cannabinus* L.) core for wood laminating adhesive, Bioresour. Technol. 101 (2010) 1355–1360. https://doi.org/10.1016/j.biortech.2009.09.048.

[396] S-I. Tohmura, G-Y. Li, T-F. Qin, Preparation and characterization of wood polyalcohol-based isocyanate adhesives, J. Appl. Polym. Sci. 98 (2005) 791–795. https://doi.org/10.1002/app.22072.

[397] L. Jasiūnas, G. Peck, D. Bridžiuvienė, L. Miknius, Mechanical, thermal properties and stability of high renewable content liquefied residual biomass derived bio-polyurethane wood adhesives, Int. J. Adhes. Adhes. 101 (2020) 102618. https://doi.org/10.1016/j.ijadhadh.2020.102618.

[398] S. Balcioglu, H. Parlakpinar, N. Vardi, E.B. Denkbas, M.G. Karaaslan, S. Gulgen, E. Taslidere, S. Koytepe, B. Ates, Design of Xylose-Based Semisynthetic Polyurethane Tissue Adhesives with Enhanced Bioactivity Properties, ACS Appl. Mater. Interfaces 8 (2016) 4456–4466. https://doi.org/10.1021/acsami.5b12279.

[399] R.A. Rackham, Use of xylan to improve bond strength (2005).

[400] O.H.H. Hsu, W.G. Glasser, Polyurethane adhesives and coatings from modified lignin, J. Appl. Polym. Sci. Appl. Polym. Symp. 378 (1975) 297–307.

[401] J.C. De Haro, C. Allegretti, A.T. Smit, S. Turri, P. D'Arrigo, G. Griffini, Biobased Polyurethane Coatings with High Biomass Content: Tailored Properties by Lignin Selection, ACS Sustain. Chem. Eng. 7 (2019) 11700–11711. https://doi.org/10.1021/acssuschemeng.9b01873.

[402] Y. Chen, H. Zhang, Z. Zhu, S. Fu, High-value utilization of hydroxymethylated lignin

in polyurethane adhesives, Int. J. Biol. Macromol. 152 (2020) 775–785. https://doi.org/10.1016/j.ijbiomac.2020.02.321.

[403] J.R. Gouveia, L.D. Antonino, G.E.S. Garcia, L.B. Tavares, A.N.B. Santos, D.J. dos Santos, Kraft lignin-containing polyurethane adhesives: the role of hydroxypropylation on thermomechanical properties, J. Adhes. (2020). https://doi.org/10.1080/00218464.2020.1784148.

[404] V. Ibrahim, G. Mamo, P-J. Gustafsson, R. Hatti-Kaul, Production and properties of adhesives formulated from laccase modified Kraft lignin, Ind. Crops Prod. 45 (2013) 343–348. https://doi.org/10.1016/j.indcrop.2012.12.051.

[405] J. Lima-García, G. Pans, C. Phanopoulos, Use of lignin in polyurethane based structural wood adhesives, J. Adhes. 94 (2018) 814–828. https://doi.org/10.1080/00218464.2017.1385458.

[406] S. Wang, Y. Yu, M. Di, Green modification of corn stalk lignin and preparation of environmentally friendly lignin-based wood adhesive, Polymers 10 (2018) 631. https://doi.org/10.3390/polym10060631.

[407] A.S. Lyadov, Y.M. Maksimova, A.S. Shakhmatova, V. V. Kirillov, O.P. Parenago, Urea (Polyurea) Greases, Russ. J. Appl. Chem. 91 (2018) 885–894. https://doi.org/10.1134/S1070427218060010.

[408] U. Chandra Sharma, N. Singh, Biogreases for Environment Friendly Lubrication, in: Environonmental Science & Engineering Vol. 1 Sustainable Development, Studium Press (2019).

[409] R. Gallego, T. Cidade, R. Sánchez, C. Valencia, J.M. Franco, Tribological behaviour of novel chemically modified biopolymer-thickened lubricating greases investigated in a steel–steel rotating ball-on-three plates tribology cell, Tribol. Int. 94 (2016) 652–660. https://doi.org/10.1016/j.triboint.2015.10.028.

[410] Y. Ma, Z. Li, H. Wang, H. Li, Synthesis and optimization of polyurethane microcapsules containing [BMIm]PF6 ionic liquid lubricant, J. Colloid Interface Sci. 534 (2019) 469–479. https://doi.org/10.1016/j.jcis.2018.09.059.

[411] T. Litters, F. Hahn, T. Goerz, H.J. Erkel, Process for the preparation of polyurea-thickened lignin derivative-based lubricating greases, such lubricant greases and use thereof (2016).

[412] J.R. Aureliano Perez, K.A. Vaught, G.P. Hansen, Low volatile organic content lubricant (2005).

[413] H.W. Parker, R.W. Tock, F. Qiao, R.S. Lenox, Elastomeric material compositions obtained from castor oil and epoxidized soybean oil (2004).

[414] Z. Dai, P. Jiang, W. Lou, P. Zhang, Y. Bao, X. Gao, J. Xia, A. Haryono, Preparation of degradable vegetable oil-based waterborne polyurethane with tunable mechanical and thermal properties, Eur. Polym. J. 139 (2020) 109994. https://doi.org/10.1016/j.eurpolymj.2020.109994.

[415] K. Mizera, J. Ryszkowska, Polyurethane elastomers from polyols based on soybean oil with a different molar ratio, Polym. Degrad. Stab. 132 (2016) 21–31. https://doi.org/10.1016/j.polymdegradstab.2016.05.004.

[416] K. Zheng, J. Zhang, J. Cheng, Morphology, structure, miscibility, and properties of

wholly soy-based semi-interpenetrating polymer networks from soy-oil-polyol-based polyurethane and modified soy protein isolate, Ind. Eng. Chem. Res. 52 (2013) 14335–14341. https://doi.org/10.1021/ie401791v.

[417] I. Javni, W. Zhang, Z.S. Petrović, Effect of different isocyanates on the properties of soy-based polyurethanes, J. Appl. Polym. Sci. 88 (2003) 2912–2916. https://doi.org/10.1002/app.11966.

[418] P.K.S. Pillai, M.C. Floros, S.S. Narine, Elastomers from Renewable Metathesized Palm Oil Polyols, ACS Sustain. Chem. Eng. 5 (2017) 5793–5799. https://doi.org/10.1021/acssuschemeng.7b00517.

[419] H.M.C.C. Somarathna, S.N. Raman, K.H. Badri, A.A. Mutalib, D. Mohotti, S.D. Ravana, Quasi-static behavior of palm-based elastomeric polyurethane: For strengthening application of structures under impulsive loadings, Polymers 8 (2016) 202. https://doi.org/10.3390/polym8050202.

[420] S. Michałowski, M.A. Mosiewicki, M. Kurańska, M.I. Aranguren, A. Prociak, Polyurethane composites synthesized using natural oil-based polyols and sisal fibers, J. Renew. Mater. 6 (2018) 426–437. https://doi.org/10.7569/JRM.2017.634163.

[421] K. Mizera, J. Ryszkowska, M. Kurańska, A. Prociak, The effect of rapeseed oil-based polyols on the thermal and mechanical properties of ureaurethane elastomers, Polym. Bull. 77 (2020) 823–846. https://doi.org/10.1007/s00289-019-02774-3.

[422] H. Blache, F. Méchin, A. Rousseau, É. Fleury, J.P. Pascault, P. Alcouffe, N. Jacquel, R. Saint-Loup, New bio-based thermoplastic polyurethane elastomers from isosorbide and rapeseed oil derivatives, Ind. Crops Prod. 121 (2018) 303–312. https://doi.org/10.1016/j.indcrop.2018.05.004.

[423] O.S. Yemul, Z.S. Petrović, Thermoplastic polyurethane elastomers from modified oleic acid, Polym. Int. 63 (2014) 1771–1776. https://doi.org/10.1002/pi.4771.

[424] K. Mizera, M. Kirpluks, U. Cabulis, M. Leszczyńska, M. Półka, J. Ryszkowska, Characterisation of ureaurethane elastomers containing tall oil based polyols, Ind. Crops Prod. 113 (2018) 98–110. https://doi.org/10.1016/j.indcrop.2018.01.019.

[425] K. Pietrzak, M. Kirpluks, U. Cabulis, J. Ryszkowska, Effect of the addition of tall oil-based polyols on the thermal and mechanical properties of ureaurethane elastomers, Polym. Degrad. Stab. 108 (2014) 201–211. https://doi.org/10.1016/j.polymdegradstab.2014.03.038.

[426] D. Pasquini, Fully Green Elastomer Composites, In: Advances in Elastomers II, Springer (2013). https://doi.org/10.1007/978-3-642-20928-4_5.

[427] N.D. Ghatge, V.B. Phadke, Elastomers from castor oil, J. Appl. Polym. Sci. 11 (1967) 629–638. https://doi.org/10.1002/app.1967.070110502.

[428] W. Zhang, Y. Zhang, H. Liang, D. Liang, H. Cao, C. Liu, Y. Qian, Q. Lu, C. Zhang, High bio-content castor oil based waterborne polyurethane/sodium lignosulfonate composites for environmental friendly UV absorption application, Ind. Crops Prod. 142 (2019) 111836. https://doi.org/10.1016/j.indcrop.2019.111836.

[429] F. Abdolhosseini, M. Kazem, B. Givi, Characterization of a Biodegradable Polyurethane Elastomer Derived from Castor Oil, Am. J. Polym. Sci. 6 (2016) 18–27.

[430] E. Hablot, D. Zheng, M. Bouquey, L. Avérous, Polyurethanes based on castor oil:

Kinetics, chemical, mechanical and thermal properties, Macromol. Mater. Eng. 293 (2008) 922–929. https://doi.org/10.1002/mame.200800185.

[431] L.B. Tavares, C.V. Boas, G.R. Schleder, A.M. Nacas, D.S. Rosa, D.J. Santos, Bio-based polyurethane prepared from Kraft lignin and modified castor oil, Express Polym. Lett. 10 (2016) 927–940. https://doi.org/10.3144/expresspolymlett.2016.86.

[432] A. Cassales, L.A. Ramos, E. Frollini, Synthesis of bio-based polyurethanes from Kraft lignin and castor oil with simultaneous film formation, Int. J. Biol. Macromol. 145 (2020) 28–41. https://doi.org/10.1016/j.ijbiomac.2019.12.173.

[433] S. Arévalo-Alquichire, M. Valero, Castor Oil Polyurethanes as Biomaterials, In: Elastomers, IntechOpen (2017). https://doi.org/10.5772/intechopen.68597.

[434] S. Oprea, Synthesis and properties of polyurethane elastomers with castor oil as crosslinker, J. Am. Oil Chem. Soc. 87 (2010) 313–320. https://doi.org/10.1007/s11746-009-1501-5.

[435] X-P. An, J-H. Chen, Y-D. Li, J. Zhu, J-B. Zeng, Rational design of sustainable polyurethanes from castor oil: towards simultaneous reinforcement and toughening, Sci. China Mater. 61 (2018) 993–1000. https://doi.org/10.1007/s40843-017-9192-8.

[436] Z. Gao, J. Peng, T. Zhong, J. Sun, X. Wang, C. Yue, Biocompatible elastomer of waterborne polyurethane based on castor oil and polyethylene glycol with cellulose nanocrystals, Carbohydr. Polym. 87 (2012) 2068–2075. https://doi.org/10.1016/j.carbpol.2011.10.027.

[437] S.N. Jaisankar, Y. Lakshminarayana, G. Radhakrishnan, T. Ramasami, Modified castor oil based polyurethane elastomers for one-shot process, Polym. - Plast. Technol. Eng. 35 (1996) 781–789. https://doi.org/10.1080/03602559608004060.

[438] S. Oprea, Dependence of fungal biodegradation of PEG/castor oil-based polyurethane elastomers on the hard-segment structure, Polym. Degrad. Stab. 95 (2010) 2396–2404. https://doi.org/10.1016/j.polymdegradstab.2010.08.013.

[439] M.F. Valero, Y. Ortegón, Polyurethane elastomers-based modified castor oil and poly(ε-caprolactone) for surface-coating applications: Synthesis, characterization, and in vitro degradation, J. Elastomers Plast. 47 (2015) 360–369.

[440] R. Ducharme, Multi-composite acoustic panel (2004).

[441] H. Bi, Z. Ren, R. Guo, M. Xu, Y. Song, Fabrication of flexible wood flour/thermoplastic polyurethane elastomer composites using fused deposition molding, Ind. Crops Prod. 122 (2018) 76–84. https://doi.org/10.1016/j.indcrop.2018.05.059.

[442] F. Mengeloğlu, V. Çavuş, Preparation of thermoplastic polyurethane-based biocomposites through injection molding: Effect of the filler type and content, BioResources 15 (2020) 5749–5763.

[443] T. Guodong, Z. Yu, X. Jiming, Z. Jianying, W. Yiwei, Rice straw liquefying method and method for synthesizing polyurethane elastomer from rice straw liquefying product (2014).

[444] S.L. Zhao, Z.H. Xue, Y.B. Li, J.T. Huang, Study on straw liquefied product synthetizing polyurethane elastomer, Adv. Mater. Res., 821-822 (2013) 977–980. https://doi.org/10.4028/www.scientific.net/AMR.821-822.977.

[445] Q. Yan, S. Zhao, H. Kang, S. Zhang, Thiol-assisted bioinspired deposition of

polyurethane onto cellulose as robust elastomer for reinforcing soy protein-based composites, J. Appl. Polym. Sci. 137 (2020) 49176. https://doi.org/10.1002/app.49176.

[446] Q. Wu, M. Henriksson, X. Liu, L.A. Berglund, A high strength nanocomposite based on microcrystalline cellulose and polyurethane, Biomacromolecules. 8 (2007) 3687–3692. https://doi.org/10.1021/bm701061t.

[447] A. Pei, J.M. Malho, J. Ruokolainen, Q. Zhou, L.A. Berglund, Strong nanocomposite reinforcement effects in polyurethane elastomer with low volume fraction of cellulose nanocrystals, Macromolecules 44 (2011) 4422–4427. https://doi.org/10.1021/ma200318k.

[448] Y. Zhu, J. Hu, H. Luo, R.J. Young, L. Deng, S. Zhang, Y. Fan, G. Ye, Rapidly switchable water-sensitive shape-memory cellulose/elastomer nano-composites, Soft Matter 8 (2012) 2509–2517. https://doi.org/10.1039/c2sm07035a.

[449] M.I. Aranguren, N.E. Marcovich, W. Salgueiro, A. Somoza, Effect of the nano-cellulose content on the properties of reinforced polyurethanes. A study using mechanical tests and positron anihilation spectroscopy, Polym. Test. 32 (2013) 115–122. https://doi.org/10.1016/j.polymertesting.2012.08.014.

[450] A. Saralegi, L. Rueda, L. Martin, A. Arbelaiz, A. Eceiza, M.A. Corcuera, From elastomeric to rigid polyurethane/cellulose nanocrystal bionanocomposites, Compos. Sci. Technol. 88 (2013) 39–47. https://doi.org/10.1016/j.compscitech.2013.08.025.

[451] M. Lee, M.H. Heo, H-H. Lee, Y-W. Kim, J. Shin, Tunable softening and toughening of individualized cellulose nanofibers-polyurethane urea elastomer composites, Carbohydr. Polym. 159 (2017) 125–135. https://doi.org/10.1016/j.carbpol.2016.12.019.

[452] Y. Lu, L. Zhang, Morphology and mechanical properties of semi-interpenetrating polymer networks from polyurethane and benzyl konjac glucomannan, Polymer 43 (2002) 3979–3986. https://doi.org/10.1016/S0032-3861(02)00206-9.

[453] S. Gao, L. Zhang, J. Cao, Synthesis and Characterization of Poly(ester urethane)/Nitrokonjac Glucomannan Semi-Interpenetrating Polymer Networks, J. Appl. Polym. Sci. 90 (2003) 2224–2228. https://doi.org/10.1002/app.12882.

[454] Y. Lu, L. Zhang, X. Zhang, Y. Zhou, Effects of secondary structure on miscibility and properties of semi-IPN from polyurethane and benzyl konjac glucomannan, Polymer 44 (2003) 6689–6696. https://doi.org/10.1016/S0032-3861(03)00594-9.

[455] H. Li, Y. Liang, P. Li, C. He, Conversion of biomass lignin to high-value polyurethane: A review, J. Bioresour. Bioprod. 5 (2020) 163–179. https://doi.org/10.1016/j.jobab.2020.07.002.

[456] H. Gang, D. Lee, K-Y. Choi, H-N. Kim, H. Ryu, D-S. Lee, B-G. Kim, Development of High Performance Polyurethane Elastomers Using Vanillin-Based Green Polyol Chain Extender Originating from Lignocellulosic Biomass, ACS Sustain. Chem. Eng. 5 (2017) 4582–4588. https://doi.org/10.1021/acssuschemeng.6b02960.

[457] R. Wang, B. Zhou, Y. Zhu, Z. Wang, Effects of lignin-derived polycarboxylic acids on the properties of waterborne polyurethane elastomers, Int. J. Polym. Sci. 2018 (2018) 7989367. https://doi.org/10.1155/2018/7989367.

[458] H. Li, J-T. Sun, C. Wang, S. Liu, D. Yuan, X. Zhou, J. Tan, L. Stubbs, C. He, High Modulus, Strength, and Toughness Polyurethane Elastomer Based on Unmodified Lignin, ACS Sustain. Chem. Eng. 5 (2017) 7942–7949.

https://doi.org/10.1021/acssuschemeng.7b01481.

[459] Y. Zhang, R. Yan, T-D. Ngo, Q. Zhao, J. Duan, X. Du, Y. Wang, B. Liu, Z. Sun, W. Hu, H. Xie, Ozone oxidized lignin-based polyurethane with improved properties, Eur. Polym. J. 117 (2019) 114–122. https://doi.org/10.1016/j.eurpolymj.2019.05.006.

[460] W. Liu, C. Fang, S. Wang, J. Huang, X. Qiu, High-Performance Lignin-Containing Polyurethane Elastomers with Dynamic Covalent Polymer Networks, Macromolecules 52 (2019) 6474–6484. https://doi.org/10.1021/acs.macromol.9b01413.

[461] C. Ciobanu, M. Ungureanu, L. Ignat, D. Ungureanu, V.I. Popa, Properties of lignin-polyurethane films prepared by casting method, Ind. Crops Prod. 20 (2004) 231–241. https://doi.org/10.1016/j.indcrop.2004.04.024.

[462] D. Kai, M.J. Tan, P.L. Chee, Y.K. Chua, Y.L. Yap, X.J. Loh, Towards lignin-based functional materials in a sustainable world, Green Chem. 18 (2016) 1175–1200. https://doi.org/10.1039/c5gc02616d.

[463] M. Culebras, A. Beaucamp, Y. Wang, M.M. Clauss, E. Frank, M.N. Collins, Biobased Structurally Compatible Polymer Blends Based on Lignin and Thermoplastic Elastomer Polyurethane as Carbon Fiber Precursors, ACS Sustain. Chem. Eng. 6 (2018) 8816–8825. https://doi.org/10.1021/acssuschemeng.8b01170.

[464] H. Li, G. Sivasankarapillai, A.G. McDonald, Lignin valorization by forming toughened thermally stimulated shape memory copolymeric elastomers: Evaluation of different fractionated industrial lignins, J. Appl. Polym. Sci. 132 (2015) 41389. https://doi.org/10.1002/app.41389.

[465] P. Frigerio, L. Zoia, M. Orlandi, T. Hanel, L. Castellani, Application of sulphur-free lignins as a filler for elastomers: Effect of hexamethylenetetramine treatment, BioResources 9 (2014) 1387–1400. https://doi.org/10.15376/biores.9.1.1387-1400.

[466] J. Zhang, Y. Chen, P. Sewell, M.A. Brook, Utilization of softwood lignin as both crosslinker and reinforcing agent in silicone elastomers, Green Chem. 17 (2015) 1811–1819. https://doi.org/10.1039/c4gc02409e.

[467] G. Engelmann, J. Ganster, Lignin Reinforcement in Thermosets Composites, In: Lignin in Polymer Composites, William Andrew (2016). https://doi.org/10.1016/B978-0-323-35565-0.00007-2.

Chapter 3:

Materials & Methods

1. Materials

1.1. Non-fractionated lignocellulose sources

Two lignocellulose sources were used as polyols and/or thickeners for the production of oleogels with lubricating properties, wheat (*Triticum aestivum* var. maestro) and barley (*Hordeum vulgare*) straw. Both wheat and barley straws were treated with *Streptomyces* MDG301 through a solid-state fermentation process. These biosources were acquired, treated and kindly supplied to our Research Centre by the Department of Biomedicine and Biotechnology of the University of Alcalá de Henares, in the framework of a collaborative project (CTQ2014-56038-C3-1R and CTQ2014-56038-C3-2R). Uninoculated and fermented systems were milled by employing a MF 10 basic microfine grinder drive (IKA, Germany) equipped with 0.25 pore size sieve prior to functionalization.

Both straws composition ranged from 30-35 wt% of lignin and 58-62 wt% of holocellulose content.

1.2. Fractionated lignocellulose sources

1.2.1. Cellulose pulp

Cellulose pulp obtained from the fractionation through solid-state fermentation (with and without inoculation with a *Streptomyces* strain) and further soda pulping process of both wheat and barley straws were likewise used as thickening or gelling agents for lubricating grease formulations. In this case, two different *Streptomyces* strains, MDG147 and MDG301 were employed. MDG301, being a thermophilic strain with an optimum temperature at 45ºC, was tested at 28 and 45ºC to evaluate the differences obtained by applying the two conditions. These fractions were likewise treated and donated by the University of Alcalá de Henares and the INIA-CIFOR Research Centre. Similar milling as mentioned in the previous section was carried out.

Cellulose pulp comprises a mix of the three main lignocellulosic components, with cellulose as the main constituent, but also including a relatively high percentage of hemicellulose and some lignin content. In general terms, concentrations were around, 63, 32 and 5 wt% of cellulose, hemicellulose and lignin, respectively.

1.2.2. Lignin

Being the most used lignocellulosic source in the present study, lignin has been employed to develop thickening or gelling agents, binders and/or fillers in the formulation of lubricating greases, adhesives and elastomers, respectively.

Alkali lignin obtained through a Kraft process, purchased from Merck (Germany), was used to test the performance of several diisocyanates as potential crosslinkers. It was also used for the optimization of the one-step processing protocol.

On the other hand, lignin obtained from the Kraft process of *Eucalyptus globulus* was tested at different lignin/HDI w/w ratio and gelling agent concentration, to optimize their values for lubricant application. This lignin was kindly supplied by the INIA-CIFOR.

Furthermore, the use of diverse residual lignin-containing fractions generated as side-streams in different conversion processes of eucalypt and pine woods as thickening agents in bio-lubricant formulations was also addressed. Thus, lignins from *Eucalyptus globulus* obtained from three different extraction processes, i.e., Kraft pulping, fermentable sugars extraction by autohydrolysis and steam explosion, and Kraft lignin from *Pinus radiata* were provided by the INIA-CIFOR. Another study was performed to study the influence of the fermentation process with *Streptomyces* MDG301 in wheat straw-derived lignin fractions for lubricating applications. The influence of the fermentation process with *Streptomyces* MDG301 and MDG147 was also evaluated for adhesive formulations. These lignins were likewise produced, treated and characterized in the framework of the collaborative project above mentioned.

Finally, Indulin AT, a Kraft lignin obtained from pine and purchased from MeadWestvaco (USA), was used as the precursor of bioelastomers with potential applications. A detailed description of this product has been reported elsewhere [1].

1.3. Castor oil

Castor oil is obtained from the seeds of *Ricinus communis*, mainly cultivated in the tropical areas of India, Africa and South America. The main characteristic which differentiates this oil from the others is that it comprises the only commercially available oil

that contains ricinoleic fatty acid, with a hydroxyl group in its hydrocarbon chain [2], in its fatty acid profile. Because of that, the worldwide supply has increased by more than 50% during the last three decades. Composition and main physical properties are depicted in Table 1 and Table 2, respectively.

Table 1. Composition of castor oil [3].

Acid name	Average percentage range (%)
Ricinoleic acid	80-94.9
Oleic acid	0-9
Linoleic acid	1.4-7
Stearic acid	0.6-2.4
Linolenic acid	<1

Table 2. Main physical properties of castor oil [2].

Physical properties	Values
Viscosity	5.5×10−1 Pa·s (25ºC)
Density	960 kg/m^3
Thermal conductivity	4.727 W/(m·ºC)
Melting point	-2 to -5ºC
Boiling point	313ºC

As established in Table 1, ricinoleic acid is the main fatty acid present in castor oil. The corresponding triglyceride, the ricinolein, is shown in Figure 1.

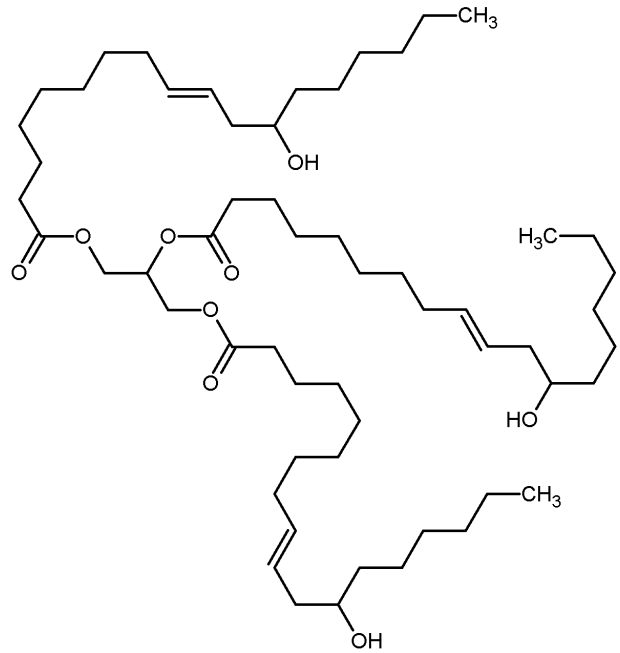

Figure 1. Ricinolein chemical structure.

Castor oil from two different sources has been targeted in this study. For the production of lubricating grease and adhesive formulations, castor oil purchased from Guinama (Spain) has been used, where has acted as both base oil and copolyol. Instead, for the production of elastomeric formulations, castor oil was purchased from Merck (Finland). The fatty acid composition of both oils has been included in Table 3.

Table 3. Fatty acid composition of both castor oils from Guinama [4] *and Merck.*

Fatty acid	Guinama (wt%)	Merck (wt%)
Palmitic C16:0	1.70	0.90
Stearic C18:0	1.96	1.10
Oleic C18:1	5.34	3.00
Ricinoleic C18:1:OH	82.48	89.7
Linoleic C18:2	7.01	3.9
Linolenic C18:3	1.51	0.4
Eicosenoic acid	-	0.3
Saturated	3.66	-
Monounsaturated	87.82	-
Polyunsaturated	8.52	-

1.4. Diisocyanates

Several diisocyanates have been evaluated as crosslinkers in this work, from linear aliphatic to aromatic ones, which are included in Table 4. These diisocyanates were acquired from Merck (Germany), with a purity >98%.

Table 4. Diisocyanates used in this study.

Diisocyanate	Formula	Structure	Molecular weight (g/mol)	Melting point (ºC)	Boiling point (ºC)
Hexamethylene diisocyanate (HDI)	$C_8H_{12}O_2N_2$	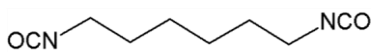	168.2	-67	255
Tolylene-2,4-diisocyanate (TDI)	$C_9H_6O_2N_2$	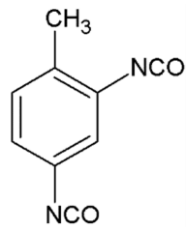	174.2	21.8	250
4,4'-methylene diphenyl diisocyanate (MDI)	$C_{15}H_{10}O_2N_2$	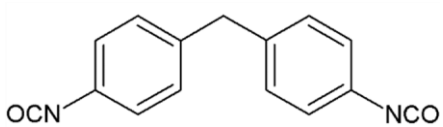	250.3	39.5	314
Isophorone diisocyanate (IDI)	$C_{12}H_{18}O_2N_2$	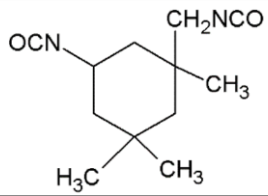	222.3	-60	158

1.5. Other chemicals

Chemicals and solvents needed to perform synthesis reactions, processing of formulations and characterization of raw, intermediate and final products were purchased from Merck (Germany). Toluene (≥99.7%) and triethylamine (analytical grade) were used as solvent and catalyst, respectively, when applying the two-step protocol in the processing of oleogels. Pyridine and acetic anhydride were used for acetylation of residual lignins. Tetrahydrofuran (THF) and 0.05 M NaOH solution were employed as eluents in GPC determinations. Intrinsic viscosity was evaluated with cupriethylendiamine solutions. Deuterated both chloroform and dimethylsulfoxide were also used in nuclear magnetic resonance characterization.

2. Synthesis protocols

2.1. Two-step protocol

The two-step protocol of polyurethane oleogel formation comprises first a functionalization of the biosource, followed by an efficient mixing with the castor oil to achieve the formation of the oleogel itself.

2.1.1. Functionalization process

The functionalization process of the biosource (lignin from different sources, wheat or barley straw) consists of the reaction between the biosource and a diisocyanate in a toluene medium using triethylamine as a catalyst. Step-by-step, a three-neck round-bottom flask was firstly filled with toluene (100 mL), which was demoisturized by sparking argon within the solvent for 30 min. Afterwards, biosource, diisocyanate and trimethylamine were added. Biosource quantity was generally 5-10 g, and the diisocyanate content was dependent on the biosource/HDI ratio, which varied from 1/1 to 1/4 w/w. Triethylamine content added was similar to that of the diisocyanate. Once all the components were included, the mixture was kept at room temperature for 24 h under vigorous agitation. After that, a rotary evaporator equipped with a water bath at 80ºC was used to separate toluene and triethylamine from the functionalized biosource. A step-by-step scheme has been included in Figure 2.

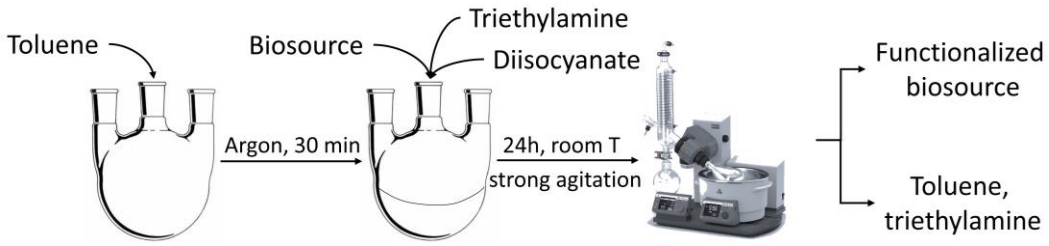

Figure 2. Schematic representation of the functionalization process.

2.1.2. Oleogel formation

Immediately after the functionalized biosource collection, this was mixed with castor oil. Straws were mixed in 15% functionalized biosource content while residual lignins varied between 20-30%. The mixture was stirred at low speed (70 rpm) in a stainless-steel open vessel for another 24 h-period by using a controlled-rotational speed mixing apparatus RW 20 (IKA, Germany), equipped with an anchor impeller. After the stirring period, samples were poured into vessels or moulds, where they were kept for curing or conditioned for testing, respectively. Both oleogels and elastomers were obtained by this procedure. A schematic illustration is included hereunder.

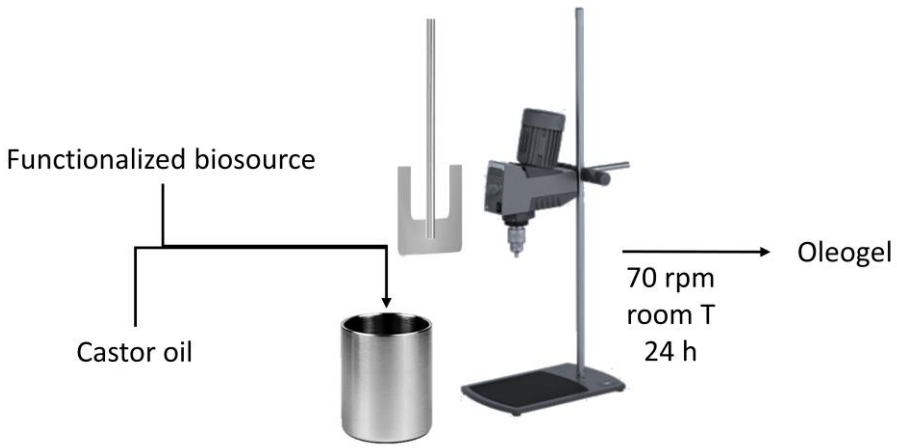

Figure 3. Oleogel formation step diagram.

2.2. One-step protocol

The one-step protocol involves the use of only castor oil, the biosource and the diisocyanate for the formation of the oleogel, with neither solvent nor catalyst taking part in the process.

Following this protocol, a stainless-steel open vessel was filled with castor oil, biosource and diisocyanate, with varying biosource/diisocyanate w/w ratio and castor oil concentrations depending on the proposed formulation. Thus, oleogels from cellulose pulp were produced using castor oil concentrations up to 90 wt%, while lignin-based systems ranged between 70-75 wt%. Instead, the formulation of lignin-based adhesives required the use of 50% castor oil. The biosource/diisocyanate ratios selected were 1/2 for cellulose pulp, 1/0.5 for lignin-based lubricating grease products and 1/4 for lignin-based adhesive formulations. More specific details of the composition can be found in the respective experimental sections of the corresponding articles, included in chapter 4. The mixture was stirred at low rates (70 rpm) by using the same mechanical stirrer mentioned in section 2.1.2, at room temperature and for 24 h in the case of lubricating grease or 48 h for adhesive formation. Illustrative information about the process has been included in Figure 4.

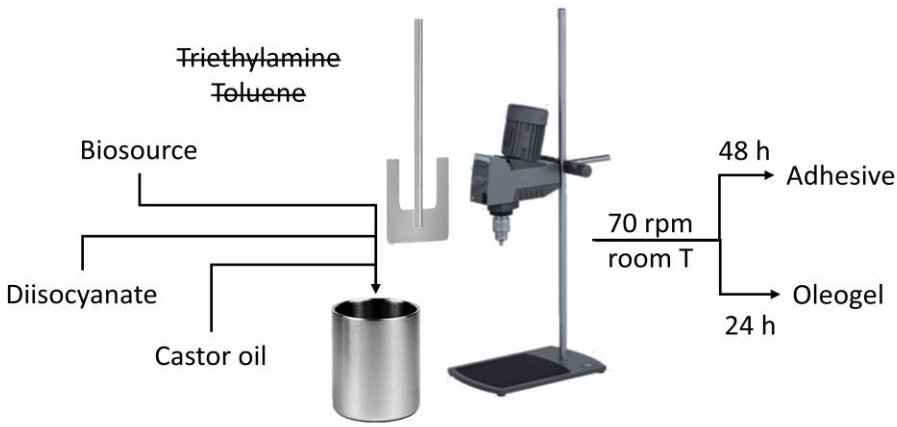

Figure 4. One-step procedure illustrative diagram.

Later, systems were stored or put into moulds for curing and testing conditioning. Eventually, the modification of several processing parameters (temperature and agitation speed) and the effect of using different diisocyanates in the oleogel characteristics obtained through this one-step protocol was studied. For that, the viscosity during the processing was

monitored for 6 h by using an ARES controlled-strain rheometer from Rheometric Scientific (UK), equipped with an anchor impeller and using a stainless-steel cylinder as mixing geometry. The dimensions and appearance of these systems have been included in Figure 5.

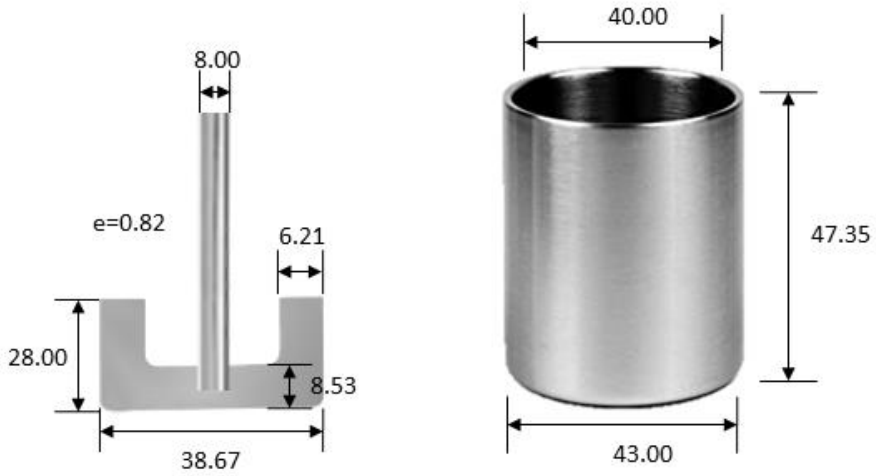

Figure 5. Dimensions of the rheo-reactor and anchor impeller used to process the bio-based polyurethanes in the rheometer. All dimensions are included in mm.

3. Characterization techniques

3.1. Thermogravimetric analysis (TGA)

The TGA was used to evaluate the thermal stability of the different biosources, intermediates and final products. In a typical experiment, 5-10 mg of the sample were placed on a platinum pan and conducted to a temperature ramp within 25-600ºC at 10ºC/min. The experiments were carried out under nitrogen atmosphere. Both Q-50 and Q500 thermal analysers (TA instruments, USA) and SII TG/DTA 6200 apparatus (Seiko, Japan) were used.

3.2. Differential scanning calorimetry (DSC)

The DSC spectra were obtained by placing from 5 to 10 mg sample in a hermetically-sealed aluminium pan, and then three temperature ramps were generally conducted. The first one, from -80 to ~200ºC, was conducted to remove the thermal history of the sample. Eventually, this ramp was also used to monitor the curing process of selected samples by evaluating the fusion enthalpy of unreacted isocyanate reactions. A second ramp was

performed from ~200 to -80ºC, after which a final step once more from -80 to ~200ºC allowed to evaluate the different thermal events (glass transition, melting temperature, etc.). Both Q100 and DSC250 apparatus (TA Instruments, USA) were the equipment used for the purpose.

3.3. Fourier transform infrared spectroscopy (FTIR)

The FTIR spectra were recorded in different ways depending on the nature of the sample. Thus, powder-like systems like lignin, cellulose pulp or straws were milled with KBr, and then moulded under compression to produce rounded pill-like pellets. For liquid- and gel-like systems, the sample was placed between two KBr discs (32 mm diameter, 3 mm thick). Both systems were later placed into a sample holder, after which the measurement was conducted between 400-500 and 4000 cm^{-1} wavenumbers, with a resolution of 4 cm^{-1}. Two different apparatus were employed, a JASCO FT/IR 4200 (Jasco Inc., Japan) and a Nicolet 380 FT-IR (Thermo Scientific, USA).

3.4. Nuclear magnetic resonance (NMR)

Four different types of NMR spectra were obtained, ^{13}C, ^{1}H, ^{31}P and 2D HSQC (two-dimensional heteronuclear single quantum coherence) NMR, whose spectra were recorded using a Bruker Avance III 500 MHz (^{13}C, ^{1}H and 2D HSQC) and a Bruker NMR Avance III 400 MHz (^{1}H NMR and ^{31}P NMR) (Bruker, USA) spectrometers at room temperature. The spectrometer III 500 MHz was equipped with a 5 nm BBFO plus with a z-gradient double-resonance probe.

The operational conditions of the NMR assays are included hereunder:

- ^{1}H NMR: pulse 45°, 4.9 μs; recycle delay, 10 s; spectral width, 10330.5 Hz; acquisition time, 3.17 s; scans number, 32.
- ^{13}C NMR: pulse 30°, 3.21 μs; recycle delay, 1 s; spectral width, 30.03 Hz; acquisition time, 1.09 s; scans number, 12500.
- ^{31}P NMR: acquisition time, 1 s; recycle delay, 5 s; scans number, 128.
- 2D HSQC: spectral widths, 4700-6200 Hz for the ^{1}H dimensions, and 20.84-22.52 Hz for ^{13}C dimensions; number of collected complex points, 1024 for ^{1}H-dimension with a recycle delay of 1 s; scans number, 32; time increments (^{13}C) 256; 1 JC-H 145 Hz; J-

coupling evolution delay set to 3.45 ms; squared cosine-bell apodization function applied in both dimensions.

3.5. Gel permeation chromatography (GPC)

The GPC measurements of acetylated lignins were performed at 35ºC and a flow rate of 1 mL/min using THF as eluent in a Waters (USA) equipment, coupled to an HPLC pump (1515 model) and a Styragel column (7.8 x 300 mm). A 2414 model refractive index apparatus was used for detection. The direct GPC measurements of lignin fractions were accomplished by using 0.05 M NaOH as mobile phase at a similar flow rate and 25ºC. The equipment used was a 1260 HPLC (Agilent, Germany) coupled with a G1315D diode array detector set at 254 nm, two columns (Phenomenex, USA) arranged in series (GPC P4000 and P5000, both 300 × 7.8 mm) and a safeguard column (35 × 7.8 mm)). The molecular weight of lignin and acetylated lignin fractions was calculated according to previous calibration with polystyrene standards.

3.6. Rheological characterization

Rheological characterization was performed by using an ARES-G2, and two other ARES controlled-strain rheometer (TA Instruments, USA), several controlled-stress rheometers such as a Physica MCR 301 and a Physica MCR302 (Anton Paar, Austria) and a MARS and a Rheoscope (Thermo Scientific, Germany). Different geometries were used depending on the consistency of the sample. Thus, for low viscous samples, 50 mm diameter serrated plate-plate geometries were used. For samples with higher consistency, 25 or 20 mm rough plates were selected. Generally, the plate-plate gap was set at 1 mm. For adhesive and elastomeric formulations, torsion geometries were used. At least two replicates of each test were always carried out.

3.6.1. Viscous flow measurements

The viscous flow measurements were generally obtained at room temperature by applying a stepped shear rate ramp from 0.01 to 100 s^{-1}, getting from 3 to 5 points per decade, evenly distributed following a logarithmic scale.

3.6.2. Strain and stress sweeps

Both strain and stress sweeps were performed from 0.01 to 100% or from 0.01 up to 1000 Pa, respectively, depending on the rheometer used, to establish the extent of the linear viscoelastic regime of each sample.

3.6.3. Small amplitude oscillatory shear and torsion tests (SAOS & SAOT)

Small amplitude oscillatory shear and torsion tests were obtained within the range of 100-0.03 rad/s, with 3-5 points per decade evenly distributed. Generally, these measurements were performed at room temperature, but occasionally, some results were obtained up to 200ºC. All measurements were performed within the linear viscoelastic regime by selecting an appropriate strain or stress value inside the mentioned range.

3.6.4. Temperature sweeps

Temperature sweeps were also performed in SAOS and SAOT modes, in which the linear viscoelastic behaviour of the sample was measured by increasing and decreasing temperature rates of 1ºC/min, usually from room temperature up to 200ºC.

3.7. Penetration tests

Both unworked and worked penetration tests of selected oleogel samples for lubricating application were performed by following ASTM D1403 standard and using a 17000-2 Seta Universal penetrometer (Stanhope-Seta, UK) equipped with one-quarter cone geometry. The values obtained from those measurements and its conversion to standard penetration values were performed according to ASTM D127 standard, which also allows to obtain NLGI grade of the corresponding oleogels tested. From three to six replicates for each sample were obtained. The working of the samples was also performed following a standard (ASTM D1831), by means of a 19400-3 Roll Stability tester (Stanhope-Seta, UK).

3.8. Tribological measurements

The friction coefficient of oleogels with lubricating grease purposes was measured in a tribological cell coupled with a Physica MCR501 (Anton Paar, Austria) rheometer by applying a constant normal force of 20 N at 10 rpm for 10 minutes, in order to achieve stationary values. The tribological cell consists of three 45°-inclined steel plates (1.4301

steel) onto which surface a 1/2″ diameter steel ball (1.4301 grade 100 steel) rotates. A schematic representation of the tribological cell is included in Figure 6.

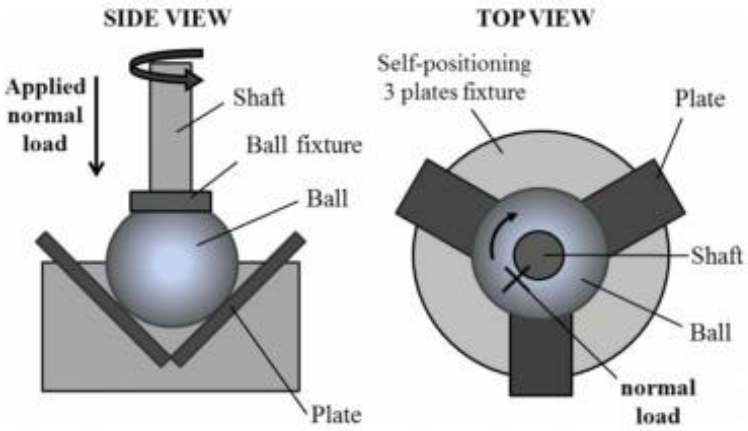

Figure 6. Schematic representation of the tribological cell used in this study [5].

3.9. Wear evaluation

The wear generated on the three surfaces of the inclined plates was evaluated by means of both the parallel-to-rotation diameter and the elliptical area of the wear mark. The measurements were obtained through optical microscopy, by using a BX51 model (Olympus, Japan) coupled to a digital camera (DP70 model, also from Olympus).

3.10. Microstructure

3.10.1. Atomic Force Microscopy (AFM)

The morphology of selected lignin-based oleogel samples was assessed by AFM, using a multimode AFM connected to a Nanoscope IV scanning probe microscope controller (Digital Instruments, Veeco Metrology Group Inc., USA). TM PPP-NCH AFM Silicon Nanosensor probes for tapping mode, applying a constant 42 N/m force and a resonance frequency of 330 kHz were employed. The typical oscillation amplitude varied between 20-100 nm. Windows and scan speed were set at 6 and 1 μm, and 1 Hz, respectively.

3.10.2. Scanning Electron Microscopy (SEM)

The surface topography of the elastomers developed in this work was observed via SEM imaging. Previously, the samples were conditioned by sputter-coating with 6 nm-thick gold layers to prevent the charging of the samples. After that, the images were acquired by using a Zeiss Sigma VP microscope (Carl Zeiss Microscopy Ltd., UK).

3.11. Water contact angle (WCA)

The WCA of the developed elastomers was measured by placing 6 µL water droplets onto the sample surface by a force tensiometer (Sigma 70, UK), equipped with a COHU solid-state CCD monochrome camera, and using OneAttension software for the appropriate calculation of the angles related to the water-sample contact.

3.12. Mechanical tests

3.12.1. Adhesion tests

The adhesion tests were performed by using an AG-IS Universal Testing Machine (Shimadzu, Japan), equipped with either a 1 or a 10 kN load cell depending on adhesion test, i.e., peeling or shear strength evaluation, respectively. All adhesion tests were carried out according to ASTM standards, i.e., D903 for metal-textile stripping, D906 for wood-wood specimens shear and D1002 for stainless-steel (SS) metal-metal shear. Usually, up to 10 specimens were measured, due to the scattered results obtained, which were treated with an analysis of variance method (ANOVA) to get centralized values and discard outliers.

3.12.2. Tensile tests

Tensile characterization of the produced elastomers was performed in both an AG-IS Universal Testing Machine (Shimadzu, Japan) and a 4204 Universal Tester (Instron, USA). Rates of 10 mm/min were applied, and a load cell of 1 kN was used.

3.12.3. Compression tests

Compressive tests of the mentioned elastomers were performed in the same equipment used for tensile characterization. Nonetheless, the load cell was switched from 1 to 10 kN depending on the sample tested. In this case, compressive rates of 5 mm/min were used.

3.12.4. Dynamic compression tests

The dynamic compression tests of the elastomers were performed in a TA.XT Plus Texture Analyser (Stable Micro Systems, UK). The given loads were calculated to achieve equivalent stresses of either 0.35 MPa or 0.70 MPa. Different testing times were also applied; from short-time tests with a duration of around 70 s to long-time ones up to 24 h. A constant compressive rate of 0.5 cycles/s was implemented.

4. References

[1] M.A. Rahman, D. De Santis, G. Spagnoli, G. Ramorino, M. Penco, V.T. Phuong, A. Lazzeri, Biocomposites based on lignin and plasticized poly(L-lactic acid), J. Appl. Polym. Sci. 129 (2013) 202–214. https://doi.org/10.1002/app.38705.

[2] V.R. Patel, G.G. Dumancas, L.C.K. Viswanath, R. Maples, B.J.J. Subong, Castor oil: Properties, uses, and optimization of processing parameters in commercial production, Lipid Insights 9 (2016) 1–12. https://doi.org/10.4137/LPI.S40233.

[3] B. Sreenivasan, N.R. Kamath, J.G. Kane, Studies on castor oil. I. Fatty acid composition of castor oil, J. Am. Oil Chem. Soc. 33 (1956) 61–66. https://doi.org/10.1007/BF02612549.

[4] L.A. Quinchia, M.A. Delgado, C. Valencia, J.M. Franco, C. Gallegos, Viscosity modification of different vegetable oils with EVA copolymer for lubricant applications, Ind. Crops Prod. 32 (2010) 607–612. https://doi.org/10.1016/j.indcrop.2010.07.011.

[5] J.E. Martín-Alfonso, C. Valencia, Tribological, rheological, and microstructural characterization of oleogels based on EVA copolymer and vegetables oils for lubricant applications, Tribol. Int. 90 (2015) 426–434. https://doi.org/10.1016/j.triboint.2015.05.004.

Chapter 4
Results & Discussion

Chapter 4. Results & Discussion

Algunos de los trabajos científicos que forman parte del capítulo IV, debido a restricciones relativas a derechos de autor, han sido retirado de la tesis. En sustitución de los artículos ofrecemos la siguiente información: referencia bibliográfica, enlace a la revista y resumen.

- Borrero-López, A. M., Blánquez, A., Valencia, C., Hernández, M., Arias, M. E., Eugenio, M. E., Fillat, Ú., & Franco, J. M. (2018). Valorization of Soda Lignin from Wheat Straw Solid-State Fermentation: Production of Oleogels. In ACS Sustainable Chemistry & Engineering (Vol. 6, Issue 4, pp. 5198–5205). American Chemical Society (ACS). https://doi.org/10.1021/acssuschemeng.7b04846

Enlace al texto completo: https://doi.org/10.1021/acssuschemeng.7b04846

RESUMEN:
This work describes the solid-state fermentation (SSF) of wheat straw with Streptomyces sp. MDG147 and further soda-pulping process to obtain wheat straw soda lignins (WSLs). Subsequently, these WSLs were NCO-functionalized with 1,6-hexamethylene diisocyanate and then dispersed in castor oil to achieve stable oleogels. The WSLs were characterized using standard analytical methods, gel permeation chromatography, Fourier transform infrared spectroscopy, differential scanning calorimetry, and thermogravimetric analysis. Rheological properties of oleogels were determined by means of small-amplitude oscillatory shear and viscous flow measurements. The enzymatic profile and production of lignin–carbohydrate complexes were recorded along the growth time of Streptomyces, whose life cycle was achieved after 7 days. NCO-functionalized WSL was able to chemically interact with castor oil via urethane bonding, providing oleogels with suitable rheological characteristics. Linear viscoelastic functions and viscosity values of oleogels were higher when wheat straw was submitted to SSF using Streptomyces, turning out in stronger oleogels.

- Borrero-López, A. M., Valencia, C., Domínguez, G., Eugenio, M. E., & Franco, J. M. (2021). Rheology and adhesion performance of adhesives formulated with lignins from agricultural waste straws subjected to solid-state fermentation. In Industrial Crops and Products (Vol. 171, p. 113876). Elsevier BV. https://doi.org/10.1016/j.indcrop.2021.113876

Enlace al texto completo: https://doi.org/10.1016/j.indcrop.2021.113876

RESUMEN:
In this study, modified residual lignins from barley and wheat straws submitted to solid-state fermentation with diverse *Streptomyces* strains were targeted as binders in eco-friendly castor oil-based polyurethane adhesive formulations. The thermo-rheological and adhesion properties of these adhesives were examined and related to the solid-state fermentation yields. Viscoelastic properties were enhanced by lignin addition, and the *Streptomyces* action generally increased the values of the linear viscoelastic functions. Adhesion performance was dominated by lignin source and further *Streptomyces* activity and can be correlated with the resulting lignocellulosic composition. Wheat straw lignin-based polyurethane adhesives showed the best performance in metal-textile peeling tests, whereas barley straw lignin provided the best achievements in terms of shear strength

in metal-metal and wood-wood joints. Overall, solid-state fermentation with *Streptomyces* demonstrated to be a suitable pretreatment to conveniently modify and improve residual lignin fractions for application as binders in environmental-friendly polyurethane adhesive formulations.

1. Study and optimization of lignin-based polyurethane formulations and processing protocol

1.1. Article 1

Rheology of lignin-based chemical oleogels prepared using diisocyanate crosslinkers: Effect of the diisocyanate and curing kinetics

A.M. Borrero-López, C. Valencia, J.M. Franco

Published in:

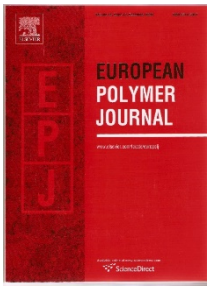

European Polymer Journal
Publishing Company: Elsevier
Editor-in-Chief: Richard Hoogenboom
Volume 89, pp 311-323
Year 2017
ISSN 0014-3057
DOI: 10.1016/j.eurpolymj.2017.02.020

Category	Journal Rank / Total number of journals	Quartile (Percentage)
Polymer Science	12/87	Q1 (87%)
Impact Factor	3.741	

European Polymer Journal 89 (2017) 311–323

Contents lists available at ScienceDirect

European Polymer Journal

journal homepage: www.elsevier.com/locate/europolj

Rheology of lignin-based chemical oleogels prepared using diisocyanate crosslinkers: Effect of the diisocyanate and curing kinetics

A.M. Borrero-López[a], C. Valencia[a,b], J.M. Franco[a,b,*]

[a] Departamento de Ingeniería Química, Campus de "El Carmen", Universidad de Huelva, Campus de Excelencia Internacional Agroalimentario (ceiA3), 21071 Huelva, Spain
[b] Pro²TecS – Chemical Product and Process Technology Center, Universidad de Huelva, 21071 Huelva, Spain

ARTICLE INFO

Keywords:
Castor oil
Diisocyanates
Lignin
Oleogel
Rheology
Urethanes

ABSTRACT

In this work, alkali lignin together with different diisocyanates (hexamethylene diisocyanate (HDI), isophorone diisocyanate (IDI), toluene diisocyanate (TDI) and 4,4′-methylenebis (phenyl isocyanate) (MDI)) have been tested as gelling agents in a castor oil medium. A two-step process comprising first lignin functionalization with a diisocyanate and then the formation of a bio-based polyurethane with gel-like characteristics by combining the functionalized lignin with castor was followed. FTIR and thermogravimetry analysis were carried out on both the gelling agents and resulting oleogels. Moreover, oleogel rheological properties were evaluated by means of small-amplitude oscillatory shear (SAOS) tests and viscous flow measurements. The influences of time-temperature processing conditions during oleogel formation, lignin/diisocyanate ratio and functionalized lignin concentration on the rheological properties of oleogels were analyzed using HDI as crosslinker. 30% (w/w) thickener concentration and room temperature processing were selected to prepare oleogels with the rest of diisocyanates considered. Under the same conditions, HDI-functionalized lignin-based oleogels showed the strongest gel-like behavior whereas TDI-, IDI- and especially MDI-functionalized lignin-based oleogels displayed weak gel-like, or even a liquid-like, behaviors as a consequence of the respective chemical structures, which guide to higher steric hindrance, diminishing the formation of urethane linkages and/or Van der Waals forces. In general, oleogels exhibited an internal curing process due to the progressive formation of urethane linkages, which is closely related to the evolving rheological properties. The kinetics of this curing process was studied and an empirical model has been proposed to predict the evolution of the rheological properties with time.

1. Introduction

In the last decades, the climate change and resources depletion have been increasing and changing the focus of research to more friendly environmental approaches. In that way, lignocellulosic materials are gaining more and more importance since they are renewable and ecological sources widespread around the world. Lignocellulosic materials include lignin, the second most abundant biopolymer after cellulose [1], which forms a random, amorphous three-dimensional network [2] and does not possess a well-defined structure but a complex combination among three main monomers (monolignols), i.e., p-hydroxyphenyl, guaiacyl and syringyl, and

* Corresponding author at: Departamento de Ingeniería Química, Campus de "El Carmen", Universidad de Huelva, 21071 Huelva, Spain.
E-mail address: franco@uhu.es (J.M. Franco).

http://dx.doi.org/10.1016/j.eurpolymj.2017.02.020
Received 23 December 2016; Received in revised form 13 February 2017; Accepted 14 February 2017
Available online 16 February 2017

some others, as aliphatic hydroxyl groups, condensed phenol units, and carboxylic acid protons [3]. Paper industry is the main producer of lignin-rich residues, where around 98% are directly burned to recover energy. For these reasons, lignin is being focused as a promising material to obtain high-value added and environmental-friendly products.

In the same direction, several industries such as those involved in the production of lubricants [4–6] and adhesives [7] also face serious environmental problems [8] and are demanding eco-friendly oleogel-like systems with suitable functional properties, which can overcome these problems. Recently, some formulations which replace mineral or synthetic oils, in the case of lubricants [9–11], or volatile organic solvents, in the case of adhesives [12,13], by vegetable oils have been reported.

On the other hand, diisocyanates (HDI, IDI, TDI, MDI…) are capable of reacting with −OH groups of many polymers, e.g. butanediol polyester [14], hydroxyl-terminated polybutadiene and butacene [15], 4,4′-{oxy-1,4-diphenyl bis(nitromethyl-idine)} diphenol [16], glycidyl azide polymer [17], as well as graphene oxide [18] and mineral [19] and castor oils [20,21], to form urethane linkages (−NH−C(O)−O−) owing to protons be transferred from −OH to the N in −NCO groups. These compounds are known to form materials with a wide variety of outstanding properties, depending on the application. In particular, some lignin-based polyurethanes have been already synthetized [1,22,23], even using castor oil as chain extender [24,25], thus adding the renewability and biodegradability characteristics sometimes desired for this type of materials. Similarly, HDI [11], TDI [13] and MDI [26,27] have demonstrated to be effective and efficient crosslinkers in oleogel formation and they can be used to chemically connect a vegetable oil and a suitable thickener agent. Among the different gelling agents in oil media, several isocyanate-functionalized cellulose and chitin derivatives have been previously proposed to form chemical gels in castor oil [28–30]. Considering the foregoing, this study is focused on combining lignin, as a well entangled, renewable, biodegradable and abundant material [31], with different diisocyanates as HDI, IDI, TDI and MDI as crosslinkers, to achieve a functionalized biopolymer which can be able to act as gelling agent in a castor oil (CO) medium. Following the methodology previously described for cellulose derivatives [32], in the present work a two-step oleogel formation which comprises firstly the lignin functionalization and secondly the formation of a chemical oleogel is proposed. This second step also involves chemical reactions, since free end-chain isocyanates, bonded to lignin or not, which had not already reacted can now react with the hydroxyl groups of the ricinoleic fatty acid chain. The main objective of this study was to investigate the influence of the type of diisocyanate crosslinker, the lignin/diisocyanate ratio, the NCO-functionalized lignin (FL) concentration and processing temperature on the rheological response of these chemical oleogels. Moreover, the kinetics of the chemical interaction between FL and CO, i.e., the curing process, was monitored by means of rheological measurements.

2. Experimental

2.1. Materials

Alkali lignin (L) obtained through a kraft process with up to 5% moisture and the different diisocyanates evaluated as crosslinkers, i.e. HDI, IDI, TDI and MDI, were purchased from Sigma-Aldrich. Purity of diisocyanate compounds was 98%, excepting for TDI (80%). Castor oil was purchased from Guinama (Spain). Fatty acid composition and main physical properties can be found elsewhere [33]. Other common reagents like toluene and triethylamine were analytical grade and also supplied by Sigma-Aldrich.

2.2. Functionalization reaction of lignin with diisocyanates

Lignin functionalization reaction was performed according to the methodology previously reported [32]. Briefly described, toluene (100 ml) was added to a round-bottom flask and maintained under argon inert atmosphere for 30 min. After that, a determined amount of lignin, followed by diisocyanate (in 1:1 and 1:2 lignin/diisocyanate weight ratios) and finally triethylamine (twice diisocyanate amount) were added and maintained for 24 h under vigorous stirring at room temperature. The functionalized lignin (FL), purified under vacuum using a rotary evaporator, was prepared immediately before being used.

FLs were intended to be always prepared maintaining the same −OH/−NCO molar ratio for a given lignin/diisocyanate ratio. In this sense, a determined amount of lignin was mixed with the same amount of HDI for 1:1 ratio or double for 1:2 ratio. To maintain the same −OH/−NCO molar ratio for the rest of diisocyanates, the amount added for IDI-, TDI- and MDI-based FLs was calculated according to the different molecular weights:

$$IDI, TDI \ or \ MDI = HDI \cdot \frac{Mw_{IDI,\ TDI\ or\ MDI}}{Mw_{HDI}} \quad (1)$$

where HDI is the quantity of HDI that would be needed to add according to the above-mentioned lignin/diisocyanate ratio and M_ws are the molecular weights of the different diisocyanates. In the forthcoming text, for the sake of simplicity, the 1:1 and 1:2 lignin/diisocyanate ratio nomenclature will be maintained in all cases, assuming the correction of weights given by Eq. (1) for each diisocyanate. The different FLs were named with the codes included in Table 1 containing information of the lignin/diisocyanate ratio and type of crosslinker.

2.3. Preparation of oleogels

FL was mixed with castor oil in a stainless-steel reactor (100 mL) and generally maintained 24 h under stirring at 70 rpm, using a controlled-rotational speed mixing device RW 20 (Ika), equipped with an anchor impeller. Processing of oleogels was generally carried out at room temperature, although the reaction was also accomplished at 70 °C in order to study processing conditions. FL

Table 1
TGA characteristic parameters of raw materials and functionalized lignin samples.

Sample	Code	T_{onset} (°C)	T_{max} (°C)	T_{final} (°C)	ΔW (%)	Residue (%)
Alkali lignin	L	27/129/249	61/164/373	92/183/407	3/4/49	44
HDI	HDI	137	172	178	99	1
TDI	TDI	116/172	155/181	159/188	84/14	2
IDI	IDI	124	177	184	100	0
MDI	MDI	174	221	227	97	3
L + HDI (1:1 ratio)	FLH	96/185/291/409	119/221/320/437	136/247/344/471.5	15/8/35/20	22
L + TDI (1:1 ratio)	FLT	102/171/275	126/195/300	143/216/322	11/17/37	35
L + IDI (1:1 ratio)	FLI	114/308	123/346	155/391	12/62	24
L + MDI (1:1 ratio)	FLM	121/303	179/333	205/361	14/46	40
L + HDI (1:2 ratio)	FLH2	98/298/429	118/344/454	134/375/475	11/41/24	24
L + TDI (1:2 ratio)	FLT2	144/266/371	160/331/391	178/341/443	16/19/25	40
L + IDI (1:2 ratio)	FLI2	100/245/318	153/261/355	174/286/393	33/8/40	19
L + MDI (1:2 ratio)	FLM2	162/321	192/345	233/363	18/47	35

concentration was modified in the range of 20–30% (w/w) in the case of HDI-based FL. For the comparison of using different diisocyanates, a 30% (w/w) concentration was selected. Oleogels obtained were stored at room temperature and they will be referred using the codes included in Table 2.

2.4. Fourier Transform Infrared Spectroscopy (FTIR)

FTIR spectra were obtained using a JASCO FT/IR 4200 (Jasco inc. Japon). The gels, some FLs and all diisocyanates were characterized using KBr disks (32 × 3 mm), where the sample was placed between both disks. For lignin and solid FLs, KBr pellets containing 10 parts of KBr and 1 part of sample were prepared by applying pressure for several minutes. In both cases, disks and pellets were placed in an adequate sample holder and FTIR were obtained between 400 and 4000 cm^{-1}, at 4 cm^{-1} resolution, in the transmission mode.

2.5. Thermogravimetric analysis (TGA)

Measurements of mass loss with temperature was evaluated in the range from room temperature to 600 °C, following a constant rise of 10 °C/min, using a Q-50 model (TA Instrument Waters, USA) under N2 purge. 5–10 mg of each sample were placed in a platinum pan previously tared and put onto the sample holder. After that, the measurement was automatically performed.

2.6. Rheological characterization

Linear viscoelasticity characterization of oleogels was carried out by means of SAOS tests in both the ARES (Rheometric Scientific) and the Rheoscope (Thermo Haake) rheometers, using roughened plate-plate geometries (25 and 20 mm, respectively, depending on the consistency of the sample, and 1 mm gap). Frequency sweep tests were performed inside the linear viscoelastic regime, in a frequency range of 0.03–100 rad/s. Strain or stress sweep tests were previously carried out to determine the linear viscoelastic range. Flow measurements were carried out in the ARES rheometer by applying an increasing stepped shear rate ramp from 0.01 to 100 s^{-1}, taking 3–5 points each decade and maintaining the shear rate for three minutes in each step. Each rheological test was performed on

Table 2
TGA characteristic parameters of oleogel samples.

Sample	Code	T_{onset} (°C)	T_{max} (°C)	T_{final} (°C)	ΔW (%)	Residue (%)
Oleogel 30%FLH H-T	O30H H-T	335/427	378/439	427/459	82/10	8
Oleogel 20%FLH	O20H	337/422	382/431	297/457	80/16	4
Oleogel 25%FLH	O25H	334/420	381/442	398/463	84/11	5
Oleogel 30%FLH	O30H	324/425	379/439	397/458	83/11	6
Oleogel 30%FLT	O30T	275/355/423	311/380.5/446	334/397/454.5	16/64/15	5
Oleogel 30%FLI	O30I	290/360/427	327/382/450	332.5/398/459	22/59/17	2
Oleogel 30%FLM	O30M	286/358/437	320/378/441	330/398/463	16/69/11	4
Oleogel 20%FLH2	O20H2	304/366/423.5	334/382/451	339.5/398/456	23/60/17	0
Oleogel 25%FLH2	O25H2	306/362/432	333/384.5/447	350/403/465	24/59/13	4
Oleogel 30%FLH2	O30H2	301/358/431	343/381/445	358/408/466	28/53/12	7
Oleogel 30%FLT2	O30T2	282/355/425	311/380.5/439	320/396.5/463	21/61/11	7
Oleogel 30%FLI2	O30I2	296/357/417	327/379/424	329/395/446	29/46/17	8
Oleogel 30%FLM2	O30M2	285/361/433	320/386/454	328/404/473	19/67/13	1

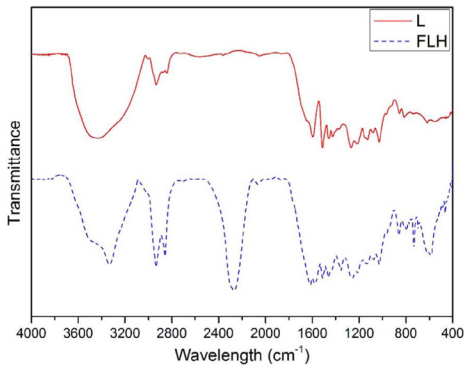

Fig. 1. Lignin and functionalized lignin FTIR spectra.

fresh samples one week after oleogel formation and replicated at least twice. Moreover, in the case of oleogels prepared with HDI, a kinetic study was programmed, for which rheological measurements were performed from just 1 h after oleogel preparation up to one week.

3. Results and discussion

3.1. Characterization of lignin and functionalized lignin samples

Lignin and functionalized lignin samples (FLs) were characterized using FTIR spectroscopy, as shown in Fig. 1. Taking into account that spectra for all FLs are very similar, only results for the 1:1 lignin/HDI weight ratio functionalization is displayed. FTIR results confirm that new bonds were created in the functionalization process, yielding new and modified peaks in the spectra. Thus, a new peak appears at around 3330 cm^{-1}, related to the N—H stretching vibration of new urethane bonds formed between —OH groups from lignin and —NCO from diisocyanates [32], and therefore the intensity of —OH stretching vibration band, centered at around 3430 cm^{-1}, is significantly diminished, so that a sharper peak was found for FL in comparison with that obtained with non-functionalized lignin in the range of 3300–3600 cm^{-1}. The two absorption bands around 2934 and 2855 cm^{-1}, corresponding to asymmetric and symmetric C—H stretching vibration of aliphatic methylene groups are widely increased in FLs as a consequence of the new six-methylene chains in HDI moieties. Also, as intended, FLs exhibit a new intense peak centered at 2270 cm^{-1}, corresponding to the stretching vibration of free isocyanate moieties. This peak is consequence of both, the free-one-side isocyanate bonded to lignin and possible non-reacted diisocyanates remained. Besides this, C=O bonds may generate two observable peaks in FTIR measurements, one related to C=O unconjugated bonds at around 1710 cm^{-1} and the second related to C=O conjugated bonds, centered at around 1620 cm^{-1} [34]. FLs spectra do not exhibit any clear signal corresponding to C=O unconjugated bonds but do show for C=O conjugated groups. Centered at around 1570 cm^{-1}, another peak related to the urethane N—H bending vibration was observed only in FL IR spectrum, demonstrating once again the formation of urethane linkages.

Thermogravimetric analyses were also used to characterize lignin and FL samples (Fig. 2). Characteristic parameters considered for each thermal event were the onset temperature (T_{onset}), temperature for the maximum weight loss rate (T_{max}), final degradation temperature (T_{final}) and weight loss (ΔW), whose values together with the final residue obtained at 600 °C are shown in Table 1.

As can be seen, apart from the loss of moisture contained in the sample up to 100 °C (≈3%) and the dehydration process of hydroxyl groups at around 165 °C, lignin show one main weight loss peak at high temperatures with an associated T_{max} at 373 °C (see Table 1), which according to the literature [35] may be attributed to the β-O-4 linkage breakdown, starting at around 250–300 °C, the aliphatic side chains cleavage, starting at around 300 °C, and disruption of C—C bonds among monolignols at around 400 °C. Moreover, the mass loss rate is very slow, yielding derivative weight loss not higher than 0.3%/°C, which is in concordance with previous results [36].

Apart from the above mentioned mass loss events, properly related to the lignin-like structure, FLs thermograms also show another main degradation peak corresponding to the disruption of free —NCO segments, starting at around 100–140 °C [28]. This thermal event depends, however, on the type of diisocyanate compound employed to functionalize the lignin. For instance, attending to the results obtained for the 1:1 lignin/diisocyanate ratio, the temperature for the maximum degradation rate of —NCO segments is 119 °C for HDI, whereas it is around 123–126 °C for TDI and IDI, and 179 °C for MDI. Similar tendency was observed for the 1:2 lignin/diisocyanate ratio. These degradation temperatures of —NCO segments in FL samples are roughly in agreement with those found in pure diisocyanates (Table 1).

Regarding the main mass loss detected in the non-functionalized lignin sample, the inclusion of diisocyanate compounds shifts the temperature for the maximum degradation rate to lower values. For instance, the lowest T_{max} value was observed for TDI-based FL sample obtained with 1:1 lignin/TDI ratio, followed by HDI-, MDI- and IDI-based FLs. Nevertheless, this difference is almost

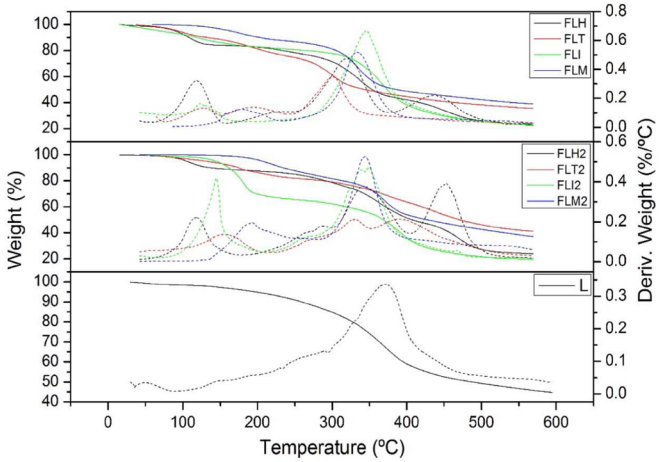

Fig. 2. TGA curves for lignin and functionalized lignin samples.

negligible for FL samples prepared with 1:2 lignin/diisocyanate ratio. Moreover, HDI-based FLs exhibit another peak at 437–454 °C which was not detected in the raw lignin, which may be attributed to a high degree of crosslinking, as previously reported for other HDI-functionalized biopolymers [28]. On the other hand, FLs generate lower residue values in comparison with the non-functionalized lignin. HDI- and IDI-based FLs show lower residue values (around 19–24%) than TDI- and MDI-based FLs (35–40%).

3.2. Characterization of oleogels

3.2.1. Influence of processing conditions

In order to optimize and gain a deeper knowledge on how processing conditions affect urethane bonds generation and therefore resulting oleogel rheological properties, the time and temperature, as two of the most important parameters during processing, are considered and modified. Two time-temperature conditions such as room temperature-24 h (RT-24) and 70 °C-3 h (HT-3) were chosen as processing conditions, whereas the HDI-based FL with 1:1 lignin/HDI ratio, at 30% w/w concentration, was selected as chemical gelling agent to compare the different processes. FTIR spectra determinations were sequentially carried out after oleogel formation. As expected, a high processing temperature increases the reaction rate between free −NCO groups in FL and available −OH groups mainly located in the CO ricinoleic fatty acid chains, as can be seen in FTIR results in Fig. 3a, where the spectra of just-

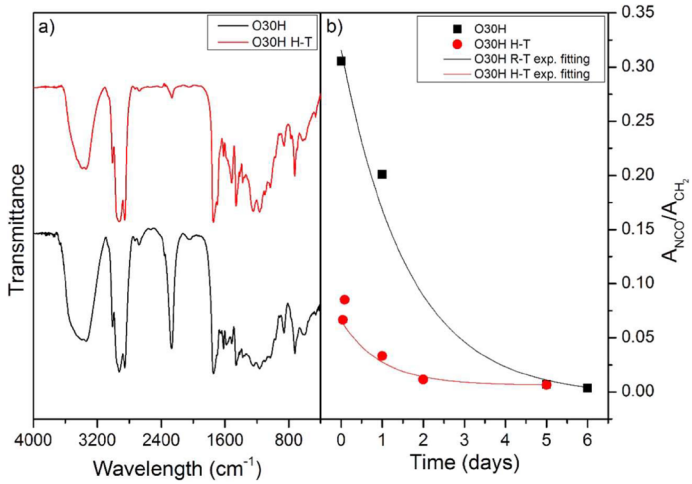

Fig. 3. (a) FTIR spectra and (b) evolution of isocyanate content with curing time for oleogels obtained applying different T-t processing conditions.

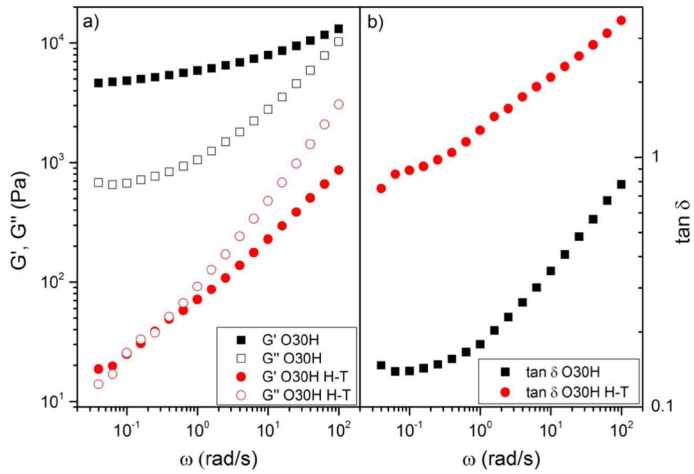

Fig. 4. Evolution of (a) the storage, G′, and loss, G″, moduli and (b) the loss tangent, tanδ, with frequency for oleogels obtained applying different T-t processing conditions.

obtained oleogels are shown. As can be seen, the NCO absorption band, at 2270 cm^{-1}, almost disappear after 3 h at 70 °C, whereas is clearly detectable after 24 h at room temperature. As well known, this residual amount of free −NCO groups still react after processing, which is called the curing process. However, despite the different kinetics during processing, as shown in Fig. 3b, the curing time is extended up to 5–6 days, independently on the processing conditions, once free −NCO groups are not detected anymore. Nevertheless, processing conditions, i.e., time-T combination, dramatically influence oleogel rheological behavior after curing. As can be seen in Fig. 4, a weak gel after curing was obtained by applying the HT-3 process, in contrast to that found when applying the RT-24 process conditions, which yields a strong gel response. This result may be explained taking into account that free isocyanates may react more randomly with different species, including themselves, at high temperatures [37], becoming other kind of linkages and limiting the chemical interaction between CO and FL, thus finally resulting much lower values of the storage (G′) and loss (G″) moduli (Fig. 4a) and significantly higher values of the loss tangent (tan δ = G″/G′) (Fig. 4b).

Regarding the viscous flow response, a shear thinning behavior was always observed in the shear rate range studied, which may be fairly well described by the power-law model:

$$\eta = K \cdot \dot{\gamma}^{n-1} \tag{2}$$

where K and n are the consistency and flow indexes, respectively. After applying the HT-3 process conditions, lower viscosity values and higher flow index than those found in the oleogel processed with RT-24 conditions were obtained (see Fig. 5 and power-law fitting parameters inset). Interestingly, in spite of all these differences found in the rheological behavior, TGA profiles (curves not shown) are almost identical for both types of oleogels (see relevant degradation temperatures in Table 2) and very similar to those reported for castor oil- and lignin-based flexible polyurethane foams [24], indicating that thermal degradation is mainly governed by

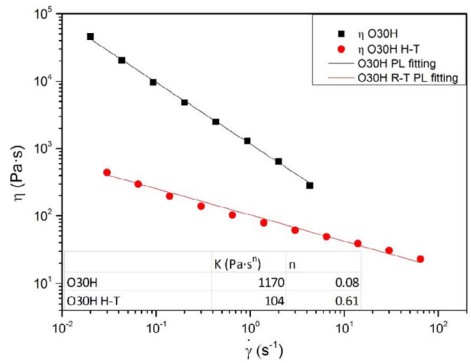

Fig. 5. Viscous flow curves of oleogels obtained applying different T-t processing conditions. (Inside: power-law fitting parameters).

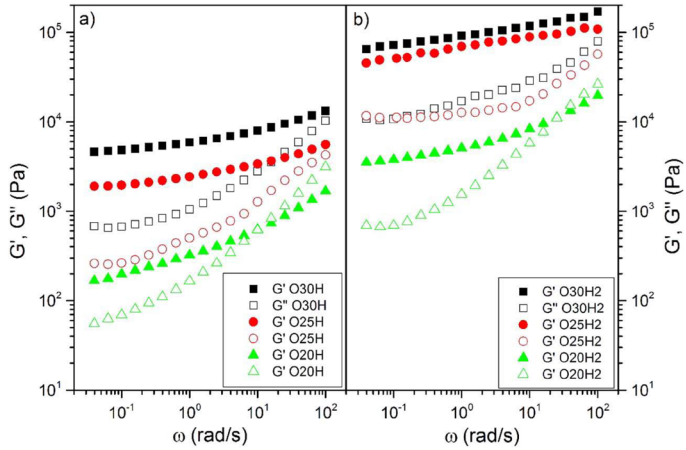

Fig. 6. Frequency dependence of SAOS functions for HDI-FL-based oleogels as a function of FL concentration (a) 1:1 lignin/HDI ratio, (b) 1:2 lignin/HDI ratio).

FL and castor oil rather than the density and type of urethane linkages.

3.2.2. Influence of functionalized lignin concentration and lignin/diisocyanate ratio

Oleogels containing different concentrations (20–30% w/w) of HDI-based FL as gelling agent were prepared and the rheological response was analyzed. Figs. 6 and 7 show the mechanical spectra obtained in the linear viscoelasticity regime and viscous flow curves, respectively, for oleogels containing 20, 25 and 30% w/w FL, and both 1:1 and 1:2 lignin/diisocyanate ratios. In general, both the SAOS functions and viscosity values increase, around one order of magnitude, when using FL with 1:2 lignin/diisocyanate ratio in relation to the 1:1 ratio. This fact is simply explained attending the higher availability of free isocyanate moieties which guides to a higher degree of crosslinking between FL and CO. However, the SAOS functions frequency dependence is not qualitatively influenced by the lignin/diisocyanate ratio. On the other hand, as expected, for both 1:1 and 1:2 lignin/diisocyanate ratios, the higher the FL concentration, the higher the G′, G″ and viscosity values are. Moreover, 20% w/w oleogels show a crossover point between G′ and G″ at relatively high frequencies, as well as higher frequency dependence of SAOS functions (see Fig. 6). This means a not well developed plateau region in the mechanical spectrum, which results in a shift of the transition region to lower frequencies, according to the typical behavior of not highly entangled gel networks [38]. A more extended plateau region with a crossover point shifted to higher frequencies was observed by increasing FL concentration. This effect was dampened by modifying the lignin/diisocyanate ratio from 1:1 to 1:2, since the degree of crosslinking is higher, as above mentioned.

Viscosity values depend on FL concentration in the same way as G′ and G″ do. Nevertheless, similar viscosity values, especially at high shear rates, were obtained for oleogels containing 25 and 30% w/w FL using the 1:2 lignin/HDI ratio. Table 3 collects the values of the power-law fitting parameters. As can be observed, K values increase with FL concentration and decrease with lignin/HDI ratio, whereas extremely low values of the flow index were generally observed, which is the consequence of the typical yielding behavior found in gel-like dispersions [39–41]. Only the oleogel prepared with 20% w/w FL and 1:1 lignin/HDI weight ratio shows a different

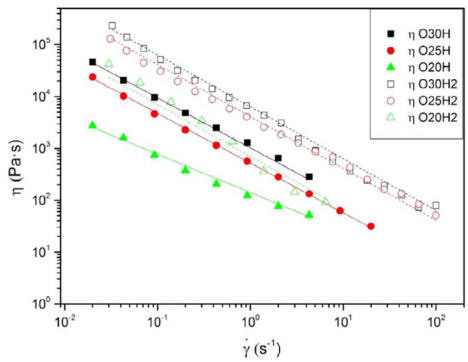

Fig. 7. Viscous flow curves for HDI-FL-based oleogels as a function of FL concentration and lignin/HDI ratio.

Table 3
K and n values for HDI, IDI, TDI and MDI-FL-based oleogels.

Samples	K ($Pa·s^n$)	n
O30H	1170	0.08
O25H	522	0.04
O20H	141	0.26
O30H2	6343	0.01
O25H2	4120	0.01
O20H2	70	0.01
O30T	126	0.60
O30I	89	0.94
O30M	14	0.91
O30I2	48,375	0.86
O30M2	52	0.93

flow behavior with an exceptionally high value of the flow index, as a result of a not so extensively crosslinked-network achieved at this concentration (see also Fig. 6).

Despite the large influence on the rheological response, FL concentration and lignin/diisocyanate ratio do not significantly affect FTIR and TGA profiles of oleogels. Since the rheological characterization was carried out just after curing (one week after processing), it is logical that FTIR spectra of all oleogels were very similar, since chemical composition is essentially the same in that moment. Regarding TGA profiles, most remarkable effect is the disappearance of the first degradation peak, corresponding to free isocyanate groups, found in FL samples (see Fig. 2), corroborating the almost complete reaction of these groups after one week of curing. Moreover, all the oleogels show a main degradation stage with T_{max} at around 379–384 °C, although the temperature range is broadened in those prepared with FLs having 1:2 lignin/diisocyanate ratio (see T_{onset} and T_{final} values in Table 2), as previously found in NCO-functionalized methylcellulose-based oleogels [28].

3.2.3. Influence of the type of diisocyanate used as crosslinker

The comparison of the rheological response of oleogels prepared with different types of diisocyanates was carried out for 30% w/w FL concentration and both 1:1 and 1:2 lignin/diisocyanate ratios. Chemical structure of different diisocyanates, i.e., conformational shape, bonds and molecular size, is one of the main factors determining the rheological behavior of resulting oleogels. Briefly described, HDI contains a small linear chain between both isocyanate groups, while the other three compounds are cyclic. TDI is an aromatic ring with isocyanates in positions 2 and 4, IDI is a cyclic hexane with three methylene groups joined and free isocyanates disposed in positions 1 and 3 and, finally, MDI is composed of two-phenyl rings joined by a methylene group and diisocyanates symmetrically disposed in *para* position respect to the methylene group. However, despite the different chemical structures, urethane bonds generated are similar and therefore oleogel FTIR spectra are analogous, although the evolution of isocyanate content with curing time is different, as will be discussed more in deep in next section.

On the other hand, regarding TGA results, for completely cured oleogels, again the first peak observed in FLs was not detected. Only one main peak centered on CO decomposition, at around 379–386 °C, with small shoulders at both sides, is evidenced in all gels (see characteristic temperatures in Table 2). Temperature ranges for these overlapped degradation peaks are similar for all oleogels and comprise thermal degradation of both CO and FL, also considering the chemical interaction between both of them. IDI-FL-based oleogels show the highest loss in both shoulders, increasing as the lignin/diisocyanate ratio increases, and the smallest peak in maximum weight loss, decreasing from 1:1 to 1:2 ratio (see Table 2).

More dramatical differences were found in the rheological responses. The evolutions of SAOS functions with frequency are compared in Fig. 8, as a function of the type of diisocyanate employed. Oleogel containing FL with 1:2 lignin/TDI ratio was not included since a rather heterogeneous sample was obtained, probably due to an excessive crosslinking degree achieved during lignin functionalization. However, as can be observed, TDI-FL-based oleogel, for 1:1 lignin/TDI ratio, shows a weak gel-like behavior, response quite close to a critical gel [42], with similar values of G′ and G″. This weak gel-like behavior may be explained attending the size, rigidity and, therefore steric hindrance of TDI molecule, much higher than HDI, which favors lower crosslinking density. This effect is even emphasized when using IDI and MDI as crosslinkers, resulting not really gels but liquid-like viscoelastic dispersions. In the case of the systems containing 1:2 lignin/IDI ratio, however, a tendency to reach a crossover point between G′ and G″ was observed at high frequencies. This rheological response is probably related with a higher difficulty when bonding and also with lower Van der Waals forces because of IDI chemical structure [14]. Supporting this, MDI, with the greater stearic hindrance, yields the lower values of G′ and G″, being $G'' \gg G'$ in the whole frequency range studied, even for the 1:2 lignin/MDI ratio.

Viscous flow measurements shown in Fig. 9 also reflect huge differences among the oleogels prepared with different diisocyanates. In general, much lower viscosity values, several orders of magnitude, and smoother shear-thinning behavior were found when using TDI, IDI and especially MDI as crosslinkers, in comparison to HDI-FL-based oleogels (see power-law parameters in Table 3). For IDI and MDI, again similar responses were displayed, both oleogels exhibiting an almost completely Newtonian behavior. Following the same tendency than that previously discussed for SAOS results, IDI-FL-based oleogel viscosity is higher than those obtained for MDI-FL-based ones, around one order of magnitude higher for the 1:1 lignin/diisocyanate ratio. Interestingly, FL containing 1:2 lignin/IDI ratio, provides an oleogel with exceptionally high and almost constant viscosity values, even higher than

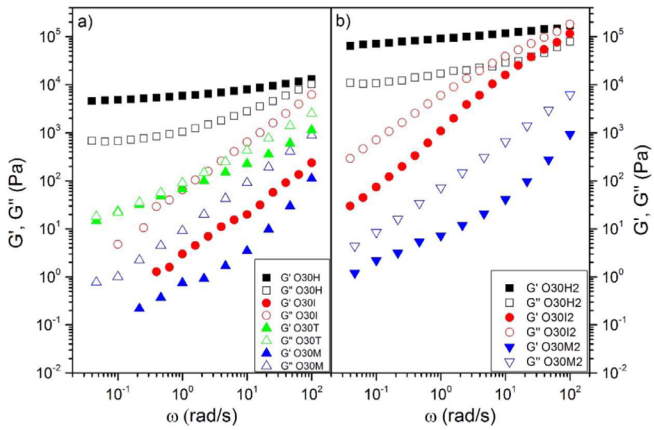

Fig. 8. Frequency dependence of SAOS functions for oleogels prepared with different types of diisocyanates (a) 1:1 lignin/diisocyanate ratio, (b) 1:2 lignin/diisocyanate ratio).

those obtained for HDI-FL-based oleogels. This extremely high viscosity values are in agreement with the high G″ values obtained at high frequencies in SAOS tests. Finally, an intermediate response was obtained with TDI-FL-based oleogel, exhibiting generally higher viscosity values, but also a lower flow index, than oleogels prepared with MDI- and IDI-based FL.

3.2.4. Curing kinetics

As explained above, FL-based oleogels undergo an internal process of curing. However, this curing process does not follow the same kinetics for the different diisocyanates considered. As can be observed in Fig. 10, the progressive disappearance of free −NCO during curing, monitored through the evolution of the −NCO intensity band in FTIR spectra, is totally different for each of the diisocyanates employed as crosslinkers. Since areas of the different bands are correlated with the concentration of functional groups in a given sample, the decrease in intensity of the isocyanate peak with curing time is a real representation of isocyanate loss by chemical reactions in the sample. As peak intensity and area depend on the quantity of sample added to the KBr plate or pellet, as well as surface exposed, changes in peak values may be due not only to isocyanate reaction inside the sample. To remove that negative effect, the area of the characteristic isocyanate band at 2270 cm^{-1} was considered relative to the areas of CH_2 groups at 2934 and 2855 cm^{-1}, which are constant for an oleogel along the whole curing process, being the evolution of isocyanate content with time considered proportional to A_{NCO}/A_{CH_2} [22]. HDI-FL-based oleogels show an exponential decay of free −NCO content with curing time, till 6–12 days after preparation when the residual free −NCO content is negligible. Similar trend was observed in IDI-FL-based oleogels, although the initial isocyanate content is higher and the kinetics much slower, achieving the total loss of −NCO groups during the second week or even longer in the case of the 1:2 lignin/IDI ratio. On the contrary, TDI-FL-based oleogels exhibited a quick decay of free −NCO content, no longer than 3–4 days, which unexpectedly does not completely disappear but remain constant at a significant level. More surprising is the behavior found in MDI-FL-based oleogels, where no decay was observed at all, being the free

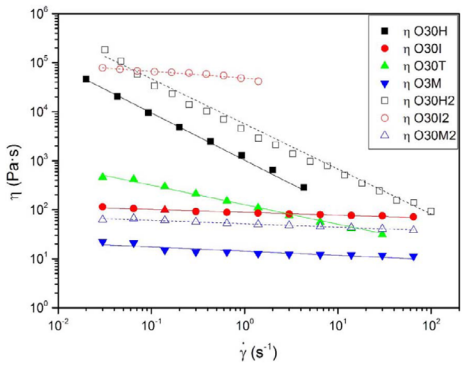

Fig. 9. Viscous flow curves of oleogels prepared with different types of diisocyanates.

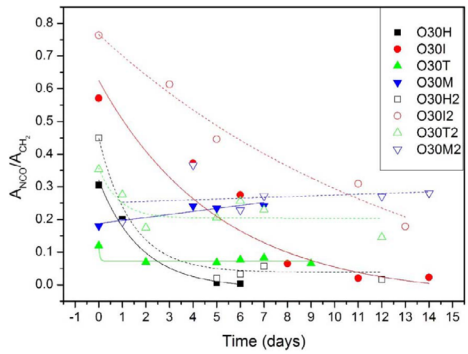

Fig. 10. Evolution of free isocyanate content with curing time for oleogels prepared with different types of diisocyanates.

−NCO content equal, or even slightly higher, to that obtained just after oleogel preparation. This means that the curing process does not occur in fact, which explains the liquid-like rheological response obtained.

Therefore, the relationship between the loss of free −NCO groups during curing and the final oleogel rheological properties seems to be closely related. Moreover, the evolution of isocyanate content also modifies the rheological properties along the curing process. Since HDI-FL-based oleogels achieved stronger gel-like characteristics, these systems have been selected at a 25% w/w FL concentration and both 1:1 and 1:2 lignin/HDI weight ratios to study more in deep the kinetics of the curing process from a rheological point of view. Fig. 11 displays a detailed evolution of A_{NCO}/A_{CH_2} with time for the two HDI-FL-based oleogels selected, showing the expected initial higher values for the oleogel prepared with FL containing 1:2 lignin/HDI ratio respect to the 1:1 ratio, as well as the exponential decay of values with curing. At the same time, SAOS measurements were performed equitably separated three times the same day of oleogel preparation, twice the following day and once per day until 1 week. Fig. 12 displays the evolution of SAOS functions with frequency for the oleogel prepared with the 1:2 lignin/HDI weight ratio FL sample and selected curing times, from 2 h to one week after preparation. As can be observed, the values of the storage and loss moduli increase with curing time predominantly during the first 24 h (Fig. 12a), which is in agreement with the evolution of free −NCO groups shown in Fig. 11. Moreover, the loss tangent (Fig. 12b) significantly decreases during these first stages of the curing process, especially at high frequencies, and remains almost constant after 24 h, also exhibiting a minimum which is shifted to higher frequencies with the progress of curing, as a consequence of the achievement of a more expanded plateau region. Measurements after one and two months were also performed to gain further insight at much longer times after completion of the curing process, roughly providing the same results than those reported for one week (data not shown).

As the plateau region of the mechanical spectrum, more or less extended, was always detected for HDI-based oleogels, the plateau modulus, G^0_N, the characteristic parameter of this region in the mechanical spectrum, which can be straightforwardly estimated as [43]:

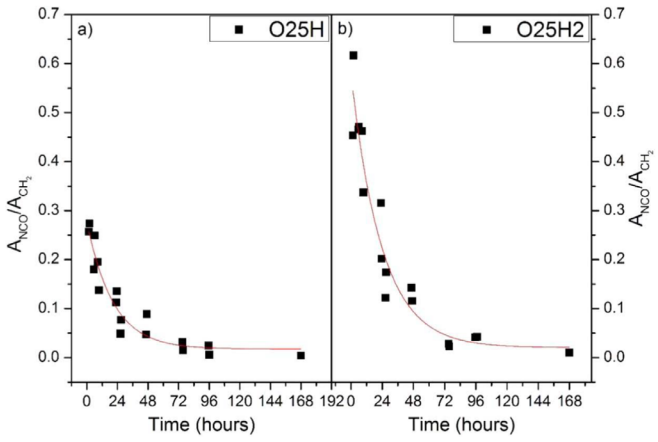

Fig. 11. Evolution of free isocyanate content with curing time for 25% HDI-FL-based oleogels (a) 1:1 lignin/diisocyanate ratio, (b) 1:2 lignin/diisocyanate ratio).

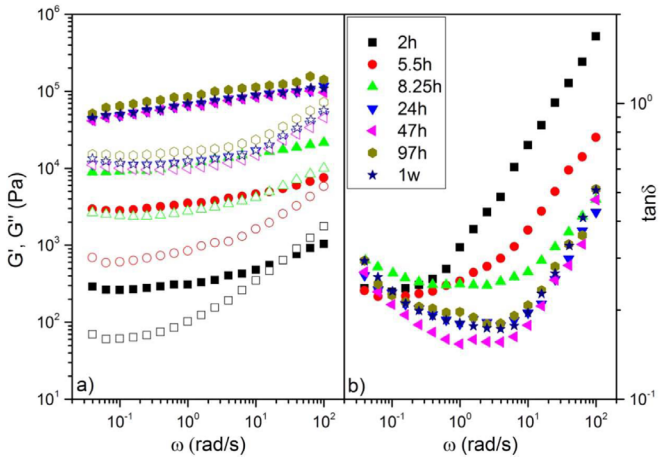

Fig. 12. Evolution of SAOS functions with curing time for O25H2 sample.

$$G_N^o = [G']_{\tan\delta \to minimum} \quad (3)$$

has been selected to analyze and model the curing kinetics. Moreover, since the loss tangent is not substantially affected by the curing process after 24 h, the whole SAOS mechanical spectrum may be determined from G^0_N values. Fig. 13 shows the evolution of the normalized plateau modulus, being $G^0_{N\text{-}0}$ and $G^0_{N\text{-}\infty}$ the values of the plateau modulus at time zero after oleogel preparation, and for the totally cured oleogel, respectively. For the HDI-FL-based oleogel containing 1:1 lignin/HDI ratio, a rather fast increase in the values of SAOS functions was obtained during the first day after processing, achieving a maximum value at around 20–30 h of ageing, still remaining approximately 25–30% of the initial free isocyanate content. However, unexpectedly, once this maximum value was reached, G′ and G″ values decreased for the following two days and finally a slight increase was observed after one week, remaining constant further on, as illustrated in Fig. 13. This evolution may be explained considering two contrary effects, on one hand the strengthening of the oleogel sample as the crosslinking degree increases through the formation of new urethane bonds chemically bonding FL and CO, and on the other hand, the relaxation of the gel network as a consequence of the non-physical equilibrium during the progress of the chemical reaction [44]. During the first hours, chemical reaction kinetics has much more importance on the rheology than any relaxation process, as free −NCO groups concentration is still high (see Fig. 11). However, after one day, available free −NCO groups have significantly diminished its concentration, and relaxation of the oleogel network gains more importance in detriment of the effect of crosslinking formation. Finally, the equilibrium is achieved once isocyanate content was negligible. On the other hand, the oleogel containing a 1:2 lignin/HDI ratio exhibits a different behavior. Even when both mentioned processes come about at the same time, isocyanate concentration is much higher than for the 1:1 lignin/HDI ratio, resulting a more extensively crosslinked network which dampens structural relaxation. Thus, the values of the SAOS moduli progressively increase after oleogel preparation, achieving the maximum value at longer times, approximately coinciding with the equilibrium, as a consequence of the higher amount of residual free −NCO groups, which obviously need more time to react completely (see Fig. 11).

The evolution of the plateau modulus with the curing time has been modeled for oleogels containing 25% w/w FLH and FLH2,

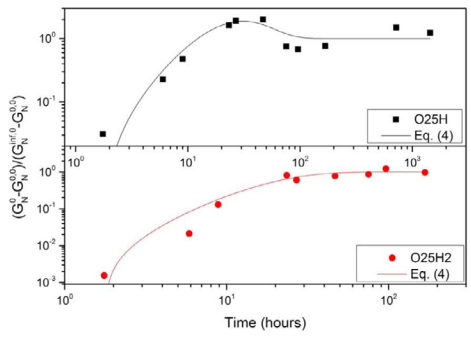

Fig. 13. Evolution of the normalized plateau modulus with curing time and fitting to Eq. (4).

Table 4
Eq. (4) fitting parameters for oleogels containing 25% w/w FLH and FLH2.

Sample	$G^0_{N\text{-}0}$ (Pa)	$G^0_{N\text{-}\infty}$ (Pa)	B (h^{-1})	A	k_1 (h^{-1})	k_2 (h^{-1})	R^2
1:1	21	4015	8.0 E-4	250	0.0805	0.0813	0.83
1:2	65	80,379	7.4 E-4	3	0.0953	0.0946	0.92

i.e., 1:1 and 1:2 FL/HDI ratios, using a modified consecutive-reaction kinetic equation:

$$\frac{G^0_N - G^0_{N-0}}{G^0_{N-\infty} - G^0_{N-0}} = \left(B \cdot t \cdot \frac{k_1}{k_2 - k_1} - 1\right) \cdot (A \cdot e^{-k_1 \cdot t} - (A-1) \cdot e^{-k_2 \cdot t}) + 1 \quad (4)$$

which takes into account both internal processes during curing, i.e., the strengthening according to isocyanate loss through the kinetic constant k_1 and structural relaxation through constant k_2, where *A* and *B* are fitting parameters considering the relative weight of both exponential terms and the absolute values of the normalized plateau modulus, respectively. As shown in Fig. 13, reasonable good fittings were obtained in both cases (see fitting parameters in Table 4).

4. Conclusions

Lignin, a promising renewable and residual polymeric material in the paper industry, has been successfully tested, along with diisocyanate crosslinkers, as gelling agent in a castor oil medium by applying a two-step oleogel preparation protocol which comprises firstly the lignin functionalization and secondly the formation of bio-based polyurethanes with gel-like characteristics by combining the functionalized lignin with castor oil. Time-temperature processing conditions influence oleogel formation and related rheological properties. A high processing temperature (70 °C) shortens oleogel preparation by accelerating the formation of new urethane linkages between the functionalized lignin and castor oil, but however yields a weak gel-like response. Oleogel rheological properties can be modulated by modifying the functionalized lignin concentration or the lignin/diisocyanate ratio in the functionalization reaction, thus varying the crosslinking density afterwards.

The chemical structure of the diisocyanate compound used as crosslinker dramatically influences oleogel rheological properties. Thus, IDI and especially MDI produce liquid-like viscoelastic dispersions, in contrast to the strong gel-like characteristics found in HDI-based oleogels, whereas an intermediate response was observed for TDI-based oleogels.

The evolution of free isocyanate content during curing, i.e., after oleogel preparation, is also influenced by the type of diisocyanate, showing an exponential decay for HDI and IDI, and small variation for TDI and MDI. The kinetics of this curing process has been analyzed from a rheological point of view and explained as two different processes occurring simultaneously, the strengthening of the samples by the formation of new urethane linkages and the gel network structural relaxation. A modified consecutive-reaction kinetic model has been proposed to describe the evolution of the plateau modulus with curing time.

Acknowledgments

This work is a part of two research projects (CTQ2014-56038-C3-1R and TEP-1499) sponsored by the MINECO-FEDER and Junta de Andalucía programmes, respectively.

References

[1] H. Jeong, J. Park, S. Kim, J. Lee, N. Ahn, H. Gyoo Roh, Preparation and characterization of thermoplastic polyurethanes using partially acetylated kraft lignin, Fibers Polym. 14 (2013) 1082–1093, http://dx.doi.org/10.1007/s12221-013-1082-7.
[2] M. Chávez Sifontes, M.E. Domine, Lignina, estructura y aplicaciones: métodos de despolimerización para la obtención de derivados aromáticos de interés industrial, Avances en Ciencias e Ingenería 4 (2013) 15–46 <http://www.exeedu.com/publishing.cl/av_cienc_ing/2013/Vol4/Nro4/3-ACI1184-13-full.pdf>.
[3] C.A. Cateto, Lignins as macromonomers for polyurethane synthesis: a comparative study on hydroxyl group determination, Polym. Polym. Compos. 21 (2013) 449–456, http://dx.doi.org/10.1002/app.
[4] C.W. Lea, European development of lubricants derived from renewable resources, Ind. Lubr. Tribol. 54 (2002) 268–274, http://dx.doi.org/10.1108/00368790210445632.
[5] B. Wilson, Lubricants and functional fluids from renewable sources, Ind. Lubr. Tribol. 50 (1998) 6–15, http://dx.doi.org/10.1108/00368799810781274.
[6] J.E. Martín-Alfonso, C. Valencia, M.C. Sánchez, J.M. Franco, C. Gallegos, Development of new lubricating grease formulations using recycled LDPE as rheology modifier additive, Eur. Polym. J. 43 (2007) 139–149, http://dx.doi.org/10.1016/j.eurpolymj.2006.09.020.
[7] D.E.Ã. Packham, Int. J. Adhes. Adhes. Technol. Sustain. 29 (2009) 248–252, http://dx.doi.org/10.1016/j.ijadhadh.2008.06.002.
[8] J.O. Metzger, M. Eissen, Concepts on the contribution of chemistry to a sustainable development, Renew. Raw Mater. 7 (2004) 569–581, http://dx.doi.org/10.1016/j.crci.2003.12.003.
[9] R. Sánchez, C. Valencia, J.M. Franco, Rheological and tribological characterization of a new acylated chitosan-based biodegradable lubricating grease: a comparative study with traditional lithium and calcium greases, Tribol. Trans. 57 (2014) 445–454, http://dx.doi.org/10.1080/10402004.2014.880541.
[10] L.A. García-Zapateiro, C. Valencia, J.M. Franco, Formulation of lubricating greases from renewable basestocks and thickener agents: a rheological approach, Ind. Crops Prod. 54 (2014) 115–121, http://dx.doi.org/10.1016/j.indcrop.2014.01.020.
[11] R. Gallego, J.F. Arteaga, C. Valencia, M.J. Diaz, J.M. Franco, Gel-like dispersions of HMDI-cross-linked lignocellulosic materials in castor oil: toward completely renewable lubricating grease formulations, ACS Sustain. Chem. Eng. 3 (2015) 2130–2141, http://dx.doi.org/10.1021/acssuschemeng.5b00389.
[12] K.P. Somani, S.S. Kansara, N.K. Patel, A.K. Rakshit, Castor oil based polyurethane adhesives for wood-to-wood bonding, Int. J. Adhes. Adhes. 23 (2003) 269–275, http://dx.doi.org/10.1016/S0143-7496(03)00044-7.
[13] B.B.R. Silva, R.M.C. Santana, M.M.C. Forte, A solventless castor oil-based PU adhesive for wood and foam substrates, Int. J. Adhes. Adhes. 30 (2010) 559–565,

http://dx.doi.org/10.1016/j.ijadhadh.2010.07.001.
[14] M.V. Pandya, D.D. Deshpande, D.G. Hundiwale, Effect of diisocyanate structure on viscoelastic, thermal, mechanical and electrical properties of cast polyurethanes, J. Appl. Polym. Sci. 32 (1986) 4959–4969, http://dx.doi.org/10.1002/app.1986.070320518.
[15] B. Lucio, J.L. De La Fuente, M.L. Cerrada, Characterization of phase structures of novel metallo-polyurethanes, Macromol. Chem. Phys. 216 (2015) 2048–2060, http://dx.doi.org/10.1002/macp.201500238.
[16] D.P. Suhas, H.M. Jeong, T.M. Aminabhavi, A.V. Raghu, Preparation and characterization of novel polyurethanes containing 4,4′-{oxy-1,4-diphenyl bis (nitromethylidine)}diphenol schiff base diol, Polym. Eng. Sci. 54 (2014) 24–32, http://dx.doi.org/10.1002/pen.23532.
[17] Z.J. Zhang, Y.J. Luo, G.P. Li, Reaction kinetics of GAP and three kinds of isocyanates with variable temperature FTIR spectrum method, Chinese J. Energetic Mater. 22 (2014) 382–385, http://dx.doi.org/10.3969/j.issn.1006-9941.2014.03.020.
[18] U. Saha, R. Jaiswal, J.P. Singh, T.H. Goswami, Diisocyanate modified graphene oxide network structure: steric effect of diisocyanates on bimolecular cross-linking degree, J. Nanopart. Res. 16 (2014), http://dx.doi.org/10.1007/s11051-014-2404-4.
[19] G. Moreno, C. Valencia, J.M. Franco, C. Gallegos, A. Diogo, J.C.M. Bordado, Influence of molecular weight and free NCO content on the rheological properties of lithium lubricating greases modified with NCO-terminated prepolymers, Eur. Polym. J. 44 (2008) 2262–2274, http://dx.doi.org/10.1016/j.eurpolymj.2008.04.047.
[20] A.A. Cuadri, F.J. Navarro, P. Partal, Isocyanate-functionalized castor oil as a novel bitumen modi fi er, Chem. Eng. Sci. 97 (2013) 320–327, http://dx.doi.org/10.1016/j.ces.2013.04.045.
[21] A.A. Cuadri, M. García-Morales, F.J. Navarro, P. Partal, Effect of transesterification degree and post-treatment on the in-service performance of NCO-functionalized vegetable oil bituminous products, Chem. Eng. Sci. 111 (2014) 126–134, http://dx.doi.org/10.1016/j.ces.2014.02.028.
[22] C.A. Cateto, M.F. Barreiro, A.E. Rodrigues, Monitoring of lignin-based polyurethane synthesis by FTIR-ATR, Ind. Crops Prod. 27 (2008) 168–174, http://dx.doi.org/10.1016/j.indcrop.2007.07.018.
[23] A. Arshanitsa, L. Krumina, G. Telysheva, T. Dizhbite, Exploring the application potential of incompletely soluble organosolv lignin as a macromonomer for polyurethane synthesis, Ind. Crop. Prod. 92 (2016) 1–12, http://dx.doi.org/10.1016/j.indcrop.2016.07.050.
[24] J. Bernardini, P. Cinelli, I. Anguillesi, M.B. Coltelli, A. Lazzeri, Flexible polyurethane foams green production employing lignin or oxypropylated lignin, Eur. Polym. J. 64 (2015) 147–156, http://dx.doi.org/10.1016/j.eurpolymj.2014.11.039.
[25] L.B. Tavares, C.V. Boas, G.R. Schleder, A.M. Nacas, D.S. Rosa, D.J. Santos, Bio-based polyurethane prepared from Kraft lignin and modified castor oil, Express Polym. Lett. 10 (2016) 927–940, http://dx.doi.org/10.3144/expresspolymlett.2016.86.
[26] D. Wolfgang Schröder, W. Klaus Jenni, Crosslinked castor oil derivatives, US Patent 5 387 658, 1995.
[27] M.M. Jin, Y.J. Luo, Preparation and characterization of nitrocellulose aerogel, Chin. J. Explos. Propel. 36 (2013) 82–86.
[28] R. Gallego, J.F. Arteaga, C. Valencia, J.M. Franco, Rheology and thermal degradation of isocyanate-functionalized methyl cellulose-based oleogels, Carbohydr. Polym. 98 (2013) 152–160, http://dx.doi.org/10.1016/j.carbpol.2013.04.104.
[29] R. Gallego, M. González, J.F. Arteaga, C. Valencia, J.M. Franco, Influence of functionalization degree on the rheological properties of isocyanate-functionalized chitin- and chitosan-based chemical oleogels for lubricant applications, Polymers 6 (2014) 1929–1947, http://dx.doi.org/10.3390/polym6071929.
[30] R. Gallego, J.F. Arteaga, C. Valencia, J.M. Franco, Thickening properties of several NCO-functionalized cellulose derivatives in castor oil, Chem. Eng. Sci. 134 (2015) 260–268, http://dx.doi.org/10.1016/j.ces.2015.05.007.
[31] J. Zakzeski, P.C.A. Bruijnincx, A.L. Jongerius, B.M. Weckhuysen, The catalytic valorization of lignin for the production of renewable chemicals, Chem. Rev. 110 (2010) 3552–3599.
[32] R. Gallego, J.F. Arteaga, C. Valencia, J.M. Franco, Chemical modification of methyl cellulose with HMDI to modulate the thickening properties in castor oil, Cellulose 20 (2013) 495–507, http://dx.doi.org/10.1007/s10570-012-9803-4.
[33] L.A. Quinchia, M.A. Delgado, C. Valencia, J.M. Franco, C. Gallegos, Viscosity modification of different vegetable oils with EVA copolymer for lubricant applications, Ind. Crops Prod. 32 (2010) 607–612, http://dx.doi.org/10.1016/j.indcrop.2010.07.011.
[34] K.K. Pandey, A study of chemical structure of soft and harwood and wood polymers by FTIR spectrscopy, J. Appl. Polym. Sci. 71 (1999) 1969–1975, http://dx.doi.org/10.1002/(sici)1097-4628(19990321)71:12<1969::aid-app6>3.0.CO;2-D.
[35] C. Liu, H. Wang, A.M. Karim, J. Sun, Y. Wang, Catalytic fast pyrolysis of lignocellulosic biomass, Chem. Soc. Rev. 43 (2014) 7594–7623, http://dx.doi.org/10.1039/C3CS60414D.
[36] H. Yang, R. Yan, H. Chen, D.H. Lee, C. Zheng, Characteristics of hemicellulose, cellulose and lignin pyrolysis, Fuel 86 (2007) 1781–1788, http://dx.doi.org/10.1016/j.fuel.2006.12.013.
[37] S. Velankar, S.L. Cooper, Microphase separation and rheological properties of polyurethane melts. 1. Effect of block length, Macromolecules 31 (1998) 9181–9192, http://dx.doi.org/10.1021/ma9811472.
[38] C. Liu, J. He, E. Van Ruymbeke, R. Keunings, C. Bailly, Evaluation of different methods for the determination of the plateau modulus and the entanglement molecular weight, Polymer 47 (2006) 4461–4479, http://dx.doi.org/10.1016/j.polymer.2006.04.054.
[39] P. Coussot, Q.D. Nguyen, H.T. Huynh, D. Bonn, Avalanche behavior in yield stress fluids, Phys. Rev. Lett. 88 (2002) 175501, http://dx.doi.org/10.1103/PhysRevLett. 88.175501.
[40] M.A. Delgado, C. Valencia, M.C. Sánchez, J.M. Franco, C. Gallegos, Thermorheological behaviour of a lithium lubricating grease, Tribol. Lett. 23 (2006) 47–54, http://dx.doi.org/10.1007/s11249-006-9109-5.
[41] G. Ovarlez, S. Cohen-addad, K. Krishan, J. Goyon, P. Coussot, On the existence of a simple yield stress fluid behavior, J. Nonnewton Fluid Mech. 193 (2013) 68–79, http://dx.doi.org/10.1016/j.jnnfm.2012.06.009.
[42] L. Lu, X. Liu, Z. Tong, Critical exponents for sol-gel transition in aqueous alginate solutions induced by cupric cations, Carbohydr. Polym. 65 (2006) 544–551, http://dx.doi.org/10.1016/j.carbpol.2006.02.010.
[43] J.E. Martín-Alfonso, J.M. Franco, Influence of polymer reprocessing cycles on the microstructure and rheological behavior of polypropylene/mineral oil oleogels, Polym. Test. 45 (2015) 12–19, http://dx.doi.org/10.1016/j.polymertesting.2015.04.016.
[44] M. Dandapat, D. Mandal, Local viscosity and solvent relaxation experienced by rod-like fl uorophores in AOT/4-chlorophenol/m-xylene organogels, Spectrochim. Acta Part A: Mol. Biomol. Spectrosc. SAA 170 (2017) 150–156, http://dx.doi.org/10.1016/j.saa.2016.07.012.

1.2. Article 2

Green and facile procedure for the preparation of liquid and gel-like polyurethanes based on castor oil and lignin: Effect of processing conditions on the rheological properties

A.M. Borrero-López, C. Valencia, J.M. Franco

Published in:

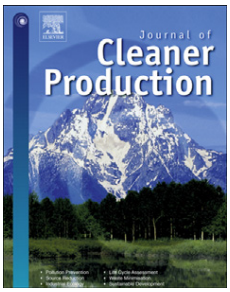

Journal of Cleaner Production
Publishing Company: Elsevier
Editor-in-Chief: JJ. Klemeš, CMVB. Almeida, Y. Wang
Volume 277, 123367
Year 2020
ISSN 0959-6526
DOI: 10.1016/j.jclepro.2020.123367

Category	Journal Rank / Total number of journals	Quartile (Percentage)
Engineering, Environmental	8/53	Q1 (86%)
Environmental Sciences	19/265	Q1 (93%)
Green & Sustainable Science & Technology	6/41	Q1 (87%)
Impact Factor	7.246	

Journal of Cleaner Production 277 (2020) 123367

Contents lists available at ScienceDirect

Journal of Cleaner Production

journal homepage: www.elsevier.com/locate/jclepro

Green and facile procedure for the preparation of liquid and gel-like polyurethanes based on castor oil and lignin: Effect of processing conditions on the rheological properties

Antonio M. Borrero-López , Concepción Valencia , José M. Franco *

Pro²TecS — Chemical Process and Product Technology Research Center, Departamento de Ingeniería Química, ETSI. Campus de "El Carmen", Universidad de Huelva, 21071, Huelva, Spain

ARTICLE INFO

Article history:
Received 11 March 2020
Received in revised form
3 July 2020
Accepted 20 July 2020
Available online 4 August 2020

Handling editor: Cecilia Maria Villas Bôas de Almeida

Keywords:
Castor oil
Lignin
Polyurethanes
Processing variables
Rheology
Solvent-free synthesis

ABSTRACT

This work presents a comprehensive study on the influence of processing variables (temperature, agitation speed) and type of diisocyanate crosslinker on the rheological properties of liquid and gel-like polyurethane formulations based on lignin and castor oil. With this aim, a green and facile one-step preparation protocol which avoids the use of any harmful catalyst or solvent was proposed. Different processing temperatures (25, 45, 70 °C), stirring speeds (23, 70, 140 rpm) and kinds of diisocyanates (hexamethylene diisocyanate, and toluene diisocyanate) were selected to process the different bio-sourced polyurethane samples. These processing variables have proven to be crucial to modulate and control the rheological (viscous and viscoelastic) properties, and curing kinetics after processing, due to the different chemical structures achieved that were elucidated by means of Fourier-transform infrared spectroscopy and differential scanning calorimetry. In general, a low processing temperature and low stirring speed favour the achievement of gel-like characteristics and/or the formation of highly viscous polyurethanes, as a consequence of a higher number of total hydrogen-bonded carbonyl groups, urethane/urea ratio and ratio of hydrogen-bonded/non-bonded urethane and urea linkages. Besides, the selected one-step process, in comparison with the reported two-step process, provides polyurethanes with similar rheological characteristics by significantly reducing the isocyanate content. Finally, lignin was demonstrated to act as an effective filler agent increasing the values of the viscoelastic moduli.

1. Introduction

The increasing interest in the development of harmless and renewable materials has driven research into bio-based polyurethanes over the last few decades. As well-known, the most widely synthetic approach to industrially produce polyurethanes (PUs) is the polycondensation reaction between polyols and polyfunctional isocyanates. This classical method allows to obtain PUs with a wide range of properties which match an extensive variety of applications such as adhesive (Díez-García et al., 2020; Tenorio-Alfonso et al., 2019), coating (Lei et al., 2020; Liang et al., 2019), construction (Zhou et al., 2016), energy storage (Lu et al., 2020) or sound absorption (Caniato et al., 2020) materials. In particular, bio-based liquid-like and gel-like PUs have been proposed as efficient alternatives for replacing traditional lubricating oils and greases. Thus, in previous studies, lignin (Borrero-López et al., 2018), lignocellulose (Gallego et al., 2015a) and cellulose derivatives (Gallego et al., 2015b) were tested as thickening agents in oily media. Some chemical components employed in the manufacture of PUs, i.e. raw materials, catalysts and solvents, may cause environmental problems as they are mainly derived from non-renewable petroleum resources (Visanko et al., 2017). Diverse strategies for the substitution of non-renewable raw materials by renewable resources have been explored to minimize the effect that these products and associated process technologies, affecting a variety of industrial sectors, could provoke in the environment. For instance, Calvo-Correas et al. (2015) developed thermally responsive and shape-memory polymers using only biomaterials such as castor oil, corn sugar and lysine. Castor oil and lignin without using solvent or catalyst involved were applied by Cassales et al. (2020) for film formation. Macocinschi et al. (2009) exploited cellulose

* Corresponding author. Departamento de Ingeniería Química, ETSI. Campus de "El Carmen", Universidad de Huelva, 21071, Huelva, Spain.
E-mail address: franco@uhu.es (J.M. Franco).

https://doi.org/10.1016/j.jclepro.2020.123367
0959-6526/

possibilities to enhance biocompatibility and adhesive properties in biomedical applications of PUs. Santan et al. (2018) also utilized castor oil as the main component for the performance of solvent- and catalyst-free adhesives at room temperature. On the other hand, a completely different approach was targeted by Strachota et al. (2008), which tested environmentally friendly catalysts for polyurethane formation. Among the different renewable resources, lignin is a highly-branched aromatic biopolymer, in most cases considered as a residue and frequently used as a low-valuable fuel in co-generation processes (Lettner et al., 2020), which is able to form networks where other compounds can physically or chemically interact or be confined due to several functional groups available in its chemical structure. On the other hand, castor oil is considered as an important renewable material, with huge possibilities in different industrial sectors and chemical applications (Mutlu and Meier, 2010), mainly as a consequence of its very interesting and particular properties such as high viscosity, good performance at low temperature and availability of free hydroxyl groups which may represent reactive sites and let hydrogen bonds be formed (Trân et al., 1997).

Attending the crosslinking properties of diisocyanates, an easy and straightforward chemical reaction between them and the hydroxyl groups available in both lignin and castor oil is expected, resulting in extensive and entangled networks (Trân et al., 1997). As well known, the chemical structure of diisocyanates influences the −NCO group reactivity (Sonnenschein, 2015). Thus, for instance, hexamethylene diisocyanate (HDI) shows the same reactivity for both isocyanate groups, while in tolylene diisocyanate (TDI), reactivity is highly influenced by the position of the −NCO group, being much more reactive the 2,4 diisocyanate than the 2,6 diisocyanate (Randall and Lee, 2003), where some isocyanate groups could be hindered (Borrero-López et al., 2017). Nevertheless, TDI, due to its aromatic character, possesses a higher reactivity compared to aliphatic diisocyanates like HDI (Hablot et al., 2008). Moreover, as a result of the chemical and morphological versatility, processing variables and conditions are crucial on polyurethanes developing, especially considering the different possible competitive and/or concurrent chemical reactions (formation of urethanes, ureas, carbodiimides, allophanates, biurets, etc.) and network arrangements that can be deeply influenced by temperature, agitation or shear and moisture conditions, among other factors. In this way, Raghunanan et al. (2018) demonstrated rheological properties to be highly dependent on humidity conditions. Furthermore, Zimmer et al. (2017), supported these results by studying dry-curing conditions in long-term analyses. The reactivity of isocyanate groups also depends on the electronegativity and steric hindrance of the other reactive group, being always higher for amines and equal for water and primary alcohols, as examples (Ionescu, 2005). Besides, not only chemical but physical interactions need to be carefully considered in elucidating PU structure, as hydrogen-bonding has demonstrated to possess a substantial effect on the macroscopic properties of polyurethanes (Yang et al., 2006). For all these reasons, PUs can lead to unexpected properties regarding different manufacturing processes and/or processing conditions, even when the same reagents and proportions are used. There are plenty of works reporting different processing conditions in the PUs synthesis, such as different solvents (toluene (Borrero-López et al., 2017), THF (Nacas et al., 2017), DMF (Suhas et al., 2014), pyridine (Cheradame et al., 1989)), catalysts (triethylamine (Gallego et al., 2015a) and DBTDL (Hablot et al., 2008)) or steps (one (Lu et al., 2002) or two (Jeong et al., 2013)). Furthermore, structural, thermal and mechanical properties of PUs have been suggested to depend on them (Hablot et al., 2008), however, no in-depth systematic studies have been performed until now.

Some previous works have been carried out on the NCO-functionalization of lignocellulosic materials and further dispersion in castor oil to achieve oleogels, foams and solid-like systems, thus involving a two-step protocol. Gallego et al. (2015a) studied different lignocellulosic fractions obtained either from different treatments or from different origins, whereas in Borrero-López et al. (2017) kraft lignin was used as polyol, in both cases for lubricant applications. On the contrary, Zhang et al. (2015) were able to produce solid PU composites through the combination of lignin modified with octadecyl isocyanate and a soybean-and-castor oil vegetable oil mix with enhanced dielectric and mechanical properties. Gómez-Fernández et al. (2017) instead performed flexible polyurethane foam formulations by NCO-functionalizing lignin and mixing with a castor oil derived polyol. Despite the two-step protocol prevents randomness in the chemical reaction of the different polyols, some drawbacks such as the use of solvents in the first functionalization step cannot be avoided. The target of the present work was to study the influence of processing variables such as temperature and agitation speed on the thermo-rheological properties of liquid and gel-like polyurethane formulations based on renewable materials like castor oil and lignin as a source of polyols. With this aim, following the principles of process intensification, a simple one-step process, free of any harmful catalyst or solvent, was selected. Moreover, aliphatic (HDI) and aromatic (TDI) diisocyanates were employed to assess the role of the crosslinker molecular structure and reactivity on the processing conditions, further curing of these bio-based PUs and their influence on the rheological properties.

2. Materials and methods

In this section, the materials employed to prepare the bio-sourced polyurethanes are described thoroughly as well as the processing methods and conditions and the characterization techniques.

2.1. Materials

The alkali lignin and the diisocyanates used in this work (HDI, 98% purity, and TDI, 80% isomer 2,4-TDI, 99% purity) were purchased from Sigma-Aldrich. Castor oil was supplied by Guinama (Spain). Fatty acid composition and main physical properties can be found elsewhere (Quinchia et al., 2010).

2.2. Processing of castor oil/lignin-based polyurethanes

Processing of castor oil/lignin-based polyurethanes was carried out *in situ* in an ARES controlled-strain rheometer (Rheometric Scientific, UK) equipped with a forced convection oven as temperature controller and a mixing geometry comprising a rotational anchor impeller and a 60 mL cylindrical vessel (schematic picture and dimensions included in Fig. S1 of supporting information). Different processing temperatures (25, 45 and 70 °C) and agitation speeds (23, 70, 140 rpm) were applied whereas 24 h was fixed as processing time. All components were added simultaneously in batches of 30 g, selecting 70 and 75 wt% castor oil concentration for HDI- and TDI-based PUs, respectively. The remaining percentage corresponded to the other two components which were generally added in lignin/diisocyanate weight ratios of 1/0.5 and 1/0.76, for HDI- and TDI-based PUs, respectively. In this way, the amount of TDI was recalculated taking into account its molecular weight, as explained elsewhere (Borrero-López et al., 2017), to maintain the same free −NCO molar content in the whole sample. For the sake of comparison, other PUs were also prepared using other lignin/diisocyanate ratios or without lignin, just replacing this with the corresponding amount of castor oil. Table 1 collects the different PU

Table 1
Nomenclature, components, concentrations and processing conditions for the PU samples studied.

Sample code	Diisocyanate	Oil concentration (%)	Lignin/diisocyanate ratio (w/w)	Stirring (rpm)	Temperature (°C)
H25	HDI	70	1/0.5	70	25
H45	HDI	70	1/0.5	70	45
H70	HDI	70	1/0.5	70	70
H25-140	HDI	70	1/0.5	140	25
H45-23	HDI	70	1/0.5	23	45
T25	TDI	75	1/0.76	70	25
T45	TDI	75	1/0.76	70	45
T70	TDI	75	1/0.76	70	70
H25 (1/1)	HDI	70	1/1	70	25
H25 (1/0.75)	HDI	70	1/0.75	70	25
H25-lignin free	HDI	90	–	70	25
H25 (1/1)-lignin free	HDI	85	–	70	25
T25-lignin free	TDI	89.21	–	70	25
H25TS(1/1)[a]	HDI	70	1/1	70	25
H25TS(1/2)[a]	HDI	70	1/2	70	25
T25TS(1/1)[a]	TDI	70	1/1	70	25

[a] Samples prepared using a two-step protocol (from Borrero-López et al., 2017).

samples prepared using the different processing conditions, types of diisocyanate and lignin/diisocyante weight ratios. After processing, samples were maintained under environmental conditions to study the curing process.

2.3. Fourier-transform infrared spectroscopy (FTIR)

FTIR spectra were obtained using a JASCO FT/IR 4200 (Jasco inc. Japan) apparatus in a 400 to 4000 cm^{-1} wavenumber range, at a resolution of 4 cm^{-1}, in the transmission mode. A small drop of the different PU samples was placed between two KBr disks (32 × 3 mm^2) to acquire the FTIR spectra.

2.4. Differential scanning calorimetry (DSC)

DSC measurements were carried out using a Q-100 calorimeter (TA Instrument Waters, USA). Curing evolution was assessed by applying temperature ramps from −80 °C to 200 °C at 10 °C/min under inert nitrogen atmosphere. Both glass transition temperatures of hard and soft segments were obtained, once the systems were fully cured (no free isocyanate available), in the second heating ramp from −80 to 200 °C in order to eliminate the thermal history of the sample (Sánchez et al., 2014).

2.5. Rheological characterization

Rheological characterization was performed in an ARES controlled-strain rheometer (Rheometric Scientific, UK). The viscosity evolution with reaction time was followed up for 24 h during the processing of castor oil/lignin-based PUs, using the previously described mixing geometry and applying the principles of the mixing rheometry technique (Aït-kadi et al., 2002; Franco et al., 2005). After processing, several different tests were performed using serrated plate-plate geometries (25 and 50 mm diameters and 1 mm gap). Small-amplitude oscillatory shear (SAOS) tests, inside the linear viscoelastic regime, were carried out from 100 to 0.03 rad/s at different temperatures (from 25 to 100 °C) several days during curing and once the sample was fully cured. Oscillatory strain sweep tests, at a frequency of 1 rad/s, were previously performed to determine the linear viscoelastic range. On the other hand, viscous flow measurements of the final products, i.e. once the curing process was totally accomplished, were carried out by applying an increasing stepped shear rate ramp from 0.01 to 100 s^{-1}, at 25 °C. All rheological tests were replicated at least twice.

3. Results and discussion

This section includes detailed description of the results obtained with regard to monitoring of the one-step processing protocol, analysis and understanding of the curing process, rheological response of the bio-based polyurethanes, FTIR structural analysis and the comparison with formulations obtained by applying a two-step processing protocol and lignin-free systems.

3.1. In situ viscosity monitoring during processing

Fig. 1a and b shows the *in situ* follow up of viscosity evolution for the incipient castor oil/lignin-based PUs, using HDI and TDI as crosslinkers, respectively, during their processing in the rheoreactor, as a function of temperature and agitation speed. As can be noticed, the modification of processing conditions, i.e. processing temperature and agitation speed, allows to obtain different control of the viscosity. Generally, the viscosity increases during processing as a consequence of the occurrence of the different reactions (Arnold et al., 1957), however, PU samples studied exhibited diverse trends in the evolution of viscosity above 300–400 min, depending on the processing conditions. With respect to HDI-containing samples, the viscosity values of incipient PUs processed at 70 rpm and 45 °C and, especially, 70 °C exceeded those found for sample H25, manufactured at 25 °C, during a significant part of the processing, despite the reciprocal influence of temperature on viscosity. Moreover, only the H70 sample achieved a constant viscosity value within the 24 h-process (Fig. 1a). The higher viscosity values observed when increasing processing temperature are due to the more pronounced initial increase, as a consequence of the boosted reactivity of the diisocyanates with temperature. This trend was observed by Abushammala (2019) when treating cellulose nanocrystals with TDI, whereas Ando (1993) observed similar tendencies when working with 4,4′-diisocyanatodiphenylmethane (MDI). Hablot et al. (2008) also obtained similar results working with castor oil and TDI, HDI and isophorone diisocyanates. In fact, the constant values finally achieved for H70 suggest no longer free isocyanate available due to the fast kinetics. On the other hand, significantly lower and higher viscosity values were obtained by increasing and decreasing the stirring speed, respectively, which is also a consequence of the shear thinning character of these samples, as discussed below. Apart from the effect of shear intensity on the viscosity of a non-Newtonian reacting mixture, the increasing agitation speed favours the contact between the three components facilitating both

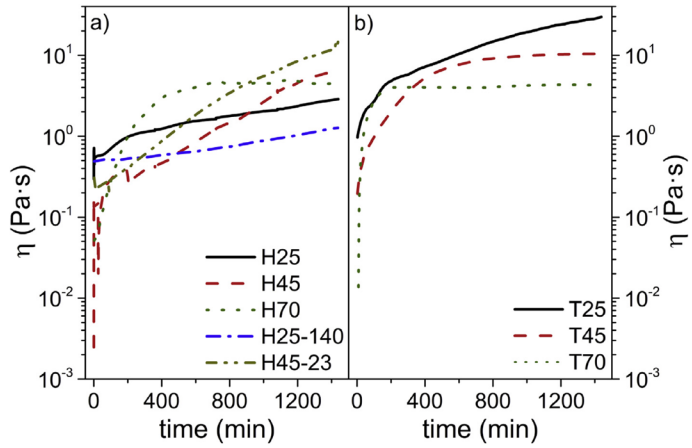

Fig. 1. Viscosity evolution during processing at different temperatures and agitation speeds for a) HDI- and b) TDI-based PUs.

urethane and urea formation (Navarchian et al., 2005), the last one promoted by the incorporation of a certain amount of air and moisture. Nonetheless, a higher agitation can also produce different rearrangements which may affect hydrogen-bonding and final structuration of the urethane and urea chains, which had already shown to be affected by temperature (Teo et al., 1997). Regarding the type of diisocyanate crosslinker, as a consequence of the much higher reactivity of TDI, higher initial slopes of the viscosity vs. time plots, i.e. higher viscosity increments at short reaction times, were found for TDI-based systems at all temperatures compared to their counterparts containing HDI (Fig. 1b). Furthermore, for the same reason, both samples processed at 45 and 70 °C tended towards a plateau in viscosity values relatively soon in this case.

3.2. Study of the curing process

Several samples studied, as inferred from the evolution of the viscosity values during processing, did not achieve the final structure just after completion of the processing treatment and, on the contrary, they require from several days to around one week, i.e. a subsequent curing process, to obtain the ultimate rheological properties. This fact is predominantly a consequence of the free-isocyanate groups still present in the matrix, which are able to react further at room temperature until their complete disappearance. Fig. 2, which shows the FTIR spectra of both HDI- and TDI-based formulations (H25 and T25, respectively) taken one day and seven days after processing, illustrates this evolution. As can be observed, there is still a significant amount of free –NCO groups one day after processing, which is easily detected by the absorption band centred at around 2270 cm^{-1}. This band is much more intense in H25, as expected. However, after one week of curing, no free isocyanate was detected in both systems. Furthermore, as can be seen, at around 3330 cm^{-1}, a narrow band overlapped to the wide absorption band centred at 3400 cm^{-1}, corresponding to hydroxyl groups, appears with the progress of curing. This band, attributed to N–H stretching vibration, confirms the urethane and urea formation (Borrero-López et al., 2017). Another band which also supports the occurrence of these reactions is that found in the range of 1745 to 1600 cm^{-1}, corresponding to the stretching vibration of carbonyl groups in different chemical environments and/or components, i.e., free (non-hydrogen-bonded) carbonyl groups in castor oil triglycerides and those free or hydrogen-bonded carbonyl groups in urethane and urea segments (Tenorio-Alfonso et al., 2019).

On the other hand, the curing process can also be quantitatively monitored taking into account the intensity of the free isocyanate absorption peak normalized with the methylene absorption bands at both 2934 and 2855 cm^{-1}, which must remain unaltered during the whole curing process (Cateto et al., 2008). For the sake of comparison and deeper insight, DSC tests have also been used for this purpose. In the samples studied, as can be illustrated for a selected formulation (H25-140) 24 h after processing (see Fig. S2 in the supporting information), an exothermic peak at around 130 °C and 140 °C for TDI- and HDI-based samples respectively, is observed. This thermal event has been associated with the temperature-promoted curing reactions of still-available –NCO groups (Bina et al., 2004) and therefore becomes less significant with the progress of curing, totally disappearing after completion of the process. The enthalpy of this thermal event has been traditionally considered a measurement of the amount of the remaining free isocyanates in the matrix. Both sets of data have been collected and displayed in Fig. 3 as a function of the curing time. As can be observed, both DSC and FTIR results evidenced a very similar trend, demonstrating their robustness and usefulness. Dashed lines in Fig. 3 are plotted to indicate the end of the processing in the rheoreactor. As can be seen, the available –NCO content decreased with time, with different kinetics depending on the processing variables. For instance, it can be shown that the induced agitation during processing favours the reaction of –NCO groups, whereas once the mixing process was finished, the evolution of free –NCO groups changed to a less pronounced trend. This fact can be clearly noticed in H25 and H25-140 samples, where much slower kinetics is observed once the processing conditions have been withdrawn. Moreover, analysing different stirring speeds, it is apparent how an increase in this processing variable led to lower values of free –NCO content because of the occurrence of faster reactions, as shown for the H25-140 sample as compared with H25. However, no significant differences were found in H45–23 and H45 samples, probably because of the influence of the higher processing temperature. On the other hand, as expected, higher processing temperatures promote a sharper decay of free –NCO content. Finally, faster curing

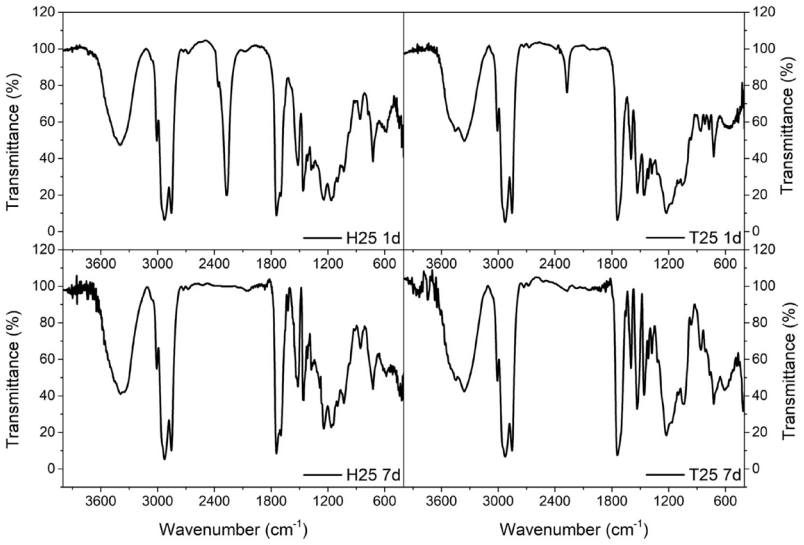

Fig. 2. FTIR spectra of PU samples at different curing times.

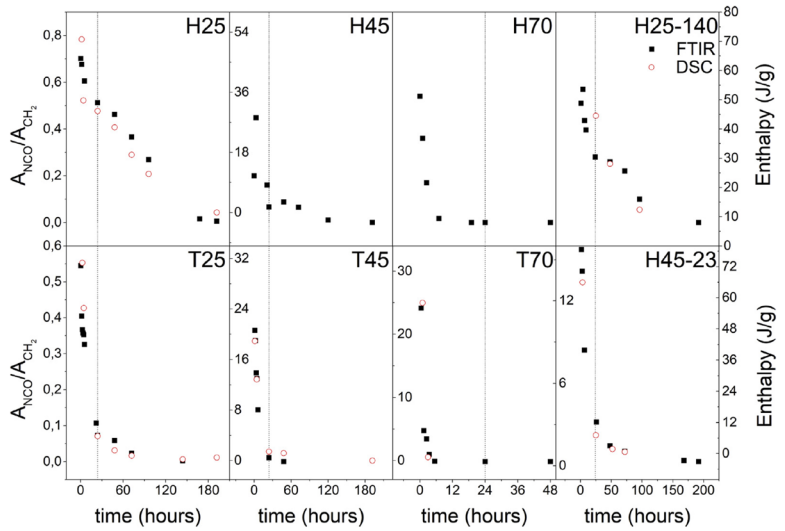

Fig. 3. Evolution of free isocyanate during curing monitored using FTIR and DSC. Vertical dashed lines are included to separate processing (left) to the curing process (right).

kinetics of TDI-based samples compared to HDI-based samples is again evidenced.

3.3. Thermo-rheological behaviour

During the curing process, it is also noticeable the change observed in the rheological response of the PU samples. Fig. 4 shows the evolution of SAOS functions (the storage, G′ and the loss, G″, moduli, respectively) of two selected HDI- and TDI-based samples, at several temperatures and different curing stages (1 and 7 days after processing). On the one hand, a dramatic increase of almost two decades in the values of both SAOS functions can be observed for H25 sample at 25 °C as a consequence of curing, whereas this increase is almost negligible for T25 sample, since

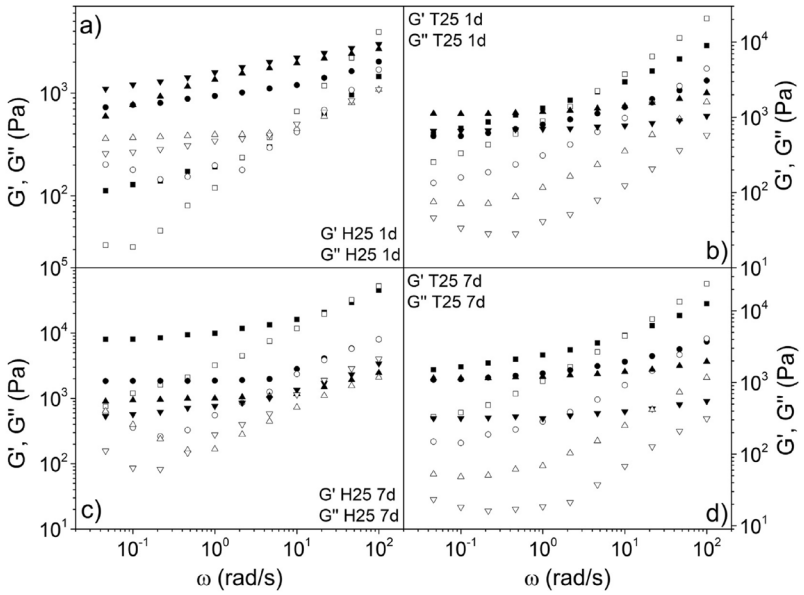

Fig. 4. Frequency dependence of the storage (G′, filled symbols) and loss (G″, hollow symbols) moduli for H25 and T25 samples at a) & b) first day and c) & d) seven days of curing respectively. (■ 25 °C, ● 50 °C, ▲ 75 °C and ▼ 100 °C).

curing is almost completed one day after processing. On the other hand, a reduction in both G′ and G″ should be observed for these isocyanate-based gel-like dispersions when increasing temperature (Gallego et al., 2015a). However, this fact only happens for totally cured samples (Fig. 4c and d) whereas for shorter curing times (Fig. 4a and b), an increase in SAOS functions with temperature is evidenced as a consequence of the free −NCO still available, being this effect much more noticeable for the HDI-based sample, which exhibited values at 100 °C up to one decade higher than those observed at 25 °C. On the contrary, as TDI-based samples have much less free −NCO content available after one day of curing, the temperature-induced changes of SAOS functions are not so relevant. Moreover, this temperature-promoted effect on the SAOS functions found on the first day of curing does not only affect the values of these functions but also the frequency dependence, indicating the achievement of different internal structures. For H25, the crossover between G' and G" found at intermediate frequencies at 25 °C, was not detected at higher temperatures, during the first day of curing (Fig. 4a). However, this crossover is apparent at 50 and 75 °C in the naturally cured sample (Fig. 4c), which reflects the different gel strength achieved depending on the curing conditions. A higher curing temperature may favour secondary reactions, leading to a higher proportion of urea bonds (Han et al., 2008), thus resulting in a more developed plateau region, as it was also demonstrated when modifying humidity conditions during curing (Raghunanan et al., 2018).

Concerning the thermo-rheological behaviour of the completely cured formulations, it is apparent for H25 how SAOS functions decrease by increasing temperature, but the overall microstructural pattern remains the same, as deduced from the same frequency dependence of the viscoelastic functions (Fig. 4c). However, T25 sample does not undergo the same thermo-rheological response. A shift in the plateau region to higher frequencies was detected by increasing temperature together with a decrease in the values of viscoelastic moduli (Fig. 4d), yielding a softening of the structure, thus suggesting a thermo-rheological simplicity.

The application of the time-temperature (t-T) superposition principle is illustrated in Fig. 5 for all completely cured samples studied in order to obtain a generalized rheological response. Excepting H25, as a consequence of the already mentioned thermo-rheological response, all the PU samples can be considered thermo-rheologically simple materials, similarly to that found in other isocyanate-based materials (Tenorio-Alfonso et al., 2019). The selected reference temperature in all these master curves was 25 °C. Several important remarks on the effect of processing variables on the PU rheological response can be deduced from these plots. The stronger gel-like responses were found at low processing temperature (25 °C), for both HDI- and TDI-based PUs, probably due to longer PU chains formed (Ando, 1993). However, H25 does not follow the t-T superposition principle, especially at temperatures lower than 75 °C, which have already been reported for large block polyurethanes due to microphase separation at those temperatures (Velankar and Cooper, 1998). In addition, a higher degree of microphase separation at relatively low NCO:OH ratios in bio-based PU adhesives has been directly related with the non-application of the t-T superposition principle as a consequence of the lower thermodynamic compatibility (Tenorio-Alfonso et al., 2019). As well-known, the degree of phase separation in PUs is strongly related to the glass transition temperatures of the soft ($T_{g,SS}$) and hard ($T_{g,HS}$) segments, resulting in higher values of $T_{g,HS}$ for higher compatibility between both microphases (Tenorio-Alfonso et al., 2019). In this respect, DSC tests performed on the PUs studied allow to conclude that H25 is the one with the lowest $T_{g,HS}$ (around 56 °C, see Table 2). On the contrary, HDI-based PUs

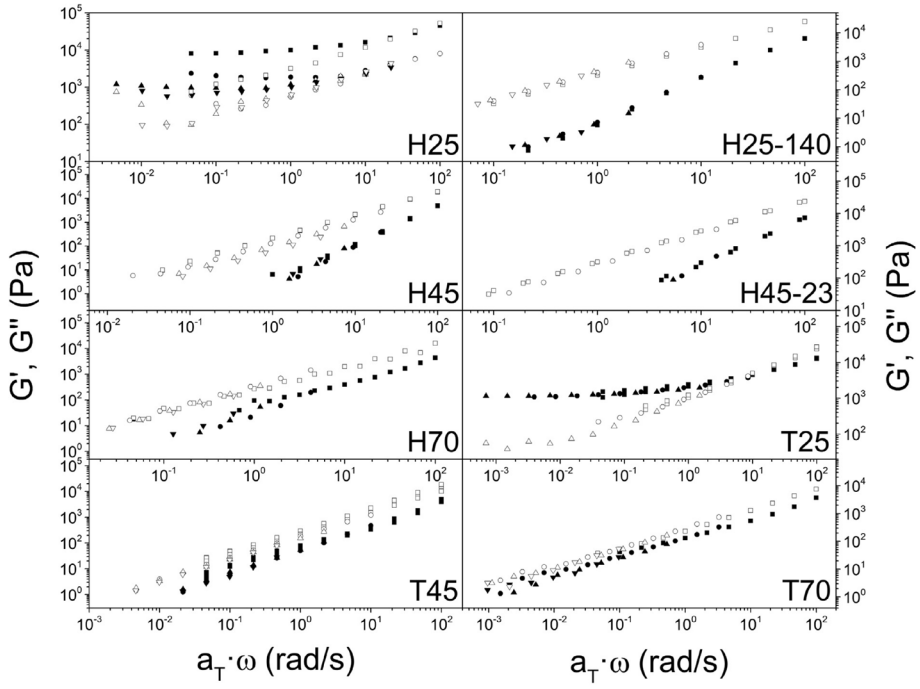

Fig. 5. Time-temperature superposition master curves of PU samples studied. (■ 25 °C, ● 50 °C, ▲ 75 °C and ▼ 100 °C).

Table 2
Pre-exponential factors and activation energies for the superposition shift factors (eq. (1)) and glass transition temperatures of soft (SS) and hard (HS) segments.

Sample	A_T	Ea (kJ/mol)	$T_{g,SS}$ (°C)	$T_{g,HS}$ (°C)
H25	–	–	−52	56
H25-140	1.41E-11	61.46	−53	82
H45	8.94E-08	39.70	−50	82
H45-23	3.54E-09	47.66	−49	89
H70	5.72E-12	62.87	−51	87
T25	4.05E-18	99.39	−45	74
T45	2.94E-12	65.57	−43	80
T70	1.15E-15	84.46	−45	72

processed at higher temperatures showed liquid-like responses. For instance, increasing the processing temperature to 45 °C favoured liquid-like properties, although some soft gel-like characteristics are again evidenced by further increasing processing temperature to 70 °C. Moreover, a high processing stirring speed (i.e. 140 rpm) also leads to liquid-like behaviour, resulting in values of the linear viscoelastic moduli slightly higher than those found when applying 70 rpm at 45 °C, demonstrating that the application of different temperatures and stirring speeds actually leads to diverse structural orders. Finally, softer gels were obtained when processing TDI-based systems at 45 and 70 °C compared to the relatively strong gel obtained at 25 °C. In fact, very similar almost critical gel behaviours were obtained at these two processing temperatures, being the T70 sample slightly stronger (i.e. closer values of G' and G"), similarly to what happened with HDI systems.

The evolution of the shift factors (a_T) applied to obtain the master curves with temperature is shown in Fig. 6. In all cases, an Arrhenius-type equation describes fairly well this evolution:

$$a_T = A_T \cdot e^{\frac{E_a}{R} \cdot \left(\frac{1}{T} - \frac{1}{T_0}\right)} \quad (1)$$

where R is the ideal gas constant (8.314 J mol^{-1} K^{-1}), T the absolute temperature (K), T_0 is the reference temperature (K), A_T is the pre-exponential factor and E_a is the activation energy (J·mol^{-1}). The values of the pre-exponential factor and the activation energies resulting from the fittings to eq. (1) are collected in Table 2. The lowest values of E_a correspond to the samples processed at 45 °C, i.e., the most liquid-like ones, which highlights the lower temperature dependence of non-highly structured materials (Velankar and Cooper, 1998). Besides, TDI-based samples generally show higher thermal susceptibility, i.e. higher E_a values, than HDI-based samples. On the other hand, slightly higher values of E_a were obtained by decreasing stirring speed.

Most of the bio-based polyurethanes processed can be categorized as liquid-like or weak gel-like systems. A modification of the power-law equation (Gabriele et al., 2001) widely used for weak gels, as for instance in fields such as lubrication (Cortés-Triviño et al., 2017) or tissue regeneration (Munarin et al., 2014), can be applied to describe the evolution of the complex modulus with frequency for the PU systems studied:

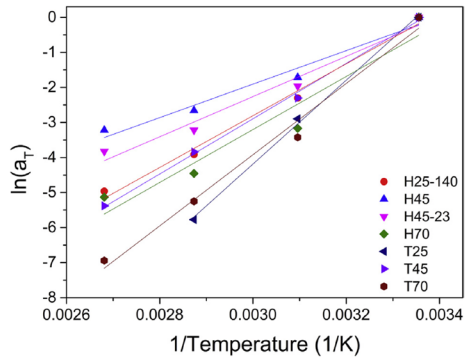

Fig. 6. Values of the superposition parameter (a_T) for PUs obtained by applying different processing conditions.

$$G^* = A \cdot \left(b + \omega^{1/n} \right) \quad (2)$$

where G* is the complex modulus, ω is the angular frequency (rad/s), A gives an idea of the gel strength or sample consistency, n is a power-law exponent, and b takes the values of 0 and 1, for liquid-like and gel-like systems, respectively.

Fig. 7 shows the evolution of G* with frequency and fittings to eq. (2) for all the systems studied, considering the time-temperature superposition. As can be seen, G* for those dispersions exhibiting weak gel-like characteristics, i.e. almost critical gels, or liquid-like responses, follows a linear evolution in log-log plots, which can be well fitted to eq. (2) being $b = 0$. However, those samples with stronger gel-like properties depict a non-linear trend in the wide frequency range studied, which can be fitted to eq. (2) for $b = 1$. For the sake of comparison, the fitting for H25 was also shown, not including G* values at 25 °C. Table 3 collects the values of eq. (2) fitting parameters for all the PU samples studied. As can be seen, an increase in processing temperature, from 45 to 70 °C, results in slightly higher values of both A and n parameters for both HDI- and TDI-based samples, as a consequence of the aforementioned structural change favoured at 70 °C. An increase in both parameters was also observed when processing stirring speed was reduced. When comparing both types of diisocyanates for 45 and 70 °C processing temperatures, TDI-based samples yielded higher values of both parameters because of its inherent structure, which has already shown to provide more rigid networks (Hablot et al., 2008). Pandya et al. (1986) associated this effect to the direct bonding of the –NCO group to the aromatic ring.

In an attempt to quantify the effect of processing parameters on the rheological properties of the PUs studied, parameters A and n obtained from the fitting to eq. (2) were intended to be correlated with processing temperature and stirring speed. As both temperature and stirring speed have been modified in the processing of PUs, simultaneously affecting the rheological response, both

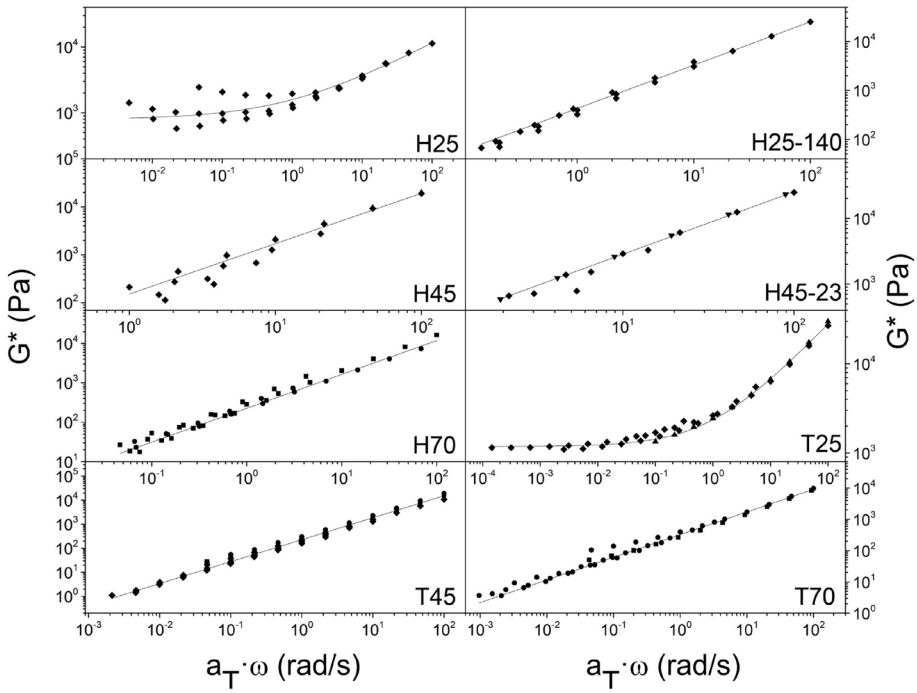

Fig. 7. Evolution of the complex modulus (G*) with frequency resulting from the time-temperature superposition for PU samples.

Table 3
Values of A, n and b parameters resulting from the fitting to eq. (2).

Samples	A (Pa·rad·s$^{1/n}$)	b	n	R^2
H25	793	1	1.77	0.959
H45	179	0	0.98	0.994
H70	227	0	1.16	0.960
H25-140	427	0	1.13	0.999
H45-23	320	0	1.05	0.998
T25	1182	1	1.47	0.995
T45	229	0	1.10	0.947
T70	325	0	1.38	0.995

variables have been combined in one single parameter which considers the severity of processing conditions:

$$S = N \cdot e^{\frac{(T-100)}{\phi}} \quad (3)$$

This equation is a modified version of the severity concept used in the pulping treatment of lignocellulosic materials which takes into account the effect of time and temperature together (Overend and Chornet, 1987). In eq. (3) S is the severity of processing conditions, N is the stirring speed, in rpm, included instead of the processing time, T is the processing temperature, in Celsius degrees, and ϕ is a constant established for the treatment of lignocellulosic materials (value 14.75).

Fig. 8 shows how A and n parameters evolve with the severity parameter for both HDI- and TDI-based PUs. From this plot, it is clearly deduced that increasing processing severity values up to around 2 reduced the values of both A and n parameters while higher values produce again an increase in both of them, basically as a consequence of the above-mentioned effect of processing at 70 °C.

3.4. Viscous flow behaviour

Fig. 9 shows the viscous flow response of the different PU systems, which was likewise affected by processing conditions. Thus, an increase in processing temperature from 25 to 45 °C or in the stirring speed led to a reduction in both the viscosity values, in most of the shear rate range studied, and the shear-thinning character, an effect which was reverted when processing at 70 °C. Thus, as a consequence of the more pronounced shear-thinning character, the viscosity of the H25 sample, at high shear rates (above 10 s^{-1}), was lower than those observed for H25–140 or H45. A similar trend was observed for TDI-based samples. When comparing both diisocyanates, viscosity values were generally higher and the shear-thinning character more pronounced for TDI-based PU systems. These results highlight again the influence of the diisocyanate on the PU rheological properties. Thus HDI, being a linear diisocyanate, is known to generate more ordered structures under the same conditions than TDI, as Suhas et al. (2014) demonstrated by means of X-ray diffraction, while hardness and opacity tests allowed Pandya et al. (1986) to reach similar conclusions. Therefore, the structuration can lead to the viscoelastic properties already mentioned, however, once the system starts to flow, the rigidity of the TDI molecule may play a more significant role, raising viscosity values instead (Hablot et al., 2008). The viscous flow responses obtained were found to fit fairly well the power-law model described hereafter:

$$\eta = K \cdot \dot{\gamma}^{m-1} \quad (4)$$

where K and m are the consistency and flow indices, respectively. Both parameters for all the systems studied have been included in Table 4, which support the statements previously discussed.

3.5. FTIR-based structural analysis

Processing variables have demonstrated to play a crucial role in the properties of liquid and gel-like PUs studied, which is logically the consequence of different chemical structures achieved during the reaction. As well-known (Chattopadhyay and Raju, 2007; Raghunanan et al., 2018), at low temperatures urethane and urea are the two main linkages than can be formed in the isocyanate

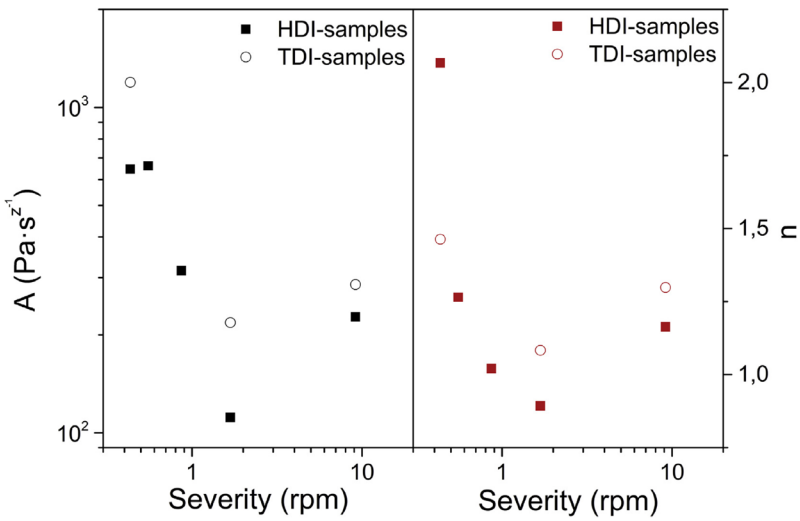

Fig. 8. Influence of processing conditions quantified in the severity parameter (eq. (3)) on A & n for HDI- (■) and TDI-samples (●).

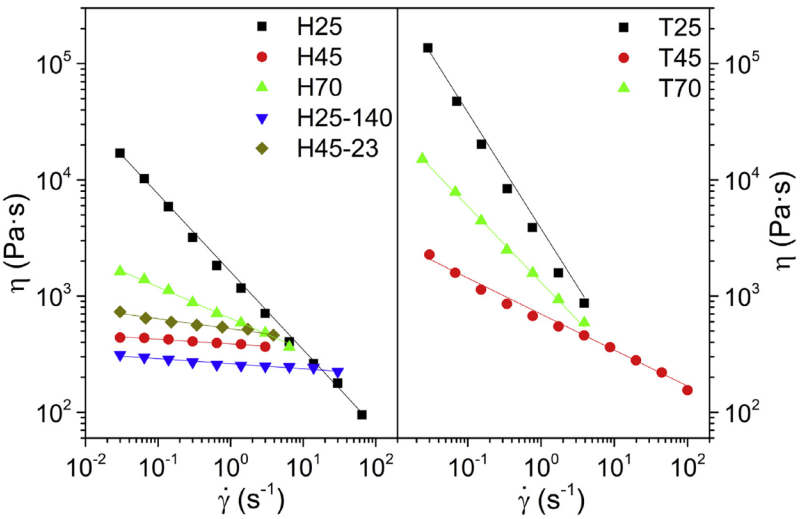

Fig. 9. Viscous flow measurements, at 25 °C, for PUs obtained by applying different processing conditions.

Table 4
K and m values resulting from the fitting to eq. (4).

Sample	K (Pa·s^m)	m
H25	1614	0.33
H45	387	0.96
H70	641	0.73
H25-140	261	0.96
H45-23	522	0.91
T25	3806	0.01
T45	699	0.69
T70	1313	0.34

Table 5
Signals resulting from the deconvolution study applied to the carbonyl stretching band.

Carbonyl Unit	Peak (cm^{-1})
Castor oil free carbonyl groups	1748
Free urethane	1739; 1732; 1724
Disordered urethane	1716
Ordered urethane	1705
Urethane with urea	1697
Free urea	1690; 1684
Disordered urea	1670; 1662
Ordered urea	1635
Methylene residual signals	1654; 1645

nucleophilic attack by the hydroxyl groups in a castor oil medium, which can be promoted and arranged in several ways depending on processing and reaction conditions, resulting in different hydrogen bonding. FTIR spectra have been obtained and used to elucidate the diverse bonds of the carbonyl groups present in these urethane and urea linkages (Yang et al., 2006). With this aim, the spectra were then submitted to a mathematical self-deconvolution procedure which enables the determination of intrinsically overlapped absorption bands. The wavenumbers of the different bands apparent after deconvolution for the PU samples studied are displayed in Table 5. The second-derivative signal of FTIR spectra provides up to 14 different signals within the main absorption band associated to the stretching vibration of the carbonyl group, which can be related to several linkages, H-bonding and/or chemical environment, as can be seen in Fig. 10 and Table 5. Bands of the carbonyl group associated with free urethanes can be found in the range 1740–1724 cm^{-1}, whereas the same groups interlinked via hydrogen bonding appear at lower wavenumbers (Rath et al., 2008). On the other hand, those bands associated with free urea groups appear at around 1685 cm^{-1}. In general, lower wavenumbers indicate higher structuration degree (Shi et al., 2008), i.e. H-bonding, being disordered ureas centred at around 1666 cm^{-1} (Ning et al., 1997) and ordered ureas at around 1638 cm^{-1} (Mishra et al., 2012).

Table 6 includes the proportion of the carbonyl groups present in the different types of bonds estimated from the relative areas of the main absorption bands obtained by applying the deconvolution procedure. As expected, the first peak at around 1748 cm^{-1}, related to free C=O moieties from castor oil triglycerides, generally corresponds to the highest peak of the deconvolution, being usually more intense for those samples exhibiting liquid-like or weak gel-like rheological properties. This fact suggests a reduction of the H-bonded carbonyl groups of castor oil (Chattopadhyay and Raju, 2007), which may cause the decrease observed in the values of the viscoelastic moduli.

In agreement with previous work (Seymour et al., 1970), a prevalence of hydrogen-bonded urethane linkages to non-bonded linkages is achieved. As expected, TDI-based samples present higher density of urethane linkages compared to HDI-based PUs, as suggested before, due to the higher reactivity of the aromatic diisocyanate, since the lower reactivity of HDI makes urea bonds be triggered by the longer contact with moisture.

Generally, the increase in the total number of hydrogen-bonded carbonyl groups, the urethane/urea ratio and the ratio of H-bonded/non-bonded carbonyl groups of both kinds of linkages, and for urethane and urea independently, results in higher gel strength or more viscous PU systems. Thus, for instance, the higher values of

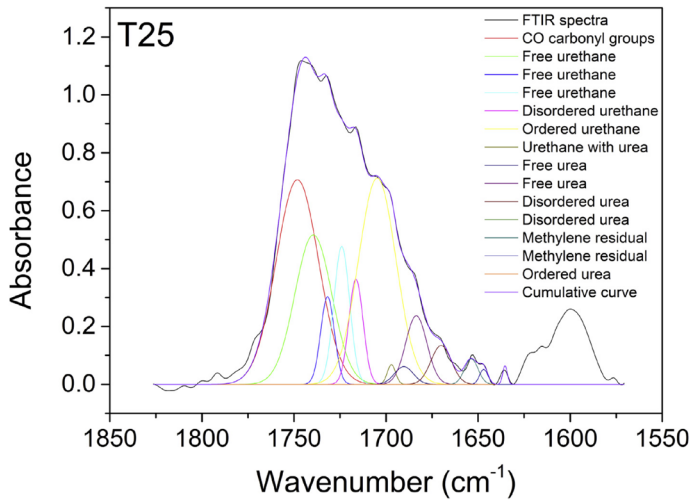

Fig. 10. FTIR spectra in the range of 1600–1800 cm^{-1} and deconvolution signals regarding carbonyl groups of castor oil and the diverse urethane and urea linkages.

Table 6
Deconvolution results for PUs obtained by applying different processing conditions expressed as proportions of the carbonyl groups present in the different types of bonds, estimated from the relative areas of the absorption bands.

	H25	H45	H70	H25-140	H45-23	T25	T45	T70
Non-H-bonded triglycerides carbonyl groups	0.31	0.33	0.24	0.32	0.23	0.29	0.27	0.35
Total urethanes	0.39	0.37	0.41	0.38	0.43	0.60	0.58	0.46
Total ureas	0.16	0.24	0.24	0.17	0.12	0.09	0.09	0.13
Total H-bonded	0.42	0.32	0.42	0.36	0.42	0.34	0.32	0.40
Urethanes/Ureas	2.37	1.57	1.72	2.26	3.53	6.84	6.37	3.62
Bonded/non-bonded urethanes	3.70	2.02	1.56	2.16	1.78	1.06	0.97	2.31
bonded/no bonded ureas	0.32	0.28	1.19	0.24	0.21	0.49	0.18	0.67
Bonded/non-bonded linkages	1.85	1.01	1.42	1.25	1.30	0.96	0.82	1.76

viscoelastic moduli observed at room temperature were consistent with the higher percentage of bonded/non-bonded ratio of urethanes and urea linkages for both HDI and TDI, and the total number of hydrogen-bonded carbonyl groups, highlighting the extreme importance of H-bonding on polyurethane formation. Finally, the slightly higher total content of urea bonds when increasing processing temperature may be explained attending the improved contact with moisture by convection and the already suggested stronger influence of temperature in urea formation compared to urethanes (Han et al., 2008).

3.6. *One-step versus two-step processing protocol*

As mentioned in the introduction section, a two-step process consisting in the functionalization of the biopolymer first and then the subsequent efficient dispersion of this in the vegetable oil has been traditionally applied to produce similar PU systems (Gallego et al., 2015a), which in principle results in a more controlled reaction between the castor oil triglycerides and the biopolymer. Here, following the process intensification principles, this two-step process has been compared with the more direct and simpler one-step process previously described, which is also more environmentally friendly, since it halves the reaction time and avoids the use of risky chemicals, like solvents (i.e. toluene) or catalysts (i.e. triethylamine). Fig. 11 shows the comparison of the rheological response of PU systems prepared using the one-step approach followed in this study with that previously reported (Borrero-López et al., 2017) for PUs prepared using a two-step processing protocol. For better understanding, two-step samples were named similarly to the one-step samples by adding TS and, in brackets, the lignin/diisocyanate ratio (see Table 1 and Fig. 11).

First, it is worth mentioning that comparable rheological response was obtained using different lignin/diisocyanate ratio and both processing protocols. In general, higher diisocyanate content was required in the two-step processing method to obtain similar gel-like characteristics. With respect to the HDI-based systems, lignin/diisocyanate ratios of 1/1 and 1/0.5, for two-step and one-step process, respectively, i.e. 15 % and 10% diisocyanate contents, yield similar gel-like behaviours when using both processing protocols (Fig. 11a). However, although G' and G″ values are quite similar, a crossover between both viscoelastic functions was found at intermediate frequencies in the one-step protocol (H25), whereas G′ was always higher than G" over the entire frequency range studied when applying the two-step protocol. This effect was not observed for lower lignin/diisocyanate ratios, i.e. higher diisocyanate content (20% for two-step and around 13% for one-step samples). Thus, once again, it is evinced that very similar viscoelastic response and values of the SAOS functions were obtained in

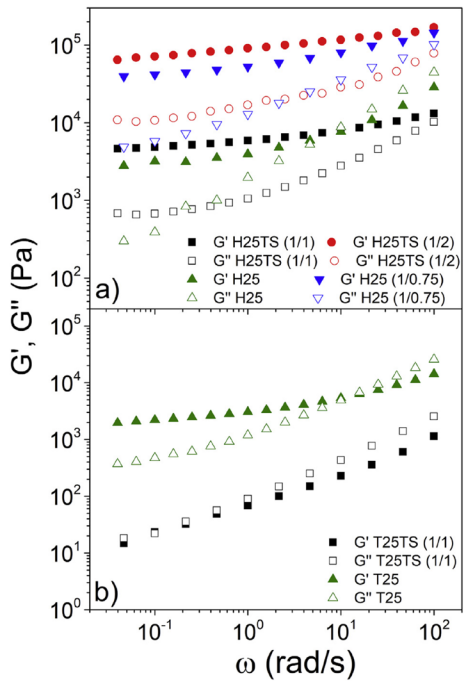

Fig. 11. Comparison of the mechanical spectra shown by PUs prepared using two-step and one-step processing protocols for a) HDI- and b) TDI-based systems.

samples prepared with the same lignin + diisocyanate content using both preparation methods, but much lower HDI content is required following the one-step process. Fig. 11b shows the same comparison for TDI-based PUs. As can be observed, in this case, different responses were obtained depending on the processing protocol and the lignin/diisocyanate weight ratio. Thus, as already mentioned, a relatively strong gel-like response, with a crossover between both SAOS functions, can be clearly noticed in the mechanical spectra of T25. This crossover point was shifted to lower frequencies when applying the two-step process, also exhibiting a rheological behaviour close to the critical gel and values of the SAOS functions several orders of magnitude lower than those obtained with the one-step process, despite the higher TDI content.

The different behaviour found with both types of diisocyanates can be explained attending the higher reactivity of TDI, which in the two-step process is able to produce a higher degree of lignin functionalization, resulting in a more crosslinked biopolymer structure, and consequently leaving lower free diisocyanate content and more difficult to be accessed by the hydroxyl groups of castor oil in the second step. On the contrary, non-aromatic diisocyanates are not able to achieve the same degree of lignin functionalization and, therefore, free diisocyanates are to a larger extent available for chemical interaction with castor oil. Consequently, a less cross-linked lignin structure which can let castor oil be introduced within the network and further react and interact through secondary-bonds may be obtained, finally favouring the gel strength.

3.7. Lignin-based versus lignin-free gel-like polyurethanes

In the one-step process protocol, lignin and castor oil are blended together with the diisocyanate, the hydroxyl groups of both molecules being in competition for free isocyanate groups. In order to assess the role of lignin in the PU structure, some systems were prepared, at 25 °C, by replacing lignin by the same amount of castor oil, using both HDI and TDI. In such a way, H25 (1/1), H25 and T25 PU samples were compared with the corresponding systems without lignin. Exceptionally, H25 (1/1) was characterized after two days of curing, since after that it becomes too stiff to perform the rheological tests. As Fig. 12 illustrates, the addition of lignin always increases the values of the SAOS functions, demonstrating a crucial filler effect that reinforces the gel strength, apart from providing a higher number of hydroxyl groups than the castor oil, able to produce urethane and urea linkages. Moreover, in HDI-based gels, lignin addition yields higher differences between the storage and loss moduli, i.e. lower values of the loss tangent, and shifts the crossover point to higher frequencies. The same filler effect produced by the lignin was observed in TDI-based PU, although in this case the crossover between G' and G" was slightly shifted to lower frequencies when lignin was added.

4. Conclusions

A green and simple one-step procedure for the preparation of bio-based liquid and gel-like polyurethanes (PUs) containing lignin and castor oil as a source of polyols was successfully followed. This study allows to conclude that processing conditions play a crucial role in the chemical structure of these PUs, significantly affecting their rheological properties. Both low processing temperature and low stirring speed favour the achievement of gel-like characteristics and/or the formation of highly viscous polyurethanes, whereas increasing either temperature or agitation fosters the development of liquid-like systems. Nonetheless, when processing temperature was raised to 70 °C, PUs were more viscous than those prepared at 45 °C. During processing, the formation of urethane and urea linkages were accelerated by increasing temperature and agitation speed and by using an aromatic diisocyanate, like TDI, with higher reactivity than an aliphatic one, like HDI, favouring the consumption of free isocyanates and minimizing the subsequent curing process. Once the curing process was accomplished, the time-temperature superposition can be satisfactorily applied in most of the polyurethanes, confirming a thermo-rheological simplicity. The processing dependent rheological properties were in concordance with the FTIR-spectra deconvolution study. Thus, those PU systems with enhanced gel-like characteristics exhibited lower content of free (non-hydrogen-bonded) carbonyl groups from castor oil triglycerides and higher ratios of urethane/urea linkages and H-bonded/non-bonded carbonyl groups of both kinds of linkages, and for urethane and urea independently, highlighting the extreme importance of H-bonding in polyurethane formation. In general, TDI-based PUs present higher density of urethane linkages compared to HDI-based PUs, whereas higher processing temperatures and higher agitation speeds result in higher contents of total urea linkages and/or lower urethane/urea ratios. In addition to this, the selected one-step process, in comparison with the traditional

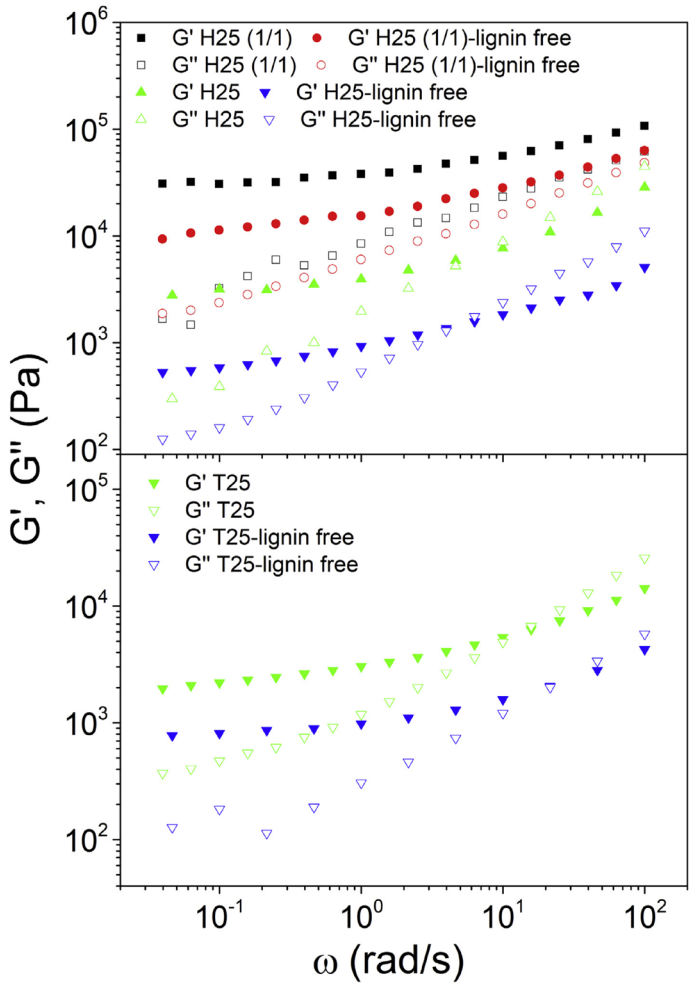

Fig. 12. Comparison of the mechanical spectra shown by PUs prepared by replacing and non-replacing lignin with the corresponding amount of castor oil, for HDI- (left) and TDI-based (right) PUs.

two-step process, turns out to be more environmentally-friendly, less time consuming and capable of providing oleogels with similar rheological characteristics significantly reducing the isocyanate content. Likewise, lignin was demonstrated to act as an effective filler agent increasing the values of the viscoelastic moduli.

CRediT authorship contribution statement

Antonio M. Borrero-López: Investigation, Data curation, Formal analysis, Writing - original draft, Writing - review & editing. **Concepción Valencia:** Conceptualization, Investigation, Methodology, Writing - original draft, Writing - review & editing, Funding acquisition, Project administration. **José M. Franco:** Conceptualization, Investigation, Formal analysis, Methodology, Supervision, Writing - original draft, Writing - review & editing, Funding acquisition, Project administration.

Declaration of competing interest

The authors declare that they have no known competing financial interests or personal relationships that could have appeared to influence the work reported in this paper.

Acknowledgements

This work is part of a research project (RTI2018-096080-B-C21) sponsored by the MICINN-FEDER I + D + i Spanish Programme. A.M.B-L. has received a Ph.D. Research Grant from the Ministerio de Educación, Cultura y Deporte (FPU16/03697). The financial support is gratefully acknowledged.

Appendix A. Supplementary data

Supplementary data to this article can be found online at https://doi.org/10.1016/j.jclepro.2020.123367.

References

Abushammala, H., 2019. On the para/ortho reactivity of isocyanate groups during the carbamation of cellulose nanocrystals using 2,4-toluene diisocyanate. Polymers 11, 1164. https://doi.org/10.3390/polym11071164.
Aït-kadi, A., Marchal, P., Choplin, L., Chrissemant, A.S., Bousmina, M., 2002. Quantitative analysis of mixer-type rheometers using the Couette analogy. Can. J. Chem. Eng. 80, 1166–1174. https://doi.org/10.1002/cjce.5450800618.
Ando, T., 1993. Effect of reaction temperature on polyurethane formation in bulk. Polym. J. 25, 1207–1209. https://doi.org/10.1295/polymj.25.1207.
Arnold, R.G., Nelson, J.A., Verbanc, J.J., 1957. Recent advances in isocyanate chemistry. Chem. Rev. 57, 47–76. https://doi.org/10.1021/cr50013a002.
Bina, C.K., Kannan, K.G., Ninan, K.N., 2004. DSC study on the effect of isocyanates and catalysts on the HTPB cure reaction. J. Therm. Anal. Calorim. 78, 753–760. https://doi.org/10.1007/s10973-004-0442-3.
Borrero López, A.M., Blánquez, A., Valencia, C., Hernández, M., Arias, M.E., Eugenio, M.E., Fillat, U., Franco, J.M., 2018. Valorization of soda lignin from wheat straw solid-state fermentation: production of oleogels. ACS Sustain. Chem. Eng. 6, 5198–5205. https://doi.org/10.1021/acssuschemeng.7b04846.
Borrero López, A.M., Valencia, C., Franco, J.M., 2017. Rheology of lignin-based chemical oleogels prepared using diisocyanate crosslinkers: effect of the diisocyanate and curing kinetics. Eur. Polym. J. 89, 311–323. https://doi.org/10.1016/j.eurpolymj.2017.02.020.
Calvo Correas, T., Santamaria-Echart, A., Saralegi, A., Martin, L., Valea, A., Corcuera, M.A., Eceiza, A., 2015. Thermally-responsive biopolyurethanes from a biobased diisocyanate. Eur. Polym. J. 70, 173–185. https://doi.org/10.1016/j.eurpolymj.2015.07.022.
Caniato, M., Kyaw Oo D'Amore, G., Kaspar, J., Gasparella, A., 2020. Sound absorption performance of sustainable foam materials: application of analytical and numerical tools for the optimization of forecasting models. Appl. Acoust. 161, 107166. https://doi.org/10.1016/j.apacoust.2019.107166.
Cassales, A., Ramos, L.A., Frollini, E., 2020. Synthesis of bio-based polyurethanes from Kraft lignin and castor oil with simultaneous film formation. Int. J. Biol. Macromol. 145, 28–41. https://doi.org/10.1016/j.ijbiomac.2019.12.173.
Cateto, C.A., Barreiro, M.F., Rodrigues, A.E., 2008. Monitoring of lignin-based polyurethane synthesis by FTIR-ATR. Ind. Crop. Prod. 27, 168–174. https://doi.org/10.1016/j.indcrop.2007.07.018.
Chattopadhyay, D.K., Raju, K.V.S.N., 2007. Structural engineering of polyurethane coatings for high performance applications. Prog. Polym. Sci. 32, 352–418. https://doi.org/10.1016/j.progpolymsci.2006.05.003.
Cheradame, H., Detoisien, M., Gandini, A., Pla, F., Roux, G., 1989. Polyurethane from kraft lignin. Br. Polym. J. 21, 269–275. https://doi.org/10.1002/pi.4980210314.
Cortés-Triviño, E., Valencia, C., Franco, J.M., 2017. Influence of epoxidation conditions on the rheological properties of gel-like dispersions of epoxidized kraft lignin in castor oil. Holzforschung 71, 777–784. https://doi.org/10.1515/hf-2017-0012.
Díez-García, I., Keddie, J.L., Eceiza, A., Tercjak, A., 2020. Optimization of adhesive performance of waterborne poly(urethane-urea)s for adhesion on high and low surface energy surfaces. Prog. Org. Coating 140, 105495. https://doi.org/10.1016/j.porgcoat.2019.105495.
Franco, J.M., Delgado, M.A., Valencia, C., Sánchez, M.C., Gallegos, C., 2005. Mixing rheometry for studying the manufacture of lubricating greases. Chem. Eng. Sci. 60, 2409–2418. https://doi.org/10.1016/j.ces.2004.10.042.
Gabriele, D., De Cindio, B., D'Antona, P., 2001. A weak gel model for foods. Rheol. Acta 40, 120–127. https://doi.org/10.1007/s003970000139.
Gallego, R., Arteaga, J.F., Valencia, C., Díaz, M.J., Franco, J.M., 2015a. Gel-like dispersions of HMDI-cross-linked lignocellulosic materials in castor oil: toward completely renewable lubricating grease formulations. ACS Sustain. Chem. Eng. 3, 2130–2141. https://doi.org/10.1021/acssuschemeng.5b00389.
Gallego, R., Arteaga, J.F., Valencia, C., Franco, J.M., 2015b. Thickening properties of several NCO-functionalized cellulose derivatives in castor oil. Chem. Eng. Sci. 134, 260–268. https://doi.org/10.1016/j.ces.2015.05.007.
Gómez-Fernández, S., Ugarte, L., Calvo-Correas, T., Peña-Rodríguez, C., Corcuera, M.A., Eceiza, A., 2017. Properties of flexible polyurethane foams containing isocyanate functionalized kraft lignin. Ind. Crop. Prod. 100, 51–64. https://doi.org/10.1016/j.indcrop.2017.02.005.
Hablot, E., Zheng, D., Bouquey, M., Avérous, L., 2008. Polyurethanes based on castor oil: kinetics, chemical, mechanical and thermal properties. Macromol. Mater. Eng. 293, 922–929. https://doi.org/10.1002/mame.200800185.
Han, J.L., Yu, C.H., Lin, Y.H., Hsieh, K.H., 2008. Kinetic study of the urethane and urea reactions of isophorone diisocyanate. J. Appl. Polym. Sci. 107, 3891–3902. https://doi.org/10.1002/app.27421.
Ionescu, M., 2005. Chemistry and Technology of Polyols for Polyurethane, Rapra Technology, Shrewsbury. https://doi.org/10.1002/pi.2159.
Jeong, H., Park, J., Kim, S., Lee, J., Ahn, N., Roh, H.G., 2013. Preparation and characterization of thermoplastic polyurethanes using partially acetylated kraft lignin. Fibers Polym. 14, 1082–1093. https://doi.org/10.1007/s12221-013-1082-7.
Lei, L., Buddingh, J., Wang, J., Liu, G., 2020. Transparent omniphobic polyurethane coatings containing partially acetylated β–cyclodextrin as the polyol. Chem. Eng. J. 380, 122554. https://doi.org/10.1016/j.cej.2019.122554.
Lettner, M., Hesser, F., Hedeler, B., Schwarzbauer, P., Stern, T., 2020. Barriers and incentives for the use of lignin-based resins: results of a comparative importance performance analysis. J. Clean. Prod. 256, 120520. https://doi.org/10.1016/j.jclepro.2020.120520.
Liang, D., Zhang, Q., Zhang, W., Liu, L., Liang, H., Quirino, R.L., Chen, J., Liu, M., Lu, Q., Zhang, C., 2019. Tunable thermo-physical performance of castor oil-based polyurethanes with tailored release of coated fertilizers. J. Clean. Prod. 210, 1207–1215. https://doi.org/10.1016/j.jclepro.2018.11.047.
Lu, Q.W., Hoye, T.R., Macosko, C.W., 2002. Reactivity of common functional groups with urethanes: models for reactive compatibilization of thermoplastic polyurethane blends. J. Polym. Sci. Polym. Chem. 40, 2310–2328. https://doi.org/10.1002/pola.10310.
Lu, X., Liang, B., Sheng, X., Yuan, T., Qu, J., 2020. Enhanced thermal conductivity of polyurethane/wood powder composite phase change materials via incorporating low loading of graphene oxide nanosheets for solar thermal energy storage. Sol. Energy Mater. Sol. Cells 208, 110391. https://doi.org/10.1016/j.solmat.2019.110391.
Macocinschi, D., Filip, D., Vlad, S., Cristea, M., Butnaru, M., 2009. Segmented biopolyurethanes for medical applications. J. Mater. Sci. Mater. Med. 20, 1659–1668. https://doi.org/10.1007/s10856-009-3731-3.
Mishra, A.K., Narayan, R., Raju, K.V.S.N., Aminabhavi, T.M., 2012. Hyperbranched polyurethane (HBPU)-urea and HBPU-imide coatings: effect of chain extender and NCO/OH ratio on their properties. Prog. Org. Coating 74, 134–141. https://doi.org/10.1016/j.porgcoat.2011.11.027.
Munarin, F., Petrini, P., Barcellona, G., Roversi, T., Piazza, L., Visai, L., Tanzi, M.C., 2014. Reactive hydroxyapatite fillers for pectin biocomposites. Mater. Sci. Eng. C 45, 154–161. https://doi.org/10.1016/J.MSEC.2014.09.003.
Mutlu, H., Meier, M.A.R., 2010. Castor oil as a renewable resource for the chemical industry. Eur. J. Lipid Sci. Technol. 112, 10–30. https://doi.org/10.1002/ejlt.200900138.
Nacas, A.M., Ito, N.M., De Sousa, R.R., Spinacé, M.A., Dos Santos, D.J., 2017. Effects of NCO:OH ratio on the mechanical properties and chemical structure of Kraft lignin–based polyurethane adhesive. J. Adhes. 93, 18–29. https://doi.org/10.1080/00218464.2016.1177793.
Navarchian, A.H., Picchioni, F., Janssen, L.P.B.M., 2005. Rheokinetics and effect of shear rate on the kinetics of linear polyurethane formation. Polym. Eng. Sci. 45, 279–287. https://doi.org/10.1002/pen.20280.
Ning, L., De-Ning, W., Sheng-Kang, Y., 1997. Hydrogen-bonding properties of segmented polyether poly(urethane urea) copolymer. Macromolecules 30, 4405–4409. https://doi.org/10.1021/ma951386e.
Overend, R.P., Chornet, E., 1987. Fractionation of lignocellulosics by steam-aqueous pretreatments. Philos. Trans. R. Soc. A 321, 523–536. https://doi.org/10.1098/rsta.1987.0029.
Pandya, M.V., Deshpande, D.D., Hundiwale, D.G., 1986. Effect of diisocyanate structure on viscoelastic, thermal, mechanical and electrical properties of cast polyurethanes. J. Appl. Polym. Sci. 32, 4959–4969. https://doi.org/10.1002/app.1986.070320518.
Quinchia, L.A., Delgado, M.A., Valencia, C., Franco, J.M., Gallegos, C., 2010. Viscosity modification of different vegetable oils with EVA copolymer for lubricant applications. Ind. Crop. Prod. 32, 607–612. https://doi.org/10.1016/j.indcrop.2010.07.011.
Raghunanan, L.C., Fernandez-Prieto, S., Martínez, I., Valencia, C., Sánchez, M.C., Franco, J.M., 2018. Molecular insights into the mechanisms of humidity-induced changes on the bulk performance of model castor oil derived polyurethane adhesives. Eur. Polym. J. 101, 291–303. https://doi.org/10.1016/j.eurpolymj.2018.02.041.
Randall, D., Lee, S., 2003. The Polyurethanes Book. Wiley, New York.
Rath, S.K., Ishack, A.M., Suryavansi, U.G., Chandrasekhar, L., Patri, M., 2008. Phase morphology and surface properties of moisture cured polyurethane-urea (MCPU) coatings: effect of catalysts. Prog. Org. Coating 62, 393–399. https://doi.org/10.1016/j.porgcoat.2008.02.004.
Sánchez, R., Valencia, C., Franco, J.M., 2014. Rheological and tribological characterization of a new acylated chitosan-based biodegradable lubricating grease: a comparative study with traditional lithium and calcium greases. Tribol. Trans. 57, 445–454. https://doi.org/10.1080/10402004.2014.880541.
Santan, H.D., James, C., Fratini, E., Martínez, I., Valencia, C., Sánchez, M.C., Franco, J.M., 2018. Structure-property relationships in solvent free adhesives derived from castor oil. Ind. Crop. Prod. 121, 90–98. https://doi.org/10.1016/j.indcrop.2018.05.012.
Seymour, R.W., Estes, G.M., Cooper, S.L., 1970. Infrared studies of segmented polyurethan elastomers. I. Hydrogen bonding. Macromolecules 3, 579–583. https://doi.org/10.1021/ma60017a021.

Shi, Y., Zhan, X., Luo, Z., Zhang, Q., 2008. Quantitative IR characterization of urea groups in waterborne polyurethanes. J. Polym. Sci. Polym. Chem. 46, 2433–2444. https://doi.org/10.1002/pola.22577.
Sonnenschein, M.F., 2015. Polyurethanes: Science, Technology, Markets, and Trends. Wiley, New York. https://doi.org/10.1002/9781118901274.
Strachota, A., Strachotová, B., Špírková, M., 2008. Comparison of environmentally friendly, selective polyurethane catalysts. Mater. Manuf. Process. 23, 566–570. https://doi.org/10.1080/10426910802157938.
Suhas, D.P., Jeong, H.M., Aminabhavi, T.M., Raghu, A.V., 2014. Preparation and characterization of novel polyurethanes containing 4,4'-{oxy-1,4-diphenyl bis(nitromethylidine)}diphenol schiff base diol. Polym. Eng. Sci. 54, 24–32. https://doi.org/10.1002/pen.23532.
Tenorio-Alfonso, A., Sánchez, M.C., Franco, J.M., 2019. Synthesis and mechanical properties of bio-sourced polyurethane adhesives obtained from castor oil and MDI-modified cellulose acetate: influence of cellulose acetate modification. Int. J. Adhesion Adhes. 95, 102404. https://doi.org/10.1016/j.ijadhadh.2019.102404.
Teo, L.S., Chen, C.Y., Kuo, J.F., 1997. Fourier transform infrared spectroscopy study on effects of temperature on hydrogen bonding in amine-containing polyurethanes and poly(urethane-urea)s. Macromolecules 30, 1793–1799. https://doi.org/10.1021/ma961035f.
Trân, N.B., Vialle, J., Pham, Q.T., 1997. Castor oil-based polyurethanes: 1. Structural characterization of castor oil—nature of intact glycerides and distribution of hydroxyl groups. Polymer 38, 2467–2473. https://doi.org/10.1016/S0032-3861(96)00791-4.
Velankar, S., Cooper, S.L., 1998. Microphase separation and rheological properties of polyurethane melts. 1. Effect of block length. Macromolecules 31, 9181–9192. https://doi.org/10.1021/ma9811472.
Visanko, M., Sirviö, J.A., Piltonen, P., Liimatainen, H., Illikainen, M., 2017. Castor oil-based biopolyurethane reinforced with wood microfibers derived from mechanical pulp. Cellulose 24, 2531–2543. https://doi.org/10.1007/s10570-017-1286-x.
Yang, B., Huang, W.M., Li, C., Li, L., 2006. Effects of moisture on the thermo-mechanical properties of a polyurethane shape memory polymer. Polymer 47, 1348–1356. https://doi.org/10.1016/j.polymer.2005.12.051.
Zhang, C., Wu, H., Kessler, M.R., 2015. High bio-content polyurethane composites with urethane modified lignin as filler. Polymer 69, 52–57. https://doi.org/10.1016/j.polymer.2015.05.046.
Zhou, X., Sain, M.M., Oksman, K., 2016. Semi-rigid biopolyurethane foams based on palm-oil polyol and reinforced with cellulose nanocrystals. Compos. Part A Appl. Sci. Manuf. 83, 56–62. https://doi.org/10.1016/j.compositesa.2015.06.008.
Zimmer, B., Nies, C., Schmitt, C., Possart, W., 2017. Chemistry, polymer dynamics and mechanical properties of a two-part polyurethane elastomer during and after crosslinking. Part I: dry conditions. Polymer 115, 77–95. https://doi.org/10.1016/j.polymer.2017.03.020.

2. Use of residual lignin fractions obtained from different physico-chemical pretreatments as gelling agent for lubricating grease application

2.1. Article 3

Valorization of Kraft lignin as thickener in castor oil for lubricant applications

A.M. Borrero-López, F. J. Santiago-Medina, C. Valencia, M. E. Eugenio, R. Martin-Sampedro, J.M. Franco

Published in:

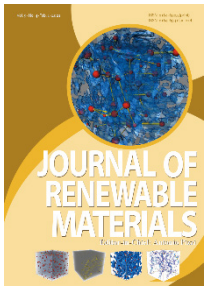

Journal of Renewable Materials
Publishing Company: Tech Science Press
Editor-in-Chief: Antonio Pizzi
Volume 6 (4), pp 347-361
Year 2018
ISSN 2164-6325
DOI: 10.7569/JRM.2017.634160

Category	Journal Rank / Total number of journals	Quartile (Percentage)
Green & Sustainable Science & Technology	30/35	Q4 (16%)
Materials Science, Composites	15/25	Q3 (42%)
Polymer Science	58/87	Q3 (34%)
Impact Factor	1.427	

Valorization of Kraft Lignin as Thickener in Castor Oil for Lubricant Applications

A. M. Borrero-López[1], F. J. Santiago-Medina[1], C. Valencia[1,2]*, M. E. Eugenio[3], R. Martin-Sampedro[3] and J. M. Franco[1,2]

[1]*Department of Chemical Engineering, University of Huelva, El Carmen Campus, Agrifood Campus of International Excellence (ceiA3), 21071 Huelva, Spain*
[2]*Pro²TecS – Chemical Process and Product Technology Research Center, University of Huelva, 21071 Huelva, Spain*
[3]*INIA-CIFOR, Ctra de la Coruña, km 7.5. 28040, Madrid, Spain*

Received April 12, 2017; Accepted August 04, 2017

ABSTRACT: It is known that large amounts of residual lignin are generated in the pulp and paper industry. A new alternative for Kraft lignin valorization, which consists of first a chemical modification using a diisocyanate and then the efficient dispersion in castor oil to achieve stable gel-like systems, is proposed in this work. Rheological properties and microstructure of these materials were determined by means of small amplitude oscillatory shear tests and viscous flow measurements and atomic force microscopy observations, respectively. Moreover, both standardized penetration tests and tribological assays, usually performed in the lubricant industry, were carried out to evaluate the performance characteristics as lubricating greases. Linear viscoelasticity functions are affected by the lignin/diisocyanate ratio and thickener concentration. The thermo-rheological response evidenced a softening temperature of around 105 °C. The microstructure of these gel-like dispersions is composed of interconnected thin fibers, homogeneously distributed in castor oil. Moreover, the NCO-functionalized lignin gel-like dispersions studied show lower friction coefficients than traditional lubricating greases.

KEYWORDS: Kraft lignin, diisocyanate, gel-like dispersion, rheology, thermal properties

1 INTRODUCTION

Lignin is nowadays considered the main aromatic renewable resource and an excellent alternative feedstock for the synthesis of value-added chemicals and polymers. Lignin extraction from lignocellulosic biomass (wood, annual plant, etc.) represents the key point to its large use for industrial applications [1]. It is the second most abundant renewable resource after cellulose [2] and mainly results from the polymerization of three monomers: p-coumaryl alcohol, coniferyl alcohol and synapyl alcohol. Each of these monolignols leads to different types of lignin units called p-hydroxyphenyl (H), guaiacyl (G) and syringyl (S), respectively. Although these monomers are the main precursors of lignin, it is well known that others can also participate in its formation, such as coniferaldehyde, acylated monolignols, etc. The resulting polymeric structure is a complex macromolecule, which contains a wide variety of functional groups and different types of bonds depending on biomass source [3]. Thus, hardwood lignin consists principally of G and S units and traces of H units, whereas softwood lignin mostly consists of G units, with low levels of H units [1]. Furthermore, not only the original source but also the method used to isolate the different lignins has an influence on their structural characteristics and, therefore, on their industrial applicability.

It is known that large amounts of residual lignin are generated in the pulp and paper industry. In the pulping manufacturing process, the lignin contained in the wood is dissolved in the process liquor, obtaining the so-called black liquor. In the case of the predominant Kraft pulping process, the black liquor is typically burned in order to obtain energy. Although previous structural modification processes are needed to increase lignin's initial poor properties, residual Kraft lignin may be otherwise used to obtain value-added products [4]. The abundance of the chemical sites in lignin structure offers different possibilities for chemical modifications. For instance, lignin has phenolic

*Corresponding author: barragan@uhu.es

DOI: 10.7569/JRM.2017.634160

hydroxyl groups and aliphatic hydroxyl groups at C-α and C-γ positions on the side chain. Phenolic hydroxyl groups are the most reactive functional groups and can significantly influence the chemical reactivity of the material. Among several polymerization methods with lignin macromonomers, lignin-based urethane polymerization has been investigated using different diisocyanates, reaction conditions and ratios of functionalities [5–7]. Moreover, lignin macromonomers have been incorporated into polycaprolactone, polyester [8], polyurethanes [6, 8–10], phenolics and urea matrices [11], or have been used to prepare and reinforce vegetable oil-based polyurethane composites [12–15].

On the other hand, there is a general tendency based on the use of natural components in a wide variety of products to promote both the replacement of non-renewable raw materials by renewable resources and the minimization of the environmental impact caused by industrial wastes [16–18]. Over the past two decades, a renewed interest in different vegetable oil-based lubricants has occurred as a result of environmental concerns. Vegetable oils with high viscosity indices, low volatility and high flash points have been employed in a series of applications over lubricants and additives in polymers, coatings and resins [19]. Moreover, a great number of research works dealing with the lubrication properties of different vegetable oils and some chemical derivatives have been reported in the past few years. Among them, castor oil is considered one of the most interesting alternative base oils, especially due to its high viscosity and good performance characteristics at low temperatures [20, 21]. Some adverse properties can be overcome by using some additives as previously reported [21, 22]. On the other hand, the replacement of traditional thickening agents in lubricating greases, such as lithium, calcium or aluminum soaps, by others derived from renewable resources, like some biopolymers, is a complicated task due to the technical efficiency of metallic soaps to impart the desired rheological, thermal and tribological properties to the bulk system. Previous research focused on the proper dispersion of different types of gelifiers, including some cellulose derivatives, in vegetable oils in order to achieve suitable gel-like characteristics and suitable lubricant performance have been reported [23–26]. In general, similar rheological and thermal characteristics to those displayed by traditional metallic soap-based greases were found but there are still some limitations regarding physical and mechanical stabilities. A significant improvement was achieved by performing the functionalization of cellulosic derivatives with isocyanate groups, which are also able to chemically interact with hydroxyl groups of castor oil, thus resulting in promising formulations [27, 28]. Following this approach, the main objective of this work was to develop and characterize new gel-like formulations, potentially applicable as biodegradable lubricating greases, based on residual Kraft lignin once chemically modified with 1,6-hexamethylene diisocyanate and properly dispersed in castor oil.

2 MATERIALS AND METHODS

2.1 Materials

Eucalyptus globulus chips were supplied by a Spanish pulp mill (Factoría La Montañanesa, Torraspapel-Lecta Group). The 1,6-Hexamethylene diisocyanate (HMDI), purum grade (≥ 98.0%), was obtained from Sigma-Aldrich. Castor oil (Guinama, Spain) was selected as lubricant base oil to prepare gel-like dispersions. All other common reagents and solvents employed were purchased from Sigma-Aldrich.

A commercial model lithium lubricating grease (Castrol Optipit, Germany) and a semi-biodegradable one based on vegetable oil and a calcium thickener (kindly supplied by Verkol, Spain) were used as benchmarks.

2.2 Kraft Pulping

Kraft cooking of *Eucalyptus globulus* chips was performed in a 26 L batch reactor furnished with a system for recirculation and heating of the cooking liquor. Prior to cooking, the chips were steamed for 5 min to facilitate impregnation of chemicals. The cooking temperature was controlled by a computer run specially developed software. Applied cooking conditions were: 16% active alkali, 20% sulphidity, 4 L kg^{-1} liquor/wood ratio, 170 °C cooking temperature, 60 min to reach cooking temperature and 30 min at cooking temperature. These conditions correspond to an H-factor of 460. The H-factor is a well-known control parameter in the pulping process that includes time and temperature as a single variable, which is calculated according to the following equation:

$$H = \int_0^t e^{\left(43.2 - \frac{16115}{T}\right)} dt$$

where T is the temperature (K) and t the cooking time (hours).

2.3 Lignin Precipitation

After Kraft pulping, lignin was precipitated from the black liquor by acidification adding sulphuric acid until pH 2.5 (initial pH was 13.2). Then, precipitated

DOI: 10.7569/JRM.2017.634160 A. M. Borrero-López et al.:Valorization of Kraft Lignin as Thickener in Castor Oil for Lubricant Applications

lignin was air dried and milled for 20 min using a Retsch agate mortar grinder (model RMO).

2.4 Kraft Lignin Functionalization

All functionalization reactions were performed in round-bottom flasks where reactants were mixed. Toluene, employed as solvent in the reaction between the lignin powder and the diisocyanate, was purified according to standard literature techniques. The 1,6-hexamethylene diisocyanate (HMDI) was stored at 4 °C.

Functionalization of Kraft lignin (KL) was carried out according to methodologies previously reported [27] and by modifying the lignin/HMDI weight ratio. The KL was added to a round-bottom flask with toluene while stirring at room temperature, becoming a suspension. Then, triethylamine (Et_3N) and HMDI were also added to the system, the last one dropwisely. The solution was vigorously stirred at room temperature for 24 h. The synthesis was carried out under inert atmosphere of argon. Afterwards, the mixture was concentrated in a rotary evaporator, resulting in a black compound. The product was prepared immediately before being used. The different proportions of KL, HMDI, Et_3N and toluene used in the reaction as well as the yield are collected in Table 1.

2.5 Preparation of Gel-Like Dispersions

Gel-like dispersion samples were prepared in an open vessel, using a controlled rotational speed mixing device RW 20 (IKA), equipped with an anchor impeller to disperse the different functionalized lignin samples in the oil. NCO-functionalized lignin was slowly added to the castor oil at concentrations of 20% and 30% (w/w) under agitation (70 rpm). The mixing process was maintained for 24 h at room temperature. Finally, the resulting dispersion was homogenized with an Ultra-Turrax T50 basic (IKA) rotor-stator turbine at 4000 rpm for 1 min. Batches of 50 g were prepared for each formulation investigated.

2.6 Characterizations

2.6.1 *Precipitated Lignin Composition*

The composition of the precipitated lignin was determined by standard analytical methods (National Renewable Energy Laboratory NREL/TP-510-42618). The sample was subjected to quantitative acid hydrolysis in two steps to determine the carbohydrate composition. The hydrolyzed liquid obtained was then analyzed for sugar content using an Agilent Technologies 1260 HPLC fitted with a refractive index detector and an Agilent Hi-Plex Pb column operated at 70 °C with Milli-Q water as mobile phase pumped at a rate of 0.6 mL. The solid residue remaining after the acid hydrolysis is considered acid-insoluble lignin (Klason lignin). Moreover, ash was also determined following the standard UNE 57050:2003.

2.6.2 *Thermogravimetric Analysis (TGA)*

Measurements of mass losses versus temperature were carried out by using a thermogravimetric analyzer, model Q-50 (TA Instrument Waters, USA) under N_2 purge. Typically, 5–10 mg of sample were placed on a platinum pan and heated from 30 to 600 °C at 10 °C/min.

2.6.3 *Fourier Transform Infrared (FTIR) Spectroscopy*

Fourier transform infrared spectroscopy spectra were obtained with a JASCO FT/IR-4200 (Jasco Inc., Japan) apparatus. A small drop of functionalized lignin or gel-like dispersion samples was placed between two KBr disks (32 × 3 mm). Then, the set was placed into an appropriate sample holder. The spectra were obtained in a wavenumber range of 400–4000 cm^{-1}, at 4 cm^{-1} resolution, in the transmission mode.

2.6.4 *Rheological Characterization of Gel-Like Dispersions*

Gel-like NCO-functionalized lignin-based dispersions were rheologically characterized in both

Table 1 Proportions of Kraft lignin (KL), hexamethylene diisocyanate (HMDI), triethylamine (Et_3N) and toluene used in the functionalization reaction and yield obtained.

Thickener code	Lignin (g)	HMDI (g)	Et_3N (g)	Toluene (ml)	Yield (%)
KL1	10	10	20	100	85
KL2	10	20	20	100	91
KL4	10	40	20	150	92

controlled-stress (HAAKE RheoScope, Thermo Fisher Scientific, Germany) and controlled-strain (ARES, Rheometric Scientific, UK) rheometers, using serrated plate-plate (20 and 25 mm diameter respectively, 1 mm gap) geometries. Small amplitude oscillatory shear (SAOS) tests were carried out inside the linear viscoelastic region in a frequency range of 0.03–100 rad/s at 25 °C. Stress sweep tests were previously performed to determine the linear viscoelastic regime. Measurements were done one day, one week, one month and four months after gel-like dispersion preparation. The SAOS tests were obtained at different temperatures carried out between 30 and 155 °C. Apparent viscosity was determined by applying a stepped shear rate ramp in a shear rate range of 10^{-2}–10^{2} s^{-1}, using plate-plate geometry (25 mm) with grooved surfaces to overcome the wall slip phenomena usually observed in lubricating greases [29]. At least two replicates of each test were carried out on fresh samples.

2.6.5 *Penetration and Tribological Tests*

Unworked penetration indexes were determined according to the ASTM D1403 standard, by using a Seta Universal penetrometer model 17000-2 with one-quarter cone geometry (Stanhope-Seta, UK). The one-quarter scale penetration values were converted into the equivalent full-scale cone penetration values, following the ASTM D217 standard. Classical consistency NLGI grade was established according to these penetration values [30]. At least three replicates of penetration measurements were done.

Tribological tests were performed in a tribology measuring cell coupled with a Physica MCR-501 rheometer. The tribological cell deals with a 1/2″ diameter steel ball (1.4301 grade 100) rotating on three 45° inclined steel plates (1.4301). The stationary friction coefficient was obtained by applying a normal force of 20 N, resulting in a maximum contact Hertzian pressure of ~1.72 GPa and setting a constant rotational speed of 10 rpm for 10 min. At least five replicates of each test were done on fresh samples at room temperature. For the sake of comparison, tribological tests were also carried out under the same conditions on two commercial lubricating greases, typical lithium grease (Castrol Optipit, Germany) and one based on vegetable oil and calcium thickener (Verkol, Spain).

2.6.6 *Atomic Force Microscopy (AFM) Observations*

Morphological observation of a selected gel-like dispersion sample was investigated with a multimode AFM connected to a Nanoscope IV scanning probe microscope controller (Digital Instruments, Veeco Metrology Group Inc., Santa Barbara, CA) using the tapping mode with phase detection imaging at room temperature. The amplitude of oscillation typically ranges from 20 nm to 100 nm. The tip lightly interacts with the sample surface during scanning, providing high-resolution images with minimum sample damage. Silicon Nanosensors TM PPP-NCH AFM probes for tapping mode with a force constant of 42 N m^{-1} and resonance frequency of 330 kHz were used. Scan speed and windows were set at 1 Hz and 6 and 1 µm, respectively.

3 RESULTS AND DISCUSSION

3.1 Composition of Kraft Lignin

The Kraft lignin (KL) contains 4.98% carbohydrates (0.49% glucose, 4.29% xylose and 0.20% arabinose), which can probably be attributed to both LCCs (lignin carbohydrates bound) and non-bounded sugars. As can be observed, the predominant elemental sugar was xylose. These results are in concordance with those found by Dos Santos *et al.* [31] and Alekhina *et al.* [32]. The latter authors explained that this fact could be due to a combination of two factors, i.e., the low solubility in acid media of the hemicellulose (xylose) and the fast degradation of the cellulose into its monomers during the cooking process and then its further decomposition into degradation products.

The acid-insoluble lignin (Klason lignin) and the acid-soluble lignin (ASL) found in the precipitated lignin were 35.96% and 8.85%, respectively (44.81% total lignin). These results are also in concordance with those found by Alekhina *et al.* [32] when they precipitated the lignin at pH 2.5 (46.90% and 10.78% of Klason lignin and ASL, respectively). However, Dos Santos *et al.* [31] found a lower amount of ASL (1.60%) with a similar value of Klason lignin (40.93%). Yasuda *et al.* [33] studied the structure and formation mechanism of ASL and concluded that it is composed of low-molecular-weight degradation products and hydrophilic derivatives of lignin. The precipitation of lignin at low pH, as in our case (pH 2.5), favors the increase of both products. Moreover, the severity of the cooking treatment conditions can also contribute to increase the ASL content in the recovery fraction due to the progressive depolymerization of the lignin with increased cooking time.

Finally, the ash content found in the precipitated lignin was 35.66% at 900 °C. This high amount can be attributed to the high content of salts presented in the sample. Similar and even higher ash contents were found by Dos Santos *et al.* [31] when they precipitated lignin at different pHs (55.8–71.6%).

DOI: 10.7569/JRM.2017.634160 A. M. Borrero-López et al.:Valorization of Kraft Lignin as Thickener in Castor Oil for Lubricant Applications

3.2 Fourier Transform Infrared Spectroscopy Analysis

Figure 1a shows the FTIR spectrum of KL sample. As reported by Boeriu *et al.* [34], lignin presents a broad band at 3424 cm^{-1}, attributed to the hydroxyl groups in phenolic and aliphatic structures, and two bands centered around 2918 and 2849 cm^{-1}, predominantly arising from CH stretching in aromatic methoxyl groups and in methyl and methylene groups of side chains. These bands are less intense for KL than those of original lignin in wood (data not shown), suggesting a decrease in the number of aliphatic methylene and methyl groups during Kraft pulping. In addition, a peak corresponding to the C=O in the unconjugated ketones, carbonyl, and ester groups stretching was observed at 1720 cm^{-1} [32]. Moreover, the spectrum shows the typical lignin triplet at 1610, 1516 and 1425 cm^{-1} band due to aromatic ring vibration. The FTIR spectrum also shows a higher intensity of the band assigned to aromatic ring breathing in S unit (1330 cm^{-1}) than in G units (1260 cm^{-1}), typically found in hardwood, and a high intensity band at 1115 cm^{-1} related to the asymmetric stretching of SO_4 groups due to the formation of salts during lignin precipitation [35, 31], in agreement with the ash content in lignin composition previously discussed.

The KL functionalization with HMDI produces a compound whose FTIR spectrum is shown in Figure 1b. The broad band of hydroxyl groups found at 3424 cm^{-1} in the unmodified Kraft lignin FTIR disappears almost completely. This is evidence of the reaction between isocyanate and OH groups of lignin. Secondly, the urethane bands were apparent at 3324 (N-H), 1739 (C=O), and 1574 cm^{-1} (N-H). Moreover, the intense peak at 2270 cm^{-1} confirms the presence of free isocyanate groups. Finally, as can be observed in Figure 1c, the reaction between free NCO in the thickener with the OH groups in the fatty acid of the castor oil is also corroborated in the spectrum of the gel-like dispersion, in which the emergence of one band at around 3336 cm^{-1}, assigned to –NH groups, and the disappearance of the free isocyanate peak at 2270 cm^{-1} can be noticed. Moreover, the inclusion of castor oil is noticed in two characteristic peaks. The first of them at 3007 cm^{-1} attributed to C=C and the second one at 1746 cm^{-1} for C=O.

Figure 2 shows the FTIR spectra for a selected gel-like dispersion (GKL2-30), as a function of ageing time (one day, one week and one month). As has been previously discussed, the intensity of the band assigned to free isocyanates (2270 cm^{-1}) is progressively reduced until being almost negligible after one month. On the contrary, a significant amount of free –NCO groups is detectable one day after preparation. This means that the reaction between free isocyanates and hydroxyl groups in such viscous medium is extremely slow, as previously reported for similar biopolyurethanes [36]. Then, there are some peaks that are well defined one month after preparation (3007, 2918, 2849 and 1746 cm^{-1}). The shape of the band at 3336 cm^{-1} is modified as a consequence of the progressive reaction between the hydroxyl groups in the fatty acid chain of castor oil and free NCO inserted in the modified lignin, which promotes the appearance of new NH groups in the urethane linkages.

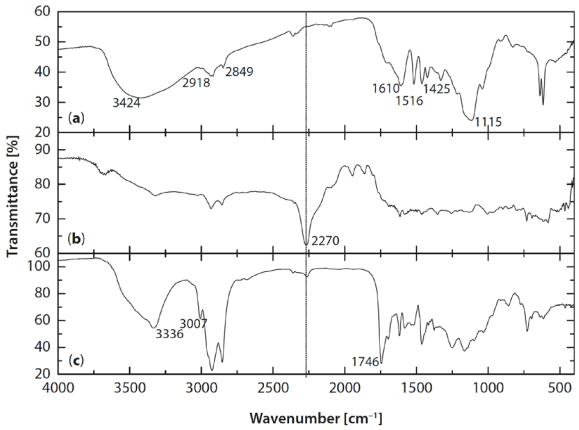

Figure 1 FTIR spectra for (**a**) Kraft lignin, (**b**) KL2 and (**c**) gel-like dispersion GKL2-30.

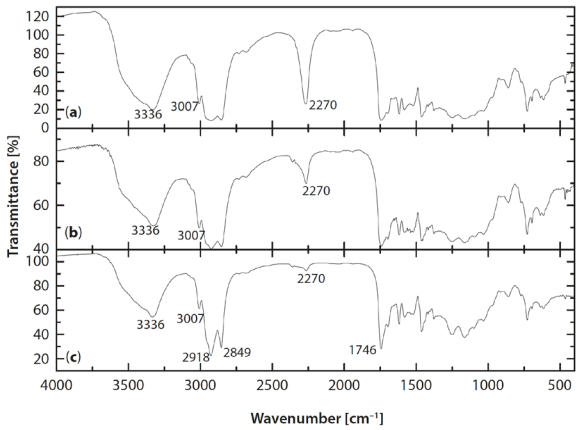

Figure 2 FTIR spectra for gel-like dispersion GKL2-30 as a function of the ageing time: (**a**) one day, (**b**) one week and (**c**) one month after their preparation.

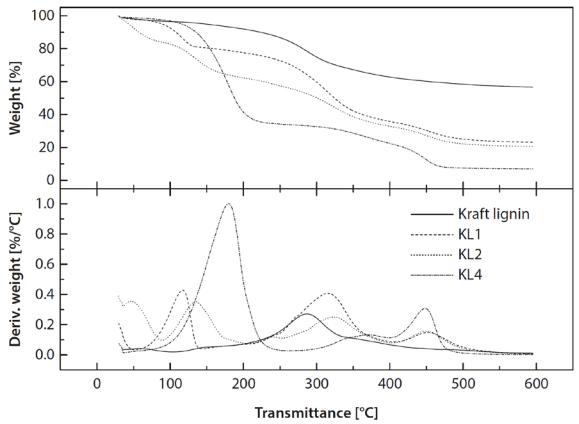

Figure 3 Thermal degradation curves, under inert atmosphere, for Kraft lignin and NCO-functionalized lignins studied.

3.3 Thermogravimetric Analysis

Thermal degradation of KL- and NCO-functionalized lignin compounds was investigated by means of thermogravimetric analysis (TGA). Figure 3 shows TGA curves in the form of weight loss versus temperature and its derivative function for KL and chemically modified lignins as a function of the functionalization degree. The temperature for the onset of thermal decomposition (T_{onset}), the temperature at which decomposition rate is maximum (T_{max}), final temperature (T_{final}), loss weight at the end of each decomposition step and the percentage of nondegraded residue have been determined from the thermograms of the different samples and collected in Table 3.

As can be observed in Figure 3 and Table 3, thermal degradation of KL, ignoring the weight loss of around 2% due to water evaporation, starts at relatively low temperature (T_{onset} = 138 °C and T_{max} = 150 °C) as a

DOI: 10.7569/JRM.2017.634160 A. M. Borrero-López et al.:Valorization of Kraft Lignin as Thickener in Castor Oil for Lubricant Applications

Table 2 Composition of gel-like dispersion formulations studied.

Thickener agent	Concentration (%, w/w)	Vegetable oil (up to 100 %, w/w)	Gel-like dispersion code
KL1	20	Castor	GKL1-20
KL2	20	Castor	GKL2-20
KL2	30	Castor	GKL2-30
KL4	20	Castor	GKL4-20

Table 3 TGA characteristic parameters for Kraft lignin, NCO-functionalized lignin samples and gel-like dispersions studied.

Sample	T_{onset} (ºC)	T_{max} (ºC)	T_{final} (ºC)	Residue (%)	ΔW (%)
Kraft Lignin	**68/138/248/416**	**58/150/288/348**	**91/195/325/443**	**57**	**2/2/24/15**
HDMI	137	172	178	1	99
KL1	94/262/411	117/316/453	134/361/502	23	17/43/17
KL2	119/293/478	135/322/449	172/371/500	21	32/32/15
KL4	140/339/463	179/371/448	211/396/474	7	65/11/17
GKL1-20	344	378/437	473	4	80/16
GKL2-20	340	374/435	475	2	84/14
GKL2-30	324	367/430	476	1	80/19
GKL4-20	327	371/444	472	0.5	85/14.5

consequence of hydroxyl groups dehydration from benzyl groups [1]. The cleavage of α- and β-aryl-alkyl-ether linkages takes place between 150 and 300 °C. At around 288 °C, aliphatic side chains start splitting off from the aromatic ring while carbon-carbon cleavage between lignin structural units occurs at around 350–443 °C. NCO-functionalized lignin thermal decomposition occurs in several stages, generally three. First, the degradation of HMDI moieties appears in the range of 118–180 °C, which is accountable for the reduction in thermal stability of this type of functionalized thickener [27]. The T_{onset} for this degradation stage takes place at around 94–140 °C, with temperatures for the maximum decomposition rate at around 117–179 °C, depending on the degree of functionalization. The second main thermal event, with temperatures for the maximum decomposition rate at 316–371 °C, is attributed to the degradation of aliphatic side chains and aromatic rings of lignin. Finally, the last stage at 411–463 °C can be associated with carbon-carbon cleavage between lignin structural units and degradation of more rigid polyurethanes due to excessive crosslinking [37]. As shown in Table 3, when the HMDI content in the modified lignin increases, the values of T_{onset}, T_{final} and T_{max} also increase in each stage. Obviously, the modified lignin sample with higher –NCO content (KL4) shows higher weight loss in the first stage (65%) and lower weight loss value (11%) in the second thermal degradation process. Furthermore, the lower amount of residue (7%) was obtained for KL4, whereas it was 57% for KL sample.

Figure 4 shows the thermal decomposition of lignin derivative-based gel-like dispersions. This decomposition takes place in one main single stage with T_{max} of around 367–378 °C, comprising several overlapped degradation events which appear as shoulders of the main peak in the derivative function. Thus, for GKL2-30 and GKL4-20, shoulders at both sides are clearly distinguished, whereas the first shoulder, located at the lower temperatures, is not apparent in GKL1-20 and GKL2-20. These overlapped thermal events comprise the thermal degradation of both NCO-functionalized lignin previously discussed and castor oil, the main component in gel-like dispersions [25]. However, the first degradation stage found in functionalized lignin was not observed in gel-like dispersions, which is indicative of the almost total completion of the reaction between free isocyanates and castor oil. Table 3 shows all TGA characteristic parameters obtained from the thermograms of gel-like dispersions, which generally evidence a higher thermal resistance than that generally exhibited by mineral oil-based lubricating greases [38].

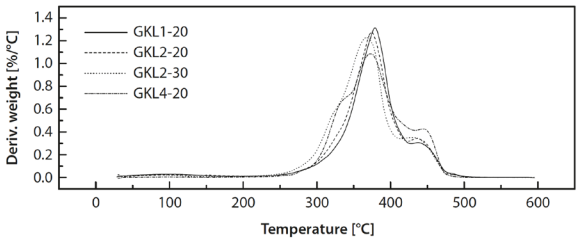

Figure 4 Thermal degradation curves, under inert atmosphere, for gel-like dispersions from NCO-functionalized lignin.

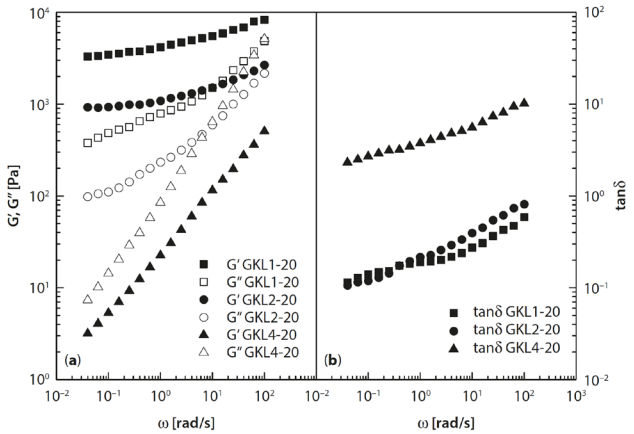

Figure 5 Frequency dependence of (**a**) the storage, G′, and loss, G″, moduli and (**b**) the loss tangent for NCO-functionalized lignin gel-like dispersions in castor oil, as a function of functionalization degree, 1 day after their preparation.

3.4 Rheological Characterization of NCO-Functionalized Lignin Gel-Like Dispersions

Figure 5 shows the SAOS response of NCO-functionalized lignin gel-like dispersions in castor oil, at a concentration of 20% w/w, one day after their preparation, as a function of the HMDI content in the modified lignin. The storage modulus, G″, generally shows higher values than the loss modulus, G″, in the whole frequency range studied, for the gel-like dispersions prepared with lower NCO contents (GKL1-20 and GKL2-20), associated with the plateau region of the mechanical spectrum, followed by the beginning of the transition region. According to Lu *et al.* [39], the gel strength of biopolymer dispersed systems is mainly dependent on the crosslinking density, which can be analyzed from SAOS measurements attending the G′ and G″ frequency dependence, i.e., the slopes of G′ and G″ versus frequency plots, and the relative elasticity, expressed in terms of the loss tangent (tan δ = G″/G′). Thus, GKL1-20 and GKL2-20 exhibit a gel-like rheological behavior with relatively low slopes of SAOS functions versus frequency plots (Figure 5a). On the contrary, the gel-like dispersion prepared with the highly functionalized lignin (GKL4-20) essentially exhibits a viscous response, with values of G″ higher than G′ in the whole frequency range studied. Moreover, the values of the loss tangent for GKL4-20 are more than one order of magnitude higher than those found for GKL1-20 and GKL2-20 (Figure 5b), thus showing a lower relative elasticity. This result obtained with sample GKL4-20 is in principle unexpected since the higher HMDI excess in lignin functionalization

DOI: 10.7569/JRM.2017.634160 A. M. Borrero-López et al.:Valorization of Kraft Lignin as Thickener in Castor Oil for Lubricant Applications

should extend the plateau region of the mechanical spectrum and reduce the slope of SAOS functions, as a result of the higher degree of crosslinking. However, the slopes of both SAOS functions vs. frequency plots suggest a certain degree of crosslinking among low-molecular-weight compounds, resulting in the typical transition region of the mechanical spectrum [40]. On the other hand, the kinetics of the reaction between free –NCO groups and castor oil triglycerides is relatively slow in such viscous medium, as confirmed in FTIR analysis (see Figure 2), and is highly dependent on the functionalization degree. This fact extremely influences the rheology of these gel-like dispersions, which can dramatically evolve with ageing time. This effect is clearly illustrated in Figure 6, where samples GKL2-20 and GKL4-20 are compared not just after preparation but one month later. As can be observed, whereas the values of SAOS functions slightly increase with time for sample GKL2-20, a dramatic increment was found for GKL4-20, also changing the frequency dependence displayed in Figure 5 to reach the typical gel-like response. This fact corroborates that the chemical interaction between the functionalized lignin and castor oil is mainly responsible for the gel-like behavior. Therefore, considering the comparison included in Figures 5 and 6 for the same concentration by weight (20%), the rheological behavior of these dispersions can be explained as a balance between a quick structuring effect caused by the polymer, favored by higher lignin/HMDI ratios, which yields higher values of the SAOS functions and lower frequency dependence from the beginning, and the excess of free HMDI, which delays the chemical interaction between the modified lignin and castor oil, probably involving competitive reactions which can produce crosslinking among polymeric chains or among triglycerides.

Regarding thickener concentration, Figure 6 also includes the mechanical spectra of the gel-like dispersion prepared with 30% w/w of NCO-functionalized lignin containing a lignin/HMDI weight ratio of 1:2 (sample GKL2-30). As can be seen, almost two orders of magnitude of both viscoelastic functions can be covered by modifying the thickener concentration between 20% and 30% (w/w). In addition to this, the evolution of viscoelastic functions with frequency slightly depends on lignin concentration. Thus, the lower NCO-functionalized lignin concentration (20%) yields a crossover of both SAOS functions at high frequencies, i.e., the beginning of the transition region (Figure 6a). On the contrary, a well-extended plateau region in the whole frequency range was obtained by increasing thickener concentration up to 30% (w/w), where G′ slightly increases with frequency and G″ displays a clear minimum at low frequencies. This evolution was typically found in other gel-like dispersions of different biopolymers in vegetable oil previously studied [24, 26] and standard lubricating greases [38]. As extensively studied, typical G′ values in lubricating greases of NLGI grade 1–2 range from 10^4 to 10^5 Pa, around one order of magnitude higher than G″ values, depending on processing conditions and compositions [38, 41], as, for instance, achieved with samples

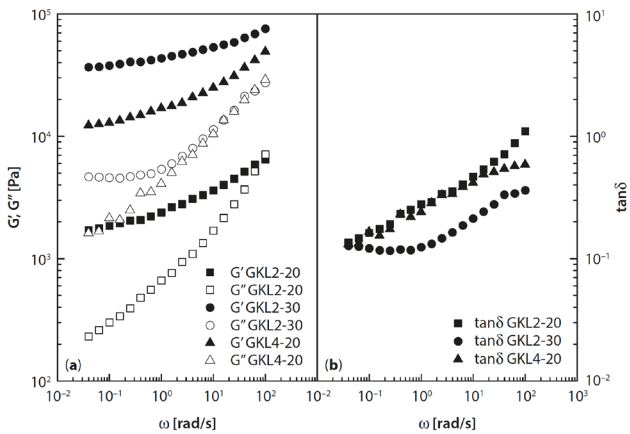

Figure 6 Frequency dependence of (**a**) the storage, G′, and loss moduli, G″, and (**b**) the loss tangent for NCO-functionalized lignin gel-like dispersions in castor oil, as a function of NCO-functionalized lignin concentration, 1 month after their preparation.

GKL2-30 and GKL4-20. Nonetheless, sample GKL4-20 becomes almost a rubber after approximately one month as a consequence of the excessive chemical crosslinking.

In relation to long-term stability, Figure 7 illustrates the influence of ageing time on the storage modulus, at 1 rad/s, for three selected NCO-functionalized lignin gel-like dispersions in castor oil (GKL2-20, GKL2-30 and GKL4-20). As can be seen, the values of G′ significantly increase during the first seven days of ageing, slightly increase until one month and then remain almost constant for a long period of time. As previously discussed, these results can be explained on the basis of the slow reactivity of residual –NCO functional groups in a highly viscous medium [36].

The influence of the temperature on the SAOS functions was also studied for a selected sample prepared using a lignin/HMDI weight ratio of 1:2 and a concentration of 30% w/w (GKL2-30). This sample was selected considering its mechanical spectrum at 25 °C, which is more similar to those found in conventional lithium lubricating greases. As can be observed in Figure 8, the linear viscoelastic functions, G′ and G″, generally decrease with temperature in the whole

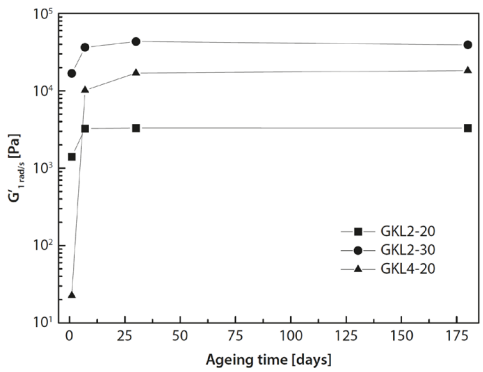

Figure 7 Evolution of the storage modulus, G′, at 1 rad/s, with the ageing time for selected NCO-functionalized lignin gel-like dispersions in castor oil.

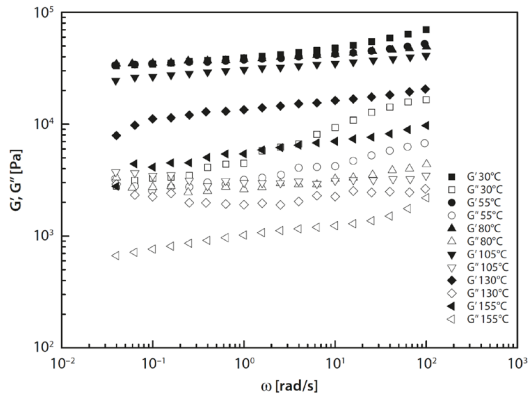

Figure 8 Evolution of the storage and loss moduli with frequency, at different temperatures, for a selected NCO-functionalized lignin gel-like dispersion (GKL2-30).

DOI: 10.7569/JRM.2017.634160 A. M. Borrero-López et al.:Valorization of Kraft Lignin as Thickener in Castor Oil for Lubricant Applications

frequency range studied, much more sharply above 105 °C. G′ frequency dependence is not significantly affected by temperature and G″ is influenced mainly at high frequencies. At temperatures higher than 155 °C, a significant "oil bleeding" is generally observed, which limits the thermo-rheological characterization. The plateau modulus, G_N^0, can be used to quantify the SAOS function-temperature dependence (Figure 9). As mentioned above, a sudden change in the slope of G_N^0 versus 1/T plot at around 105 °C was clearly seen, thus indicating a much higher thermal susceptibility of sample studied at temperatures above this critical temperature. This critical temperature matches fairly well with that referred for the softening point of traditional lithium lubricating greases, which is around 110 °C. Two different Arrhenius-type relationships are proposed to describe the evolution of G_N^0 with temperature in both temperature ranges, as previously reported [28, 42]:

$$G_N^o = A \cdot e^{(E_a/R)\cdot(1/T)} \quad (1)$$

where E_a is a fitting parameter that gives information about the gel-like dispersion thermal dependence, with a physical meaning similar to an activation energy (J mol^{-1}), R is the gas constant (8.314 J mol^{-1} K^{-1}), T is the absolute temperature (K), and A is the pre-exponential factor (Pa). Equation 1 fits the experimental plateau modulus values for the selected sample, in the whole temperature range studied, fairly well ($R^2 > 0.90$, see Figure 9). The activation energy values resulting from this fitting were 1.3 kJ mol^{-1} in the low temperature range and 50 kJ mol^{-1} in the high temperature range. These values are similar to those obtained for standard lithium greases in the low temperature range (1–2 kJ mol^{-1}) and higher than those reported in the high-temperature range (18–20 kJ mol^{-1}) [42]. However, this thermal dependence is lower than that shown by other biodegradable lubricating greases based on castor oil and lignocellulose pulps from different origins and/or submitted to different crosslinking treatments with hexamethylene diisocyanate [28].

From a rheological point of view, the formulation of new lubricating greases needs the characterization of both linear viscoelastic and viscous flow behaviors. The viscous flow behavior of NCO-functionalized lignin gel-like dispersions seems to be not so significantly affected by the amount of HMDI used to modify the lignin. However, the concentration of thickener used in the formulation affects the viscosity, as can be seen in Figure 10, where viscous flow curves of gel-like dispersions containing a lignin/HMDI weight ratio of 1:1 and 1:2 and concentrations of 20% and 30% w/w have been compared. The power-law model fits the viscous flow behavior of these gel-like dispersions fairly well ($R^2 > 0.99$) in the experimental range of shear rates studied,

$$\eta = k \cdot \dot{\gamma}^{n-1} \quad (2)$$

where "k" and "n" are the consistency and flow indexes respectively. The values of these fitting parameters are shown in Figure 10. As can be observed, the values of the consistency and flow indexes slightly decrease with the lignin/HMDI weight ratio, the latter one being extremely low, especially for GKL1-20, as typically found in lubricating greases, which have been traditionally considered classical yielding materials. GKL2-30 displays the higher consistency index,

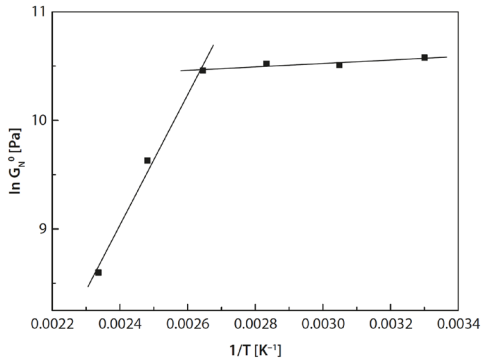

Figure 9 Evolution of the plateau modulus with temperature and Arrhenius' fitting (solid line) for a selected NCO-functionalized lignin gel-like dispersion (GKL2-30).

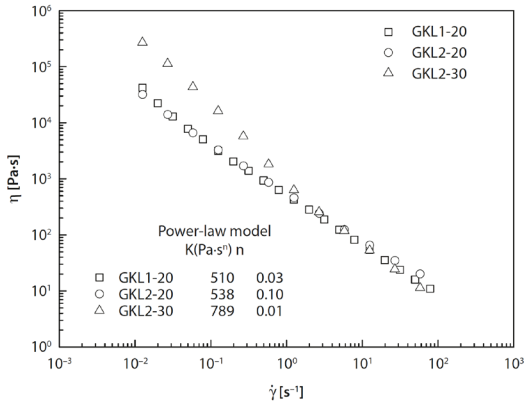

Figure 10 Viscous flow curves for NCO-functionalized lignin gel-like dispersions studied, at 25 °C, as a function of HMDI/lignin weight ratio and concentration.

which may be attributed to the higher thickener concentration.

3.5 AFM Analysis of NCO-Functionalized Lignin Gel-Like Dispersions

Figure 11 shows the microstructure of a selected NCO-functionalized lignin gel-like dispersion (GKL2-20), evaluated by using the AFM technique. The advantage of this technique in contrast to classical electron microscopy observations is that the sample does not need to be modified since the experiments can be carried out under atmospheric pressure. Thus, both scanning (SEM) and transmission (TEM) electron microscopy techniques are vacuum based and the sample must be submitted to either a freezing treatment or oil removal. Appropriate microstructural characterization of conventional lubricating greases and lignocellulose pulp gel-like dispersions were previously reported just by simply heating the sample at a temperature below the dropping point and then cooling down to room temperature in order to obtain a very smooth surface [43]. In this work, the sample was prepared following the same protocol. As can be noticed, the microstructure of this sample is composed of interconnected thin fibers, forming a three-dimensional network, which are distributed in a continuous oil medium. Average fiber thickness and length are around 24–30 nm and 178–230 nm, respectively. These chemically modified lignin dispersions show more densely grouped, thinner and shorter fibers than those found for conventional lubricating

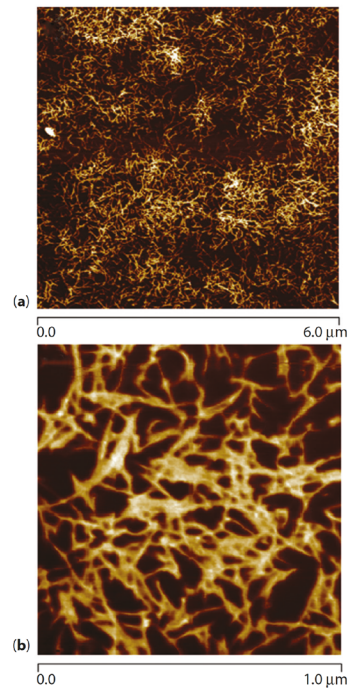

Figure 11 AFM micrographs for selected NCO-functionalized lignin gel-like dispersion (GKL2-20): (**a**) window size 6 µm; (**b**) window size 1 µm.

DOI: 10.7569/JRM.2017.634160 A. M. Borrero-López et al.:Valorization of Kraft Lignin as Thickener in Castor Oil for Lubricant Applications

greases and HMDI-crosslinked lignocellulose pulp gel-like dispersions, previously described [28, 43].

3.6 Lubrication Performance Properties of NCO-Functionalized Lignin Gel-Like Dispersions

The lubrication properties of NCO-functionalized lignin gel-like dispersions studied were evaluated by means of penetration tests and tribological experiments, and the results have been compared with those shown by commercial lithium and calcium lubricating greases. Penetration of standard cone geometries inside a given lubricating grease sample is a common practice in the lubricant industry to determine grease consistency, which is obviously related to the rheological properties. The NLGI grade is a commonly accepted parameter to classify lubricating greases as a function of their consistency obtained as penetration index [30]. Table 4 shows unworked penetration values of gel-like dispersions studied, along with the corresponding NLGI grade, and friction coefficients obtained in the tribological cell. The gel-like dispersion with the higher thickener concentration and lignin/HMDI weight ratio of 1:2 is more viscous (see Figure 10) and therefore shows lower unworked penetration value and higher NLGI grade. Beside this, a decrease of lignin/HMDI weight ratio in the thickener results in a decrease of unworked penetration and higher NLGI grade. On the other hand, all samples studied provide similar friction coefficient values which are lower than those obtained for the commercial lubricating greases under the same tribological conditions. Although friction coefficient depends on operating conditions and wear mechanisms, this is a relevant result since the main purpose of using lubricants in a tribological contact is the reduction of friction as much as possible. In this sense, the model gel-like dispersions studied in this work show a reduction of 16–22% in the friction coefficient with respect to the two standard commercial greases used as references.

4 CONCLUSIONS

This work describes a potential form of industrial valorization of residual Kraft lignin via modification with HMDI and subsequent dispersion in castor oil to obtain gel-like dispersions with suitable and promising properties to be used as biodegradable lubricating greases. Rheological functions of these gel-like dispersions are qualitatively and quantitatively affected by the lignin/HMDI weight ratio and modified lignin concentration. In most cases, the values of the storage modulus are always higher than those found for the loss modulus in a wide frequency range, displaying the plateau region of the mechanical spectrum which is characteristic of particle gels and lubricating greases among them. The rheological functions evolve with ageing time, up to around one month after preparation, as a consequence of an internal curing process where free isocyanates react with castor oil triglycerides. The effect of the curing process is especially dramatic for the sample containing a lignin/HMDI weight ratio of 1:4, which exhibits a predominant viscous response immediately after preparation and becomes almost a rubber after one month. In particular, the frequency dependence of SAOS functions of 30% modified lignin gel-like dispersion with 1:2 lignin/HMDI weight ratio is very similar to that found for traditional NLGI 2 lithium lubricating greases. In relation to long-term rheological stability, the values of SAOS functions significantly increase during the first seven days of ageing, slightly increase up to one month and then remain almost constant for a long period. The thermo-rheological response evidences a softening temperature of around 105 °C. The unworked penetration values and related NLGI grade is essentially viscosity dependent. An increase in lignin functionalization degree results in a decrease of the unworked penetration for the same concentration. All samples studied provide similar friction coefficient values in a tribological contact, lower than those obtained with standard commercial lubricating greases.

Table 4 Penetration, NLGI and friction coefficient for samples studied.

Sample	Unworked penetration (dmm)	NLGI	Friction coefficient
GKL1-20	330	1	0.086
GKL2-20	287	2	0.083
GKL2-30	198	4	0.089
Lithium-based grease	260	2–3	0.108
Calcium-based grease	279	2	0.107

ACKNOWLEDGMENTS

This work is part of two research projects (CTQ2014-56038-C3-1R and RTA2015-00051-00-00) sponsored by MINECO-FEDER (70% European cofunding rate) and INIA programs, respectively.

REFERENCES

1. S. Laurichesse and L. Avérous, Chemical modification of lignins: Towards biobased polymers. *Prog. Polym. Sci.* **39**, 1266–1290 (2014).
2. I.H. Bolker, *Natural and Synthetic Polymers: An Introduction*, Marcel Dekker, New York (1974).
3. A. Tejado, C. Peña, J. Labidi, J.M. Echevarria, and I. Mondragon, Physico-chemical characterization of lignins from different sources for use in phenol-formaldehyde resin synthesis. *Bioresour Technol*. **98**, 1655–1663 (2007).
4. X. Du, J. Li, and M.E. Lindström, Modification of industrial softwood Kraft lignin using Mannich reaction with and without phenolation pretreatment. *Ind. Crops Prod*. **52**, 729–735 (2014).
5. C. Bonini, M. D'Auria, L. Emanuele, R. Ferri, R. Pucciatiello, and A.R. Sabia, Polyurethanes and polyesters from lignin. *J. Appl. Polym. Sci.* **98**(3), 1451–1456 (2005).
6. D.V. Evtuguin, J.P. Andreolety, and A. Gandini, Polyurethanes based on oxygen-organosolv lignin. *Eur. Polym. J*. **34**(8), 1163–1169 (1998).
7. H. Hatakeyama and T. Hatakeyama, Thermal Properties of isolated and in situ lignin, in *Lignin and Lignans: Advances in Chemistry*, C. Heitner, D. Dimmel, and J. Schmidt (Eds.), pp. 301–319, CRC Press, Boca Raton (2011).
8. T. Hatakeyama, Y. Izuta, S. Hirose, and H. Hatakeyama, Phase transitions of lignin-based polycaprolactones and their polyurethane derivatives. *Polymer* **43**(4), 1177–1182 (2002).
9. J. Bernardini, P. Cinelli, I. Anguillesi, M.B. Coltelli, and A. Lazzeri, Flexible polyurethane foams green production employing lignin or oxypropylated lignin. *Eur. Polym. J*. **64**, 147–156 (2015).
10. C.Q. Zhang, H.C. Wu, and M.R. Kessler, High bio-content polyurethane composites with urethane modified lignin as filler. *Polymer* **69**, 52–57 (2015).
11. D. Feldman, M. Lacasse, and L.M. Beznaczuk, Lignin-polymer systems and some applications. *Prog. Polym. Sci*. **12**, 271–276 (1986).
12. P.C. Mileo, M.F. Oliveria, S.M. Luz, G.J.M. Rocha, and A.R. Gonçalves, Thermal and Chemicals characterization of sugarcane bagasse cellulose/lignin-reinforced composites. *Polym. Bull*. **73**, 3163–3174 (2016).
13. A. Lee and Y.L. Deng, Green polyurethane from lignin and soybean oil through non-isocyanate reactions. *Eur. Polym. J*. **63**, 67–73 (2015).
14. X.G. Luo, A. Mohanty, and M. Misra, Lignin as a reactive reinforcing filler for water-blow rigid biofoam composites from soy oil-based polyurethane. *Ind. Crops Prod*. **47**, 13–19 (2013).
15. L.B. Tavares, C.V. Boas, G.R. Schleder, S.M. Nacas, D.S. Rosa, and D.J. Santos, Bio-based polyurethane prepared from Kraft lignin and modified castor oil. *Express Polym. Lett*. **11**, 927–940 (2016).
16. J.W. Bartz, Lubricants and the environment. *Tribol. Int*. **31**, 35–47 (1998).
17. C.W. Lea, European development of lubricants derived from renewable resources. *Ind. Lubr. Tribol*. **54**, 268–274 (2002).
18. S. Boyde, Green lubricants. Environmental benefits and impacts of lubrication. *Green Chem*. **4**, 293–307 (2002).
19. F.S. Guner, Y. Yagci, and A.T. Erciyes, Polymers from triglyceride oils. *Prog. Polym. Sci*. **31**, 633–670 (2006).
20. L.A. Quinchia, M.A. Delgado, J.M. Franco, H.A. Spikes, and C. Gallegos, Low-temperature flow behaviour of vegetable oil-based lubricants. *Ind. Crops Prod*. **37**, 383–388 (2012).
21. S. Asadauskas, J.M. Perez, and J.L. Duda, Lubrication properties of castor oil. Potential basestock for biodegradable lubricants. *Lubr. Eng*. **53**, 35–41 (1997).
22. S.Z. Erhan, B.K. Sharma, and J.M. Perez, Oxidation and low temperature stability of vegetable oil-based lubricants. *Ind. Crops Prod*. **24**, 292–299 (2006).
23. R. Sánchez, J.M. Franco, M.A. Delgado, C. Valencia, and C. Gallegos, Effect of thermo-mechanical processing on the rheology of oleogels potentially applicable as biodegradable lubricating greases. *Chem. Eng. Res. Des*. **86**, 1073–1082 (2008).
24. R. Sánchez, J.M. Franco, M.A. Delgado, C. Valencia, and C. Gallegos, Thermal and mechanical characterization of cellulosic derivatives-based oleogels potencially applicable as bio-lubricating grease: Influence of ethyl cellulose molecular weight. *Carbohydr. Polym*. **83**, 151–158 (2011).
25. N. Nuñez, J.E. Martín-Alfonso, M.E. Eugenio, C. Valencia, M.J. Díaz, and J.M. Franco, Preparation and characterization of gel-like dispersions based on cellulosic pulps and castor oil for lubricating applications. *Ind. Eng. Chem. Res*. **50**, 5618–5627 (2011).
26. N. Nuñez, J.E. Martín-Alfonso, C. Valencia, M.C. Sánchez, and J.M. Franco, Rheology of new green lubricating grease formulations containing cellulose pulp and its methylated derivative as thickener agents. *Ind. Crops Prod*. **37**, 500–507 (2012).
27. R. Gallego, J.F. Arteaga, C. Valencia, and J.M. Franco, Rheology and thermal degradation of isocyanate-functionalized methyl cellulose-based oleogels. *Carbohydr. Polym*. **98**, 152–160 (2013).
28. R. Gallego, J.F. Arteaga, C. Valencia, M.J. Díaz, and J.M. Franco, Gel-like dispersions of HMDI-cross-linked lignocellulosic materials in castor oil: Toward completely renewable lubricating grease formulations. *ACS Sus. Chem. Eng*. **3**, 2130–2141 (2015).
29. C. Balan and J.M. Franco, Influence of the geometry on the transient and steady flow of lubricating greases. *Tribol. Trans*. **44**, 53–58 (2001).
30. National Lubricating Grease Institute, *NLGI: Lubricating Greases Guide*, NLGI, Kansas (2006).

31. P.S.B. Dos Santos, X. Erdocia, D.A. Gatto, and J. Labidi, Characterization of Kraft lignin separated by gradient acid precipitation. *Ind. Crops Prod.* **55**, 149–154 (2014).
32. M. Alekhina, O. Ershova, A. Ebert, S. Heikkinen, and H. Sixta, Softwood kraft lignin for value-added applications: Fractionation and structural characterization. *Ind. Crops Prod.* **66**, 220–228 (2015).
33. S. Yasuda, K. Fukushima, and A. Kakehi, Formation and chemical structures of acid-soluble lignin I: Sulphuric acid treatment, time and acid-soluble lignin content of hardwood. *J. Wood Sci.* **47**, 69–72 (2001).
34. C.G. Boeriu, D. Bravo, R.J.A. Gosselink, and J.E.G. Van Dam, Characterization of structure-dependent functional properties of lignin with infrared spectroscopy. *Ind. Crops Prod.* **20**, 205–218 (2004).
35. D. Ibarra, M.I. Chávez, J. Rencoret, J.C. Del Río, A. Gutiérrez, J. Romero. S. Camarero, M.J. Martínez, J. Jiménez-Barbero, and A.T. Martínez, Lignin modification during Eucalyptus globulus kraft pulping followed by totally chlorine-free bleaching: A two-dimensional nuclear magnetic resonance, Fourier transform infrared, and pyrolysis-gas chromatography/mass spectrometry study. *J. Agric. Food Chem.* **55**, 3477–3490 (2007).
36. A.M. Borrero-López, C. Valencia, and J.M. Franco, Rheology of lignin-based chemical oleogels prepared using diisocyanate crosslinkers: Effect of the diisocyanate and curing kinetics. *Eur. Polym. J.* **89**, 311–323 (2017).
37. C.V. Mythili, A. Malar Retna, and S. Gopalakrishnan, Synthesis, mechanical, thermal and chemical properties of polyurethanes based on cardanol. *Bull. Mater. Sci.* **27**, 235–241 (2004).
38. J.E. Martín-Alfonso, C. Valencia, M.C. Sánchez, J.M. Franco, and C. Gallegos, Rheological modification of lubricating greases with recycled polymers from different plastic waste. *Ind. Eng. Chem. Res.* **48**, 4136–4144 (2009).
39. L. Lu, X. Liu, and Z. Tsong, Critical exponents for sol-gel transition in aqueous alginate solutions induced by cupric cations. *Carbohydr. Polym.* **65**, 544–551 (2006).
40. J.D. Ferry, *Viscoelastic Properties of Polymers*, 3rd ed., John Wiley & Sons, New York (1980).
41. J.M. Franco, M.A. Delgado, C. Valencia, M.C. Sánchez, and C. Gallegos, Mixing rheometry for studying the manufacture of lubricating greases. *Chem. Eng. Sci.* **60**, 2409–2418 (2005).
42. M.A. Delgado, C. Valencia, M.C. Sanchez, J.M. Franco, and C. Gallegos, Thermorheological behaviour of a lithium lubricating grease. *Tribol. Lett.* **23**, 47–53 (2006).
43. C. Roman, C. Valencia, and J.M. Franco, AFM and SEM assessment of lubricating grease microstructures: Influence of sample preparation protocol, frictional working conditions and composition. *Tribol. Lett.* **63**(20), 1–12 (2016).

2.2. Article 4

Evaluation of lignin-enriched side-streams from different biomass conversion processes as thickeners in bio-lubricant formulations

A.M. Borrero-López, R. Martin-Sampedro, D. Ibarra, C. Valencia, M. E. Eugenio, J.M. Franco

Published in:

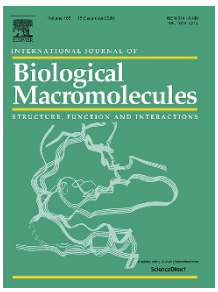

International Journal of Biological Macromolecules
Publishing Company: Elsevier
Editor-in-Chief: A. Dong, JF. Kennedy
Volume 162, pp 1398-1413
Year 2020
ISSN 0141-8130
DOI: 10.1016/j.ijbiomac.2020.07.292

Category	Journal Rank / Total number of journals	Quartile (Percentage)
Biochemistry & Molecular Biology	51/297	Q1 (83%)
Chemistry, Applied	10/71	Q1 (87%)
Polymer Science	9/89	Q1 (90%)
Impact Factor	5.162	

International Journal of Biological Macromolecules 162 (2020) 1398–1413

Contents lists available at ScienceDirect

International Journal of Biological Macromolecules

journal homepage: http://www.elsevier.com/locate/ijbiomac

Evaluation of lignin-enriched side-streams from different biomass conversion processes as thickeners in bio-lubricant formulations

Antonio M. Borrero-López [a], Raquel Martín-Sampedro [b], David Ibarra [b], Concepción Valencia [a,*], María E. Eugenio [b], José M. Franco [a]

[a] Pro2TecS - Chemical Process and Product Technology Research Center, Dept. Ingeniería Química, ETSI, Campus de El Carmen, Universidad de Huelva, 21071 Huelva, Spain
[b] INIA-CIFOR, Forestry Products Department, Ctra. de la Coruña Km 7.5, Madrid 28040, Spain

ARTICLE INFO

Article history:
Received 21 May 2020
Received in revised form 14 July 2020
Accepted 20 July 2020
Available online 6 August 2020

Keywords:
Residual lignin
Oleogel
Rheology

ABSTRACT

This study explores the suitability of residual lignin-containing fractions generated as side-streams in different conversion processes of eucalypt and pine woods as thickening agents in bio-lubricant formulations. These conversion processes included fermentable sugars extraction by autohydrolysis or steam explosion and kraft pulping. Structural properties of lignin fractions were characterized by FTIR, ^{1}H and ^{13}C NMR, two-dimensional NMR, TGA and SEC, whereas their compositions were analysed by standard analytical methods. On the other hand, chemical oleogels were prepared with NCO-functionalized residual lignin fractions, and characterized by means of rheological, tribological and AFM techniques. Hydrolysis lignin fractions exhibited a great content of carbohydrates, especially glucose (46.0–48.5%), xylose (4.3–15.6%) and lignin (32.5–39.9%) with a well-maintained structure, displaying the main inter-unit linkages and low phenolic content. By contrast, kraft lignin fractions presented a lower carbohydrate content, mainly xylose (3.4–4.3%), and higher content (44.9–67%) of severely degraded lignin, showing a dramatic reduction of inter-unit linkages, and thereby high phenolic content. The rheological response of NCO-functionalized lignin fractions-based oleogels is highly influenced by the composition and chemical structure of residual lignin fractions. Moreover, these oleogels presented suitable tribological properties with values of the friction coefficient lower than those typically exhibited by standard lubricating greases.

1. Introduction

The improvement of energy security, renewability of end-use products and goods, and the reduction of greenhouse emissions should be favoured through the transformation of lignocellulosic biomass into chemicals and fuels. This scheme, nowadays known as biorefinery, involves the selective fractionation of the main constituents of lignocellulose (cellulose, hemicellulose and lignin), and their conversion into materials, chemicals, and fuels. Thus, polysaccharides can be used for the production of materials such as cellulosic pulp, and more recently, nanofibrillated cellulose [1]; or can also be transformed into fermentable monomeric sugars from which alcohols, organic acids, alkanes, lipids, etc., can be obtained [2,3]. However, the exploitation of the other main components of lignocellulose, i.e., lignin, is much less studied. Lignin is usually present in the residual fractions generated as side-streams in the carbohydrates-based conversion processes, such as paper pulp and bioethanol industries [4–6], being generally burned to obtain energy. Instead, lignin could be used for the manufacture of new high added-value products [7], improving the sustainability and competitiveness of these lignocellulosic transformation processes.

Conventional lubricating greases can be considered colloidal suspensions, including a solid thickening agent, typically a metallic soap, dispersed in a liquid matrix, traditionally a mineral oil, forming a three-dimensional gel-like network [8]. As a result of the increased environmental awareness, different studies have proposed alternative green formulations obtained from renewable resources, like those containing vegetable-derived oils or glycerol esters instead of the traditional mineral oils [9,10], or biopolymers-derived thickeners as a replacement for the classical metallic soaps. Among these biopolymers, the use of some cellulosic materials such as paper pulps and different cellulose derivatives has been reported [11–13]. In these studies, comparable rheological and thermal properties to those shown by traditional lubricating greases were obtained, however, the physical and mechanical stabilities turned out to be seriously compromised. Further studies have shown substantial improvements in the development of these cellulose-based

* Corresponding author at: Departamento de Ingeniería Química, ETSI, Campus de "El Carmen", Universidad de Huelva, 21071 Huelva, Spain.
E-mail addresses: am.borrero@diq.uhu.es (A.M. Borrero-López), r.martin.sampedro@csic.es (R. Martín-Sampedro), ibarra.david@inia.es (D. Ibarra), barragan@diq.uhu.es, barragan@uhu.es (C. Valencia), mariaeugenia@inia.es (M.E. Eugenio), franco@uhu.es (J.M. Franco).

https://doi.org/10.1016/j.ijbiomac.2020.07.292
0141-8130/

bio-thickeners by functionalizing the cellulose derivatives with isocyanate groups [14,15]. Recently, this approach has been also applied to modify different lignins in order to be subsequently dispersed in castor oil to produce bio-lubricating greases with promising properties [16,17].

A thorough understanding of the composition and structure of residual lignins is imperative to develop new and efficient valorization pathways, including bio-lubricants production. In contrast to cellulose and hemicelluloses, the chemical structure and other related features of lignin have not been as accurately determined, due to the difficulties arisen in its extraction and composition and structural characterization. The problem of a detailed structural description of lignin is mainly related to the different nature of the numerous units that make it up, which are not usually repeated on a regular basis, and the variability of its composition and structure depending on its source. In general, lignin derives from three basic phenylpropanoid units (*p*-hydroxyphenyl (H), guayacil (G), and syringyl (S) units) and their acetylated forms, which react in the cell wall, through peroxidase catalyzed oxidation reactions (via radical intermediates) to eventually form lignin polymers with a large number of functional groups and bonds [18]. The H/G/S units amount and ratio differ depending on the biomass type. Thus, for instance, softwood lignin is enriched in G units also containing a small quantity of H units, whereas hardwood lignin mainly comprises G and S units. Lignins from non-woody plants also contain H units together with G and S units [18]. Moreover, not only the original source but also the technology for lignin extraction has an impact on the purity, molecular weight and chemical functionalities of the isolated lignins and, consequently on their potential valorization [19].

This study explores the valorization of different residual lignin-enriched fractions as thickening agents, via isocyanate functionalization, in the production of bio-lubricating greases. The lignin fractions were generated in different conversion processes of eucalypt and pine woods of interest, including fermentable sugars extraction (using autohydrolysis or steam explosion followed by enzymatic hydrolysis), and cellulosic pulp production (using a classical kraft pulping approach). The main advantage of producing the different residual lignins in the laboratory under controlled conditions is to cover a relatively wide range of compositions and physico-chemical characteristics, in order to evaluate the influence of these in the ultimate properties of the potential end-use lubricants. Apart from the chemical composition determined by standardized analytical methods, lignin chemical structure was comprehensively evaluated by means of Fourier transform infrared spectroscopy (FTIR), ^{1}H and ^{13}C nuclear magnetic resonance (^{1}H and ^{13}C NMR), two dimensional NMR (2D NMR), size exclusion chromatography (SEC), and thermogravimetric analysis (TGA). The NCO-functionalized lignin fractions structure was likewise assessed by FTIR, NMR and TGA techniques. Then, a relationship between the chemical composition and structure of the lignin fractions and their suitability as thickeners in bio-lubricant formulations was established. With this purpose, the rheological, tribological and microstructural properties of the resulting residual lignin fractions-based oleogels obtained were also studied.

2. Materials and methods

2.1. Raw materials and reagents

Eucalyptus globulus wood was kindly supplied by La Montañanesa pulp mill (Torraspapel-Lecta Group, Zaragoza, Spain). *Pinus radiata* wood was obtained from the material available at INIA-CIFOR (Madrid, Spain). The materials were air-dried and then homogenized and stored in polyethylene bags, in a single stock to avoid differences in composition and water content. The woods were ground and sieved to select chips with a size of 0.5–1.5 cm length and 1–2 mm width, and then stored at 25 °C. Chemicals and solvents were acquired from Merck (Barcelona, Spain), Panreac (Barcelona, Spain) or Sigma-Aldrich (Madrid, Spain). Hydrolytic enzymes were donated by Novozymes (Bagsvaerd, Denmark). Castor oil from Guinama (Valencia, Spain) was used as base oil to prepare the oleogels.

2.2. Procedures for obtaining residual lignin-containing fractions

2.2.1. Autohydrolysis and steam explosion followed by enzymatic hydrolysis

Autohydrolysis of eucalypt samples (pieces between 0.25 and 0.20 mm from chips grounded and sieved) was performed in an autoclave (Trade Raypa S.L.) at the following conditions: 135 °C, 30 min, and liquid to solid ratio of 6/1 (water/wood). Steam explosion of eucalypt chips (pre-moistened at 25 °C for 16 h) was carried out in a 26 L stainless steel digester at 195 °C for 20 min.

The samples resulting from autohydrolysis and steam explosion pretreatments were vacuum-filtered and thoroughly washed. Then, the insoluble solid fractions were subjected to enzymatic hydrolysis at 5% w/w solid concentration in 50 mM sodium citrate buffer (pH 4.8), 50 °C, 120 rpm, and 72 h. For that, a cellulolytic complex (Celluclast 1.5 L, 5 filter paper units (FPU)/g of dry sample), supplemented with β-glucosidase (Novozym 188, 5 IU/g of dry sample) was used.

After enzymatic hydrolysis, the resulting hydrolysates were filtered and the insoluble solids fractions, i.e. the residual lignin-containing fractions referenced as AHL and SEL from autohydrolysis and steam explosion pretreatments respectively, were collected, dried at 60 °C overnight, and homogenized using a Retsch mill [20].

2.2.2. Kraft pulping

Kraft pulping of eucalypt and pine chips was carried out in a 26 L batch reactor furnished with a system for recirculation and heating of the pulping liquor, at the following conditions: 16% active alkali, 20% sulfidity, 4 L kg^{-1} liquor/wood ratio, 170 °C cooking temperature, 60 min to reach pulping temperature and 30 min at pulping temperature (H-factor of 460). Chips were steamed for 5 min to facilitate the impregnation of chemicals before starting the pulping. Afterwards, the resulting kraft pulps (insoluble solids fractions) were filtered and the black liquors were recovered. Then, residual lignin-containing fractions (referenced as EKL and PKL from eucalypt and pine kraft pulping, respectively) were recovered from black liquors by acid precipitation (pH lowered to 2.5 with concentrated sulfuric acid). EKL and PKL lignin fractions were filtered, dried at 60 °C overnight and finally homogenized using a Retsch mill [21].

2.3. Analytical methods

The composition of the residual lignin-containing fractions (AHL, SEL, EKL, and PKL) was determined by standard analytical methods [22]. Thus, the samples were subjected to quantitative acid hydrolysis in two steps to determine the carbohydrate composition, being the hydrolysed liquids analysed by high-performance liquid chromatography (1260 HPLC, Agilent, Waldbronn, Germany; fitted with a G1362A refractive index detector; and equipped with an Agilent Hi-PlexPb column operated at 70 °C with Milli-Q water as mobile phase pumped at a rate of 0.6 mL min^{-1}). The solid residues remaining after the acid hydrolysis were considered acid-insoluble lignin (Klason lignin). Moreover, ash content was determined following the standard UNE 57050:2003.

2.4. Fourier transform infrared (FTIR) spectroscopy

FTIR spectra were performed using a JASCO FT/IR-4200 (Jasco Inc., Japan) apparatus. Lignin fractions were dispersed in KBr to obtain disks. Then, the disk was put in a sample holder. NCO-functionalized lignins were directly measured instead. The spectra were collected in a wavenumber range of 400–4000 cm^{-1}, in the transmission mode, at 4 cm^{-1} resolution.

2.5. Nuclear magnetic resonance (NMR)

Prior to ^{1}H and ^{13}C nuclear magnetic resonance (^{1}H and ^{13}C NMR) experiments, lignin fractions were acetylated by mixing samples (1 g) with anhydride acetic (30 mL) and pyridine (30 mL) for 48 h at room temperature. Then, the reaction mixture was transferred into cold water (300 mL) to obtain a solid that was filtered and washed with water.

^{1}H and ^{13}C NMR experiments of acetylated lignin fractions were carried out at 25 °C in a Bruker AVANCE 500 MHz (Bruker, USA) spectrometer equipped with a 5 mm BBFO plus with a z-gradient double-resonance probe. Chemical shifts were referred to tetramethylsilane. $CDCl_3$ was used as solvent, except for PKL which was dissolved in DMSO-d_6. ^{1}H NMR experiments were carried out under the following operation conditions: pulse 45° (μs) 4.9 (AHL, pulse 30° (μs) 2.875); recycle delay (s) 10 (AHL, 10); spectral width (Hz) 10,330.5 (AHL, 6172.84); acquisition time (s) 3.17 (AHL, 5.3); scans number 32 (AHL, 64). ^{13}C NMR experiments were carried out under the following operation conditions: pulse 30° (μs) 3.21 (AHL, 4); recycle delay (s) 1 (AHL, 10); spectral width (Hz) 30,030 (AHL, 29,761); acquisition time (s) 1.09 (AHL, 5.3); scans number 12,500 (AHL, 13,360).

^{13}C–^{1}H two-dimensional nuclear magnetic resonance (2D NMR) analysis of lignin fractions and NCO-functionalized lignins (dissolved in 0.75 mL of deuterated dimethylsulfoxide, DMSO-d_6) was recorded at 25 °C in the same spectrometer. HSQC (heteronuclear single quantum correlation) experiment was recorded under the following operation conditions: spectral widths, 5000 (EKL), 5252 (PKL), 6172 (AHL), and 4771 (SEL) Hz for the ^{1}H dimensions, and 22,522 Hz for ^{13}C dimensions (AHL, 20,843); number of collected complex points, 1024 for ^{1}H-dimension with a recycle delay of 1 s (AHL, 1676); scans number 32; time increments (13C) 256; 1 JC-H (Hz): 145; *J*-coupling evolution delay set to 3.45 ms; squared cosine-bell apodization function applied in both dimensions. Residual DMSO (from DMSO-d_6) was used as internal reference (δ_C/δ_H 39.6/2.5 ppm).

2.6. Size exclusion chromatography (SEC)

SEC analysis (weight-average (M_w), number-average (M_n) molecular weights, and polydispersity (M_w/M_n)) of lignin fractions was performed by HPLC (1260 HPLC, Agilent, Waldbronn, Germany; fitted with a G1315D diode array detector; and equipped with two columns (Phenomenex) coupled in series (GPC P4000 and P5000, both 300 × 7.8 mm) and a safeguard column (35 × 7.8 mm)). The samples were analysed at 254 nm using NaOH (0.05 M) as a mobile phase pumped at a rate of 1 mL min^{-1} at 25 °C for 30 min. Prior to SEC analysis, lignin fractions were dissolved at a final concentration of 0.5 g L^{-1} in NaOH (0.05 M). Polystyrene sulfonated standards (peak average molecular weights of 4210, 9740, 65,400, 470,000, PSS-Polymer Standards Service) were used for calibration purposes.

2.7. Thermogravimetric analysis (TGA)

Mass loss versus temperature curves were determined under N_2 purge in a thermogravimetric analyser Q-50 (TA Instruments, New Castle, USA). Lignin fractions and NCO-functionalized lignins (5–10 mg) were placed on platinum pans and heated from 30 °C to 600 °C, at 10 °C min^{-1}.

2.8. Functionalization of residual lignin fractions and oleogel preparation

NCO-functionalization was performed by using hexamethylene diisocyanate (HDI) and selecting a 1/2 w/w residual lignin fraction/HDI ratio according to the methodology previously reported [16,17]. NCO-functionalized lignin samples have been named as FAHL, FSEL, FEKL and FPKL.

The preparation of chemical oleogels was carried out following the procedure detailed by Borrero-López et al. [16], wherein the NCO-functionalized lignin samples, at 20% w/w concentration, were dispersed in castor oil at room temperature for 24 h, using a RW 20 IKA stirrer outfitted with an anchor impeller. Subsequently, the oleogels were stored at room temperature and characterized after one month, to ensure the complete curing of the samples [23]. Oleogel samples have been named as GAHL, GSEL, GEKL and GPKL for those prepared with lignins obtained from the autohydrolysis, steam explosion and eucalypt and pine kraft pulping treatments, respectively.

2.9. Rheological characterization of residual lignin fractions-based oleogels

Rheological measurements were conducted using controlled-stress (Rheoscope, Haake, Germany) and controlled-strain (ARES, Rheometric Scientific, UK) rheometers. Small-amplitude oscillatory shear (SAOS) tests were carried out using a serrated plate-and-plate geometry (20 mm diameter and 1 mm gap), in the linear viscoelastic regime and frequency range of 0.03–100 rad s^{-1}, at 25 °C. Viscous flow tests were performed in a shear rate range of 10^{-2}–10^{2} s^{-1}, using a serrated plate-plate geometry (25 diameter and 1 mm gap). At least two replicates of each test on fresh samples were made.

2.10. Microstructural characterization of residual lignin fractions-based oleogels

Morphological observations of oleogels samples were made using a multimode AFM connected to a Nanoscope IV scanning probe microscope controller (Digital Instruments, Veeco Metrology Group Inc., Santa Barbara, CA) in the tapping mode with phase detection imaging. Silicon Nanosensors TM PPP-NCH AFM probes with a constant force of 42 N m^{-1} and resonance frequency of 330 kHz were utilized. Scan speed and window size were fixed to 1 Hz and 6 μm, respectively.

2.11. Mechanical stability and tribological characterization of residual lignin fractions-based oleogels

Unworked penetration indexes were determined using a Seta Universal penetrometer model 17000-2 with one-quarter cone geometry (Stanhope-Seta, UK), following the ASTM D1403 standard. One-quarter scale penetration values were transformed into the equivalent full-scale cone penetration values, following the ASTM D217 standard. The classical NLGI consistency grade was determined according to these penetration values [8]. Five replicates of penetration measurements were done.

A tribology measuring cell connected to a Physica MCR-501 rheometer was used to carry out the tribological tests. The tribological cell is composed of a 1/2″ diameter steel ball (1.4301 grade 100) that rotates on three steel plates (1.4301) inclined 45°. The stationary friction coefficient was measured at room temperature by applying a normal force of 20 N, resulting in a maximum contact Hertzian pressure of ~1.72 GPa, and setting a constant rotational speed of 10 rpm for 10 min. At least five replicates of each test were done using fresh oleogel samples as lubricants. For the sake of comparison, the same tribological test was also performed under the same conditions using a commercial lithium lubricating grease [24].

3. Results and discussion

3.1. Chemical analysis of residual lignin-containing fractions

In the context of biorefineries, lignocellulose conversion processes typically involve access to carbohydrates contained in the plant wall that will be later transformed into materials, chemicals, and fuels. For that, biomass must first be subjected to a pretreatment stage in order to produce an extensive modification of lignocellulose, mainly through

lignin degradation, solubilization of hemicellulose and breaking the crystalline structure of cellulose [2]. Among the pretreatment technologies that act on lignin, kraft pulping using NaOH and Na_2S is the most extensively used in the pulp and paper industry [25], whereas hydrothermal processes such as autohydrolysis and steam explosion are specially designed for hemicellulose hydrolysis and solubilization, being more employed for fermentable sugars production [2].

Table 1 displays the chemical composition of the different residual lignin-containing fractions recovered after enzymatic hydrolysis of autohydrolysed eucalypt (AHL) and steam-exploded eucalypt (SEL), as well as those precipitated from eucalypt (EKL) and pine (PKL) kraft black liquors. In general, the total lignin content detected in kraft lignin fractions (44.8% and 67.0% for EKL and PKL, respectively) was higher than those found in the hydrolysis-derived lignin fractions (40.0% and 32.5% for SEL and AHL, respectively). The latter instead showed a much higher carbohydrates content, around 52.7–61.9%, compared to EKL and PKL samples (5.0–4.5%). This higher carbohydrate content observed in lignin fractions obtained from the hydrolysis treatments could be explained by the hydrolytic enzymes doses used herein. Whereas the majority of studies for sugars and bioethanol production uses 15 FPU and 15 IU/g of dry sample of cellulase and β-glucosidase enzymes [26,27], respectively, or even higher [5], the enzyme doses applied in this study were considerably lower (5 FPU and 5 IU/g of dry sample of cellulase and β-glucosidase enzymes, respectively). Then, lower enzyme doses reduce saccharification yields and, consequently a higher sugar content remains in hydrolysis lignin fractions [28]. Among the carbohydrates, glucose was the major sugar in both hydrolysis lignin fractions (46.0–48.5%), whereas xylose was predominant in the AHL sample (15.6%) compared to SEL sample (4.3%). During hydrothermal pretreatments, lignocellulosic biomass is exposed to water at high temperature and pressure for a short time, where acetyl groups are solubilized, promoting the hydrolysis and solubilization of hemicelluloses by cleavage of glycosidic bonds in hemicelluloses and lignin-hemicelluloses linkages [29,30]. Nevertheless, the hemicelluloses removal level varies in function of the pretreatment conditions and severity [29–31]. Then, AHL lignin fraction showed a higher xylose content, according to the lower severity of the autohydrolysis pretreatment ($S_0 = 2.5$), while SEL lignin fraction exhibited a lower xylose amount in agreement to the higher severity of the steam-explosion pretreatment ($S_0 = 4.09$).

Regarding kraft lignin fractions, both samples also showed slight amounts of xylose (Table 1), in agreement with other studies on eucalypt and pine kraft lignins [21,32]. Carbohydrates are solubilized from biomass during kraft pulping. This effect, known as peeling reaction, includes a sequential depolymerization of the carbohydrates, especially affecting hemicellulosic hexoses like glucomannan and to a lesser extent pentoses as xylan [25]. Afterwards, co-precipitation of hemicelluloses together with lignins is due to acidification of black pulping liquors, which is described by the lower solubility of hemicelluloses in acidic media [32]. Nonetheless, the pH value of pulping black liquors for lignin extraction defines the amount of carbohydrates co-precipitated, leading to a higher sugars content as pH decreases [32]. In addition, it is also known that hemicelluloses can also be linked to these isolated lignins in the form of lignin-carbohydrates complexes [21,33]. On the other hand, a great content of ashes was observed for both kraft lignin fractions, being especially higher for the EKL sample. Ashes are related to the inorganic matter existing in the sample, and in this case, probably to the high amount in Na_2SO_4 salts produced during the acid precipitation step to obtain lignin fractions from pulping black liquor [34]. Moreover, it is known that hardwood normally consumes lower amount of chemical reagents during pulping process (due to the higher amount of S units, easier to remove during pulping) [35] compared to softwood and, consequently, higher amount of NaOH remains in the black liquor favouring Na_2SO_4 formation when H_2SO_4 is added [36], which could explain the higher amount of ashes observed in EKL sample.

Table 1
Chemical composition (%) of residual lignin-containing fractions obtained from eucalypt and pine wood conversion processes.

	Klason lignin	Soluble lignin	Total lignin	Glucose	Xylose	Arabinose	Ash[a]
AHL	27.52	4.92	32.44	46.04	15.63	0.25	<0.5
SEL	38.82	1.12	39.94	48.40	4.30	0.00	<0.5
EKL	35.95	8.85	44.81	0.49	4.29	0.20	33.66
PKL	60.50	6.50	67.00	0.45	3.36	0.72	16.00

[a] Ash content determined at 900 °C.

The impurities detected in lignin fractions, mainly sugars, may have significant effects on their applicability, and based on requirements of the target application some lignin purification procedures may be needed [37]. Nevertheless, in the case of bio-lubricants production, the presence of carbohydrates may have a positive effect in the functionalization reaction with diisocyanates as an additional source of polyols, as discussed below. In this sense, previous studies have reported that the reaction between the hydroxyl groups from cellulose, e.g., cellulosic pulps, cellulose derivatives, etc., and –NCO groups of diisocyanates generates a suitable biopolymer to be mixed with castor oil giving rise to oleogels with lubricating properties [15,38].

3.2. FTIR and NMR spectroscopic analysis of residual lignin-containing fractions

FTIR spectra of lignin fractions are displayed in Fig. 1, being the corresponding bands assigned by comparison with other lignin spectra previously reported [4–6,35,39]. According to the chemical composition described above, the FTIR spectra show the typical lignin bands, including those at 1615, 1517, and 1423 cm^{-1} associated to the aromatic skeleton vibrations; at 2930 and 2850 cm^{-1} corresponding to the asymmetrical and symmetrical stretching vibrations of methylene groups, respectively; and that appearing at 1457 cm^{-1} due to asymmetric vibrations and deformation. Moreover, a predominance of bands assigned to S units was observed for eucalypt AHL, SEL and EKl lignins (Fig. 1a, b, and c), similarly to other lignins derived from hardwoods [5,6,35,40,41], with bands at 1327–1324 cm^{-1} (ring breathing) and 831–829 cm^{-1} (out of plane C–H bending vibration). On the contrary, pine kraft lignin (PKL) spectrum (Fig. 1d) shows prevalence bands corresponding to G units at 1262 cm^{-1} (ring breathing) and 853 cm^{-1} (out of plane C–H bending vibration) [39].

The band at 1732 cm^{-1} (unconjugated C=O stretching) attributed to lignin oxidation was clearly visible in AHL and PKL samples (Fig. 1a and d). Nevertheless, the carbonyl groups of hemicelluloses could also contribute to this band [32], particularly in the case of AHL lignin fraction according to its higher xylose content. On the other hand, conjugated C=O groups at 1645 cm^{-1} can also be observed in all spectra, contributing to the widening of the 1615 cm^{-1} band. This band could also be associated with lignin oxidation as well as to amide bonds from enzymes used during enzymatic hydrolysis, mainly in the case of AHL and SEL samples (Fig. 1a and b).

Regarding the presence of carbohydrates, different bands attributed to cellulose and hemicelluloses were observed in all spectra, being especially pronounced in hydrolysis lignin fractions (AHL and SEL, Fig. 1a and b, respectively) according to their higher carbohydrates content. Thus, a carbohydrate region with characteristic cellulose and hemicelluloses bands at 1156 (C–O asymmetric vibration), 1114 (C–OH skeletal vibration), and 1030 cm^{-1} (C–O stretching vibration) are apparent, in the same way that FTIR spectra of lignin-containing side streams recently described for bioethanol production of different agriculture residues and energy dedicated crops [4–6]. By contrast, according to the great ash content found for both kraft lignin fractions (EKL and PKL, Fig. 1c and d, respectively), the carbohydrate region of their FTIR spectra is overlapped by a broad band at 1114 cm^{-1} related to the asymmetric

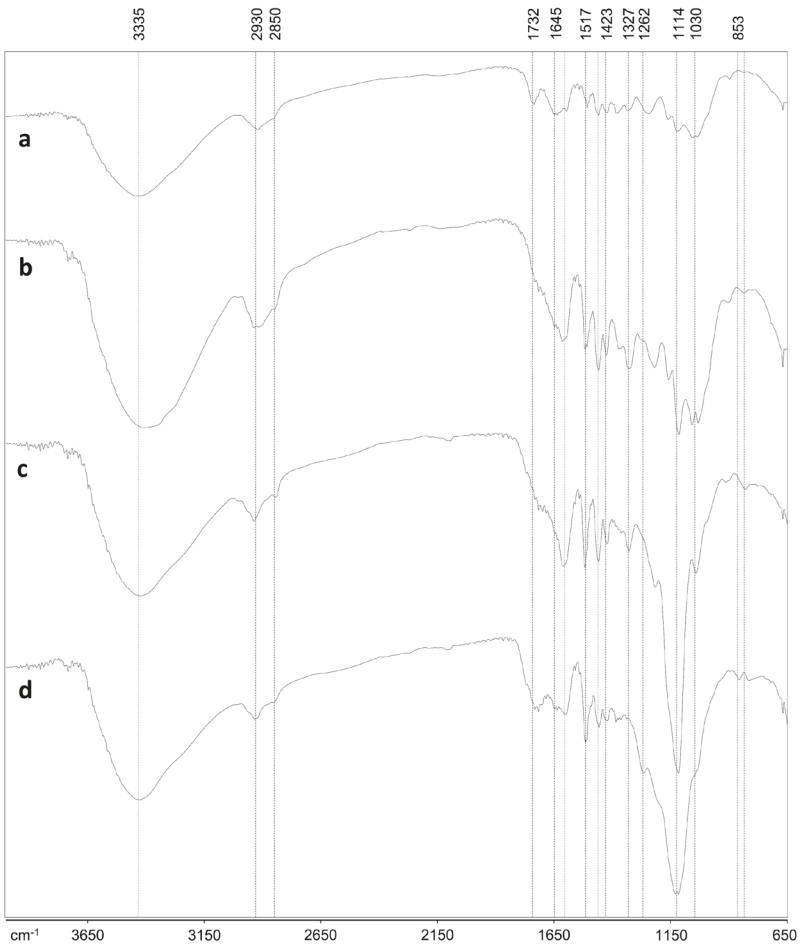

Fig. 1. FTIR spectra of AHL (a), SEL (b), EKL (c), and PKL (d) lignin-containing fractions.

stretching of $SO_4^{=}$ groups [34], resulting from the salts generated during the acid precipitation for lignin recovery from kraft black liquors.

Fig. 2 shows 2D NMR HSQC spectra of hydrolysis lignin fractions (AHL and SEL), while Fig. 3 displays 2D NMR HSQC spectra of kraft lignin fractions (EKL and PKL). Fig. 4 illustrates the corresponding ^{13}C NMR spectra of acetylated lignin fractions, whereas Fig. 5 the corresponding ^{1}H NMR spectra. Finally, Fig. 6 displays the lignin substructures identified in these residual lignin fractions by the different NMR analysis. The main 2D NMR signals are listed in Table S1 (in the Supporting information), whereas Table S2 (in the Supporting information) displays ^{1}H NMR and ^{13}C NMR signals. All signals were assigned according to those previously described in the literature [4–6,21,40–47].

Around δ_C/δ_H 0–50/0–4.5 ppm of 2D NMR HSQC spectra, ascribed to the non-oxygenated aliphatic region, a great diversity of saturated aliphatic moieties were detected in all lignin fractions (Figs. 2 and 3), showing higher intensities in EKL and PKL spectra (Fig. 3). Some signals around δ_H 0.8–1.6 ppm are attributed to extractives, whereas others about δ_H 1.6–2.6 ppm could correspond to different groups resulting from lignin degradation [44,48].

Around δ_C/δ_H 50–95/2.6–5.6 ppm, assigned to the oxygenated aliphatic region, the cross-signals of methoxyl groups and the different inter-unit linkages of lignins can be detected (Table S1 in the Supporting information). Then, AHL and SEL fractions spectra presented lignin signals attributed to *β-O-4′* substructures (A) (Fig. 2), including those assigned to C_α–H_α correlations for *β-O-4′* substructures of G and S units, C_β–H_β correlations of *β-O-4′* S units, and C_γ–H_γ correlations partly overlapped with other signals. AHL and SEL fractions spectra also displayed pronounced lignin signals for resinol (*β-β′*) substructures (B) (Fig. 2), showing C_α–H_α, C_β–H_β, and the double C_γ–H_γ correlations. Signals of phenylcoumaran (*β-5′*) substructures (C) were also slightly observable (signal corresponding to C_α–H_α correlation) in SEL lignin spectrum (Fig. 2b). By contrast, this signal was absent in the AHL lignin spectrum (Fig. 2a).

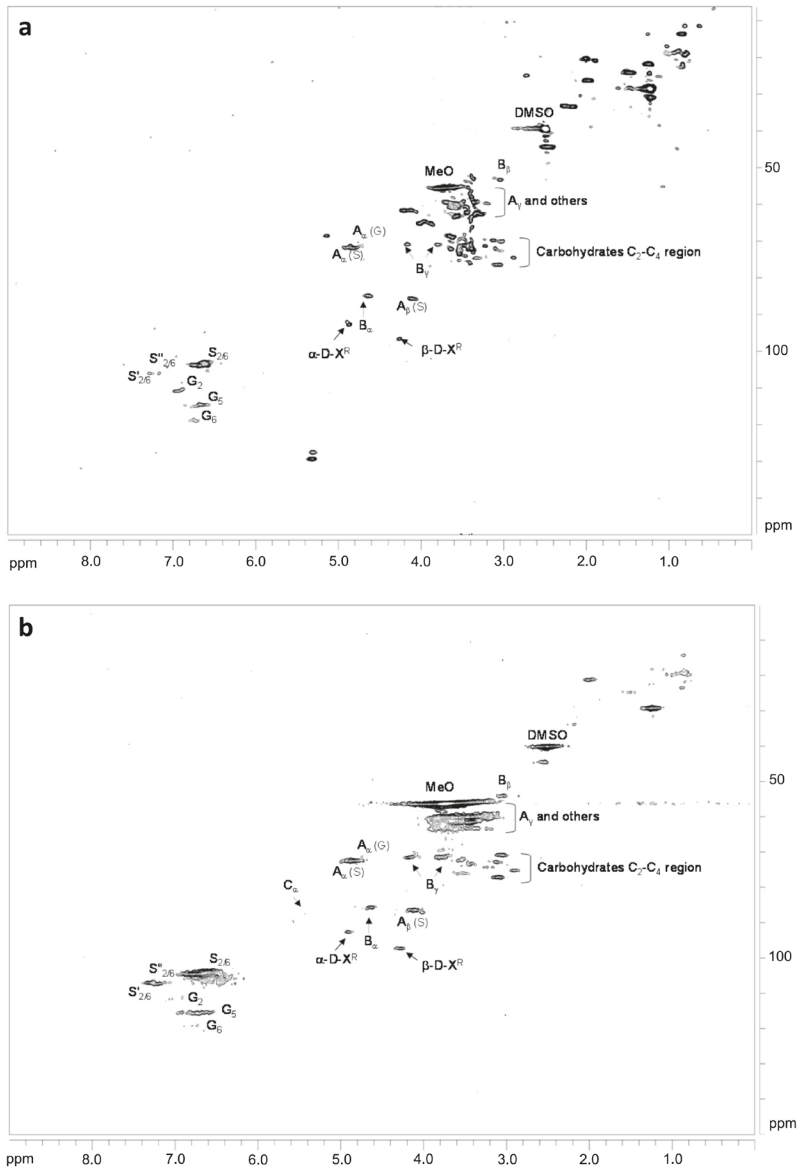

Fig. 2. HSQC 2D-NMR spectra, δ_C/δ_H 0–150/0–90 ppm region, of AHL (a) and SEL (b) lignin-containing fractions. The aliphatic, oxygenated aliphatic, and aromatic regions are observed. Cross-signals of the residual DMSO is indicated.

Compared to AHL and SEL lignin fractions (Fig. 2a and b, respectively) from saccharification processes, the oxygenated aliphatic region of EKL and PKL fractions spectra from kraft pulping showed rather low intensity of lignin signals assigned to *β-O-4′* substructures (A) (Fig. 3), together with a new signal identified in eucalypt kraft lignin as C_{β}–H_{β} correlation for *β-O-4′* substructures with a conjugated carbonyl or

Fig. 3. HSQC 2D-NMR spectra, δ_C/δ_H 0–150/0–90 ppm region, of EKL (a) and PKL (b) lignin-containing fractions. The aliphatic, oxygenated aliphatic, and aromatic regions are observed. Cross-signals of the residual DMSO is indicated.

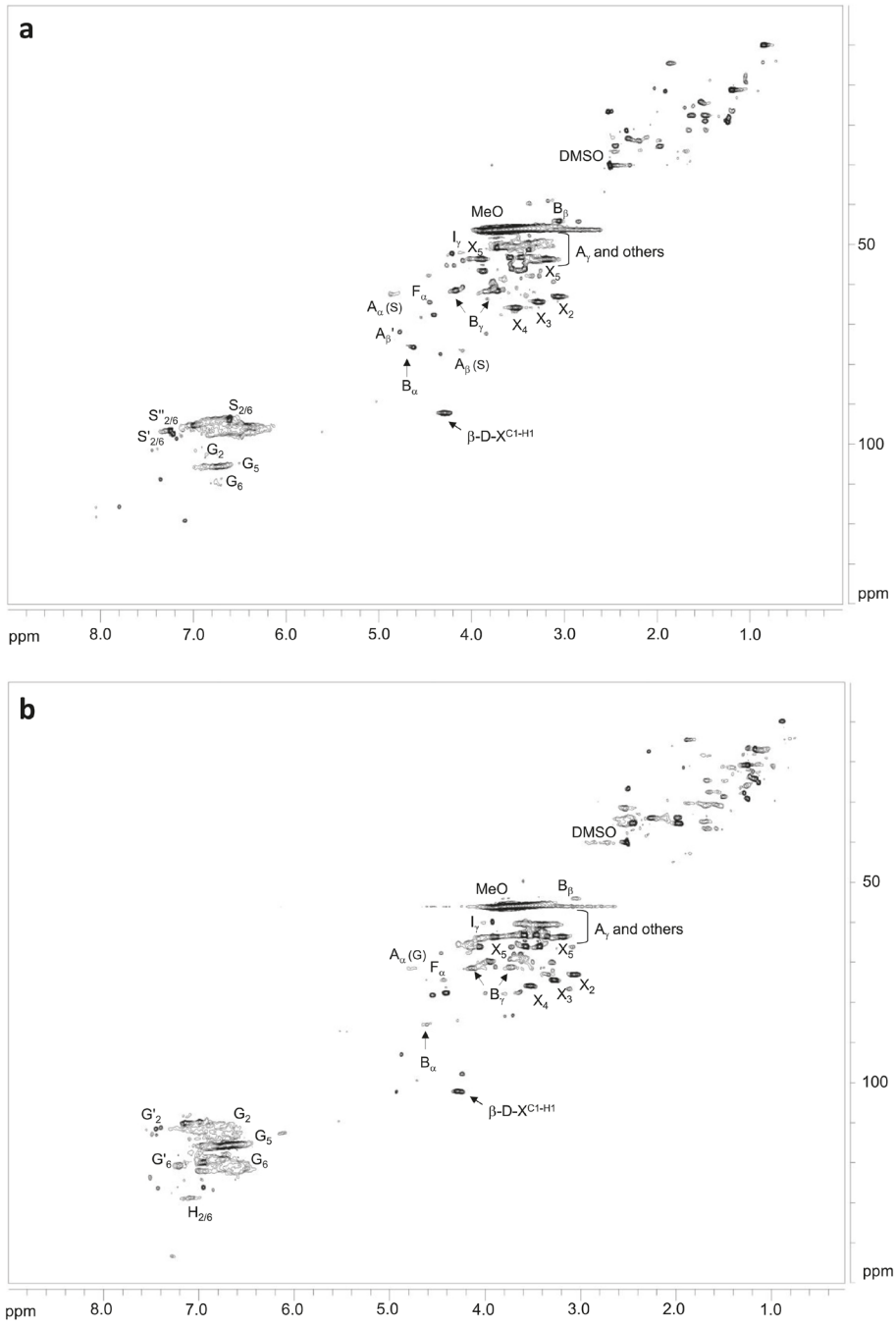
a
DMSO
MeO
Bβ
Iγ
X5
Aγ and others
X5
Fα
Aα (S)
Bγ
X4
X3
X2
Aβ'
Aβ (S)
Bα
S''2/6
S2/6
S'2/6
G2
G5
G6
β-D-XC1-H1
50
100
ppm
ppm 8.0 7.0 6.0 5.0 4.0 3.0 2.0 1.0
b
DMSO
MeO
Bβ
Iγ
Aγ and others
Aα (G)
X5
X5
Fα
Bγ
X4
X3
X2
Bα
β-D-XC1-H1
G'2
G2
G5
G'6
G6
H2/6
50
100
ppm
ppm 8.0 7.0 6.0 5.0 4.0 3.0 2.0 1.0

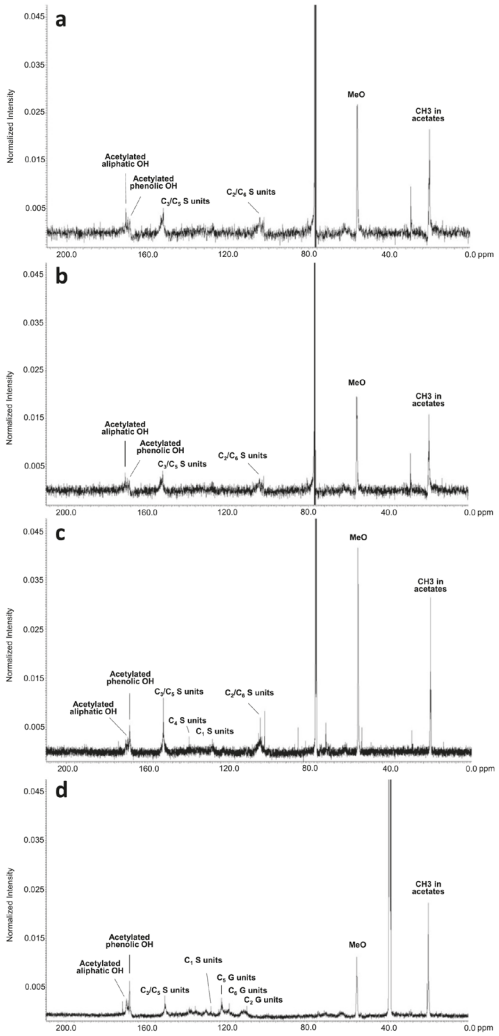

Fig. 4. ^{13}C NMR spectra of AHL (a), SEL (b), EKL (c), and PKL (d) acetylated lignin-containing fractions (PKL dissolved in DMSO-d_6 instead of $CDCl_3$).

carboxyl group (Fig. 3a). All these effects are indicative of a higher β-O-4′ linkage degradation during kraft pulping of eucalypt and pine [21,32,35,46,49], and consequently, a higher lignin content with available phenolic hydroxyl groups, as also confirmed by ^{1}H NMR and ^{13}C NMR experiments. Moreover, signals corresponding to phenylcoumaran substructures (C) were also absent. Only correlations assigned to resinol substructures (B) were observable, together with a new C_α–H_α signal recognized as lignin terminal structure with a carboxyl in C_β (F). This terminal structure has been already reported as intermediate in side-chains cleavage of eucalypt and pine kraft lignins [44,46], which possibly reveals a greater shortening of aliphatic chains during pulping processes. Lastly, other signals found in the oxygenated region of the spectra of both kraft lignin fractions correspond to the C_γ–H_γ correlations of cinnamyl alcohol end-groups (I).

The oxygenated aliphatic region of all spectra also shows a set of signals around δ_C/δ_H 68–78/2.8–3.6 ppm attributed to carbohydrates, both hexose and pentose units (Figs. 2 and 3). According to the higher glucose content determined for AHL and SEL lignin fractions, their spectra presented mostly signals from hexose units together with the reducing ends of (1 → 4) α-D-xylopyranosyl units (α-D-X^R) and (1 → 4) β-D-xylopyranosyl units (β-D-X^R) (Fig. 2). This fact was also observed in 2D NMR spectra of lignin-containing side streams generated during bioethanol production from steam-exploded materials of wheat straw, forage sorghum, poplar wood, and olive tree pruning, being glucose the main carbohydrate existent [4–6]. In contrast, EKL and PKL lignins spectra from kraft pulping mainly show correlation in xylan chains (C_2–H_2, C_3–H_3, C_4–H_4, and C_5–H_5) and the C_1–H_1 cross-signal of (1 → 4) β-D-Xylopyranosyl units (β-D-$X^{C1\text{-}H1}$) (Fig. 3), which is consistent with the xylose content determined for these kraft lignin fractions, and other studies on eucalypt and pine kraft lignins [21,32].

Finally, around δ_C/δ_H 95–150/5.6–9.0 ppm, corresponding to the aromatic region, residual lignin fractions spectra show correlations associated with the aromatic rings of the different S and G lignin units depending on lignocellulose source. Then, a pronounced signal assigned to the $C_{2,6}$–$H_{2,6}$ correlation in S lignin units was observed for residual fractions AHL, SEL and EKL from eucalypt (Figs. 2a and b, and 3a), in agreement with other studies [21,31,46,49]. In addition, signals described for $C_{2,6}$–$H_{2,6}$ correlation in S units with a C_α bearing a carbonyl (S′) or carboxyl (S″) group [46] are also present in all eucalypt spectra. Regarding signals associated with G lignin units, C_2–H_2, C_5–H_5, and C_6–H_6 cross-signals were also visible in AHL, SEL, and EKL lignin fractions spectra. By contrast, the PKL spectrum from pine residual fraction only showed signals related to G units (Fig. 3b), which is typical of softwood materials [21,44,45]. Besides, signals attributed to C_2–H_2 and C_6–H_6 correlation in G units with oxidized C_α (G′) were also present in PKL spectrum [50], together with a signal corresponding to $C_{2,6}$–$H_{2,6}$ correlations in H lignin units. In support of 2D NMR experiments, ^{13}C NMR spectra of acetylated residual lignins also confirmed the predominance of S units in eucalypt lignins (Fig. 4a, b, and c), and the prevalence of G units in pine lignin (Fig. 4d).

Moreover, the abundance of lignin inter-unit linkages, S/G ratio, and aromatic OH/aliphatic OH ratio of the different residual lignins were also determined from the integration of ^{13}C–^{1}H correlation peaks in the HSQC and ^{1}H NMR spectra (Table 2). It is well well-known that β-*O*-4′ substructures depolymerization is the principal reaction during hydrothermal pretreatments [29–31,51,52]. This phenomenon is due to the acid-promoted cleavage of alkyl–aryl ether β-*O*-4′ linkages by the action of acetic and uronic acids produced during the pretreatment from the acetylated lignocellulose components [51]. Acidolysis of glycosidic bonds in hemicelluloses is also produced, together with the degradation of β-β′ resinols, and β-5′ phenylcoumarans [29,30,52]. Nevertheless, the lignin depolymerization level varies with the hydrothermal pretreatment conditions and severity [29–31]. Accordingly, AHL and SEL lignins studied herein still showed different inter-unit linkages, with higher contents for AHL lignin (β-*O*-4′ alkyl–aryl ether, 49.6 linkages per 100 aromatic units; and β-β′ resinols, 17.25 linkages per 100 aromatic units), according to the lower severity of the autohydrolysis pretreatment ($S_0 = 2.5$). By contrast, SEL lignin showed lower amounts of inter-unit linkages (β-*O*-4′ alkyl–aryl ether, 24 linkages per 100 aromatic units; and β-β′ resinols, 8.5 linkages per 100 aromatic units), according to the higher severity of steam-explosion pretreatment ($S_0 = 4.09$). Similar lignin depolymerization was described by Araya et al. [31] when eucalypt biomass was submitted to different autohydrolysis pretreatment conditions, observing higher lignin degradation as severity conditions increased. On the other hand, kraft pulping has also been widely employed for lignin removal in the pulp and paper industry [25]. In this case, the alkaline conditions used in this process lead to the hydrolysis of β-*O*-4′ alkyl–aryl ether bonds

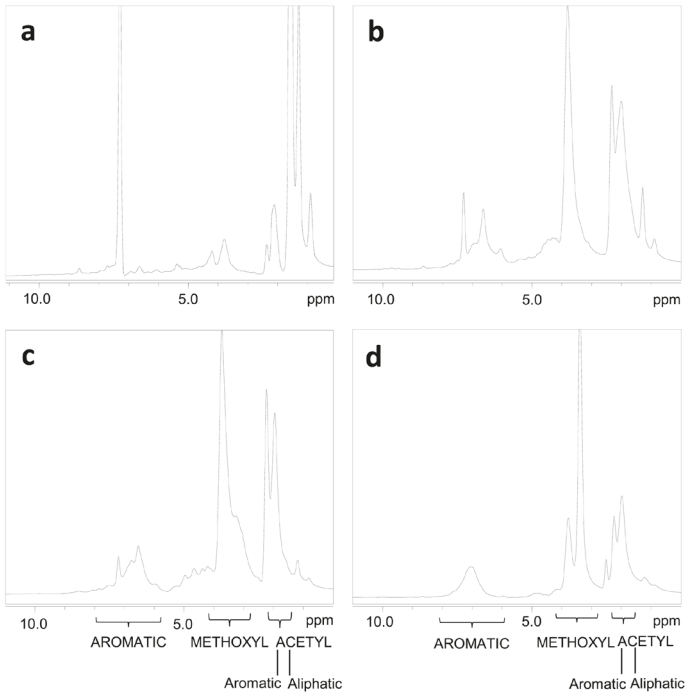

Fig. 5. ^{1}H NMR spectra of AHL (a), SEL (b), EKL (c), and PKL (d) acetylated lignin-containing fractions. Regions from aromatic, methoxy, and acetyls from aliphatic OH and phenolic OH are indicated.

and glycosidic linkages in hemicelluloses [21,32,46,49]. Nevertheless, as already mentioned for hydrothermal pretreatments, the lignin depolymerization level also varies depending on the alkaline pulping conditions and severity [32,49]. The quantification of EKL and PKL lignin fractions indicated a wide breakdown of β-*O*-4′ substructures (4.82 and 7.13 linkages per 100 aromatics for eucalypt and pine kraft lignins, respectively), and some of them oxidized, as previously observed for EKL sample (Fig. 3a). β-β′ resinols partially resist the kraft pulping [21,32,46,49], as the quantities indicate (4.9 and 5.7 for EKL and PKL, respectively). In comparison to AHL and SEL lignins, the extensive lignin depolymerization observed for EKL and PKL lignins led to lignin-containing residual fractions with a higher hydroxyl group content. These hydroxyl groups were mostly phenolic hydroxyl groups, as could be inferred from the ^{13}C NMR and ^{1}H NMR spectra of acetylated lignins (Figs. 4 and 5, respectively).

The integration of aromatic and aliphatic acetyl groups (2.5–2.2 and 2.2–1.9 ppm, respectively) in ^{1}H NMR spectra (Fig. 5) allowed to establish the ratio between phenolic and aliphatic hydroxyl groups, which shows higher values for kraft lignins, especially EKL sample (Table 2). In the same way, ^{13}C NMR spectra of EKL and PKL samples (Fig. 4c and d) also displayed higher intensities of the phenolic hydroxyl bands than those of the aliphatic hydroxyl bands (including primary and secondary aliphatic hydroxyls). By contrast, this effect was not observed in ^{13}C NMR spectra of AHL and SEL (Fig. 4a and b).

Finally, S units are predominant in all lignins from eucalypt (AHL, SEL, and EKL), exhibiting much higher S/G ratios compared to pine kraft lignin (PKL) (Table 2). Among eucalypt lignins, AHL lignin showed a slightly higher ratio (1.90) than SEL sample (1.65). Generally, hydrothermal pretreatments produce a substantial decrease of S/G ratios, as reported by Samuel et al. [29,30] for the steam pretreatment of poplar and switchgrass, and Araya et al. [31] in the course of an autohydrolysis pretreatment of eucalypt. On the contrary, EKL lignin displayed a higher S/G ratio since an increase of S units is generally produced as a result of their preferential removal from biomass during the kraft pulping [46,49].

3.3. SEC analysis of residual lignin-containing fractions

Table 3 displays the weight-average (M_w) and number (M_n) molecular weights, and polydispersity (M_w/M_n) values for the residual lignin-containing fractions studied. In line with the fact that lignins obtained from hydrolysis treatments (AHL and SEL) were less degraded than kraft lignins (EKL and PKL), as can be deduced from NMR analysis (see Section 3.2), their Mw values were slightly higher (Mw = 4275 and 4380 g mol^{-1} for AHL and SEL, respectively) than those shown by kraft lignins (Mw = 3040 and 3690 g mol^{-1} for EKL and PKL, respectively). As commented above, the acidic conditions created during autohydrolysis and steam explosion pre-treatments can lead to a cleavage of β-*O*-4′ linkages and, consequently, to a reduction of the molecular weight of lignin [51,53]. Nevertheless, possible condensation reactions can take place under acid-catalyzed conditions of hydrothermal pretreatments, which can affect the molecular weight of lignin [51,53]. This fact is especially relevant among lignin molecules present in solid residues during hydrothermal processes, as the AHL and SEL lignin fractions studied herein. Contrary, the main reaction produced in the lignin solubilized during kraft pulping is the alkaline hydrolysis of β-*O*-4′ alkyl–aryl ether bonds, yielding a more important reduction in molecular weight [32,41].

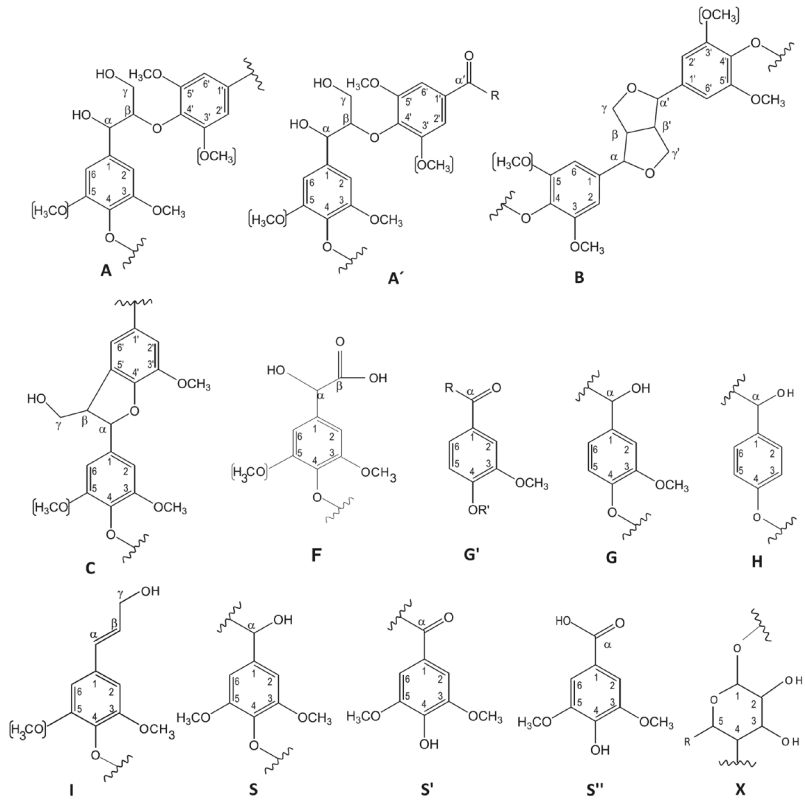

Fig. 6. Main lignin and carbohydrate structures identified in residual lignin-containing fractions from eucalypt and pine: **A**, *β-O-4′*; **A′**, *β-O-4′* with C_{α}′ bearing carbonyl or carboxyl groups; **B**, resinols with *β-β′*, *α-O-γ′*, and *γ-O-α′* linkages; **C**, phenylcoumarans with *α-O-4′* and *β-5′* linkages; **F**, Ar–CHOH–COOH; **G**, guaiacyl unit; **G′**, oxidized guaiacyl unit in C_{α}; **H**, *p*-hydroxyphenyl unit; **S**, syringyl unit; **S′**, oxidized syringyl units with a C_{α} ketone; **S″**, oxidized syringyl units with a C_{α} carboxyl; **X**, xylopyranose (R, OH).

Finally, it must be noticed that hydrolysis lignins were not completely soluble in the alkali solution used as eluent, the high-molecular-weight fraction, probably containing LCCs complexes, being presumably the one that was not completely solubilized [54]. Therefore, the molecular weight of these hydrolysis lignins is possibly slightly underestimated. On the contrary, kraft lignins were completely dissolved in alkali eluent, showing low molecular weight values according to its high degradation inferred from NMR analysis.

Table 2
Abundance of lignin inter-unit linkages expressed as linkage per 100 aromatic units (and as relative percentage of the total linkages considered in brackets) and S/G ratio from integration of ^{13}C–^{1}H correlation peaks in the HSQC spectra of residual lignin-containing fractions from eucalypt and pine. OH_{phe}/OH_{ali} from ^{1}H NMR spectra is also showed.

	AHL	SEL	EKL	PKL
β-O-4′ (**A**)	49.57 (74.2)	23.98 (69.8)	4.82 (49.6)	7.13 (55.6)
Resinols (**B**)	17.25 (25.8)	8.49 (24.7)	4.89 (50.4)	5.69 (44.4)
Phenylcoumarans (**C**)	0	1.88 (5.5)	0	0
S/**G** ratio	1.90	1.65	2.71	0.10
OH_{phe}/OH_{ali}	0.26	0.46	0.73	0.54

Abundances of *β-O-4′*, resinols, and phenylcoumarans, were estimated from C_{α}–H_{α} correlations. $C_{2,6}$–$H_{2,6}$ correlations from S units and C_2–H_2 correlations from G units were used to estimate the S/G lignin ratios.

3.4. Thermogravimetric analysis (TGA) of residual lignin-containing fractions

The thermal degradation processes of the residual lignin fractions were conducted under nitrogen atmosphere (Fig. 7). The residual lignin-containing fractions collected after saccharification of autohydrolysed and steam-exploded eucalypt chips (AHL and SEL) were compared with the lignin fractions recovered from eucalypt and pine kraft black liquors (EKL and PKL). Without taking into account the small mass loss found at around 70–80 °C, which is about 3%, mainly corresponding to the removal of residual water, the thermal degradation of lignin fractions takes place in two main steps (see Fig. 7), with

Table 3
Weight average (M_w) and number-average (M_n) and polidispersity (M_w/M_n) of residual lignin-containing fractions from eucalypt and pine.

	Residual lignin fractions			
	AHL	SEL	EKL	PKL
M_w indicate (g/moL)	4275	4380	3040	3690
M_n indicate (g/moL)	2270	2275	2210	2125
M_w/M_n	1.88	1.92	1.37	1.73

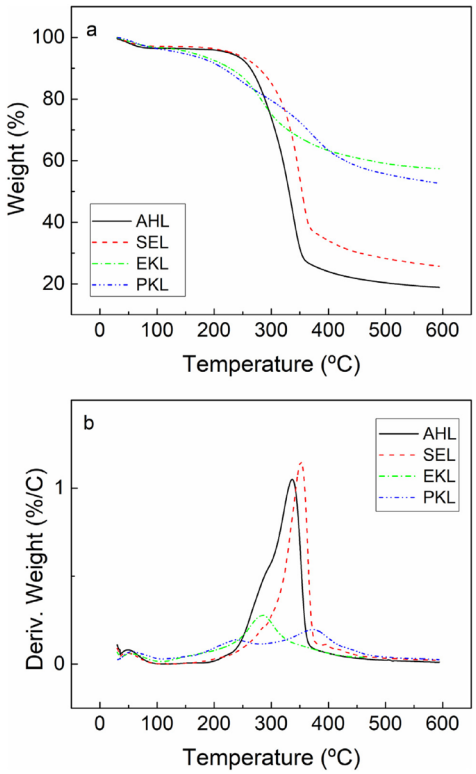

Fig. 7. Thermogravimetric curves under nitrogen purge for AHL, SEL, EKL and PKL lignin-containing fractions.

those detected in the AHL, EKL and SEL samples being overlapped between them. The main characteristic parameters of these thermal events and final residue values can be seen in Table 4. The thermal stability of lignin-containing fractions is significantly favoured by applying the autohydrolysis and steam explosion treatments, which may noticeably expand the temperature of processability and the range of applications of potential materials prepared from these residual fractions.

It is well-known that hemicellulose volatilizes between 200 and 350 °C and cellulose at around 350 °C, while lignin volatilization happens over an extended temperature range of 200–700 °C [55]. According to this, residual lignin fractions obtained from hydrolysis treatments, with higher carbohydrate content and less chemically degraded, showed higher thermal degradation temperatures as well as much lower amount of final residue (20–25 wt% at 600 °C). However, kraft lignin fractions, more chemically degraded and having lower carbohydrate content as well as higher quantity of C–C thermostable linkages (β-β′) [56], displayed a much wider range of thermal degradation temperatures, together with a higher quantity of residue (52–57 wt% at 600 °C) due to the higher content of ashes, principally for EKL sample.

Table 4
TGA characteristics parameters for residual lignin-containing fractions and resulting NCO-functionalized samples.

Sample	T_{onset} (°C)	T_{max} (°C)	Residue (%)	ΔW (%)
AHL	236	292/338	22	78
SEL	212	285/351	24	76
EKL	138	348	57	43
PKL	199/325	240/373	48	16/26
FAHL	124/208/320/453	156/270/345/475	21	17/18/26/18
FSEL	133/210/309/447	162/261/354/477	11	42/13/25/10
FEKL	119/293/426	135/322/451	24	32/32/15
FPKL	99/245/428	128/335/448	11	39/35/7

3.5. NCO-functionalized lignins characterization

Lignin functionalization with HDI was verified by using some of the techniques previously described i.e., FTIR, NMR and TGA. Some relevant differences in the FTIR spectra were observed after NCO-functionalization of lignin fractions. As shown in Fig. 8, new stretching bands may be clearly detected as a consequence of free isocyanate presence and urethane formation. Thus, the wide presence of free NCO reactive groups generates an intense peak in the spectra, centred at around 2270 cm^{-1}, due to the NCO stretching vibration [57]. Moreover, the successful formation of urethane bonds is confirmed by the N—H bending vibration band which appears at 1570 cm^{-1}. Unfortunately, no differences between the diverse NCO-functionalized lignins could be prompted by using this technique due to the intense NCO-peak, which masked the possible differences that could be observed regarding the other bands. The formation of these urethane bonds is also associated with a reduction in the number of hydroxyl groups. Thereby, the wide peak related to the stretching of hydroxyl groups was partially replaced by a narrower peak at around 3330 cm^{-1}, related to the stretching vibration of the N—H bond formed in urethane linkages [23]. Finally, the intensity of both aliphatic methylene bands was significantly increased as a consequence of the HDI 6-carbon chain incorporation to the functionalized lignin structure and free HDI.

^{1}H and 2D NMR tests were also performed in an attempt to establish the differences between lignin and its functionalized counterpart. Despite the complexity of the functionalized system, i.e. non-reacted both lignin and HDI, lignin units reacted with one terminal NCO group, thus forming a urethane bond, with the other NCO group available for subsequent reaction with CO and even lignin units reacted with both terminal NCO groups of HDI, some remarkable facts can be highlighted. As may be observed in Fig. S1 (in the Supporting information) for a selected sample (FPKL), significant differences respecting the non-modified lignin spectra were found within the aromatic band. Although very small, some new peaks at around 8.76 and 8.26 ppm

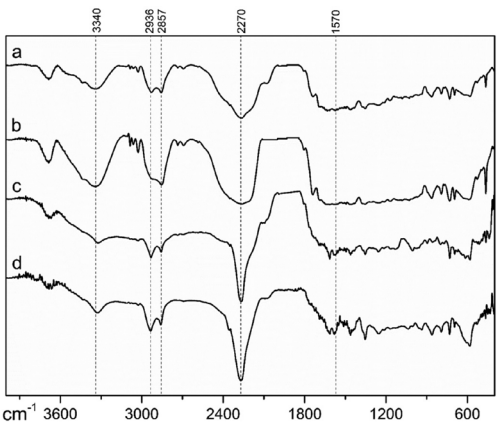

Fig. 8. FTIR spectra for FAHL (a), FSEL (b), FEKL (c), and FPKL (d) NCO-functionalized lignin-containing fractions.

were found after functionalization, which are attributable to the hydrogen atoms of the urethane group [58,59]. On the other hand, while the results of non-functionalized residual lignin fractions show a wide band of aromatic units, the spectra of NCO-functionalized lignin exhibited only two narrow peaks centred at 7.25 and 7.18 ppm, which can be assigned to aromatic protons of lignin units bearing a urethane group. As discussed below regarding the 2D NMR spectrum, it is hypothesized that the formation of urethane groups adjacent to aromatic lignin units would intensify these signals in this region of the ^{1}H NMR. Within the range from 3 to 3.90 ppm, apart from the methoxy groups in lignin (3.55 ppm), signals of methylene adjacent to NCO and urethane groups of HDI can also be identified (at around 3.09 ppm) [58–61]. The presence of urea linkages formed by isocyanate groups in the presence of humidity, presumably occurring during sample storage, was confirmed by the appearance of peaks at around 4.02, 4.25, 4.98, 5.18 and 5.80 ppm [62]. At lower chemical shifts (1.33, 1.24 ppm), more aliphatic units joined to urethane and NCO groups can be likewise reported [58,60].

Regarding the 2D NMR spectrum (see Fig. S2 in the Supporting information), significant differences respecting the non-functionalized lignin sample were once again observed. In the non-oxygenated aliphatic region (δ_C/δ_H 0–50/0–4.5 ppm), the presence of the six-methylene carbon chain of HDI, increased the density of the signals in this region, as expected. In the oxygenated aliphatic region (δ_C/δ_H 50–95/2.6–5.6 ppm), the areas previously attributed to β-O-4 linkages and methoxy groups were significantly reduced. On the other hand, in the aromatic region, the intensity associated with G lignin units, C_2–H_2, C_5–H_5, and C_6–H_6 cross-signals, decreased and new signals with strong intensities appeared at 125.5/7.1 ppm and 128.6/7.2 ppm, which were tentatively assigned to aromatic C—H correlations of lignin units bearing a urethane group. The finding of these new signals supports IR results thus confirming the functionalization of lignin units by formation of urethane bonds. Nevertheless, this fact should be more rigorously confirmed by HMBC (heteronuclear multiple bond correlation) experiments in further studies. Furthermore, the foreseen presence of urethane bonds at high chemical shifts (around 153.0/8.2 ppm) could not be observed by HSQC experiments, being again necessary HMBC experiments for its identification (through correlations of aromatic protons of lignin with the carbonyl carbon of the urethane group) [63].

On the other hand, thermogravimetric curves are depicted in Fig. S3 (in the Supporting information) and main characteristic thermal degradation parameters are collected in Table 4. As previously discussed, lignin fractions only showed one or two degradation events. On the contrary, the functionalized lignins exhibited up to four main degradation steps. The first one (T_{max} of 128–162 °C) was related to the cleavage of free –NCO segments and the evaporation of some remaining free HDI molecules [23,61], while the second and third ones were in correspondence with the lignin structure. Another new fourth degradation event was found at T_{max} of around 448–477 °C, which can be related to more complex structures generated by the crosslinking [15]. Both the first and the last degradation events are strongly interrelated as a decrease in the mass loss in the first one has a direct relationship with an increase in the last one. In any case, these new degradation events detected in the TGA curves of the modified lignin samples corroborate the functionalization intended. As seen in Table 4, the FAHL sample exhibited the lowest and the highest mass loss in the first and fourth thermal degradation steps respectively, indicating that extensively crosslinking was achieved prior to the proper oleogel formation. On the other hand, even though cellulose content in SEL was very similar to AHL, the lower hemicellulose and higher lignin content led to minor crosslinking. This fact occurs as a consequence of the higher hydroxyl content of both cellulose and hemicellulose [64] and the noticeable steric impedance provided by lignin structure, which reduce isocyanate reactivity to the biopolymer [15,23]. In general, the higher the lignin content, the greater hindrance to promote crosslinking. Finally, FEKL shows a slightly higher amount of mass loss than FPKL in the fourth thermal degradation stage, suggesting a higher degree of crosslinking, probably due to its higher proportion of phenolic hydroxyl groups, more reactive to –NCO.

3.6. Functional properties of NCO-functionalized residual lignin-containing fractions-based oleogels

The rheological response of the residual lignin-containing fractions-based oleogels studied is significantly affected by the conversion process of eucalypt and pine woods from which the residual lignin fractions were obtained. Fig. 9a depicts the evolution of SAOS functions with frequency, inside the linear viscoelastic range, for oleogels manufactured with castor oil and NCO-functionalized lignin fractions recovered after saccharification of autohydrolysed (AHL) or steam-exploded (SEL) eucalypt wood compared to those prepared with NCO-functionalized lignin fractions recovered from eucalypt (EKL) and pine (PKL) kraft black liquors. As reported elsewhere [14], the presence of free –NCO groups in the functionalized lignin structure, verified and discussed in the previous section, allows the formation and stabilization of chemical oleogels as a result of the interaction between these –NCO groups and castor oil –OH groups.

In all cases, the mechanical spectra exhibit the typical gel-like behaviour, with a "plateau" region in the low-frequency range considered and a tendency to reach the glass transition region at high frequencies. Therefore, the values of the storage modulus (G′) are roughly one-decade higher than those found for the loss modulus (G″) at low frequencies, whereas both viscoelastic functions tend to reach a crossover at high frequencies. Both the frequency dependence and the values of the SAOS functions obtained for the oleogel prepared with AHL sample (GAHL) are very similar to those exhibited by the most commonly employed lubricating greases, i.e. NLGI grade 2 lithium or calcium greases, which typically show G′ values around 10^4 Pa, one order of magnitude higher than G″, in a wide frequency range [65]. Nonetheless, a more extended plateau region, i.e. lower frequency dependence, was generally displayed by commercial lubricating greases for similar thickener concentrations. On the other hand, the highest values of SAOS functions were achieved for GAHL, followed by GSEL, GEKL, and GPKL. That is, softer gels were obtained when using kraft lignins as thickeners. In addition, the values of the loss tangent ($\tan\delta = G''/G'$) are plotted versus frequency (Fig. 9b), indicating slightly higher relative elasticity for oleogels prepared with lignins derived from hydrolysis treatments (AHL and SEL). According to the detailed chemical characterization presented above, this may be a consequence of the higher amount of carbohydrates that hydrolysis lignin fractions contain, together with the not so degraded chemical structure, displaying a higher number of inter-unit linkages, such as alkyl–aryl ether and resinol, and slightly higher average molecular weight. Moreover, attending to the TGA results, the presence of carbohydrates favours the formation of a more crosslinked structure after functionalization, which must enhance the rheological properties, especially in the case of AHL. On the contrary, GEKL and GPKL oleogels showed lower values of G′ and G″ moduli and relative elasticity due to a dramatic decrease of lignin inter-unit linkages and, therefore, a rather pronounced depolymerization degree during kraft pulping, as commented above. The presence of certain amounts of carbohydrates in the hydrolysis residual fractions is also beneficial since they provide an additional source of polyols which are able to react with HDI in the functionalization reaction, as previously discussed. Furthermore, as described for oleogels physically stabilized with cellulose pulp [11], a decrease in the lignin/cellulose ratio increased the values of the SAOS functions. On the other hand, despite lignins were derived from the same process, GEKL sample displayed values of the viscoelastic functions higher than those found for GPKL, which may be explained attending to the higher content of available phenolic hydroxyl groups in EKL as compared to PKL. As well known [66], phenolic hydroxyl groups in lignin are highly reactive groups, thus favouring isocyanate functionalization as previously described [17] and fostering a relatively more crosslinked structure as TGA results suggest. In support of the

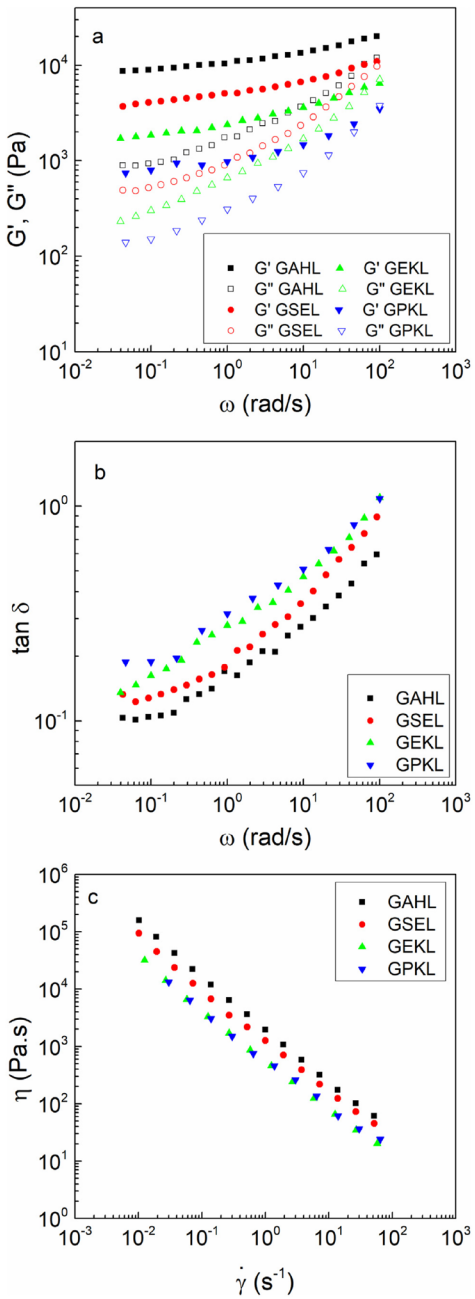

Fig. 9. Frequency dependence of the storage, G′, and loss, G″, moduli (a), the loss tangent (b), and the viscous flow curves (c) for residual lignin-containing fractions-based oleogels.

Table 5
Power-law model fitting parameters of the viscous flow curves, penetration, NLGI grade and friction coefficient for residual lignin-containing fractions-based oleogels studied.

Oleogels	K (Pa·s^n)	n	R^2	Unworked penetration (dmm)	NLGI grade	Friction coefficient
GAHL	2088	0.06	0.997	221	3	0.074
GSEL	1324	0.08	0.998	227	3	0.082
GEKL	596	0.10	0.995	287	2	0.083
GPKL	595	0.12	0.998	243	3	0.076

aforementioned arguments, compared to other polyurethane oleogels based on lignocellulose or cellulose derivatives, these lignin-enriched fractions generally requires a higher amount of crosslinker for achieving similar viscoelastic response [14,38].

Regarding viscous flow measurements, a highly pronounced shear-thinning behaviour was found for all the samples studied (Fig. 9c). These flow curves can be fitted fairly well by the power-law model:

$$\eta = K \cdot \dot{\gamma}^{n-1}$$

where K and n are the consistency and flow indexes, respectively. Table 5 lists the values of these fitting parameters for the samples studied. As can be seen, the consistency index follows the same tendency previously discussed for the SAOS functions. Thus, oleogels prepared with hydrolysis lignin fractions are more viscous, in the whole shear rate range studied, than lignins derived from the kraft pulping process. However, in this latter case, almost identical viscous flow curves were obtained (GEKL and GPKL gels). Overall, the rheological behaviour of these oleogels can be modulated attending to the chemical composition and structure of the lignin-containing residual fractions in order to achieve the appropriate consistency and viscoelasticity for lubricant applications.

Moreover, oleogels exhibit different structural morphologies depending on the conversion process as demonstrated by AFM observations for eucalypt woods (Fig. 10). Thus, more densely clustered and thicker fibers and a generally more interconnected three-dimensional network were observed for GAHL oleogel, which very much resemble the microstructure of traditional lithium greases [67]. Instead, GEKL displays a less compact structure with shorter and thinner fibers and more separation among them.

Finally, the lubrication performance of these oleogels was studied by means of penetration and friction tests and the results were compared with those obtained by a typical lithium lubricating grease. The penetration of a standard cone geometry was used to establish grease consistency. The NLGI grade is a common parameter to classify lubricating greases as a function of their consistency. Table 5 displays the unworked penetration values of oleogels studied, together with the corresponding NLGI grade, and the values of the friction coefficient obtained in a tribological cell. Most of the samples studied showed lower unworked penetration values than commercial NLGI 2–3 lubricating greases [65] and can be classified as NLGI 3 greases, excepting GEKL which is slightly softer. This means that NCO-functionalized lignin fractions provide higher, or similar in the worse cases, consistency to the oil phase than the traditional metallic soaps and therefore may be considered effective thickening agents. On the other hand, all residual lignin-containing fractions-based oleogels provided satisfactory values of the friction coefficient, significantly lower than those found for commercial lithium and calcium lubricating greases [65] and cellulose pulp-based polyurethane oleogels [38].

4. Conclusions

Residual lignin-containing fractions recovered after saccharification of autohydrolysed eucalypt (AHL) and steam-exploded eucalypt (SEL) had clearly different features compared to lignin fractions recovered from eucalypt (EKL) and pine (PKL) kraft black liquors; a higher amount

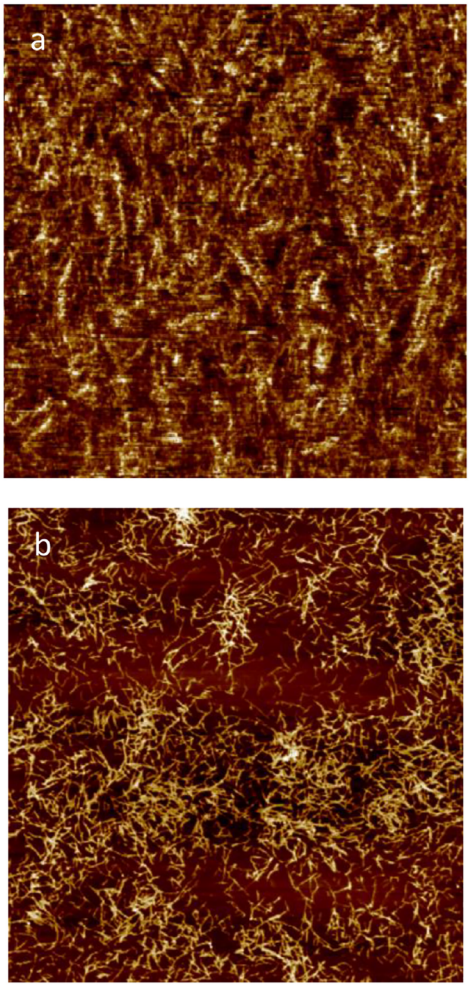

Fig. 10. AFM micrographs for selected residual lignin-containing fractions-based oleogels samples: a) GAHL and b) GEKL.

of inter-unit linkages (mainly alkyl–aryl ether and resinol), translating into slightly higher molar mass, together with lower content of phenolic hydroxyl groups. AHL and SEL lignin fractions also contained a significant amount of carbohydrates, mainly glucose. Contrary, kraft lignin fractions revealed a certain amount of xylose together with a dramatical reduction in inter-units linkages (despite resinol linkages partially resisted) and therefore lower molar mass and higher phenolic content, indicating rather harsh lignin depolymerization degree and chemical degradation during kraft pulping, which also contributed to an expanded range of thermal degradation temperatures. All eucalypt lignins exhibited a majority of syringyl (S) units, especially EKL sample, because of a major S lignin solubilization during kraft pulping. By contrast, PKL sample was clearly composed by guayacil (G) units, typical from softwood materials. Lignin-enriched fractions were successfully functionalized with HDI, resulting a more extensively crosslinked structure in the case of AHL sample.

Oleogels were subsequently obtained by dispersing the NCO-functionalized lignin fractions in castor oil. The rheological response and microstructure of NCO-functionalized residual lignin-containing fractions-based chemical oleogels studied were significantly affected by the conversion process of eucalypt and pine woods. Linear viscoelasticity functions and viscosity values of resulting oleogels obtained were higher when hydrolysis lignin fractions were used as thickeners, which is mainly found to be a consequence of both the higher carbohydrates content and molecular weight. This fact was especially relevant for the oleogel generated from AHL, which exhibited the least degraded chemical structure. As a result, the use of NCO-functionalized hydrolysis lignin fractions as thickening agents provides oleogels with very similar rheological characteristics to those found in commercial lubricating greases. On the other hand, all the lignin fractions-based oleogels used as lubricants in a tribological contact provided very satisfactory values of the friction coefficient, lower than that provided by a typical lithium lubricating grease. Overall, residual lignin-containing fractions resulting from hydrolysis and kraft pulping biomass conversion processes can be used as suitable thickening agents, once conveniently functionalized, to produce bio-based oleogels with appropriate lubricating properties, whereas their composition and chemical structure serve to modulate the functional properties of these.

CRediT authorship contribution statement

Antonio M Borrero-López: Investigation, Data curation, Formal analysis, Writing - original draft, Writing - review & editing
Raquel Martín-Sampedro: Investigation, Data curation, Formal analysis, Writing - original draft, Writing - review & editing
David Ibarra: Conceptualization, Investigation, Methodology, Writing - original draft, Writing - review & editing, Funding acquisition, Project administration
Concepción Valencia: Conceptualization, Investigation, Methodology, Writing - original draft, Writing - review & editing, Funding acquisition, Project administration
María E. Eugenio: Conceptualization, Investigation, Methodology, Writing - original draft, Writing - review & editing, Funding acquisition, Project administration
José M. Franco: Conceptualization, Investigation, Formal analysis, Methodology, Supervision, Writing - original draft, Writing - review & editing, Funding acquisition, Project administration.

Acknowledgements

This work is part of two coordinated research projects (RTI2018-096080-B-C21 and RTI2018-096080-B-C22) sponsored by MICIU-FEDER and another sponsored by the Comunidad de Madrid (SUSTEC-CM S2018/EMT-4348). One of the authors, A.M.B.-L., has received a Ph. D. Research Grant from the Ministerio de Educación, Cultura y Deporte (FPU16/03697). We gratefully acknowledge their financial support.

Appendix A. Supplementary data

Supplementary data to this article can be found online at https://doi.org/10.1016/j.ijbiomac.2020.07.292.

References

[1] Ú. Fillat, B. Wicklein, R. Martín-Sampedro, D. Ibarra, E. Ruiz-Hitzky, C. Valencia, A. Sarrión, E. Castro, M.E. Eugenio, Assessing cellulose nanofiber production from olive tree pruning residue, Carbohydr. Polym. 179 (2018) 252–261, https://doi.org/10.1016/j.carbpol.2017.09.072.
[2] A.D. Moreno, L. Olsson, Pretreatment of lignocellulosic feedstocks, in: R.K. Sani, R.N. Krishnaraj (Eds.), Extremophilic Enzymatic Processing of Lignocellulosic Feedstocks

to Bioenergy, vols. 1–308, Springer, New York 2017, pp. 31–52, https://doi.org/10.1007/978-3-319-54684-1_3.
[3] R. Parajuli, T. Dalgaard, U. Jørgensen, A.P.S. Adamsen, M.T. Knudsen, M. Birkved, M. Gylling, J.K. Schjørring, Biorefining in the prevailing energy and materials crisis: a review of sustainable pathways for biorefinery value chains and sustainability assessment methodologies, Renew. Sust. Energ. Rev. 43 (2015) 244–263, https://doi.org/10.1016/j.rser.2014.11.041.
[4] J.I. Santos, R. Martín-Sampedro, Ú. Fillat, J.M. Oliva, M.J. Negro, M. Ballesteros, M.E. Eugenio, D. Ibarra, Evaluating lignin-rich residues from biochemical ethanol production of wheat straw and olive tree pruning by FTIR and 2D-NMR, Int. J. Polym. Sci. 314891 (2015)https://doi.org/10.1155/2015/314891.
[5] J.I. Santos, Ú. Fillat, R. Martín-Sampedro, I. Ballesteros, P. Manzanares, M. Ballesteros, M.E. Eugenio, D. Ibarra, Lignin-enriched fermentation residues from bioethanol production of fast-growing poplar and forage sorghum, Bioresources 10 (2015) 5215–5232, https://doi.org/10.15376/biores.10.3.5215-5232.
[6] J.I. Santos, Ú. Fillat, R. Martín-Sampedro, M.E. Eugenio, M.J. Negro, I. Ballesteros, A. Rodríguez, D. Ibarra, Evaluation of lignins from side-streams generated in an olive tree pruning-based biorefinery: bioethanol production and alkaline pulping, Int. J. Biol. Macromol. 105 (2017) 238–251, https://doi.org/10.1016/j.ijbiomac.2017.07.030.
[7] A.J. Ragauskas, G.T. Beckham, M.J. Biddy, R. Chandra, F. Chen, M.F. Davis, B.H. Davison, R.A. Dixon, P. Gilna, M. Keller, P. Langan, A.K. Naskar, J.N. Saddler, T.J. Tschaplinski, G.A. Tuskan, C.E. Wyman, Lignin valorization: improving lignin processing in the biorefinery, Science 344 (2014), 1246843. https://doi.org/10.1126/science.1246843.
[8] NLGI, Lubricating Greases Guide, fifth ed., 2006 Kansas City.
[9] T.M. Panchal, A. Patel, D.D. Chauhan, M. Thomas, J.V. Patel, A methodological review on bio-lubricants from vegetable oil based resources, Renew. Sust. Energ. Rev. 70 (2017) 65–70, https://doi.org/10.1016/j.rser.2016.11.105.
[10] N.A. Zainal, N.W.M. Zulkifli, M. Gulzar, H.H. Masjuki, A review on the chemistry, production, and technological potential of bio-based lubricants, Renew. Sust. Energ. Rev. 82 (2018) 80–102, https://doi.org/10.1016/j.rser.2017.09.004.
[11] N. Núñez, J.E. Martín-Alfonso, M.E. Eugenio, C. Valencia, M.J. Díaz, J.M. Franco, Preparation and characterization of gel-like dispersions based on cellulosic pulps and castor oil for lubricant applications, Ind. Eng. Chem. Res. 50 (2011) 5618–5627, https://doi.org/10.1021/ie1025584.
[12] N. Núñez, J.E. Martín-Alfonso, C. Valencia, M.C. Sánchez, J.M. Franco, Rheology of new green lubricating grease formulations containing cellulose pulp and its methylated derivative as thickener agents, Ind. Crop. Prod. 37 (2012) 500–507, https://doi.org/10.1016/j.indcrop.2011.07.027.
[13] J.E. Martín-Alfonso, N. Núñez, C. Valencia, J.M. Franco, M.J. Díaz, Formulation of new biodegradable lubricating greases using ethylated cellulose pulp as thickener agent, J. Ind. Eng. Chem. 17 (2011) 818–823, https://doi.org/10.1016/j.jiec.2011.09.003.
[14] R. Gallego, J.F. Arteaga, C. Valencia, J.M. Franco, Chemical modification of methyl cellulose with HMDI to modulate the thickening properties in castor oil, Cellulose 20 (2013) 495–507, https://doi.org/10.1007/s10570-012-9803-4.
[15] R. Gallego, J.F. Arteaga, C. Valencia, J.M. Franco, Thickening properties of several NCO-functionalized cellulose derivatives in castor oil, Chem. Eng. Sci. 134 (2015) 260–268, https://doi.org/10.1016/j.ces.2015.05.007.
[16] A.M. Borrero-López, A. Blánquez, C. Valencia, M. Hernández, M.E. Arias, M.E. Eugenio, Ú. Fillat, J.M. Franco, Valorization of soda lignin from wheat straw solid-state fermentation: production of oleogels, ACS Sustain. Chem. Eng. 6 (2018) 5198–5205, https://doi.org/10.1021/acssuschemeng.7b04846.
[17] A.M. Borrero-López, F.J. Santiago-Medina, C. Valencia, M.E. Eugenio, J.M. Franco, Valorization of kraft lignin as thickener in castor oil for lubricant applications, J. Renew. Mater. 6 (2018) 347–361, https://doi.org/10.7569/JRM.2017.634160.
[18] Á.T. Martínez, F.J. Ruiz-Dueñas, M.J. Martínez, J.C. del Río, A. Gutiérrez, Enzymatic delignification of plant cell wall: from nature to mill, Curr. Opin. Biotechnol. 20 (2009) 348–357, https://doi.org/10.1016/j.copbio.2009.05.002.
[19] T.Q. Yuan, F. Xu, R.C. Sun, Role of lignin in a biorefinery: separation characterization and valorization, J. Chem. Technol. Biotechnol. 88 (2013) 346–352, https://doi.org/10.1002/jctb.3996.
[20] P. Sannigrahi, A.J. Ragauskas, Characterization of fermentation residues from the production of bio-ethanol from lignocellulosic feedstocks, J. Biobased Mater. Bio. 5 (2011) 514–519, https://doi.org/10.1166/jbmb.2011.1170.
[21] C. Fernández-Costas, S. Gouveia, M.A. Sanromán, D. Moldes, Structural characterization of kraft lignins from different spent cooking liquors by 1D and 2D Nuclear Magnetic Resonance spectroscopy, Biomass Bioenergy 63 (2014) 156–166, https://doi.org/10.1016/j.biombioe.2014.02.020.
[22] National Renewable Energy Laboratory, NREL, Chemical analysis and testing laboratory analytical procedures, Retrieved from http://www.eere.energy.gov/biomass/analytical procedures.html 2010.
[23] A.M. Borrero-López, C. Valencia, J.M. Franco, Rheology of lignin-based chemical oleogels prepared using diisocyanate crosslinkers: effect of the diisocyanate and curing kinetics, Eur. Polym. J. 89 (2017) 311–323, https://doi.org/10.1016/j.eurpolymj.2017.02.020.
[24] R. Gallego, T. Cidade, R. Sánchez, C. Valencia, J.M. Franco, Tribological behaviour of novel chemically modified biopolymer-thickened lubricating greases investigated in a steel–steel rotating ball-on-three plates tribology cell, Tribol. Int. 94 (2016) 652–660, https://doi.org/10.1016/j.triboint.2015.10.028.
[25] E. Brännvall, Overview of pulp and paper processes, in: M. Ek, G. Gellerstedt, G. Henriksson (Eds.), Pulping Chemistry and Technology, De Gruyter, Berlin 2009, pp. 1–12, https://doi.org/10.1515/9783110213423.1.
[26] A.D. Moreno, D. Ibarra, P. Alvira, E. Tomás-Pejó, M. Ballesteros, Exploring laccase and mediators behavior during saccharification and fermentation of steam-exploded wheat straw for bioethanol production, J. Chem. Technol. Biotechnol. 91 (2015) 1816–1825, https://doi.org/10.1002/jctb.4774.
[27] R. Martín-Sampedro, Ú. Fillat, D. Ibarra, M.E. Eugenio, Use of new endophytic fungi as pretreatment to enhance enzymatic saccharification of Eucalyptus globulus, Bioresour. Technol. 196 (2015) 383–390, https://doi.org/10.1016/j.biortech.2015.07.088.
[28] P. Alvira, M. Ballesteros, M.J. Negro, Progress on enzymatic saccharification technologies for biofuels production, in: V.K. Gupta, M.G. Tuohy (Eds.), Biofuel Technol. Recent Dev, Springer, New York 2013, pp. 145–169, https://doi.org/10.1007/978-3-642-34519-7_6.
[29] R. Samuel, M. Foston, N. Jiang, L. Allison, A.J. Ragauskas, Structural changes in switchgrass lignin and hemicelluloses during pretreatments by NMR analysis, Polym. Degrad. Stab. 96 (2011) 2002–2009, https://doi.org/10.1016/j.polymdegradstab.2011.08.015.
[30] R. Samuel, M. Foston, N. Jaing, S. Cao, L. Allison, M. Studer, C. Wyman, A.J. Ragauskas, HSQC (heteronuclear single quantum coherence) ^{13}C-^{1}H correlation spectra of whole biomass in perdeuterated pyridinium chloride-DMSO system: an effective tool for evaluating pretreatment, Fuel 90 (2011) 2836–2842, https://doi.org/10.1016/j.fuel.2011.04.021.
[31] F. Araya, E. Troncoso, R.T. Mendonça, J. Freer, Condensed lignin structures and relocalization achieved at high severities in autohydrolysis of Eucalyptus globulus wood and their relationship with cellulose accessibility, Biotechnol. Bioeng. 112 (2015) 1783–1791, https://doi.org/10.1002/bit.25604.
[32] M. Alekhina, O. Ershova, A. Ebert, S. Heikkinen, H. Sixta, Softwood kraft lignin for value-added applications: fractionation and structural characterization, Ind. Crop. Prod. 66 (2015) 220–228, https://doi.org/10.1016/j.indcrop.2014.12.021.
[33] G. Henriksson, M. Lawoko, M.E. Eugenio, G. Gellerstedt, Lignin-carbohydrate network in wood and pulps: a determinant for reactivity, Holzforschung 61 (2007) 668–674, https://doi.org/10.1515/HF.2007.097.
[34] P.S.B. dos Santos, X. Erdocia, D.A. Gatto, J. Labidi, Characterisation of Kraft lignin separated by gradient acid precipitation, Ind. Crop. Prod. 55 (2014) 149–154, https://doi.org/10.1016/j.indcrop.2014.01.023.
[35] D. Ibarra, J.C. Del Río, A. Gutiérrez, I.M. Rodríguez, J. Romero, M.J. Martínez, Á.T. Martínez, Chemical characterization of residual lignins from eucalypt paper pulps, J. Anal. Appl. Pyrol. 74 (2005) 116–122, https://doi.org/10.1016/j.jaap.2004.12.009.
[36] R. Prado, X. Erdocia, J. Labidi, Lignin extraction and purification with ionic liquids, J. Chem. Technol. Biotechnol. 88 (2012) 1248–1257, https://doi.org/10.1002/jctb.3965.
[37] A. Vishtal, A. Kraslawski, Challenges in industrial applications of technical lignins, BioResources. 6 (2011) 3547–3568.
[38] R. Gallego, J.F. Arteaga, C. Valencia, M.J. Díaz, J.M. Franco, Gel-like dispersions of HMDI-cross-linked lignocellulosic materials in castor oil: toward completely renewable lubricating grease formulations, ACS Sustain. Chem. Eng. 3 (2015) 2130–2141, https://doi.org/10.1021/acssuschemeng.5b00389.
[39] A.T. Martínez, G. Almendros, F.J. González-Vila, R. Fründ, Solid-state spectroscopic analysis of lignins from several Austral hardwoods, Solid State Nucl. Magn. Reson. 15 (1999) 41–48, https://doi.org/10.1016/S0926-2040(99)00045-4.
[40] R. Martín-Sampedro, J.I. Santos, M.E. Eugenio, B. Wicklein, L. Jiménez-López, D. Ibarra, Chemical and thermal analysis of lignin streams from *Robinia pseudoacacia* L. generated during organosolv and acid hydrolysis pre-treatments and subsequent enzymatic hydrolysis, Int. J. Biol. Macromol. 140 (2019) 311–322, https://doi.org/10.1016/j.ijbiomac.2019.08.029.
[41] R. Martín-Sampedro, J.I. Santos, Ú. Fillat, B. Wicklein, M.E. Eugenio, D. Ibarra, Characterization of lignins from *Populus alba* L. generated as by-products in different transformation processes: kraft pulping, organosolv and acid hydrolysis, Int. J. Biol. Macromol. 126 (2019) 18–29, https://doi.org/10.1016/j.ijbiomac.2018.12.158.
[42] J. Ralph, L. Landucci, NMR of lignins, in: C. Heitner, D.R. Dimmel, J.A. Schmidt (Eds.), Lignin and Lignans; Advances in Chemistry, CRC press, Boca Raton 2010, pp. 137–234, https://doi.org/10.1201/ebk1574444865.
[43] S. Ralph, L. Landucci, J. Ralph, NMR database of lignin and cell wall model compounds, NMR database, US Forest Products Laboratory, Madison, WI2006 , Available at http://ars.usda.gov/Services/docs.htm?docids10491. (Accessed July 2017).
[44] M.Y. Balakshin, E.A. Capanema, C.L. Chen, H.S. Gracz, Elucidation of the structures of residual and dissolved pine kraft lignins using an HMQC NMR technique, J. Agric. Food Chem. 51 (2003) 6116–6127, https://doi.org/10.1021/jf034372d.
[45] E.A. Capanema, M.Y. Balakshin, C.L. Chen, J.S. Gratzl, H. Gracz, Structural analysis of residual and technical lignins by ^{1}H-^{13}C correlation 2D NMR-spectroscopy, Holzforschung 55 (2001) 302–308, https://doi.org/10.1515/HF.2001.050.
[46] D. Ibarra, M.I. Chávez, J. Rencoret, J.C. Del Río, A. Gutiérrez, J. Romero, S. Camarero, M.J. Martínez, J. Jiménez-Barbero, A.T. Martínez, Lignin modification during *Eucalyptus globulus* kraft pulping followed by totally chlorine-free bleaching: a two-dimensional nuclear magnetic resonance, Fourier transform infrared, and pyrolysis-gas chromatography/mass spectrometry study, J. Agric. Food Chem. 55 (2007) 3477–3490, https://doi.org/10.1021/jf063728t.
[47] T.M. Liitiä, S.L. Maunu, B. Hortling, M. Toikka, I. Kilpeläinen, Analysis of technical lignins by two- and three-dimensional NMR spectroscopy, J. Agric. Food Chem. 51 (2003) 2136–2143, https://doi.org/10.1021/jf0204349.
[48] R. Martin-Sampedro, E.A. Capanema, I. Hoeger, J.C. Villar, O.J. Rojas, Lignin changes after steam explosion and laccase-mediator treatment of eucalyptus wood chips, J. Agric. Food Chem. 59 (2011) 8761–8769, https://doi.org/10.1021/jf201605f.
[49] P. Prinsen, J. Rencoret, A. Gutiérrez, T. Liitiä, T. Tamminen, J.L. Colodette, M.Á. Berbis, J. Jiménez-Barbero, Á.T. Martínez, J.C. Del Río, Modification of the lignin structure during alkaline delignification of eucalyptus wood by kraft, soda-AQ, and soda-O_2 cooking, Ind. Eng. Chem. Res. 52 (2013) 15702–15712, https://doi.org/10.1021/ie401364d.

[50] J.L. Wen, B.L. Xue, F. Xu, R.C. Sun, A. Pinkert, Unmasking the structural features and property of lignin from bamboo, Ind. Crop. Prod. 42 (2013) 332–343, https://doi.org/10.1016/j.indcrop.2012.05.041.
[51] J. Li, G. Henriksson, G. Gellerstedt, Lignin depolymerization/repolymerization and its critical role for delignification of aspen wood by steam explosion, Bioresour. Technol. 98 (2007) 3061–3068, https://doi.org/10.1016/j.biortech.2006.10.018.
[52] D.J. Yelle, P. Kaparaju, C.G. Hunt, K. Hirth, H. Kim, J. Ralph, C. Felby, Two-dimensional NMR evidence for cleavage of lignin and xylan substituents in wheat straw through hydrothermal pretreatment and enzymatic hydrolysis, Bioenergy Res. 6 (2013) 211–221, https://doi.org/10.1007/s12155-012-9247-6.
[53] H. Wang, Z. Liu, L. Hui, L. Ma, X. Zheng, J. Li, Y. Zhang, Understanding the structural changes of lignin in poplar following steam explosion pretreatment, Holzforschung 74 (2020) 275–285, https://doi.org/10.1515/hf-2019-0087.
[54] A. Toledano, X. Erdocia, L. Serrano, J. Labidi, Influence of extraction treatment on olive tree (*Olea europaea*) pruning lignin structure, Environ. Prog. Sustain. Energy 32 (2013) 1187–1194, https://doi.org/10.1002/ep.11725.
[55] A.G. Barneto, J.A. Carmona, J.E. Martín-Alfonso, L. Jímenez-Alcaide, Use of autocatalytic kinetics to obtain composition of lignocellulosic materials, Bioresour. Technol. 100 (2009) 3963–3973, https://doi.org/10.1016/j.biortech.2009.03.048.
[56] A. Tejado, C. Peña, J. Labidi, J.M. Echeverria, I. Mondragon, Physico-chemical characterization of lignins from different sources for use in phenol-formaldehyde resin synthesis, Bioresour. Technol. 98 (2007) 1655–1663, https://doi.org/10.1016/j.biortech.2006.05.042.
[57] M. Chauhan, M. Gupta, B. Singh, A.K. Singh, V.K. Gupta, Effect of functionalized lignin on the properties of lignin-isocyanate prepolymer blends and composites, Eur. Polym. J. 52 (2014) 32–43, https://doi.org/10.1016/j.eurpolymj.2013.12.016.
[58] M. Pegoraro, A. Galbiati, G. Ricca, ^{1}H nuclear magnetic resonance study of polyurethane prepolymers from toluene diisocyanate and polypropylene glycol, J. Appl. Polym. Sci. 87 (2001) 347–357.
[59] H.J. Kim, M.S. Kang, J.C. Knowles, M.S. Gong, Synthesis of highly elastic biocompatible polyurethanes based on bio-based isosorbide and poly(tetramethylene glycol) and their properties, J. Biomater. Appl. 29 (2014) 454–464, https://doi.org/10.1177/0885328214533737.
[60] M. Hajikhani, M.M. Khanghahi, M. Shahrousvand, J. Mohammadi-Rovshandeh, A. Babaei, S.M.H. Khademi, Intelligent superabsorbents based on a xanthan gum/poly (acrylic acid) semi-interpenetrating polymer network for application in drug delivery systems, Int. J. Biol. Macromol. 139 (2019) 509–520, https://doi.org/10.1016/j.ijbiomac.2019.07.221.
[61] L.C. Raghunanan, S. Fernandez-Prieto, I. Martínez, C. Valencia, M.C. Sánchez, J.M. Franco, Molecular insights into the mechanisms of humidity-induced changes on the bulk performance of model castor oil derived polyurethane adhesives, Eur. Polym. J. 101 (2018) 291–303, https://doi.org/10.1016/j.eurpolymj.2018.02.041.
[62] Q. Yu, D. Li, M. Cai, F. Zhou, W. Liu, Supramolecular gel lubricants based on amino acid derivative gelators, Tribol. Lett. 61 (2016) 16, https://doi.org/10.1007/s11249-015-0634-y.
[63] M.V. Pergal, I.S. Stefanovic, D. Godevac, V. Antic, V. Milacic, S. Ostojic, J. Rogan, J. Djonlagic, Structural, thermal and surface characterization of thermoplastic polyurethanes based on poly(dimethylsiloxane), J. Serbian Chem. Soc. 79 (2014) 843–866, https://doi.org/10.2298/JSC130819149P.
[64] H. Ben, X. Chen, G. Han, Y. Shao, W. Jiang, Y. Pu, A.J. Ragauskas, Characterization of whole biomasses in pyridine based ionic liquid at low temperature by ^{31}P NMR: an approach to quantitatively measure hydroxyl groups in biomass as their original structures, Front. Energy Res. 6 (2018) 13, https://doi.org/10.3389/fenrg.2018.00013.
[65] R. Sánchez, C. Valencia, J.M. Franco, Rheological and tribological characterization of a new acylated chitosan-based biodegradable lubricating grease: a comparative study with traditional lithium and calcium greases, Tribol. Trans. 57 (2014) 445–454, https://doi.org/10.1080/10402004.2014.880541.
[66] S. Laurichesse, L. Avérous, Chemical modification of lignins: towards biobased polymers, Prog. Polym. Sci. 39 (2014) 1266–1290, https://doi.org/10.1016/j.progpolymsci.2013.11.004.
[67] M.C. Sanchez, J.M. Franco, C. Valencia, C. Gallegos, F. Urquiola, R. Urchegui, Atomic force microscopy and thermorheological characterization of lubricating greases, Tribol. Lett. 41 (2011) 463–470, https://doi.org/10.1007/s11249-010-9734-x.

3. Use of lignocellulose from solid-state fermentation with *Streptomyces* as thickening agent for lubricating grease formulations

3.1. Article 5

Influence of solid-state fermentation with *Streptomyces* on the ability of wheat and barley straws to thicken castor oil for lubricating purposes

A.M. Borrero-López, A. Blánquez, C. Valencia, M. Hernández, M.E. Arias, J.M. Franco

Published in:

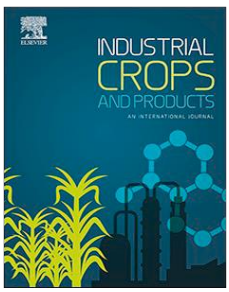

Industrial Crops & Products
Publishing Company: Elsevier
Editor-in-Chief: M. Berti, E. Frollini, O. Koul, R.C. Sun
Volume 140, 111625
Year 2019
ISSN 0926-6690
DOI: 10.1016/j.indcrop.2019.111625

Category	Journal Rank / Total number of journals	Quartile (Percentage)
Agricultural Engineering	2/13	Q1 (88%)
Agronomy	8/91	Q1 (92%)
Impact Factor	4.244	

Industrial Crops & Products 140 (2019) 111625

Contents lists available at ScienceDirect

Industrial Crops & Products

journal homepage: www.elsevier.com/locate/indcrop

Influence of solid-state fermentation with *Streptomyces* on the ability of wheat and barley straws to thicken castor oil for lubricating purposes

Antonio M. Borrero-López[a], Alba Blánquez[b], Concepción Valencia[a,*], Manuel Hernández[b], María E. Arias[b], José M. Franco[a]

[a] *Pro²TecS – Chemical Process and Product Technology Research Centre, Departamento de Ingeniería Química. ETSI, Campus de "El Carmen". Universidad de Huelva, 21071, Huelva, Spain*

[b] *Departamento de Biomedicina y Biotecnología, Universidad de Alcalá, 28805 Alcalá de Henares, Madrid, Spain*

ARTICLE INFO

Keywords:
Straw lignocellulosic residues
Streptomyces
Oleogel
Rheology
Lubricating grease
Solid-state fermentation

ABSTRACT

This work reports the influence of solid-state fermentation (SSF) of two agricultural residues, wheat and barley straws, by using *Streptomyces* MDG301 strain, on their capacity to thicken and structure castor oil via cross-linking with hexamethylene diisocyanate in order to obtain gel-like systems. The analytical composition of the lignocellulosic residues and the enzymatic profile of the strain on both substrates were screened in order to establish the best conditions to achieve optimal oleogel properties. A different rheological response was found for oleogels obtained from each residue. This result could be explained in terms of the different enzymatic profile observed when the microorganism grow on these substrates. Thus, a notable difference in the production levels of CMCase and xylanase activities were detected. The assessment of the resulting oleogels as potential lubricating grease formulations was carried out by means of rheological characterization at different temperatures and tribological and mechanical stability tests. Overall, these oleogels demonstrate to possess similar rheological and tribological characteristics compared to other commercial lubricating greases.

1. Introduction

Lignocellulosic biomass is emerging as a promising renewable resource that can be converted to both biochemicals and biofuels, which represent realistic alternatives to fossil fuels and petrochemicals (Aramrueang et al., 2017; Himmel et al., 2007; Mupondwa et al., 2018). A substantial part of lignocellulosic biomass comes from wheat and barley straws, with great potential owing to their widespread production and low cost (Kim and Dale, 2004; Malhi et al., 2006; Sarkar et al., 2012). These residues also offer promising expectations to be converted into high added-value products (Chen et al., 2007; Duque et al., 2014; Huang et al., 2019; Nabarlatz et al., 2007; Robinson et al., 2002). Containing cellulose, hemicellulose and lignin as main components, the combination of the three of them generates an entangled structure which linkages are principally glycosidic (Van Dyk and Pletschke, 2012).

Nevertheless, not always green procedures and harmless reagents are used when processing straws, thereby generating hazardous wastes (Chen et al., 2007; Robinson et al., 2002). Therefore, green and eco-friendly methodologies are necessary to harness lignocellulosic biomass. This green chemistry is easily reachable by using microorganisms able to modify the structure of lignocellulose through enzymatic mechanisms. Some of these microorganisms such as *Streptomyces* can solubilize lignin from lignocellulosic residues through the production of hemicellulolytic (xylanases, mannanases) and oxidative (laccases, peroxidases) enzymes obtaining lignin-carbohydrate complexes (Acid-Precipitable Polymeric Lignin, APPL) (Antonopoulos et al., 2001; Moya et al., 2010). These actinobacteria are able to break those glycosidic linkages which join the different lignocellulosic units, transforming the material under less severe conditions than in other chemical treatments (Nabarlatz et al., 2007). However, some pretreatments in order to aid enzymatic activity are frequently carried out (García-Aparicio et al., 2006; Rosgaard et al., 2007; Van Dyk and Pletschke, 2012).

On the other hand, through the growing interest in eco-friendly bioproducts and thanks to the entangled structure and available functional groups in the components of wheat and barley straws, they are potentially suitable for thickening and structure oil media and subsequently for oleogel formation, via chemical gelation. Previous studies demonstrated that, using hexamethylene diisocyanate (HDI) as cross-linker, cellulose (Gallego et al., 2013a), cellulose pulp (Gallego et al., 2015) or lignin (Borrero-López et al., 2018a, b; Borrero-López et al., 2017), can effectively act as thickening agents in vegetable oil media,

* Corresponding author.
E-mail address: barragan@uhu.es (C. Valencia).

https://doi.org/10.1016/j.indcrop.2019.111625
Received 15 March 2019; Received in revised form 26 July 2019; Accepted 29 July 2019

resulting oleogels based on renewable resources with applications in the lubricant industry (González et al., 2016), among others. In this work, a further attempt to achieve bio-based thickening agents from raw, miscellaneous and waste materials such as wheat and barley straws was explored. HDI is able to act as crosslinker due to its affinity for hydroxyl groups, forming urethane bonds, either between the different hydroxyl groups of the straw components or between the lignocellulosic material and the castor oil, which has previously been pointed out as the determining factor in oleogel stabilization (Gallego et al., 2013a).

According to what exposed above, the main focus of the present work is to study the relevance of *Streptomyces* MDG301 strain action through SSF in two different substrates, barley and wheat straws, to obtain suitable thickeners by further inducing crosslinking with HDI in castor oil. These oleogels have been tested rheologically, tribologically and through penetration and mechanical stability tests in order to evaluate the performance as lubricating greases.

2. Experimental Methods

2.1. Raw materials, chemicals and microorganism strain

The lignocellulosic residues used as fermentation substrates, i.e., wheat straw (*Triticum aestivum* var. *maestro*) and barley straw (*Hordeum vulgare*), were both kindly furnished by local farmers from the province of Guadalajara (Spain). HDI, along with all other common reagents (culture media components, enzyme substrates and buffers) and solvents (extraction procedures), were purchased from Sigma-Aldrich. Castor oil was obtained from Guinama (Spain).

The microorganism used for this study was isolated from volcanic soils in Nicaragua. The strain was classified as *Streptomyces* sp. based on morphology and subsequently cell wall chemotype (Anderson and Wellington, 2001). The strain is deposited into MICRODEG Collection of the Biomedicine and Biotechnology Department of the University of Alcalá as *Streptomyces* sp. MDG 301.

2.2. Solid-state fermentation of both barley and wheat straws

Previous to SSF process, both wheat and barley straws were ground in a 40-mesh screen-coupled Janke and Kunkel A-10 equipment and air-dried for 24 h at 50 °C. To facilitate the colonization of the substrate unplugged 2 L flasks containing 10 g wheat straw were steamed for 1 h. The flasks were plugged with cotton stoppers and autoclaved for 20 min at 121 °C (Blánquez et al., 2017). On the other hand, the preinoculum was simultaneously prepared by growing standardized spore suspensions of the strain (107 colony forming units per mL; cfu mL^{-1}) in 250 mL Erlenmeyer flasks containing saline basal medium (MBM) [per liter: 0.5 g of K_2HPO_4, 0.5 g of $MgSO_4$ $7H_2O$, 0.01 g of $FeSO_4$, 0.05 $CaCl_2$ and 0.01 g of NaCl] (Crawford, 1978) supplemented with 0.6% (w/v) yeast extract. The cultures were incubated by shaking at 45 °C overnight until the beginning of exponential phase of growth was achieved.

The SSF was performed by adding 56 mL of the preinoculum to 250 mL flasks containing 10 g of each residue and maintaining the cultures at 45 °C for 2, 4 and 7 days. In all samples, enzymatic activities and APPL and alkali lignin yields were determined. In order to get enough quantity of fermented biomass for oleogel production, the SSF was scale up in two five-tray bioreactors containing a total of 1 kg of each residue to which 5.6 L of preinoculum was added. Substrates were aseptically distributed into the trays (200 g per tray) and incubated at 45 °C and keeping 90–95% relative humidity by blowing humidified sterile air filtered through a 0.22 µm nominal cut-off membrane every 12 h. Uninoculated controls were incubated under the same conditions (Borrero-López et al., 2018a).

2.3. APPL and alkali-lignin extraction and enzymatic analysis

APPL and alkali-lignin extraction along with enzymatic content analyses were performed following the protocol previously described (Borrero-López et al., 2018a).

For enzyme assays, 10 g of transformed substrates were extracted with 40 mL distilled water after 2, 4 and 7 days growth. The mixtures were sonicated for 15 min and then filtered through Whatman no. 1 filter paper to obtain the crude enzyme extract (Berrocal et al., 1997) in which the following enzymes were measured:

- Peroxidase activity (EC 1.11.1.7) was assayed using 2,6-dimethoxyphenol (2,6-DMP) as substrate. One unit of peroxidase activity is defined as the amount of enzyme required to oxidize one µmol of 2,6-DMP per minute (ε = 27,500 M^{-1} cm^{-1}) (Hernández et al., 2001).
- Laccase activity (EC 1.10.3.2) was determined by the oxidation of 2,2-azino-bis-(3-ethylbenzthiazoline-6-sulphonic acid) (ABTS). One unit of laccase activity is defined as the amount of enzyme required to oxidize one µmol of ABTS per minute (ε = 29,300 M^{-1} cm^{-1}) (Moya et al., 2010).
- Xylanase (EC 3.2.1.8), mannanase (EC 3.2.1.78) and carboxymethylcellulase (EC 3.2.1.4) activities were determined by the release of reducing sugars using Somogyi-Nelson reactive (Somogyi, 1945). For the reaction, 25 µL enzyme extract was mixed with 75 µL phosphate buffer 50 mM pH 7.0 and with the specific substrate for each enzyme; xylan, mannan and carboxymethyl-cellulose (CMC), respectively. The absorbance was determined at 540 nm and one unit of xylanase, mannanase or CMCase activity is defined as the amount of enzyme required to release 1 µmol of xylose, mannose or glucose per minute, respectively.

2.4. Functionalization of lignocellulosic residues

Fermented wheat and barley straws were washed several times with distilled water and vacuum filtered in order to remove salts and other water-soluble components included in the preinocula and not consumed by the *Streptomyces* MDG301 (S. MDG301). Further, drying at 60 °C was performed until no water was released, checked by performing thermogravimetric analyses. Final milling to a 0.25 mm maximum size employing a rotatory miller IKA MF 10 basic WERKE was performed for both uninoculated and fermented samples.

Functionalization reaction was accomplished by selecting 1:2 w/w straw/HDI ratio by following a protocol described elsewhere (Borrero-López et al., 2017). Summarising, straws were introduced in a two-neck round-bottom vessel where 100 mL toluene were softly stirred under inert atmosphere for 30 min. Subsequently, both reagents, straw and HDI, were added together with triethylamine, which acts as a catalyst. Functionalization reaction was held under stirring at room temperature for 24 h. After that, residual toluene and triethylamine were eliminated by using a rotary evaporator.

2.5. Preparation of oleogels

The functionalized straws (NCO-Barley, NCO-Wheat, NCO-Fermented Barley, NCO-Fermented Wheat) were mixed with castor oil, at 15% w/w concentration and room temperature, for 24 h, using a RW 20 IKA stirrer outfitted with an anchor-shape agitator. Finally, oleogels were stored at room temperature for further characterization. Oleogel samples have been named as OBarley, OWheat, OFermented Barley and OFermented Wheat respectively depending on the type of straw used to prepare them.

2.6. Characterization methods

The analysis of main components of control and fermented

lignocellulosic residues was carried out once residues were dried overnight at 60 °C. Extractives were removed with ether-petroleum (10 ml g^{-1} straw) in a soxhlet for 1 h, and water-soluble components also were obtained by refluxing the samples in a soxhlet for 6 h. The Klason lignin content of the extracted substrate was estimated after hydrolysis of polysaccharides with 72% v/v H_2SO_4 for 1 h at 30 °C, then with 4% v/v H_2SO_4 at 120 °C for 1 h and finally maintained at 4 °C for 48 h. Precipitated Klason lignin was obtained by filtration through a Whatman no. 1 filter paper and its dry weight was estimated. Acid-soluble lignin was determined after removing the Klason lignin in the acidified supernatants by measuring the absorbance at 205 nm. Ash content was determined gravimetrically after leaving the residues at 575 ± 25 °C for 5 h (Berrocal et al., 2000).

Fourier Transform Infrared (FTIR) spectra were performed using a JASCO FT/IR 4200 (Jasco Inc. Japan), from 400 to 4000 cm^{-1} wavenumber, at a 4 cm^{-1} resolution. Thermogravimetric analysis (TGA) measurements were carried out from room temperature to 600 °C, working with a Q50 analyser (TA Instrument Waters, USA).

Rheological characterization of the oleogels was performed with an ARES (Rheometric Scientific, UK), equipped with 25 and 50 mm serrated plate-plate geometries. Small amplitude oscillatory shear (SAOS) tests within the linear viscoelastic regime were carried out in a frequency range of 0.03–100 rad/s from 25 to 150 °C. Viscous flow measurements were performed at room temperature between 0.03 and 100 s^{-1}. At least two replicates of each measurement were carried out.

The friction coefficient was obtained in a tribological measuring cell, coupled to a Physica MCR-501 rheometer (Anton Paar, Austria), which uses a 6.35 mm steel ball rotating on three 45° positioned steel rectangular-shape plates where the lubricant is placed (Gallego et al., 2016), by applying a constant normal load of 20 N and at a constant rotational speed of 10 min^{-1}. These conditions were held for 10 min in order to achieve stationary values of the friction coefficient. At least five replicates were carried out.

Penetration of both unworked and worked oleogels were obtained by following ASTM D1403 standard, employing a 17000-2 Seta Universal penetrometer coupled with one-quarter cone geometry and then re-scaled using ASTM D217 standard to provide standard penetration values. ASTM D217 was also applied to get the NLGI grade of the oleogels. The samples were worked by following ASTM D1831 standard using a 19400-3 Roll Stability tester (Stanhope-Seta, UK). At least five replicates of penetration measurements were carried out.

2.7. Statistics

The enzymatic production and lignin-based fractions solubilisation (i.e. APPL and alkali-lignin) were analysed by using factorial ANOVA implemented in Statistica v8.0 software. Time was considered as a fixed factor. The differences among groups were analysed using Kruskal-Wallis test.

3. Results

3.1. APPL and alkali-lignin yields from fermented substrates

From both wheat and barley straws submitted to SSF with *S.* MDG301 strain, solubilised lignin estimated as APPL and alkali-lignin extracted with NaOH were quantified (Fig. 1A and B). The differences found in the amount of APPL solubilised by the strain along the time course of growth on both substrates were not significant regardless of the substrate (Kruskal-Wallis test: H(2,N = 9) = 5,6 p = 00,608). When comparing the results obtained on both substrates, it could be observed that the quantity of APPL obtained from wheat straw was significantly higher than that obtained from barley straw (Kruskal-Wallis test: H (1,N = 6) = 385 p = 00,495). The maximum solubilisation of APPL was reached the seventh day of incubation with both substrates.

When an alkaline extraction with 0.1 M NaOH was applied to the fermented substrates, the yield of lignin obtained was much higher than that obtained with water (APPL). The amount of alkali-lignin obtained from fermented barley straw along the time course of growth were much more significant (Kruskal-Wallis test: H(2, N = 9) = 7,2 p = 00,273) and much higher than those obtained with other strains (Borrero-López et al., 2018a). In every day of sampling (2, 4 and 7 days), wheat straw was again the substrate from which a greater amount of alkali-lignin was extracted after its fermentation with the *Streptomyces* strain showing significant differences with that obtained from barley straw (Kruskal-Wallis test: H(1,N = 6) = 385 p = 00,495). As occurred with APPL, the highest amount of alkali-lignin was obtained the seventh day of incubation, regardless the substrate.

Taking into account these results, it could be concluded that the optimal conditions to achieve the highest solubilisation of lignin (APPL) and the greater extraction of alkali-lignin from fermented substrates corresponded to wheat straw fermented with *S.* MDG301 strain for 7 days.

3.2. Enzyme activities determination in aqueous extracts from fermented substrates

Along the time of incubation of the two inoculated substrates with *S.* MDG301 strain under SSF conditions, three hydrolytic enzyme activities (xylanase EC 3.2.1.8, mannanase EC 3.2.1.78 and carboxymethyl cellulase (CMCase) EC 3.2.1.203) and two oxidative enzyme activities (laccase EC 1.10.3.2 and peroxidase EC 1.11.1.7) involved in lignocellulose degradation were screened. In the extracts obtained from both fermented substrates, neither laccase nor peroxidase activities were detected, probably due to the adsorption of these enzymes to the substrates, which makes difficult their recovery (Kiiskinen et al., 2004; Saarinen et al., 2009). However, the hydrolytic enzyme activities could be detected in these extracts. The production level of xylanase activity by the strain during the time of incubation showed significant differences between both substrates. Thus, the maximum xylanase activity on wheat straw was 45.12 U g^{-1} (Fig. 2A) and on barley straw was 32.45 U g^{-1} (Fig. 2B), both after 7 days of incubation.

Regarding CMCase activity, the results showed again a significantly higher production rate of the enzyme activity on wheat straw (maximum activity: 11.85 U g^{-1}) than on barley straw (1.80 U g^{-1}) (Kruskal-Wallis test: H(1,N = 6) = 385 p = 00,495). On barley straw, differences found in CMCase activity along the time of incubation were not significant and the production levels of this enzyme were around six times lower than those obtained from wheat straw. In contrast with the production pattern of xylanase activity, for which an increase along the time course of growth was observed on both substrates, the maximum production of CMCase activity was reached at the second day of incubation, maintaining this value along the time (Fig. 2A).

Although wheat straw resulted to be more efficient for the production of the two above described enzymes, in the case of mannanase, barley straw was the only substrate on which this enzyme activity was detected. However, there were no significant differences in the mannanase activity detected along the time course of growth (Kruskal-Wallis test: H(2,N = 9) = 595 p = 00,509). As occurred with CMCase, the maximum of mannanase activity was detected after two days of fermentation (1.58 U g^{-1}) (Fig. 2B).

In a previous work, it was demonstrated that the *Streptomyces* MDG147 strain grown under SSF conditions on wheat straw at 28 °C produced the highest xylanase and mannanase activities after 4 days of incubation, along with a simultaneous noticeable lignin solubilisation estimated as APPL. In the same work and taking into account that the ratio arabinoxylan/glucomannane in non-woody angiosperms is 20:1.3, the main role for lignin solubilisation from the lignocellulosic residue was attributed just to the production of xylanase activity (Borrero-

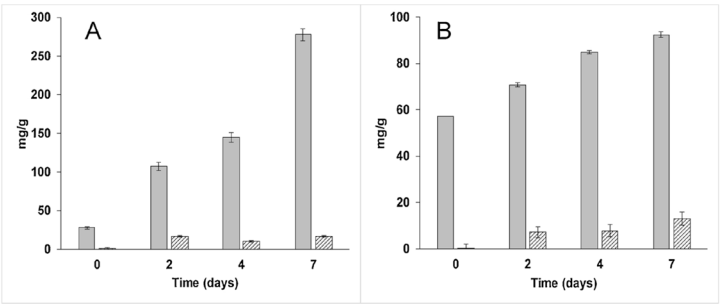

Fig. 1. Quantity of Alkali-lignin (grey) and APPL (striped) per gram obtained from wheat (A) and barley (B) straws fermented with *Streptomyces* sp. MDG301 along the time course of growth. All values are the mean of three determinations ± SD.

López et al., 2018a).

In the present study, the comparison of the results obtained on both wheat straw and barley straw lignocellulosic substrates allow to conclude that the highest levels of xylanase and CMCase activities were achieved when the strain *S.* MDG301 was grown at 45 °C on wheat straw for 7 and 2 days, respectively. In parallel, the highest lignin solubilisation rate from the residue (estimated as APPL) was detected after 7 days of growth. From these results, an involvement of xylanase and CMCase activities in lignin solubilisation from wheat straw by the *S.* MDG301 strain could be inferred. It is noticeable the important role of xylanase activity in the solubilisation of the residue by *Streptomyces* and the possible contribution in some strains of this genus of other hydrolytic enzymes such as CMCase in this process.

Nevertheless, it is important to remark the important role generally attributed to oxidative enzymes such as laccases and peroxidases in lignin solubilisation and/or degradation from lignocellulosic substrates by streptomycetes (Berrocal et al., 1997; Blánquez et al., 2017), in spite of the difficulties to detect them in SSF fermentation conditions.

3.3. Characterization of uninoculated, fermented and NCO-functionalized straws

To assess the effects of growth of the *S.* MDG301 strain under SSF conditions on the composition of wheat and barley straw samples, both control (uninoculated) and fermented (after 7 days submitted to SSF) straws were analysed (Table 1).

The Klason lignin content was reduced in both barley and wheat straws after 7 days of fermentation (Zeng et al., 2013), reaching 26.4% and 17.9% loss, respectively. This decrease could be attributed to the presence of oxidative enzymes above mentioned although they could not be detected in the assayed conditions. On the other hand, an enrichment in holocellulose content by 5.2% was detected in barley straw.

Table 1
Composition of barley and wheat straws studied.

	Barley Straw (%) (control)	Wheat Straw (%) (control)	Fermented Barley (%)	Fermented Wheat (%)
Extractives	4.61 ± 0.56	4.56 ± 0.12	4.85 ± 0.12	4.22 ± 0.12
Water-soluble	8.16 ± 0.55	7.96 ± 1.75	11.43 ± 2.50	13.45 ± 1.31
Acid-soluble lignin	2.54 ± 0.16	2.19 ± 0.13	2.43 ± 0.40	2.07 ± 0.29
Klason lignin	25.15 ± 1.51	24.53 ± 2.55	18.5 ± 3.81	20.14 ± 2.6
Holocellulose	58.94 ± 0.94	59.63 ± 4.15	61.98 ± 2.01	58.84 ± 2.38
Ash	0.60 ± 0.06	1.13 ± 0.04	0.82 ± 0.16	1.27 ± 0.06

However, in fermented wheat straw, the percentage of hollocellulose remains similar to the control. It is important to notice that the water-soluble fraction, containing short oligosaccharides, increased up to 40% and 70% for barley straw and wheat straw initial values, respectively. These trends found in the analytical results are similar to those already obtained for wheat straw treatment with another *Streptomyces* strain (Zeng et al., 2013).

The differences found in the composition of both fermented substrates could be attributed to the different hydrolytic enzymes production pattern. Thus, the high production of xylanase activity together with the low level of CMCase activity detected in barley straw could explain the enrichment of hollocellulose in this substrate mainly due to the inability to degrade cellulose, and therefore the stronger influence of oxidative enzymes produced. Furthermore, it also explains the lower concentration of water-soluble fraction obtained. However, for wheat straw, the stronger combined action of xylanase and CMCase activity could produce a simultaneous degradation of both xylan and cellulose and as a consequence, the water-soluble fraction became much higher

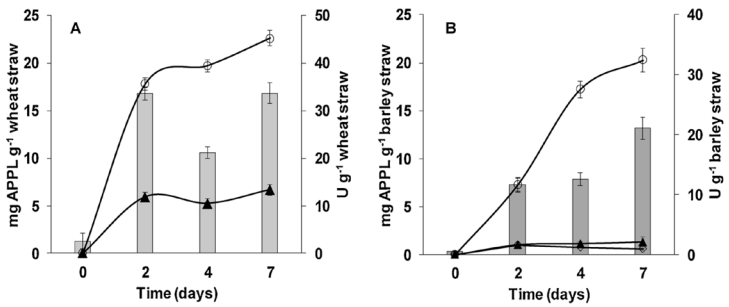

Fig. 2. Production of extracellular xylanase (O), mannanase (◊) and CMCase (▲) activities and estimation of APPL yield (bars) during the growth of *Streptomyces* sp. MDG301 in solid-state fermentation on wheat straw (A) and barley straw (B) at 45 °C. All values are the mean of three determinations ± SD.

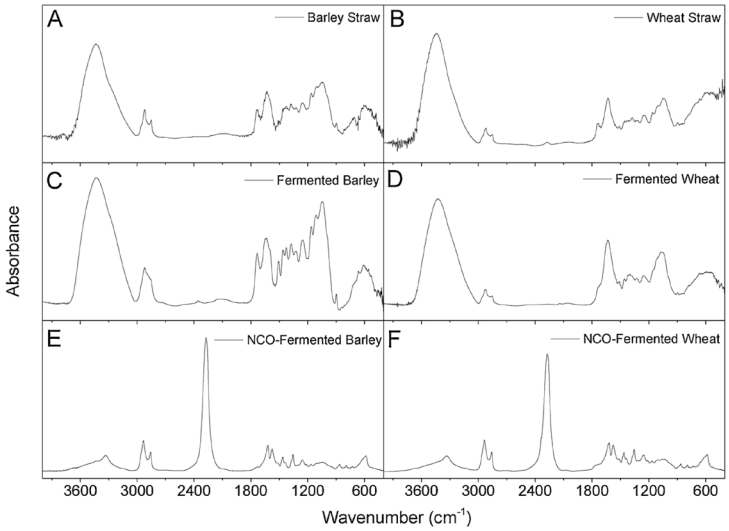

Fig. 3. FTIR spectra of uninoculated (A & B), fermented (C & D) and further NCO-functionalized (E & F) barley and wheat straws.

in this substrate. Nevertheless, this was not translated into a lower holocellulose content due to the combined activity of the oxidative enzymes, which finally makes even the holocellulose concentration for both uninoculated and fermented wheat straws.

FTIR spectroscopy was also used to study the different modifications in the chemical structure of the different lignocellulosic raw materials carried out by S. MDG301 action and after functionalization with HDI (see Fig. 3). All the samples present the typical spectrum of lignocellulosic materials corresponding to cellulose, hemicellulose and lignin as main constituents. One of the most prominent bands found in the spectra is centred around 3430 cm^{-1}, associated to the O—H stretching vibrations in their main components. When comparing untreated and fermented straws, an increase in the intensity of these peaks can be observed prompted by *Streptomyces* action, demonstrating the creation of new hydroxyl groups by cleavage of the different linkages through enzymatic action (Borrero-López et al., 2018a). Approximately around 1733–1737 cm^{-1}, an incipient peak was shown for both straws which can be assigned to two possible structures. The first one is related to ester bonds of hemicelluloses, both acetyl and uronic, whilst the second one is given by COOH groups of both p-coumaric and coniferic acids included in lignin-type structures (Alemdar and Sain, 2008a, 2008b). This band appears narrower and shifted to lower wavenumbers in fermented samples, which confirms the partial elimination of these structures by *Streptomyces* action (Zeng et al., 2013).

Wheat straw lignocellulosic material exhibits a wide peak centred at 1633 cm^{-1}, due to the contribution of absorbed water (Johar et al., 2012). Nonetheless, for barley straw samples, this contribution is clearly split into two different peaks, being the first one (1633 cm^{-1}) due to the adsorbed water, and the second one, focused at 1601 cm^{-1}, of much higher intensity for the fermented sample, attributed to C=C stretching of aromatic units of lignin. Even though for barley straw the whole lignin concentration was reduced, this increment may be consequence of the structure alteration which let previously not so-accessible bonds to be observed better now. This increment is not as clear for wheat straw due to the much higher concentration of absorbed water. In addition to this, the peak at around 1513 cm^{-1} together with the peak at around 1420 cm^{-1} are both also characteristic of the aromatic skeleton vibration of lignin, present in both cases, weaker for both untreated straws (Meng et al., 2014), supporting what established above.

Besides, a wide peak corresponding to the overlapping stretching vibrations of C–O from aryl ethers (1274 cm^{-1}) and C–O and O—H from phenoxy structures (1222 cm^{-1}) (Meng et al., 2014) can be detected. This wide peak, attributed by Zeng et al. (2013) to guaiacyl and syringyl units, should be reduced in intensity after SSF with *Streptomyces*. Nonetheless, in our case an increase in intensity was observed, again probably as a consequence of lignin improved accessibility.

Another important peak is observed around 896 cm^{-1}, attributed to β-glycosidic linkages of the cellulose structure (Sun et al., 2005), which is decreased by means of the SSF treatment with *Streptomyces* for wheat straw, similarly to what was previously observed for lignin β—O—4 bonds (Borrero-López et al., 2018a). Nonetheless, this reduction is not so clearly exhibited for barley straw, probably due to the low level of CMCase activity previously discussed.

Finally, once NCO-functionalization was performed, not significant differences in the FTIR spectra can be observed, which are eventually masked by the high intensity absorption peak attributed to the stretching of free NCO groups, located at around 2270 cm^{-1} (see Fig. 3E & F).

Thermogravimetric analysis may also provide useful information about the different thermal degradation pattern of wheat and barley straws caused by the effect of SSF and further modification with HDI. Fig. 4 depicts TGA curves for both non-functionalized and functionalized straws, showing the weight loss percentage and the derivative curve versus temperature. As can be seen, a similar trend for all non-functionalized samples was followed. Initially, a weight loss close to 5% regarding humidity content is observed, followed by the main event at around 322–359 °C due to the degradation of the main components of the different straws. Characteristic thermal parameters determined from the thermogram (onset temperature (T_{onset}), temperature for the maximum decomposition rate (T_{max}) and final temperature in each decomposition step (T_{final}), along with the weight-loss percentage corresponding to each step and the percentage of non-degraded residue at the end of the process) are collected in Table 2. As can be seen in Fig. 4B, T_{max} is higher for the original barley straw than for wheat straw. On the contrary, Fermented Barley possess the lowest T_{max} while

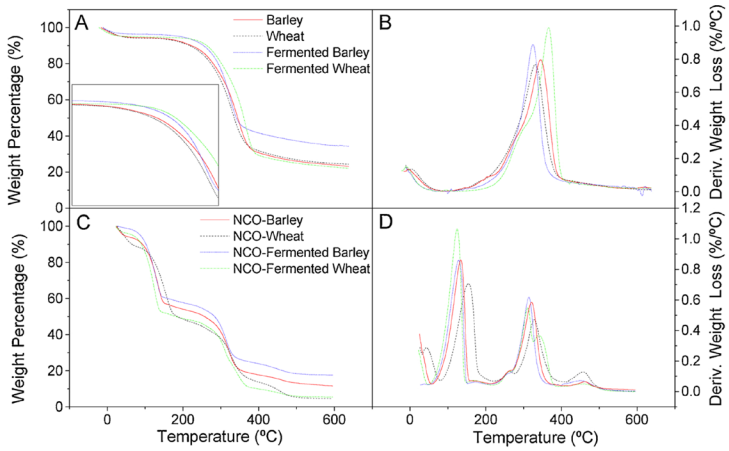

Fig. 4. Thermogravimetric curves of both non-functionalized (A & B) and functionalized straws (C & D).

Fermented Wheat the highest. Final residue amounts obtained are around 22–24%, except for Fermented Barley, which is slightly higher. Probably, Fermented Wheat does not increase its residue due to the CMCase action, which also eliminates cellulose-based complexes.

Regarding NCO-functionalized straws, apart from the first solvent loss, three main degradation stages can be appreciated. The first one at around T_{max} of 124–155 °C corresponds to the evaporation of remaining free HDI molecules (Gallego et al., 2013b; Raghunanan et al., 2018) still available for subsequent reaction with straw components and/or castor oil during the subsequent oleogel forming process. A higher content of free HDI implies a lower degree of crosslinking, which is clearly observed for NCO-Fermented Wheat, whilst for the other samples this content remained quite close. This fact may be consequence of the higher enzymatic activity focused on easily accessible structures, thus leaving less-accessible hydroxyl groups for crosslinking with HDI. The second event at around 314–342 °C, as for non-functionalized straws, is due to the degradation of the main components of the lignocellulosic materials. For NCO-Fermented Wheat sample, this event depicts even a visible split of the peaks in the derivative curve (Fig. 4D), suggesting a more resistant structure to appear consequence of the enzymatic action. This difference could not be observed for NCO-Fermented Barley, due to the lower degree of enzymatic production and subsequent lower degree of structural modification. Finally, the third thermal event, at around T_{max} of 480–494 °C, is characteristic of highly entangled structuration promoted by NCO-crosslinking (Gallego et al., 2013b). These structures are favoured by SSF treatment only for barley straw, whereas non-treated wheat straw shows the highest weight loss (see Table 2), consequence of the statements above commented.

3.4. Rheological and tribological characterization of oleogels

Typical viscoelastic behaviour of commercial lithium lubricating greases implies values of the storage modulus (G') close to 10^4 Pa and values of the loss modulus (G") around one order of magnitude lower, along with a well-developed plateau region within a wide frequency range, characteristic of gel-like colloidal systems. Moreover, a highly pronounced shear thinning behaviour is typically found in the viscous flow response of greases (Martín-Alfonso et al., 2011). As displayed in Fig. 5A, where the SAOS functions are plotted versus the frequency within the linear viscoelastic range at 25 °C, the above-mentioned behaviour is reproduced by all the oleogels studied, showing the OWheat sample the higher values of the viscoelastic functions, followed by OFermented Barley, OBarley and finally OFermented Wheat oleogel. This behaviour should be in part related with holocellulose and lignin contents of the straw samples studied (see Table 1). In principle, as previously reported (Núñez et al., 2011), a reduction in lignin content as a result of the enzymatic activity should increase the values of the viscoelastic moduli in both fermented straw-based oleogels, result which was only found in barley straw-based oleogel. In addition, this barley straw sample submitted to SSF, showed an increased holocellulose content, favouring higher values of viscoelastic moduli in the oleogel than the control (uninoculated) straw. The main reason would be the higher content of high molecular weight (non-degraded) cellulose as well as the favourable reactivity of free NCO groups with linear polymers rather than branched polymers. Therefore, the contradictory influence of SSF on the linear viscoelastic response of barley and wheat straw-based oleogels can be explained by focusing on different enzyme production pattern. As wheat straw produced CMCase in a much higher

Table 2
Thermal characteristic parameters of non-functionalized and functionalized barley and wheat straws.

	T_{onset} (ºC)	T_{max} (ºC)	T_{final} (ºC)	Weight loss (%)	Residue (%)
Barley	254	339	364	72	23
Wheat	273	328	352	70	24
Fermented Barley	277	322	341	62	34
Fermented Wheat	267	359	375	73	22
NCO-Barley	104/248/445	134/321/463	145/340/480	39/37/6	12
NCO-Wheat	118/249/437	155/329/458	171/350/482	41/34/9	5
NCO-Fermented Barley	100/238/421	129/314/451	141/329/482	41/33/7	18
NCO-Fermented Wheat	87/244/332/444	124/312/342/456	136/317/365/494	48/24/14/5	5

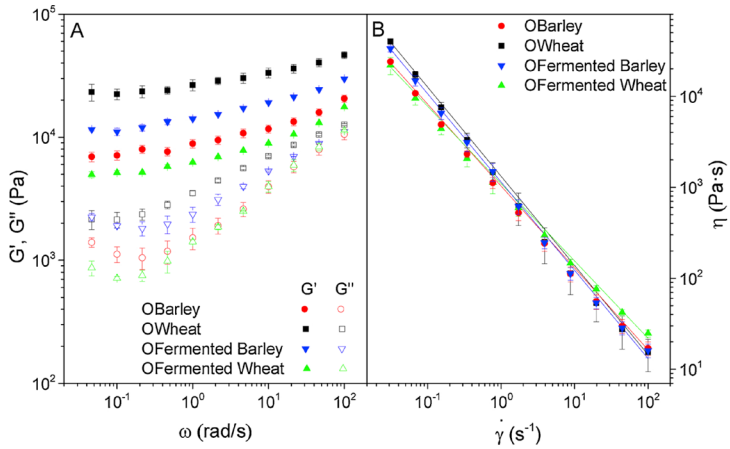

Fig. 5. Linear viscoelastic functions (A) and viscous flow curves (B) for the oleogels performed with NCO-functionalized fermented and uninoculated straws. Standard deviation has been included in the form of error bars.

level than barley straw, it was expected to see a decrease in the SAOS functions of Fermented Wheat-based oleogel as a consequence of a more extensive degradation of cellulose. On the contrary, a positive influence of the predominant xylanase action is expected since this enzyme eminently affects branched biopolymers. However, the influence of both enzymes should not be of the same grade, otherwise Fermented Wheat-based oleogel would not show such dramatic drop of both viscoelastic moduli. Considering both xylanase and CMCase maximum activities, a simple mathematical model can be drawn to evaluate the relative influence of the actions of both enzymes. Thus, the plateau modulus, G_N^0, a characteristic parameter of the plateau region of the mechanical spectrum, defined as the extrapolation of the contribution of entanglements to G' at high frequencies (Baumgaertel et al., 1992), was estimated for all samples as shown elsewhere (Borrero-López et al., 2017; Sánchez et al., 2014), and then the ratio of the plateau moduli for the control and fermented straw-based oleogels was evaluated as a function of the xylanase and CMCase relative maximum activity percentage respecting the total enzymatic activity determined in each fermented straw, as follows:

$$G^0_{N,(FB,FW)} = G^0_{N,(B,W)} \cdot \frac{[Xylanase\ (\%)]^b}{[CMCase\ (\%)]^a} \quad (1)$$

The results demonstrated a positive influence of xylanase activity whereas a negative and twofold stronger influence was shown by CMCase, being *a* and *b* parameters 1.82 and 0.97 values, respectively, which supports the previous discussion. In addition, as previously discussed, the lower crosslinking degree achieved in HDI-modified Fermented Wheat sample, as a result of the higher enzymatic activity, favours the decrease in the linear viscoelastic functions found in the corresponding oleogel.

Regarding the viscous flow measurements, Fig. 5B shows the apparent viscosity versus shear rate plots for the different oleogels studied. As can be seen, very similar viscosity values and a markedly shear-thinning behaviour were observed in all cases. Viscous flow curves were fitted by using the power-law model (Eq. 2):

$$\eta = K \cdot \dot{\gamma}^{n-1} \quad (2)$$

where *K* and *n* are the consistency and flow indexes, respectively. Table 3 shows the values of *K* and *n* for all the oleogels studied. Only slight differences in viscosity are found at low and/or high shear rates, resulting very similar values of K (the viscosity at 1 s^{-1}). The same tendency found for the SAOS functions can be appreciated at low shear rates, i.e. contrary effect of SSF in barley and wheat straw-based oleogels, respectively, whereas Fermented Wheat-based oleogel tends to have high viscosity at high shear rates. Flow indexes were quite close to 0, varying from 0.02 for OWheat to 0.15 for OFermented Wheat, which are characteristic of yielding materials such as lubricating greases (Delgado et al., 2019; Sánchez et al., 2014).

In addition, the evaluation of the thermo-rheological behaviour is important to predict the lubrication performance in grease lubricated contacts, which under working conditions may be significantly heated due to friction. Accordingly, the straw-based oleogels developed were also tested up to 150 °C (see evolution of SAOS functions with frequency from 25 to 150 °C in the supporting information, Fig. S1). As can be observed, the linear viscoelastic functions decrease with temperature in a similar way for all the oleogels studied. Fig. 6 shows G_N^0 vs. the reciprocal temperature plots for the four oleogels studied. In all cases, two different trends were observed, the first one, from 25 to 75 °C, where a moderate decrease of G_N^0 with temperature is noticed, and above 75 °C, where a more important decrease in this parameter was experienced. Two Arrhenius-type equations were applied to describe the evolution of G_N^0 with temperature for each oleogel (see Eq. (3)), in both temperature ranges:

$$G^0_N = A \cdot e^{(E_a/R)\cdot(1/T)} \quad (3)$$

where A is the pre-exponential factor (Pa), E_a is a parameter which determines the thermal dependence, similar to the activation energy (J/mol), R is the gas constant (8.314 J/mol K) and T is the absolute temperature (K). A and E_a values resulting from the fitting to Eq. (3) are shown in Table 4. In general, compared to the results obtained for other lignocellulosic-based oleogels and traditional metallic soap-based lubricating greases, the activation energy values obtained in both the low (5.8–13.4 kJ/mol) and the high (33.8–51.2 kJ/mol) temperature ranges are slightly higher to those obtained for commercial lithium greases, but similar to those found for calcium greases (Sánchez et al., 2014), or much lower than those reported for other biodegradable lubricating greases based on castor oil and lignocellulose in the high temperature range (Borrero-López et al., 2018b; Gallego et al., 2015). It is worth mentioning that the more important xylan degradation in fermented wheat straw because of enzymatic activity softens the change of tendency at 75 °C, being less pronounced (see Fig. 6).

Tribological tests were also carried out to assess the lubrication

Table 3
Friction coefficient values measured in a tribological contact, penetration measurements and power-law model indexes for the oleogels studied.

Samples	Friction Coefficient	Unworked penetration (mm/10)	Worked penetration (mm/10)	Penetration variation (mm/10)	NLGI grade	K (Pa·s^n)	n
OBarley	0.091 ± 0.007	235 ± 21	368 ± 11	133	3	1031	0.10
OWheat	0.095 ± 0.002	209 ± 9	247 ± 4	38	3-4	1319	0.02
OFermented Barley	0.092 ± 0.003	234 ± 8	300 ± 4	66	3	1141	0.03
OFermented Wheat	0.095 ± 0.002	281 ± 15	392 ± 1	111	2	1098	0.15

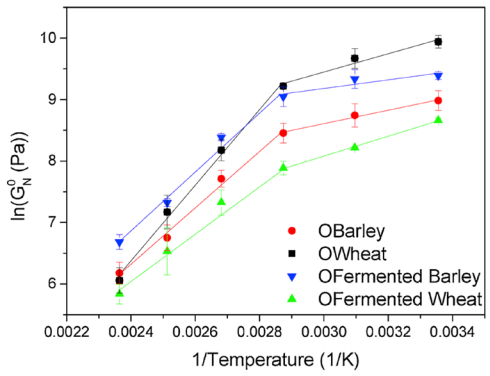

Fig. 6. Evolution of the plateau modulus with the reciprocal temperature and corresponding Arrhenius fitting for the oleogels studied. Standard deviation has been included in the form of error bars.

Table 4
Eq. (3) fitting parameters for the oleogels studied.

Samples		25–75 °C	75–150 °C
OBarley	A (Pa)	208.5	9.2E-3
	Ea (kJ/mol)	9.1	38.1
OWheat	A (Pa)	146.9	2.2E-4
	Ea (kJ/mol)	12.4	51.2
OFermented Barley	A (Pa)	1184.4	9.7E-3
	Ea (kJ/mol)	5.8	39.8
OFermented Wheat	A (Pa)	25.5	2.4E-2
	Ea (kJ/mol)	13.4	33.8

performance of these oleogels. The friction coefficient values obtained for the four oleogels were displayed in Table 3. In all cases, very similar values were obtained, always below 0.10, which imply outstanding values, lower than those obtained for commercial lithium and calcium-based lubricating greases under the same conditions (Borrero-López et al., 2018b; Gallego et al., 2016) and close to those obtained from waste lignin-based oleogels (Borrero-López et al., 2018b).

Besides, oleogels were also characterized by means of penetration tests, which allow to classify greases in terms of NLGI grades, attending to their consistency, as determines the mechanical stability after working. Table 3 shows both unworked and worked penetration values, including penetration variation, as well as the associated NLGI grade. As expected, unworked penetration values of the samples studied increased inversely to the viscosity and values of linear viscoelastic functions, providing lower NLGI grade for Fermented Wheat-based oleogels (NLGI 2), and higher grade for OWheat (NLGI 3–4). Typically, NLGI grade ranges from NLGI 000, for liquid-like greases, to NLGI 6 for hard greases. Most common greases suitable for a wider range of applications are those with NLGI grades 1–3, and more specifically NLGI 2. The penetration variation, calculated after application of the shear rolling test is also shown in Table 3. Since penetration variation is

Table 5
Recovery of the plateau modulus for the oleogels studied.

Samples	Recovery (Percentage of initial value) (%)		
	After Rolling	Day 7	Day 40
OBarley	2.6	9	22
OWheat	1.6	8	17
OFermented Barley	3.5	13	23
OFermented Wheat	0.7	10	15

recommended to be lower as possible, the mechanical stability of these samples is rather poor, only being acceptable that exhibited by the OWheat sample.

The severe drop in consistency values experienced by the four oleogels after application of the shear rolling test was extrapolated to the linear viscoelastic functions, which suffered a reduction of around 96–99% of the initial G_N^0 values, being the largest softening observed for fermented samples (see Table 5). Nevertheless, a partial recovery of the structure was observed when SAOS functions were monitored along a determined period of time after the application of the rolling test, reaching stationary values at around 40 days. For the sake of comparison, the G_N^0 values at different recovery times, obtained from frequency sweeps (raw SAOS curves shown in Fig. S2 of SI) were used to estimate the recovery percentage (see Table 5). As can be seen, after 1 week, around 10–13% of recovery has been achieved for fermented straws-based oleogels, while uninoculated-based ones only reached 8–9%. After forty days, no recovery is any longer observed, at which plateau modulus was able to raise up to 23% of that found in the initial (non-sheared) barley-based oleogels while only around 15–17% was finally recovered for wheat straw-based oleogels, independently of the SSF, demonstrating a higher capacity of structural recovery for barley-based systems and again the importance of the original structure of the straw.

4. Conclusions

Wheat and barley straws were successfully modified by *Streptomyces* MDG301 action through a SSF process. The differences found in the enzymatic pattern of xylanase, CMCase and mannanase detected on both substrates as well as their different level of activity, could explain the different yield of APPL and alkali-lignin obtained. As long-chain cellulose is a key component on strengthening oleogels, elevated CMCase activity found on wheat straw generated oleogels with lower values of the linear viscoelastic functions, contrary to that observed on fermented barley straw-based oleogels, where the activity of CMCase was much lower and xylan elimination led to a stronger network which increased the values of SAOS functions. Straw-based oleogels were assessed for potential lubrication applications, as bio-sourced lubricating greases, demonstrating typical and suitable rheological behaviour from room temperature to 150 °C. Tribological tests demonstrated outstanding frictional behaviour, with values of the frictional coefficient below those obtained for commercial lubricating greases. On the other hand, consistency values ranged these samples in NLGI grades between 2 to 4. Nonetheless, straw-based oleogels presented relatively poor mechanical stability, thus penetration variation was far from ideal, but

comparable or even better than some calcium greases and other lignocellulosic-based gel-like dispersions. After working tests, barley straw-based oleogels demonstrated better structural recovery.

Declaration of Competing Interest

The authors declare no competing financial interest.

Acknowledgements

This work is part of two coordinated research projects (CTQ2014-56038- C3-1R and CTQ2014-56038-C3-2R) sponsored by MINECO-FEDER. A.M.B-L. has received a Ph.D. Research Grant from the Ministerio de Educación, Cultura y Deporte (FPU16/03697). We gratefully acknowledge its financial support.

Appendix A. Supplementary data

Supplementary material related to this article can be found, in the online version, at doi:https://doi.org/10.1016/j.indcrop.2019.111625.

References

Alemdar, A., Sain, M., 2008a. Isolation and characterization of nanofibers from agricultural residues - Wheat straw and soy hulls. Bioresour. Technol. 99, 1664–1671. https://doi.org/10.1016/j.biortech.2007.04.029.

Alemdar, A., Sain, M., 2008b. Biocomposites from wheat straw nanofibers: morphology, thermal and mechanical properties. Compos. Sci. Technol. 68, 557–565. https://doi.org/10.1016/j.compscitech.2007.05.044.

Anderson, A.S., Wellington, E.M.H., 2001. The taxonomy of *Streptomyces* and related genera. Int. J. Syst. Evol. Microbiol. 51, 797–814. https://doi.org/10.1099/00207713-51-3-797.

Antonopoulos, V.T., Hernandez, M., Arias, M.E., Mavrakos, E., Ball, A.S., 2001. The use of extracellular enzymes from *Streptomyces albus* ATCC 3005 for the bleaching of eucalyptus kraft pulp. Appl. Microbiol. Biotechnol. 57, 92–97. https://doi.org/10.1007/s002530100740.

Aramrueang, N., Zicari, S.M., Zhang, R., 2017. Characterization and compositional analysis of agricultural crops and residues for ethanol production in California. Biomass Bioenergy 105, 288–297. https://doi.org/10.1016/j.biombioe.2017.07.013.

Baumgaertel, M., De Rosa, M.E., Machado, J., Masse, M., Winter, H.H., 1992. The relaxation time spectrum of nearly monodisperse polybutadiene melts. Rheol. Acta 31, 75–76.

Berrocal, M., Ball, A.S., Huerta, S., Barrasa, J.M., Hernández, M., Pérez-Leblic, M.I., Arias, M.E., 2000. Biological upgrading of wheat straw through solid-state fermentation with *Streptomyces cyaneus*. Appl. Microbiol. Biotechnol. 54, 764–771. https://doi.org/10.1007/s002530000454.

Berrocal, M.M., Rodríguez, J., Ball, A.S., Pérez-Leblic, M.I., Arias, M.E., 1997. Solubilisation and mineralisation of [14C]lignocellulose from wheat straw by *Streptomyces cyaneus* CECT 3335 during growth in solid-state fermentation. Appl. Microbiol. Biotechnol. 48, 379–384. https://doi.org/10.1007/s002530051066.

Blánquez, A., Ball, A.S., González-Pérez, J.A., Jiménez-Morillo, N.T., González-Vila, F., Arias, M.E., Hernández, M., 2017. Laccase SilA from *Streptomyces ipomoeae* CECT 3341, a key enzyme for the degradation of lignin from agricultural residues? PLoS One 12, 1–15. https://doi.org/10.1371/journal.pone.0187649.

Borrero-López, A.M., Blánquez, A., Valencia, C., Hernández, M., Arias, M.E., Eugenio, M.E., Fillat, Ú., Franco, J.M., 2018a. Valorization of soda lignin from wheat straw solid-state fermentation: production of oleogels. ACS Sustain. Chem. Eng. 6, 5198–5205. https://doi.org/10.1021/acssuschemeng.7b04846.

Borrero-López, A.M., Santiago-Medina, F.J., Valencia, C., Eugenio, M.E., Franco, J.M., 2018b. Valorization of kraft lignin as thickener in Castor oil for lubricant applications. J. Renew. Mater. 6, 1–15. https://doi.org/10.7569/JRM.2017.634160.

Borrero-López, A.M., Valencia, C., Franco, J.M., 2017. Rheology of lignin-based chemical oleogels prepared using diisocyanate crosslinkers: effect of the diisocyanate and curing kinetics. Eur. Polym. J. 89, 311–323. https://doi.org/10.1016/j.eurpolymj.2017.02.020.

Chen, Y., Sharma-Shivappa, R.R., Keshwani, D., Chen, C., 2007. Potential of agricultural residues and hay for bioethanol production. Appl. Biochem. Biotechnol. 142, 276–290. https://doi.org/10.1007/s12010-007-0026-3.

Crawford, D.L., 1978. Lignocellulose decomposition by selected *Streptomyces* strains. Appl. Environ. Microbiol. 35, 1041–1045.

Delgado, M., Secouard, S., Valencia, C., Franco, J., 2019. On the steady-state flow and yielding behaviour of lubricating greases. Fluids 4, 6. https://doi.org/10.3390/fluids4010006.

Duque, A., Manzanares, P., Ballesteros, I., Negro, M.J., Oliva, J.M., González, A., Ballesteros, M., 2014. Sugar production from barley straw biomass pretreated by combined alkali and enzymatic extrusion. Bioresour. Technol. 158, 262–268. https://doi.org/10.1016/j.biortech.2014.02.041.

Gallego, R., Arteaga, J.F., Valencia, C., Díaz, M.J., Franco, J.M., 2015. Gel-like dispersions of HMDI-Cross-Linked lignocellulosic materials in Castor oil: toward completely renewable lubricating grease formulations. ACS Sustain. Chem. Eng. 3, 2130–2141. https://doi.org/10.1021/acssuschemeng.5b00389.

Gallego, R., Arteaga, J.F., Valencia, C., Franco, J.M., 2013a. Chemical modification of methyl cellulose with HMDI to modulate the thickening properties in castor oil. Cellulose 20, 495–507. https://doi.org/10.1007/s10570-012-9803-4.

Gallego, R., Arteaga, J.F., Valencia, C., Franco, J.M., 2013b. Rheology and thermal degradation of isocyanate-functionalized methyl cellulose-based oleogels. Carbohydr. Polym. 98, 152–160. https://doi.org/10.1016/j.carbpol.2013.04.104.

Gallego, R., Cidade, T., Sánchez, R., Valencia, C., Franco, J.M., 2016. Tribological behaviour of novel chemically modified biopolymer-thickened lubricating greases investigated in a steel–steel rotating ball-on-three plates tribology cell. Tribol. Int. 94, 652–660. https://doi.org/10.1016/j.triboint.2015.10.028.

García-Aparicio, M.P., Ballesteros, I., González, A., Oliva, J.M., Ballesteros, M., Negro, M.J., 2006. Effect of inhibitors released during steam-explosion pretreatment of barley straw on enzymatic hydrolysis. Appl. Biochem. Biotechnol. 129, 278–288. https://doi.org/10.1385/ABAB:129:1:278.

Hernández, M., Hernández-Coronado, M.J., Montiel, M.D., Rodríguez, J., Pérez-Leblic, M.I., Bocchini, P., Galletti, G.C., Arias, M.E., 2001. Pyrolysis/gas chromatography/mass spectrometry as a useful technique to evaluate the ligninolytic action of streptomycetes on wheat straw. J. Anal. Appl. Pyrolysis 58–59, 539–551.

Himmel, M.E., Ding, S.Y., Johnson, D.K., Adney, W.S., Nimlos, M.R., Brady, J.W., Foust, T.D., 2007. Biomass recalcitrance: engineering plants and enzymes for biofuels production. Science 315, 804–807. https://doi.org/10.1126/science.1137016.

Huang, C., Tian, L., Qi, G., Chen, X., Chen, X., Luo, M., Huang, Q., Xiong, L., Li, H., 2019. Hydrotropic pretreatment on wheat straw for efficient biobutanol production. Biomass Bioenergy 122, 76–83. https://doi.org/10.1016/j.biombioe.2019.01.039.

Johar, N., Ahmad, I., Dufresne, A., 2012. Extraction, preparation and characterization of cellulose fibres and nanocrystals from rice husk. Ind. Crops Prod. 37, 93–99. https://doi.org/10.1016/j.indcrop.2011.12.016.

Kiiskinen, L.L., Palonen, H., Linder, M., Viikari, L., Kruus, K., 2004. Laccase from *Melanocarpus albomyces* binds effectively to cellulose. FEBS Lett. 576, 251–255. https://doi.org/10.1016/j.febslet.2004.08.040.

Kim, S., Dale, B.E., 2004. Global potential bioethanol production from wasted crops and crop residues. Biomass Bioenergy 26, 361–375. https://doi.org/10.1016/j.biombioe.2003.08.002.

Malhi, S.S., Lemke, R., Wang, Z.H., Chhabra, B.S., 2006. Tillage, nitrogen and crop residue effects on crop yield, nutrient uptake, soil quality, and greenhouse gas emissions. Soil Tillage Res. 90, 171–183. https://doi.org/10.1016/j.still.2005.09.001.

Martín-Alfonso, J.E., Valencia, C., Sánchez, M.C., Franco, J.M., Gallegos, C., 2011. Evaluation of different polyolefins as rheology modifier additives in lubricating grease formulations. Mater. Chem. Phys. 128, 530–538. https://doi.org/10.1016/j.matchemphys.2011.03.046.

Meng, F., Yu, J., Tahmasebi, A., Han, Y., Zhao, H., Lucas, J., Wall, T., 2014. Characteristics of chars from low-temperature pyrolysis of lignite. Energy Fuels 28, 275–284. https://doi.org/10.1021/ef401423s.

Moya, R., Hernández, M., García-Martín, A.B., Ball, A.S., Arias, M.E., 2010. Contributions to a better comprehension of redox-mediated decolouration and detoxification of azo dyes by a laccase produced by *Streptomyces cyaneus* CECT 3335. Bioresour. Technol. 101, 2224–2229. https://doi.org/10.1016/j.biortech.2009.11.061.

Mupondwa, E., Li, X., Tabil, L., 2018. Integrated bioethanol production from triticale grain and lignocellulosic straw in Western Canada. Ind. Crops Prod. 117, 75–87. https://doi.org/10.1016/j.indcrop.2018.02.070.

Nabarlatz, D., Ebringerová, A., Montané, D., 2007. Autohydrolysis of agricultural by-products for the production of xylo-oligosaccharides. Carbohydr. Polym. 69, 20–28. https://doi.org/10.1016/j.carbpol.2006.08.020.

Núñez, N., Martín-Alfonso, J.E., Eugenio, M.E., Valencia, C., Díaz, M.J., Franco, J.M., 2011. Preparation and characterization of gel-like dispersions based on cellulosic pulps and castor oil for lubricant applications. Ind. Eng. Chem. Res. 50, 5618–5627. https://doi.org/10.1021/ie1025584.

Raghunanan, L.C., Martínez, I., Valencia, C., Sánchez, M.C., Franco, J.M., 2018. Unexpected selectivity in the functionalization of neat Castor oil under benign catalyst-free conditions. ACS Sustain. Chem. Eng. 6, 7212–7215. https://doi.org/10.1021/acssuschemeng.8b00979.

Robinson, T., Chandran, B., Nigam, P., 2002. Effect of pretreatments of three waste residues, wheat straw, corncobs and barley husks on dye adsorption. Bioresour. Technol. 85, 119–124. https://doi.org/10.1016/S0960-8524(02)00099-8.

Rosgaard, L., Pedersen, S., Meyer, A.S., 2007. Comparison of different pretreatment strategies for enzymatic hydrolysis of wheat and barley straw. Appl. Biochem. Biotechnol. 143, 284–296. https://doi.org/10.1007/s12010-007-8001-6.

Sánchez, R., Valencia, C., Franco, J.M., 2014. Rheological and tribological characterization of a new acylated chitosan-based biodegradable lubricating grease: a comparative study with traditional lithium and calcium greases. Tribol. Trans. 57, 445–454. https://doi.org/10.1080/10402004.2014.880541.

Sarkar, N., Ghosh, S.K., Bannerjee, S., Aikat, K., 2012. Bioethanol production from agricultural wastes: an overview. Renew. Energy 37, 19–27. https://doi.org/10.1016/j.renene.2011.06.045.

Somogyi, M., 1945. A new reagent for determinations of sugars. J. Biol. Chem. 160, 61–68.

Sun, X.F., Xu, F., Sun, R.C., Fowler, P., Baird, M.S., 2005. Characteristics of degraded cellulose obtained from steam-exploded wheat straw. Carbohydr. Res. 340, 97–106. https://doi.org/10.1016/j.carres.2004.10.022.

Saarinen, T., Orelma, H., Grönqvist, S., Andberg, M., Holappa, S., Laine, J., 2009. Adsorption of different laccases on cellulose and lignin surfaces. BioResources 4, 94–110.

González, M., Gallego, R., González-Delgado, J.A., Arrteaga, J.F., Valencia, C., Franco, J.M., 2016. Impact of natural sources-derived antioxidants on the oxidative stability

and rheological properties of castor oil based-lubricating greases. Ind. Crops Prod. 87, 297–303. https://doi.org/10.1016/j.indcrop.2016.04.068.
Van Dyk, J.S., Pletschke, B.I., 2012. A review of lignocellulose bioconversion using enzymatic hydrolysis and synergistic cooperation between enzymes-factors affecting enzymes, conversion and synergy. Biotechnol. Adv. 30, 1458–1480. https://doi.org/10.1016/j.biotechadv.2012.03.002.
Zeng, J., Singh, D., Laskar, D.D., Chen, S., 2013. Degradation of native wheat straw lignin by *Streptomyces viridosporus* T7A. Int. J. Environ. Sci. Technol. 10, 165–174. https://doi.org/10.1007/s13762-012-0085-z.

3.2. Article 6

Cellulose Pulp- and Castor Oil-Based Polyurethanes for Lubricating Applications: Influence of *Streptomyces* Action on Barley and Wheat Straws

A.M. Borrero-López, C. Valencia, A. Blánquez, M. Hernández, M.E. Eugenio, J.M. Franco

Published in:

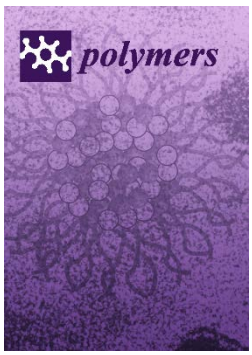

Polymers
Publishing Company: MDPI
Editor-in-Chief: A. Pizzi, A. Böker, V. Mavrantzas, M. Kröger, F. Wiesbrock, S. Yusha, H. Yoon, D. Bikiaris, MA. López, G. Malucelli, FP. La Mantia
Volume 12 (12), 2822
Year 2020
ISSN 2073-4360
DOI: 10.3390/polym12122822

Category	Journal Rank / Total number of journals	Quartile (Percentage)
Polymer Science	16/89	Q1 (83%)
Impact Factor	3.426	

polymers

MDPI

Article

Cellulose Pulp- and Castor Oil-Based Polyurethanes for Lubricating Applications: Influence of *Streptomyces* Action on Barley and Wheat Straws

Antonio M. Borrero-López [1], Concepción Valencia [1,*], Alba Blánquez [2], Manuel Hernández [2], María E. Eugenio [3] and José M. Franco [1]

[1] Pro2TecS—Chemical Process and Product Technology Research Centre, Departamento de Ingeniería Química, ETSI, Campus de "El Carmen", Universidad de Huelva, 21071 Huelva, Spain; am.borrero@diq.uhu.es (A.M.B.-L.); franco@uhu.es (J.M.F.)

[2] Departamento de Biomedicina y Biotecnología, Universidad de Alcalá, 28805 Alcalá de Henares, Spain; alba.blanquez@edu.uah.es (A.B.); manuel.hernandez@uah.es (M.H.)

[3] Forest Research Centre, Forest Products Department, INIA, 28040 Madrid, Spain; mariaeugenia@inia.es

* Correspondence: barragan@uhu.es; Tel.: +34-959218201

Received: 27 October 2020; Accepted: 25 November 2020; Published: 27 November 2020

check for updates

Abstract: The replacement of mineral oils and non-renewable gelling agents is an imperative requirement for the lubricant industry in the near future. In this framework, cellulose pulp and castor oil are proposed as sustainable substitutes for these components. Biological treatment has been explored and evaluated to enhance the dispersing and thickening properties of cellulose pulp in oil media. *Streptomyces* sp. MDG147 and MDG301 strains were employed to modify agricultural wheat and barley straw residues from which cellulose pulp was obtained afterwards. In addition, an environmentally friendly process for the production of cellulose-pulp-/castor-oil-based polyurethanes was applied, in which neither catalysts nor harmful solvents were used, resulting in chemical oleogels. These oleogels were rheologically and tribologically characterized to evaluate their performance as lubricating greases. The enzymatic activity pattern developed was dependent on the raw material, the strain type, and the temperature, influencing the cellulose pulp's composition, polymerization degree, and crystallinity. These modified characteristics tuned the rheological behavior of the different oleogels, providing a beneficial range of viscoelastic responses and viscosity values that were generally favored by the *Streptomyces* action. Furthermore, the friction coefficient and dimensions of wear scars measured in a tribological contact were comparable to, or even lower than, those found with commercial and other bio-based lubricating greases that have previously been studied.

Keywords: cellulose pulp; lubricating grease; oleogel; polyurethane; rheology; solid-state fermentation; *Streptomyces*; tribology

1. Introduction

Current research is being driven by the mandatory necessity of finding new materials and proceedings that will enable harmful industrial processes, end-use products, and non-renewable energy sources to be replaced by greener alternatives, such as natural, renewable, or bio-based products and non-hazardous techniques that meet the trends of Green Chemistry [1].

Among the most studied bioresources, cellulose is undoubtedly the principal one. As a consequence of being the most abundant biopolymer on Earth, research has focused on many alternative fields, such as composites [2], tissue regeneration [3], chemical products [4,5], biosensors [6], energy storage [7],

etc. Such diverse applications are possible because of cellulose's main chemical and physical properties, which make of it an outstanding biopolymer. The linear chemical structure—based on glucose and linked by β(1–4) glycosidic bonds—and the numerous hydroxyl groups that allow the formation of a crystalline structure through hydrogen bonding [8] are some of its most interesting features. The fibrous structure and ability to form macromolecular networks have prompted the possibility of using cellulose to produce different gel-like structures, such as aerogels [9,10], hydrogels [11,12], or oleogels [13–15], for a wide variety of applications.

The development of bio-based oleogels may represent a new market niche in the lubricant industry with interesting perspectives for the future, since metallic soap-based thickening agents and mineral oils, the main components in lubricating grease formulations, may have to be replaced soon as a consequence of more restrictive politics [16,17]. At the Chemical Process and Product Technology Research Center (Pro2TecS, Universidad de Huelva), we have dedicated our efforts over the last two decades to the development of eco-friendly oleogels, attempting to provide them with outstanding functional properties so they can be proposed as efficient alternatives to traditional lubricating greases, as well as to the comprehensive characterization of the rheological and tribological behaviors of both commercial and bio-based lubricating greases [18,19]. More specifically, this research has been focused on the finding of suitable and sustainable gelling or thickening agents in oily media by following diverse approaches. Among the different raw materials, biopolymers such as chitosan and chitin [20], lignin [16,21–23], cellulose derivatives [14], and more complex lignocellulosic materials [17,24,25] have been used to thicken or gelify vegetable oils. Furthermore, chemical modifications, such as epoxidation [24], methylation [26,27], ethylation [28], acylation [20], or polyurethane formation [29], were applied to either decrease the polarity of these biopolymers—thus increasing the affinity by the oil medium—or promote the formation of chemical gels and more stable networks by generating covalent bonds between the biopolymer and the vegetable oil. Nonetheless, despite the fact that these final formulations can be considered bio-based, inert, and non-toxic materials, some of these procedures involve the use of hazardous chemicals and solvents; therefore, alternative processes and methodologies must be further explored. This is the case, for instance, of polyurethane-based materials, which are usually synthesized using toluene or other harmful solvents [30], as well as triethylamine or dibutyltindilaurate as catalysts [31]. Thus, procedures free of both catalysts and solvents have lately been focused upon [29].

On the other hand, bio-source modification has also widely been targeted in order to provide systems with better properties for certain applications, rather than the consequent use of harmful chemicals [32]. To overcome the challenge, biological treatments have been acutely pointed out as a greener alternative to chemical modifications. Fungi [33,34] and bacteria [16,35–37] are among the most used precursors, and are capable of altering the biomass through a degradation process. Some actinobacteria, like the genus *Streptomyces*, produce cellulolytic, hemicellulolytic, and ligninolytic enzymes, which break the main linkages that join cellulose, hemicellulose, and lignin, respectively [38]. The resulting bioproducts may achieve better characteristics than the non-modified ones, since this linkage breakdown is known to increase the content of functional groups, thus facilitating further reactions and altering the original structural features, which may favor the formation of more appropriate oleogels, as demonstrated in previous work on lignin-enriched streams [16]. Following this research line, the preparation of polyurethane oleogels with lubricating grease properties based on cellulose pulp and castor oil was targeted in this work. Several cellulose pulp samples were obtained from barley and wheat straws after being subjected to biological modification (solid-state fermentation) through the action of the *Streptomyces* sp. MDG147 and MDG301 strains. Afterwards, chemical oleogels were prepared by directly mixing the castor oil, cellulose pulp, and the diisocyanate crosslinker at room temperature, avoiding the use of harmful catalysts, solvents, and energy-consuming processes. Finally, the effect of the biological treatment on the rheological and some performance properties was evaluated.

2. Materials and Methods

2.1. Materials

Wheat (*Triticum aestivum* var. *maestro*) and barley (*Hordeum vulgare*) straws were kindly provided by farmers from Guadalajara (Spain). Hexamethylene diisocyanate (HDI) (>98% purity) was purchased from Merck (Darmstadt, Germany). Castor oil, with fatty acid contents of 5.3%, 7.0%, and 82.5% of oleic, linoleic, and ricinoleic acids, respectively, was supplied by Guinama (Valencia, Spain). All other common solvents and reagents used to perform the solid-state fermentation and soda pulping were acquired from Merck.

2.2. Solid-State Fermentation

Wheat and barley straws were submitted to solid-state fermentation (SSF) treatments by selecting two different types of *Streptomyces* sp. MDG147 and MDG301 strains. The first one finds its optimum working temperature at 28 °C, while the latter is considered a thermophilic strain, reaching an optimum activity at 45 °C. MDG301 activity was tested at 45 °C on both wheat and barley straws (samples CPW301.45 and CPB301.45) and 28 °C on wheat straw (sample CPW301), whereas MDG147 activity was evaluated only on barley straw (CPB147). More detailed information about preinoculum acquisition, SSF process, and enzymatic activity monitoring system can be found elsewhere [39]. Uninoculated samples followed a similar treatment for further comparison.

2.3. Soda Pulping

Once SSF was accomplished, a soda pulping process was carried out to separate both holocellulosic and lignin-enriched phases. This process has been thoroughly described in previous work [16]. Uninoculated wheat and barley straws were also submitted to soda pulping and were taken as references. Finally, large cellulosic pulp clusters obtained after soda pulping were milled by using a rotary miller MF 10 basic WERKE (IKA, Staufen, Germany) equipped with a 0.25 mm mesh.

2.4. Oleogel Processing

A green and straightforward procedure to prepare gel-like polyurethanes, which avoids the use of solvents and catalysts, was followed [29]. In brief, cellulose pulps were directly blended with HDI (1/2 cellulose pulp/HDI weight ratio) and castor oil (85% or 90% w/w) under stirring at room temperature (~20 °C) for 24 h using an RW20 (IKA, Staufen, Germany) equipped with an anchor impeller at 70 rpm.

2.5. Characterization Techniques

Cellulose pulp composition was determined by following the National Renewable Energy Laboratory's standard analytical methods (NREL/TP-510-42618). Samples were subjected to acid hydrolysis to determine the carbohydrate composition. The liquids resulting from the hydrolysis were then analyzed to determine the sugar contents using high-performance liquid chromatography (1260 HPLC, Agilent, Waldbronn, Germany) fitted with a G1362A refractive index detector (Agilent, Waldbronn, Germany) and equipped with an Hi-PlexPb column (Agilent, Waldbronn, Germany) operated at 70 °C. Ultrapure water (A10 Milli-Q, Millipore, Burlington, MA, USA) was used as a mobile phase, and was pumped at a rate of 0.6 mL min^{-1}. UV -Visible spectrophotometry (Jasco V-500, Jasco, Japan) at 205 nm was used to quantify acid-soluble lignin. The solid residue obtained after the acid hydrolysis was considered acid-insoluble lignin (called Klason lignin). Extractives and ashes of the samples were analyzed according to the NREL/TP-510-42619 and UNE 57050:2003 standards, respectively. Intrinsic viscosity [η] was calculated by following the ISO/FDIS 5351:2010 standard,

from which the polymerization degree (DP) was obtained by applying the following equations indicated in the SCAN-CM 15:88 standard:

$$\begin{array}{c} DP = \frac{[\eta]}{0.42} \; for \; DP < 950 \\ DP^{0.76} = \frac{[\eta]}{2.28} \; for \; DP > 950 \end{array} \quad (1)$$

Thermogravimetric analysis (TGA) was performed by applying a ramp increasing at 10 °C/min from room temperature up to 600 °C in a Q-50 apparatus (TA Instrument Waters, New Castle, DE, USA), while Fourier transform infrared (FTIR) spectra were collected in a JASCO FTIR 4200 spectrometer (Jasco Inc., Tokyo, Japan) with wavenumbers from 400 to 4000 cm^{-1} and with a 4 cm^{-1} resolution.

Both linear viscoelasticity and viscous flow tests were performed in a controlled stress rheometer, MARS (Thermo Scientific, Darmstadt Germany), using a serrated plate–plate geometry (20 mm diameter and 1 mm gap). Frequency sweeps were carried out from 100 to 0.03 rad/s within the linear viscoelastic range, which was previously estimated by performing stress sweeps at 1 Hz, whereas viscous flow curves were obtained by applying an increasing stepped shear rate ramp within the 0.01–100 s^{-1} range.

Friction coefficient values were obtained in a Physica MCR-501 rheometer (Anton Paar, Graz, Austria) equipped with a tribological cell, consisting of a 6.35 mm diameter steel ball spinning on three 45°-inclined rectangular-shaped steel plates, on which the oleogel specimens acting as lubricants were spread. A constant normal load and a rotational speed of 20 N and 10 min^{-1}, respectively, were applied for 10 min. This time was long enough to achieve stationary values of the friction coefficient. Five replicates were performed for each oleogel sample. The wear scars thereby produced in the steel plates were analyzed through optical microscopy using an Olympus microscope, BX51 model (Tokyo, Japan), from which both the parallel-to-the-rotation diameter and the typically elliptical wear area were determined. The data supplied here represent the mean of the three plates.

3. Results

3.1. Cellulose Pulp Composition

The composition of the different cellulose pulps obtained from barley and wheat straws, whether or not submitted to bacterial action in solid-state fermentation, is included in Table 1. In general, these results are supported by the enzymatic activity pattern of the diverse *Streptomyces* strains shown in Figure 1. This figure only displays the enzymatic activity of CMCase and hemicellulases, as laccases and peroxidases are known to remain attached to the substrate, which does not allow their separation for quantification [40,41]. These enzymatic profiles accurately reflect hemicellulose's typical structure [42], as hemicellulase activities suggest a higher concentration of xylan units compared to mannans.

Table 1. Composition of the cellulose pulp samples.

Sample	Klason Lignin (%)	Soluble Lignin (%)	Glucose (%)	Xylose (%)	Arabinose (%)	Extracts (%)	Ashes (%)
CPB	2.2 ± 0.2	0.3 ± 0.1	62.2 ± 0.5	30.3 ± 0.5	3.2 ± 0.2	0.66	1.2 ± 0.2
CPB147	2.1 ± 0.3	0.3 ± 0.0	65.3 ± 0.8	28.1 ± 2.1	3.0 ± 0.2	0.44	1.3 ± 0.2
CPB301.45	3.5 ± 0.3	0.4 ± 0.0	64.2 ± 1.3	27.6 ± 0.7	3.1 ± 0.0	0.41	1.2 ± 0.0
CPW	6.3 ± 0.3	1.1 ± 0.1	55.5 ± 2.6	21.6 ± 1.8	1.1 ± 0.3	5.08	1.2 ± 0.2
CPW301	6.3 ± 0.6	0.3 ± 0.2	62.0 ± 2.2	29.7 ± 0.7	2.5 ± 0.0	1.14	0.6 ± 0.4
CPW301.45	4.0 ± 1.4	0.4 ± 0.0	61.2 ± 3.5	31.1 ± 3.7	4.3 ± 2.5	0.27	1.3 ± 0.3

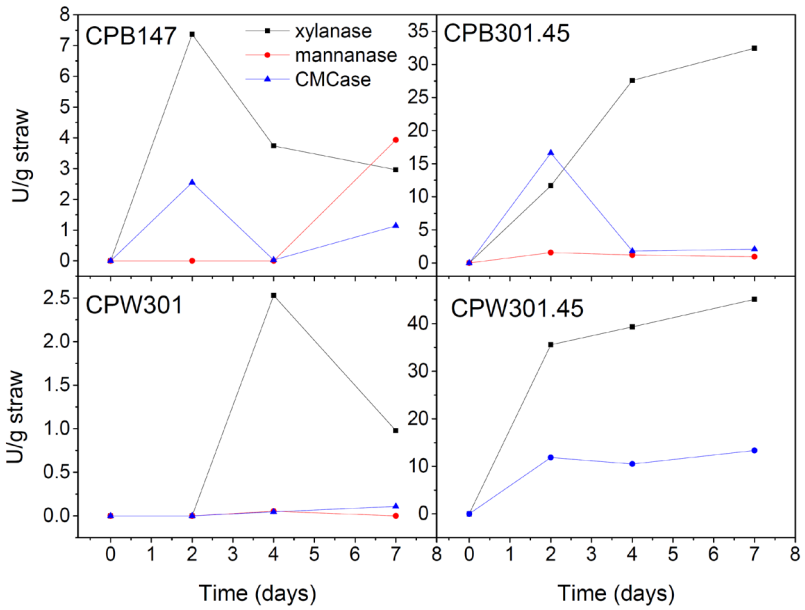

Figure 1. Enzymatic profiles for both wheat and barley straws treated under different conditions in the solid-state fermentation.

In barley-straw-derived cellulose pulps, it can be seen how the xylose concentration in systems previously fermented with MDG301 (CPB301.45) and MDG147 (CPB147) is slightly lower in comparison to the uninoculated one (CPB), which reveals the xylanase activity of these strains (see Figure 1). However, although the final xylanase concentration was more than 10 times higher for MDG301 compared to MDG147, xylose concentrations in the corresponding cellulose pulps did not differ significantly. This fact can be explained by also taking into account the higher activity of CMCase, which balances both hemicellulose and cellulose losses. As a consequence, the glucose concentration in cellulose pulps was generally increased by enzymatic action, and this increment was higher in the case of the MDG147 strain due to the lower CMCase production during SSF. Regarding the lignin content, similar concentrations for CPB (uninoculated) and CPB147 were observed. However, this content increased due to the MDG301 action, which may have been a consequence of a lower laccase production compared to the other enzymes.

In the case of wheat straw, only MDG301 was considered; nonetheless, this strain was tested at optimum (45 °C, cellulose pulp sample CPW301.45) and non-optimum conditions (28 °C, cellulose pulp sample CPW301). The enzymatic profile shown in Figure 1 allows the confirmation of these non-optimum conditions, as xylanase only achieved less than 10% activity on the fourth day and around 2% on the seventh day compared to the optimum conditions. Moreover, slightly lower glucose content and higher xylose content were respectively obtained in sample CPW301.45 in comparison with CPW301 as a consequence of the higher CMCase/xylanase enzymatic ratio. In any case, both the glucose and xylose concentrations in the cellulose pulps obtained from wheat straw submitted to SSF significantly differ from those obtained from the uninoculated wheat straw (CPW). Moreover, these results were not similar to those observed for barley straw, highlighting the importance of the bioresource. For instance, acting on wheat straw, at optimum conditions, MDG301 was able to deeply degrade lignin's structure, reaching around 60% concentration with respect to the reference

content, i.e., the uninoculated system, while the application of non-optimum temperature only exerted a slight influence on the soluble lignin content. On the other hand, CMCase and xylanase activities obtained at optimum temperature were much higher than those observed for barley straw. Nonetheless, despite these remarkable activities, the overall concentrations of glucose and xylose increased with respect to the reference system due to a more important loss of alternative extractives and both Klason and soluble lignin occurring simultaneously. The different responses of diverse enzymatic strains in similar bio-sources have already been reported for endoglucanases [43].

3.2. TGA and FTIR Spectroscopy of Cellulose Pulps

The main characteristic parameters of cellulose pulps' thermal degradation patterns—obtained from the TGA curves depicted in Figure 2—are presented in Table 2, i.e., the temperatures at which degradation steps begin (T_{onset}) and end (T_{final}), the temperature for the maximum degradation rate (T_{max}), the weight losses (ΔW), and the final residue values.

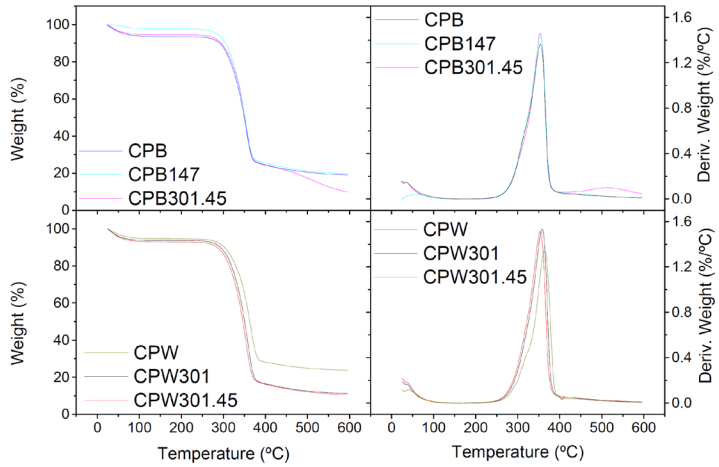

Figure 2. TGA curves, expressed as both the weight loss percentage and the associated derivative function, of (**top**) barley- and (**bottom**) wheat-straw-derived cellulose pulps.

Table 2. Characteristic thermogravimetric analysis (TGA) parameters of the cellulose pulps studied.

Sample	T_{onset} (°C)	T_{max} (°C)	T_{final} (°C)	ΔW (%)	Residue (%)
CPB	290	355	368	75	19
CPB147	288	354	368	78	20
CPB301.45	288/473	355/515	368/553	72/13	10
CPW	293	364	380	71	24
CPW301	291	358	373	82	11
CPW301.45	286	354	370	82	11

Unlike the differences reported for straws submitted to SSF treatments with *Streptomyces* and the corresponding lignin fractions obtained [16,33], the TGA profiles of cellulose pulps were very similar and not very influenced by the SSF treatments. Thus, all of them exhibited an initial water loss of around 5–7% and a similar prominent main degradation event centered at around 354–364 °C as a consequence of the cellulose chain breakage [44]; however, some remarks may be pointed out. Both CPB and CPB147 cellulose pulps demonstrated similar final residue values of around 19–20%. Nonetheless, a deeper modification was again noticed due to MDG301 action, since an additional weight-loss stage can be

detected at around 515 °C, finally reaching only 10% residue. This means that MDG301 action favors the degradation of initially stronger chemical structures, as the higher enzymatic activity can lead to the breakage of more hydrogen bonds, finally making it easier to thermally degrade cellulose [43]. On the other hand, for cellulose pulps obtained from wheat straw, very similar TGA profiles were found once submitted to SSF treatments with MDG301, regardless of the application of optimum or non-optimum temperatures, with residues of around 11% despite the already-discussed differences observed in the enzymatic patterns. On the contrary, cellulose pulp obtained from uninoculated wheat straw (CPW) exhibited higher T_{max} and residue values. These results allow us to conclude that, even though the enzymatic activity at non-optimum temperature was much smaller, it enables the removal of more easily thermally degradable products, as mentioned above, suggesting similar preferential targets regardless of the temperature.

The FTIR spectra of all the cellulose pulps studied were also very similar (see Figure 3), as the compositions were not excessively different. However, as mentioned in the introduction section, cellulose pulps may show a certain degree of crystallinity, a consequence of hydrogen bonding, which can be addressed by evaluating the peaks centered around 1430 and 893 cm^{-1} [45]. These two peaks are due to symmetric CH_2 bending vibration and C–O–C units of glucose, respectively, which are considered markers of crystallinity and amorphous behavior, respectively. Hence, the absorbance ratio between both peaks (A_{1430}/A_{893}) is considered an index to evaluate the relative crystallinity of different samples (Table 3). Therefore, higher relative crystallinity indices were obtained for cellulose pulp samples obtained from fermented barley straw in comparison to that obtained from the uninoculated one. This fact may be a consequence of the higher cellulose content and more hydroxyl groups available, which may induce hydrogen bonding. Nonetheless, the opposite behavior was, once again, observed for cellulose pulps obtained from wheat straw, where fermented samples exhibited a clear reduction in the relative crystallinity index, which is probably due to the extreme levels of the MDG301 enzymatic activity compared to those measured in barley straw (see Figure 1), then leading to very degraded systems that were not able to generate crystalline structures to such a degree, i.e., breaking of hydrogen bonding [43].

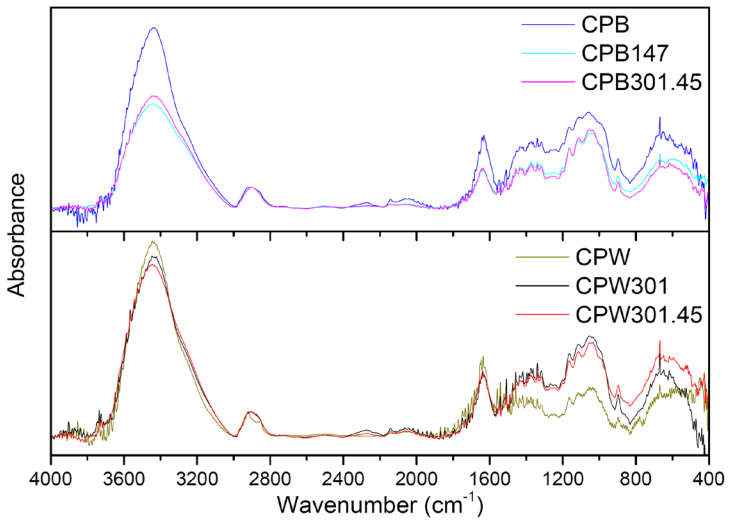

Figure 3. Fourier transform infrared (FTIR) spectra of (**top**) barley- and (**bottom**) wheat-straw-based pulps.

Table 3. Relative crystallinity index, energy related to hydrogen bonds (E_H), and polymerization degree of the cellulose pulps studied.

	Relative Crystallinity Index	E_H (kJ)	Intrinsic Viscosity (cm^3/g)	Polymerization Degree
CPB	1.24	11.31	494	1185
CPB147	1.29	11.18	492	1178
CPB301.45	1.51	11.31	700	1875
CPW	2.03	11.24	397	944
CPW301	1.45	11.31	544	1344
CPW301.45	1.10	10.78	608	1556

It is also well known that FTIR bands are shifted to lower wavenumbers when stronger interactions are formed; thereby, the strength of hydrogen bonding within the cellulose structure can also be evaluated using FTIR spectra. Thus, the higher the shifting, the higher the energy of the linkage, as expressed in Equation (2) [46]:

$$E_H = \frac{1}{K} \cdot \frac{(v_0 - v)}{v_0} \quad (2)$$

where v_0 and v are the initial wavenumber corresponding to the stretching absorption of –OH groups (3600 cm^{-1}) and the wavenumber for –OH groups once SSF-induced structural changes have occurred, respectively, whereas K is a constant whose value is 4.02×10^{-3} kJ. In this case, the E_H values are quite similar for most of the samples (see Table 3). Nonetheless, once again, the lowest energy was evinced by the CPW301-45 sample, supporting the higher degree of biological modification deduced from other techniques and analyses.

3.3. Polymerization Degree of Cellulose Pulps

The polymerization degrees of cellulose pulp samples estimated from Equation (1) have also been included in Table 3. In general, the MDG301 strain was able to produce cellulose pulps with a higher polymerization degree, especially when the strain worked at its optimum temperature. In principle, these results may be unexpected, but can be explained considering the degradation and possibly further elimination during pulping of numerous easily accessible structures and/or low-molecular-weight segments. This increment in DP has already been observed in other cellulose pulps where preferential removal of xylan was accomplished [47]. Actually, this fact results in higher proportions of stronger networks and longer cellulose chains, leading to an increase in intrinsic viscosity. Nonetheless, the MDG147 strain did not exert any influence on this parameter.

3.4. Rheology of Cellulose-Pulp-Based Oleogels

Polyurethane oleogels were obtained by simply mixing the different cellulose pulps obtained from barley and wheat straws and HDI in the castor oil medium, as detailed for lignin-based polyurethanes [29]. Using 10–15% *w/w* of thickener agent (cellulose pulp and HDI at 1/2 weight ratio), the typical gel-like response of lubricating greases was achieved, covering a relatively wide range of values for the linear viscoelastic functions [19,48], as can be seen in Figure 4. Although the frequency dependence of the small-amplitude oscillatory shear (SAOS) functions was similar in all cases, in general, higher values of both the storage, G', and the loss, G'', moduli were found when the cellulose pulps from fermented straws were used. For cellulose pulps derived from barley straw (Figure 4a), higher increments of the SAOS functions were observed when the straw was modified with the strain MDG147 (sample CPB147-15) in comparison with that modified with MDG301 (sample CPB301.45-15). This result is a consequence of the synergetic effect of both the higher cellulose content caused by the lower CMCase production and the lower lignin content, which may be due to a higher laccase production. These two opposite effects caused by cellulose and lignin concentrations have already

been reported to modulate the viscoelastic response of non-modified cellulose pulp dispersions in vegetable oils [25].

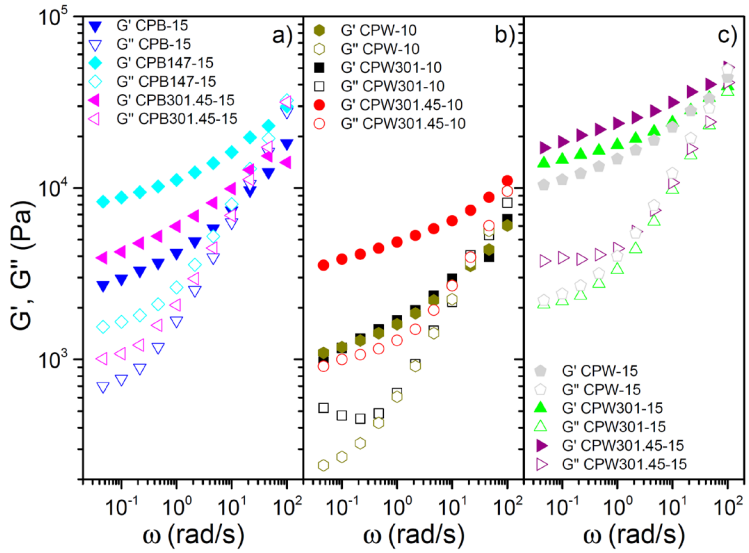

Figure 4. Evolution of the storage and loss moduli with frequency for oleogels containing (**a**) 15% barley-straw-derived cellulose-pulp-based thickener, (**b**) 10% wheat-straw-derived cellulose-pulp-based thickener, and (**c**) 15% wheat-straw-derived cellulose-pulp-based thickener.

Regarding the cellulose pulps derived from wheat straw, the slight rheological modification achieved in the polyurethane oleogels by the action of MDG301 at non-optimum temperature can be clearly observed for both thickener percentages (Figure 4b,c), as the viscoelastic response is almost identical to that obtained with the uninoculated wheat-straw-derived cellulose pulp. On the contrary, the action of the MDG301 strain at its optimum temperature (sample CPW301.45) was able to produce a noticeable increment in the SAOS functions, especially when using a 10% thickener concentration. Nonetheless, this difference is dampened to some extent at higher concentration, viz. 15%, due to the higher diisocyanate content, which can mask the biopolymer influence, as already found in previous work with lignin-based polyurethanes [22]. Again, the highest viscoelastic moduli were concomitant with the wheat-straw-derived cellulose pulps' composition, as the highest glucose/lignin ratio was shown by the sample CPW301.45 compared to the other cellulose pulps obtained from wheat straw. Furthermore, as already demonstrated in a previous work regarding lignin-based oleogels [16], a higher enzymatic activity may somehow modify the lignocellulosic structure, making it more feasible for reaction with HDI by increasing the number of available hydroxyl groups, and thus yielding stronger crosslinked networks. In addition, along with the composition, a higher polymerization degree was also pointed out to significantly increase the viscoelastic functions of physically stabilized cellulose pulp dispersions [25]. The linear viscoelastic behavior of these bio-based oleogels is similar to that shown by commercial lithium lubricating greases, which traditionally exhibit G' values of around 10^4 Pa and G" values around one order of magnitude lower, although a more extended plateau region within the frequency range studied is generally found [19].

Regarding the viscous flow behavior of these polyurethane oleogels, a markedly shear-thinning response was obtained in all cases, as shown in Figure 5, with a viscosity decay of several decades with the increasing shear rate, which is also a distinctive characteristic of traditional lubricating greases [49].

This power-law evolution, generally associated with very low values of the flow index, is, however, part of a more general and complex viscous flow behavior of this type of material (see, for instance, [18]). In fact, at very low shear rates, a tendency to achieve constant high viscosity values should be observed, although the controversy about the existence of an apparent yield stress value is still open, whereas at very high shear rates, again, constant values of limiting viscosity must be reached. However, reliable viscosity data above 100 s^{-1} are not easy to obtain in rotational rheometers as a consequence of different flow problems, like the fracture of the sample.

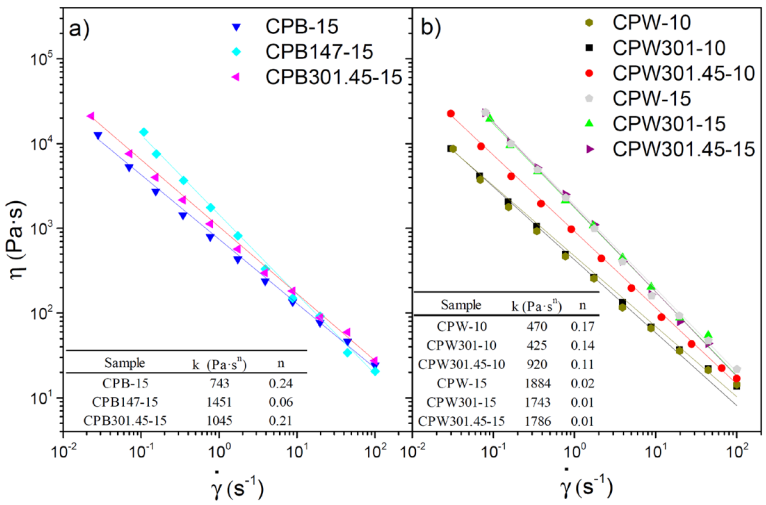

Figure 5. Viscous flow curves of polyurethane oleogels prepared with (**a**) barley- and (**b**) wheat-straw-derived cellulose pulps. Values of the consistency and flow indexes are also included as an inset.

Similarly to what was discussed for the viscoelastic response, generally, the highest viscosity values were obtained for the oleogels prepared with cellulose pulps containing higher glucose/lignin ratios. Nonetheless, at high shear rates, this tendency may be dampened, or even reversed, since more structured oleogels tend to exhibit a stronger shear-thinning character, as observed for the CPB147-15 oleogel (Figure 5a). Finally, almost identical viscosity curves were obtained for all the polyurethane oleogels prepared with wheat-straw-derived cellulose-pulp-based thickeners at 15 wt.%, revealing once again that, at this concentration, the rheological response is mainly governed by the crosslinker.

In all cases, the power-law model fits the viscous flow behavior fairly well within the shear rate range studied:

$$\eta = k \cdot \dot{\gamma}^{n-1} \quad (3)$$

where k and n are the consistency and flow indexes, respectively. The values of these fitting parameters are listed in the insets of Figure 5. As can be seen, extremely low values of the flow index, n, were always obtained, especially for the most structured systems, as discussed above, which is representative of the yielding behavior typically exhibited by lubricating greases [18]. Moreover, the k values of these oleogels are also close to those shown by commercial calcium and lithium lubricating greases and model polyolefin-thickened lithium greases, which exhibited values in the range of 600–1500 Pa·s^n [19,49], again highlighting the rheological similarity between the traditional products and the obtained ones. Finally, it is worth mentioning that the samples showing higher values of the viscoelastic functions also exhibit higher k values.

3.5. Tribological Performance

In order to test the lubrication performance of these cellulose-pulp-based polyurethane oleogels, friction and wear were assessed in a ball-on-three inclined plate steel–steel tribological contact [50] at both constant rotating speed and normal load. In all cases, highly satisfactory values of the friction coefficient were obtained, lower than those obtained when conventional greases [19] or previously functionalized cellulose-based oleogels [17] were used as lubricants. In general, the values of the friction coefficient tend to increase with the viscosity of the oleogel sample used as lubricant at high shear rates. Thus, for instance, very similar values of the friction coefficient were found for all the oleogels prepared with barley-straw-derived cellulose pulps, which presented almost identical viscosity values at high shear rates (see Figure 5a). On the contrary, cellulose pulp obtained from wheat straw submitted to SSF treatment with the MDG301 strain at its optimum temperature provided oleogels that produced slightly higher values of the friction coefficient in the tribological contact. As the oil medium was the same in all oleogel samples, these differences must be attributed to the thickener. Either the cellulose pulps containing higher cellulose pulp/lignin ratios—presumably yielding more crosslinked networks and also generally having higher DP values—favor oil entrapment, thus preventing its release, or simply the whole oleogel sample, including the thickener, can penetrate in the lubricating contact, and the highest friction is just a consequence of the higher viscosity [18]. Since the wear scars associated with the friction experiments were generally reduced when fermented-straw-derived cellulose pulps were used as a thickener agent, the second assumption seems to be more feasible. The observation of the wear scars generated during the friction tests (see some examples in Figure 6) allows us to conclude that the main wear mechanism was abrasion, supporting the idea that thickener particles penetrate into the mating surface, thus contributing to increased friction, especially at higher concentrations. These marks were evaluated in terms of both parallel-to-spin diameter and scar area (data shown in Table 4). As mentioned above, lower scar sizes were measured when cellulose pulps obtained from straw submitted to SSF treatments were employed, especially those resulting from the MDG301 action at its optimum temperature. Overall, outstanding wear values were obtained, lower than those found with commercial and other bio-based lubricating greases [51,52].

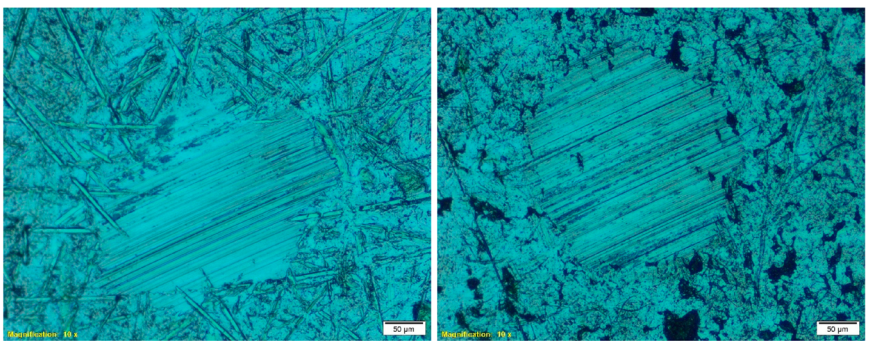

Figure 6. Selected pictures of wear marks produced during the tribological tests when using polyurethane oleogels prepared with barley- (CPB147-15) (**left**) or wheat- (CPW301.45-10) (**right**) straw-derived cellulose pulps as lubricants.

Table 4. Values of the friction coefficient and sizes of wear scars.

Oleogels	Friction Coefficient	Wear Scar Surface (μm^2)	Wear Scar Diameter (μm)
CPB-15	0.081 ± 0.003	55,640 ± 2803	315 ± 32
CPB147-15	0.082 ± 0.003	41,024 ± 14,467	263 ± 69
CPB301.45-15	0.089 ± 0.006	28,551 ± 5918	190 ± 28
CPW-10	0.077 ± 0.003	35,669 ± 5704	217 ± 24
CPW301-10	0.077 ± 0.006	105,796 ± 7362	366 ± 2
CPW301.45-10	0.085 ± 0.006	63,314 ± 13,295	286 ± 23
CPW-15	0.099 ± 0.010	35,148 ± 504	215 ± 23
CPW301-15	0.088 ± 0.010	22,306 ± 11,749	161 ± 23
CPW301.45-15	0.108 ± 0.013	25,205 ± 3769	193 ± 30

4. Conclusions

The modification of the lignocellulosic structures of both wheat and barley straw was accomplished through the action of the *Streptomyces* sp. MDG147 and MDG301 strains, also leading to alteration of the derived cellulosic pulps, which were further used to prepare polyurethane oleogels. This modification, as demonstrated by the lignocellulosic composition, is a reflection of the enzymatic activity pattern developed, which was also demonstrated to significantly affect the crystalline structure and polymerization degree of cellulose. The MDG301 strain caused more important modifications of the cellulose pulps, especially on those derived from wheat straw, when working at its optimum temperature, generally yielding a higher cellulose/lignin ratio and polymerization degree. These modifications had direct and significant impacts on the rheological and tribological behaviors of the polyurethane oleogels prepared with these cellulose pulps. SSF treatments to which the wheat and barley straws were previously subjected proved to be effective in enhancing the strength of the resulting oleogels, thereby increasing the values of both linear viscoelastic functions and viscosity. In addition, these oleogels showed outstanding frictional and wear behaviors when used as lubricants in a tribological contact, with similar or even lower values of both the friction coefficient and the size of resulting wear marks than those found in commercial lubricating greases. Overall, fermented-straw-derived cellulose pulps can be conclusively proposed as effective thickeners for preparing polyurethane oleogels with tunable properties depending on the biological modifications, as well as a potential substitute for non-renewable gelling agents in lubricating grease formulations.

Author Contributions: Conceptualization: A.M.B.-L., C.V., M.H., M.E.E., and J.M.F.; Formal analysis: A.M.B.-L., A.B., and M.E.E.; Funding acquisition: C.V., M.E.E., and J.M.F.; Investigation: A.M.B.-L. and A.B.; Methodology: A.M.B.-L., C.V., M.H., and M.E.E.; Project administration: M.E.E. and J.M.F.; Supervision: C.V. and J.M.F.; Writing—original draft: A.M.B.-L.; Writing—review and editing: J.M.F. All authors have read and agreed to the published version of the manuscript.

Funding: This work is part of two coordinated research projects (RTI2018-096080-B-C21 and RTI2018-096080-B-C22) sponsored by MICIU-FEDER. A.M.B.-L. has received a Ph.D. Research Grant from the Ministerio de Educación, Cultura y Deporte (FPU16/03697). We gratefully acknowledge the financial support.

Conflicts of Interest: The authors declare no conflict of interest.

References

1. Cao, Z.; Fan, Z.; Chen, Y.; Li, M.; Shen, T.; Zhu, C.; Ying, H. Efficient preparation of 5-hydroxymethylfurfural from cellulose in a biphasic system over hafnyl phosphates. *Appl. Catal. B Environ.* **2019**, *244*, 170–177. [CrossRef]
2. Choi, H.Y.; Jeong, Y.G. Microstructures and piezoelectric performance of eco-friendly composite films based on nanocellulose and barium titanate nanoparticle. *Compos. Part B Eng.* **2019**, *168*, 58–65. [CrossRef]
3. Younesi, M.; Akkus, A.; Akkus, O. Microbially-derived nanofibrous cellulose polymer for connective tissue regeneration. *Mater. Sci. Eng. C* **2019**, *99*, 96–102. [CrossRef] [PubMed]

4. Amarasekara, A.S.; Gutierrez Reyes, C.D. Brønsted acidic ionic liquid catalyzed one-pot conversion of cellulose to furanic biocrude and identification of the products using LC-MS. *Renew. Energy* **2019**, *136*, 352–357. [CrossRef]
5. Wu, Q.; Zhang, G.; Gao, M.; Cao, S.; Li, L.; Liu, S.; Xie, C.; Huang, L.; Yu, S.; Ragauskas, A.J. Clean production of 5-hydroxymethylfurfural from cellulose using a hydrothermal/biomass-based carbon catalyst. *J. Clean. Prod.* **2019**, *213*, 1096–1102. [CrossRef]
6. Manan, F.A.A.; Hong, W.W.; Abdullah, J.; Yusof, N.A.; Ahmad, I. Nanocrystalline cellulose decorated quantum dots based tyrosinase biosensor for phenol determination. *Mater. Sci. Eng. C* **2019**, *99*, 37–46. [CrossRef]
7. Konuklu, Y.; Erzin, F.; Akar, H.B.; Turan, A.M. Cellulose-based myristic acid composites for thermal energy storage applications. *Sol. Energy Mater. Sol. Cells* **2019**, *193*, 85–91. [CrossRef]
8. Vasiljevic, L.; Pavlović, S. Biodegradable polymers based on proteins and carbohydrates. In *Advances in Applications of Industrial Biomaterials*; Pellicer, E., Nikolic, D., Sort, J., Baró, M.D., Zivic, F., Grujovic, N., Grujic, R., Pelemis, S., Eds.; Springer: New York, NY, USA, 2017; pp. 87–101. [CrossRef]
9. Tripathi, A.; Parsons, G.N.; Khan, S.A.; Rojas, O.J. Synthesis of organic aerogels with tailorable morphology and strength by controlled solvent swelling following Hansen solubility. *Sci. Rep.* **2018**, *8*, 2106. [CrossRef]
10. Tripathi, A.; Parsons, G.N.; Rojas, O.J.; Khan, S.A. Featherlight, mechanically robust cellulose ester aerogels for environmental remediation. *ACS Omega* **2017**, *2*, 4297–4305. [CrossRef]
11. Wang, Q.; Wang, Y.; Chen, L. A green composite hydrogel based on cellulose and clay as efficient absorbent of colored organic effluent. *Carbohydr. Polym.* **2019**, *210*, 314–321. [CrossRef]
12. Singh, A.; Sarkar, D.J.; Mittal, S.; Dhaka, R.; Maiti, P.; Singh, A.; Raghav, T.; Solanki, D.; Ahmed, N.; Singh, S.B. Zeolite reinforced carboxymethyl cellulose-Na^+-*g*-*cl*-poly(AAm) hydrogel composites with pH responsive phosphate release behavior. *J. Appl. Polym. Sci.* **2019**, *136*, 47332. [CrossRef]
13. Gallego, R.; Arteaga, J.F.; Valencia, C.; Franco, J.M. Chemical modification of methyl cellulose with HMDI to modulate the thickening properties in castor oil. *Cellulose* **2013**, *20*, 495–507. [CrossRef]
14. Gallego, R.; Arteaga, J.F.; Valencia, C.; Franco, J.M. Thickening properties of several NCO-functionalized cellulose derivatives in castor oil. *Chem. Eng. Sci.* **2015**, *134*, 260–268. [CrossRef]
15. Gallego, R.; Arteaga, J.F.; Valencia, C.; Franco, J.M. Rheology and thermal degradation of isocyanate-functionalized methyl cellulose-based oleogels. *Carbohydr. Polym.* **2013**, *98*, 152–160. [CrossRef] [PubMed]
16. Borrero-López, A.M.; Blánquez, A.; Valencia, C.; Hernández, M.; Arias, M.E.; Eugenio, M.E.; Fillat, Ú.; Franco, J.M. Valorization of soda lignin from wheat straw solid-state fermentation: Production of oleogels. *ACS Sustain. Chem. Eng.* **2018**, *6*, 5198–5205. [CrossRef]
17. Gallego, R.; Arteaga, J.F.; Valencia, C.; Díaz, M.J.; Franco, J.M. Gel-like dispersions of HMDI-cross-linked lignocellulosic materials in castor oil: Toward completely renewable lubricating grease formulations. *ACS Sustain. Chem. Eng.* **2015**, *3*, 2130–2141. [CrossRef]
18. Delgado, M.; Secouard, S.; Valencia, C.; Franco, J. On the Steady-State Flow and Yielding Behaviour of Lubricating Greases. *Fluids* **2019**, *4*, 6. [CrossRef]
19. Sánchez, R.; Valencia, C.; Franco, J.M. Rheological and Tribological Characterization of a New Acylated Chitosan-Based Biodegradable Lubricating Grease: A Comparative Study with Traditional Lithium and Calcium Greases. *Tribol. Trans.* **2014**, *57*, 445–454. [CrossRef]
20. Sánchez, R.; Stringari, G.B.; Franco, J.M.; Valencia, C.; Gallegos, C. Use of chitin, chitosan and acylated derivatives as thickener agents of vegetable oils for bio-lubricant applications. *Carbohydr. Polym.* **2011**, *85*, 705–714. [CrossRef]
21. Borrero-López, A.M.; Martín-Sampedro, R.; Ibarra, D.; Valencia, C.; Eugenio, M.E.; Franco, J.M. Evaluation of lignin-enriched side-streams from different biomass conversion processes as thickeners in bio-lubricant formulations. *Int. J. Biol. Macromol.* **2020**, *162*, 1398–1413. [CrossRef]
22. Borrero-López, A.M.; Valencia, C.; Franco, J.M. Rheology of lignin-based chemical oleogels prepared using diisocyanate crosslinkers: Effect of the diisocyanate and curing kinetics. *Eur. Polym. J.* **2017**, *89*, 311–323. [CrossRef]
23. Cortés-Triviño, E.; Valencia, C.; Franco, J.M. Influence of epoxidation conditions on the rheological properties of gel-like dispersions of epoxidized kraft lignin in castor oil. *Holzforschung* **2017**, *71*, 777–784. [CrossRef]

24. Cortés-Triviño, E.; Valencia, C.; Delgado, M.A.; Franco, J.M. Rheology of epoxidized cellulose pulp gel-like dispersions in castor oil: Influence of epoxidation degree and the epoxide chemical structure. *Carbohydr. Polym.* **2018**, *199*, 563–571. [CrossRef]
25. Núñez, N.; Martín-Alfonso, J.E.; Eugenio, M.E.; Valencia, C.; Díaz, M.J.; Franco, J.M. Preparation and characterization of gel-like dispersions based on cellulosic pulps and castor oil for lubricant applications. *Ind. Eng. Chem. Res.* **2011**, *50*, 5618–5627. [CrossRef]
26. Núñez, N.; Martín-Alfonso, J.E.; Valencia, C.; Sánchez, M.C.; Franco, J.M. Rheology of new green lubricating grease formulations containing cellulose pulp and its methylated derivative as thickener agents. *Ind. Crops Prod.* **2012**, *37*, 500–507. [CrossRef]
27. Martín-Alfonso, J.E.; Yañez, R.; Valencia, C.; Franco, J.M.; Díaz, M.J. Optimization of the methylation conditions of kraft cellulose pulp for its use as a thickener agent in biodegradable lubricating greases. *Ind. Eng. Chem. Res.* **2009**, *48*, 6765–6771. [CrossRef]
28. Martín-Alfonso, J.E.; Núñez, N.; Valencia, C.; Franco, J.M.; Díaz, M.J. Formulation of new biodegradable lubricating greases using ethylated cellulose pulp as thickener agent. *J. Ind. Eng. Chem.* **2011**, *17*, 818–823. [CrossRef]
29. Borrero-López, A.M.; Valencia, C.; Franco, J.M. Green and facile procedure for the preparation of liquid and gel-like polyurethanes based on castor oil and lignin: Effect of processing conditions on the rheological properties. *J. Clean. Prod.* **2020**, *277*, 123367. [CrossRef]
30. Thomas, V.; Jayabalan, M. Studies on the effect of virtual crosslinking on the hydrolytic stability of novel aliphatic polyurethane ureas for blood contact applications. *J. Biomed. Mater. Res.* **2001**, *56*, 144–157. [CrossRef]
31. Panda, S.S.; Panda, B.P.; Mohanty, S.; Nayak, S.K. The castor oil based water borne polyurethane dispersion; effect of -NCO/OH content: Synthesis, characterization and properties. *Green Process. Synth.* **2016**, *6*, 341–351. [CrossRef]
32. Labafzadeh, S.R. Cellulose-Based Materials. Ph.D. Thesis, University of Helsinki, Helsinki, Finland, 2015.
33. Huang, L.; Sun, N.; Ban, L.; Wang, Y.; Yang, H. Ability of different edible fungi to degrade crop straw. *AMB Express* **2019**, *9*, 4. [CrossRef] [PubMed]
34. Becarelli, S.; Chicca, I.; Siracusa, G.; La China, S.; Gentini, A.; Lorenzi, R.; Munz, G.; Petroni, G.; Levin, D.B.; Di Gregorio, S. Hydrocarbonoclastic Ascomycetes to enhance co-composting of total petroleum hydrocarbon (TPH) contaminated dredged sediments and lignocellulosic matrices. *New Biotechnol.* **2019**, *50*, 27–36. [CrossRef] [PubMed]
35. Vila-Costa, M.; Sebastián, M.; Pizarro, M.; Cerro-Gálvez, E.; Lundin, D.; Gasol, J.M.; Dachs, J. Microbial consumption of organophosphate esters in seawater under phosphorus limited conditions. *Sci. Rep.* **2019**, *9*, 233. [CrossRef] [PubMed]
36. Saarela, M.H. Safety aspects of next generation probiotics. *Curr. Opin. Food Sci.* **2019**, *30*, 8–13. [CrossRef]
37. Kasli, I.M.; Thomas, O.R.T.; Overton, T.W. Use of a design of experiments approach to optimise production of a recombinant antibody fragment in the periplasm of *Escherichia coli*: Selection of signal peptide and optimal growth conditions. *AMB Express* **2019**, *9*, 5. [CrossRef] [PubMed]
38. Arias, M.E.; Blánquez, A.; Hernández, M.; Rodríguez, J.; Ball, A.S.; Jiménez-Morillo, N.T.; González-Vila, F.J.; González-Pérez, J.A. Role of a thermostable laccase produced by *Streptomyces ipomoeae* in the degradation of wheat straw lignin in solid state fermentation. *J. Anal. Appl. Pyrolysis* **2016**, *122*, 202–208. [CrossRef]
39. Borrero-López, A.M.; Blánquez, A.; Valencia, C.; Hernández, M.; Arias, M.E.; Franco, J.M. Influence of solid-state fermentation with *Streptomyces* on the ability of wheat and barley straws to thicken castor oil for lubricating purposes. *Ind. Crops Prod.* **2019**, *140*, 111625. [CrossRef]
40. Kiiskinen, L.L.; Palonen, H.; Linder, M.; Viikari, L.; Kruus, K. Laccase from *Melanocarpus albomyces* binds effectively to cellulose. *FEBS Lett.* **2004**, *576*, 251–255. [CrossRef]
41. Saarinen, T.; Orelma, H.; Grönqvist, S.; Andberg, M.; Holappa, S.; Laine, J. Adsorption of different laccases on cellulose and lignin surfaces. *Bioresources* **2009**, *4*, 94–110.
42. De Souza, W.R. Microbial degradation of lignocellulosic biomass. In *Sustainable Degradation of Lignocellulosic Biomass—Techniques, Applications and Commercialization*; Chandel, A., Ed.; IntechOpen: London, UK, 2013; pp. 207–248. [CrossRef]
43. Quintana, E. Enzymatic and Chemical Treatments to Obtain Pulps with High-Cellulose Content. Ph.D. Thesis, Universitat Politècnica de Catalunya, Barcelona, Spain, 2016.

44. Liu, C.; Wang, H.; Karim, A.M.; Sun, J.; Wang, Y. Catalytic fast pyrolysis of lignocellulosic biomass. *Chem. Soc. Rev.* **2014**, *43*, 7594–7623. [CrossRef] [PubMed]
45. Ciolacu, D.; Ciolacu, F.; Popa, V.I. Amorphous cellulose—Structure and characterization. *Cell. Chem. Technol.* **2011**, *45*, 13–21.
46. Ciolacu, D.; Kovac, J.; Kokol, V. The effect of the cellulose-binding domain from *Clostridium cellulovorans* on the supramolecular structure of cellulose fibers. *Carbohydr. Res.* **2010**, *345*, 621–630. [CrossRef] [PubMed]
47. Janzon, R.; Puls, J.; Bohn, A.; Potthast, A.; Saake, B. Upgrading of paper grade pulps to dissolving pulps by nitren extraction: Yields, molecular and supramolecular structures of nitren extracted pulps. *Cellulose* **2008**, *15*, 739. [CrossRef]
48. Martín-Alfonso, J.E.; Valencia, C.; Sánchez, M.C.; Franco, J.M.; Gallegos, C. Evaluation of different polyolefins as rheology modifier additives in lubricating grease formulations. *Mater. Chem. Phys.* **2011**, *128*, 530–538. [CrossRef]
49. Martín-Alfonso, J.E.; Valencia, C.; Sánchez, M.C.; Franco, J.M.; Gallegos, C. Rheological modification of lubricating greases with recycled polymers from different plastics waste. *Ind. Eng. Chem. Res.* **2009**, *48*, 4136–4144. [CrossRef]
50. Heyer, P.; Läuger, J. Correlation between friction and flow of lubricating greases in a new tribometer device. *Lubr. Sci.* **2009**, *21*, 253–268. [CrossRef]
51. Delgado, M.A.; Cortés-Triviño, E.; Valencia, C.; Franco, J.M. Tribological study of epoxide-functionalized alkali lignin-based gel-like biogreases. *Tribol. Int.* **2020**, *146*, 106231. [CrossRef]
52. Gallego, R.; Cidade, T.; Sánchez, R.; Valencia, C.; Franco, J.M. Tribological behaviour of novel chemically modified biopolymer-thickened lubricating greases investigated in a steel–steel rotating ball-on-three plates tribology cell. *Tribol. Int.* **2016**, *94*, 652–660. [CrossRef]

3.3. Article 7

Valorization of Soda Lignin from Wheat Straw Solid-State Fermentation: Production of Oleogels

A.M. Borrero-López, A. Blánquez, C. Valencia, M. Hernández, M.E. Arias, M.E. Eugenio, U. Fillat, J.M. Franco

Published in:

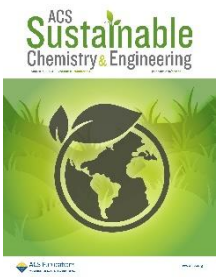

ACS Sustainable Chemistry & Engineering
Publishing Company: ACS
Editor-in-Chief: DT. Allen
Volume 6, pp 9198-5205
Year 2018
ISSN 2168-0485
DOI: 10.1021/acssuschemeng.7b04846

Category	Journal Rank / Total number of journals	Quartile (Percentage)
Chemistry, Multidisciplinary	26/172	Q1 (85%)
Green & Sustainable Science & Technology	5/35	Q1 (87%)
Engineering, Chemical	9/138	Q1 (94%)
Impact Factor	6.970	

4. Use of lignin from solid-state fermentation with *Streptomyces* as binder for adhesive formulations

4.1. Article 8

Rheology and adhesion performance of bio-sourced adhesives formulated with lignins from agricultural waste straws submitted to solid-state fermentation

A.M. Borrero-López, C. Valencia, G. Domínguez, M.E. Eugenio, J.M. Franco

Submitted to:

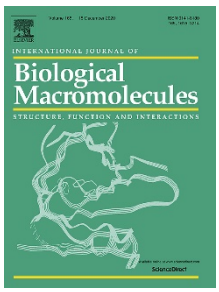

International Journal of Biological Macromolecules
Publishing Company: Elsevier
Editor-in-Chief: A. Dong, JF. Kennedy
Year 2021
ISSN 0141-8130

Category	Journal Rank / Total number of journals	Quartile (Percentage)
Biochemistry & Molecular Biology	51/297	Q1 (83%)
Chemistry, Applied	10/71	Q1 (87%)
Polymer Science	9/89	Q1 (90%)
Impact Factor	5.162	

5. Use of lignin as filler for elastomeric cushioning formulations

5.1. Article 9

Lignin effect in castor oil-based elastomers: Reaching new limits in rheological and cushioning behaviors

A.M. Borrero-López, L. Wang, C. Valencia, J.M. Franco, O.J. Rojas

Published in:

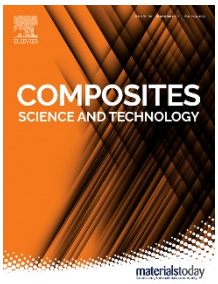

Composites Science & Technology
Publishing Company: Elsevier
Editor-in-Chief: Karl Schulte
Volume 203, 108602
Year 2021
ISSN 0266-3538
DOI: 10.1016/j.compscitech.2020.108602

Category	Journal Rank / Total number of journals	Quartile (Percentage)
Material Science, Composites	2/26	Q1 (94%)
Impact Factor	7.094	

Composites Science and Technology 203 (2021) 108602

Contents lists available at ScienceDirect

Composites Science and Technology

journal homepage: http://www.elsevier.com/locate/compscitech

Lignin effect in castor oil-based elastomers: Reaching new limits in rheological and cushioning behaviors

Antonio M. Borrero-López [a,*], Ling Wang [b], Concepción Valencia [a], José M. Franco [a], Orlando J. Rojas [b,c]

[a] Pro²TecS – Chemical Process and Product Technology Research Centre, Dept. Ingeniería Química, ETSI, Universidad de Huelva, 21071, Huelva, Spain
[b] Department of Bioproducts and Biosystems, School of Chemical Engineering, Aalto University, P.O. Box 16300, FIN-00076, Espoo, Finland
[c] Bioproducts Institute, Departments of Chemical and Biological Engineering, Chemistry and Wood Science, 2360 East Mall, The University of British Columbia, Vancouver, BC V6T 1Z3, Canada

ARTICLE INFO

Keywords:
Polymer-matrix composites
Particle-reinforcement
Rheological properties
Mechanical testing
Bio-based composites

ABSTRACT

Lignin is demonstrated as an unprecedented reinforcing material that tailors the rheological and cushioning properties of castor oil-based polyurethane elastomers, expanding their viscoelastic moduli by four orders of magnitude. The tensile strain at break was triplicated in the presence of lignin while the Young modulus and the stress at break were enhanced 17- and 7-fold, respectively. Remarkably, in compression tests, lignin addition increased the stresses at break by more than 88-fold, whereas the strain at failure shifted from 50 to 93%. Dynamic mechanical compression tests indicated outstanding cushioning and resistance performance. Overall, the results demonstrate a performance not reached before for biosourced elastomeric materials, fitting the demands of a wide range of applications.

1. Introduction

Owing to factors such as resource sufficiency and the need for greener materials, there is a high demand for biobased materials that are able to substitute or enhance those based on non-renewable sources [1]. According to the biorefinery concept, chemical intermediates and end-use materials can be produced in an integrated industrial process under the principles of green chemistry and engineering [2]. As a by-product of cellulosic pulp production, lignin may play a fundamental role since it is otherwise combusted for energy and chemical recovery [3]. Its production, amounting >50 million tons annually, makes lignin a widely available and low-cost bioresource suitable to substitute or partially replace non-renewables in given applications [4]. For instance, lignin possesses abundant functional groups, such as phenolic and aliphatic hydroxyl, carbonyl, carboxyl and methoxyl groups, which are available throughout a complex aromatic macromolecular structure [5], combining main phenylpropane units, namely, syringyl, guaiacyl and *p*-hydroxyphenyl. Technical lignin has been proposed as a key component or intermediate for end-use products, such as lubricating greases [6,7], foams [3], adhesives, coatings, or fine chemicals, among others [8].

Lignin has been used as a component in polyurethanes based on non-renewable polyols but full replacement of the latter, i.e., as the main component, has been challenging [3]. Moreover, environmentally friendly, fully biosourced and biodegradable or partially biodegradable bioproducts have considered composites of lignin with castor oil [6,7,9], poly (ε-caprolactone) [10] or polylactic acid [11], all of which replace petroleum-based counterparts while maintaining the expected performance. Specially, compared to other vegetable oils, castor oil displays a high viscosity and thermal stability. Its low cost, availability and purity make castor oil a significant alternative precursor for bioproducts and biochemicals [12]. Combined with lignin, the hydroxyl groups present in castor oil's fatty acid chains make them attractive as polyol source in polyurethanes (PU). Depending on diisocyanate type, processing, and composition, lignin- and castor oil-based PUs allow a great range of possible materials and applications, including oleogels, thermoplastics, elastomers, films, foams or composites [6,7,13–16]. In particular, owing to their cushioning and resilience properties, related elastomers have been applied for flooring (sport indoor courts), footwear, surfboards, car interiors and household products [17]. Nonetheless, castor oil-based PU elastomers generally exhibit poor mechanical performance due to the dangling fatty acid chains of triglycerides [18]. The mechanical

* Corresponding author.
E-mail address: am.borrero@diq.uhu.es (A.M. Borrero-López).

https://doi.org/10.1016/j.compscitech.2020.108602
Received 18 September 2020; Received in revised form 27 November 2020; Accepted 3 December 2020
Available online 8 December 2020

properties, however, can be adjusted considering the soft segments (SS) (basically castor oil domains) and hard segments (HS) (urea/urethane bonds) in PUs, with a superior strength observed at lower thermodynamic compatibility [18]. Upgrading the HS content may be possible by increasing diisocyanate concentration; unfortunately, this comes at the cost of reduced ductility [18,19]. As a consequence, nanoparticles, natural compounds, ceramic platelets and biopolymers have been used as fillers to adjust the crosslinking density needed and to increase both strength and resistance [19–21]. It is in this domain where lignin can play a determining role, e.g., acting as reinforcement in the PU structure and improving the mechanical properties [3,17]. Jeong et al. [16] developed polyethylene glycol (PEG) and acetylated lignin-based PUs with outstanding elastomeric properties, whose elongations at break were >2000%. Likewise, Zhang et al. [22] proposed PEG-based PU elastomers with excellent tensile properties using oxidized lignin as copolymer. By using polypropylene glycol as copolymer, Lang et al. [23] demonstrated lignin addition of up to 60% to increase the elastomeric viscoelastic functions, by up to six-fold, compared to the lignin-free system. In the search for fully-renewable copolymers, castor oil alone led to PUs with relatively poor elastomeric properties, with elongations <130% [12–15]. However, improved tensile properties were found by combining castor oil with polycaprolactone [24] or PEG [25,26]. Moreover, castor oil- and lignin-based elastomers crosslinked with diphenylmethane-4,4′-diisocyanate (MDI) showed good tensile results, but mainly when castor oil was chemically modified to increase the hydroxyl index [13]. Despite these advances, no reports exist on the mechanical evaluation of related elastomers considering the response to static and dynamic compression, relevant to cushioning applications. Indeed, energy loss, compressibility and elongation, recoverability after strain and fatigue endurance are some of the main properties needed in suitable cushioning elastomers.

In this study, castor oil, lignin and hexamethylene diisocyanate (HDI) were used as oleo-based, eco-friendly and efficient PU elastomer. The rheological and cushioning properties were investigated, in light of the role of lignin compared to other well-known fillers (such as cellulose and silica nanoparticles).

2. Materials & methods

2.1. Materials

Castor oil, hexamethylene diisocyanate (HDI), silica nanoparticles (40–63 μm), toluene and triethylamine were purchased from Merck (Finland) and used as received. Indulin AT, a purified form of kraft pine lignin, in the following referred only as lignin, was obtained from MeadWestvaco (USA). Detailed information about it can be found elsewhere [27]. Cellulose was directly obtained by milling paper produced from softwood (pine) fibers.

2.2. Lignin functionalization and preparation of the oleo-PU

The oleo-PUs were produced by following a two-step process [7], with lignin first functionalized with HDI, and subsequently dispersed in castor oil (see Fig. 1). In brief, in the first step, 100 mL toluene and a certain amount of lignin were introduced and sealed in a three-neck round bottom flask. Following, a 30-min conditioning that removed residual moisture was carried out by sparging nitrogen into the lignin-toluene system. HDI and triethylamine catalyst were then added. The concentrations of the HDI (8.33–25 wt%) and the catalyst (1/1 HDI/catalyst w/w ratio) were varied in order to investigate their effect on the mechanical properties of the ensuing PUs. The mixture was maintained for 24 h at room temperature under vigorous agitation, followed by rotary evaporation to recover toluene and the catalyst (80 °C), resulting in the functionalized lignin. In a second step, the functionalized lignin was immediately introduced in a 100 mL stainless-steel reactor together with castor oil, and the mixture was

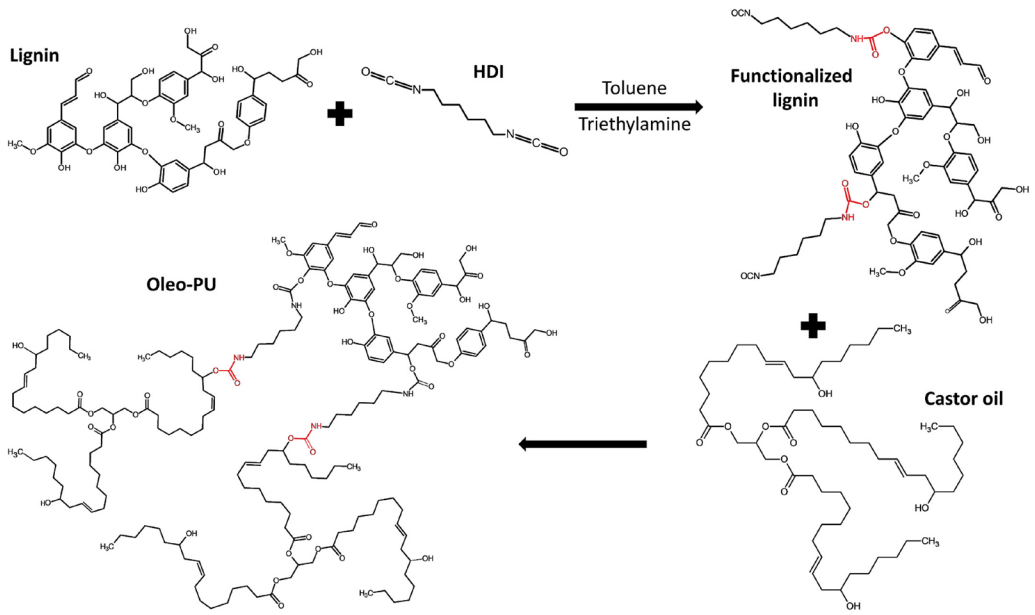

Fig. 1. Reaction scheme for lignin functionalization and oleo-PU formation through crosslinking with castor oil. The urethane links formed in each step are marked in red. (For interpretation of the references to colour in this figure legend, the reader is referred to the Web version of this article.)

gently stirred at 70 rpm by using a magnetic stirrer (RW 20 model, IKA, Germany) for another 24 h at room temperature. Once the process was completed, the mixture was poured into molds for curing (one month) and to completely purge any remaining isocyanates in the mixture. The respective oleo-polyurethane sample ("oleo-PU" or, for simplicity, "PU") was then subjected to mechanical and rheological characterization. The preparation of the reference sample (lignin-free polyurethane), termed herein as "PU0", was carried following the same procedure described above, except for replacing lignin in this first step with an equivalent amount of castor oil (1/2 castor oil/HDI w/w ratio in this case).

Lignin loading (4.16–16.67 wt%) was adjusted with respect to castor oil, to evaluate its role and to compare the obtained PUs with the reference as well as those obtained by using other fillers, namely, silica nanoparticles and cellulose (8.33 wt%, 1/2 filler/HDI ratio). The samples studied are listed in Table 1, and referred to as "PUX(Y)" where "X" represents the lignin concentration and "Y" the lignin/HDI w/w ratio.

2.3. Characterization

The thermal stability of the different samples was assessed by thermogravimetry (Q500 thermal analyser, TA Instruments, USA). The testing protocol used heating to 600 °C (10 °C·min^{-1}), with a conditioning step at 30 °C. The experiments were performed under nitrogen atmosphere.

Fourier transform infrared spectroscopy (FTIR) measurements were collected by using a Nicolet 380 FT-IR (Thermo Scientific, USA) spectrometer. Measurements were performed from 500 to 4000 cm^{-1} wavenumbers with a resolution of 4 cm^{-1}.

Differential scanning calorimetry (DSC) spectra were obtained by using a Q100 equipment (TA Instruments, USA). In order to eliminate the thermal history, a cycle was first applied by heating the sample from −80 to 250 °C (10 °C·min^{-1}) followed by cooling to −80 °C at the same rate. Immediately thereafter, a new heating cycle was performed.

The surface topography of the PU samples was analyzed by means of field emission scanning electron microscopy (SEM) using a Zeiss Sigma VP microscope (Carl Zeiss Microscopy Ltd, UK). Prior to imaging, the samples were sputter-coated with 6 nm-thick gold layer.

The water contact angle (WCA) of the PUs was measured with a force tensiometer (Sigma 70, UK) equipped with a COHU solid-state CCD monochrome camera. A 6 μL water droplet was placed on the surface of the PUs, and the angle was carefully calculated by using the OneAttension software.

Strain sweeps, small-amplitude oscillatory shear and torsional (SAOS and SAOT) tests at different temperatures, and temperature sweeps were performed by using an Ares-G2 (TA Instruments, USA) equipped with either a rough plate-plate or a torsional geometry, depending on the consistency of the sample. The temperature was controlled by using a convection oven coupled to the rheometer. Generally, SAOS & SAOT tests were carried out between 0.03 and 100 rad s^{-1}, at 25 °C, and eventually at higher constant temperatures, in the range of 40–200 °C.

Table 1
Composition of the oleo-PUs.

Sample	Castor oil (wt%)	Lignin (wt%)	HDI (wt%)
PU0	83.33	0	16.67
PU8(1/2)	75.00	8.33	16.67
PU4(1/4)	79.16	4.16	16.67
PU17(1/1)	66.66	16.67	16.67
PU8(1/1)	83.34	8.33	8.33
PU8(1/3)	66.66	8.33	25.00
		Cellulose (wt%)	
CEL-PU	75.00	8.33	16.67
		Silica nanoparticles (wt%)	
SIL-PU	75.00	8.33	16.67

For the temperature sweeps (1 rad s^{-1}), a constant heating ramp (1 °C·min^{-1}) was applied from 30 °C to 200 °C, followed by a cooling step at the same decreasing rate, down to 30 °C. The rheological tests were carried out within the linear viscoelastic range, previously identified by performing strain sweeps at the lowest and the highest temperatures.

Static tensile and compression tests were performed indistinctly in an AG-IS Universal Testing Machine (Shimadzu, Japan) and a 4204 Universal Tester (Instron, USA). Rates of 10 and 5 mm min^{-1} were applied for the tensile and compression tests, respectively. Different load cells, from 1 kN to 10 kN, were used depending on the toughness of the sample. The compression results were well fitted to the model of Bian et al. (2018) [28]:

$$\sigma_c = A\cdot(e^{B\cdot\gamma_c} - 1) \quad (1)$$

where A and B are fitting parameters and γ_c represents the compressive strain of the sample.

Dynamic mechanical compression analyses were carried out using a TA.XT Plus Texture Analyser (Stable Micro Systems, UK). Given loads (equivalent to 0.35–0.70 MPa) and test lengths (70 s–24 h) were applied at a constant compressive rate of 0.5 cycles·s^{-1}. The cushioning performance, determined as the energy the system is able to dissipate per unit area, was evaluated by the cushioning factor (CF) [1]:

$$CF = \frac{T\cdot L}{E} \quad (2)$$

where T is the initial thickness of the test specimen, L the load at the maximum strain applied and E the required energy to produce the deformation (area under the curve of the load applied vs. the strain achieved), respectively.

3. Results and discussion

3.1. Thermogravimetric and FTIR analysis

The thermal decomposition profiles and FTIR spectra of castor oil and lignin, the functionalized castor oil and lignin, both at 1/2 biosource/HDI weight ratio, and the PU0 and PU8(1/2) systems are described in detail in the Supporting Information document. Compared to the functionalized castor oil, and due to the higher –OH group content, a lower free HDI content (and consequently a higher crosslinked structure) was observed in the thermograms of the functionalized lignin (see Fig. S1 and Table S1, Supporting Information). The results were related to the thermogravimetric observations of the corresponding oleogels with the free HDI content in the functionalized specimens tracking with the HDI available during the second step. Therefore, a more extensive crosslinking during the second step was achieved at a higher remaining free HDI content, which resulted in greater mass loss at temperatures higher than those corresponding to the main loss event, characteristic of the non-modified castor oil. The urethane formation was likewise confirmed in the FTIR spectra of functionalized castor oil and lignin, by observing the new peaks emerging from N–H stretching vibration (see Fig. S2). Moreover, the intensity of the peak at around 2270 cm^{-1} in the oleo-PU spectra allowed to follow the curing process and to ensure a complete reaction of free isocyanates.

3.2. Microstructural and topographical analysis

SEM micrographs of both the surface and the cross section of selected oleo-PUs are displayed in Fig. S3. Quite smooth surfaces were observed for both PU0 and PU8(1/2), with some small clusters apparent at low magnifications. Nonetheless, some large features also appeared for PU8 (1/2), which became more prominent in cross section images, as a consequence of the colloidal size of the lignin [27]. Some cracks were identified, especially in PU8(1/2). However, images obtained at higher

magnification showed more uniform and homogeneous microstructures for PU8(1/2), considering both surface and cross sections. These observations suggest a compatibilizing effect of lignin, in agreement with results for other types of lignin-containing PUs [29].

The WCA for the surface and cross sections are reported in Table S1. A higher WCA (9–10%) was recorded for the surface compared to the cross section, reflecting a more hydrophilic composition in the core of the PU. Unexpectedly, PU0 showed a hydrophilic character (WCA<90 °C), indicating that the addition of HDI to the castor oil matrix increased the surface energy of the mixture, as previously reported [30]. The hydrophobic character in the PU structure was partially recovered in the presence of lignin, probably due to the contribution of the aromatic skeleton and the random assembly of hydrocarbons, especially on the surface, where WCA >90° [31], even though the core still remained hydrophilic.

3.3. Rheological behavior

The mechanical and rheological properties of the oleo-PU elastomers varied over a broad range, depending on the HDI, lignin and castor oil concentrations (Table 1). In particular, as shown in Fig. 2, the values of the storage, G` and the loss, G`` moduli in the linear viscoelasticity regime spanned over a four-order of magnitude (note that pure elastomeric materials are included in Fig. 2a, whereas those showing a distinctive soft gel-like behavior are shown separately in Fig. 2b). The visual appearance of the oleo-PUs is shown in Fig. S4 (Supporting Information).

We compare the PU0 and PU8(1/2) samples to evaluate the effect of partial replacement of castor oil with lignin: slight differences in the storage moduli were noted, although the relative elastic response was slightly enhanced in PU0 (lower G``). The addition of lignin likely hindered castor oil structuration and hence crystallinity, thus providing lower relative elasticity to the system [32]. Nonetheless, it is worth mentioning that strain sweeps performed with PU8(1/2) in the torsional mode demonstrated outstanding flexibility of the specimen. Video S1 (Supporting Information), for example, shows a sample withstanding up to 720° counter- and clockwise twisting without breaking. As shown in the thermogravimetric spectra (Fig. S1), a higher free-HDI content was present in PU0 for reaction during the second preparation step (Fig. 1), which likely increased crosslinking, favoring the ultimate elastic response.

Supplementary video related to this article can be found at http s://doi.org/10.1016/j.compscitech.2020.108602

Taking PU8(1/2) as a reference for the lignin-based systems, we note

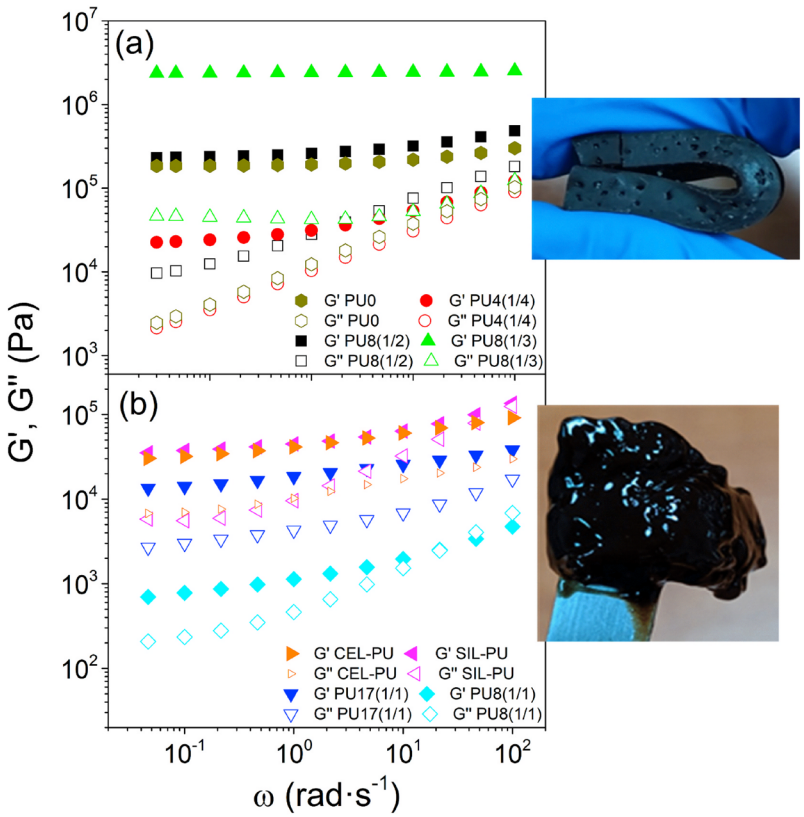

Fig. 2. Evolution of linear viscoelastic moduli with oscillatory frequency at 25 °C for the castor oil-based oleo-PU (PU0), and those reinforced with either lignin, cellulose (CEL-PU) or silica nanoparticles (SIL-PU). Samples showing elastomeric behavior (Fig. 2a) and soft or gel behavior (Fig. 2b) are shown. Selected photos for each system are also included to illustrate the differences (PU8(1/2), and PU8(1/1) respectively).

that an increase in the lignin content, to achieve lignin/HDI ratio of 1 (sample PU17(1/1)), failed to reach the desired elastomeric properties, as a consequence of the lower free –NCO content available for reaction with the castor oil during the second step. Indeed, similar behavior was observed for PU8(1/1), with a lower lignin content but the same lignin/HDI ratio. As a result, both PU17(1/1) and PU8(1/1) produced gel-like dispersions that are better suited for other applications, as previously reported [6,7]. In contrast, a higher relative diisocyanate content was obtained by decreasing the lignin content in the sample (PU4(1/4) with lignin/HDI ratio reduced to 1/4), which is expected to favor cross-linking. However, the viscoelastic properties did not reach the values as those found for 1/2 lignin/HDI ratio. This observation can be explained by considering the possible high crosslinking degree achieved during the first preparation step, which reduced the compatibilization of the functionalized lignin with castor oil during the second step, as already shown in the case of other, more reactive diisocyanates [7].

When the HDI concentration was increased, for a given lignin content, a more fully developed plateau zone was observed for the viscoelastic moduli, with much higher values, implying an enhanced elastic response (the storage and loss moduli differed by almost two orders of magnitude, see PU8(1/3) in Fig. 2a). As expected, a higher HDI concentration improves crosslinking [18,19].

Cellulose and silica nanoparticles, which are well-known oil-structuring agents [33] were tested at a filler/HDI ratio of 1/2 (Table 1) and compared with the results obtained with lignin. Noting that the viscoelastic moduli of the oleo-PUs obtained with cellulose and silica (CEL-PU and SIL-PU, respectively) were comparable to those of PU4(1/4) (Fig. 2b), the performance is clearly lower, in terms of stiffness and elasticity, compared to the lignin counterparts (Fig. S4). The results highlight the comparatively better effect of lignin as a reinforcing agent.

The thermo-rheological response of the elastomers was determined to explore potential applications. As such, the PU8(1/2) sample was subjected to oscillatory torsional deformation (SAOT) in the 25–200 °C range (Fig. 3). In general, a similar frequency dependence was found in the temperature range evaluated, especially below 140 °C (Fig. 3a and 3b). As can be observed, similar storage modulus values were achieved in the range of temperatures 25 to 40 °C as well as 80 to 140 °C. In contrast, a significant drop was observed from 40 to 80 °C and above 140 °C, which suggests an alteration of the elastomeric structure at those temperatures. The DSC thermogram (Fig. S5, Supporting Information) confirms the presence of two glass transition temperatures centered around 55 and 171 °C, related to HDI [34], which explains the dramatic drop in the viscoelastic functions. These results have been observed for large block polyurethanes due to microphase separation [35]. The evolution with frequency of both viscoelastic functions, up to 200 °C, has been supplemented with a temperature sweep (1 rad s^{-1}), as shown in Fig. 3c, which confirmed reduced G′ values in the ranges 45–80 °C and 160–185 °C. The assessment of the temperature effect on the rheological properties of the elastomer was also considered by running a subsequent cooling ramp, from 200 °C down to room temperature. As can be observed in Fig. 3c, the viscoelastic functions were drastically affected by the application of heating/cooling cycles, with no recovery of the initial values. Instead, G′ at 200 °C was maintained during cooling, whilst the G″ followed a similar trend compared to the increasing temperature ramp, but yielding lower values. Therefore, the relative elastic properties of the sample were dramatically reduced upon restoring room temperature conditions, with a shift of the loss tangent (G"/G') from 0.11 to 0.23.

3.4. Mechanical performance

The mechanical properties of the oleo-PU elastomers were evaluated by performing static compression and tension tests. The compression profiles of the oleo-PU elastomers showed a variety of compression

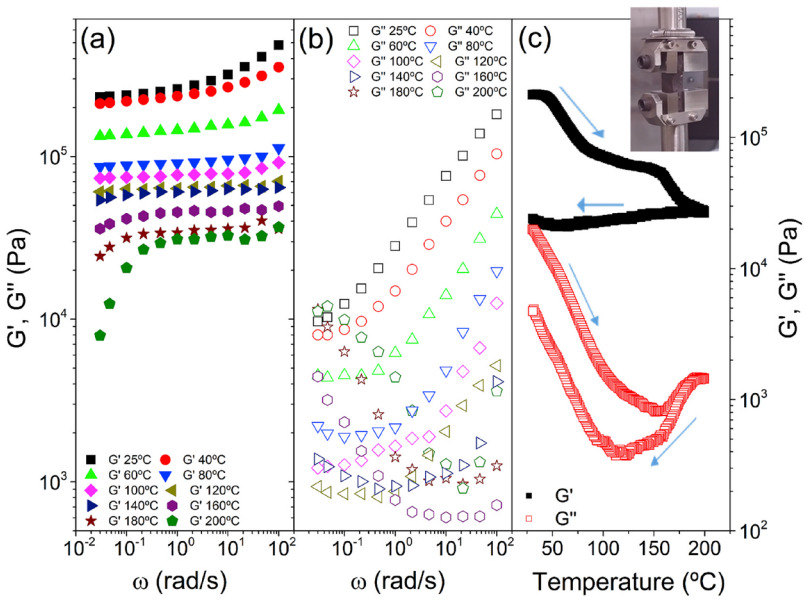

Fig. 3. Frequency-temperature dependence of the (a) storage and (b) loss moduli, within the 25–200 °C range. (c) Evolution of G' (■) and G" (□) for the PU8(1/2) sample undergoing subsequent heating (up to 200 °C) and cooling (down to 25 °C) cycles. The arrows indicate the time-evolution of the heating-cooling test. Inset: photograph of the sample in the torsional geometry during the test.

responses, depending on lignin, castor oil and HDI contents (see Fig. S6). All the elastomers exhibited an exponential increase of the compressive stress [36], σ_c, which follows equation (1). For comparison Table 2 lists the *A* and *B* parameters of Eq, 1 along with the σ_c values when reaching 20% and 50% strain and at failure.

From the data in Fig. S6 and Table 2, it is concluded that the lignin-free sample (PU0) exhibited the poorest mechanical performance, with <50% strain and a very low compressive stress (0.76 MPa) causing total failure (Video S2, Supporting Information), despite the relatively high elasticity exhibited in oscillatory torsional tests performed inside the linear viscoelastic regime. When castor oil was partially replaced with lignin, a remarkable improvement in performance was observed. Related effects have been reported in the literature for lignin as a filler in elastomers [17]. The PU4(1/4) sample, with only a 4.17 wt% lignin, withstood > 88% strain without failure, associated to a compressive stress at break that is 4-times higher compared to the value observed for PU0 (3 MPa). Besides, the softer viscoelastic behavior determined in SAOT tests was reflected in very low stress values needed to produce 20% and 50% strains. Doubling the lignin concentration (8.33 wt% lignin) endowed a substantially improved compressive mechanical response, as can be observed in PU8(1/2), where a compressive stress as high as ~67 MPa was necessary to break the sample, far better than that reported for other rubber or elastomeric materials [36,37] (see Video S3, Supporting Information) and comparable to high-impact composites based on alumina platelets [21]. Interestingly, the stress at 20 and 50% strain did not exceed those of PU0, demonstrating simultaneously a soft but very strong behavior at low and high deformations, respectively. We further note, however, that the mechanical properties were compromised at the highest lignin content, such as in the PU17(1/1) sample, which showed a gel-like rheological response, as previously discussed.

Supplementary video related to this article can be found at https://doi.org/10.1016/j.compscitech.2020.108602

The influence of a higher crosslinking degree was analyzed by comparing PU8(1/2) and PU8(1/3) at differing HDI concentrations. As expected, a stiffer and more brittle material was produced by increasing crosslinking [18,19]. A higher compressive stress was needed from the very beginning to compress the sample, as observed by the higher values of stress at 20 and 50% strains, whereas failure took place at much lower values, 19 MPa stress and 69% strain.

According to the parameters in Eq. (1), the highest *B* values are associated with samples that are capable of holding higher strains without failure. On the other hand, *A* is associated with the slope of the initial trend compared to the final values, indicating PU8(1/2) with the lowest *A*, followed by PU4(1/4) and PU8(1/3), which is the strongest PU.

The oleo-PU elastomers were subjected to tensile tests (Fig. 4 and Fig. S7). The tensile stress and elongation at break as well as Young modulus were determined (Table 3). Apart from Zhang et al. (2019), who reported remarkable elongations (~120%) in tensile tests performed with castor oil-based PUs [15], the rather poor mechanical performance observed in our reference system (PU0) is in agreement with other studies, which have shown values of elongation at break lower than 32% [12–14]. As in the compression tests, partial substitution of castor oil with lignin resulted in a better performance; although, the elongational properties depended on lignin and HDI concentration, as already shown in the literature [13]. The PU4(1/4) sample (4.17 wt% of lignin) showed a significant improvement in elongation at break (209%), more than 3 times higher than that obtained in the absence of lignin (62%). However, the softer rheological characteristics demanded a lower stress for the completion of the failure, also exhibiting a lower value of the Young modulus. A strengthening of the systems occurred by increasing either the lignin or the HDI content (increasing both the Young modulus and the stress at break). This effect was more pronounced for the PU8(1/3) sample, as a consequence of the increased crosslinking, as previously discussed. However, brittleness was severely compromised for the same reason, yielding much lower elongation at break [9,12]. Compared to PU4(1/4), the increased lignin loading in sample PU8(1/2) led to similar values of the strain at break, whereas higher Young modulus and stress at break were recorded. Even though the extensibility is still far from that found in other biocompatible composites especially designed for 3D printing [20], the results highlight the possibility of tuning the tensile properties according to the lignin content and lignin/HDI ratio, e.g., to fit the requirements of a given application.

3.5. Dynamic mechanical compression

Based on the compression and tensile results, PU8(1/2) was selected as the best elastomer for a wide variety of applications, and therefore we carried out a comprehensive study on the response of this system, to short- and long-term dynamic compression tests. Fig. 5 summarizes the short-time responses to dynamic compression tests (0.70 MPa/200 kg equivalent force, 0.5 cycles/s, during 70 s) of PU8(1/2) and PU0. As can be observed, excellent recovery properties at short times were observed for PU8(1/2), from which only very slight variations in successive strain cycles were observed. In contrast, PU0 failed during the first cycle, showing a continuous strain increase up to the end of the test. A quite interesting feature was observed upon unloading of the elastomeric sample, namely, PU8(1/2) underwent reverse loops at high strains. This "catapult" phenomenon has been observed in nature and indicates a fast release of the absorbed energy [38].

The effect of temperature and applied load in short-time dynamic compression tests can be evaluated from Fig. S8 (Supporting Information). The higher the temperature or loading, the higher the maximum strains achieved, as can be expected considering the relatively strong influence of temperature on the rheological properties. Furthermore, the effect of temperature turned out to be more critical in samples subjected to lower loads.

We discuss next the influence of temperature and applied load on the long-term dynamic compression response of PU8(1/2). The evolution of the compressive strain was followed after the completion of the 24 h-tests at different temperatures and loads. A clear relationship between compressive strain and time (plotted in a logarithmic scale) is observed (Fig. 6).

The relationship between maximum compressive strains and time observed in Fig. 6 is independent of the load applied, within the studied range, as very similar slopes were observed by applying 0.35 MPa and 0.70 MPa (100 or 200 kg force, respectively). Unlike load, the temperature noticeably affected the strain evolution with time, i.e., time effects became more limited at higher temperatures, possibly due to the

Table 2
Mechanical performance of elastomers in compression tests (data include the average value and standard deviation).

Sample	Compression parameters, Eq. 1		Stress at 20% strain (MPa)	Stress at 50% strain (MPa)	Stress at failure (MPa)	Strain at failure (%)
	A (MPa)	B ($\%^{-1}$)				
PU0	0.150	0.036	0.16 ± 0.01	0.75 ± 0.07	0.76 ± 0.09	50.7 ± 0.90
PU8(1/2)	3.72E-4	0.132	0.13 ± 0.02	0.72 ± 0.07	67.3 ± 9.86	93.7 ± 1.14
PU4(1/4)	2.85E-3	0.089	0.01 ± 0.01	0.13 ± 0.08	3.08 ± 0.15	88.6 ± 0.44
PU8(1/3)	0.528	0.059	1.38 ± 0.38	6.04 ± 2.23	19.1 ± 3.05	69.0 ± 4.08

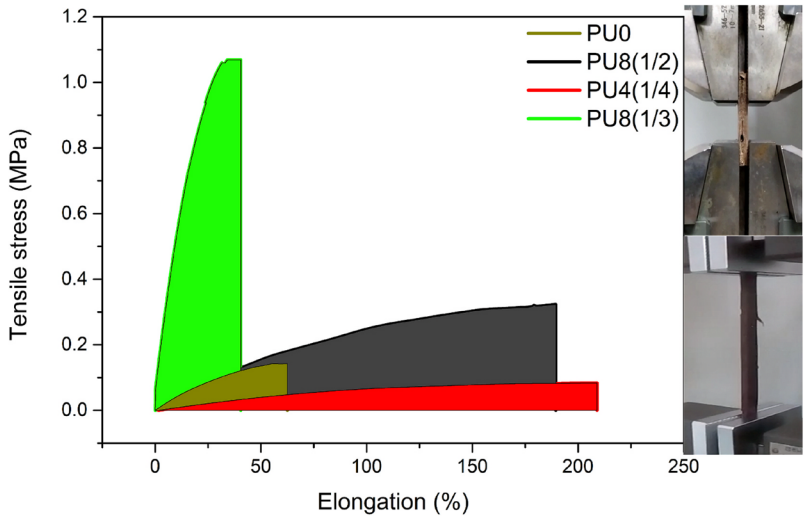

Fig. 4. Results of tensile tests (10 mm min^{-1} elongation rate) comparing the average tensile profiles for the different elastomers. The different replicates have been included in Fig. S7 (Supporting Information). Images of two elastomeric samples used in the tests (PU8(1/3), top and PU4(1/4), down) are included.

Table 3
Average and standard deviation values of the Young modulus, tensile stress and elongation at break obtained from tensile tests.

PU elastomer	Young modulus (MPa)	Tensile stress at break (kPa)	Elongation at break (%)
PU0	0.42 ± 0.02	145 ± 11	63 ± 8
PU8(1/2)	0.51 ± 0.02	323 ± 28	189 ± 17
PU4(1/4)	0.10 ± 0.02	80 ± 9	209 ± 42
PU8(1/3)	7.54 ± 1.24	1118 ± 172	35 ± 14

softening of the oleo-PU, as previously discussed. Some examples of cycles at different compression times are included in Fig. S9, which shows that the hysteresis loops did not change during the course of the tests [36]. This fact implies that the energy absorption of the material is not time-dependent, which substantially exceeds the results reported for other PU systems and commercial cushioning midsoles [16,39].

Compression tests were also performed after the 24-h essays in order to assess the fatigue effects in terms of mechanical properties. The compression remained unaltered for strains up to ca. 85%, after which failure started to occur (Fig. S10), slightly decreasing both the compressive stress and strain due to fatigue. However, these results are still far better than those reported for other cushioning materials [16, 36].

The evolution of the energy loss during different short-time strain cycles was evaluated. As can be seen in Fig. S11, the PU8(1/2) system is able to release higher energy than provided at low strains, probably due to some structurally-stored energy. Both loading and unloading cycles became closer to each other when increasing the strain, as the mechanical spectra evolved following the typical hysteresis losses exhibited by elastomers and rubbers, where a positive energy loss occurs [36]. Nevertheless, there is always a quick energy release immediately after unloading. We studied the evolution of the hysteresis losses, calculated by the difference between the areas under the compressive force curves in the loading and unloading cycles. Values from −12% up to 40% were recorded and plotted in Fig. 6 for increasing strains, indicating that PU8 (1/2) absorbed more energy under higher compression (Fig. 6). The energy absorption in our oleo-PU is similar to that reported for reference systems used as shoe soles for use under high loading [39].

In order to provide a quantitative reference to the cushioning properties, the cushioning factor (CF) was calculated from equation (2). Noting that CF < 8 is recommended for cushioning materials such as shoe soles [1], Fig. 7 (inset table) indicates that PU8(1/2) fully met such performance, with deformations higher than 35%, indicating excellent cushioning under high loading.

4. Conclusions

We demonstrate the strengthening effect of lignin as a filler in castor oil/HDI elastomers. Despite the reduced elasticity observed from rheological measurements, the addition of lignin promoted excellent performance as far as the tensile and compression behavior. Adjusting lignin or HDI concentration allows tailoring the rheological properties, from very soft to strong materials. The tensile strain at break of lignin-loaded polyurethanes was triplicated by replacing a small fraction of castor oil with lignin (4.17 wt%). At higher lignin content, 8.33 wt%, the PU maintained the elongation but presented 17- and 7-fold increases in the Young modulus and the stress at break, respectively. The increase in HDI concentration significantly enhanced the Young modulus and compressive stress at break with a simultaneous reduction of elongation. According to the compression tests, lignin addition (4.17 wt%) withstood > 88% strain without failure, an improvement of >38% compared to PU0, and exhibited a 4-times higher stress at break (3 MPa). A superior lignin addition (8.33 wt%), extended the outstanding properties, with a strain at failure of 93%, while the stress at break was 88-fold higher compared to the reference system, with values of 67 MPa, a record performance for biobased-polyurethane elastomers. Simultaneously, the sample exhibited similar stresses to produce 20 and 50% strains, thereby showing both soft and hard behavior depending on the strain applied. When isocyanate concentration was raised, higher stresses were needed to achieve 20 and 50% strains, however, the ultimate compressive strain was reduced. The optimum mechanical response was observed in elastomers with 8.33 wt% lignin and 1/2

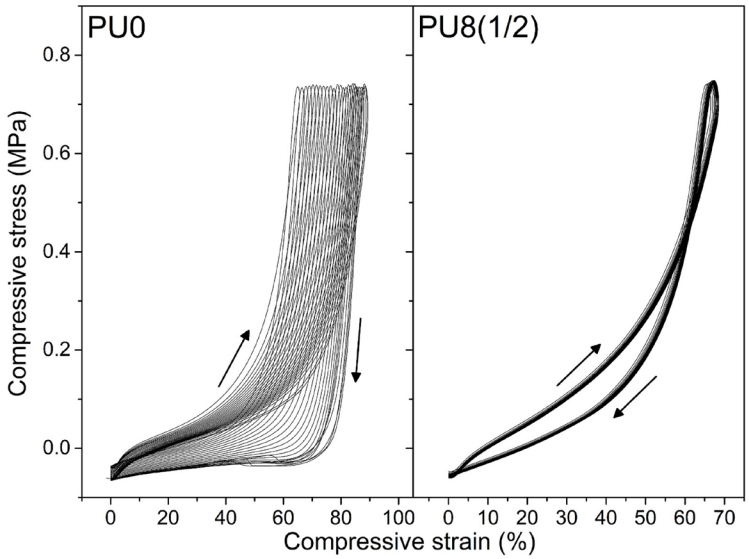

Fig. 5. Effect of lignin addition in the dynamic compression response of castor oil-based elastomer (PU0 and PU8(1/2)) evaluated in short-term (70 s) tests. Arrows are added to indicate successive compression cycles.

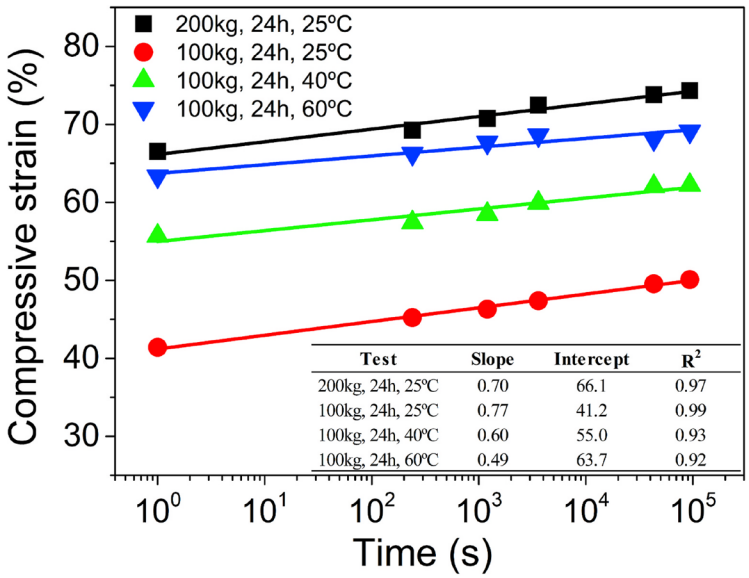

Fig. 6. Maximum compressive strains of PU8(1/2) with time during 24 h dynamic compression tests and measured under 100 (●) and 200 (■) kg compression loads at room temperature. Tests at 40 (▲) and 60 (▼) °C under 100 kg are also included. Inset: Values of the slope, intercept and coefficient of determination of the fits.

lignin/HDI ratio. Such systems demonstrated outstanding short- and long-term dynamic compression properties, such as time-independent energy absorption evolution, outstanding resilience in long term high-load fatigue tests and a fast release of the absorbed energy during the compression. These facts make lignin-loaded oleo-PU formulations highly suitable as cushioning material for diverse applications.

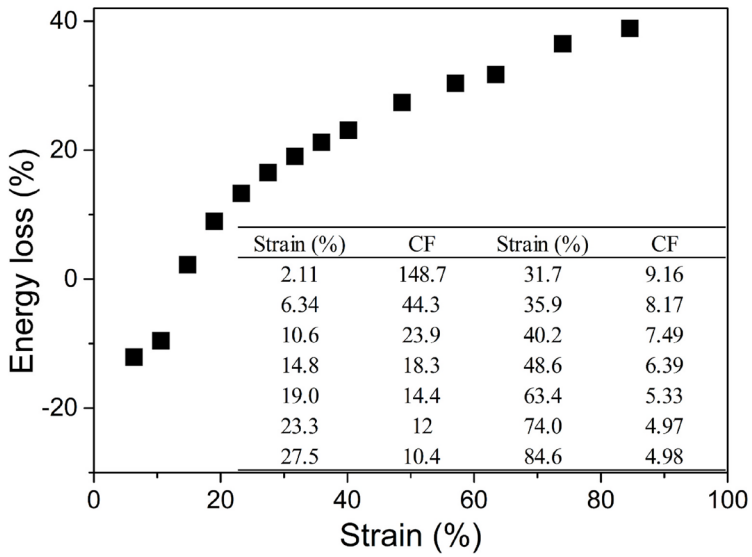

Strain (%)	CF	Strain (%)	CF
2.11	148.7	31.7	9.16
6.34	44.3	35.9	8.17
10.6	23.9	40.2	7.49
14.8	18.3	48.6	6.39
19.0	14.4	63.4	5.33
23.3	12	74.0	4.97
27.5	10.4	84.6	4.98

Fig. 7. Cushioning performance PU8(1/2): energy loss and cushioning factor (CF) (inset) as a function of the maximum strain applied.

CRediT authorship contribution statement

Antonio M. Borrero-López: Conceptualization, Funding acquisition, Investigation, Methodology, Writing - original draft. **Ling Wang:** Investigation, Methodology, Supervision, Writing - review & editing. **Concepción Valencia:** Funding acquisition, Supervision, Writing - review & editing. **José M. Franco:** Funding acquisition, Project administration, Supervision, Writing - review & editing. **Orlando J. Rojas:** Resources, Supervision, Project administration, Writing - review & editing.

Declaration of competing interest

The authors declare that they have no known competing financial interests or personal relationships that could have appeared to influence the work reported in this paper.

Acknowledgments

This work is part of a research project (RTI2018-096080-B-C21) sponsored by the MICINN-FEDER I + D + i Spanish Programme. A.M.B-L. acknowledges the Ph.D. Research Grant FPU16/03697 from MECD (Spain) and EST17/00875 and EST18/00577 grants from MEFP (Spain) which made possible the collaboration with the Aalto University.

Appendix A. Supplementary data

Supplementary data to this article can be found online at https://doi.org/10.1016/j.compscitech.2020.108602.

References

[1] M. Mukherjee, S.A. Gurusamy-Thangavelu, D.K. Chelike, A. Alagumalai, B.N. Das, S.N. Jaisankar, A.B. Mandal, Biodegradable polyurethane foam as shoe insole to reduce footwear waste: optimization by morphological physicochemical and mechanical properties, Appl. Surf. Sci. 499 (2020) 143966, https://doi.org/10.1016/j.apsusc.2019.143966.

[2] S. Octave, D. Thomas, Biorefinery: toward an industrial metabolism, Biochimie 91 (2009) 659–664, https://doi.org/10.1016/j.biochi.2009.03.015.

[3] S. Wang, W. Liu, D. Yang, X. Qiu, Highly resilient lignin-containing polyurethane foam, Ind. Eng. Chem. Res. 58 (2019) 496–504, https://doi.org/10.1021/acs.iecr.8b05072.

[4] B.M. Upton, A.M. Kasko, Strategies for the conversion of lignin to high-value polymeric materials: review and perspective, Chem. Rev. 116 (2016) 2275–2306, https://doi.org/10.1021/acs.chemrev.5b00345.

[5] M. Balakshin, E.A. Capanema, X. Zhu, I. Sulaeva, A. Potthast, T. Rosenau, O. Rojas, Spruce milled wood lignin: linear, branched or cross-linked? Green Chem. 22 (2020) 3985–4001, https://doi.org/10.1039/D0GC00964D.

[6] A.M. Borrero-López, A. Blánquez, C. Valencia, M. Hernández, M.E. Arias, M. E. Eugenio, Ú. Fillat, J.M. Franco, Valorization of soda lignin from wheat straw solid-state fermentation: production of oleogels, ACS Sustain. Chem. Eng. 6 (2018) 5198–5205, https://doi.org/10.1021/acssuschemeng.7b04846.

[7] A.M. Borrero-López, C. Valencia, J.M. Franco, Rheology of lignin-based chemical oleogels prepared using diisocyanate crosslinkers: effect of the diisocyanate and curing kinetics, Eur. Polym. J. 89 (2017) 311–323, https://doi.org/10.1016/j.eurpolymj.2017.02.020.

[8] D. Kai, M.J. Tan, P.L. Chee, Y.K. Chua, Y.L. Yap, X.J. Loh, Towards lignin-based functional materials in a sustainable world, Green Chem. 18 (2016) 1175–1200, https://doi.org/10.1039/c5gc02616d.

[9] M. Visanko, J.A. Sirviö, P. Piltonen, H. Liimatainen, M. Illikainen, Castor oil-based biopolyurethane reinforced with wood microfibers derived from mechanical pulp, Cellulose 24 (2017) 2531–2543, https://doi.org/10.1007/s10570-017-1286-x.

[10] R. Liang, J. Zhao, B. Li, P. Cai, X.J. Loh, C. Xu, P. Chen, D. Kai, L. Zheng, Implantable and degradable antioxidant poly(ε-caprolactone)-lignin nanofiber membrane for effective osteoarthritis treatment, Biomaterials 230 (2019) 119601, https://doi.org/10.1016/j.biomaterials.2019.119601.

[11] S.Y. Park, J.Y. Kim, H.J. Youn, J.W. Choi, Utilization of lignin fractions in UV resistant lignin-PLA biocomposites via lignin-lactide grafting, Int. J. Biol. Macromol. 138 (2019) 1029–1034, https://doi.org/10.1016/j.ijbiomac.2019.07.157.

[12] E. Hablot, D. Zheng, M. Bouquey, L. Avérous, Polyurethanes based on castor oil: kinetics, chemical, mechanical and thermal properties, Macromol. Mater. Eng. 293 (2008) 922–929, https://doi.org/10.1002/mame.200800185.

[13] L.B. Tavares, C.V. Boas, G.R. Schleder, A.M. Nacas, D.S. Rosa, D.J. Santos, Bio-based polyurethane prepared from Kraft lignin and modified castor oil, Express Polym. Lett. 10 (2016) 927–940, https://doi.org/10.3144/expresspolymlett.2016.86.

[14] A. Cassales, L.A. Ramos, E. Frollini, Synthesis of bio-based polyurethanes from Kraft lignin and castor oil with simultaneous film formation, Int. J. Biol. Macromol. 145 (2020) 28–41, https://doi.org/10.1016/j.ijbiomac.2019.12.173.

[15] W. Zhang, Y. Zhang, H. Liang, D. Liang, H. Cao, C. Liu, Y. Qian, Q. Lu, C. Zhang, High bio-content castor oil based waterborne polyurethane/sodium lignosulfonate composites for environmental friendly UV absorption application, Ind. Crop. Prod. 142 (2019) 111836, https://doi.org/10.1016/j.indcrop.2019.111836.

[16] H. Jeong, J. Park, S. Kim, J. Lee, N. Ahn, H. gyoo Roh, Preparation and characterization of thermoplastic polyurethanes using partially acetylated kraft lignin, Fibers Polym. 14 (2013) 1082–1093, https://doi.org/10.1007/s12221-013-1082-7.
[17] M. Alinejad, C. Henry, S. Nikafshar, A. Gondaliya, S. Bagheri, N. Chen, S.K. Singh, D.B. Hodge, M. Nejad, Lignin-based polyurethanes: opportunities for bio-based foams, elastomers, coatings and adhesives, Polymers 11 (2019) 1202, https://doi.org/10.3390/polym11071202.
[18] J. Zhang, M. Yao, J. Chen, Z. Jiang, Y. Ma, Synthesis and properties of polyurethane elastomers based on renewable castor oil polyols, J. Appl. Polym. Sci. 136 (2019) 47309, https://doi.org/10.1002/app.47309.
[19] X.P. An, J.H. Chen, Y.D. Li, J. Zhu, J.B. Zeng, Rational design of sustainable polyurethanes from castor oil: towards simultaneous reinforcement and toughening, Sci. China Mater. 61 (2018) 993–1000, https://doi.org/10.1007/s40843-017-9192-8.
[20] J.M. Koo, J. Kang, S.H. Shin, J. Jegal, H.G. Cha, S. Choy, M. Hakkarainen, J. Park, D.X. Oh, S.Y. Hwang, Biobased thermoplastic elastomer with seamless 3D-Printability and superior mechanical properties empowered by in-situ polymerization in the presence of nanocellulose, Compos. Sci. Technol. 185 (2020) 107885, https://doi.org/10.1016/j.compscitech.2019.107885.
[21] R.G. Crookes, H. Wu, S.J. Martin, C. Kay, G.W. Critchlow, Bio-inspired platelet reinforced elastomeric-ceramic composites for impact and high strain rate applications, Compos. Sci. Technol. 184 (2019) 107857, https://doi.org/10.1016/j.compscitech.2019.107857.
[22] Y. Zhang, R. Yan, T. dung Ngo, Q. Zhao, J. Duan, X. Du, Y. Wang, B. Liu, Z. Sun, W. Hu, H. Xie, Ozone oxidized lignin-based polyurethane with improved properties, Eur. Polym. J. 117 (2019) 114–122, https://doi.org/10.1016/j.eurpolymj.2019.05.006.
[23] J.M. Lang, U.M. Shrestha, M. Dadmun, The effect of plant source on the properties of lignin-based polyurethanes, Front. Energy Res. 6 (2018) 4, https://doi.org/10.3389/fenrg.2018.00004.
[24] S.M. Hong, J.R. Cha, J.G. Kim, Preparation of body-temperature-triggered shape-memory polyurethane with biocompatibility using isosorbide and castor oil, Polym. Test. 91 (2020) 106852, https://doi.org/10.1016/j.polymertesting.2020.106852.
[25] Z. Gao, J. Peng, T. Zhong, J. Sun, X. Wang, C. Yue, Biocompatible elastomer of waterborne polyurethane based on castor oil and polyethylene glycol with cellulose nanocrystals, Carbohydr. Polym. 87 (2012) 2068–2075, https://doi.org/10.1016/j.carbpol.2011.10.027.
[26] S. Oprea, Dependence of fungal biodegradation of PEG/castor oil-based polyurethane elastomers on the hard-segment structure, Polym. Degrad. Stabil. 95 (2010) 2396–2404, https://doi.org/10.1016/j.polymdegradstab.2010.08.013.
[27] M.A. Rahman, D. De Santis, G. Spagnoli, G. Ramorino, M. Penco, V.T. Phuong, A. Lazzeri, Biocomposites based on lignin and plasticized poly(L-lactic acid), J. Appl. Polym. Sci. 129 (2013) 202–214, https://doi.org/10.1002/app.38705.
[28] H. Bian, L. Wei, C. Lin, Q. Ma, H. Dai, J.Y. Zhu, Lignin-containing cellulose nanofibril-reinforced polyvinyl alcohol hydrogels, ACS Sustain. Chem. Eng. 6 (2018) 4821–4828, https://doi.org/10.1021/acssuschemeng.7b04172.
[29] C.W. Park, W.J. Youe, S.Y. Han, J.S. Park, E.A. Lee, J.Y. Park, G.J. Kwon, S.J. Kim, S.H. Lee, Influence of lignin and polymeric diphenylmethane diisocyante addition on the properties of poly(butylene succinate)/wood flour composite, Polymers 11 (2019) 1161, https://doi.org/10.3390/polym11071161.
[30] A.D. Macalino, V.A. Salen, L.Q. Reyes, Castor oil based polyurethanes: synthesis and characterization, IOP Conf. Ser. Mater. Sci. Eng. 229 (2017), 012016, https://doi.org/10.1088/1757-899X/229/1/012016.
[31] W. Horwath, Carbon cycling: the dynamics and formation of organic matter, in: E. A. Paul (Ed.), Soil Microbiology, Ecology and Biochemistry, fourth ed., Elsevier Inc., Amsterdam, 2015, pp. 339–382, https://doi.org/10.1016/b978-0-12-415955-6.00012-8.
[32] P. Mousavioun, P.J. Halley, W.O.S. Doherty, Thermophysical properties and rheology of PHB/lignin blends, Ind. Crop. Prod. 50 (2013) 270–275, https://doi.org/10.1016/j.indcrop.2013.07.026.
[33] A.R. Patel, Alternative Routes to Oil Structuring, Springer, Berlin, 2015, https://doi.org/10.1007/978-3-319-19138-6.
[34] Q. Luo, J. Chen, P. Gnanasekar, X. Ma, D. Qin, H. Na, J. Zhu, N. Yan, A facile preparation strategy of polycaprolactone (PCL)-based biodegradable polyurethane elastomer with a highly efficient shape memory effect, New J. Chem. 44 (2020) 658–662, https://doi.org/10.1039/c9nj05189a.
[35] S. Velankar, S.L. Cooper, Microphase separation and rheological properties of polyurethane melts. 1. Effect of block length, Macromolecules 31 (1998) 9181–9192, https://doi.org/10.1021/ma9811472.
[36] C. Delgado-Sánchez, G. Amaral-Labat, L.I. Grishechko, A. Sánchez-Sánchez, V. Fierro, A. Pizzi, A. Celzard, Fire-resistant tannin-ethylene glycol gels working as rubber springs with tuneable elastic properties, J. Mater. Chem. A. 5 (2017) 14720–14732, https://doi.org/10.1039/c7ta03768f.
[37] K. Haraguchi, Synthesis and properties of soft nanocomposite materials with novel organic/inorganic network structures, Polym. J. 43 (2011) 223–241, https://doi.org/10.1038/pj.2010.141.
[38] R.M. Alexander, H.C. Bennet-Clark, Storage of elastic strain energy in muscle and other tissues, Nature 265 (1977) 114–117, https://doi.org/10.1038/265114a0.
[39] L. Wang, Y. Hong, J.X. Li, Durability of running shoes with ethylene vinyl acetate or polyurethane midsoles, J. Sports Sci. 30 (2012) 1787–1792, https://doi.org/10.1080/02640414.2012.723819.

Chapter 5
Conclusions

The following general conclusions can be drawn from the research carried out in the context of this PhD Thesis:

- A number of lignocellulosic materials, including wheat and barley straws, cellulose pulps and residual lignin from different origins, were able to successfully act as thickeners, binders o reinforcing agents in castor oil through chemical reaction with diisocyanates, thus generating bio-based polyurethanes with diverse industrial applications, such as lubricating greases, cushioning materials and/or adhesives, depending on biosource/diisocyanate weight ratio, castor oil concentration and formulation protocol.

- The rheological characteristics of lignin- and castor oil-based polyurethanes produced by following a two-step processing protocol demonstrated to be highly dependent on nature and chemical structure of the diisocyanate selected. More reactive aromatic diisocyanates promoted the formation of highly crosslinked networks during the first step, involving the reaction with the lignocellulosic material, which hindered the castor oil structuring that takes place in the second step, compromising the oleogel strength. The cyclic structure of IDI likewise dampened a suitable gel formation. Only HDI, with a linear aliphatic structure, led to the achievement of enhanced gel-like characteristics.

- The mechanical behaviour of polyurethanes developed by applying one-step procedure with residual lignin and castor oil as main components were also severely affected by diisocyanate nature, as expected, but also by the imposed processing conditions, i.e., temperature and stirring speed. Polyurethanes produced at room temperature and under low stirring conditions exhibited gel-like characteristics, whereas an increase in temperature and/or stirring speed resulted in liquid-like properties of the final products, which was associated to a faster curing. The comparison between the two-step and the one-step processing protocol allows to conclude that gel-like properties are more easily obtained by the simpler and faster process, which also needed a lower crosslinker content to get similar rheological responses.

- The gel-like properties of lignin-based polyurethanes can also be modulated by the biosource/HDI weight ratio and castor oil content. Suitable gel-like characteristics,

comparable to those shown by commercial lithium lubricating greases, were optimally achieved with 1/2 biosource/HDI weight ratio and 70% wt. castor oil content.

- The rheological properties can likewise be tailored by using differently-sourced lignins and/or by applying different pretreatments. Therefore, a higher carbohydrate content, higher molecular weight and lower phenolic content, obtained by producing residual lignin through mild pretreatments, was concomitant with the formulation of oleogels with enhanced viscoelastic properties. The differently-sourced residual lignins similarly provided diverse outcomes, basically attributed to the differences in phenolic hydroxyl groups content.

- A more environmentally-friendly biological pretreatment, the solid-state fermentation with *Streptomyces*, was applied to modify the lignocellulose structure. Both inoculated and fermented barley and wheat straws, as well as the cellulose pulps and lignin-enriched fractions obtained from them, were successfully used as gelling agents in castor oil. Once more, the straw source type highly influenced the rheological properties of the oleogels, nonetheless, they also experienced different behaviour when fermented, as a consequence of the different enzymatic patterns. Thus, whereas fermented barley straw produced an increase in the viscoelastic functions of derived oleogels, the opposite effect was found with fermented wheat straw, as a consequence of the stronger CMCase activity in wheat straw. Regarding the cellulose pulps, the solid-state fermentation was always responsible for an improvement in the linear viscoelastic functions of all developed oleogels, atrributted to the increase of hydroxyl groups availability and the higher polymerization degree obtained. Lastly, fermented lignin-based oleogels also experienced an enhancement of the viscoelastic properties in comparison to oleogels produced with non-fermented lignins, again due to the higher content of hydroxyl groups induced by the main breakdown of lignin linkages, which are available to further react with the diisocyanates.

- In general, all the oleogels performed with the different lignocellulosic sources exhibited good lubricant properties, with friction coefficient values that were comparable or even lower than those obtained with commercial lubricating greases and similarly preventing wear.

- The stickiness and rheological properties of lignin- and castor oil-based polyurethane adhesives herein formulated demonstrated to be strongly dependent on lignin origin and solid-state fermentation conditions, exhibiting very good adhesion properties in wood-wood joints, as expected, but also in other surfaces like stainless steel-stainless steel and stainless steel-textile joints.

- Outstanding both static and dynamic compressive, tensile and torsional properties were obtained by the inclusion of lignin in castor oil-based polyurethane elastomers, enhancing stress at break, strain at failure and being able to withstand massive loads for long periods. Moreover, the modification of the lignin/HDI ratio and castor oil concentration allowed the mechanical behaviour of the elastomers to be tailored. These characteristics make these products highly suitable as cushioning materials.

Annex I

1. Contributions to congresses and conferences derived from the work performed in Ph.D.

- Title of the contribution: Valorization of kraft lignin as thickener in castor oil for lubricant applications
  Type of contribution: Poster
  Congress: Lignocost
  Presenting author: No
  City: Régua, Portugal
  Opening date: 13/11/2019
  Closing date: 14/11/2019
  Authors: Antonio María Borrero López; Francisco José Santiago Medina; Concepción Valencia Barragán; María Eugenia Eugenio; Raquel Martín Sampedro; José María Franco.

- Title of the contribution: Adhesion and rheological properties of lignin-based polyurethanes: Influence of the solid-state fermentation pretreatment applied on barley Straw
  Type of contribution: Poster
  Congress: ANQUE-ICCE-CIBIQ 2019
  Presenting author: No
  City: Santander, Cantabria, Spain
  Opening date: 19/06/2019
  Closing date: 21/06/2019
  Organizing committee: Asociación de Química e Ingeniería Química de Cantabria
  Authors: Antonio María Borrero López; Concepción Valencia Barragán; José María Franco.

- Title of the contribution: Influence of lignin functionalization with laccase on the rheological properties of polyurethane-based oleogels
  Type of contribution: Poster
  Congress: Iberian Meeting on Rheology (IBEREO 2019)
  Corresponding author: No
  City: Oporto, Portugal
  Opening date: 04/09/2019
  Closing date: 06/09/2019
  Organizing committee: Spanish Group of Rheology
  (GER) & Portuguese Society of Rheology (SPR)
  Authors: Antonio María Borrero López; Concepción Valencia Barragán; José Enrique Martín Alfonso; José María Franco Gómez.

- Title of the contribution: Lignin-based polyurethanes with adhesion properties: a comprehensive study of lignin
  modification with Streptomyces
  Type of contribution: Oral presentation
  Congress: Iberian Meeting on Rheology (IBEREO 2019)

Corresponding author: Yes
City: Oporto, Portugal
Opening date: 04/09/2019
Closing date: 06/09/2019
Organizing committee: Spanish Group of Rheology (GER) & Portuguese Society of Rheology (SPR)
Authors: Antonio María Borrero López; Concepción Valencia Barragán; José María Franco Gómez.

- Title of the contribution: Solid-state fermentation with streptomyces to enhance the thickening properties of cellulose pulp and lignin in castor oil
  Type of contribution: Oral presentation
  Congress: X Congreso Jóvenes Investigadores en Polímeros (JIP 2019)
  Corresponding author: Yes
  City: Burgos, Castile and Leon, Spain
  Opening date: 20/05/2019
  Closing date: 23/05/2019
  Organizing committee: Universidad de Burgos
  Authors: Antonio María Borrero López; Concepción Valencia Barragán; José María Franco Gómez.
  Published in: "Polímeros para el siglo XXI. X Congreso Jóvenes Investigadores en Polímeros (JIP 2019)".

- Title of the contribution: Solid-state fermentation as potential tool to modify lignin from wheat straw: production of oleogels
  Type of contribution: Oral presentation
  Congress: IV Jornadas de Doctorandos from Universidad de Huelva
  Corresponding author: Yes
  City: Huelva, Andalucía, Spain
  Opening date: 08/11/2018
  Closing date: 09/11/2018
  Organizing committee: Universidad de Huelva
  Authors: Antonio María Borrero López; Concepción Valencia Barragán; José María Franco Gómez

- Title of the contribution: Propiedades reológicas y adhesivas de poliuretanos basados en lignina modificada y aceite de ricino: influencia de la fermentación en estado sólido con Streptomyces
  Type of contribution: Poster
  Congress: Conferencia Internacional de Nanogateway (Mission 10000) 2018
  Corresponding author: No
  City: Braga, Portugal
  Opening date: 17/10/2018
  Closing date: 17/10/2018
  Organizing committee: International Iberian Nanotechnology Laboratory
  Authors: Antonio María Borrero López; Concepción Valencia Barragán; José María Franco Gómez.

- Title of the contribution: Processing temperature impact on the rheological behaviour of castor oil and lignin-based polyurethanes
  Type of contribution: Poster
  Congress: XV Reunión del grupo especializado de Polímeros GEP (RSEQ, RSEF)
  Corresponding author: No
  City: Punta Umbría (Huelva), Andalucía, Spain.
  Opening date: 24/09/2018
  Closing date: 27/09/2018
  Organizing committee: Grupo Especializado de Polímeros
  Authors: Antonio María Borrero López; Francisco José Santiago Medina; Concepción Valencia Barragán; José María Franco Gómez.

- Title of the contribution: Influence of processing variables on the rheological properties of one-step processed castor oil/lignin-based gel-like polyurethanes
  Type of contribution: Oral presentation
  Congress: 82nd Prague meeting on Macromolecules – Polymer Networks and Gels
  Corresponding author: Yes
  City: Prague, Czech Republic
  Opening date: 17/06/2018
  Closing date: 21/06/2018
  Organizing committee: Polymer Networks Group, IUPAC, IMC, CSCH, EPF
  Authors: Antonio María Borrero López; Concepción Valencia Barragán; José María Franco Gómez.

- Título of the contribution: NCO-Functionalized wheat and barley straws-based oleogels: influence of solid-state fermentation
  Type of contribution: Poster
  Congress: 82nd Prague meeting on Macromolecules –Polymer Networks and Gels
  Corresponding author: No
  City: Prague, Czech Republic
  Opening date: 17/06/2018
  Closing date: 21/06/2018
  Organizing committee: Polymer Networks Group, IUPAC, IMC, CSCH, EPF
  Authors: Antonio María Borrero López; Concepción Valencia Barragán; José María Franco Gómez.

- Title of the contribution: Elaboración de una grasa lubricante biodegradable a partir de paja de cebada fermentada con Streptomyces sp. MDG 301
  Type of contribution: Poster
  Congress: VII Congreso Nacional de Microbiología y Biotecnología Microbiana
  City: Cádiz, Andalucía, Spain
  Corresponding author: No
  Opening date: 06/06/2018
  Closing date: 08/06/2018
  Organizing committee: Grupo de Microbiología Aplicada y Biotecnología Fúngica
  Authors: Alba Blánquez; Gabriela Domínguez; Carmen Fajardo; Antonio María Borrero López; Concepción Valencia; María E. Arias; Manuel Hernández; Juana Rodríguez.

Published in: "Microbiología Industrial y Biotecnología Microbiana: Actas del VII CMIBM 2018"

- Title of the contribution: Funcionalización de ligninas mediante la lacasa SilA de S. ipomoeae CECT 3341 para la obtención de polímeros de utilidad industrial
  Type of contribution: Poster
  Congress: VII Congreso Nacional de Microbiología y Biotecnología Microbiana
  City: Cádiz, Andalucía, Spain
  Corresponding author: No
  Opening date: 06/06/2018
  Closing date: 08/06/2018
  Organizing committee: Grupo de Microbiología Aplicada y Biotecnología Fúngica
  Authors: Gabriela Domínguez; Alba Blánquez; Rodrigo Serrano; Antonio María Borrero López; Concepción Valencia; Francisco Guillén; María E. Arias; Manuel Hernández.
  Published in: "Microbiología Industrial y Biotecnología Microbiana: Actas del VII CMIBM 2018"

- Title of the contribution: Desarrollo de nuevos agentes espesantes basados en fracciones lignocelulósicas para formulaciones biodegradables tipo gel en fase oleosa con diversas aplicaciones industriales
  Type of contribution: Poster
  Congress: I Jornadas Doctorales en Energías Renovables
  Corresponding author: Yes
  City: Jaén, Andalucía, Spain
  Opening date: 09/05/2018
  Closing date: 11/05/2018
  Organizing committee: Centro de Estudios Avanzados en Energía y Medio Ambiente from Universidad de Jaén
  Authors: Antonio María Borrero López; Concepción Valencia Barragán; José María Franco Gómez.

- Title of the contribution: Bio-based polyurethanes for industrial applications
  Type of contribution: Oral presentation
  Congress: III Jornadas de Doctorandos from Universidad de Huelva
  Corresponding author: Yes
  City: Huelva, Andalucía, Spain
  Opening date: 02/11/2017
  Closing date: 03/11/2017
  Organizing committee: Universidad de Huelva
  Authors: Antonio María Borrero López; Concepción Valencia Barragán; José María Franco Gómez.

- Title of the contribution: Effect of preparation protocol on the rheological properties of chemically modified alkali lignin-based oleogels
  Type of contribution: Poster
  Congress: 10th World Congress of Chemical Engineering
  Corresponding author: No
  City: Barcelona, Catalonia, Spain

Opening date: 01/10/2017
Closing date: 05/10/2017
Organizing committee: EFCE-Spain Group
Authors: Antonio María Borrero López; Concepción Valencia Barragán; José María Franco Gómez.

- Title of the contribution: Influence of processing conditions on the rheological behaviour of NCO-functionalized lignin-based gel-like dispersions
  Type of contribution: Oral presentation
  Congress: Iberian Meeting on Rheology (IBEREO 2017)
  Corresponding author: Yes
  City: Valencia, Valencian Community, Spain
  Opening date: 06/09/2017
  Closing date: 08/09/2017
  Organizing committee: Grupo Español de Reología & Sociedade Portuguesa de Reologia
  Authors: Antonio María Borrero López; Concepción Valencia Barragán; José María Franco Gómez.

- Title of the contribution: Rheological properties of lignin-based oleogels prepared using different diisocyanate crosslinkers
  Type of contribution: Oral presentation
  Congress: IX Congreso de Jóvenes Investigadores en Polímeros
  Corresponding author: Yes
  City: Tarragona, Catalonia, Spain
  Opening date: 05/06/2017
  Closing date: 08/06/2017
  Organizing committee: Universidad Rovira i Virgili & Grupo Especializado de Polímeros
  Antonio María Borrero López; Concepción Valencia Barragán; José María Franco Gómez.

- Title of the contribution: Formulation and characterization of oleogels based on chemically modified waste lignins for potential lubricant applications
  Type of contribution: Poster
  Congress: Fifth International Symposium Frontiers in Polymer Science
  Corresponding author: Yes
  City: Seville, Andalucía, Spain
  Opening date: 17/05/2017
  Closing date: 19/05/2017
  Organizing committee: Elsevier
  Authors: Antonio María Borrero López; Concepción Valencia Barragán; José María Franco Gómez.

2. Other contributions related to the work performed in Ph.D.

2.1. Articles

The present Ph.D. thesis has led to the publication of other articles not directly concerned with the work initially planned but related to, mainly as a consequence of the collaboration with other research groups. Three different articles regarding the hydrothermal carbonization of lignocellulosic biomass have been published along the course of the thesis, which have demonstrated that suitable compounds with other interesting industrial applications can be obtained from this harmless procedure.

- Borrero-López, A.M.; Fierro, V.; Jeder, A.; Ouederni, A.; Masson, E.; Celzard, A. High added-value products from the hydrothermal carbonisation of olive stones. *Environ. Sci. Pollut. Res.* **2017**, *24*, 9859–9869, doi:10.1007/s11356-016-7807-6. (Q2, IF:2.800, Environmental Sciences 83/242)
- Borrero-López, A.M.; Masson, E.; Celzard, A.; Fierro, V. Modelling the reactions of cellulose, hemicellulose and lignin submitted to hydrothermal treatment. *Ind. Crops Prod.* **2018**, *124*, 919–930, doi:10.1016/j.indcrop.2018.08.045. (Q1, IF: 4.191, Agronomy 3/89)
- Borrero-López, A.M.; Masson, E.; Celzard, A.; Fierro, V. Modelling the production of solid and liquid products from the hydrothermal carbonisation of two biomasses. *Ind. Crops Prod.* **2020**, *151*, 112452, doi:10.1016/j.indcrop.2020.112452. (Q1, IF: 4.244, Agronomy 8/91)

On the other hand, the oleogels obtained in this thesis have been evaluated in terms of sustainability and ecotoxicity in the context of the collaboration with the University of Alcalá de Henares, which have derived into the publication:

- Fajardo, C.; Blánquez, A.; Domínguez, G.; Borrero-López, A.M.; Valencia, C.; Hernández, M.; Arias, M.E.; Rodríguez, J. Assessment of Sustainability of Bio Treated Lignocellulose-Based Oleogels. *Polymers* **2021**, *13*, 267, doi:10.3390/polym13020267. (Q1, IF: 3.426, Polymer Science 16/89)

Moreover, another publication dealing with the modification of lignin with laccase at different concentrations and environmental conditions has also been published:

- Domínguez, G.; Blánquez, A.; Borrero-López, A.M.; Valencia, C.; Eugenio, M.E. Arias, M.E. Rodríguez, J.; Hernández, M. Eco-friendly oleogels from functionalized Kraft lignin with laccase SilA from *Streptomyces ipomoeae*: an opportunity to replace commercial lubricants. *ACS Sus. Chem. Eng.* **2021,** *9*, 4611–4616. https://doi.org/10.1021/acssuschemeng.1c00113. (Q1, IF: 7.632, Chemical Engineering 8/143)

2.2. Congresses

During the course of the Ph.D. thesis, a number of posters and oral presentations in both national and international congresses and conferences have been carried out, and are detailed hereunder:

- No contributtion
  Congress: Congreso Internacional Cambio Climático SOCC 2017
  City: Huelva, Andalucía, Spain
  Opening date: 10/05/2017
  Closing date: 12/05/2017
  Organizing committee: Junta de Andalucía, Diputación de Huelva & Ayuntamiento de Huelva

- Title of the contribution: Nitrogen doped carbon materials as electrocatalysts for oxygen reduction reaction
  Type of contribution: Poster
  Congress: The World Conference on Carbon: Common fundamentals, remarkably versatile applications
  Corresponding author: No
  City: State College, USA
  Opening date: 10/07/2016
  Closing date: 15/07/2016
  Organizing committee: American Carbon Society
  Authors: María Jesús Nieto Monge; Giovanni Lemes; Antonio María Borrero López; C. Alegre; Rafael Moliner; M. V. Martínez Huerta; M. C. Goya; E. Pastor; María Jesús Lázaro Elorri.

- Title of the contribution: Towards an efficient synthesis of NiO/heteroatom (N, S or B)-doped graphene nanocomposites
  Type of contribution: Poster
  Congress: The World Conference on Carbon: Common fundamentals, remarkably versatile applications

Corresponding author: No
City: State College, USA
Opening date: 10/07/2016
Closing date: 15/07/2016
Organizing committee: American Carbon Society
Authors: Giovanni Lemes; José Manuel Luque Centeno; Antonio María Borrero López; Sara Pérez Rodríguez; C. Montero; L. M. Rivera; M. V. Martínez Huerta; E. Pastor; Rafael Moliner; María Jesús Lázaro Elorri.

- Title of the contribution: Electrocatalizadores basados en grafenos dopados para pilas de combustible
  Congress: II Encuentro de Jóvenes Investigadores de la SECAT
  Corresponding author: No
  City: Ciudad Real, Castile-La Mancha, Spain
  Opening date: 27/06/2016
  Closing date: 27/06/2016
  Organizing committee: Asociación Española de Catálisis
  Authors: Giovanni Lemes; Sara Pérez Rodríguez; Antonio María Borrero López; José Manuel Luque Centeno; M. V. Martínez Huerta; E. Pastor; María Jesús Lázaro Elorri.

- Title of the contribution: Nitrogen doped carbon materials as electrocatalysts for oxygen reduction reaction
  Congress: World Hydrogen Energy Conference
  Corresponding author: No
  City: Zaragoza, Aragon, Spain
  Opening date: 13/06/2016
  Closing date: 16/06/2016
  Organizing committee: Asociación Española del Hidrógeno
  Authors: Giovanni Lemes; Antonio María Borrero López; María Jesús Nieto Monge; C. Alegre; Rafael Moliner; María Jesús Lázaro Elorri; M. V. Martínez Huerta; M. C. Goya; E. Pastor.

List of Figures & Tables

1. List of Figures

Chapter 2: State of the art

Chapter 3: Materials & Methods

2. List of Tables

Chapter 2: State of the art

Chapter 3: Materials & Methods